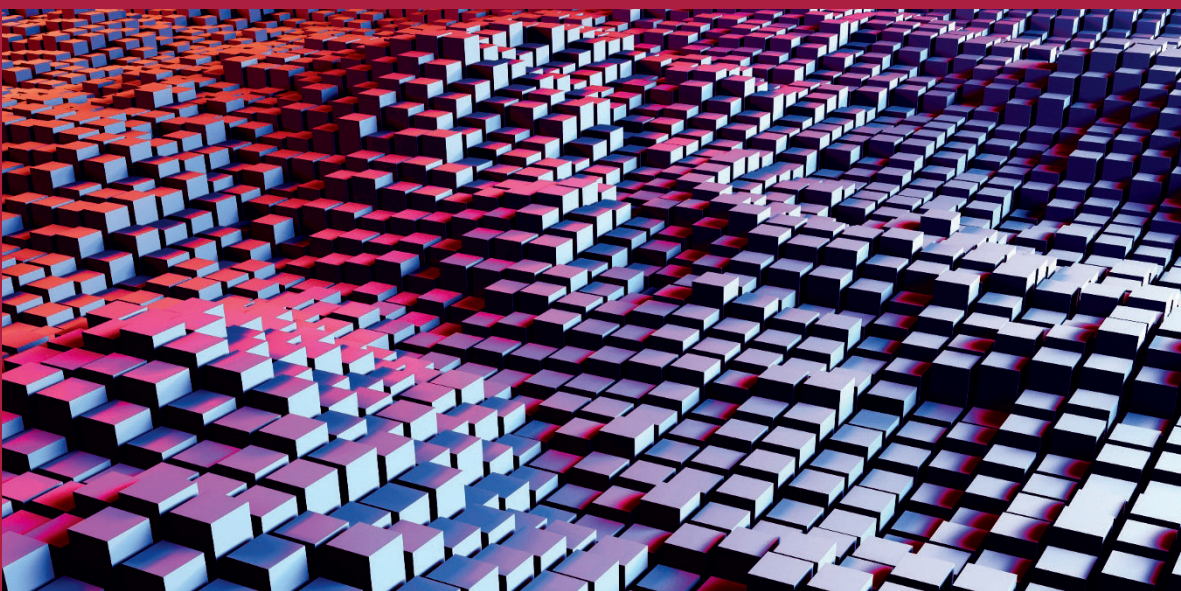


**MATERIALS SCIENCE SERIES**



# **Dyes and Chromophores in Polymer Science**

**Edited by  
Jacques Lalevée  
Jean-Pierre Fouassier**

**ISTE**

**WILEY**



## Dyes and Chromophores in Polymer Science



*Series Editor*  
*Yves Rémond*

---

# **Dyes and Chromophores in Polymer Science**

---

*Edited by*

Jacques Lalevée  
Jean-Pierre Fouassier

**ISTE**

**WILEY**

First published 2015 in Great Britain and the United States by ISTE Ltd and John Wiley & Sons, Inc.

Apart from any fair dealing for the purposes of research or private study, or criticism or review, as permitted under the Copyright, Designs and Patents Act 1988, this publication may only be reproduced, stored or transmitted, in any form or by any means, with the prior permission in writing of the publishers, or in the case of reprographic reproduction in accordance with the terms and licenses issued by the CLA. Enquiries concerning reproduction outside these terms should be sent to the publishers at the undermentioned address:

ISTE Ltd  
27-37 St George's Road  
London SW19 4EU  
UK

[www.iste.co.uk](http://www.iste.co.uk)

John Wiley & Sons, Inc.  
111 River Street  
Hoboken, NJ 07030  
USA

[www.wiley.com](http://www.wiley.com)

© ISTE Ltd 2015

The rights of Jacques Lalevée and Jean-Pierre Fouassier to be identified as the authors of this work have been asserted by them in accordance with the Copyright, Designs and Patents Act 1988.

Library of Congress Control Number: 2015932910

---

British Library Cataloguing-in-Publication Data  
A CIP record for this book is available from the British Library  
ISBN 978-1-84821-742-3

---

---

# Contents

---

<b>PREFACE</b> . . . . .	xi
<b>CHAPTER 1. TRENDS IN DYE PHOTOSENSITIZED RADICAL POLYMERIZATION REACTIONS</b> . . . . .	1
Jacques LALEVÉE and Jean-Pierre FOUASSIER	
1.1. Introduction. . . . .	1
1.2. A brief overview of dye-based PISs . . . . .	6
1.2.1. Dye one-component systems . . . . .	6
1.2.2. Dye two-component systems . . . . .	7
1.2.3. Dye three-component systems . . . . .	10
1.3. A discussion on specific or recent developments in dye-based photoinitiating systems . . . . .	12
1.3.1. Dyes for use with polychromatic visible lights . . . . .	14
1.3.2. Dyes for blue, green and red laser light-induced polymerizations. . . . .	16
1.3.3. Dyes as part of PISs in the medical area . . . . .	18
1.3.4. Dyes in controlled radical photopolymerization reactions . . . . .	19
1.3.5. Photoinitiation under soft irradiation conditions: novel three-component systems . . . . .	19
1.3.6. Dyes with red-shifted absorptions and high molar extinction coefficients . . . . .	22
1.3.7. Performances of novel three-component PISs in low-viscosity matrices under LEDs/laser diodes and low-intensity household devices . . . . .	23
1.3.8. Recoverable dyes: the concept of photoinitiator catalysts . . . . .	25
1.3.9. Metal-based dyes: recent perspectives . . . . .	26
1.3.10. Dyes under sunlight exposure. . . . .	27

1.3.11. Dye-based PISs as a source of mediator radicals: application to FRPCP . . . . .	27
1.3.12. Dyes exhibiting a dual radical/cationic behavior: application to concomitant radical/cationic photopolymerizations. . . . .	28
1.3.13. Dyes in thiol-ene photopolymerizations. . . . .	29
1.3.14. Dyes for the manufacture of photopolymerizable panchromatic films. . . . .	29
1.3.15. Dyes for polymerization of in situ nanoparticle containing films. . . . .	30
1.4. Dye-based photoinitiating systems: properties, efficiency and reactivity . . . . .	31
1.5. Trends and perspectives . . . . .	32
1.6. Bibliography . . . . .	34
<b>CHAPTER 2. SENSITIZATION OF CATIONIC PHOTOPOLYMERIZATIONS . . . . .</b>	<b>45</b>
James CRIVELLO	
2.1. Introduction. . . . .	45
2.2. Photosensitization of onium salts . . . . .	48
2.3. Synthesis of long wavelength absorbing photoinitiators . . . . .	50
2.4. Photosensitization of onium salt cationic photoinitiators . . . . .	51
2.5. Early dye sensitization studies. . . . .	55
2.6. Polynuclear aromatic hydrocarbons and their derivatives. . . . .	56
2.7. Phenothiazine photosensitizers . . . . .	60
2.8. Carbazole photosensitizers. . . . .	62
2.9. Thioxanthone photosensitizers . . . . .	63
2.10. Curcumin as a photosensitizer . . . . .	64
2.11. Quinoxaline photosensitizers. . . . .	65
2.12. Miscellaneous electron-transfer photosensitizers . . . . .	66
2.13. Free-radical-promoted photosensitization . . . . .	66
2.14. Conclusions . . . . .	70
2.15. Bibliography . . . . .	71
<b>CHAPTER 3. CONTROLLED PHOTOPOLYMERIZATION AND NOVEL ARCHITECTURES . . . . .</b>	<b>81</b>
Sean DORAN, Omer Suat TASKIN, Mehmet Atilla TASDELEN and Yusuf YAĞCI	
3.1. Introduction. . . . .	81
3.2. Photoinitiated controlled radical polymerizations . . . . .	84
3.2.1. Photoiniferter . . . . .	84
3.2.2. Photoinitiated nitroxide-mediated radical polymerization . . . . .	87
3.2.3. Photoinitiated atom transfer radical polymerization . . . . .	89

3.2.4. Photoinitiated RAFT polymerization . . . . .	97
3.3. Photoinitiated living ionic polymerization. . . . .	102
3.3.1. Living cationic photopolymerization . . . . .	102
3.3.2. Living anionic photopolymerization. . . . .	106
3.4. Acknowledgments . . . . .	108
3.5. Bibliography . . . . .	109
<b>CHAPTER 4. APPLIED PHOTOCHEMISTRY IN DENTAL MATERIALS: FROM BEGINNINGS TO STATE OF THE ART . . . . .</b>	<b>123</b>
Joachim E. KLEE, Maximilian MAIER and Christoph P. FIK	
4.1. Photoinitiated free radical polymerization. . . . .	123
4.1.1. Introduction: from ultraviolet to visible light curing . . . . .	123
4.1.2. The camphorquinone/amine system . . . . .	124
4.1.3. Acyl phosphine oxides. . . . .	127
4.1.4. Various other photoinitiator systems . . . . .	129
4.2. Cationic photopolymerization . . . . .	133
4.3. Conclusion . . . . .	134
4.4. Bibliography . . . . .	134
<b>CHAPTER 5. PHOTINITIATED CROSS-LINKING IN OLEDs: AN EFFICIENT TOOL FOR ADDRESSING THE SOLUTION-PROCESSED DEVICES ELABORATION AND STABILITY ISSUES . . . . .</b>	<b>139</b>
Frédéric DUMUR and Didier GIGMES	
5.1. Introduction. . . . .	139
5.2. Cross-linking of light-emitting materials . . . . .	141
5.2.1. Polymer-based light-emitting materials . . . . .	141
5.2.2. Small-molecule-based light-emitting materials . . . . .	154
5.3. Cross-linking of charge-transport materials. . . . .	157
5.3.1. Polymer-based hole-transport materials. . . . .	157
5.3.2. Polymer-based electron-transport/injection materials. . . . .	165
5.3.3. Small-molecule-based hole-transport materials . . . . .	167
5.4. Conclusion . . . . .	169
5.5. Bibliography . . . . .	170
<b>CHAPTER 6. POLYMERS AS LIGHT-HARVESTING DYES IN DYE-SENSITIZED SOLAR CELLS . . . . .</b>	<b>183</b>
Thanh-Tuân BUI, Xavier SALLENAVE and Fabrice GOUBARD	
6.1. Introduction. . . . .	183
6.2. Characterization of DSSC devices . . . . .	185
6.3. Poly(3-thiophenylacetic acid)-based polymers . . . . .	188

---

6.4. Phenylenevinylene-based polymers . . . . .	194
6.5. Triphenylamine-based polymer . . . . .	195
6.6. Fluorene-based polymers . . . . .	196
6.7. Dye polymers with acceptor–donor structure . . . . .	197
6.8. Polymer containing metal complexes . . . . .	199
6.9. Conclusion . . . . .	205
6.10. Bibliography . . . . .	206
<b>CHAPTER 7. NIR-DYES FOR PHOTOPOLYMERS AND LASER DRYING IN THE GRAPHIC INDUSTRY . . . . .</b>	<b>213</b>
Bernd STREHMEL, Thomas BRÖMME, Christian SCHMITZ, Knut REINER, Steffen ERNST and Dietmar KEIL	
7.1. Introduction . . . . .	213
7.2. Computer to plate systems . . . . .	216
7.2.1. Technical remarks . . . . .	216
7.2.2. Photochemical aspects of photoinitiation using NIR lasers . . . . .	218
7.2.3. Importance of thermal deactivation . . . . .	230
7.2.4. Contrast materials and color on demand . . . . .	232
7.2.5. Sensitivity . . . . .	236
7.3. Laser-drying and offset-printing . . . . .	239
7.3.1. Principle of laser-drying . . . . .	239
7.3.2. Chemical systems . . . . .	241
7.4. Conclusions and outlook . . . . .	243
7.5. Acknowledgments . . . . .	244
7.6. Bibliography . . . . .	244
<b>CHAPTER 8. DYES AND PHOTOPOLYMERS . . . . .</b>	<b>251</b>
Yue QI and John T. SHERIDAN	
8.1. Photopolymer . . . . .	251
8.2. Dye study of the photopolymer materials . . . . .	260
8.3. Conclusion . . . . .	271
8.4. Bibliography . . . . .	272
<b>CHAPTER 9. ADVANCED STRATEGIES FOR SPATIALLY RESOLVED SURFACE DESIGN VIA PHOTOCHEMICAL METHODS . . . . .</b>	<b>279</b>
Anja S. GOLDMANN, Guillaume DELAITTRE, Jan O. MUELLER and Christopher BARNER-KOWOLLIK	
9.1. Introduction . . . . .	279
9.2. Inorganic surfaces . . . . .	282
9.3. Bio and bioinspired surfaces . . . . .	296

9.4. Cross-linking . . . . .	309
9.5. Conclusion . . . . .	314
9.6. Bibliography . . . . .	315

**CHAPTER 10. PHOTOSYNTHESIZED HIGH-PERFORMANCE BIOMATERIALS . . . . .**

327

Julien BABINOT, Estelle RENARD, Valérie LANGLOIS and Davy-Louis VERSACE

10.1. Introduction . . . . .	327
10.2. Surface photografting methodology . . . . .	329
10.2.1. Photoinduced “grafting-from” method . . . . .	329
10.2.2. Benzophenone and derivatives . . . . .	329
10.2.3. Ketones and derivatives . . . . .	331
10.2.4. Photo-oxidation process . . . . .	333
10.2.5. Photoiniferters for living/controlled surface photografting . . . . .	334
10.2.6. Triarylsulfonium salts . . . . .	335
10.3. Photoinduced “grafting-to” procedure . . . . .	337
10.3.1. Aryl azides chemistry . . . . .	337
10.3.2. Anthraquinone-derived monomers . . . . .	337
10.4. Achievements and biomedical applications of the photosynthesized materials . . . . .	339
10.4.1. Achievements . . . . .	339
10.4.2. Stimuli-responsive materials . . . . .	341
10.4.3. Modification of membranes . . . . .	343
10.4.4. Biomedical applications . . . . .	344
10.4.5. Enzymes and proteins immobilization . . . . .	347
10.4.6. Cell adhesion and compatibility . . . . .	348
10.5. Conclusion . . . . .	350
10.6. Bibliography . . . . .	350

**CHAPTER 11. LIGHT-CURED LUMINESCENT COATINGS FOR PHOTOVOLTAIC DEVICES . . . . .**

361

Federico BELLA, Gianmarco GRIFFINI, Roberta BONGIOVANNI and Stefano TURRI

11.1. Photovoltaics: technology, devices and spectral management . . . . .	361
11.1.1. Energy demand and photovoltaic converters . . . . .	361
11.1.2. Spectral management for photovoltaics: principles, materials and applications . . . . .	364

11.2. Photocurable luminescent downshifting layers and dye-sensitized solar cells. . . . .	371
11.3. Luminescent solar concentrators. . . . .	378
11.4. Bibliography . . . . .	385
<b>CHAPTER 12. POLYMERS WITH PHOTOINDUCED SELF-HEALING PROPERTIES . . . . .</b>	<b>393</b>
Julien POLY	
12.1. Introduction . . . . .	393
12.2. Healing based on photo-reversible cycloadditions . . . . .	395
12.3. Healing based on photoinduced homolytic dissociations of covalent bonds. . . . .	399
12.4. Photoinduced healing in supramolecular polymers and related systems . . . . .	408
12.5. Healing based on photothermally induced phase transitions or photo-isomerizations . . . . .	413
12.6. Conclusion and perspectives . . . . .	416
12.7. Bibliography . . . . .	418
<b>LIST OF AUTHORS . . . . .</b>	<b>423</b>
<b>INDEX . . . . .</b>	<b>427</b>

---

## Preface

---

Light is involved in various chemical processes and its use in material science, and more particularly in polymer science, is growing in great strides. In this book, the use of light as a stimulus for chemical events encountered in the polymer science area is presented. Very different and important applications in polymer synthesis, data storage, photovoltaics (dye-sensitized solar cells), organic light-emitting devices (OLED) technology or biology use this innovative approach, for example.

One of the most challenging aspects in the field of chemistry is the design and development of high-performance systems requiring low energy consumption and with a low ecological impact. Today, photochemistry using visible light sources has become very attractive as a visible light is characterized by intrinsic advantages compared to an ultraviolet (UV) light (e.g. safety and availability of eco-friendly and cheap sources such as sunlight, halogen lamps, laser diodes and light-emitting diodes (LEDs)). Therefore, the use of visible light will be particularly emphasized.

The first three chapters of this book deal with the fundamentals in visible-light-induced polymer synthesis: free radical photopolymerization (Chapter 1), cationic photopolymerization (Chapter 2) and controlled radical photopolymerization (Chapter 3). Then, different applications in high-tech sectors are provided: curing of dental materials (Chapter 4), photoinitiated cross-linking in OLEDs (Chapter 5), photopolymers and laser drying in the graphic industry (Chapter 7), data storage using photopolymers (Chapter 8), surface modifications and design (Chapter 9), biology (Chapter 10), photovoltaic devices (Chapter 11) and self-healing of polymers induced by

light (Chapter 12). Special mention of the use of dyes in dye-sensitized solar cells (DSSC) is also given (Chapter 6).

We believe that these exciting topics related to the development of photosensitive systems using dyes and various chromophores in polymer science and technology will be helpful for many readers (R&D researchers, engineers, technicians, university people, students, etc.). The examples presented in this book are still subject to fantastic evolutions and we hope they will herald a bright future in the coming years. We also hope that this book will provide the readers with a useful background in these different fields.

We would like to thank all the authors for their excellent work and all the fascinating discussions.

Professor Jean-Pierre FOUASSIER

Professor Jacques LALEVÉE

March 2015

---

# Trends in Dye Photosensitized Radical Polymerization Reactions

---

In this chapter, visible light-induced radical polymerization reactions in the 380–800 nm range are reviewed. The role of the absorbing species (dye) and the complete multicomponent photoinitiating systems (PISs) (dye and additives) are then emphasized. The original works on the dye-based PISs that have been proposed over the years are also outlined. However, this chapter is mainly focused on the latest developments, in the 2010–2014 period, and the actual trends of research, in particular the novel perspectives of applications under soft irradiation conditions.

## 1.1. Introduction

Dye photosensitized polymerization (DPP) (see [FOU 12a]) is a common expression often employed [OST 54, EAT 86, MON 93] to refer to a series of reactions where a dye<sup>1</sup> (i) is excited by light [1.1a]<sup>2</sup>, (ii) leads [1.1b], alone or through primary or subsequent reactions involving one or more

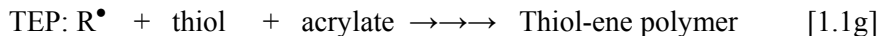
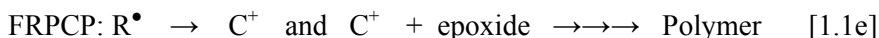
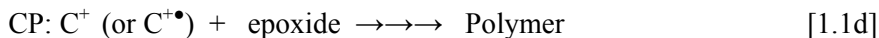
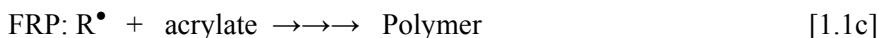
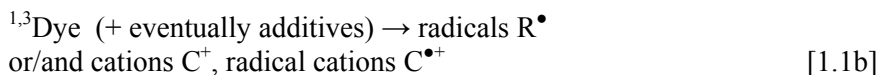
---

Chapter written by Jacques LALEVÉE and Jean-Pierre FOUASSIER.

1 Originally, the term “dye” referred to a colored molecule used to color various materials in the dyeing industry. Originally, in the early papers on dye sensitized polymerization reactions, the term “dye” refers to a molecule that absorbs in the visible wavelength range. Later on, colored molecules usable in other areas (dye lasers, solar cells, OLEDs, etc.) were also defined as dyes. Here, we call “dye” any substance absorbing in the defined 380–800 nm range.

2 <sup>1</sup>Dye stands for the first excited singlet state of the dye and is formed under excitation by light; <sup>3</sup>Dye is the triplet state of the dye generated from <sup>1</sup>Dye through an intersystem crossing.

additional compounds, to radicals, cations or cation radicals, and (iii) initiates a free radical polymerization (FRP) [1.1c], a cationic polymerization (CP) [1.1d], a free radical promoted cationic photopolymerization (FRPCP) [1.1e], a concomitant cationic/radical polymerization (hybrid cure) (CCRP) [1.1f], a thiol-ene photopolymerization (TEP) [1.1g] or cross-linking reactions of prepolymers or polymers (this last point will not be covered here).



Therefore, by analogy with the term “initiator” in thermal polymerizations, the dye is also usually presented as a photoinitiator (PI), i.e. a substance that absorbs light and participates in the photoinitiation of a polymerization reaction. In the sense of photochemistry [TUR 90], however, it can also play the true role of a photosensitizer (PS) in some specific reactions<sup>3</sup>. Sometimes, there is an apparent ambiguity with the words “photoinitiator” and “photosensitizer” in papers dealing with

---

<sup>3</sup> In mechanistic photochemistry, the term “photosensitization” is limited to cases in which the PS is not consumed in the reaction (for example, in a PS/PI couple, the energy moves from the excited PS to a PI-excited state through an energy transfer). However, by extension, this term is also used for a photosensitization process through an electron transfer: in this case, the PS/PI interaction results in the formation of radical ions, PS being, therefore, destroyed.

photopolymerization. For the sake of clarity and convenience, we consider here that dye-based PISs can be classified into one-component PIS (I\_Dye, [1.1a, 1.2]), two-component PIS (II\_Dye, i.e. a dye and one additive ([1.1a], [1.3]–[1.5])), three-component PIS (III\_Dye, i.e. a dye and two additives), etc. The additives can be electron donors (EDs) [1.3], electron acceptors (EAs) [1.4], hydrogen donors (HDs) [1.5] or electron/proton donors (EPDs) [1.6].



DPP reactions have been largely applied in various traditional and recently high-tech areas, such as radiation curing, imaging, graphic arts, optics, dentistry, medicine and nanomaterials (see [FOU 12a] and other relevant books [LAS 90, BOT 91, PAP 92, FOU 93b, KRO 94, REI 89, FOU 95a, SCR 97, KOL 97, DAV 99, NEC 99, FOU 99, CRI 99, FOU 01, DIE 02, BEL 03, FOU 06, SCH 07a, SCH 07b, LAC 08, MIS 09, ALL 10, FOU 10a, GRE 10, MAC 07]). For the past 50 years [OST 54], the large choice of available dyes and additives, and the possibility to tune the absorption in a given PIS by only changing the dye, has led to numerous research works. Recent developments have progressively allowed the use of increasingly less intense visible light sources. An important topic is now concerned with the adaptation of DPPs to irradiations with newly developed laser diodes and light emitting diodes (LEDs) for specific applications.

In many sectors, radical photopolymerization reactions are used more often than cationic photopolymerizations [FOU 12a, CRI 99, BEL 03, GRE 10]. Two historical facts can explain this difference. First, in industrial applications, the benefits versus the drawbacks are very often in favor of the radical processes. Second, many radical PISs have been successfully developed since the beginning of the 1960s. In contrast, industrial cationic PIs are only quasi-based on iodonium and sulfonium salts [CRI 79]

(still largely used today) that are sensitive in the ultraviolet (UV). Later on, dialkylphenacylsulfonium, N-alkoxypyridinium, thianthrenium and ferrocenium salts, that absorb in the near UV/visible or visible range, have also been proposed [FOU 12a, CRI 99, BEL 03, KAH 10]. The photosensitization of onium salts in the visible range remains rather difficult (although successful results have been reached along the past years [FOU 12a, KAH 10]). Recent, promising developments using FRPCP should likely overcome this issue (see [FOU 12a, KAH 10] and below).

Thousands of papers have been already published in the field of DPPs. Before writing a novel review chapter, one question we can ask is: how can we present the most up-to-date situation? The first possibility, as is very often done, consists of providing a broad overview of the available systems which results in a qualitative list of PI, PS and compound/additive combinations. For obvious reasons, it is impossible to discuss their relative efficiency as the experimental conditions are completely different from one paper to another (film vs. solution, high-viscosity media vs. low-viscosity media, in laminate vs. under air, high light intensity vs. low light intensity, short exposure time vs. long exposure time, etc.). It could even happen that a proposed system (presented as a new system) is in the end not interesting from a practical point of view. The main interest of such reviews undoubtedly remains the gathering of the available systems. The second possibility, as sometimes encountered, consists of presenting the systems that are effectively used in a given field of applications. This represents a real interest as only the efficient systems are reported in that case. However, it requires us to have a review paper for each domain of applications. The third possibility, that is rather rare, consists of outlining the key points and the breakthroughs in the design of ever more reactive and efficient compounds, discussing the relative interest of the different systems toward the different uses, comparing the performances when possible and stressing the actual trends of development at a given time.

A recent book provides a detailed analysis of the encountered systems up to 2010/2011 (large overview, mechanism, reactivity and efficiency) [FOU 12a]; other previous books on the subject include [LAS 90, BOT 91, PAP 92, FOU 93b, KRO 94, REI 89, FOU 95a, SCR 97, KOL 97, DAV 99, NEC 99, FOU 99, CRI 99, FOU 01, DIE 02, BEL 03, FOU 06, SCH 07a, SCH 07b, LAC 08, MIS 09, ALL 10, FOU 10a, GRE 10] and [MAC 07].

Many review papers typically focusing on dyes as PIs or PSs [EAT 86, FOU 90, SCH 90b, URA 03, FOU 03, FOU 93a, FOU 95b, FOU 95c, FOU 00, TIM 93, CUN 93, GRE 93, CRI 93, FOU 11, FOU 10b, YAG 10, FOU 07, FOU 12b, FOU 12c, LAL 11b, XIA 15, LAL 15, SHA 14] or partly dealing with photoinitiation under visible lights [PAC 01, LAL 09b, LAL 09, LAL 10, LAL 12, IVA 10, MUF 10, LAL 14b, BON 14, SAN 14] have also been already published. As a result, we chose here to (i) provide a very brief overview of the PISs developed over the last 50 years, (ii) focus on the most recent literature and (iii) illustrate the today's trends of development. Examples of these trends will concern the search of novel dyes for (i) polychromatic light excitations, (ii) blue, green and red laser light-induced polymerizations, (iii) photoinitiation under soft irradiation conditions, (iv) sunlight exposure, (v) enhanced absorption properties (red-shifted spectra and high molar extinction coefficients), (vi) the use as photoinitiator catalysts (PICs), (vii) dual radical/cationic PISs, (viii) performances attained under specific LED and laser diode exposures, (ix) concomitant radical/cationic photopolymerizations and the elaboration of interpenetrated polymer networks (IPNs), (x) TEPs, (xi) photopolymerizable panchromatic films or (xii) the manufacture of *in situ* nanoparticle (NP) containing films.

Our review here is limited to systems operating in dye photosensitized radical polymerizations (DPRPs) (see Figure 1.1). Their behavior in FRPCP reactions will be only evoked as all CPs are specifically covered in another covered in Chapter 2 of this book. In the same way, the role of dyes as part of PISs in the medical area, controlled radical photopolymerization reactions, printing technologies, stereolithography, optics or dyes under two-photon excitation are also discussed in detail in other chapters of this book.

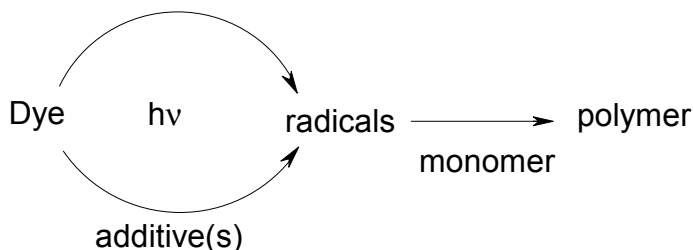


**Figure 1.1.** Chemical mechanisms for dye photosensitized radical polymerizations

## 1.2. A brief overview of dye-based PISs

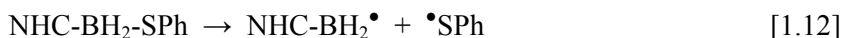
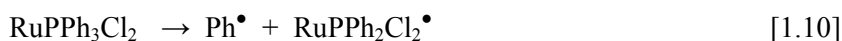
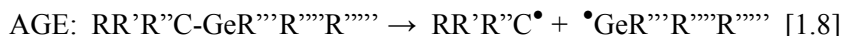
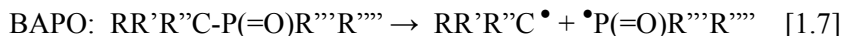
As stated in the previous section, various presentations of DPP reactions are available in review papers [EAT 86, FOU 90, SCH 90b, URA 03, FOU 03, FOU 93a, FOU 95b, FOU 95c, FOU 00, TIM 93, CUN 93, GRE 93, CRI 93, FOU 11, FOU 10b, YAG 10, FOU 07, FOU 12b, FOU 12c, LAL 11b, XIA 15, PAC 01, LAL 09b, LAL 09, LAL 10, LAL 12, IVA 10, MUF 10, LAL 14b], in general books [LAS 90, BOT 91, PAP 92, FOU 93b, KRO 94, REI 89, FOU 95a, SCR 97, KOL 97, DAV 99, NEC 99, FOU 99, CRI 99, FOU 01, DIE 02, BEL 03, FOU 06, SCH 07a, SCH 07b, LAC 08, MIS 09, ALL 10, FOU 10a, GRE 10, MAC 07] and in a recent specialized monograph [FOU 12a]. In this section, a short survey is done on DPRP which helps us to outline several particular points; examples of some specific papers are also mentioned. More detailed developments of recently proposed PISs are provided in section 1.3.

### 1.2.1. Dye one-component systems

Contrary to the UV sensitive PI area where many efficient compounds are known, visible light radical one-component PISs are limited because (i) they require a specific synthesis and (ii) the finding of easily cleavable bonds is not trivial (contrary to the easy cleavage of various molecules under UV lights, e.g. the largely used ketones [FOU 12a, DIE 02], or other cleavables C–S, S–S, Se–Se, Si–Si, S–Si and C–Ge bonds that have also been revisited [FOU 12a]).

Examples of visible PIs concern (bis)benzoyl phosphine oxides (BAPOs) [MOS 10, DEC 01, ZAL 14, MEE 14], and titanocenes Tit ([ROL 86, LAL 09c, TEH 11, KIT 13]; see also some modified ketones [ROS 09] and particular diketones [BIB 02] in sections 1.3.9 and 1.3.15). Recently, acylgermanes (AGEs) [GAN 08, NES 13, THE 10], bisgermyl derivatives [THE 10] (when going from mono-germyl ketones to bisgermyl ketone, a strongly red-shifted transition up to ~514 nm is noted), dibenzoyl diethyl germanes [YUK 09], cleavable thioxanthenes (TXs) (TX-OSi and TX-Si) [LAL 09c, LAL 11], and di- and trifunctional structures [TEH 13] have been disclosed. Some ruthenium complexes RuPPh<sub>3</sub>Cl<sub>2</sub> [VER 13a], zirconocene derivatives Cp<sub>2</sub>ZrCl<sub>2</sub> [VER 13b] or N-heterocyclic-boryl sulfides NHC-BH<sub>2</sub>-SPh [TEL 13b] might be a novel way for cleavable compounds, but progress

has to be made to extend the photosensitivity to visible lights. Upon excitation, these compounds undergo a fast homolytic cleavage of a given bond leading to two radicals (see [1.7]–[1.12]). Novel adequate modification of usual cleavable ketone scaffolds enables a dramatic improvement of the bathochromic absorption properties (see sections 1.3.5 and 1.3.6).



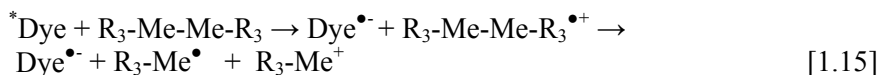
### 1.2.2. Dye two-component systems

Contrary to the restricted number of cleavable PIs, there are a large number of two-component PISs [FOU 12a] as it is quite easy to find a dye and a suitable additive able to work according to primary electron transfer<sup>4</sup> [REH 70], electron/proton transfer or direct hydrogen abstraction (see reactions [1.4], [1.5] or [1.6]). Examples of papers can be found in [FOU 12b, FOU 12c, LAL 11b, XIA 15, LAL 15, LAL 14b, JED 10, KAB 10, TAR 10, GRO 01, KAB 07, PIE 11, KUM 12, KOR 13, KAR 14, JIA 11, GUO 13, ESE 13, CUI 11, BAI 13, ALZ 14] and [XU 12]. Well-known examples of dyes include modified benzophenone (BP) (e.g. the Michler's ketone), TX, camphorquinone (CQ) and ketocoumarin derivatives, hydrocarbons, xanthenic dyes (Rose Bengal, Eosin, etc.), azines, thiazines (methylene blue, thionine, etc.), phenoxazines, riboflavines, acridines,

<sup>4</sup> The free energy change  $\Delta G$  of the reaction must be positive for getting a favorable electron transfer reaction.  $\Delta G$  is often calculated from the classical Rehm–Weller equation.  $\Delta G = E_{\text{ox}} - E_{\text{red}} - E_{\text{S}}$  (or  $E_{\text{T}}$ ) +  $C$ , where  $E_{\text{ox}}$ ,  $E_{\text{red}}$ ,  $E_{\text{S}}$  (or  $E_{\text{T}}$ ) and  $C$  are the oxidation potentials of the electron donors, the reduction potential of the electron acceptors, the excited singlet (or triplet) state energies of the dye and the electrostatic interaction energy for the initially formed ion pair, generally considered as negligible in polar solvents.

acridones, phenoxazones, benzopyranones, enzofuranones, phenosafranines, thiopyronines, polymethines (cyanines, merocyanines, carbocyanines, etc.), phthalocyanines, pyrromethenes, fluorones (rhodamines, etc.), quinolinones, julolidine dyes, quinoxaline dyes, styryl dyes, crystal violet, pyrylium and thiopyrylium salts, styrylquinolinium salts, aminostyryl benzothiazolinium salts, squarylium salts, quinoline imidazopyridinium salts, benzimidazoles, etc. Many PISs described below as three-component PISs [XIA 15, TEH 13b, LAL 84, TEH 13a, TEH 12a, TEH 13e, TEH 11, TEH 13c, TEH 13d, TEH 12b, TEH 12c, TEL 13a, XIA 13] can also work as two-component systems into some extent. A lot of novel recent structures (e.g. [XIA 15, TEH 13b, LAL 84, TEH 13a, TEH 12a, TEH 13e, TEH 11, TEH 13c, TEH 13d, TEH 12b, TEH 12c, TEL 13a, XIA 13b] and others, see below) are presented in section 1.3.5.

Examples of additives are the following: EA = iodonium salt, e.g. diphenyliodonium hexafluorophosphate (more rarely, a sulfonium salt) and related derivatives<sup>5</sup> [1.13], alkyl halide, e.g. phenacyl bromide [1.14] and triazine, e.g. 2,4,6-tris(trichloromethyl)-1,3,5-triazine; ED = borate disulfide, group IVb dimetal [1.15]; HD = alcohol, THF, thiol, benzoxazine, aldehyde, acetal, silane (e.g. tris(trimethylsilyl)silane = (TMS)<sub>3</sub>Si-H) [1.16]), germane, borane, stannane, alkoxyamine, silyloxyamine, polymer substrate, etc.; EPD = amine [1.17], thiol, etc. The generated radicals (e.g. Ph<sup>•</sup>, R<sup>•</sup>, R<sub>3</sub>Si<sup>•</sup>, RR'C<sup>(•)</sup>NR''R''' in [1.13]–[1.17]<sup>6</sup>) are the initiating species. Efficient novel or newly modified dye structures in the Dye/amine, Dye/iodonium salt or Dye/silane two-component PISs have been proposed within the last 4 years (see section 1.3.5).



<sup>5</sup> In this case, we can say that the dye acts as a photosensitizer for the iodonium salt decomposition.

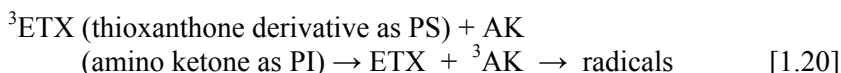
<sup>6</sup> The symbol <sup>\*</sup>Dye refers to the dye in an excited state (the singlet state <sup>1</sup>Dye or eventually the triplet state <sup>3</sup>Dye).



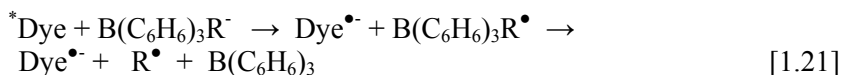
The interaction of dyes with hydroperoxides and peroxides leads to oxyl radicals ([1.18], [1.19]), e.g. in ferrocenium salt/cumylhydroperoxide and diketone/benzoyl peroxide (see references in [FOU 12]).



Finding a dye that is able to work as a PS and to decompose a cleavable PI through a triplet-triplet energy transfer has been vigorously researched. This was not really successful, however, as increasing the ground state absorption wavelengths results in a decreasing of the first excited singlet state energy and the triplet state energy<sup>7</sup>: one famous example (but relatively old) in the photocurable coating area is known [RIS 92] [1.20].



Another particularly interesting system is based on a dye-borate ion pair<sup>8</sup> where an intramolecular electron transfer occurs and results in the generation of radicals [1.21]. Changing the cationic dye moiety<sup>9</sup> enables a tuning of the absorption (e.g. see [EAT 86, MON 93, JED 10, KAB 07, GRI 99, SCH 90a, MUR 93]).



Linking together two reactive moieties instead of having two separate reactants (e.g. in Eosin-oxime ester [BUR 99] or dye-triazine [KAW 13]) facilitates efficient intramolecular interactions (generally through electron

7 Remember that a favorable triplet-triplet energy transfer only occurs if the triplet energy level of the donor is higher than that of the acceptor.

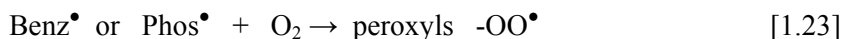
8 If isolated, the dye-borate ion pair can be considered as a one-component system.

9 The symbol "Dye" in our text can refer either to a neutral dye or a cationic dye; in the last case, the symbol "Dye•-" obviously corresponds to a radical species and not to a radical anion.

transfer) which avoids the necessary diffusion process of the reactants (unfortunately restricted in viscous media<sup>10</sup>) arising in an intermolecular approach.

Various by-side interactions can also improve the efficiency of II\_Dye and III\_Dye PISs (see below) in for example the coumarin derivative/titanocene system [ALL 04].

Recently, some cleavable ketones mixed with a suitable additive led to an increased efficiency, such as in the BAPO/silane couple [EL 09] where the primarily formed benzoyl (Benz<sup>•</sup>) and phosphinoyl (Phos<sup>•</sup>) radicals lead to peroxy radicals that are further quenched by the silane [1.22]–[1.24].



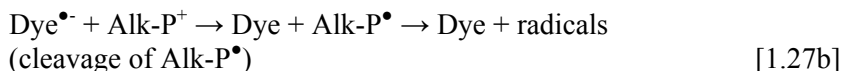
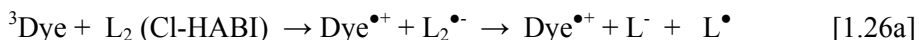
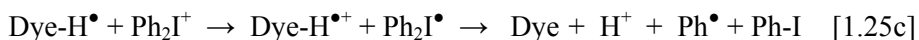
### 1.2.3. Dye three-component systems

Very often, the initiating ability of two-component PISs is dramatically improved by adding a third partner (e.g. see [FOU 12a]). This strategy has been known for many years (see [TIM 93]), is well documented and is still currently used (see [FOU 93c]). More or less old examples of such three-component systems are: Dye/bromo compound/Ph<sub>2</sub>I<sup>+</sup> with Dye = benzophenone, isopropyl thioxanthone, merocyanine, etc.; Dye/amine/maleimide with Dye = benzophenone, etc.; Dye/amine/diphenyl iodonium salt with Dye = eosin, ketocoumarin, methylene blue, thioxanthene dye, fluorone dye, etc.; Dye/borate salt/triazine derivative with Dye = cyanine dye, styrylquinolinium dye, etc.; Dye/borate salt/alkoxypyridinium salt with Dye = carbocyanine dye, etc.; PI/amine/triazine derivative with Dye = pyromethene dye, Rose Bengal, etc.; Dye/hexabisimidazole derivative (e.g. Cl-HABI)/thiol with PI = styrylnaphthothiazole dye, diethylamino benzophenone, julolidine dye, etc.; Dye/amine (or

<sup>10</sup> All bimolecular rate constants level off in a viscous media (the maximum value being that of the diffusion rate constant).

hydroperoxide)/ferrocenium salt with Dye = Rose Bengal and coumarin; and Dye/amine/BAPO with Dye = camphorquinone.

The observed mechanisms depend on the nature of the three compounds. For example (see [FOU 12a]), when using Dye/amine AH/diphenyl iodonium salt  $\text{Ph}_2\text{I}^+$  (e.g. with Dye = ketocoumarin) [FOU 93c], the increased polymerization efficiency is easily explained by the quenching of the  $\text{Dye-H}^\bullet$  radicals by the iodonium salt [1.25]<sup>11</sup> in a way similar to the case of the ketyl-type  $\text{K}^\bullet$  radicals in ketones (both  $\text{Dye-H}^\bullet$  and  $\text{K}^\bullet$  are known as scavenging radicals of the growing macromolecular chains); moreover, new initiating phenyls are formed. In Dye/Cl-HABI ( $\text{L}_2$ )/thiol, the Dye/ $\text{L}_2$  electron transfer generates a dissociative radical anion  $\text{L}_2^{\bullet-}$  that yields a lophyl anion  $\text{L}^-$  and a lophyl radical  $\text{L}^\bullet$  which abstracts a hydrogen on the thiol, the thiyl being the initiating radical [4] [1.26]. In Dye/borate/alkoxyppyridinium salt, the initially formed reduced dye is oxidized by the salt [1.27]; a lot of papers deal with the role of many various additives to the Dye/borate couple (e.g. [FOU 12a, XIA 15, KAB 10, TAR 10, GRO 01, KAB 07]). In other III\_Dye systems, the mechanisms can become much more complicated [FOU 12a, FOU 03, XIA 15].



Mixing four components can even improve the performance (but the mechanisms are rather intricate), e.g. in Rose Bengal/amine/hydroperoxide/ferrocenium salt (proposed for the photocuring of white and

---

11 If starting from a cationic dye, the symbol “Dye-H<sup>•</sup>” obviously corresponds to the leuco form of the dye.

colored paints) or diethylamino BP/Cl-HABI/N-phenyl glycine/diphenyl iodonium salt (usable in laser direct imaging (LDI) applications).

More recently [XIA 15, TEH 13b, LAL 84, TEH 13a, TEH 12a, TEH 13e, TEH 11, TEH 13c, TEH 13d, TEH 12b, TEH 12c, TEL 13a], the Dye/silane/diphenyl iodonium salt systems (with Dye = thioxanthone, camphorquinone, thiopyrilium salt, Eosin, Ru or Ir complex, violanthrone, newly synthesized structures, etc.) appear as versatile and fascinating PISs exhibiting promising initiating properties of various monomers (acrylates as well as epoxides or vinyl ethers) in various experimental conditions (air/laminate, high/low intensity, 380–635 nm excitation lights and low/high-viscosity media). As they are based on a different concept, these silane containing systems will be presented and discussed in detail in section 1.3.5.

### 1.3. A discussion on specific or recent developments in dye-based photoinitiating systems

The main research direction in this area (other questions related to the design of systems that are appropriate for further end-uses in practical applications, e.g. solubility, compatibility, toxicity, handling, costing, etc., are not considered here) is governed by the requirements of an enhanced polymerization efficiency, i.e. higher polymerization rates ( $R_p$ ) and final conversions ( $C_f$ ). Within this, two special points are:

#### *1) How do we get high $R_p$ and $C_f$ ?*

We know, for a given monomer, that  $R_p$  in FRP is a function of the amount of absorbed energy ( $I_{\text{abs}}$ ) and the initiation quantum yield  $\Phi_i$ :  $R_p = k_p/k_t^{0.5} (\Phi_i I_{\text{abs}})^{0.5}$ ,  $k_p$  and  $k_t$  being the propagation and termination rate constants of the monomer, respectively. The  $I_{\text{abs}}$  quantity depends on the incident light intensity  $I_0$ <sup>12</sup> of the source and the molar extinction coefficients  $\epsilon$  of the dye (and obviously, path length  $l$  and reactant concentration  $C$ ):  $I_{\text{abs}} = I_0 (1 - 10^{-\epsilon cl})$ . The term “ $\Phi_i$ ” exhibits a rather complex dependence on the monomolecular  $k_c$  and bimolecular rate constants  $k_r$  of the different interaction processes leading to radicals, the bimolecular rate constants  $k_q$  of the quenching processes and the concentrations of the reactants. The

<sup>12</sup> The term “intensity”, which is generally used truly, corresponds to an “irradiance” and is defined as a luminous power per surface unit or, eventually, as a number of photons per surface unit.

possibility to have a high  $R_p$  (and often, as a consequence, a high  $C_f$ ) is achieved using (i) highly absorbing dyes (high  $\epsilon$  and excellent matching between the absorption spectrum of the dye and the emission spectrum of the light source) and (ii) dyes exhibiting a high photochemical/chemical reactivity (high  $k_c$  and  $k_r$ ) leading to very reactive radicals toward an acrylate double bond. The trivial effect of the experimental conditions (increase in the concentrations and the use of high  $I_0$ ) obviously ensures an enhancement of the  $R_p$ s.

2) *How can we overcome the oxygen inhibition effect?*

Three factors result in a strong oxygen inhibition of FRP and FRPCP: (i) the  $^3\text{Dye}$  triplet state or  $^1\text{Dye}$  singlet state quenching by  $\text{O}_2$  (in very reactive dyes having short-lived excited states, this quenching is fortunately not competitive); (ii) the scavenging of the initiating  $\text{R}^\bullet$  and propagating radicals  $\text{R}(\text{M})_n^\bullet$  by  $\text{O}_2$  [1.28]–[1.30] which is nearly a diffusion-controlled reaction; (iii) the formation of peroxy radicals (not usable for the FRP initiation), peroxides  $\text{ROOR}'$  and hydroperoxides  $\text{ROOH}$ . Therefore, the polymerization reactions can start in the film only as soon as oxygen is consumed (see [FOU 12a] and a review in [CLA 13]). In highly viscous or thick samples (e.g. epoxy acrylate matrices), the reoxygenation process is slow and a short inhibition period is observed. In very low viscosity media (e.g. di- or trifunctional monomers, such as trimethylolpropane triacrylate (TMPTA) or (3,4-epoxycyclohexane)methyl 3,4-epoxycyclohexylcarboxylate (EPOX)), the reoxygenation remains efficient, thereby reducing the monomer conversions. In addition, when the light intensity is attenuated, the oxygen inhibition has a dramatic effect on the polymerization profile, due to the lowering of the initial  $\text{O}_2$  consumption process and the decreasing of the initiating radical concentration.



To boost the polymerization under air, the first idea was to overcome the detrimental oxygen effect by using various strategies, as recently reviewed in [FOU 12a] and [CLA 13]. Among them, increasing the light intensity or the

PI concentration remains, although somewhat inerting, the largely used strategy both in academic and industrial experiments ([FOU 12a]).

When high-intensity sources are better avoided, a second method, developed over the past few years, consists of taking advantage of the presence of oxygen. For example (see more details in section 1.3.5), the use of adequate PI/iodonium salt/silane (or NVK) successfully led to an efficient FRPCP of low-viscosity matrices under air using sources delivering  $\sim 50\text{--}100\text{ mW/cm}^2$ ; in the same conditions, acrylate final conversions in FRP do not exceed 25–30% but are acceptable in laminate ( $\sim 50\text{--}60\%$ ; see [XIA 15]) in contrast with CQ or Eosin-based PISs that work poorly. Another example that might be considered as a newly discovered strategy (see details in section 1.3.5) relates to the use of Dye/UV PI (such as 2,2-dimethoxy-2-phenylacetophenone (DMPA) or BAPOs) combinations, e.g.  $\text{Cp}_2\text{TiCl}_2$  (or  $\text{Cp}_2\text{ZrCl}_2$ )/DMPA or Ti (iso)propoxide/BAPO, that ensure a significant reduction of the usual oxygen inhibition process. The effect on the conversion is much more visible (final TMPTA conversion under air: 60% with  $\text{Cp}_2\text{TiCl}_2$ /DMPA vs. 35% with DMPA alone). Moreover, Ti and Zr NPs are *in situ* generated during the course of the reaction (see section 1.3.15). This concept has still to be applied to visible light absorbing systems.

An innovative highly efficient strategy using a photoredox reaction in a photolabile superbase/peroxide couple makes the polymerization of TMPTA under air possible with  $\sim 90\%$  conversions upon a light intensity of  $20\text{ mW/cm}^2$  [HE 12]. Due to the self-propagating effect of this living system, the photocrosslinking of thick material or highly pigmented systems should also be possible. No details on the encountered mechanisms are available. This process, which is unfortunately restricted to wavelengths of  $<300\text{ nm}$ , deserves to be studied for the design of visible light absorbing photobases.

### 1.3.1. Dyes for use with polychromatic visible lights

The main goals in visible light-induced polymerization reactions in the radiation curing area for applications in, for example, coatings, adhesives, paints and drying of printing inks are [FOU 12a, FOU 95a, SCR 97, OLL 97, DAV 99, BEL 03, FOU 06, SCH 07a, SCH 07b]: (i) developing PISs able to

absorb the visible lights that are very often lost when employing conventional mercury lamps and usual PIs (output irradiance up to a few  $\text{W}/\text{cm}^2$  and even more); (ii) avoiding the absorption of the matrix and additives (e.g. light stabilizers or pigments); (iii) ensuring a spectral window where the dye absorbs alone; (iv) moving the operating procedure toward a UV-free exposure (realized by using, e.g., doped Hg lamps, Xe-Hg lamps, Xe lamps, LEDs and laser diodes) which avoids the use of the harmful first-generation UV lamps delivering UV-B and UV-C rays and generating ozone; (v) improving the cure rate and the cure-through depth due to the better penetration of lights having longer wavelengths; (vi) developing soft and sunlight curing. In recent years, high-intensity LEDs and laser diodes operating at well-defined near-UV and visible wavelengths have been proposed. Today, in industrial applications, LED technology facilitates highly packed arrays operating nominally at 385, 395, 405, 420, 455, 470 or 477 nm, together with a suitable safety, a high light intensity (up to approximately a few  $\text{W}/\text{cm}^2$  for industrial LED arrays), a low heat generation, low energy consumption, low cost and low maintenance. The development of laser diode arrangements also ensures high-intensity monochromatic irradiations from the blue to the red part of the spectrum.

It seems today [FOU 12a] that many PISs can meet the challenges of high-performance systems for RP under 380–650 nm lights even under air when using high-intensity sources (approximately a few  $\text{W}/\text{cm}^2$ ). A drawback (which could be a serious limitation in applications, e.g. for clear coatings or white paints) is obviously a possible residual coloration of the final material due to the remaining dye and the photolysis products: studies need to be conducted in this direction to eliminate, or at least limit, the problem.

Examples of recently developed visible PISs include some original and novel systems, but they are generally slightly modified derivatives of known existing structures already extensively studied, e.g. N-substituted quinoxalinobenzothiazine/iodonium salt for hybrid polymerization [POD 11]; ketocoumarin/triazine/thiol, pyrromethenes [TAR 10], safranine/diphenylborinate system and TX-based thia-naphthacene-12-one; various substituted thioxanones, spiropyran, cyanines, styrylquinolinium structures and related compounds [KAB 10], and zinc phthalocyanine/additive; and the proposal of heterogeneous mesoporous graphitic carbon nitride/amine and colloidal graphene oxide is more original. All these

systems operate (with more or less success) in FRP under Hg or Xe-Hg lamps or LED exposures with 50–500 mW/cm<sup>2</sup> intensities at least in laminated films or in deaerated solutions and sometimes under air in appropriate matrices.

In recent years, the proposal of the Dye/iodonium salt/silane combinations and the synthesis of many novel dyes have paved the way for the design of very efficient PISs. They easily work in FRP (most of them are noted in [XIA 15, TEH 13b, LAL 84, TEH 13a, TEH 12a, TEH 13e, TEH 11, TEH 13c, TEH 13d, TEH 12b, TEH 12c, TEL 13a]); see also section 1.3.5). Remarkably, under intensities in the 2–100 mW/cm<sup>2</sup> range, these combinations (i) behave as dual PISs (sources of both radicals, cations and radical cations) and allow not only an FRP but also an FRPCP, a CCRP (hybrid cure) or a TEP; (ii) allow FRPCP and CCRP reactions in low-viscosity matrices under air; (iii) ensure, at the moment, an acceptable FRP of low-viscosity acrylates (e.g. ~100 cP for TMPTA and 57 cp for polyethyleneglycol 400 diacrylate (PEGDA)) in laminate (conversions under air do not exceed 25%) and (iv) make possible the polymerization of viscous methacrylates (bisphenol A-glycidyl methacrylate (bis-GMA)/triethyleneglycol dimethacrylate (TEGDMA) blends 70/30% w/w) or viscous acrylates (e.g. 14,500 cP for an epoxyacrylate/HDDA blend) under air with excellent yields.

### **1.3.2. Dyes for blue, green and red laser light-induced polymerizations**

Blue and green laser light-sensitive PISs in laminate, under high light intensities or in viscous media, are largely encountered as they are obviously similar to those employed under polychromatic visible light. Many studies have been originally devoted to systems that can be more specifically excited by (i) coherent laser sources such as the Ar<sup>+</sup> laser at 488–514 nm, e.g. for holographic recording (HR), and manufacture of holographic optical elements (HOEs); (ii) easily drivable laser beams, e.g. for computer-to-plate (CTP) applications (see, e.g., [FOU 12a, FOU 03]); (iii) laser beams as high-intensity monochromatic sources (e.g. laser diodes at 405, 457, 473, 532 or 635 nm in [XIA 15]) or (iv) direct imaging device sources (see, for example, at 405 nm with a GaN laser). Typical laser diodes emit lights with nominal intensities of 10–100 mW/cm<sup>2</sup>; continuous-wave lasers deliver at 10 W/cm<sup>2</sup>.

Instead of laser beams, high-power LEDs need to be used in CTP, printing inks or 3D modeling/printing.

Examples of well-known PISs working under laser lights in this blue-green area include the Eosin/amine, Eosin/amine/bromo compound, ketocoumarin/amine/iodonium salt, thioxanthene dye/amine/iodonium salt, erythrosin/amine, julolidine dye/Cl-HABI/thiol, cyanines and related compound/borate/additive systems, pyrromethine/amine/triazine or styryl naphthothiazole dye/Cl-HABI/thiol systems and Cl-HABI-based systems. A lot of novel Dye/iodonium salts/silanes can also work (e.g. [XIA 15]; see sections 1.3.5 and 1.3.6).

In contrast, few reports concern dyes usable under red or near-infrared radiation (IR) laser lights in laminate. The use of the methylene blue/amine system, under the HeNe laser at 632 nm, has often been explored in the past [CAP 89]. Polymethines, thiazines, squarylium-triazine dyads have been proposed for the manufacture of HR and HOE. Some Dye/iodonium salt/silane PISs have also been mentioned but the efficiency in FRP, contrary to that attained in FRPCP, still remains relatively low under air; CCRP and TEP, however, are feasible (e.g. [XIA 15]; see section 1.3.12 and 1.3.13). A novel compound based on a dye-iodonium salt intra ion-pair (where the dye derives from a 1,3-bis(dicyanomethylene) indane skeleton) works under a 635 nm light with an efficiency slightly lower than that of BM/amine [TEL 14].

Upconversion emission materials can convert IR into visible light via a multiphoton absorption process. For example, using the multicolor upconversion luminescence of rare earth-doped nanophosphors UCNPs, the photopolymerization of PEGDA microspheres under NIR lights (laser diode at 980 nm) using, for example, NaYF<sub>4</sub>:Er<sup>3+</sup>, Yb<sup>3+</sup> in the presence of Eosin was achieved (the green emission of the UCNP leads to a radiative absorption of the dye and then to initiating radicals; the radical formation mechanism does not seem to be fully understood) [XIA 13].

The two-photon absorption-induced polymerization (TPAP) is based on the nonlinear optical property of the absorbing materials. The absorption of light by a molecule is usually a one-photon process (i.e. one photon  $\nu$  is used to generate a given excited state). Under intense laser beams, the

simultaneous two-photon absorption (TPA) (characterized by a TPA cross-section which is different from the usual one-photon absorption cross-section) facilitates the formation of the same excited state using a photon  $\nu''$  (with  $\nu'' = \nu/2$ ) so that the excitation wavelength can be moved from the UV up to NIR lights. Compounds exhibiting D- $\pi$ -D, D- $\pi$ -A, A- $\pi$ -A or D- $\pi$ -A- $\pi$ -D structures, where D,  $\pi$  and A stand for a donor, a charge transfer system and an acceptor, are suitable. The synthesis of well-adapted compounds has received a considerable attention (see [LI 11]).

Near-field optical techniques (evanescent waves and field enhancement), as well as TPAP, facilitate the manufacture of nano-objects. The light is confined in a nanometric volume which enables high luminous power densities: even low reactivity PISs can work in these conditions. For example, although they are not very efficient in usual film photopolymerization under conventional light excitations (see below), some polymethine dye/amine systems could appear as excellent candidates as NIR PISs in TPAP for the manufacture of microtips perfectly self-aligned on the surface of vertical-cavity surface emitting lasers (VCSELs).

Efforts have been made for the development of systems usable for CTP technology, LDI purposes, stereolithography or 3D printing. Stereolithography (usual rapid prototyping technology using conventional PISs and laser arrangements), nanostereolithography (using TPAP), CTP, LDI, as well as applications of dyes in optics, imaging and nanotechnology are discussed in detail in other chapters of this book.

### **1.3.3. Dyes as part of PISs in the medical area**

DPRP reactions are encountered in the fields of medicine (tissue engineering, bone rebuilding, artificial items, coatings, adhesives, hydrogels, etc.), dentistry (see in Chapter 4) and ophthalmology (plastic eyeglasses, organic glasses, etc.). In most of the applications, three of the key points are (e.g. in tooth care): (i) avoiding the presence of UV rays; (ii) using PISs (dye and additives) exhibiting no toxicity (e.g. germlyl ketones, Eosin and CQ) and (iii) operating under low visible light intensities. PISs described in section 1.3.5 might be potentially interesting starting systems. Extensive work is carried out on the CQ/amine system and its substitutes. The theoretical analysis and experimental characterization of the

reciprocity law in BisGMA/TEGDMA films have been investigated. We will detail the use of dyes in dentistry applications in later chapters.

#### **1.3.4. *Dyes in controlled radical photopolymerization reactions***

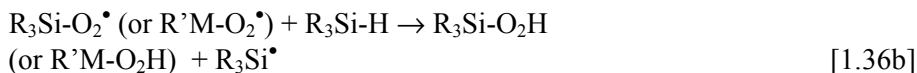
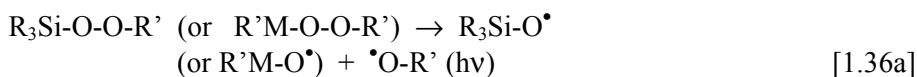
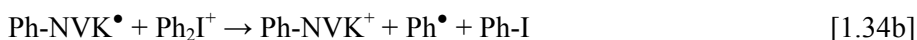
Contrary to the conventional radical photopolymerizations, where the radical generation is irreversible, controlled or living radical photopolymerizations avoid the simultaneous initiation, propagation and termination steps by temporarily blocking, in a reversible manner, the growing polymer chains. They thereby enable a control of the final properties of the constituted polymer (such as the number of average molecular weight  $M_n$  and the molecular weight distribution MWD) and the preparation of novel architectures. The control can be made possible using photoiniferters, photo nitroxide-mediated photopolymerization (NMP), photo atom transfer radical polymerization (ATRP) or photo reversible addition-fragmentation transfer (RAFT). Relatively little is known about the control of photopolymerization reactions. Visible light-induced controlled processes (NMP, RAFT and ATRP), sometimes even under sunlight, have also been described. This is also discussed later in this book.

#### **1.3.5. *Photoinitiation under soft irradiation conditions: novel three-component systems***

In the past 3–4 years, huge efforts have been deployed to develop PISs able to initiate the polymerization of low-viscosity matrices (radical or cationic) under soft irradiation conditions, i.e. visible lights, low intensity (2–30 mW/cm<sup>2</sup>) and under air [LAL 14a]. They require the design of particularly reactive systems and involve novel strategies for an efficient production of radical or cationic initiating species. Such systems can successfully operate in high-viscosity media or/and under intense light sources.

As stated above, the low incident light intensity of a given source must be counterbalanced by an initiation quantum yield  $\Phi_i$  as high as possible and enhanced absorption properties of the dye in order to achieve high  $R_p$  and  $C_f$ . The most performant new PISs are the recently developed Dye/silane (or NVK)/iodonium salt three-component systems where two significant

features appear [LAL 12]. First, both a silyl radical [1.31]–[1.32] and a silylium cation [1.33] are generated in any case, provided that the redox potentials are obviously adequate. As these reactions only depend on the starting absorbing dye, the radical/cation production can occur at any excitation wavelength: such versatile and tunable PISs have not been disclosed before in the literature. Tris(trimethyl) silane ((TMS)<sub>3</sub>SiH) is the best example of a silane usable in these PISs. Most of these PISs involve the particular and classical diphenyliodonium hexafluorophosphate; commercial and less toxic iodonium salts (e.g. diphenyliodonium tri(pentafluorophenyl) borate [FOU 12a] or substituted iodonium salts avoiding a benzene release) can also be used. The same behavior is observed with *N*-vinylcarbazole (NVK) (which is a cheaper compound) instead of (TMS)<sub>3</sub>SiH [1.34]. Second, silyl radicals consume oxygen [1.35], scavenge peroxy (R'M-O<sub>2</sub>•) and oxyl (R'M-O•) radicals inherently present in the medium and regenerate new silyls [1.36]. The oxygen inhibition that is detrimental in FRP, CCRP, TEP and FRPCP (see section 1.3) is reduced.

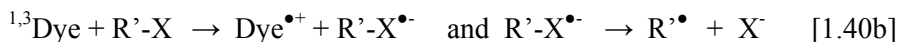
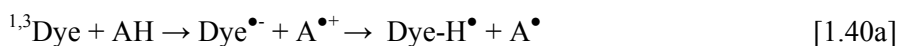


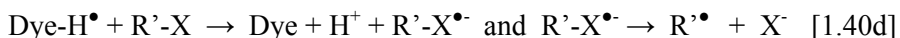
A large number of Dye/iodonium salt/silane (or NVK) combinations (with Dye = organic and organometallic compounds) usable under blue to red lights have been very recently proposed [XIA 15]. Examples of Dye include strongly modified known starting structures as well as totally novel skeletons, e.g. modified TXs, BPs, Mischler's ketone, anthraquinones or benzoin ethers, chalcones, acridinedione (ACs), chlorotriazines, naphthalenes, anthracenes, pyrenes, polyenic structures, naphthalimides, naphthalic anhydrides, naphthalimide-phthalimides, phenazines, pentacenes, thiophenes, perylenes, benzo pyrazo isoquinoline, isoquinolinones, squaraines and indolines, BODIPYs, pyrromethenes; diketopyrrolopyrroles, chromones, boranils, pyridinium dyes, indanediones, violanthrones, julolidines and fluorenones, malonates and malonitriles, thiobarbituric acid, fluoranthenes, star-shaped structures, BP-naphthalimides, polyoxometallates, Ru, Ir, Ti, Zn, Cu, Fe or Zr complexes.

The use of new metal-based compounds as Dye has also been recently proposed to enhance performance [XIA 15]: these compounds allow us to decompose the peroxy radicals through an  $S_H2$  reaction as in the case of metal(IV) amines [1.37] and the ROOH through photosensitization with metal carbonyls MeCarb [1.38], new initiating  $R_1\cdot$  and silyl radicals being formed [1.37], [1.39]. The  $Cp_2TiCl_2$  (or  $Cp_2ZrCl_2$ )/DMPA couples and Ti propoxide/BAPO also ensure a significant reduction of the oxygen inhibition through the same  $S_H2$  reaction.



Other efficient three-component systems are based on the Dye/amine AH/alkyl halide  $R'-X$  combinations. Examples of Dye are hydrocarbons, indanones, thiobarbituric acid, ruthenium or iridium complexes, etc. (see also below). They work according to the sequence [1.40],  $R'\cdot$  and  $A\cdot$  being the initiating radicals.





### 1.3.6. *Dyes with red-shifted absorptions and high molar extinction coefficients*

To fulfill the conditions recalled above in order to get a high polymerization efficiency, efforts have been recently made to develop dyes with high molar extinction coefficients (to absorb more light) and red-shifted absorptions (to recover more photons in the visible range when using polychromatic lights or to be more closely adapted to the imposed emission lines of LEDs or lasers). Successful results were obtained by a tailor-made design of extensively delocalized structures. Of course, the strategy is not completely novel but up to now, it was restricted to the introduction of usual small size ED or acceptor substituents.

Recent developments have allowed us to reach really huge molar extinction coefficients  $\epsilon$  and well-adapted absorptions in visible light for a large panel of new dyes. This was made possible by large and strong coupling of the  $\pi$  molecular orbitals of two or more moieties, e.g. a truxene core Tr with three BPs (or TX, dimethoxyacetophenone and AC) units [TEH 13b], a triazine nucleus with BP or pyrene branches [TEH 12a] or a triphenylamine core with three thiophene derivatives containing arms: this led to the concept of light-harvesting large PIs. The high  $\epsilon$  values that have never been attained before in the case of modified ketones (e.g. = 105,000 and 123,000  $\text{M}^{-1}\text{cm}^{-1}$  for Tr-BP and Tr-TX vs. 150 and 6,000 for BP and TX at the absorption maximum at  $\lambda > 300$  nm – Figure 1.1) can be compared with those of, for example, Eosin (typically, 90,000  $\text{M}^{-1}\text{cm}^{-1}$ ).

The design of such large structures might rapidly be faced with a problem of solubility in organic matrices. To overcome this possible limitation, smaller size structures have been synthesized such as push-pull arrangements consisting of substituted D- $\pi$ -A structures with ED (D) and EA (A) functionalities at both ends of a planar conjugated spacer. The strong light absorption of these push-pull dyes in the visible region results from important charge transfer optical transitions [XIA 15]. Still, high  $\epsilon$  values are obtained.

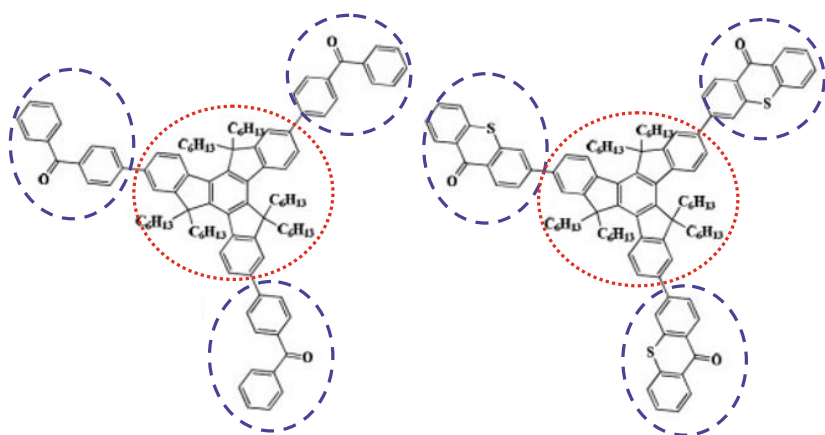


Figure 1.2. Examples of light-harvesting large photoinitiators

### 1.3.7. Performances of novel three-component PISs in low-viscosity matrices under LEDs/laser diodes and low-intensity household devices

Photopolymerization reactions under LEDs, laser diodes or household devices attract great interest; controlled photopolymerizations have been reported under household fluorescent lamps (e.g. ATRP, see [XIA 15]). As the photosensitivity of the formulations is dramatically enhanced (as resulting from quite high  $\Phi_i$  and excellent light absorptions; see below), our novel systems [XIA 15, TEH 13b, LAL 84, TEH 13a, TEH 12a, TEH 13e, TEH 11, TEH 13c, TEH 13d, TEH 12b, TEH 12c, TEL 13a] generally allow us to carry out polymerization reactions under very soft irradiation conditions using visible lights delivered by, for example, household halogen lamps ( $12 \text{ mW/cm}^2$  in the 370–800 nm range), fluorescence bulbs ( $15 \text{ mW/cm}^2$ ) and UV, violet, purple, blue, green, red or white LEDs ( $7\text{--}20 \text{ mW/cm}^2$ ) or even the Sun ( $<5 \text{ mW/cm}^2$  in the near UV-visible range). A recent review of this has been published in [LAL 14a].

In these conditions, most of the many new families of dyes detailed above incorporated in low-viscosity matrices easily work under air (FRPCP of diepoxides or CCRP acrylate/diepoxide blends) or in laminate (thiol-acrylate mixture in TEP). In contrast, low-viscosity acrylate formulations (e.g. TMPTA) can only operate, up to now, in laminate; quite excellent

conversion-time profiles for the FRP of TMPTA are therefore obtained. Interestingly, in highly viscous media (e.g. an epoxyacrylate oligomer dissolved in hexanediol diacrylate (Ep)), FRP is feasible under air in the presence of these PISs, even upon very low light intensity (e.g. sunlight exposure,  $2 \text{ mW/cm}^2$ ).

These systems [XIA 15] and other systems can obviously be used under higher intensity Xe lamp, LED and laser diodes ( $50\text{--}100 \text{ mW/cm}^2$ ); the level of performance still increases. Compared to references such as Eosin/amine or CQ/amine for green and blue light exposure, respectively, they exhibit an excellent photoinitiation ability for the FRP of TMPTA films in laminate. The efficiency remains relatively lower under air (but the references do not work at all). Interestingly, using higher viscosity matrices based on methacrylates (e.g. Bis-GMA/TEGDMA), FRP becomes really feasible under air, e.g. upon exposure to blue laser diodes at 405 or 457 nm (final conversions  $> 50\%$  instead of 25% for TMPTA). In these matrices, novel PISs are noticeably more efficient than the reference systems based on CQ or bisphosphine oxides. Finally, these PISs facilitate easy FRPCP (useful for the manufacture of low-shrinkage cationic coatings at long wavelengths) and CCRP.

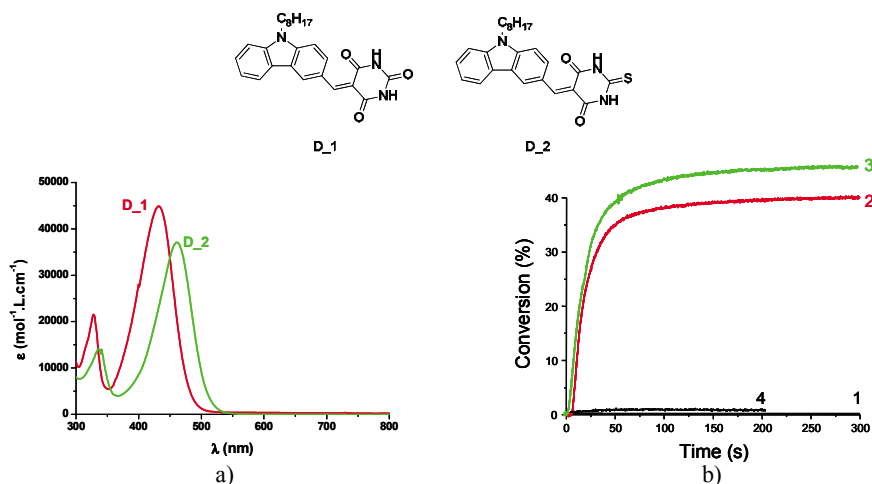


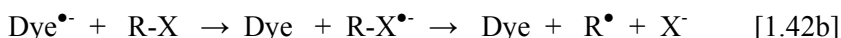
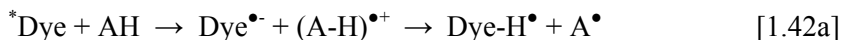
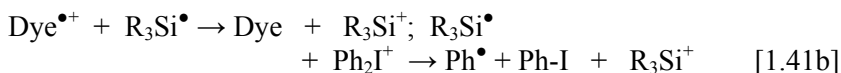
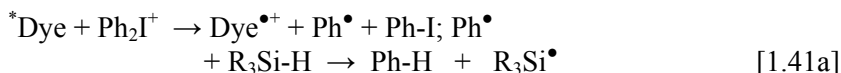
**Figure 1.3.** Examples of push-pull dyes used in PISs: a) UV-vis absorption spectra and b) typical polymerization profiles for emission wavelength 473 nm

Although interesting performances are achieved with Dye/iodonium salt/silane (or NVK) in the purple-blue-green range, the situation in the red region is more complex to get tack-free coatings from low-viscosity films, especially under air. Indeed, only low TMPTA conversions (approximately 20%) are reached in laminate (using, for example, perylene derivatives in the presence of methyl diethanolamine or methyl diethanolamine/phenacyl bromide; laser diode exposure at 635 nm; 100 mW/cm<sup>2</sup>) [XIA 15]. The CCRP of an epoxide (EPOX)/acrylate (TMPTA) blend under the same laser diode is, however, efficiently achieved under air (e.g. using an anthraquinone derivative as Dye). All the other checked PISs sometimes mentioned in the literature (e.g. cyanine/amine, cyanine/iodonium salt) do not significantly work in the FRP of TMPTA in our experimental conditions under red lights. On the opposite, the squarylium-triazine linked dye/ferrocene combination is claimed as efficient under a 635 nm source (10 mW/cm<sup>2</sup>) but for the polymerization of very viscous media (pentaerythritol tetraacrylate dissolved in a polymeric methacrylate binder; MW: 535,000 g/mol) and in laminate. Today (see also again section 1.3.2), radical polymerization reactions under red/near IR lights under air still remain a great challenge contrary to the FRPCP at 635 nm under air where successful results have been obtained, for the first time, using dye/iodonium salt/NVK systems where a Dye stands for, for example, a perylene, a violanthrone, a pentacene or an anthraquinone derivative.

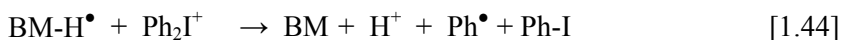
### 1.3.8. Recoverable dyes: the concept of photoinitiator catalysts

A recent research direction was focused on the use of the photoredox catalysis (well-known and largely employed in organic synthesis [XIA 15, SHI 10]) in the polymerization area where the development of sustainable radical-mediated chemical processes under very soft irradiation conditions can be of interest (see a review in [LAL 14b]). The goal is twofold: (i) getting a PI regeneration while keeping a high reactivity/efficiency and (ii) using interesting and promising colored structures. Metal containing dyes (e.g. ruthenium and iridium-based organometallic complexes) and metal-free organic dyes (e.g. Eosin, hydrocarbons and modified ketones) have been tested. Excellent visible-light absorptions, long-lived excited states and suitable redox potentials are decisive for the dye. The excitation under low light intensities from the UV to the near IR upon exposure to polychromatic lights (even sunlight), or purple, blue, green, yellow or red laser lines, is feasible. Three-component systems are usually encountered, e.g. Dye/silane

(or NVK)/iodonium salt (with, for example, Dye = Ru or Ir complex) or Dye/amine/alkylhalide (with, for example, Dye = hydrocarbon scaffold). The observed mechanisms involve oxidation [1.41] or reduction [1.42] cycles in the former and the latter systems, respectively. The dye is regenerated and can, therefore, be considered as a PIC. In [1.41]–[1.42], radicals and cations are simultaneously generated so that these PISs exhibit a dual behavior and can ensure FRP, CP, FRPCP and the formation of, for example, epoxy/acrylate IPNs.



A novel visible-light organic photoredox catalytic system based on methylene blue BM/amine/iodonium salt has been proposed [AGU 14]. Such BM-based systems containing a hydrogen-donating amine are well-known (see section 1.3.2) but relatively less efficient; the originality here is the use of a sacrificial sterically hindered amine shAH that decomposes, after electron transfer [1.43], into closed-shell products instead of open-shell (radical) intermediates. Thus, even if the light is switched off, the formed leuco BM can slowly react with the iodonium salt, generate a phenyl radical and initiate an FRP [1.44]. Therefore, this system makes the storage of light-energy and a release in the dark possible: the polymerization of thick coatings is claimed.



### 1.3.9. Metal-based dyes: recent perspectives

Metal-based PIs have been well-known for many years [CUN 93]; in particular, the titanocenes for exposure to visible light sources represent a famous (and even unique) example [ROL 86]. A strong revival of interest

has been devoted to the design of novel compounds involving various metals such as titanium, zirconium, zinc, platinum, nickel, iron, molybdenum and copper. As mentioned before (section 1.3.5), interesting results have been gained when using these novel metal-based dyes containing PISs. In most of the cases (Ti, Zr, Zn, Mo, Cu and Ti), FRP under air is feasible but the excitation is mostly restricted to UV/near UV lights so far.

### 1.3.10. *Dyes under sunlight exposure*

Despite the numerous works on visible light-induced FRP, CP or FRPCP, the sunlight curing (which has several interesting characteristics: no volatile organic compound (VOC) release, no energy consumption, no irradiation device and the possibility of curing large-dimensional pieces or surfaces) is relatively little documented (see, for example, reviews in [FOU 03, LAL 11b] and [XIA 15]). In the 1990s, FRP applications have been noted in outdoor paints for crack-bridging applications, anti-soiling properties or the fabrication of glass fiber-reinforced composites [REH 91, EIS 97]. IPNs can be obtained in CCRP or TPE. To overcome the strong oxygen inhibition effect in such a low light intensity exposure, highly viscous monomer/polymeric binder containing matrices, elastomeric latexes or waterborne latexes, were used. BP, CQ or BAPO derivatives were the usual PIs [EIS 97]. Recently, the addition of a silane to BAPO reduced the irradiation time to get a tack-free epoxy acrylate coating from 1 h to 12 mn exposure under air; as before, this was ascribed to the oxygen consumption by the radicals, the quenching of the formed peroxy radicals and the generation of silyl radicals (see reactions [1.36a]–[1.36c]) [EL 09]. Up until now however, under sunlight, tack-free coatings cannot be obtained with low-viscosity monomers such as TMPTA or ethoxylated pentaerythritol tetraacrylate (EPT). Sunlight-controlled polymerization reactions (RAFT and ATRP) are currently being investigated.

### 1.3.11. *Dye-based PISs as a source of mediator radicals: application to FRPCP*

As known for many years [FOU 12a, XIA 15, LED 78, TEH 10b], in FRPCP ([1.16]–[1.17], [1.41]), the excited dye undergoes the formation of a radical  $R^{\bullet}$  that is oxidized by an iodonium salt and generates a cation suitable for the ring opening reaction of epoxides [1.45]. The originally

proposed Dye/onium salt PIS, however, only works in oxygen-free media under near-UV light (Dye = benzoin ethers, phosphine oxides). The other radical  $R^{\bullet}$  might eventually be usable for FRP. It is obvious that any change of Dye leads to a different radical and a different cation.



An interesting development was the proposal of using the suitable Dye/iodonium salt/silane (or NVK) systems presented above for FRP (see [XIA 15] and the references therein). Indeed, in this case, in contrast with [1.45a] and [1.45b], the primarily formed radicals and the initiating cations are the same ( $R_3Si^{\bullet}$  and  $R_3Si^+$ ), whatever the dye. Therefore, changing the dye allows us to tune the absorption over the visible range (see reactions [1.31]–[1.33]); moreover, reactions under air are feasible due to the presence of the silane. This sequence of reaction is really versatile and ensures the possibility of FRPCP reactions at any wavelength. A lot of novel dyes are currently being proposed by us (e.g. Ir, Ru, Cu, Pt complexes, naphthalenes, pentacenes, naphthalimides, perylenes, phenazines, thiophenes, indolines, squaraines, violanthrones, chromones, chalcones, BPs, TXs, Michler's ketones, etc., as shown in references above). The FRPCP of epoxides under air is feasible at wavelengths ranging from the blue to the red, delivered by high-intensity light sources (Xe-Hg or Xe lamps, LEDs and laser diodes) or low-intensity devices (household halogen lamps, fluorescent bulbs and sun). In the cationic photopolymerization area, this (i) certainly represents a real progress; (ii) overcomes the drawback of the hard photosensitization of the iodonium salt decomposition which prevents efficient CP at long wavelength and (iii) should probably extend the use of CP in industrial applications under visible lights.

Cationic photopolymerizations are detailed later in the book.

### **1.3.12. Dyes exhibiting a dual radical/cationic behavior: application to concomitant radical/cationic photopolymerizations**

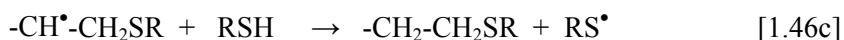
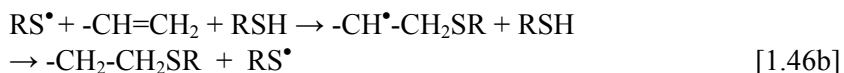
The formation of IPNs combining the properties of the two polymer backbones can be achieved using the hybrid cure technique where a blend of a radical and a cationic monomer/oligomer is photopolymerized. The consecutive two-step irradiation procedure is the most common: two PIs

(radical and cationic) are used; two different irradiation wavelengths are employed; the two monomers consecutively polymerize. The starting point of the reaction is driven by a selective and separate excitation of the two PIs depending on the wavelengths used.

A one-step procedure now becomes feasible using the dual behavior of particular dyes able to generate both radical and cationic species and allowing a simultaneous or concomitant radical/cationic photopolymerization reaction of acrylate (e.g. (TMPTA)/diepoxide or divinylether) blends (see a recent review in [XIA 14]) that can be achieved under blue to red lights.

### 1.3.13. Dyes in thiol-ene photopolymerizations

TEP involves a stoichiometric reaction of a multifunctional olefin and a multifunctional thiol (e.g. thiol-vinyl ether, thiol-allyl ether, thiol-acrylate and thiol-yne). The reaction is a step-growth addition of the thiol to the double bond [1.46a]–[1.46c]: formation of a thiyl radical, addition of the thiyl to the ene structure, regeneration of a thiyl, etc.; termination occurs through recombination and disproportionation reactions.



BP was originally introduced as PI for TEP under UV light excitation. Later on, other ketones were proposed. Recently, the TEP of a trithiol/divinylether mixture under exposure of a very soft halogen lamp, or laser diodes at 473, 457 or 635 nm, has been successfully achieved using various novel dyes [XIA 15].

### 1.3.14. *Dyes for the manufacture of photopolymerizable panchromatic films*

Multicolor PISs (exhibiting a particular absorption spectrum with red tails or broad spectrum) have been proposed [XIA 15]. The high

performance of the dyes reported above enables the preparation of panchromatic polymerizable films sensitive to UV-to-red lights using dyes with broad absorption spectra or a mixture of several suitable dyes. For example, the combination of blue-green and red light-sensitive perylene derivatives and an iodonium salt ensures the manufacture of a panchromatic thiol-ene polymerizable film (400–650 nm) usable under various household LED bulbs irradiations (i.e. blue, green, yellow or red lights).

### 1.3.15. Dyes for polymerization of *in situ* nanoparticle containing films

Upon a photochemical activation, the generation of NPs of metals or metal-based compounds (Ag, Au, Pd, Cu, Zr, Ti, etc.) can be realized in solution and films using the reduction of a metallic salt  $\text{Me}^+\text{S}^-$  [FOU 12a]. A specific case is concerned with the *in situ* incorporation of NPs in an organic monomer/oligomer matrix that photopolymerizes at the same time. A convenient PIS should produce both an initiating radical and a radical capable of reducing the salt: successful formation of Ag, Au or Cu NPs [1.47a]–[1.47b] has been already observed. Metal-functionalized PIs (e.g. a gold-thiophene derivative, an Ag-TX derivative or an Ag-diaminofluorene-derived dye) have also been proposed. As all these NPs are produced in a polyacrylate film, oxygen inhibition plays a detrimental role. As before, the phenomenon is amplified in low viscosity and thin media.



Therefore, the use of other PISs containing a silane or NVK (Dye/iodonium salt/NVK) can be useful for the formation of silver NPs ([1.48a] and [1.48b]) under air. Moreover, it ensures an excitation wavelength only depending on the dye [XIA 15]: the reaction can be carried out over the 350–700 nm range.



An interesting and really promising approach (reported in section 1.3.5) involving a  $\text{S}_{\text{H}2}$  process has been recently proposed ([1.49a] and [1.49b]). Metal salts are obviously not reduced in this case but other metal-centered

structures that do not exist as metal salts can safely work: this procedure can extend the number of metal NPs that can be photochemically generated *in situ*. According to this procedure, polymerized TMPTA films with Ti-based NPs, Zr-based NPs and Zr fillers were easily obtained under air. Very recently, a titanium isopropoxide/iodonium salt has ensured a clean *in situ* production of Ti NPs in a photopolymerized cationic matrix under air, but the mechanism might be different.



Using Dye/amine/alkyl bromide, iridium-containing photoluminescent polyacrylate films have also been manufactured. Polyoxometallate (POM)/polymer hybrid materials exhibiting modified mechanical properties (polymerized EPOX/TMPTA matrix with inserted POM clusters [XIA 15]) were synthesized in a one-step process using a silicon or phosphor polyoxomolybdate/iodonium salt/silane system.

#### 1.4. Dye-based photoinitiating systems: properties, efficiency and reactivity

Many studies have been carried out on the excited state processes in PIs and PISs using a lot of powerful techniques (see [FOU 12a]), e.g. nanosecond [SCH 90b, FOU 10b, YAG 10], picosecond or femtosecond spectroscopy [FRI 14], time-resolved Fourier Transform Infrared (FTIR) spectroscopy [FOU 12a], photothermal techniques [FOU 12a], PLP-ESI-MS [FRI 14], CIDNP, CIDEP and ESR spectroscopy [FOU 12a]. When looking at all the papers on dye-based PISs, a tempting question that arises is how is it possible to drive the performance? Their practical efficiency ( $R_p$  and  $C_f$ ) in polymerization reactions under given experimental conditions is easily accessible but the comparison from one paper to another is rather impossible (as very different polymerization conditions are used). Such a comparison can only be carried out within one paper as we have done for the numerous PISs recently developed by ourselves [XIA 15]. The efficiency of PISs must not be confused with their photochemical/chemical reactivity. The reactivity is an intrinsic characteristic which is not dependent on the experimental conditions. Improving reactivity and designing PISs with better absorption properties and an enhanced reactivity are some key challenges.

Let us consider our proposed series of PISs. They usually work according to the different sets of reactions shown above. The formation of the initiating species mainly (and often quasi-exclusively) occurs in the first excited singlet state  $S_1$  of the dye. In the Dye/iodonium salt/silane system, the primary interactions with the iodonium salt exhibit almost diffusion-controlled rate constants and highly negative free energy changes. In the Dye/amine/alkylbromide system, the Dye/amine interaction predominates and is largely favorable. In reactive systems, photolysis is very fast. Even with these favorable factors, however, large discrepancies in the reactivity/efficiency scale are observed when going from one PIS to another. Indeed, a competition of the Dye/iodonium salt (or amine) interaction with the other deactivation pathways of Dye occurs (radiative and non-radiative processes; the monomer quenching is usually low in  $S_1$  and negligible). As a result, the quantum yield of electron transfer  $\Phi_{eT}$  is more or less important but it is often  $>0.5$ . Moreover, unpredictable back electron transfer reactions (which reduce  $\Phi_{eT}$ ) are likely to occur. Unfortunately, their occurrence is not well understood and hence cannot yet be overcome. These back-reactions certainly play a detrimental role as it is amazing to see that two PISs exhibiting very large differences in absorption properties (and both having almost similar  $\Phi_{eT}$  and leading to the same efficient radicals toward the addition to the acrylate function) can lead to relatively small  $R_p$  differences. A complete understanding of the reactivity is not yet accessible. The most open *a priori* factor is certainly the absorption. MO considerations and calculations safely help the design of dyes exhibiting suitable required ground state absorptions.

### 1.5. Trends and perspectives

The dye-based radical PISs described throughout this chapter will continue to be encountered in a large variety of reactions in the radiation curing field (photopolymerization and cross-linking of multifunctional acrylates, TEP, photopolymerization of waterborne light curable systems, photopolymerization of powder-coating formulations, controlled RAFT, ATRP, NMP photopolymerization reactions, dual cure and hybrid cure photopolymerizations, etc.), the imaging and laser imaging field (writing of complex relief patterns for the manufacture of microcircuits and CTP systems, printing inks, stereolithography, 3D microscale-structured materials, manufacture of optical elements, etc.) or the medical and dentistry fields.

These PISs can initiate the photopolymerization of synthetic, as well as renewable, monomers/oligomers. A careful adaptation of the PISs to novel light sources avoiding the harmful mercury lamps emitting UVA and UVB or even UVC rays has been possible, and today, polychromatic visible light irradiation devices (Xe, Hg-Xe and doped lamps), quasi-monochromatic devices (LED arrangements) or monochromatic devices (laser diode arrays) can be safely used.

Over the last 30 years, the development of efficient radical two-component systems and above all three-component PISs (through a careful selection of suitable interactions between the different compounds) has led to a great improvement in the attained performance. Many of them can also behave as cationic PISs in FRPCP. There is still a place for innovative chemistries involving multicomponent systems.

The recent input of the silyl (or germyl and boryl) radical chemistry has enabled a decisive step for the designing of high-performance photopolymerizable materials being able to operate in severe experimental conditions (aerated media, exposure to sunlight and household fluorescent lamps or LED bulbs, low-viscosity matrices and low film thicknesses). A large number of the novel PISs presented here exhibit an improved photosensitivity (compared to that of the existing reference systems) in the blue-to-red wavelength range, even in aerated media, both working under high- and low-intensity sources. Various photocurable matrices can be used: radical, cationic, thiol-ene and radical/cationic monomers blends. The development of PISs for water-reducible as well as water-based dispersions upon visible light exposure under air needs to be investigated. Photopolymerization reactions for various potential applications involving soft irradiation conditions become feasible. The *in situ* incorporation of NPs in a photopolymerizable matrix can be achieved at any excitation wavelength. Curing under standard household fluorescent bulbs for indoor applications can be envisaged. Sunlight-induced polymerization might also be a promising way for a practical low-cost outdoor curing process, especially designed for the drying of paints and the manufacture of large-dimensional items.

Undoubtedly, new opportunities have arisen thanks to these developments. The already high-level performance helps to improve the development of existing applications and to prospect for new applications involving, for example, aerated media, low light intensities, visible lights,

very low viscosity monomers, thin films, blue-to-red household LEDs, laser lines, industrial LEDs and sunlight curing.

Even more efficient systems are likely to be designed in the future through the exploration of novel organic skeletons, substituted structures (to take into account specific end-use properties), metal organometallic complexes and metal-free organic compounds (as PICs in photoredox reactions), cheaper and non-toxic metal complexes (e.g. copper- or iron-based), PI/control agents for controlled photopolymerization reactions and more. When going to exposures to low-intensity lights, the search for highly absorbing systems becomes crucial. The design of molecules exhibiting a red-shifted absorption is challenging. In a different way, the careful choice of the dye-based PISs and the design of two-photon sensitive dyes for laser-induced polymerization open up interesting routes in the nanotechnology field.

All of these examples outline the crucial role of the dye in the formulation and the last developments should initiate novel possible applications for the future. Considering the high efficiency already attained today and the large potential expected in many innovative applications (e.g. in optics, holography, dentistry, medicine, imaging, manufacture of micro- and nano-structured materials, etc.), the development of radical PISs adapted to visible and NIR lights should continue.

## 1.6. Bibliography

- [AGU 14] AGUIRRE-SOTO A., LIM C.-H., HWANG A.T. *et al.*, *J. Am. Chem. Soc.*, vol. 136, pp. 7418–7427, 2014.
- [ALL 04] ALLONAS X., OBEID H., FOUASSIER J.P. *et al.*, *J. Photopolymer Science and Technology*, vol. 17, pp. 35–42, 2004.
- [ALL 10] ALLEN N.S. (ed.), *Photochemistry and Photophysics of Polymer Materials*, Wiley, Hoboken, 2010.
- [ALZ 14] ALZHRANI A.A., ERBSE A.A., BOWMAN C.N., *Polym. Chem.*, vol. 14, pp. 1874–1882, 2014.
- [BAI 13] BAI J., SHI Z., *J. Appl. Polym. Sci.*, vol. 128, pp. 1785–1791, 2013.
- [BEL 03] BELFIED K.D., CRIVELLO J.V. (eds), *Photoinitiated Polymerization*, ACS Symposium Series 847, Washington, DC, 2003.

- [BIB 02] BIBAUT-RENAULD C., BURGET D., FOUASSIER J.P. *et al.*, *J. Polym. Sci. Part A: Polym. Chem.*, vol. 40, pp. 3171–3181, 2002.
- [BON 14] BONGIOVANNI R., SANGERMANO M., “UV-curing science and technology”, *Encyclopedia of Polymer Science and Technology*, 2014.
- [BOT 91] BOTTCHEH H., *Technical Applications of Photochemistry*, Deutscher Verlag für Grundstoffindustrie, Leipzig, 1991.
- [BUR 99] BURGET D., FOUASSIER J.P., AMAT-GUERRI F. *et al.*, *Acta Polymer*, vol. 50, pp. 337–346, 1999.
- [CAP 89] CAPOLLA CARRE C., LOUGNOT D.J. *et al.*, *Applied Optics*, vol. 28, pp. 4050–4052, 1989.
- [CLA 13] CLARK LIGON S., HUSAR B., WUTZEL H. *et al.*, *Chem. Rev.*, 2013.
- [CRI 79] CRIVELLO J.V., LAM J.H., *J. Polym. Sci. Part A: Polym. Chem.*, vol. 17, pp. 977–982, 1979.
- [CRI 93] CRIVELLO J.V., in FOUASSIER J.P., RABEK J.F. (eds), *Radiation Curing in Polymer Science and Technology*, vol. 2, Elsevier, Barking, UK, pp. 435–472, 1993.
- [CRI 99] CRIVELLO J.V., DIETLIKER K., in BRADLEY G. (ed.), *Photoinitiators for Free Radical, Cationic and Anionic Photopolymerization*, Surface Coatings Technology Series, vol. 3, Wiley, 1999.
- [CUI 11] CUI R., WANG K., MA G. *et al.*, *J. Appl. Polym. Sci.*, vol. 120, pp. 2754–2759, 2011.
- [CUN 93] CUNNINGHAM A.F., DESOBRY V., in FOUASSIER J.P., RABEK J.F. (eds), *Radiation Curing in Polymer Science and Technology*, vol. 2, Elsevier, Barking, UK, pp. 323–374, 1993.
- [DAV 99] DAVIDSON S., *Exploring the Science, Technology and Application of UV and EB Curing*, Sita Technology Ltd, London, 1999.
- [DEC 01] DECKER C., ZAHOUILY K., DECKER D. *et al.*, “Performance analysis of acylphosphine oxides in photoinitiated polymerization”, *Polymer*, vol. 42, pp. 7551–7560, 2001.
- [DIE 02] DIETLIKER K., *A Compilation of Photoinitiators Commercially Available for UV Today*, Sita Technology Ltd, London, 2002.
- [EAT 86] EATON D.F., in HAMMOND D.H., GOLLNICK G.S. (eds), *Advances in Photochemistry*, vol. 13, Wiley, NY, pp. 427–487, 1986.

- [EIS 97] EISELÉ G., FOUASSIER J.P., REEB R., *J. Polym. Sci. Part A*, vol. 35, pp. 2333–2345, 1997.
- [EL 09] EL-ROZ M., LALEVÉE J., ALLONAS X. *et al.*, *Macromolecules*, vol. 42, pp. 8725–8732, 2009.
- [ESE 13] ESEN D.S., ARSU N., DA SILVA J.P. *et al.*, *J. Polym. Sci. Part A: Polym. Chem.*, vol. 51, pp. 1865–1871, 2013.
- [FOU 90] FOUASSIER J.P., *Prog. in Org. Coatings*, vol. 18, pp. 227–250, 1990.
- [FOU 93a] FOUASSIER J.P., in FOUASSIER J.P., RABEK J.F. (eds), *Radiation Curing in Polymer Science and Technology*, Elsevier, Barking, UK, vol. 1, pp. 49–118 and vol. 2, pp. 1–62, 1993.
- [FOU 93b] FOUASSIER J.P., RABEK J.F. (eds), *Radiation Curing in Polymer Science and Technology*, Chapman & Hall, London, 1993.
- [FOU 93c] FOUASSIER J.P., RUHLMANN D., TAKIMOTO Y. *et al.*, *J. Polym. Sci., Part A: Polym. Chem.*, vol. 31, pp. 2245–2248, 1993.
- [FOU 95a] FOUASSIER J.P., *Photoinitiation, Photopolymerization, Photocuring*, Hanser, München, 1995.
- [FOU 95b] FOUASSIER J.P., RUHLMANN D., GRAFF B. *et al.*, *Progr. Org. Coat.*, vol. 25, pp. 235–271, 1995.
- [FOU 95c] FOUASSIER J.P., RUHLMANN D., GRAFF B. *et al.*, *Progr. Org. Coat.*, vol. 25, pp. 169–202, 1995.
- [FOU 99] FOUASSIER J.P. (ed.), “Photosensitive systems for photopolymerization reactions”, *Trends in Photochemistry & Photobiology*, vol. 5, Research Trends, Trivandrum, India, 1999.
- [FOU 00] FOUASSIER J.P., *Recent Res. Devel., Polymer Science*, vol. 4, Research Trends, Trivandrum, India, pp. 131–145, 2000.
- [FOU 01] FOUASSIER J.P., *Light Induced Polymerization Reactions, Trends in Photochemistry & Photobiology*, vol. 7, Research Trends, Trivandrum, India, 2001.
- [FOU 03] FOUASSIER J.P., ALLONAS X., BURGET D., *Prog. in Org. Coatings*, vol. 47, pp. 16–36, 2003.
- [FOU 06] FOUASSIER J.P. (ed.), *Photochemistry and UV Curing*, Research Signpost, Trivandrum, India, 2006.

- [FOU 07] FOUASSIER J.P., ALLONAS X., LALEVÉE J., in MATYJASZEWSKI K., GNANOU Y., LEIBLER L. (eds), *Macromolecular Engineering: From Precise Macromolecular Synthesis to Macroscopic Materials Properties and Applications*, vol. 1, Wiley-VCH, Weinheim, pp. 643–672, 2007.
- [FOU 10a] FOUASSIER J.P., ALLONAS X. (eds), *Basics of Photopolymerization Reactions*, Research Signpost, Trivandrum, India, 2010.
- [FOU 10b] FOUASSIER J.P., ALLONAS X., LALEVÉE J. *et al.*, in ALLEN N.S. (ed.), *Photochemistry and Photophysics of Polymer Materials*, Wiley, pp. 351–420, 2010.
- [FOU 11] FOUASSIER J.P., LALEVÉE J., MORLET-SAVARY F. *et al.*, in BECKER R. (ed.), *Materials, Advances in Dyes and Pigments*, Hindawi.com, 2011.
- [FOU 12a] FOUASSIER J.P., LALEVÉE J., *Photoinitiators for Polymer Synthesis: Scope, Reactivity and Efficiency*, Wiley VCH, Weinheim, 2012.
- [FOU 12b] FOUASSIER J.P., LALEVÉE J., *RSC Advances*, vol. 2, pp. 2621–2629, 2012.
- [FOU 12c] FOUASSIER J.P., LALEVÉE J., “Design of chromophores for photoinitiators of polymerization: brief survey and recent achievements”, in MOLIERE A., VIGNERON E. (eds), *New Development in Chromophore Research*, pp. 212–254, Nova Sciences, New York, 2012.
- [FRI 14] FRICK E., ERNST H.A., VOLL D. *et al.*, *Polym. Chem.*, vol. 5, pp. 5053–5068, 2014.
- [GAN 08] GANSTER B., FISCHER U.K., MOSZNER N. *et al.*, *Macromolecules*, vol. 41, pp. 2394–2400, 2008.
- [GRE 93] GREEN W.A., TIMMS A.W., in FOUASSIER J.P., RABEK J.F. (eds), *Radiation Curing in Polymer Science and Technology*, vol. 2, Elsevier, Barking, UK, pp. 375–434, 1993.
- [GRE 10] GREEN W.A., *Industrial Photoinitiators*, CRC Press, Boca Raton, 2010.
- [GRI 99] GRINEVICH O., SERGUIEVSKI P., SARKER A.M. *et al.*, *Macromolecules*, vol. 32, pp. 328–330, 1999.
- [GRO 01] GROTZINGER C., BURGET D., JACQUES P. *et al.*, *Macromol Chem Phys.*, vol. 202, pp. 3513–3522, 2001.
- [GUO 13] GUO R., GAO Y., WU M. *et al.*, *Polymer*, vol. 54, pp. 4940–4947, 2013.
- [HE 12] HE M., HUANG X., HUANG Y. *et al.*, *Polymer*, vol. 53, pp. 3172–3177, 2012.

- [IVA 10] IVAN M.G., SCAIANO J.C., “Photoimaging and photolithographic process in polymers”, in ALLEN N.S. (ed.), *Handbook on Photochemistry and Photophysics of Polymer Materials*, Wiley, Hoboken, NJ, pp. 479–508, 2010.
- [JED 10] JEDRZEJEWSKA B., URBANSKI S., *J. Appl. Polym. Sci.*, vol. 118, pp. 1395–1405, 2010.
- [JIA 11] JIANG M., WANG K., MA G. *et al.*, *J Appl Polym Sci.*, vol. 121, pp. 2013–2017, 2011.
- [KAB 07] KABATC J., ZASADA M., PAĆZKOWSKI J., *J Polym Sci. Part A: Polym Chem.*, vol. 45, pp. 3626–3636, 2007.
- [KAB 10] KABATC J., KRZYŻANOWSKA E., JEDRZEJEWSKA B. *et al.*, *J. Appl. Polym. Sci.*, vol. 118, pp. 165–172, 2010.
- [KAH 10] KAHVECI M.U., GORKEM A.G., YAGCI Y., “Photoinitiated cationic polymerization: reactivity and mechanistic aspects”, in ALLEN N.S. (ed.), *Handbook on Photochemistry and Photophysics of Polymer Materials*, Wiley, Hoboken, NJ, pp. 421–478, 2010.
- [KAR 14] KARAHAN O., BALTA D.K., ARSU N. *et al.*, *J Photochem Photobiol A.*, vol. 274, pp. 43–49, 2014.
- [KAW 13] KAWAMURA K., LEY C., SCHMITT J. *et al.*, *J. Polym. Sci., Part A: Polym. Chem.*, vol. 51, pp. 4325–4330, 2013.
- [KIT 13] KITANO H., RAMACHANDRAN K., BOWDEN N.B. *et al.*, *J. Appl. Polym. Sci.*, vol. 128, pp. 611–618, 2013.
- [KOR 13] KORKUT S.E., TEMEL G., BALTA D.K. *et al.*, *J. Lumin.*, vol. 136, pp. 389–394, 2013.
- [KRO 94] KRONGAUZ V., TRIFUNAC A. (eds), *Photoresponsive Polymers*, Chapman and Hall, New York, 1994.
- [KUM 12] KUMBARACI V., AYDOGAN B., TALINLI N. *et al.*, *J Polym Sci. Part A: Polym Chem.*, vol. 50, pp. 2612–2618, 2012.
- [LAC 08] LACKNER M. (ed.), *Lasers in Chemistry*, Wiley-VCH, Weinheim, 2008.
- [LAL 09a] LALEVÉE J., BLANCHARD N., CHANY A.C. *et al.*, *Macromolecules*, vol. 42, pp. 6031–6037, 2009.
- [LAL 09b] LALEVEE J., EL ROZ M., ALLONAS X. *et al.*, “On the silyl radical chemistry in photopolymerization reactions”, in WYMAN E., SKIEF M.C. (eds), *Organosilanes: Properties, Performance and Applications*, Chapter 6, Nova Science Publishers, pp. 124–156, Hauppauge, NY, 2009.

- [LAL 09c] LALEVÉE J., EL ROZ M., TEHFE M.A. *et al.*, *Macromolecules*, vol. 42, pp. 8669–8674, 2009.
- [LAL 10] LALEVÉE J., TEHFE M.A., ALLONAS X. *et al.*, “Photoinitiating systems based on unusual radicals”, in ACKRINE W.J. (ed.), *Polymer Initiators*, Chapter 8, Nova Science Publishers, Inc., pp. 34–68, 2010.
- [LAL 11a] LALEVÉE J., BLANCHARD N., FRIES C. *et al.*, *Polym. Chem.*, vol. 2, pp. 1077–1084, 2011.
- [LAL 11b] LALEVÉE J., FOUASSIER J.P., *Polymer Chemistry*, vol. 2, pp. 1107–1113, 2011.
- [LAL 12] LALEVÉE J., FOUASSIER J.P., “Overview of radical initiation”, in STUDER A., CHATGILIALOGLU C. (eds), *Encyclopedia of Radicals in Chemistry, Biology and Materials*, vol. 1, Chapter 2, Wiley, New York, NY, pp. 1–34, 2012.
- [LAL 14a] LALEVÉE J., MORLET-SAVARY F., DIETLIN C. *et al.*, “Photochemistry and radical chemistry under low intensity visible light sources: application to photopolymerization reactions”, in WALTON J.C. (ed.), *Free Radicals and Radical Ions, Molecules*, available at: <http://www.mdpi.com/journal/molecules>, 2014.
- [LAL 14b] LALEVÉE J., XIAO P., TELITEL S. *et al.*, *Beilstein J. Org. Chem.*, vol. 10, pp. 863–876, 2014.
- [LAL 15] LALEVÉE J., FOUASSIER J.P., *RSC Photochemistry Reports*, vol. 42, pp. 215–232, 2015.
- [LAS 90] FOUASSIER J.P., RABEK J.F. (eds), *Lasers in Polymer Science and Technology: Applications*, CRC Press, Boca Raton, 1990.
- [LED 78] LEDWITH A., *Polymer*, vol. 19, pp. 1217–1219, 1978.
- [LI 11] LI Z., SIKLOS M., PUCHER N. *et al.*, *J. Polym. Sci. Part A: Polym. Chem.*, vol. 49, pp. 3688–3699, 2011.
- [MAT 07] MATYJASZEWSKI K., GNANOU Y., LEIBLER L. (eds), *Macromolecular Engineering: From Precise Macromolecular Synthesis to Macroscopic Materials Properties and Applications*, vol. 1, Wiley-VCH, Weinheim, pp. 643–672, 2007.
- [MEE 14] MEEREIS C.T.W., LEAL F.B., LIMA G.S. *et al.*, *Dental Materials*, vol. 30, pp. 945–953, 2014.
- [MIS 09] MISHRA M.K., YAGCI Y. (eds), *Handbook of Vinyl Polymers*, CRC Press, Boca Raton, 2009.
- [MON 93] MONROE B.M., WEED G.C., *Chem. Rev.*, vol. 93, pp. 435–448, 1993.

- [MOS 10] MOSZNER N., LAMPARTH I., ANGERMANN J. *et al.*, *Beilstein J. Org. Chem.*, vol. 6, pp. 1–9, 2010.
- [MUF 10] MUFTUOGLI A.E., TASDELEN M.A., YAGCI Y., “Photografting of polymeric materials”, in ALLEN N.S. (ed.), *Handbook on Photochemistry and Photophysics of Polymer Materials*, Wiley, Hoboken, NJ, pp. 509–540, 2010.
- [MUR 93] MURPHY S.T., CHAOFENG Z., MIERS J.B. *et al.*, *J. Phys. Chem.*, vol. 97, pp. 13152–13157, 1993.
- [NEC 99] NECKERS D.C., *UV and EB at the Millennium*, Sita Technology Ltd, London, 1999.
- [NES 13] NESHCHADIN D., ROSSPEINTNER A., GRIESSER M. *et al.*, *J. Am. Chem. Soc.*, vol. 135, pp. 17314–17321, 2013.
- [OLL 97] OLLDRING K., HOLMAN R. (eds), *Chemistry & Technology of UV & EB Formulation for Coatings, Inks and Paints*, vol. 1–8, John Wiley and Sita Technology Ltd, London, 1997.
- [OST 54] OSTER G., *Nature*, vol. 173, pp. 300–301, 1954.
- [PAC 01] PACZKOWSKI J., NECKERS D.C., *Electron Transfer in Chemistry*, vol. 5, pp. 516–585, 2001.
- [PAP 92] PAPPAS S.P., *UV-Curing: Science and Technology*, Tech. Mark. Corp., Stamford, 1986, Plenum Press, New York, 1992.
- [PIE 11] PIETRZAK M., WRZYSZCZYŃSKI A., *J. Appl. Polym. Sci.*, vol. 122, pp. 2604–2608, 2011.
- [POD 11] PODSIADLY R., PODEMSKA K., SZYMCZAK A.M., *Dyes and Pigments*, vol. 91, pp. 422–426, 2011.
- [REH 70] REHM D., WELLER., *Isro. J. Chem.*, vol. 8, 259–271, 1970.
- [REH 91] REHMER G., RAU M.G., WISTUBA E. *et al.*, *Eur. Pat.*, p. 417568, 1991.
- [REI 89] REISER A., *Photoreactive Polymers: The Science and Technology of Resists*, Wiley, New York, 1989.
- [RIS 92] RIST G., BORER A., DIETLIKER K. *et al.*, *Macromolecules*, vol. 25, pp. 4182–4193, 1992.
- [ROL 86] ROLOFF A., MEIER K., RIEDIKER M., *Pure Appl. Chem.*, vol. 58, pp. 1267–1273, 1986.
- [ROS 09] ROSSPEINTNER A., GRIESSER M., PUCHER N. *et al.*, *Macromolecules*, vol. 42, pp. 8034–8038, 2009.

- [SAN 14] SANGERMANO M., RAZZA N., CRIVELLO J.V., *Macromolecular Materials and Engineering*, vol. 229, pp. 775–793, 2014.
- [SCH 90a] SCHUSTER G.B., *Pure & App. Chem.*, vol. 62, pp. 1565–1572, 1990.
- [SCH 90b] SCHNABEL W., in FOUASSIER J.P., RABEK J.F. (eds), *Lasers in Polymer Science and Technology*, vol. 2, CRC Press, Boca Raton, pp. 95–143, 1990.
- [SCH 07a] SCHWALM R., *UV Coatings: Basics, Recent Developments and New Applications*, Elsevier, Oxford, UK, 2007.
- [SCH 07b] SCHNABEL W., *Polymer and Light*, Wiley-VCH, Weinheim, 2007.
- [SCR 97] SCRANTON A.B., BOWMAN A., PEIFFER R.W. (eds), *Photopolymerization: Fundamentals and Applications*, ACS Symposium Series 673, Washington, DC, 1997.
- [SHA 14] SHAO J., HUANG Y., FAN Q., *Polym. Chem.*, vol. 5, pp. 4195–4210, 2014.
- [SHI 10] SHIH H.-W., VANDER WAL M.N., GRANGE R.L. *et al.*, *J. Am. Chem. Soc.*, vol. 132, pp. 13600–13603, 2010.
- [TAR 10] TARZI O., ALLONAS X., LEY C. *et al.*, *J. Polym. Sci. Part A*, vol. 48, pp. 2594–2603, 2010.
- [TEH 10a] TEHFE M.A., BLANCHARD N., FRIES C. *et al.*, *Macromol. Rapid Comm.*, vol. 31, pp. 473–478, 2010.
- [TEH 10b] TEHFE M.A., LALEVÉE J., GIGMES D. *et al.*, *Macromolecules*, vol. 43, pp. 1364–1370, 2010.
- [TEH 11] TEHFE M.A., LALEVÉE J., FOUASSIER J.P., *Macromolecules*, vol. 44, pp. 8374–8379, 2011.
- [TEH 12a] TEHFE M.A., DUMUR F., MORLET-SAVARY F. *et al.*, *Macromolecules*, vol. 45, pp. 8639–8647, 2012.
- [TEH 12b] TEHFE M.A., LALEVÉE J., MORLET-SAVARY F. *et al.*, *ACS Macro Lett.*, vol. 1, pp. 198–203, 2012.
- [TEH 12c] TEHFE M.A., LALEVÉE J., TELITEL S. *et al.*, *Macromolecules*, vol. 45, pp. 4454–4460, 2012.
- [TEH 13a] TEHFE M.A., DUMUR F., CONTAL E. *et al.*, *Polym. Chem.*, vol. 4, pp. 1625–1634, 2013.

- [TEH 13b] TEHFE M.A., DUMUR F., GRAFF B. *et al.*, *Macromolecules*, vol. 46, pp. 736–746, 2013.
- [TEH 13c] TEHFE M.A., DUMUR F., GRAFF B. *et al.*, *Polym. Chem.*, vol. 4, pp. 2313–2324, 2013.
- [TEH 13d] TEHFE M.A., DUMUR F., GRAFF B. *et al.*, *Macromol. Rapid Comm.*, vol. 34, pp. 239–245, 2013.
- [TEH 13e] TEHFE M.A., ZEIN-FAKIH A., LALEVÉE J. *et al.*, *Eur. Polym. J.*, vol. 49, pp. 567–574, 2013.
- [TEL 13a] TELITEL S., SCHWEITZER S., MORLET-SAVARY F. *et al.*, *Macromolecules*, vol. 46, pp. 43–48, 2013.
- [TEL 13b] TELITEL S., VALLET A.-L., SCHWEIZER S. *et al.*, *J. Am. Chem. Soc.*, vol. 135, pp. 16938–16947, 2013.
- [TEL 14] TELITEL S., DUMUR F., KAVALLI T. *et al.*, *RSC Advances*, vol. 4, pp. 15930–15936, 2014.
- [TIM 93] TIMPE H.J., in FOUASSIER J.P. (ed.), *Radiation Curing in Polymer Science and Technology*, vol. 2, Elsevier, Barking, UK, pp. 575–602, 1993.
- [TUR 90] TURRO N.J., *Modern Molecular Photochemistry*, University Science Books, New York, 1990.
- [URA 03] URANO T., *J. Photopolym. Sci. and Tech.*, vol. 16, pp. 129–156, 2003.
- [VER 13a] VERSACE D.V., BASTIDA J.C., LORENZINI C. *et al.*, *Macromolecules*, vol. 46, pp. 8808–8815, 2013.
- [VER 13b] VERSACE D.L., DALMAS F., FOUASSIER J.P. *et al.*, *ACS Macro Lett.*, vol. 2, pp. 341–345, 2013.
- [XIA 13a] XIAO Q., JI Y., XIAO Z. *et al.*, *Chem. Commun.*, vol. 49, pp. 1527–1529, 2013.
- [XIA 13b] XIAO P., SIMONET-JEGAT C., DUMUR F. *et al.*, *Polym. Chem.*, vol. 4, pp. 4526–4530, 2013.
- [XIA 14] XIAO P., FOUASSIER J.P., LALEVÉE J., “Photochemical production of interpenetrating polymer networks; simultaneous initiation of radical and cationic polymerization reactions”, in SPERLING L.H. (ed.), *Photopolymerization of Acrylate/Epoxy Blends, Polymers*, Special Issue “Interpenetrating Polymer Networks”, available at <http://www.mdpi.com>, 2014.

- [XIA 15] XIAO P., ZHANG J., DUMUR F. *et al.*, *Prog. in Polym. Sci.*, vol. 41, pp. 32–66, February 2015.
- [XU 12] XU J., MA G., WANG K. *et al.*, *J. Nie J. Appl. Polym. Sci.*, vol. 123, pp. 725–731, 2012.
- [YAG 10] YAGCI Y., JOCKUSCH S., TURRO N.J., *Macromolecules*, vol. 43, pp. 6245–6260, 2010.
- [YUK 09] YUKSEL DURMAZ Y., KUKUT M., MONSZNER N. *et al.*, *Macromolecules*, vol. 42, pp. 2899–2902, 2009.
- [ZAL 14] ZALIBERA M., STÉBÉ P.-N., DIETLIKER K. *et al.*, *European Journal of Organic Chemistry*, vol. 2, pp. 331–337, 2014.



---

# Sensitization of Cationic Photopolymerizations

---

## 2.1. Introduction

The field of photopolymerization chemistry has shown no evidence of slowing down. Rather, this area of polymer chemistry continues to advance at a rapid pace as new applications are found and as the attractive productivity, environmental and energy saving benefits are realized. Once limited primarily to thin film applications found mainly in coatings, printing inks and adhesives, photopolymerizations are increasingly being harnessed for the preparation of advanced materials to serve the design engineering, transportation, aerospace, electronic, optoelectronic, dental and medical materials related industries. Each of these fields of application has its own materials and processing requirements and these requirements strongly influence the specific type of photopolymerization that is used. At the present time, there are four major types of photochemical processes that are applied to polymer-forming reactions. These are:

- 1) photoinduced condensation reactions;
- 2) photoinitiated free radical polymerizations;
- 3) photoinitiated cationic polymerizations;
- 4) photoinitiated anionic polymerizations.

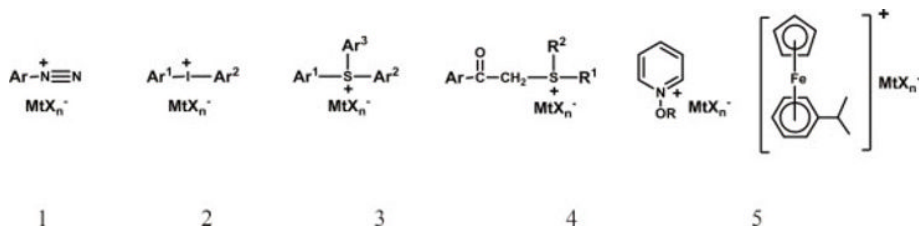
---

Chapter written by James CRIVELLO.

The term “photopolymerization” is widely applied to all four processes listed above despite the fact that photochemistry is involved in the actual bond making process of polymerization only in the first case. In the other three cases, photochemistry is operative only in the reactions involved in the generation of the reactive species that perform the initiation step of a chain reaction polymerization. From a practical standpoint, photoinduced condensation reactions are rarely employed at present. Previously, they were used in the photolithographic production of integrated circuits. However, these systems have largely been superseded by the intrinsically much more photosensitive photoinitiated polymerizations listed in categories 2–4. This is simply because photoinduced condensation polymerizations require the absorption of a minimum of one photon of light for the incorporation of every repeat unit into a polymer chain. However, most photochemically mediated condensation reactions have quantum yields considerably less than 1 and this makes them inefficient and highly energy consumptive. In contrast, photoinitiated polymerizations require only a small number of photons to generate reactive species formed by the photolysis of a photoinitiator. These reactive species subsequently catalytically consume the monomer by a chain reaction process. The field of photoinitiated chain reaction polymerizations is dominated by those in category 2 involving free radicals. Currently, the field of photoinitiated anionic polymerizations is the focus of much attention and is undergoing considerable growth. This chapter will focus specifically on the sensitization of photoinitiated cationic polymerizations as listed in category 3.

Several classes of different cationic photoinitiators have been described in the literature [CRI 78a, CRI 93]. However, only six of these have received substantial attention by both academic and industrial researchers. Formulas 1–6 below depict the general chemical structures for these photoinitiators. Among these, diaryliodonium, 2, and triarylsulfonium salts, 3, have reached commercialization, while dialkylphenacylsulfonium salts, 4, and N-alkoxypyridinium, 5, remain under active research at the present time. Diazonium salts, 1, were intensively investigated as cationic photoinitiators in the 1960s–1980s but have largely been abandoned due to the inability to stabilize their monomer solutions toward spontaneous thermally induced initiation. Ferrocenium salts ( $\eta^5$ -cyclopentadienyl(arene)iron(II) salts), 6, as cationic photoinitiators were the focus of considerable past research efforts [LOH 86, MEI 83, MEI 86], including their photosensitization [GAU 86]. The use of electron-rich donor molecules such as polynuclear aromatic hydrocarbons as photosensitizers (PSs) suggests that the mechanism of

photosensitization may involve an electron-transfer process. However, at the present time, there appears to be little activity in this area. Most likely, this is due to the fact that they have not found significant commercial applications. Accordingly, most of the focus of this chapter on photosensitization will be directed toward diaryliodonium and triarylsulfonium salts with brief mentions of the research on dialkylphenacylsulfonium salts and N-alkoxyppyridinium salts.



As shown in Diagram 2.1, there is a detailed version of the proposed mechanism for the ultraviolet (UV)-induced photolysis of diaryliodonium salt photoinitiators [DEK 90, DEK 91, DEV 87]. A very similar mechanism has been proposed for the photodecomposition of triarylsulfonium salts [DEK 87]. Briefly, the absorption of light results in the excitation of the diaryliodonium salt and the subsequent carbon–iodine bond cleavage results from decay from both the excited singlet and triplet manifolds to generate an array of species by both homolytic and heterolytic processes. These species, specifically the aryl cations and the aryliodine cation radicals, decay further by interaction with proton donor species to afford protonic acids that are indicated in the diagram as HMTX<sub>n</sub>. Consequently, the specific acid that is generated on photolysis is predetermined by the anion that is associated with the positively charged diaryliodonium cation in the starting salt. For example, the selection of a diaryliodonium salt bearing the SbF<sub>6</sub><sup>-</sup> anion will generate the exceedingly powerful protonic acid, HSbF<sub>6</sub>, on photolysis. Cationic polymerization results when the photolysis of such a diaryliodonium salt is conducted in the presence of an appropriate monomer. The direct protonation of the monomer by HSbF<sub>6</sub> results in the formation of carbon-, oxygen-, sulfur- or nitrogen-centered cationic species that are capable of undergoing the repetitive addition of monomer molecules in a chain reaction to form a polymer. Analogously, diaryliodonium salt photoinitiators with anions that give strong acids such as HBF<sub>4</sub>, HPF<sub>6</sub>, HAsF<sub>6</sub>, (C<sub>6</sub>F<sub>5</sub>)<sub>4</sub>BH and CF<sub>3</sub>SO<sub>3</sub>H may also be used to initiate the cationic polymerizations of electron-rich vinyl monomers and also to carry out the

ring-opening polymerizations of various heterocyclic compounds such as epoxides, oxetanes, tetrahydrofuran, thiiranes, 1,3-dioxolane, 1,3,5-trioxane, lactones and N-t-butylaziridine.

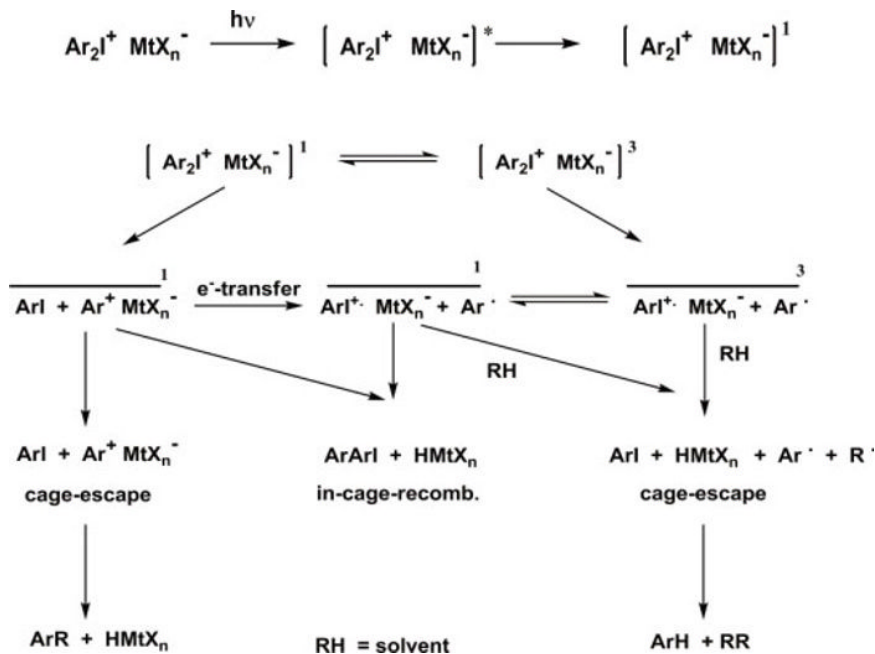


**Diagram 2.1.** Mechanism of the photolysis of diaryliodonium salts

## 2.2. Photosensitization of onium salts

Aryl onium salts within classes 2 and 3 typically absorb strongly at relatively short wavelengths (~200–300 nm) in the UV region of the spectrum and their quantum yields for photolysis in this region are quite high ( $\Phi = 0.2\text{--}0.9$ ). However, their absorption at longer UV and visible wavelengths is either very poor or non-existent. This makes these photoinitiators ill-suited for applications in which light irradiation of those wavelengths is used. Figure 2.1 shows a schematic correlation between specific practical applications of photopolymerizations and the wavelength of light needed to address them. Medical and dental applications are high in this list and the requirement for long wavelength sensitivity originates from the need to avoid the use of dermatologically damaging short wavelength

UV radiation. Similarly, stereolithography that relies on the use of lasers and graphic arts imaging that employs light-emitting diode (LED) light sources for the imagewise photopolymerization of liquid monomers are additional examples of applications where sensitivity to long wavelength UV or visible radiation is required. Finally, the potential uses of systems that allow solar irradiation to carry out polymerization reactions have many potential practical applications such as for the in-field construction of composite boats, piping and roofing panels. It is also worth noting that the narrow absorption range of aryl onium salt cationic photoinitiators 2 and 3 is also a limiting factor for their photoresponse even when broadband light sources such as mercury and xenon arc lamps are used as irradiation sources. While these sources do emit light in the short wavelength UV region, most of their emission is at long UV wavelengths and in the visible region. Consequently, these long wavelength photons are lost and unavailable for use in the photopolymerization process. Worse still, the absorption of these wavelengths by the sample can often result in its undesirable heating as well as in other detrimental photoproducts. The efficiency of the overall photopolymerization process could be markedly improved if the intrinsic absorption characteristics of the photoinitiators were broader or could be “tuned” to optimally match the emission maxima of the specific light source.

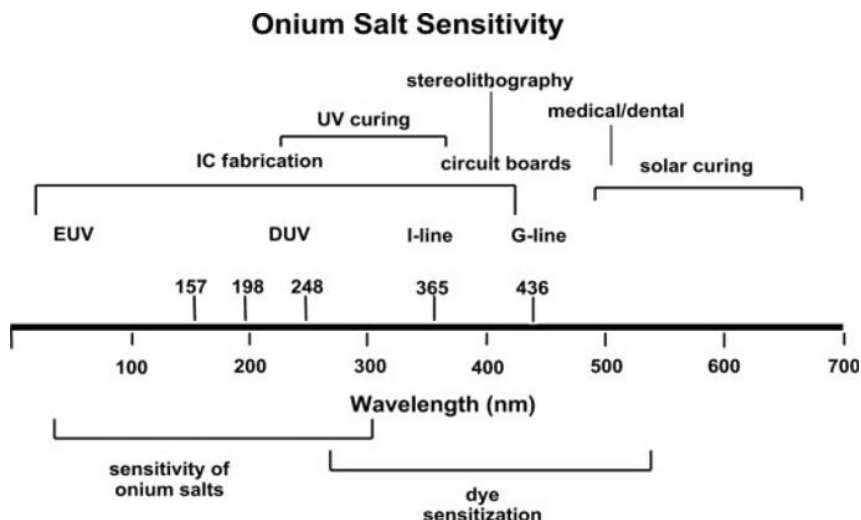
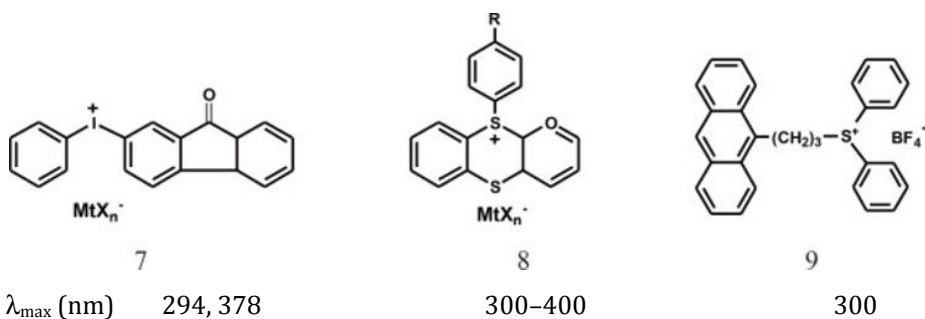


**Figure 2.1.** Relationship between the wavelength sensitivity and application for onium salt cationic photoinitiators

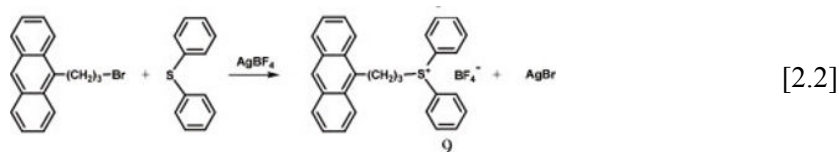
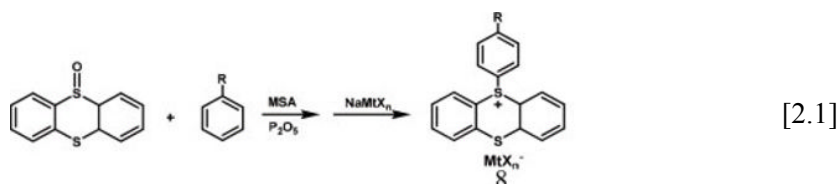
### 2.3. Synthesis of long wavelength absorbing photoinitiators

On the basis of the above-mentioned considerations, there is clearly a need for extending the range of the spectral sensitivity of onium salt cationic photoinitiators to the long wavelength UV and visible regions of the spectrum. Two major strategies for achieving this goal have been attempted. The first of these is to synthesize photoinitiators with the inclusion of chromophores that will endow them with the desired absorption characteristics. An additional concept is to prepare onium salts bearing light absorbing groups that can interact to provide an intramolecular photosensitization. While these would appear to be simple enough strategies, the available synthetic methods for onium salt photoinitiators do not always allow for a straightforward route to the preparation of the desired compounds. Often, this has needed the use of indirect, complicated and, consequently, uneconomical preparative methods.

Nevertheless, syntheses of several diaryliodonium and triarylsulfonium salts that incorporate long wavelength absorbing chromophores have been successfully accomplished and their structures 7–9 are presented below. The replacement of one of the phenyl rings in a diphenyliodonium salt with a fluorenone moiety as shown in structure 7 results in the generation of a diaryliodonium salt with two absorption bands at 294 and 378 nm [FOU 94, HAR 01]. Both the absorption and the fluorescence spectra of 7 closely resemble those of fluorenone. Unfortunately, despite the long wavelength absorption of 7, photopolymerization studies showed that it was not more efficient as a photoinitiator than simple diphenyliodonium salts that do not possess the fluorenone chromophore.



The synthesis of 5-arylthianthrenium salts, **8**, [CRI 02a, CRI 04] can be carried out by the condensation of thianthrene-S-oxide with various aromatic compounds bearing electron-donating substituents, R, as depicted in equation [2.1]. A mixture of methanesulfonic acid and phosphorous pentoxide serves as an acid catalyst and dehydrating agent for this reaction. Replacement of the methanesulfonate anion by a metathetical reaction with NaMTX<sub>n</sub> affords the desired active photoinitiator, **8**. Depending on the specific R substituent, 5-arylthianthrenium photoinitiators have UV absorption maxima in the range of 300–400 nm.



The synthesis of a sulfonium salt bearing a photosensitizing anthracene moiety in the same molecule was described by Pappas *et al.* [PAP 03]. Details of the synthesis of **9** are presented in equation [2.2]. The objective of this work was to improve the efficiency of electron-transfer photosensitization by an intramolecular interaction by incorporating the anthracene within the same sulfonium salt molecule. Indeed, **9** bearing the tetrafluoroborate anion was observed to show excellent activity in the 300 nm region due to the presence of the strongly absorbing anthracene chromophore.

#### 2.4. Photosensitization of onium salt cationic photoinitiators

Due to the complications surrounding the synthesis of long wavelength chromophore-bearing onium salt photoinitiators, alternative strategies for spectral sensitivity broadening were sought and attention was turned to the possibility of the use of photosensitization. Photosensitization is an attractive strategy for spectral broadening since it makes use of simple, easy to prepare onium salt photoinitiators and simply adds a second PS molecule.

There is much precedent in the literature for this approach and there are several methods of conducting the photosensitization of a photolysis reaction. In this chapter, the term “photosensitization” will be applied to any method by which a light-absorbing compound induces the onium salt decomposition resulting in the liberation of a strong Brønsted acid that is capable of initiating a cationic polymerization.

The first method involves “classical” or energy-transfer photosensitization in which the PS molecule is the primary light absorbing species that, on excitation, transfers the energy to a target molecule causing it to become excited and to undergo photolytic decomposition [LEE 69]. The prime requirement for classical energy-transfer photosensitization is that the energy of the excited state of the PS must be greater than that of the target molecule so that the overall transfer process is energetically downhill. In this type of photosensitization, the PS functions simply as an energy carrier and is recovered chemically unchanged after the photosensitization process. There are few documented examples of the application of classical energy-transfer photosensitization to onium salt photolysis [DAV 82].

A second photochemical process called “electron-transfer photosensitization” is, in reality, a photoinduced redox reaction [EBE 87, PAP 84a, PAP 84b] and this method of photosensitization has been much more successful for the extension of the spectral sensitivity of onium salt cationic photoinitiators into the long wavelength UV and visible spectral regions. Electron-transfer photosensitization is a well-understood process and a general mechanism for this process as exemplified for diaryliodonium salts is shown in Diagram 2.2.

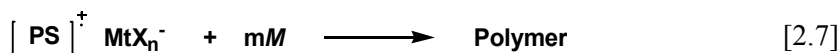
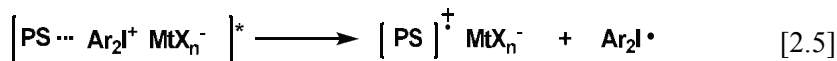


**Diagram 2.2.** Mechanism for the electron-transfer photosensitization of diaryliodonium salts

The first step of the mechanism involves the absorption of light by the PS and this step is followed by the formation of an excited state complex (exciplex). Then, the decay of the exciplex takes place with the transfer of an electron from the excited PS to the diaryliodonium salt. As a result, the PS molecule is oxidized to give the cation-radical,  $PS^+$  while at the same time, the onium salt is reduced and an unstable iodine-centered radical,  $Ar-I-Ar$ , is produced. Back electron transfer is avoided by the rapid, irreversible decomposition of this latter diaryliodine free radical into fragments that subsequently undergo further reactions in the system. Ultimately, the cation radical species,  $PS^+$ , is responsible for initiating the cationic polymerization of a monomer,  $M$ . This occurs via the direct attack of the cation-radical on the monomer as well as by secondary reactions with proton donor species that generate the protonic acid,  $HMtX_n$ . It is worth noting that during electron-transfer photosensitization, the PS is chemically reactive and is consumed during the irradiation process. This can easily be visually observed during an electron-transfer photosensitization either by the formation of a strongly colored cation-radical species or by the shift in color as the PS cation-radical undergoes further reaction during photopolymerization. In some cases, this is advantageous since the PS is “bleached”, allowing light to penetrate deeper into the sample. In other instances, further reaction of the generated cation radicals undergoes reactions that lead to the formation of even more highly absorbing species than the starting PS. This can result in the opposite effect.

A particularly graphic example of electron-transfer photosensitization is the interaction of diphenyliodonium salts with perylene. Exposure of a dichloromethane solution of a mixture of these two compounds to UV light for 2 s results in the formation of the intensely blue-colored and relatively stable perylene cation-radical. The blue color remains in solution in air for a considerable time until it slowly fades. When this photolysis reaction is conducted in the presence of a cationically polymerizable monomer, the blue color of the perylene cation-radical is very transient.

The fact that onium salts 1–5 undergo photosensitization via an electron-transfer mechanism is not surprising. The positively charged iodine, sulfur

and nitrogen atoms in these compounds are all in high oxidation states. For example, diaryliodonium salts, 2, belong to the general class of hypervalent iodine compounds and can be considered oxidants [BAN 66]. Similar considerations apply to the diazonium, 1, sulfonium, 3 and 4, and N-alkoxypyridinium salts, 5. Typical complementary electron-transfer PSs are electron-rich compounds that are reducing agents in their excited states. The criteria for electron-transfer photosensitization have been expressed mathematically in the Rehm–Weller equation shown below [LEE 69]:

$$\Delta G = (E_{\text{sens}}^{\text{ox}} - E_{\text{onium}}^{\text{red}}) - E^* \quad [2.8]$$

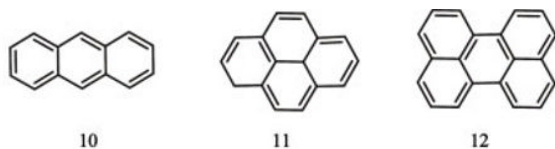
A negative free energy for electron-transfer photosensitization is obtained when the difference between the oxidation potential of the PS,  $E_{\text{sens}}^{\text{ox}}$ , and the reduction potential of the onium salt,  $E_{\text{onium}}^{\text{red}}$ , is smaller than the energy of the excited state of the PS,  $E^*$ . The magnitudes of the  $E_{\text{sens}}^{\text{ox}}$  and  $E^*$  parameters are known for many common PSs and the  $E_{\text{onium}}^{\text{red}}$  values can be obtained by polarography. The respective approximate  $E_{\text{onium}}^{\text{red}}$  values for the onium salts 1–5 are: diazonium salts  $-1.5$  kcal/mol [ELO 69], diaryliodonium salts  $-5$  kcal/mol, triphenylsulfonium salts  $-28$  kcal/mol [CRI 85], dialkylphenacylsulfonium salts  $-14.5$  kcal/mol [SAV 67] and N-alkoxypyridinium salts  $-16$  kcal/mol [YAG 93]. This is also the order of decreasing ease of electron-transfer photosensitization among onium salts 1–5. The Rehm–Weller equation allows the prediction when the electron-transfer photosensitization of a given onium salt–photoinitiator combination can occur with the proviso that the magnitude of the  $\Delta G$  values should be at least  $-10$  kcal/mol. Due to the differences in the  $\Delta G$  values, some PSs work with certain onium salts and not others. For example, thioxanthenes are good PSs for diaryliodonium salts but generally not for triarylsulfonium salts. The only other consideration for a PS to be used with onium salts is that it may not contain basic groups that inhibit or terminate cationic vinyl or ring-opening polymerizations. Using the Rehm–Weller equation, it is also possible to calculate the longest wavelength of light capable of supplying sufficient excitation energy to electron-transfer photosensitize a given onium salt. For example, for diaryliodonium salts, it is approximately 475 nm.



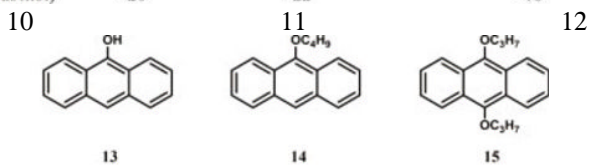
## 2.6. Polynuclear aromatic hydrocarbons and their derivatives

At very nearly the same time that diaryliodonium salts were discovered to be efficient cationic photoinitiators, triarylsulfonium salts were also shown to possess excellent characteristics as photoinitiators. Accordingly, an effort was launched to determine whether it was possible to photosensitize the photolysis of this new class of photoinitiators. As a result of a screening process, electron-rich polynuclear aromatic hydrocarbons were observed first to be excellent electron-transfer PSs for triarylsulfonium salts, and then also for diaryliodonium salts [CRI 79]. Listed below are the absorption maxima and the  $\Delta G$  values for photoexcited electron-transfer for anthracene, 10, pyrene, 11, and perylene, 12, with diaryliodonium and triarylsulfonium salts. The  $\Delta G$  values were calculated from data appearing in two literature sources [MUR 73, EHL 06]. It is interesting to note that in all cases with these three, four and five ring polynuclear aromatic hydrocarbons, the  $\Delta G$  values are quite large and negative reflecting a strong driving force for excited state electron transfer. The experimental observation that electron-transfer photosensitization with these three compounds and both diaryliodonium and triarylsulfonium salts is quite efficient appears to confirm this conclusion. Additional members of this class of compounds, including chrysene, coronene, benzanthracene, rubrene, dibenzanthracene and even pitch derived from coal tar or petroleum residues, were also found to provide good photosensitization characteristics. However, many of these compounds are toxic and even carcinogenic. In addition, unsubstituted polynuclear aromatic hydrocarbons including anthracene, pyrene and perylene have limited solubility in most common monomers and their solubility appears to decrease with an increase in the number of fused aromatic rings. For these reasons, work with the parent unsubstituted polynuclear aromatic hydrocarbons was not pursued further. Instead, several alkyl- and hydroxyl-substituted anthracene derivatives with enhanced solubility characteristics were examined for use as PSs. Work in this laboratory focused on the use of anthrone, 13, 9-n-butoxyanthracene, 14, and 2-ethyl-9,10-dimethoxyanthracene, 17 [CRI 03a, CRI 03b]. 9,10-Di-n-propoxyanthracene, 15, and 9,10-di-n-butoxyanthracene, 16, are commercially available for use as PSs from the Kawasaki-Kasei Company. The UV absorption spectra of all the anthracene derivatives are very similar to anthracene, although slightly shifted to longer wavelengths. All the anthracene derivatives were more efficient PSs than anthracene for diaryliodonium, triarylsulfonium and also dialkylphenacylsulfonium salt

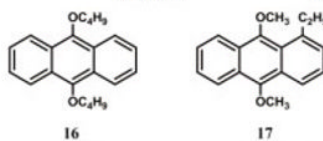
cationic photoinitiators. The best photosensitization effects were realized using the 9,10-dialkoxysubstituted anthracene derivatives 15, 16 and 17. Toba *et al.* have extended this work using the same anthracene PSs to eight onium tetrakis(pentafluorophenyl)borates as photoinitiators [TOB 99]. This same investigator [TOB 00] has reported the use of anthracene-photosensitized diaryliodonium salts in the polymerizations of vinyl ethers. Likewise, Scranton *et al.* [NEL 94, NEL 95] used time-resolved fluorescence spectroscopy to study the 9,10-dimethylantracene-photosensitized diaryliodonium salt cationic photopolymerization of divinyl ether monomers. Another approach to making anthracene PSs compatible in photopolymerizable systems is to incorporate the PS into a monomer structure [CRI 05a]. An example of an epoxy monomer containing an anthracene photosensitizing group is shown in structure 18 below:



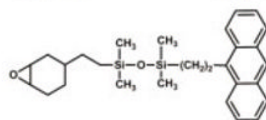
$\lambda_{\text{max}}$ (nm)	220, 251, 356, 375	271, 294, 318, 334	390, 411, 439
$\Delta G_{\text{I}^-}$ (kcal/mol)	-40	-42	-38
$\Delta G_{\text{S}^+}$ (kcal/mol)	-20	-22	-18



$\lambda_{\text{max}}$ (nm)	308, 367	368, 388	381, 403
-----------------------------	----------	----------	----------



$\lambda_{\text{max}}$ (nm)	381, 403	380, 401
-----------------------------	----------	----------



18

Pyrene, 11, is an inexpensive and readily available aromatic hydrocarbon that displays a relatively low order of toxicity. Pyrene was easily derivatized by the pathways shown in Diagram 2.3 to give three interesting PSs, 19–21 [CRI 02a].

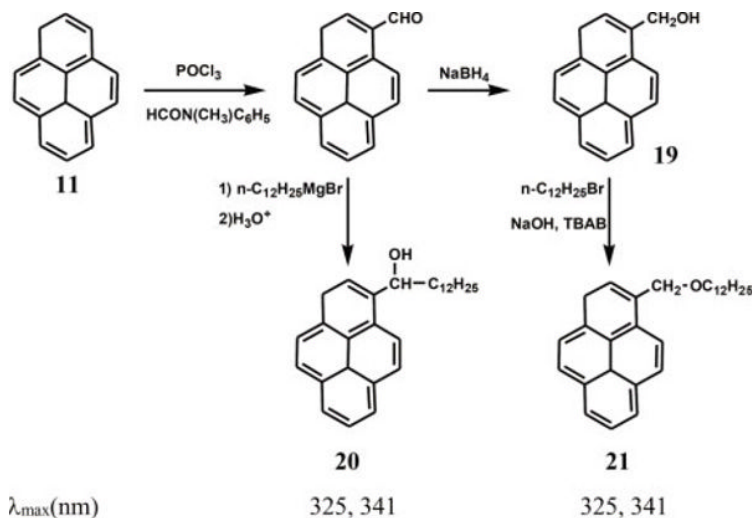
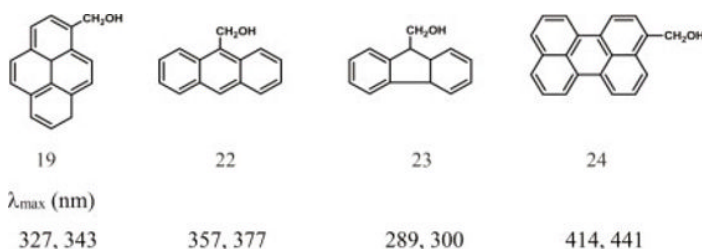


**Diagram 2.3.** Synthesis of modified pyrene photosensitizers

1-Pyrenemethanol, 19, is readily soluble in various epoxide monomers and has the advantage that it undergoes acid catalyzed and radical reactions that covalently bind it into the polymer matrix as photopolymerization proceeds. Similar considerations apply to compound 20 which, in addition to the reactive benzylic hydroxyl group, has a long alkyl chain that markedly improves solubility in a variety of vinyl and heterocyclic monomers. Like the above anthracene compounds, pyrene and its derivatives 19–21 are active as PSs for diaryliodonium, triarylsulfonium and also dialkylphenacylsulfonium salts.

The strategy of functionalizing polynuclear aromatic hydrocarbons by appending a hydroxymethyl group as described above for pyrene was also applied to a number of additional polynuclear aromatic compounds [HUA 02]. The structures of some of these compounds (22–24) along with the longest wavelengths of their absorption maxima are depicted below. On photolysis in the presence of an onium salt photoacid generator and a

monomer, they not only undergo acid-catalyzed additions to epoxy monomers, but also participate in free radical reactions that in the case of diaryliodonium salts result in the assisted decomposition of the onium salt [CRI 02b].



As mentioned previously, the  $E_{\text{red}}^{1/2}$  value determined by polarography for N-alkoxy pyridinium salts is of the order of  $-16$  kcal/mol. This indicates that N-alkoxy pyridinium salts would be expected to undergo facile reduction by photoexcited electron-rich compounds. Indeed, electron-transfer photosensitization by typical excited state electron donors such as anthracene, perylene, thioxanthene [YAG 93] and trimethoxybenzene [YAG 93] has been reported.

Diagram 2.4 depicts the proposed mechanism of the electron-transfer photosensitization of a typical alkoxy pyridinium photoinitiator, 25, by excited anthracene [YAG 94]. As shown in equation [2.11], the alkoxy pyridine radical, 26, undergoes further irreversible decomposition to give pyridine and an alkoxy radical.

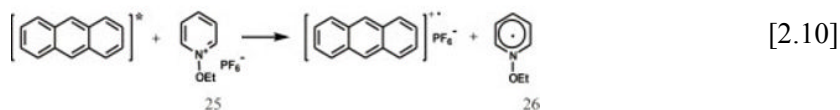
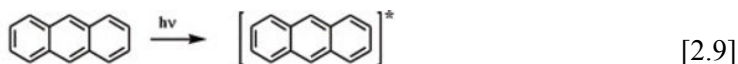
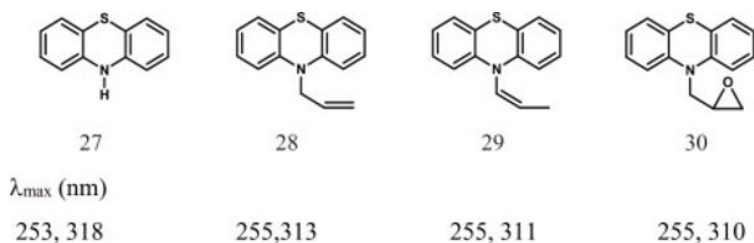


**Diagram 2.4.** Photosensitization of N-ethoxy pyridinium hexafluorophosphate by anthracene

## 2.7. Phenothiazine photosensitizers

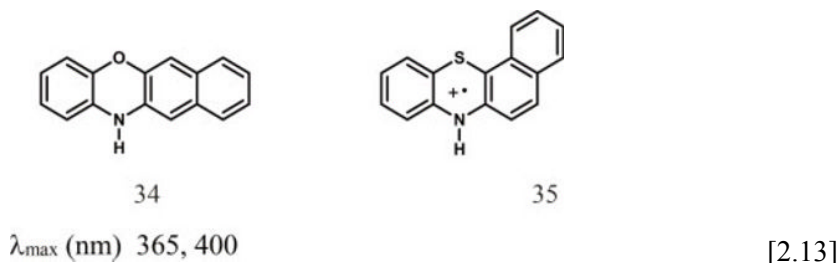
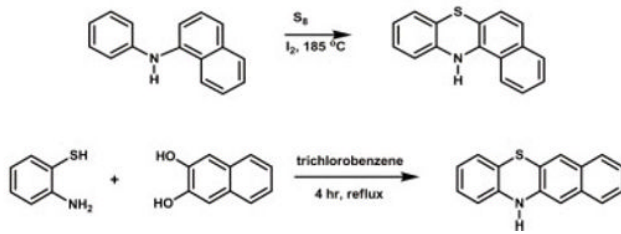
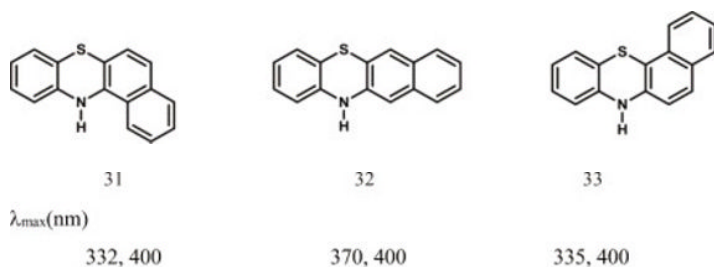
10-Phenothiazine, 27, and a wide variety of other phenothiazine derivatives (28–30) with substitution on the nitrogen and/or the aromatic rings are excellent electron-transfer PSs for diaryliodonium salt, dialkylphenacylsulfonium salt and triarylsulfonium salt photoinitiators [GOM 01, GOM 02]. Phenothiazine compounds are readily synthesized by simple, straightforward methods that allow them to be tailored for both wavelength sensitivity and for solubility purposes. Phenothiazines have low oxidation potentials and are therefore good reducing agents both in their ground and excited states. The calculated  $\Delta G_{T^+}$  for 10-phenothiazine photosensitization of diaryliodonium salts is  $-46$  kcal/mol and the  $\Delta G_{S^+}$  values for triarylsulfonium salts and dialkylphenacylsulfonium salts are, respectively,  $-23$  and  $-26.3$  kcal/mol. A mechanistic study of the phenothiazine-photosensitized polymerization of tetrahydrofuran by triphenylsulfonium hexafluoroarsenate was performed by Rodrigues and Neumann [ROD 01] that confirmed the proposed electron-transfer mechanism.



The phenothiazines 27–30 shown above provide a maximum wavelength sensitivity broadening to approximately 315 nm. PS compounds 29 and 30 bear cationically polymerizable functional groups. Consequently, these PS monomers can be expected to undergo copolymerization with conventional vinyl ether and epoxide monomers. Alternatively, they can be subjected to polymerization and the resulting polymers bearing pendant phenothiazine groups used as PSs. Both approaches have been explored and result in successful photosensitization [GOM 02].

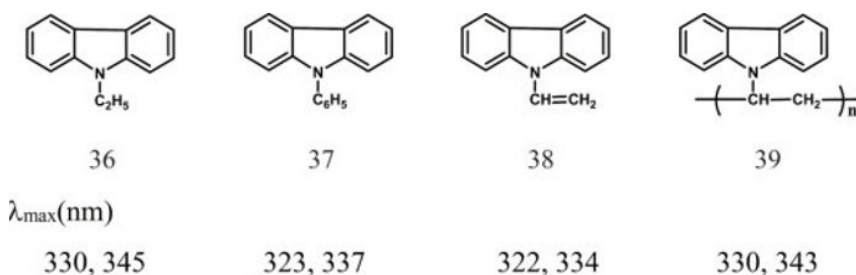
A further spectral sensitivity extension to the 400 nm region was achieved by extending the conjugation in phenothiazine systems through the addition of a fused aromatic ring to the parent phenothiazine ring system

[CRI 08]. All three isomeric benzophenothiazines, 31, 32 and 33, were prepared and characterized. Shown in equations [2.12] and [2.13] are the simple, one-step methods that were used to give the desired benzophenothiazines in good yields. In a similar manner, 12H-benzo[b]phenoxazine, 34, was also prepared using a variation of the route shown in equation [2.13]. Using a 400 nm optical cutoff filter interposed between a medium pressure mercury arc lamp and the sample, the benzophenothiazine and benzo[b]phenoxazine photosensitized polymerizations of several cationically polymerizable monomers were successfully carried out with diaryliodonium, dialkylphenacylsulfonium and triarylsulfonium salt photoinitiators. It was interesting to note that when the irradiation of the above onium salt photoinitiators was conducted at 400 nm in dichloromethane in the presence of the benzophenothiazine PSs, deep blue, red and purple benzophenothiazinium cation-radicals, e.g. 35, were formed.



## 2.8. Carbazole photosensitizers

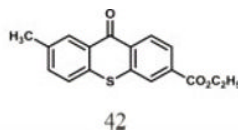
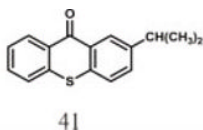
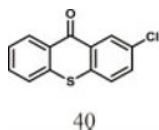
The nitrogen atom of a pyrrole ring is not basic. The reason that is generally given is that protonation of the nitrogen atom results in the loss of the aromatic character of the ring [WAD 03]. Further reduction in the basicity of a pyrrole can be achieved by fusing aromatic groups onto the ring. Consequently, indole and carbazole are even less basic than pyrrole. It was observed that N-alkyl- and N-aryl-substituted carbazoles are quite excellent PSs for onium salt photolysis [CHE 00, HUA 00, HUA 03].



It is particularly interesting to use the N-vinylcarbazole, 38, as an electron-transfer PS. This compound readily improves the photopolymerization response of diaryliodonium, triarylsulfonium and dialkylphenacylsulfonium salts to UV irradiation in the 300 nm region as well as the overall response to the broadband UV emission of a mercury arc lamp. In addition, it is worth noting that 38 is well known to be a very reactive monomer toward cationic polymerization. Thus, under the usual conditions of photoinitiated cationic polymerization, 38 undergoes polymerization to give poly(N-vinylcarbazole), 39. Moreover, further experiments showed that the resulting polymer 39 is itself a good PS for onium salts. Since 39 is a readily available commercially produced monomer, it can be used as a non-toxic, non-volatile PS for various onium-salt-induced cationic polymerizations. In addition, it has been shown that the free radical copolymerization of 38 with other vinyl monomers such as diethyl fumarate gives 1:1 alternating copolymers that are also useful as PSs [CRI 01].

## 2.9. Thioxanthone photosensitizers

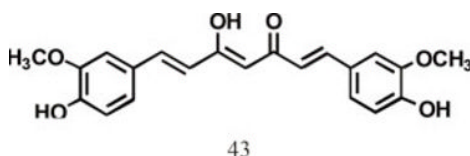
Thioxanthenes are among the most widely employed compounds used to achieve long wavelength sensitivity for photoinitiated free radical polymerizations. Thioxanthenes initiate free radical photopolymerization by a bimolecular mechanism in which the photoexcited thioxanthone triplet abstracts a proton from a proton donor molecule to generate a pair of radicals. It was discovered [FOU 89] that thioxanthenes are also active electron-transfer PSs for diaryliodonium salts. Using the Rehm–Weller equation, a  $\Delta G$  value of  $-22$  kcal/mol has been calculated for the electron-transfer from excited thioxanthone to a diphenyliodonium salt. Other aromatic ketones, benzophenone and acetophenone give  $\Delta G$  values of  $-9$  and  $-7$  kcal/mol, respectively, and consequently, they are not useful as PSs for diaryliodonium salts. Thioxanthenes do not appear to be efficient electron-transfer PSs for triarylsulfonium salts due to the considerably higher reduction potentials of these onium salts as compared to diaryliodonium salts. Excited state quenching studies by Fouassier *et al.* [FOU 94, MAN 92] appear to confirm the electron-transfer mechanism of photosensitization with a variety of different substituted thioxanthone compounds. Since thioxanthenes are widely used in free radical photopolymerizations, a number of these compounds are readily available from commercial sources. For this reason, the use of thioxanthenes as photoinitiators in onium salt photoinitiated cationic polymerizations is very attractive and widespread. The structures of three representative thioxanthone compounds, 40–42, studied for this purpose are shown below. The main spectral region in which these compounds are useful PSs is from 254 to 313 nm. However, photosensitization studies of onium salts conducted at 355 nm with 2-chlorothioxanthone, 40, showed that a band at 430 nm corresponding to the 2-chlorothioxanthone radical-cation was formed. Cho and Hong [CHO 05] have carried out detailed cationic UV photocuring studies with 2,4-diethylthioxanthone employing the widely used 2,3-epoxycyclohexylmethyl 3',4'-epoxycyclohexane carboxylate as a difunctional monomer.



The use of isopropylthioxanthone as a PS for two-photon sensitized cationic polymerizations was described by Boiko *et al.* [BOI 01]. The Yagci research group [TAS 08] has also been active in this area and has published the results of their study of the use of benzophenone and benzodioxinone as two-photon sensitizers for the diaryliodonium salt polymerization of cyclohexene oxide. These polymerizations are of growing interest since they can be used to spatially define three-dimensional images for the production of solid polymeric objects.

## 2.10. Curcumin as a photosensitizer

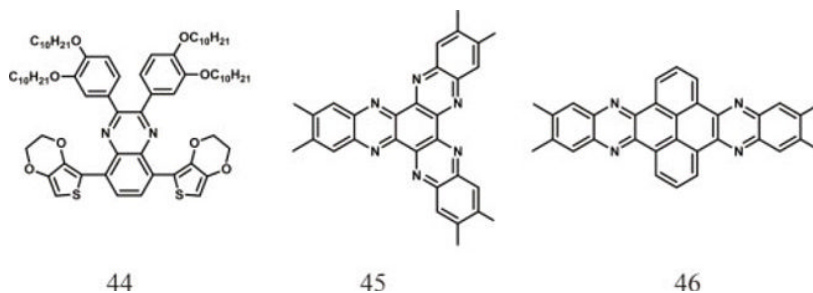
The naturally occurring bright yellow–orange dye, curcumin, 43, is a major constituent of the common spice, turmeric [CRI 05b]. In addition to its use as a food flavoring and coloring agent, curcumin is also employed as a medicinal agent and as a sunscreen. It is also readily available, low cost and is highly soluble in a wide assortment of polar and non-polar monomers, functional oligomers and polymers. Curcumin is a particularly interesting and useful PS for diaryliodonium salts in the visible region of the spectrum. As a result of the extended conjugation present in this molecule, curcumin has a strong absorption band at 427 nm ( $\epsilon = 55,000$ ) with a tail absorption that extends to at least 540 nm.



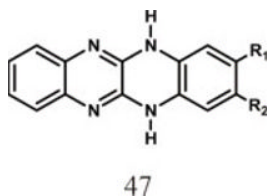
On irradiation in the presence of an epoxy monomer and a diaryliodonium salt photoinitiator, it has been observed that the initial bright yellow color of curcumin shifts to deep orange. On continued irradiation or simply standing in ambient light, the photopolymer is bleached resulting ultimately in a pale-yellow-colored cross-linked epoxy polymer.

## 2.11. Quinoxaline photosensitizers

Recently, there have been two reports of the development of conjugated aromatic quinoxalines (phenazines) as electron-transfer PSs for diaryliodonium salt cationic photoinitiators. The first of these from the Toppare group [BUL 10] describes the use of the complex substituted and highly electron-rich quinoxaline, 44, with absorption bands at 327 and 420 nm as a PS for the polymerization of epoxide monomers. A similar study was conducted by Fouassier and Lalevée *et al.* [TEH 14] with highly conjugated quinoxaline compounds 45 and 46 as PSs for diphenyliodonium hexafluorophosphate. The authors state that these two compounds show particularly high performance in the 350–425 nm range that is convenient for use with LED light sources. Presumably, the methyl groups substituted about the periphery of compounds 45 and 46 enhance their solubility in monomers. The use of these photosensitized systems with two different epoxide monomers was demonstrated.

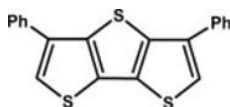


Related to these PSs are the fluoflavin dyes, 47, reported by Nerewska *et al.* [NAR 10]. These authors have shown that they can be used to photosensitize both the diaryliodonium and triarylsulfonium salt photopolymerization of cyclohexene oxide at wavelengths in the region of 415 nm. The R<sub>1</sub> and R<sub>2</sub> groups in 47 are hydrogen, methyl, bromine or chlorine.



## 2.12. Miscellaneous electron-transfer photosensitizers

A wide assortment of additional electron-transfer PSs for diaryliodonium salts have been described in the journal and patent literature. These include: ketocoumarins [FOU 88], 9,10-phenanthraquinone [BAU 86], Mannich bases [DE 88b], 1,3-indanediones [TEH 13], benzoquinonylsulfanyl derivatives [SUG 03], acridinediones [SEL 01] and dimethylaminobenzylidene derivatives [ICH 87]. In addition, the use of dyes such as eosine and Rhodamine [DE 88a, DE 89] have been employed to provide photosensitization in the visible region of the spectrum. A particularly interesting system devised by Yagci *et al.* [AYD 08] is the dithienothiophene, 48, used with diphenyliodonium hexafluorophosphate to carry out the cationic photopolymerizations of cyclohexene oxide, 3,4-epoxycyclohexylmethyl 3',4'-epoxycyclohexane carboxylate, N-vinyl carbazole, n-butyl vinyl ether and styrene. These investigators have further applied this system to the preparation of metallic silver-filled epoxy nanocomposites [YAG 11].



48

## 2.13. Free-radical-promoted photosensitization

An indirect method by which spectral broadening of the sensitivity of diaryliodonium salts can be achieved is by a so-called “free-radical-promoted photosensitization”. It has already been noted that onium salts are oxidants. In particular, diaryliodonium salts possess low reduction potentials that allow their facile reaction with photogenerated oxidizable free radicals. Several research groups [LED 79, YAG 88, KLE 85, CRI 98, MOW 00] have explored this area using easily oxidized free radicals generated by Norrish type I photoreactions. For example, unimolecular free radical photoinitiators such as 2,2-dimethoxy-2-phenylacetophenone undergo efficient photolysis by an  $\alpha$ -cleavage reaction as shown in equation [2.14] of Diagram 2.5 to afford the benzoyl, 49, and dimethoxyphenylmethyl, 50, radicals. The reduction of a diaryliodonium salt (equation [2.15]) by 50 generates the dimethoxyphenylmethyl carbocation 51. Thereafter, 51

initiates cationic ring-opening polymerization as shown in equation [2.16] by direct electrophilic attack on the heterocyclic monomer. The diphenyliodonium free radical, 52, irreversibly fragments to give a phenyl radical and iodobenzene (equation [2.17]). By the selection of a free radical photoinitiator with the appropriate absorption characteristics, it is possible to conduct the polymerization of heterocyclic monomers using long wavelength UV and even visible light.

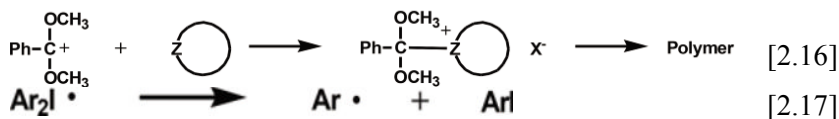
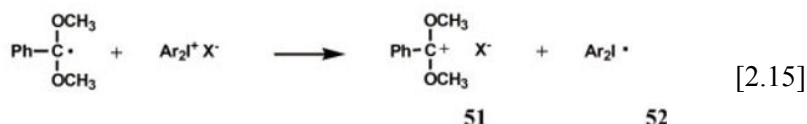
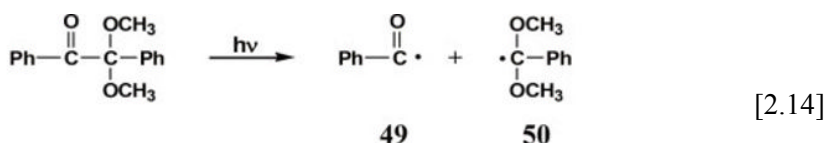
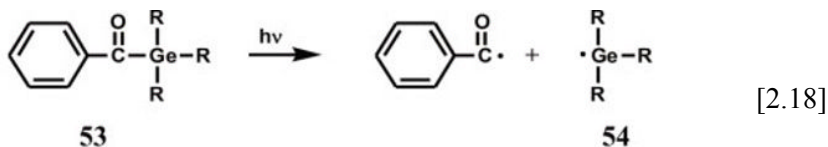


**Diagram 2.5.** Proposed mechanism for the free-radical-promoted photosensitization of diaryliodonium salts

Recently, Yagci *et al.* [DUR 08] have described several interesting and novel free-radical-promoted cationic photoinitiator systems based on the same general principles outlined above. One of the most interesting shown in Diagram 2.6 involves the use of acylgermaines, 53, as photochemical sources of free radicals. These compounds conveniently absorb in the 350–420 nm region and undergo an  $\alpha$ -cleavage (equation [2.18]) to form the benzoyl and germyl radicals, 54. In subsequent steps, 54 is oxidized by the diaryliodonium salt to form the germanium-centered cation, 55 (equation [2.19]). This latter species initiates the polymerization of the monomer (cyclohexene oxide) by a direct electrophilic attack similar to that shown in equation [2.16]. Another class of free radical photoinitiators that the Yagci

group has employed together with diaryliodonium salts for free-radical-promoted cationic polymerization is bisacyl phosphine oxides as, for example, 56 [DUR 03]. In this case, it was proposed that a photogenerated phosphorous-centered free radical reduces the diaryliodonium salt.



(18)

R = alkyl

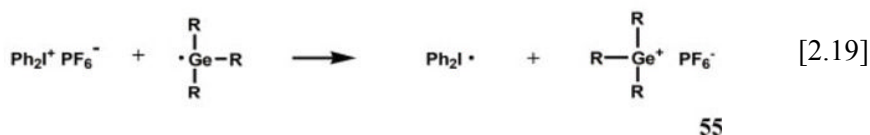
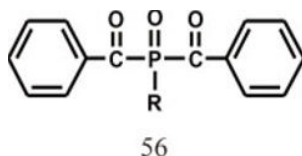
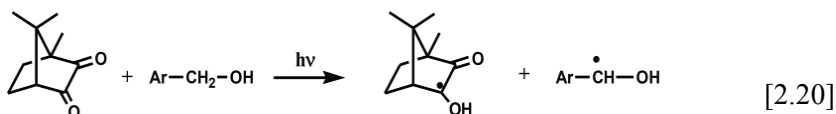


**Diagram 2.6.** Free-radical-promoted photosensitization of diaryliodonium salts



An example of a bimolecular photoinitiator that generates free radicals by a hydrogen abstraction process is the combination of camphorquinone with a benzyl alcohol (equation [2.20]) [CRI 08]. The carbon-centered free radical, 57, is capable of reducing a diaryliodonium salt in a similar manner to that shown previously in Diagram 2.5.



Recently, Lalevée *et al.* [LAL 07, LAL 08a] have reported analogous systems involving the use of aromatic ketones such as benzophenone, thioxanthone, camphorquinone or eosine together with a silane or germane as a hydrogen donor [LAL 08b, LAL 08c]. For example, as depicted in equation [2.21] of Diagram 2.7, the photolysis of benzophenone in the presence of tris(trimethylsiloxy)silane generates the silyl radical 58. This latter species is oxidized by a diaryliodonium salt (equation [2.22]) to yield the silylium cation 59 that is able to directly or indirectly initiate cationic ring-opening polymerizations. The wavelength sensitivity of this system is determined by choice of the specific aryl ketone. A study of the ring-opening polymerizations of epoxide monomers was conducted using these silane-mediated initiator systems.

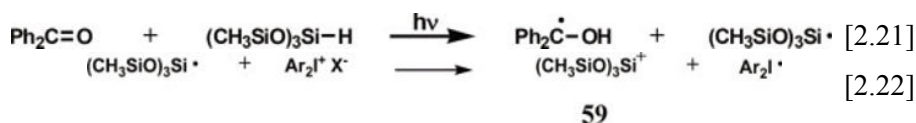


**Diagram 2.7.** Radical-promoted cationic photopolymerization by silanes

The general principle of generating oxidizable free radicals using long wavelength irradiation and using them to decompose diaryliodonium salts by a redox process has also been exploited by Bi and Neckers [BI 94]. These workers used visible light irradiation to generate free radicals by hydrogen abstraction from non-basic aromatic amines bearing benzylic protons by a variety of xanthene dyes. The carbon-centered free radicals thus produced are subsequently oxidized by the diaryliodonium salt to generate carbocations that were shown to initiate the cationic ring-opening polymerizations of epoxides. A similar report of the use of related systems was published by Ichimura *et al.* [ICH 87] and used for photoresist applications.

An interesting approach for the use of allyl sulfonium salts as photoinitiators for cationic ring-opening polymerizations was published by Yagci *et al.* [DEN 95] incorporating the elements of a free-radical-promoted cationic system together with a photoinduced free radical

addition-fragmentation system similar to radical addition-fragmentation transfer (RAFT) chemistry. Since allyl sulfonium salts absorb only at short wavelengths in the UV, there is a general need to photosensitize these compounds. Subsequently, these workers have shown that a variety of compounds are capable of performing the desired photosensitization. Among these are aromatic ketones such as benzophenone and thioxanthone; polynuclear aromatic compounds such as anthracene and perylene and conjugated heterocyclic compounds like phenothiazine. On the basis of free energy calculations using the Rehm–Weller equation, an electron-transfer mechanism analogous to that depicted in Diagram 2.2 has been proposed to account for the photosensitization and is shown in Diagram 2.8 [DEN 96]. Irradiation of the PS results in its excitation (equation [2.23]) and this is followed by electron transfer to the allylic sulfonium salt 60 to yield the cation radical 61 and a sulfur-centered radical 62 (equation [2.24]). Subsequent interaction of the PS radical-cation, 61, either directly with the monomer or indirectly by hydrogen abstraction processes, results in the initiation of the cationic polymerization of cyclohexene oxide, n-butyl vinyl ether or N-vinylcarbazole.

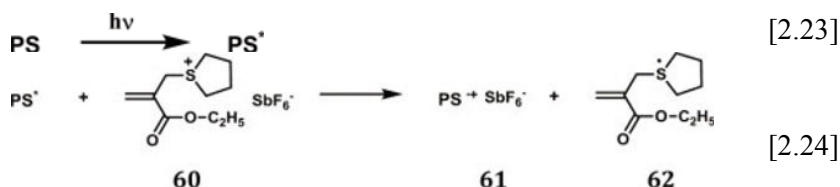


**Diagram 2.8.** Proposed mechanism for the electron-transfer photosensitization of an allyl sulfonium salt

## 2.14. Conclusions

Through the use of photosensitization, the spectral response of onium salt photoinitiators has been remarkably broadened, allowing cationic photopolymerizations to be carried out using wavelengths throughout the entire UV region and well into the visible range as well. This has made it possible to address a wide range of current and emerging applications with this technology that employ light sources that emit in the long wavelength region of the electromagnetic spectrum. In addition, the use of PSs affords a practical means of improving the response in many current applications that

employ broadband UV and UV/visible light by providing a means to capture a greater portion of the available emission from the light source. Thus, PSs cannot only improve the photoresponse of a UV cure system, they also offer a number of attractive trade-offs. For example, higher photosensitivity means higher productivity with greater energy savings. Alternatively, cost savings can be realized through a reduction in the photoinitiator concentration and the use of lower priced and less reactive monomers.

## 2.15. Bibliography

- [AYD 08] AYDOGAN B., GUNDOGAN A.S., OZTURK T. *et al.*, “A dithienothiophene derivative as a long-wavelength photosensitizer for onium salt photoinitiated cationic polymerization”, *Macromolecules*, vol. 41, no. 10, pp. 3468–3471, 2008.
- [BAN 66] BANKS D.F., “Organic polyvalent iodine compounds”, *Chemical Reviews*, vol. 66, no. 33, pp. 243–266, 1966.
- [BAU 86] BAUMANN H., OERTEL U., TIMPE H.-J., “Lichtinitiierte polymer- und polymerisationsreaktionen. 28. photopolymerisation mit der Initiatorkombination 9,10-phenanthrenchinon-aryloniumverbindungen”, *European Polymer Journal*, vol. 22, no. 4, pp. 313–318, 1986.
- [BI 94] BI Y., NECKERS D.C., “A visible light initiating system for free radical promoted cationic polymerization”, *Macromolecules*, vol. 27, no. 14, pp. 3683–3693, 1994.
- [BOI 01] BOIKO Y., COSTA J.M., WANG M. *et al.*, “Cationic two-photon induced polymerization with high dynamic range”, *Optics Express*, vol. 8, no. 10, pp. 571–584, 2001.
- [BUL 10] BULUT U., GUNBAS G.E., TOPPARE L., “A quinoxaline derivative as a long wavelength photosensitizer for diaryliodonium salts”, *Journal of Polymer Science; Part A: Polymer Chemistry*, vol. 48, no. 1, pp. 209–213, 2010.
- [CHE 00] CHEN Y., YAMMSMURA, T., IGARASHI K., “Photosensitization of carbazole derivatives in cationic polymerization with a novel sensitivity to near-UV light”, *Journal of Polymer Science; Part A: Polymer Chemistry*, vol. 38, no. 1, pp. 90–100, 2000.

- [CHO 05] CHO J.-D., HONG J.-W., "Photocuring kinetics of UV-initiated cationic polymerization of a cycloaliphatic diepoxide system photosensitized by thioxanthone", *European Polymer Journal*, vol. 41, no. 2, pp. 367–374, 2005.
- [CRI 78a] CRIVELLO J.V., "Photoinitiated cationic polymerization", in PAPPAS S.P. (ed.), *UV Curing: Science and Technology*, Technology Marketing Corp., Stamford, CT, pp. 23–76, 1978.
- [CRI 78b] CRIVELLO J.V., LAM J.H.W., "Dye sensitized photoinitiated cationic polymerization", *Journal of Polymer Science; Part A: Polymer Chemistry*, vol. 16, pp. 2441–2451, 1978.
- [CRI 79] CRIVELLO J.V., LAM J.H.W., "Dye sensitized photoinitiated cationic polymerization. The system: perylene triarylsulfonium salts", *Journal of Polymer Science; Part A: Polymer Chemistry*, vol. 17, pp. 1059–1065, 1979.
- [CRI 85] CRIVELLO J.V., LEE J.L., "Recent advances in thermally and photochemically initiated cationic polymerization", *Polymer Journal*, vol. 17, no. 11, pp. 73–83, 1985.
- [CRI 93] CRIVELLO J.V., "Photo- and thermal catalysts for cationic polymerization", in BRUNELLE D.J. (ed.), *Ring-Opening Polymerization Mechanisms, Catalysis, Structure, Utility*, Hanser, Munich, pp. 157–196, 1993.
- [CRI 98] CRIVELLO J.V., LIU S., "Free radical induced acceleration of cationic polymerization", *Chemistry of Materials*, vol. 10, no. 11, pp. 3724–3731, 1998.
- [CRI 01] CRIVELLO J.V., HUA Y., GOMURASHVILI Z., "Monomeric and polymeric carbazole photosensitizers for photoinitiated cationic polymerization", *Macromolecular Chemistry and Physics*, vol. 202, pp. 2133–2141, 2001.
- [CRI 02a] CRIVELLO J.V., JIANG F., "The development of pyrene photosensitizers for cationic photoinitiators", *Chemistry of Materials*, vol. 14, pp. 4858–4866, 2002.
- [CRI 02b] CRIVELLO J.V., ORTIZ R.A., "Benzyl alcohols as accelerators in the photoinitiated cationic polymerization of epoxide monomers", *Journal of Polymer Science; Part A: Polymer Chemistry*, vol. 40, no. 14, pp. 2298–2309, 2002.
- [CRI 02c] CRIVELLO J.V., MA J., JIANG F.M., "Synthesis and photoactivity of novel 5-arylthianthrenium salt cationic photoinitiators", *Journal of Polymer Science; Part A: Polymer Chemistry*, vol. 40, no. 20, pp. 3465–3480, 2002.

- [CRI 03a] CRIVELLO J.V., JANG M., “The development of anthracene photosensitizers for photoinitiated cationic polymerizations”, *ACS Polymer Preprints*, vol. 44, no. 1, pp. 845–849, 2003.
- [CRI 03b] CRIVELLO J.V., JANG M., “Anthracene electron-transfer photosensitizers for onium salt induced cationic photopolymerizations”, *Journal of Photochemical and Photobiology*, vol. 159, no. 2, pp. 173–188, 2003.
- [CRI 04] CRIVELLO J.V., MA J., JIANG F.M. *et al.*, “Advances in the design of photoinitiators, photosensitizers and monomers for photoinitiated cationic polymerization”, *Macromolecular Symposia*, vol. 215, pp. 165–177, 2004.
- [CRI 05a] CRIVELLO J.V., JANG M., “Synthesis of monomer and polymer-bound photosensitizers”, *Journal of Macromolecular Science, Pure and Applied Chemistry*, vol. A42, no. 1, pp. 1–19, 2005.
- [CRI 05b] CRIVELLO J.V., BULUT U., “A naturally occurring long wavelength photosensitizer for diaryliodonium salts”, *Journal of Polymer Science; Part A: Polymer Chemistry*, vol. 43, pp. 5217–5231, 2005.
- [CRI 08] CRIVELLO J.V., “Benzophenothiazine and benzophenoxaxine photosensitizers for triarylsulfonium salt cationic photoinitiators”, *Journal of Polymer Science; Part A: Polymer Chemistry*, vol. 46, no. 11, pp. 3820–3829, 2008.
- [DAV 82] DAVIDSON R.S., GOODIN J.W., “Some studies on the photo-initiated cationic polymerisation of epoxides”, *European Polymer Journal*, vol. 18, no. 7, pp. 589–595, 1982.
- [DEK 87] DEKTAR J.L., HACKER N.P., “A new mechanism for photodecomposition and acid formation from triphenylsulphonium salts”, *Journal of the Chemical Society Chemical Communications*, vol. 38, pp. 1591–1592, 1987.
- [DEK 90] DEKTAR J.L., HACKER N.P., “Photochemistry of diaryliodonium salts”, *Journal of Organic Chemistry*, vol. 55, pp. 639–647, 1990.
- [DEK 91] DEKTAR J.L., HACKER N.P., “Comparison of the photochemistry of diarylchloronium, diarylbromonium, and diaryliodonium salts”, *Journal of Organic Chemistry*, vol. 56, pp. 1838–1844, 1991.
- [DEN 95] DENIZLIGIL S., MCARDLE C., YAGCI Y., “Photochemically and thermally induced radical promoted cationic polymerization using an allylic sulfonium salt”, *Polymer*, vol. 36, pp. 3093–3098, 1995.

- [DEN 96] DENIZLIGIL S., RESUL R., YAGCI Y. *et al.*, “Photosensitized cationic polymerization using allyl sulfonium salt”, *Macromolecular Chemistry and Physics*, vol. 197, pp. 1233–1240, 1996.
- [DEV 87] DEVOE R.J., SAHYUN M.R.V., SERPONE M. *et al.*, “Transient intermediates in the photolysis of iodonium cations”, *Canadian Journal of Chemistry*, vol. 65, pp. 2342–2349, 1987.
- [DE 88a] DE VOE R.J., MITRA S., “Polymeric Manich bases as photosensitizers”, *ACS Polymer Preprints*, vol. 29, pp. 522–524, 1988.
- [DE 88b] DE VOE R.J., SAHYUN M.R.V., SCHMIDT E., “Electron transfer sensitized photolysis of onium salts”, in HERBERT A. (ed.), *SPSE Proceedings – Photochem Imaging, Summer Symposium*, SPSE, Springfield, VA, pp. 21–36, 1988.
- [DE 89] DE VOE R.J., SAHYUN M.R.V., SCHMIDT E., “Electron transfer sensitized photolysis of 'onium salts”, *Journal of Imaging Science*, vol. 33, no. 2, pp. 39–43, 1989.
- [DOS 96] DOSSOW D., ZHU Q.Q., HIZAL G. *et al.*, “Photosensitized cationic polymerization of cyclohexene oxide: a mechanistic study concerning the use of pyridinium-type salts”, *Polymer*, vol. 37, no. 13, pp. 2821–2826, 1996.
- [DUR 03] DURSUN C., DEGRIMENCI M., YAGCI Y. *et al.*, “Free radical promoted cationic polymerization by using bisacylphosphine oxide photoinitiators: substituent effect on the reactivity of phosphinoyl radicals”, *Polymer*, vol. 44, no. 24, pp. 7389–7396, 2003.
- [DUR 08] DURMAZ Y.Y., MOSZNER N., YAGCI Y., “Visible light initiated free radical promoted cationic polymerization using acylgermane based photoinitiator in the presence of onium salts”, *Macromolecules*, vol. 41, no. 18, pp. 6714–6718, 2008.
- [EBE 87] EBERSON L., *Electron Transfer Reactions in Organic Chemistry*, Springer-Verlag, Berlin, pp. 146–163, 1987.
- [EHL 06] EHLE C., RAHMAN G.M.A., JUX N. *et al.*, “Interactions in single wall carbon nanotubes/pyrene/porphrin hybrids”, *Journal of the American Chemical Society*, vol. 128, no. 34, pp. 11222–11231, 2006.
- [ELO 69] ELOFSON R.M., GADALLAH F.F., “Substituent effects in the polarography of aromatic diazonium salts”, *Journal of Organic Chemistry*, vol. 34, no. 4, pp. 854–857, 1969

- [FOU 88] FOUASSIER J.P., CHESNEAU E., "Polymérisation induite sous irradiation laser visible, 3. Un nouveau système photosensible performant", *Makromolekulare Chemie, Rapid. Communications*, vol. 9, pp. 223–227, 1988.
- [FOU 89] FOUASSIER J.P., BURR D., CRIVELLO J.V., "Time-resolved laser spectroscopy of the sensitized photolysis of iodonium salts", *Journal of Photochemistry and Photobiology: Chemistry*, vol. 49, pp. 317–324, 1989.
- [FOU 94] FOUASSIER J.P., BURR D., CRIVELLO J.V., "Photochemistry and photopolymerization activity of diaryliodonium salts", *Journal of Macromolecular Science – Pure and Applied Chemistry*, vol. A31, no. 6, pp. 677–705, 1994.
- [GAU 86] GAUBE H.G., "Photosensitization of iron-arene complexes", *SME Technical Paper FC86-843, RadTech '86 Conference Proceedings*, Baltimore, MD, pp. 15–29, 8–11 September 1986.
- [GOM 01] GOMURASVILI Z., CRIVELLO J.V., "Phenothiazine photosensitizers for photoinitiated cationic polymerization", *Journal of Polymer Science; Part A: Polymer Chemistry*, vol. 39, no. 8, pp. 1187–1197, 2001.
- [GOM 02] GOMURASVILI Z., CRIVELLO J.V., "Monomeric and polymeric phenothiazine photosensitizers for photoinitiated cationic polymerization", *Macromolecules*, vol. 35, no. 8, pp. 2962–2969, 2002.
- [HAR 01] HARTWIG A., HARDER A., LÜHRING A. *et al.*, "9-Oxo-9H-fluoren-2-yl)-phenyl-iodonium hexafluoroantimonate(V) – a photoinitiator for the cationic polymerisation of epoxides", *European Polymer Journal*, vol. 37, pp. 1449–1455, 2001.
- [HIZ 94] HIZAL G., YAGCI Y., SCHNABEL W., "Photoacid generation by stepwise two-photon scheme 1", *Polymer*, vol. 35, pp. 2428–2431, 1994.
- [HUA 00] HUA Y., CRIVELLO J.V., "Synergistic interaction of epoxides and N-vinylcarbazole during photoinitiated cationic polymerization", *Journal of Polymer Science; Part A: Polymer Chemistry*, vol. 38, pp. 3697–3709, 2000.
- [HUA 02] HUA Y., JIANG F.M., CRIVELLO J.V., "Photosensitization of onium salt induced with hydroxymethylated polynuclear aromatic hydrocarbons", *Chemistry of Materials*, vol. 14, no. 5, pp. 2369–2377, 2002.
- [HUA 03] HUA Y., CRIVELLO J.V., "Photosensitization of onium salt initiated cationic photopolymerizations by carbazole monomers", in BELFIELD K.D., CRIVELLO J.V. (eds), *Photoinitiated Polymerization*, ACS Symposium Series 847, ACS, Washington, DC, pp. 219–230, 2003.

- [ICH 87] ICHIMURA K., KAMEYAMA A., HAYASHI K., "Photosensitive resins containing p-dimethylaminobenzylidene derivatives and diphenyliodonium salt as photoinitiators", *Journal of Applied Polymer Science*, vol. 34, pp. 2747–2756, 1987.
- [KLE 85] KLEMM E., FLAMMERSHEIM H.-J., MÄRTIN R. *et al.*, "Versuche zur stufenweisen epoxid/methacrylat-photopolymerisation mit diaryliodoniumsalz-photoinitiatoren", *Angewandte Makromolekulare Chemie*, vol. 135, pp. 131–138, 1985.
- [LAL 07] LALEVÉE J., EL-ROZ M., DIRANI A. *et al.*, "New highly efficient radical photoinitiators based on Si–Si bond cleavage", *Macromolecules*, vol. 40, pp. 8527–8530, 2007.
- [LAL 08a] LALEVÉE J., EL-ROZ M., ALLONAS X. *et al.*, "Silanes as new highly efficient co-initiators for radical polymerization in aerated media", *Macromolecules*, vol. 46, no. 6, pp. 2008–2010, 2008.
- [LAL 08b] LALEVÉE J., DIRANI A., EL-ROZ, M. *et al.*, "Germanes as efficient cointiators in radical and cationic photopolymerizations", *Journal of Polymer Science; Part A: Polymer Chemistry*, vol. 46, no. 6, pp. 3042–3047, 2008.
- [LAL 08c] LALEVÉE J., EL-ROZ M., ALLONAS X. *et al.*, "Free-radical-promoted cationic photopolymerization under visible light in aerated media: new and highly efficient silane-containing initiating systems", *Journal of Polymer Science; Part A: Polymer Chemistry*, vol. 46, no. 6, pp. 2010–2014, 2008.
- [LED 79] LEDWITH A., "New initiation systems for cationic polymerisation", *Macromolecular Chemistry and Physics*, vol. 3, pp. 348–358, 1979.
- [LEE 69] LEERMAKERS P.A., "Fundamental concepts", in LAMOLA A.A., TURRO N.J. (eds), *Energy Transfer and Organic Photochemistry*, Interscience, New York, pp. 1–15, 1969.
- [LOH 86] LOHSE F., ZWEIFEL H., "Photocrosslinking of epoxy resins", *Advances in Polymer Science*, vol. 78, pp. 61–78, 1986.
- [MAN 92] MANIVANNAN G., FOUASSIER J.P., CRIVELLO J.V., "Chlorothioxanthone-onium salts: efficient photoinitiators of cationic polymerization", *Journal of Polymer Science; Part A: Polymer Chemistry*, vol. 30, pp. 1999–2001, 1992.
- [MEI 83] MEIER K., BÜHLER N., ZWEIFEL H. *et al.*, Curable compositions containing metallocene complexes, activated primers obtained there from and their use, European Patent Application No. 094915, May 1983.

- [MEI 86] MEIER K., ZWEIFEL H., "Photoinitiated cationic polymerization with iron-arene complexes", *Journal of Radiation Curing*, vol. 13, no. 4, pp. 26–32, 1986.
- [MOW 00] MOWERS W.A., CRIVELLO J.V., RAJARAMAN S., "Free radical acceleration of photoinitiated cationic polymerization by a hybrid system", RadTech Report, pp. 34–41, March/April 2000.
- [MUR 73] MUROV S.L., *Handbook of Photochemistry*, Marcel Dekker, Inc., New York, pp. 3–23, 1973.
- [NAR 10] NAREWSKA J., STRZELCZYK R., PODSIADLY R., "Fluoflavin dyes as electron transfer photosensitizers for onium salt induced cationic photopolymerization", *Journal of Photochemistry and Photobiology A: Chemistry*, vol. 30, pp. 68–74, 2010.
- [NEL 94] NELSON E.W., CARTER T.P., SCRANTON A.B., "Fluorescence monitoring of cationic photopolymerizations: divinyl ether polymerizations photosensitized by anthracene derivatives", *Macromolecules*, vol. 27, no. 4, pp. 1013–1019, 1994.
- [NEL 95] NELSON E.W., CARTER T.P., SCRANTON A.B., "The role of the triplet state in the photosensitization of cationic polymerizations by anthracene", *Journal of Polymer Science; Part A: Polymer Chemistry*, vol. 33, no. 2, pp. 247–256, 1995.
- [PAP 84a] PAPPAS S.P., GATECHAIR L.R., JILEK J.H., "Photoinitiation of cationic polymerization III: photosensitization of diaryliodonium and triarylsulfonium salts", *Journal of Polymer Science; Part A: Polymer Chemistry*, vol. 22, no. 1, pp. 77–84, 1984.
- [PAP 84b] PAPPAS S.P., PAPPAS B.C., GATECHAIR L.R., "Photoinitiation of cationic polymerization IV: direct and sensitized photolysis of aryl iodonium and sulfonium salts", *Polymer Photochemistry*, vol. 5, nos. 1–6, pp. 1–22, 1984.
- [PAP 03] PAPPAS S.P., TILLEY M.G., PAPPAS B.C., "Anthracene-bound sulfonium salts: highly efficient photoinitiators for cationic polymerization: a new synthesis of sulfonium salts which avoids the use of silver salts", *Journal of Photochemistry and Photobiology*, vol. 159, no. 2, pp. 161–171, 2003.
- [ROD 01] RODRIGUES M.R., NEUMANN M.G., "Cationic photopolymerization of tetrahydrofuran: a mechanistic study of the use of a sulfonium salt-phenothiazine initiator system", *Journal of Polymer Science; Part A: Polymer Chemistry*, vol. 39, no. 1, pp. 46–55, 2001.

- [SAV 67] SAVEANT J.M., VIANELLO E., “Potential-sweep voltammetry: theoretical analysis of monomerization and dimerization mechanisms”, *Electrochimica Acta*, vol. 12, no. 12, pp. 1545–1561, 1967.
- [SEL 01] SELVARAJU C., SIVAKUMAR A., RAMMAMURTHY P., “Excited state reactions of acridinedione dyes with onium salts: mechanistic details”, *Journal of Photochemistry and Photobiology A: Chemistry*, vol. 138, no. 3, pp. 213–226, 2001.
- [SUG 03] SUGIYAMA K., QU W., SHIRAI M. *et al.*, “Visible light-induced cationic polymerization of epoxides sensitized by benzoquinonylsulfanyl derivatives”, *Chemistry Letters*, vol. 32, no. 1, pp. 92–93, 2003.
- [TAS 08] TASDELEN M.A., KUMBARACI V., JOCKUSCH S. *et al.*, “Photoacid generation by stepwise two-photon absorption: photoinitiated cationic polymerization of cyclohexene oxide by using benzodioxinone in the presence of iodonium salt”, *Macromolecules*, vol. 41, pp. 295–297, 2008.
- [TEH 13] TEHFE M.-A., DUMUR F., GRAFF D. *et al.*, “Blue-to-red light sensitive push–pull structured photoinitiators: indanedione derivatives for radical and cationic photopolymerization reactions”, *Macromolecules*, vol. 46, no. 9, pp. 3332–3341, 2013.
- [TEH 14] TEHFE M.-A., DUMUR F., XIAO P. *et al.*, “Photoinitiators based on a phenazine scaffold: high performance system upon near-UV or visible LED (385, 395 and 405 nm) irradiations”, *Polymer*, vol. 55, no. 10, pp. 2285–2293, 2014.
- [TOB 99] TOBA Y., SAITO M., USUI Y., “Cationic photopolymerization of epoxides by direct and sensitized photolysis of onium tetrakis(pentafluorophenyl)borate initiators”, *Macromolecules*, vol. 32, no. 10, pp. 3209–3215, 1999.
- [TOB 00] TOBA Y., “Anthracene-sensitized polymerization of vinyl ethers by onium tetrakis(pentafluorophenyl)borate initiators”, *Journal of Polymer Science; Part A: Polymer Chemistry*, vol. 38, no. 6, pp. 982–987, 2000.
- [WAD 03] WADE JR. L.G., *Organic Chemistry*, 5th ed., Prentice-Hall, Upper Saddle River, NJ, pp. 698–699, 2003.
- [YAG 88] YAGCI Y., LEDWITH A., “Mechanistic and kinetic studies on the photoinitiated polymerization of tetrahydrofuran”, *Journal of Polymer Science; Part A: Polymer Chemistry*, vol. 26, pp. 1911–1918, 1988.
- [YAG 93] YAGCI Y., LUKAC I., SCHNABEL W., “Photosensitized cationic polymerization using N-ethoxy-2-methylpyridinium salts”, *Polymer*, vol. 34, pp. 1130–1133, 1993.

- [YAG 94] YAGCI Y., SCHNABEL W., “Direct and sensitized photoinitiated cationic polymerization using pyridinium salts”, *Macromolecular Symposia*, vol. 85, no. 1, pp. 115–127, 1994.
- [YAG 11] YAGCI Y., SAHIN O., OZTURK T. *et al.*, “Synthesis of silver/epoxy nanocomposites by visible light sensitization using highly conjugated thiophene derivatives”, *Reactive and Functional Polymers*, vol. 71, no. 8, pp. 857–862, 2011.



---

# Controlled Photopolymerization and Novel Architectures

---

## 3.1. Introduction

Photopolymerization can be described broadly as polymerization propagated by radical or ionic moieties as a direct consequence of a photochemical reaction. The advantages of photopolymerization include high rates of polymerization and environmental benefits from elimination of volatile organic solvents. The intrinsic nature of photopolymerization being able to occur at ambient temperature brings with it advantages which are used by polymer chemists throughout the field to develop novel architectures along with greener, more environmentally friendly processes. As the polymerization occurs at ambient temperature, thermally sensitive materials can be incorporated into the structure during polymerization. Lack of a need to use solvent is also a common feature of photopolymerizations; this reduces the emission of volatile organic compounds making them in turn “greener” processes. The use of light as the initiating source for the polymerization can also negate the need for use of harsher or more toxic initiators [YAĞ 10].

Polymerizations that do not occur at room temperature can be made to occur at this temperature under UV or visible light irradiations. Upon

---

Chapter written by Sean DORAN, Omer Suat TASKIN, Mehmet Atilla TASDELEN and Yusuf YAĞCI.

absorption of a mole of photons of 365 nm wavelength, the energy available for a polymerization process to take place is approximately 130 times greater than that available at ambient temperature (25°C) under thermal conditions, 327 kJ mol<sup>-1</sup> compared with 2.5 kJ mol<sup>-1</sup> respectively [YAĞ 98]. Absorption of a mole of photons of 254 nm wavelength (471 kJ mol<sup>-1</sup>) leads to 160 times the energy being available than would be thermally (2.5 kJ mol<sup>-1</sup>) at this temperature [DEC 98, DEC 02, AND 01]. This energy provided by UV and visible light can be used to overcome the activation barrier related to the initiation of polymerization which otherwise would not occur at room temperature. The absorption of light by the photon-absorbing moiety (photoinitiator) will typically cause it to occupy energetic states which will ultimately lead it to undergo a transformation bringing about the initiation of polymerization. The photochemically derived polymerization initiating moieties can be radical or ionic in nature. There are numerous classes of photoinitiators differing in the nature of the active species produced upon irradiation and they will be discussed later in detail [DIZ 13, DIZ 11, TAS 07b, TAS 06b, TAS 09, TAS 07a, TAS 08a]. Unlike polymerizations under thermal control, the use of photoinitiated systems gives access to spatial and temporal control which otherwise would not be available. Spatial control in photopolymerizations refers to the ability to control where polymerization occurs in 2D or 3D space [LEE 08]. This can be realized by shining the appropriate wavelength light on pre-prepared liquid mixtures of monomer/photoinitiator with any potential additives [TAS 11c]. This type of process has classically been applied in the field of coatings, films and adhesives because the photoinitiating light by its nature cannot penetrate far beneath the surface so polymerization occurs in the 2D plane. It has been shown however that the light source can be focused within a volume to achieve 3D polymerization control as well. Temporal control of the polymerization process obtained by using a photoinitiating system refers to the simplicity of being able to switch on and off a light source. This is a more convenient approach when compared to polymerizations which are driven forward thermally which require a heating up and cooling down period. The source of light is either turned on or off, which means that the exact quantum yield for the specific process in consideration is either affected or not. Under thermal conditions however, there is a time delay between applying heat and the time at which the monomer solution has heated up to the desired temperature and equilibrated throughout. During this process, there is a gradient of temperature and therefore a gradient of energy

available to initiate and propagate polymerization which can result in a broadening of the polydispersity of the obtained polymer. This is also true for the cooling down period as the temperature will not revert from high to ambient instantly, again, producing a gradient of energy available to initiate and propagate polymerization. Turning off the light instantly removes the energy source and so the halting of polymerization can be quicker. Of course, it has been shown that certain photoinitiated polymerization processes will continue for some time in the dark, this is especially true for photoinitiating systems that require only catalytic amounts of photoinitiator [TAS 06a].

Well-defined polymers with a controlled chain-length, architecture, functionality and narrow molecular weight distribution are of considerable scientific and industrial interest due to their attractive features. The synthesis of well-defined polymers has been possible because of recent significant progress in controlled polymerization techniques. These methods are based on establishing a rapid dynamic equilibrium between a minute amount of growing chains and a large majority of dormant species and are more tolerant of functional groups and impurities. Moreover, the rate of initiation must exceed the rate of propagation. Therefore, all the propagating polymer chains are formed simultaneously and grow at the same rate. If these requirements did not occur, the first chains formed would be longer than those initiated later and the molecular weight distribution of the propagating chains would broaden. If all of these criteria have been fulfilled, the polymerization where propagating center of growing chain does not terminate and does not undergo chain transfer reactions. As a result of the development of controlled polymerization methods, synthetic polymer chemists are now able to construct, in a precise manner, a wide variety of polymer architectures that were previously inaccessible using uncontrolled chain-growth methods such as free-radical polymerizations. The most widely used controlled polymerization methods are the iniferter method, nitroxide-mediated radical polymerization (NMRP), atom transfer radical polymerization (ATRP), cobalt-mediated radical polymerization, organoiodine-mediated radical polymerization, organotellurium-mediated radical polymerization and reversible addition-fragmentation chain transfer (RAFT) polymerization for radical-based systems and living cationic and anionic polymerizations for ionic-based systems. Although with limited success, there have been a number of attempts to conduct such controlled

polymerization methods by photochemical stimuli. Recent approaches with regard to achieving photoinitiated controlled polymerization control in both ionic [KAH 07, KAH 08a, KAH 08b, KAH 09] and radical systems [TAS 11a, TAS 11b, TAS 10a, TAS 08b] are based on the stabilization of unstable growing species by the reversible formation of the corresponding covalent and dormant species that rapidly exchange. It has been estimated that energy costs can be reduced 30% by switching from thermal polymerization to photoinitiated polymerization. In this chapter, the current state of the art is summarized and an overview on photoinitiated controlled polymerization for both radical and cationic systems and their potential application in the preparation of complex linear and cross-linked macromolecular structures is described.

## **3.2. Photoinitiated controlled radical polymerizations**

### **3.2.1. Photoiniferter**

One of the earliest attempts to develop a photoinitiated controlled radical polymerization was realized by Otsu *et al.* using the initiator-chain transfer-termination (iniferter) concept. In the last two decades, appropriate photoiniferters have been developed including diphenyl disulfide, tetraethylthiuram disulfide, benzyl diethyldithiocarbamate and 2-phenylethyl diethyldithiocarbamate. In the earlier studies, the dithiocarbamate (DTC) type photoiniferters were used for the polymerization of vinyl monomers under UV irradiation. The propagating polymer chain end was always a DTC group, which can photodissociate into a reactive propagating radical and a less reactive small radical DTC<sup>•</sup> resulting in successive insertion of monomers into the dissociated bond. A large number of monomers, such as styrene (St), methyl methacrylate (MMA), *n*-butyl acrylate (*n*-BA), acrylamide, acrylonitrile and methyl acrylonitrile can be polymerized in a controlled manner with photoiniferters. The control of the polymerization decreases from St to MMA, and disappears in the case of acrylates. The structures and compositions of the final polymers were not controlled very well and the polymers displayed relatively broad molecular weight distribution, poor initiation efficiency and much higher molecular weight than theoretical values [OTS 82]. This was attributed to slow initiation, slow exchange, direct reaction of counter radicals (DTC<sup>•</sup>) with monomers,

degradative transfer of photoiniferter molecules and undesired irreversible termination reactions. To overcome these drawbacks, a combination of photoiniferter with ATRP or RAFT techniques was reported by several groups. The results confirmed that this approach gave a better control in the formation of polymers having a photolabile group.

Qin *et al.* reported a photoinitiated ATRP employing 2,2-dimethoxy-2-phenylacetophenone (DMPA) as photoinitiator and ferric tri(*N,N*-diethyldithiocarbamate) [Fe(DTC)<sub>3</sub>] as catalyst for polymerization of MMA in toluene. Upon UV irradiation, the DMPA molecule produced two active radicals that could reduce Fe(DTC)<sub>3</sub> giving R–DTC and the lower oxidation state metal salt, Fe(DTC)<sub>2</sub>. Activation then proceeded by UV light irradiation with DTC acting as a reversible transfer group [QIN 01]. Kwak *et al.* realized another similar approach including a combination of ATRP and photoiniferter polymerization using a DTC photoiniferter. Upon UV irradiation, DTC molecules rapidly generate carbon-centered radicals that induce radical propagation and were deactivated by a copper complex. It was reported that due to the fast deactivation of radicals by the copper complex, unwanted chain transfer reactions in iniferter polymerization could be suppressed. The use of 2-(*N,N*-diethyldithiocarbamyl) isobutyric acid ethyl ester (EMADTC) as an iniferter with a ratio of MMA/EMADTC/Cu(I)Br/HMTETA = 200/1/1/1 in 50% (v/v) anisole offered a well-controlled polymerization under UV light irradiation. The polymerization process proceeded very slowly due to the slow activation of the dormant species by copper catalyst at 30°C in the dark, while it went on 25 times faster upon UV irradiation [QIN 01, KWA 11, KWA 10].

In 2008, synthesis and application of phenacyl morpholine-4-dithiocarbamate (PMDTC), which acted as both photoiniferter and RAFT agent in the vinyl polymerization, were reported by Tasdelen *et al.* [TAS 08b]. The PMDC possesses excellent optical absorption properties in the near UV spectral region, ensuring efficient light absorption from most UV light sources. The PMDC molecule containing a good leaving phenylacyl group (R group) and an electron rich morpholine group (Z group) was designed deliberately. The utilization of PMDC as photoinitiator and RAFT agent was tested for the radical polymerization of St under UV light irradiation. The results showed that molecular weight was linearly increased with monomer conversion, while the molecular weight distribution became

slightly narrower as monomer conversion increased. To further demonstrate the “living” character of the polymerization, the resulted PSt sample was used as a macro-RAFT agent for block copolymerization with methyl acrylate (MA) under similar experimental conditions. The GPC peak of PSt macroinitiator ( $M_n = 2,400$  g/mol, PDI = 1.47) shifted to a lower elution time after the block copolymer formation ( $M_n = 33,000$  g/mol, PDI = 1.37). The PDI of the block copolymer is slightly narrower than that of the initial polymer. This suggests most of the chains are still active during the process of the block polymerization reaction.

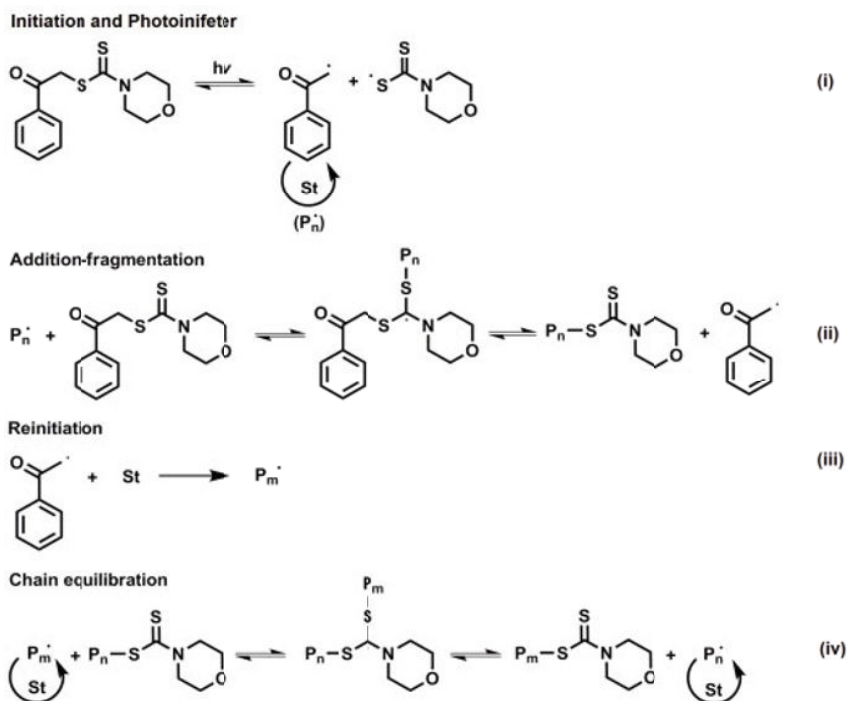


**Diagram 3.1.** Postulated mechanism of photoiniferter/RAFT polymerization of St

The proposed mechanism of the polymerization includes that both RAFT and reversible termination mechanisms are operative in the system (Diagram 3.1). Their activity of the RAFT mechanism was confirmed first by carrying out polymerization of St in the presence of PMDTC and TMDPO at  $\lambda < 365$  nm where TMDPO is active but PMDTC is not active. In

this way, a well-defined polymer with low polydispersity was obtained and the PMDTC acted as a RAFT agent, as direct photolysis of the C-S bond and the reversible termination mechanism did not occur. However, the PSt-DTC was used as a photoiniferter in the polymerization of MA under UV conditions without additional photoinitiator. The block copolymer formation proved the activity of the reversible termination mechanism. Suitable control levels were achieved in both cases.

### 3.2.2. Photoinitiated nitroxide-mediated radical polymerization

The NMRP is one of the most widely used CRP methods for vinyl monomers. It usually avails of nitroxyl radicals (nitroxides) or alkoxyamines to impart livingness into the reaction as can be observed in Diagram 3.2. The NMRP using 2,2,6,6-tetramethylpiperidine-1-oxyl (TEMPO) is very commonplace and effective for a limited amount of monomers [YOU 00, DEV 97, MAR 94, GRA 98, MAT 95]. However, much work has been done on expanding the gamut of monomers that NMRP using TEMPO can be carried out with. This often involves the modification of the nitroxide structure, the use of alkoxyamine adducts and the use of additives. So another approach of endowing photopolymerization with controlled/living behavior has been the use of photoinduced NMRP, which has been rigorously explored by a number of research groups. In the first study, Scaiano *et al.* showed that laser-flash irradiation of alkoxyamines generates nitroxides and alkyl radicals through a homolytic process [GOT 07]. Although the photosensitization step was successful, only limited numbers of radicals were generated in these systems. Moreover, they did not perform any polymerization study to see the relative contribution of these molecules in the polymerization.

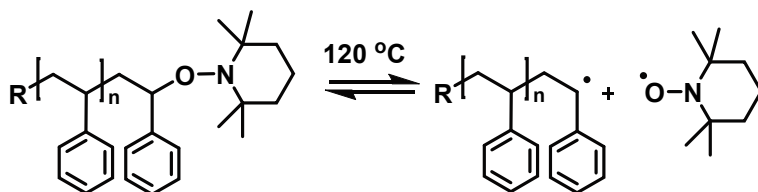


**Diagram 3.2.** General mechanism of nitroxide mediated radical polymerization

Several attempts were also made to covalently attach different chromophoric groups to the TEMPO moiety [YOU 00, GOT 07]. Although, some success was achieved, the conditions for true C/LRP were not attained, because the energy transfer from the sensitizer (“antenna”) to the C-O bond was not found to be efficient enough to activate the process [GRA 98, MAT 95]. More recently, Neckers and Lalevée groups [GUI 10] reported new alkoxyamines possessing a chromophore group with various positions to facilitate the homolysis of alkoxyamine. Guillaneuf *et al.* have reported the synthesis of an alkoxyamine with a chromophore directly attached to the aminoxyl function which undergoes primarily C-O dissociation upon UV radiation as seen in Diagram 3.3 [GUI 10]. The obtained alkoxyamine was able to act as a photoiniferter toward photoinitiated NMRP of *n*-BA; linear chain growth of the polymer was observed and it was described as having a partial living character. The reversible reaction between the polymeric radical and the nitroxide leads to a reduction in the contribution of irreversible bimolecular termination. A very recent study revealed that light sensitive alkoxyamines were applied in both thermally- and photochemically-induced polymerizations for macromolecular syntheses including block copolymer, post-modification of polymer coatings for application in patterning and photografting [MOR 15].

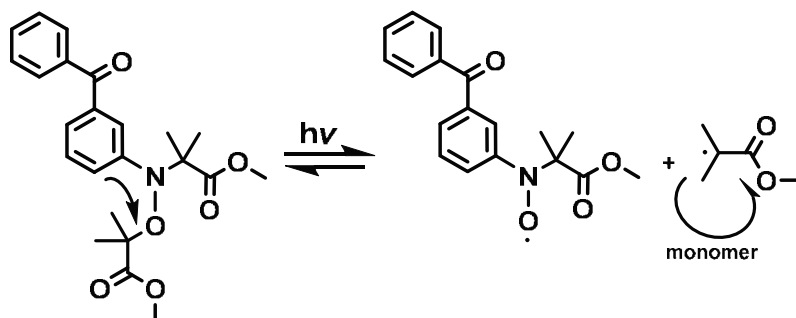


**Diagram 3.3.** Photoinduced NMRP of vinyl monomers with an alkoxyamine possessing a chromophoric benzophenone molecule

Yoshida *et al.* have reported the photopolymerization of MMA using azobis(4-methoxy-2,4-dimethylvaleronitrile) as an initiator with 4-methoxy-TEMPO (Me-TEMPO) as a mediator in the presence of a diaryliodonium salt namely, bis(alkylphenyl)iodonium hexafluorophosphate [YOS 12]. The diaryliodonium salt behaves as the photoacid generator and PMMA with a

1.4 PDI value could be obtained with high conversion. It is understood that the mechanism of the reaction proceeds through an electron transfer between the excited diaryliodonium salt and the nitroxide during the propagation process [YOS 10a]. Similarly, the use of a triarylsulfonium salt, namely (4-*tert*-butylphenyl)-diphenylsulfonium triflate, as the photoacid generator in the same process for controlled photoinduced NMRP of MMA has also been reported [YOS 10b]. However, the mechanism still has unclear points as the function of the iodonium salt is unknown.

### 3.2.3. Photoinitiated atom transfer radical polymerization

The ATRP is one of the most frequently used controlled radical polymerizations due to its simplicity, broad applicability and ability to prepare previously inaccessible well-defined polymers with complex architecture. This process is based on a redox reaction involving a transition metal complex in which a halide atom (especially Cl or Br) is reversibly transferred between a growing radical and a dormant species. It is noted that the atom transfer step is the key step in the reaction responsible for uniform polymer chain growth. The ATRP was independently reported by the Matyjaszewski, Sawamoto and Percec groups in 1995 [WAN 95a, WAN 95b, KAT 95, PER 95].

A first attempt to integrate a photochemical activation in the ATRP process is the use of light as an accelerator in classical ATRP. The visible light irradiation increases the rate of ATRP but also enhances the living character of the polymerization [GUA 00]. In 2000, Guan and Smart reported photo-enhanced ATRP of MMA by visible light irradiation. They observed considerable enhancement in the rate of polymerization under visible light irradiation as compared to the dark conditions. The polymerization of MMA (with  $[MMA]/[R-Cl]/[CuCl]/[Ligand] = 100/0.1/0.3/1$  ratio) reached 41% of monomer conversion after 16 h at 80°C in the dark, whereas employing visible light to the same conditions gave 100% of monomer conversion having molecular weights near to the theoretical values with narrow molecular weight distributions. Though the exact effect of the light was not clear, they attributed it to the acceleration of the activation of the inner-sphere complex between the catalyst (Cu(I)) and the alkyl chloride (R-X), or through the activation of the catalyst alone by light [GUA 00]. Later on, this effect was reinvestigated by Matyjaszewski

*et al.* and the  $k_{\text{act}}$  constants of ATRP system under UV and without UV irradiation were found to be quite similar, 0.10 and 0.092  $\text{M}^{-1} \text{s}^{-1}$  [KWA 10].

Copper and some other d-metal complexes are known as potential light-sensitive compounds and go through photoredox reactions during UV-irradiation. Moreover, the photoproducts of copper complexes can initiate the polymerization of various vinyl monomers in both aqueous and organic media. Previous spectroscopic studies indicated that Cu(II) complex has three distinct absorption bands at 250, 300 and 640 nm. Under UV irradiation, the d-d ligand field transition band centered at 640 nm of  $\text{CuBr}_2/\text{PMDETA}$  catalyst diminishes and gives rise to the lower energy shoulder (Figure 3.1). However, the formation of Cu(I) cannot be monitored due to overlapping with the characteristic peak of Cu(II) complex at 300 nm. The strong absorption at this wavelength corresponding to the ligand-to-metal charge-transfer transition is responsible for the photoreduction of Cu(II) to Cu(I) [KAT 95, FOR 12, TAS 12b].

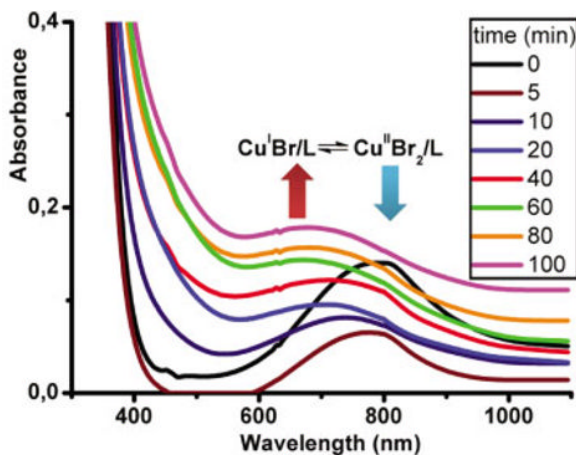


**Figure 3.1.** Typical UV/Vis spectral changes of the  $\text{CuBr}_2/\text{PMDETA}$  by UV irradiation at 350 nm. (Reproduced with permission from [TAS 11b]. Copyright 2011 John Wiley & Sons)

A series of well-defined PMMA were successfully prepared by reduction of Cu(II) to Cu(I) upon UV irradiation and subsequent activation of alkyl halide. A linear relationship was observed between monomer consumption and polymerization time and evolution of molecular weight versus

conversion confirmed the well-controlled process. The experimental molecular weights of the obtained polymers were in good agreement with the theoretical values. In the following study, the addition of a small amount of methanol facilitated to conduct the process in the homogeneous system, as methanol exclusively penetrates the solubility of Cu(II) complexes in the polymerization mixture. Applying the homogeneous polymerization of MMA could significantly increase the rate of polymerization in comparison with the heterogeneous system, and the control over molecular weights under the homogeneous system was also improved. In both works, the livingness of the obtained polymers was confirmed by chain extension experiments. The amount of Cu(II) catalyst used in these studies was equivalent with respect to the initiator [TAS 11b, TAS 10a, KWA 10, KAT 95, TAS 12a].

Very recently, Matyjaszewski *et al.* reported the use of visible light and sunlight for ATRP of various acrylates mediated by ppm level of Cu catalyst without the use of any photoinitiator or reducing agent [KON 12]. A variety of monomers including poly(ethylene glycol) methyl ether acrylate, *tert*-butyl acrylate (*t*-BA), MA, ethyl acrylate (EA), MMA and St, as well as functional initiators in different solvents were tested. There are three distinct pathways for photochemical (re)generation of Cu(I) activator including (1) direct photochemical reduction of the Cu(II) complexes by excess free amine moieties, (2) unimolecular reduction of the Cu(II) complex, (3) photochemical radical generation either directly from the alkyl halide, ligand, or via interaction of ligand with either monomer or with alkyl halides. Both experimental and simulation results show that the photochemically-mediated reduction of Cu(II) complexes by an excess of amine groups is dominant for (re)generation of Cu(I) activator [RIB 14a, RIB 14b, ANA 14a, ANA 14b, ANA 14c, MOS 12].

The ability of other transition metals such as iridium (Ir), and ruthenium (Ru), as alternatives to the cupric catalyst system, are being investigated to succeed photoinitiated ATRP. Recently Hawker *et al.* investigated the Ir-based photoredox system that can be utilized in order to control the polymerization of methacrylate monomers [FOR 12]. The *fac*-[Ir(ppy)<sub>3</sub>] (ppy = 2-pyridylphenyl) was used as the catalyst which affords photoexcited *fac*-[Ir(ppy)<sub>3</sub>]\* species upon irradiation under visible light. The photoexcited Ir<sup>III</sup>\* captured a halogen atom from alkyl halide to form initiating radicals as well as highly oxidized Ir<sup>IV</sup> complex. This Ir<sup>IV</sup> could then react with the

propagating radical to generate initial Ir<sup>III</sup> complex in the ground state. The process is applied on a variety of acrylate monomers including MA, EA, *n*-BA and *tert*-BA. The nature of the *fac*-[Ir(ppy)<sub>3</sub>] catalyst tolerates carboxylic acid functionality such as acrylic acid. The block and random copolymers of acrylic acid with other (meth)acrylates can be obtained by either macroinitiator or along the backbone of random copolymer with up to 50 mole percent of acrylic acid [TRE 14]. The process also established spatiotemporal control over the patterning of polymer brushes using the same catalytic system under visible light irradiation [POE 13, FOR 13].

Acylphosphine oxides are well-known *Type I* photoinitiators that are easily cleaved upon irradiation forming corresponding radicals. The copper (II) phenyl-2,4,6-trimethylbenzoylphosphinate (Cu<sup>II</sup>(AP)<sub>2</sub>)/PMDETA complex is not only a catalyst for the photoinitiated ATRP but also copper(I)-catalyzed azide–alkyne cycloaddition (CuAAC) click reaction. Exposing the Cu<sup>II</sup>(AP)<sub>2</sub>/PMDETA complex with visible light source causes a decrease in the absorbance peak between 550 and 800 nm as the process is monitored by UV–vis spectrum. This may be due to the transformation from the Cu(II) d<sup>9</sup> configuration to the Cu(I) d<sup>10</sup> configuration in agreement with the previous results for the *in-situ* generation of Cu(I) from Cu(II) using photoinitiators. During the visible light irradiation of Cu<sup>II</sup>(AP)<sub>2</sub>/PMDETA complex, the photogenerated radicals either lead to reduction of Cu(II) to Cu(I) or directly initiate the polymerization of (meth)acrylates, thus leading to the relatively high polydispersity indexes (PDI; 1.36–1.65) [TAS 10b, TAS 13, XI 14].

In the indirect system, the polymerization activators, Cu<sup>I</sup>X/L can be generated from Cu<sup>II</sup>X<sub>2</sub>/L under UV or visible light irradiation through the help of photoinitiators. Many UV and visible light free radical photoinitiators were reported to be powerful promoters for photoinitiated ATRP. For this purpose, the photoinitiated reverse ATRP in the absence of alkyl halide and photoinitiated SR&NI ATRP in the presence of alkyl halide were extensively investigated using commercially available photoinitiators. Photoinitiated reverse ATRP was performed with the Cu<sup>II</sup>Br<sub>2</sub>/PMDETA system in conjunction with several photoinitiators belonging to both *Type I* class, such as 2,2-dimethoxy-2-phenyl acetophenone, (2,4,6-trimethylbenzoyl) diphenylphosphine oxide (BAPO) and *Type II* class such as benzophenone, at room temperature. Even though the polymerization of

MMA could be initiated in the absence of alkyl halide, loss of control over the polymerization process was observed. The type and concentration of photoinitiators directly effects the photoinduced reverse ATRP. Photoinitiated SR&NI ATRP was successfully applied to MMA in the presence of alkyl halide. The molecular weights increased with conversion, and they were in good agreement with the theoretical values (Diagram 3.4) [TAS 11a, DAD 14b, DON 08].

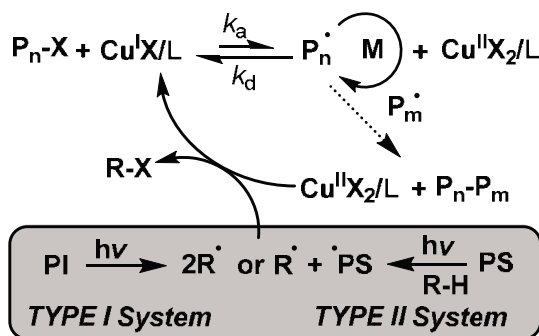


**Diagram 3.4.** Proposed mechanism for dye-sensitized SR&NI ATRP using Type I or Type II photoinitiating systems (PI: photoinitiator; PS: photosensitizer and R-H: hydrogen donor)

Subsequently, the photoinitiated reverse ATRP by employing camphorquinone/benzhydrol (CQ/Bzh) as the initiating system was also developed. Both the Bzh and PMDETA ligand could act as the hydrogen donor to form ketyl radicals (inactive toward the monomer) from the photoexcited CQ. The ketyl radicals, however, reduce the Cu(II) complex to Cu(I) activator and simultaneously generate the mineral acid (HX, where X is Cl or Br). In the following step, HX reacts with the acrylic monomer to form the R-X compound (Markovnikov addition), which is responsible for the initiation of photoinduced ATRP (Diagram 3.5). The main benefit of this approach is that it simultaneously forms alkyl halide initiator by the addition of acid released from the redox process to the monomer. The experimental molecular weights are considerably higher than theoretical values and the obtained polymers showed slightly broad molecular weight distributions ranging from 1.13 to 1.51 in the process. The photoinduced SR&NI ATRP of MMA under the same conditions is also presented and the system leads to a better control of the polymerization as reflected by the improved molecular weight distribution and chain end functionality [TAS 14].

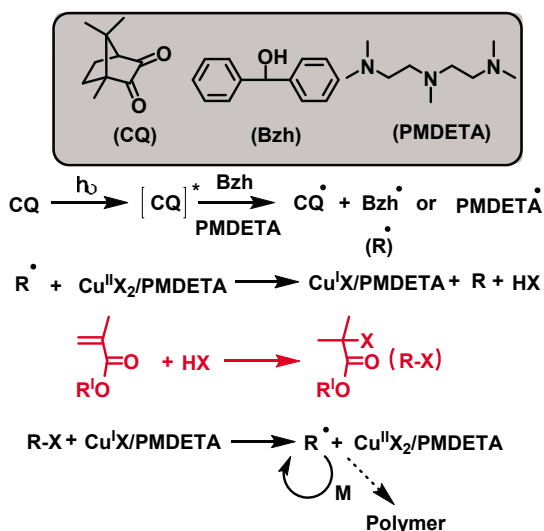


**Diagram 3.5.** Mechanistic scheme for photoinduced reverse ATRP using camphorquinone/benzhydrol

Recently, our group investigated the photoinitiated ATRP to extend its spectral sensitivity to the visible range by either adding a dye or a visible light photoinitiator. The key steps of the initiation mechanism in the case of dye systems involve the dye molecule acting as a light absorber, while an amine co-initiator is the reducing agent for the excited dye. The primary photochemical reaction involves the excited dye molecules abstracting an electron from the amine molecules to form radical-cation/radical-anion pairs. After the proton transfer, some of the radicals are in the system. These radicals are not only able to add to monomer molecules to initiate growth of polymer chains but also can reduce the Cu(II) to Cu(I), which is used as activator in the ATRP. Generally, only the radicals generated from the amine component are reactive enough to activate the polymerization. The radicals generated from the dye molecules are believed either to act mostly as radical chain terminators or to undergo other reactions leading to bleaching of the dye. Although, the molecular weights increase with conversion linearly, the experimental molecular weights are considerably higher than theoretical values in the dye-sensitized systems. In addition, the molecular weight distributions are relatively high, ranging from 1.28 to 1.60 and reasonable control are observed under visible light irradiation. However, bis(2-methyl-2-propanyl)(phenyl)phosphine oxide as *Type I* photoinitiator is used in the

same process. The resulting polymers have very narrow molecular weight distributions ranging from 1.11 to 1.18 and the molecular weight values are close to the theoretical values. Compared to the dye-sensitized SR&NI ATRP, it shows better control of molecular weight and distribution under the similar experimental conditions [YAĞ 10, YAĞ 99, CIF 14].

Another versatile approach for photoinduced ATRP is based on the photolysis of dimanganese decacarbonyl ( $\text{Mn}_2(\text{CO})_{10}$ ) under visible light or sunlight illumination. The photoredox behavior of  $\text{Mn}_2(\text{CO})_{10}$  in the system is followed by means of UV-vis spectroscopy. Optical absorption of the polymerization solution ( $[\text{MMA}]/[\text{EtBP}]/[\text{Cu}(\text{II})\text{Br}_2]/[\text{PMDETA}]/[\text{Mn}_2(\text{CO})_{10}]$ ) is found to decrease upon irradiation, indicating the reaction of  $\text{Mn}_2(\text{CO})_{10}$  with either  $\text{P}_n\text{-Br}$  or  $\text{Cu}^{\text{II}}\text{Br}_2/\text{PMDETA}$ . Admittedly, the appearance of a new peak at 455 nm upon irradiation, when alkyl halide was absent, corresponded to the ligand-to-metal charge-transfer transition of a copper metal. This indicated a direct reduction of Cu(II) to Cu(I) by  $\text{Mn}(\text{CO})_5$  radicals. The radicals formed were reported to abstract halogen atoms from alkyl halides to generate carbon-centered radicals or reducing Cu(II) to Cu(I) directly, which was used as an activator in the ATRP of vinyl monomers such as MMA, MA and St. The growth of the polymer chain is manipulated by either varying the  $\text{Mn}_2(\text{CO})_{10}$  concentration or adjusting the light intensity, which changed the concentration of the Cu(I) catalyst. Moreover, this method is also used to synthesize graft copolymers from commercially available poly(vinyl chloride) (PVC) without additional modification. The chlorine atoms of PVC can act as initiation sites for the direct grafting of MMA by visible light induced ATRP. The molecular weight measurements showed a monomodal molecular weight distribution and a significant shift of the peak value toward higher molecular weights. This confirmed the successful graft copolymerization without detectable free homopolymer formation (Diagram 3.6) [CIF 13a, CIF 14].

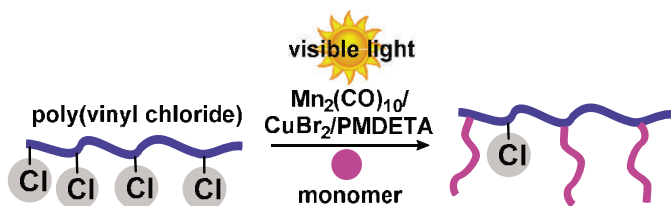


**Diagram 3.6.** Direct grafting of methyl methacrylate onto PVC via visible light induced ATRP using  $\text{Mn}_2(\text{CO})_{10}$

More recently, the photoinitiated ATRP has been implemented in the inverse microemulsion polymerization of oligo(ethylene glycol) monomethyl ether methacrylate. Two different initiation systems including SR&NI ATRP and a combination of AGET and ICAR ATRP are developed under UV light. A stable and bluish water/oil inverse microemulsion is generated after mixing polymerization solutions (aqueous phase:  $\text{Cu}^{\text{II}}\text{Br}_2$ , PMDETA or TPMA as a ligand and PEO-Br as a macroinitiator, PEG 550 as a co-stabilizer, OEOMA as a monomer and water as a solvent; oil phase: a mixture of polyoxyethylene (3) oleyl ether ( $\text{PEO}_3\text{C}_{18}$ ) and polyoxyethylene (6) oleyl ether ( $\text{PEO}_6\text{C}_{18}$ ) as surfactants and hexane as solvent) forming small aqueous monomer swollen “micelles”/droplets with the copper catalyst precursors encapsulated inside. The photoinitiated SR&NI ATRP is initiated by activating the catalysts via UV light irradiation of water-soluble photoinitiator (Irgacure 2959). However, in the AGET&ICAR ATRP system, direct photolysis of  $\text{Cu}(\text{II})/\text{TPMA}$  deactivator complex can also induce a redox reaction between  $\text{Cu}(\text{II})/\text{TPMA}$  and  $\text{Cu}(\text{I})/\text{TPMA}$  activator plus bromine radical to start the polymerization and then continue to regenerate the activator lost in the bi-radical termination process. Not only photoinitiated SR&NI ATRP, but also photoinitiated AGET & ICAR ATRP, produce nanometer-sized particles with narrow and monomodal size distribution. Moreover, the polymers obtained by two systems have molecular weight values close to the theoretical values and relatively narrow PDI ranging from 1.20 to 1.40. The method is particularly advantageous for tuning the particle size which could be manipulated by changing the aqueous phase fraction and controlling growth of polymer chains by switching on/off the UV light [DON 08, CIF 13a, CIF 13b].

In another strategy, our group reported photoinitiated ATRP of MMA using zinc oxide (ZnO) and iron doped zinc oxide (Fe/ZnO) semiconductor nanoparticles. The photoactivated semiconductor nanoparticles successfully reduce air-stable  $\text{Cu}(\text{II})$  to the activator  $\text{Cu}(\text{I})$  species. The activation mechanism is similar to AGET ATRP and is based on one-electron-transfer from the nanoparticles to the catalyst. Like  $\text{TiO}_2$  nanoparticles, ZnO nanoparticles also absorb UV light and release electrons in the conduction band. The released electrons can reduce  $\text{Cu}(\text{II})$  to  $\text{Cu}(\text{I})$  species, which operate the ATRP process. The addition of Fe in ZnO nanoparticles increased the absorbance at higher wavelengths, as well as enhanced the rate of polymerization of the system. The system also has temporal control for the growth of polymer chains, which can be manipulated by switching on/off

the UV light. Attractive features of this system included no use of expensive compounds, metals and conventional radical initiators [DAD 14a, ZHU 11].

In another attempt, mesoporous graphitic carbon nitride (mpg-C<sub>3</sub>N<sub>4</sub>) composed of only C and N atoms, was employed as an ecofriendly photocatalyst for the activation of photoinitiated ATRP of vinyl monomers such as MMA, MA and St. The mpg-C<sub>3</sub>N<sub>4</sub> possesses a high surface area (~200 m<sup>2</sup> g<sup>-1</sup>) that makes it more sensitive and active toward light. The proposed mechanism of the process is continuous regeneration of copper catalyst in a hybrid mechanism of AGET and ICAR ATRP. The light-irradiated electrons from the conduction band of mpg-C<sub>3</sub>N<sub>4</sub> with their large reduction potential can reduce the present Cu<sup>II</sup>/L to Cu<sup>I</sup>/L species which reacts with alkyl halide to form radicals capable of initiating ATRP [DAD 14b].

### 3.2.4. Photoinitiated RAFT polymerization

Since its invention in 1998, the reversible addition-fragmentation chain transfer (RAFT) polymerization has grown into one of the most important CRP techniques for the synthesis of well-defined functional polymers [CHI 98]. The RAFT process is a very convenient and easy method from a practical point of view and only requires the use of pure solvents, the necessity to degas the reaction solution, a regular control over the reaction temperature, and the addition of an appropriate chain transfer agent to the solution of monomer and initiator. Moreover, the main advantage of the RAFT process is its tolerance to a wide range of monomers bearing different functionalities such as acids, acid salts, hydroxy groups and tertiary amines. It enables the synthesis of a wide variety of well-defined polymers with very narrow polydispersity indexes without the need for protection and deprotection steps. In the RAFT polymerization, a chain transfer agent, also called the RAFT agent, is used to operate the polymerization process, allowing it to occur in a controlled manner. The key step in a successful RAFT process is the reversible addition-fragmentation sequence between propagating chain radicals and the RAFT agent. With respect to the RAFT agent, it has been noted that the Z- group should activate the C = S double bond toward radical addition while the R- group should be a good radical leaving group capable of re-initiating polymerization.

The first successful photoinduced RAFT polymerization at low temperature has been reported by Pan *et al.* [YOU 02] who polymerized St,

MA and n-BA with a dibenzyl trithiocarbonate (DBTC) under UV light between 254 and 366 nm. Low yields are achieved over a long period of time; 12–52% MA conversion under UV irradiation over a time period of 15–50 h. This method is also applied for the synthesis of an ABA-type block copolymer made up of PMA-*b*-PSt-*b*-PMA beginning from a PMA-S-C(=S)-S-PMA macroinitiator with complete conversion to block copolymer, i.e. no homopolymer is detected. In another study, the well-defined polystyrene is successfully prepared with 1-phenylethyl phenyldithioacetate as the RAFT agent under UV radiation without additional photoinitiator [QUI 02]. A linear evolution of number-average molecular weight with conversion is reached up to a maximum conversion of 16%. At high conversion, degradation of the terminal dithioester group results in a chain termination. It is also noted that molecular weight distributions of the obtained polymers are broadened by both high conversion and high doses of UV radiation.

In the beginning, there was some controversy over the mechanism of such photoinitiated CRP availing of such dithiocarbonyl species. Pan *et al.* explained the mechanism of the reaction as reversible termination polymerization as can be seen outlined in Diagram 3.7 [QUI 02]. The basis of this proposed mechanism is that the scission of a bond is directly related to its bond length, bond energy and bond order and the weakest bond is always broken first when subjected to UV radiation of appropriate wavelength. It is deduced that since the C-S single bond is the weakest bond in comparison to the vinyl monomer, it is thus decomposed first to form a stable dithio radical and a benzyl radical. The benzyl radical can initiate the polymerization while the more stable dithio radical cannot start polymerization but can reversibly scavenge growing chains forming dormant chains to imbue the controlled manner of the process.

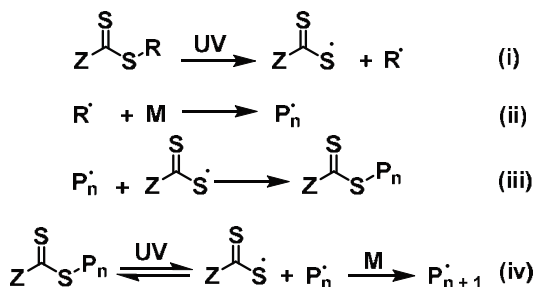


**Diagram 3.7.** The proposed mechanism of reversible termination polymerization

However it was argued that DBTC is known to induce CRP of MMA under thermal conditions using AIBN as initiator through the RAFT mechanism and addition of radicals to the C=S double bond [MAY 00]. It is therefore argued that there should be no reason for such a mechanism not to take place under UV conditions as well. It is also put forward that homolytic cleavage under UV irradiation has also been shown to occur on the monomer and since the MMA monomer is in much greater abundance compared with the dithio species, the probability that homolytic cleavage will only occur on the C-S bond is very low. It is proved that C-S cleavage does take place in the course of polymerization under UV irradiation; however, it is not the process imparting livingness into the polymerization. Homolytic cleavage, as suggested, leads to products that further decompose under UV radiation and thus reduce the controlled/living aspect of the polymerization. This seems intuitive from the nature that the polydispersity broadens greatly as polymerizations are carried out up to 48 h in length.

Later, it was shown by Cai and coworkers that the conversion of polymerization of MA and St by UV induced RAFT could be greatly increased up to 85% while maintaining low polydispersities [LU 05]. They discovered the key aspect to achieve this lay in fine-tuning the wavelength of UV light applied. They showed that *S*-dodecyl-*S'*-( $\alpha,\alpha'$ -dimethyl- $\alpha''$ -acetic acid) trithiocarbonate (DDMAT) and cumyldithiobenzoate (CDB), two CTAs, were readily photolysed at full-wave UV radiation, DDMAT however was slower than CDB (Diagram 3.8). By filtering out the short-wave UV radiation ( $\lambda \leq 313$  nm) through soda glass, the photolysis of the CTA could be dramatically reduced. This also however suppressed the initiation of polymerization and so a photoinitiator needed to be used in conjunction. Acylphosphines are excellent photoinitiators that photolyze quickly to form benzoyl and phosphonyl radicals when exposed to UV radiation [SLU 96, KOL 96]. One such acylphosphine is (2,4,6-trimethylbenzoyl)diphenylphosphine oxide (TPO) which shows long-wave UV absorption at wavelengths that DDMAT does not show. Due to this, the combination of the DDMAT CTA with TPO photoinitiator facilitated the achievement of a very efficient RAFT polymerization of MA and St under UV irradiation yielding high conversions and low polydispersity. The controlled/livingness of the polymerization was evident from the proportional increase of the number-average molecular weight with respect to conversion maintaining a PDI of  $< 1.1$  (conversion = 88%,  $M_n = 11,500$ ).

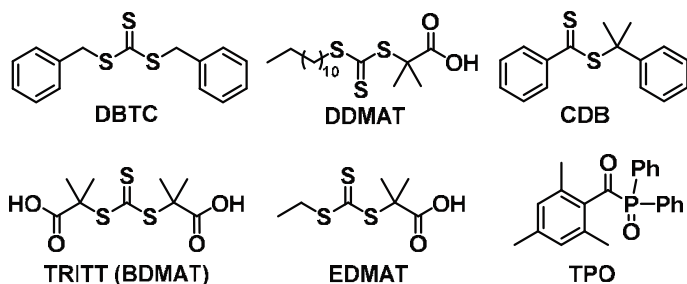


**Diagram 3.8.** Various RAFT agents employed in photoinitiated RAFT polymerizations

One of the attractions of the standard thermally induced RAFT polymerization as outlined earlier is its effectiveness toward a range of monomers without the need for protection/de-protection steps. In 2007, the effectiveness of RAFT polymerization under UV irradiation of acrylic acid (AA) carried out in water was reported [MUT 07]. The RAFT agent, S,S-bis(R,R'-dimethyl-R''-acetic acid) trithiocarbonate (TRITT also known as BDMAT) was employed in absence of additional photoinitiator under UV irradiation at 365 nm in water and at room temperature. It was reported that the initiation of polymerization of AA was due to R group radicals derived from the CTA TRITT. It was found that the conversion was linearly proportional to the number-average molecular weight when AA/TRITT = 600 and polymerizations gave PDI values  $\leq 1.1$ . It was also noted that over 50% polymer conversion could be achieved after only 5 h of polymerization, while maintaining a low PDI of 1.08 ( $M_n = 23,000 \text{ g mol}^{-1}$ ). Increasing the ratio of AA/TRITT moved the polymerization to higher molecular weights faster, achieving  $23,000 \text{ g mol}^{-1}$  in 3 h. This served to indicate the very controlled nature of the UV-initiated RAFT polymerization of AA carried out in this fashion. The authors underlined how resulting polymers obtained with 50% conversion after 5 h maintained their yellow color indicating the chromophoric trithiocarbonate had not decomposed as had happened in the work outlined by Davis *et al.* Attention was also drawn to how the conditions were environmentally friendly using water as a solvent and carried out at ambient temperatures.

Vinyl acetate (VAc) is one of the most difficult monomers to polymerize in a controlled/living manner. It must be polymerized by a radical mechanism and only a few studies have been reported with well-defined MW and PDI [IOV 03, YAM 04, KOU 08, KOU 08, WAK 01, YAN 10,

DEB 05]. Recently, the group of Kwak and coworkers has reported the use of xanthates as RAFT agent using together with bis(2,4,6-trimethylbenzoyl) phenylphosphine oxide (BAPO) as photoinitiator under UV irradiation to effectively polymerize VAc in a controlled manner (Diagram 3.9). A screening of xanthate RAFT agents was carried out to gauge their resistance to UV decomposition and it was found that methyl(ethoxycarbonothioyl) sulfanylacetate (MESA) and methyl(isopropoxyxycarbonothioyl) sulfanylacetate (MPSA) were very stable under UV irradiation. A stable xanthate RAFT agent was critical to ensure an effective RAFT mechanism and to suppress the photoiniferter or reversible termination process. The UV induced RAFT polymerizations of VAc mediated by MESA and photoinitiated by BAPO, carried out at 60°C, yielded PAVc ( $M_n = 10,500 \text{ g mol}^{-1}$ , PDI = 1.23) after just one hour with 73% conversion.

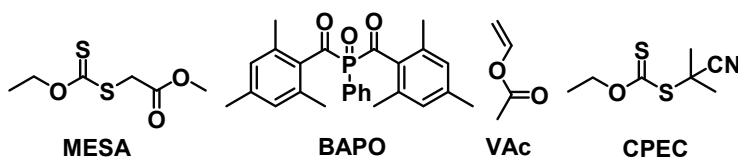


**Diagram 3.9.** Key components of the UV-induced RAFT polymerization of vinyl acetate

The proof of the concept was provided as no polymer was formed when no UV radiation was applied neither was any obtained without the use of the photoinitiator BAPO, indicating the stability of the RAFT agent and absence of photoiniferter process. In the absence of the RAFT agent MESA, an uncontrolled process was observed which results in the formation of a polymer of PDI = 3.35. However, the authors noted that loss of control was observed on approaching higher conversions and attributed this to instability of the xanthate-polymer chain adduct toward UV radiation and beginning of reversible termination mechanism.

Several groups have also reported the synthesis of polystyrene [RAN 07], poly(methyl methacrylate) [VEE 11] and poly(styrene-*alt*-maleic anhydride) [WU 03] via photoinitiated RAFT polymerization. However, this method exhibits some limitations such as low conversions even at long

polymerization times. The molecular weight distribution broadened significantly at long irradiation times due to the decomposition of the chain transfer agent moieties at the polymer ends. There have been a number of attempts to improve the photoinduced RAFT polymerization. For example, the degradation of chain transfer agent at the polymer ends can be minimized either by cutting-off the short-wave UV radiation using a filter or higher monomer conversion can be reached by the addition of a commercially available photoinitiator to the polymerization media.

### **3.3. Photoinitiated living ionic polymerization**

#### **3.3.1. *Living cationic photopolymerization***

The vast majority of progress made in the field of polymer chemistry in recent times has been based around controlled radical polymerization. However, significant strides have been made with regard to polymerizations which are propagated by ionic species. The drawbacks, which radical polymerizations suffer from, include the transitory nature of radical species and their great inhibition by oxygen. Also, monomer to polymer conversion in radical polymerization often leads to the problem of shrinkage and shrinkage-induced stress. Polymerizations propagated by ionic species typically do not suffer the same drawbacks as radical polymerizations such as oxygen inhibition and radical-based termination processes. Photogeneration of ionic species can be beneficial as the photogenerated ionic species can be longer lived than radical species and so polymerization can continue in the dark, once initiated. In this regard, there has been much research carried out toward investigating the scope of polymerization propagated by photo-generated ionic species [SHI 96]. And with respect to this, there has been much effort put into the development of photoinitiated cationic and anionic polymerization systems [TAS 08a, DOS 96, YAĞ 90, YAĞ 88b, YAĞ 92b, YAĞ 88a, BOT 91, KAS 03b, DEN 95, HIZ 94, ORA 09].

Crivello and coworkers were the first to report the use of iodonium and sulfonium salts as photoinitiators in cationic polymerization back in the 1970s [CRI 78, CRI 77, CRI 79]. Since then, research into this field has led to the development of a variety of onium salts commonly known as

photoacid generators for the generation of cations in high quantum yield [YAĚ 10]. The iodonium [CRI 77], sulfonium [CRI 79, DEN 95] and alkoxyopyridinium [YAĚ 92a, YAĚ 97, YAĚ 93] salts are particularly important cationic photoinitiators because of their thermal stability, their efficiency toward generating reactive species upon photolysis and general solubility in the relevant monomers [GOM 01]. Upon irradiation of light, the onium salt or photoinitiator undergoes photolysis or decomposition. This leads to the formation of a radical cation which reacts with either solvent or monomer which thereafter forms a Brønsted acid. It is the acid which then initiates polymerization. This process has been studied and investigated extensively as applied toward the polymerization of various epoxy and vinyl ethers [YAĚ 38, CRI 01, CRI 99, FOU 94, CRI 84].

It has been reported that the synthesis of well-defined macromolecules with structural control can also be achieved by living cationic polymerization of appropriate monomers [FAU 87]. A key to the success of the living cationic polymerization of vinyl ethers is the stabilization of the unstable carbocations via suitable nucleophilic counterion. There are two ways to stabilize the carbocations: (1) generation of a suitable nucleophilic counterion resulting from the initiator and the catalyst, and (2) addition of nucleophilic agents to the polymerization media. In the first way, Bronsted acids like hydrogen iodide are employed as the initiators, while Lewis acids like zinc iodide are employed as the catalysts (Diagram 3.10) [KAM 91, MIY 84, KAM 92a, KAM 92b].

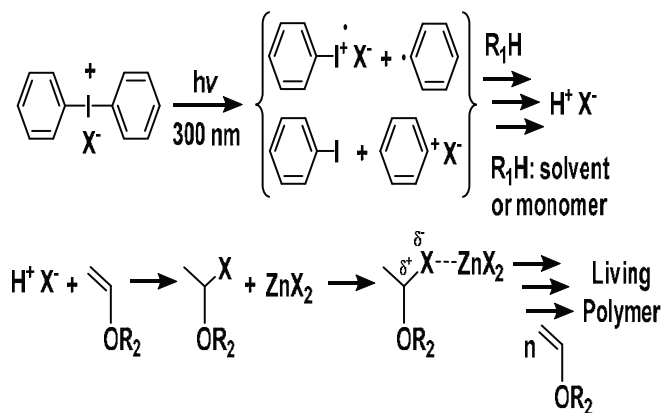


**Diagram 3.10.** Photoinitiated living cationic polymerization of isobutyl vinyl ether by iodonium salts and zinc halides

Recently, photoinduced living cationic polymerization of isobutyl vinyl ether (IBVE) in the presence of various diphenyliodonium salts and zinc halides was reported by Mah and coworkers [KAH 07, KAH 08b, KWO 06, KWO 04]. Photochemically generated protonic acid reacts with IBVE to form the corresponding monomer adduct. Terminal carbon-halide bond of the adduct is activated by the coordinating effect of zinc halide (equation 116). This activation leads to generation of suitable nucleophilic counterion by stabilizing the growing carbocation (equation 117). Thus, chain breaking processes are prevented and living cationic polymerization of IBVE proceeds. This approach was successfully employed also in free radical promoted and sensitized systems. The main advantage of these systems is the use of onium salts with highly nucleophilic counter ions such as bromide and chloride. It is well known that the onium compounds with non-nucleophilic counter ion of especially  $\text{SbF}_6^-$  and  $\text{AsF}_6^-$ , exhibit high toxicity and low cost efficiency because of their central heavy metals. Duan *et al.* and Gebel reported that long-term exposure of these metal salts to human skin led to increased incidences of various cancers [GEB 97, DUA 05]. Furthermore, the preparation of such initiators from their corresponding onium salts with halides requires additional steps, i.e. counter anion exchange; this thus makes them expensive [YAG 98, CRI 77].

This concept was further extended to totally eliminate the use of iodonium salts as the component of the photoinitiating system [KAH 09]. The cationic polymerization of vinyl ethers was initiated upon irradiation at  $\lambda = 350 \text{ nm}$  with vinyl halides in the presence of zinc iodide. A mechanism involving the formation of an adduct between the monomer and the products yielded from the photoinduced homolysis of the vinyl halide followed by electron transfer is proposed. In the subsequent step, the terminal carbon-halide bond in this adduct is activated by the coordinating effect of zinc iodide. This polymerization exhibited some characteristics of pseudo-living cationic polymerization.

In the second way, the addition of nucleophilic agents to the polymerization media has been used to suppress side reactions. For example, when the polymerization is performed in the presence of dimethyl sulfide, the polymers obtained display characteristics of living polymerization such as narrow polydispersity and well-defined chain end functionality due to suppression of side reactions [PER 87]. In this case, the polymerization

reaches an equilibrium between the alkoxy-carbenium ion (growing chain) and trialkylsulfonium species (Diagram 3.11) [PER 87]. Indeed, the latter reaction is predominant; thus, chain transfer and termination reactions are prevented to lead to living polymerization.

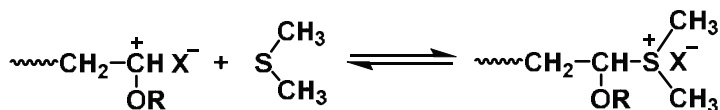


**Diagram 3.11.** Equilibrium between alkoxy-carbenium ion (growing chain) and trialkylsulfonium salt

Similar to the strategy employed in vinyl ether polymerization, the addition of sulfides was considered as a way to achieve living cationic polymerization of epoxides. The effect of additional sulfides on onium salt induced photoinitiated cationic ring opening polymerization of epoxides was reported by Crivello [FAL 05]. Polymerization profiles of the monomers like cyclohexene oxide and 1,2-epoxyhexane were monitored by optical pyrometry and real-time FT-IR spectroscopy. Dialkyl sulfides inhibit the polymerization rate as a result of its nucleophilic nature, which competes with monomers to attack to the growing chain end cation, and even overwhelms it. However, if sulfides with moderate basicity like diaryl sulfides and thianthrene are used, the polymerization is retarded. The polymerization rates and monomer conversions are decreased with increasing amount of aryl sulfides. Diagram 3.12 demonstrates the attack of the sulfide group on the growing oxonium ion instead of the epoxide monomer. Thus, the nucleophilic nature of the sulfide determines the role of the additive in the polymerization. Retardation of the ring opening polymerization of epoxides, may be employed in order to prevent chain transfer and termination reactions and living conditions can thus be attained.

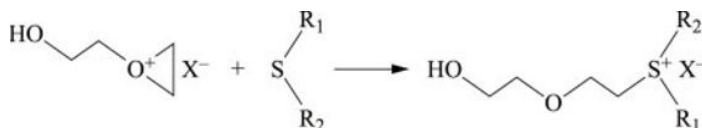


**Diagram 3.12.** Reaction of sulfide group with growing oxonium ion

### 3.3.2. Living anionic photopolymerization

The level of research and development which has been carried out with respect to photoinduced anionic polymerization has not nearly been as great as has been carried out for the photoinduced radical and cationic systems [SUY 09]. However, there are several types of reactions that can be catalyzed by base and are important on an industrial scale such as the formation of urethane from alcohols and isocyanates, epoxy ring-opening by nucleophiles and Michael addition reactions. Base catalysis could even be thought to hold some advantages as it is generally not as sensitive toward oxygen and moisture such as the radical and cationic systems are, respectively. However, one of the main drawbacks in using base catalyzed processes in polymerization is the lack of successful and efficient photoinitiating systems. In 1987, Fukuchi *et al.* reported the first work regarding photoinduced anionic polymerization when they published their work concerning the anionic coordination polymerization of epoxides by a titanium tetraisopropoxide and photochemically derived phenol catalyst system (Diagram 3.13) [FUK 87].

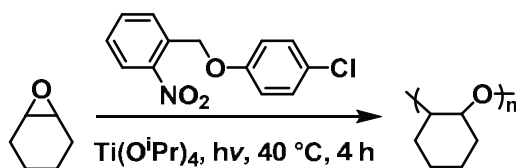


**Diagram 3.13.** First reported photoinduced anionic polymerization by Fukuchi *et al.*

There are some examples of the use of so-called photobase generators in the preparation of polymers by anionic means. Photobase generators are compounds that produce bases upon irradiation with light, examples include cobalt complexes O-acyloximines and benzyloxycarbonyl derivatives. PBGs are generally important in polymer science due to their application in photoinitiated transformation of polymeric materials and epoxy resins. Kotal *et al.* have reported the anionic polymerization of alkyl 2-cyanoacrylates initiated by anionic species upon the irradiation of group 8 metallocenes [YAM 98, YAM 99, YAM 00, SAN 02, BRI 02, DIN 03, SAN 05,

YAM 07]. For example, they have reported the implementation of the  $\text{Pt}(\text{acac})_2$  complex toward the photoinitiated anionic polymerization of ethyl- $\alpha$ -cyanoacrylate (ECA) [PAL 95]. It is understood that the initiating species were free acetylacetonate anions freed by UV excitation of the complex (Diagram 3.14).

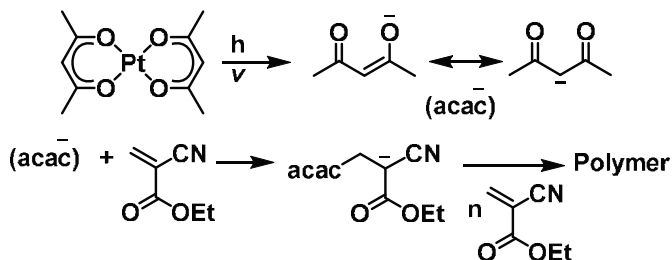


**Diagram 3.14.**  $\text{Pt}(\text{acac})_2$  used as a photoinitiator for the photoinduced anionic polymerization of ECA

Also, it has been shown that the polymerization of alkyl cyanoacrylates can be driven forward by tertiary amines such as pyridine whereby the active mechanism is thought to move through a zwitterionic pathway [JOH 81]. Through work emanating from the authors' laboratory, it has also been shown that weak photobase generator systems can be used to initiate a zwitterionic pathway toward a photoinitiated anionic polymerization of cyano acrylates. *N*-Alkoxypyridinium and *N*-phenacylpyridinium type salts were described as the active initiators for these systems (Diagram 3.15) [ARS 96, ONE 99, KAS 03a].

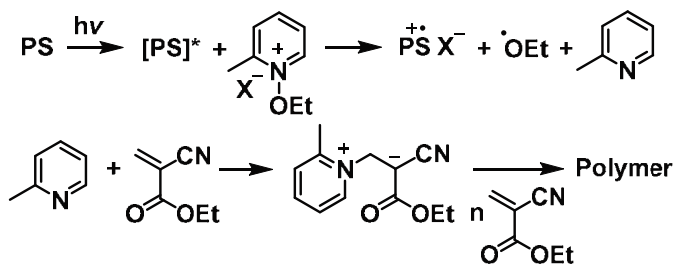


**Diagram 3.15.** *N*-alkoxypyridinium salt used for the photoinitiated anionic polymerization of ECA

Manners reported that sila[1]ferrocenophanes undergo ring-opening polymerization when treated with  $\text{Na}[\text{C}_5\text{H}_5]$  and UV light (Diagram 3.16) [TAN 06]. This reaction proceeds through a Si-Cp bond cleavage mechanism as the incoming Cp anion displaces one of the Cp ligands in the ferrocenophane. This reaction exhibits characteristics of living polymerizations such as controlling of molecular weight, narrowing molecular weight distributions and enabling block copolymer synthesis as anionic ring-opening polymerization initiated by strong nucleophilic bases such as *n*-butyl lithium [TAN 04, MUS 13]. Recently a new monomer type, dicarba[2]ferrocenophanes, bearing alternative bridging moieties, has been used in photoinitiated anionic polymerization. The photoinitiated polymerization of dicarba[2]ferrocenophanes affords soluble polyferrocenylethylene products with narrow polydispersities [HER 09b]. The control of molecular weight was effectively demonstrated through variation of the monomer to initiator ratios. Moreover, the synthetic capability of this technique was explored through the addition of dimethylsila[1]-ferrocenophane as a second monomer to the polyferrocenylethylene macroinitiator to obtain polyferrocenylethylene-*b*-polyferrocenylsilane block copolymer. In another study, synthesis of cyclic polyferrocenylsilanes has been successfully synthesized by photoinduced anionic polymerization of dimethylsila[1]ferrocenophane in the presence of a Lewis base such as 4,4'-dimethyl-2,2'-bipyridine [HER 09a].

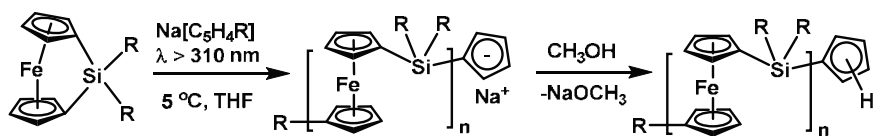


**Diagram 3.16.** Photoinitiated anionic polymerization of ferrocenophanes

### 3.4. Acknowledgments

One of the authors (Sean Doran) of this chapter would like to acknowledge and thank TUBITAK for the 2236 Co-Funded Brain Circulation Scheme (co-circulation scheme) partially supported by the ECFP7 Marie Curie Actions-People-COFUND and coordinated by BIIDEB as a source of funding.

### 3.5. Bibliography

- [AND 01] ANDRZEJEWSKA E., “Photopolymerization kinetics of multifunctional monomers”, *Progress in Polymer Science*, vol. 26, pp. 605–665, 2001.
- [ARS 96] ARSU N., ONEN A., YAĞCI Y., “Photoinitiated zwitterionic polymerization of alkyl cyanoacrylates by pyridinium salts”, *Macromolecules*, vol. 29, pp. 8973–8974, 1996.
- [ANA 14a] ANASTASAKI A., NIKOLAOU V., PAPPAS G.S. *et al.*, “Photoinduced sequence-control via one pot living radical polymerization of acrylates”, *Chemical Science*, vol. 5, pp. 3536–3542, 2014.
- [ANA 14b] ANASTASAKI A., NIKOLAOU V., SIMULA A. *et al.*, “Electrophoretic mobility of double-stranded DNA in polymer solutions and gels with tuned structures”, *Macromolecules*, vol. 47, pp. 3852–3859, 2014.
- [ANA 14c] ANASTASAKI A., NIKOLAOU V., ZHANG Q. *et al.*, “Copper(II)/tertiary amine synergy in photoinduced living radical polymerization: accelerated synthesis of  $\omega$ -functional and  $\alpha,\omega$ -heterofunctional poly(acrylates)”, *Journal of American Chemical Society*, vol. 136, pp. 1141–1149, 2014.
- [BOT 91] BOTTCHE A., HASEBE K., HIZAL G. *et al.*, “Initiation of cationic polymerization via oxidation of free radicals using pyridinium salts”, *Polymer*, vol. 32, pp. 2289–2293, 1991.
- [BRI 02] BRINKMANN N.R., SCHAEFER H.F., SANDERSON C.T. *et al.*, “Can the radical anion of alkyl-2-cyanoacrylates initiate anionic polymerization of These instant adhesive monomers”, *Journal of Physical Chemistry A*, vol. 106, pp. 847–853, 2002.
- [CIF 13a] CIFTCI M., BATAT P., DEMIREL A.L. *et al.*, “Visible light-induced grafting from polyolefins”, *Macromolecules*, vol. 46, pp. 6395–6401, 2013.
- [CIF 13b] CIFTCI M., TASDELEN M.A., LI W. *et al.*, “Photoinitiated ATRP in inverse microemulsion”, *Macromolecules*, vol. 46, pp. 9537–9543, 2013.
- [CIF 14] CIFTCI M., TASDELEN M.A., YAĞCI Y., “Sunlight induced atom transfer radical polymerization by using dimanganese decacarbonyl”, *Polymer Chemistry*, vol. 5, pp. 600–606, 2014.
- [CHI 98] CHIEFARI J., CHONG Y.K., ERCOLE F. *et al.*, “Living free-radical polymerization by reversible addition–fragmentation chain transfer: The RAFT process”, *Macromolecules*, vol. 31, pp. 5559–5562, 1998.

- [CRI 77] CRIVELLO J.V., LAM J.H.W., “Diaryliodonium salts. A new class of photoinitiators for cationic polymerization”, *Macromolecules*, vol. 10, pp. 1307–1315, 1977.
- [CRI 78] CRIVELLO J.V., LAM J.H.W., “Dye-sensitized photoinitiated cationic polymerization”, *Journal of Polymer Science Part A: Polymer Chemistry*, vol. 16, pp. 2441–2451, 1978.
- [CRI 79] CRIVELLO J.V., LAM J.H.W., “Photoinitiated cationic polymerization with triarylsulfonium salts”, *Journal of Polymer Science Part A: Polymer Chemistry*, vol. 17, pp. 977–999, 1979.
- [CRI 84] CRIVELLO J.V., “Cationic polymerization – Iodonium and sulfonium salt photoinitiators”, *Advances in Polymer Science*, vol. 62, pp. 1–48, 1984.
- [CRI 99] CRIVELLO J.V., “The discovery and development of onium salt cationic photoinitiators”, *Journal of Polymer Science Part A: Polymer Chemistry*, vol. 37, pp. 4241–4254, 1999.
- [CRI 01] CRIVELLO J.V., SANGERMANO M., “Visible and long-wavelength photoinitiated cationic polymerization”, *Journal of Polymer Science Part A: Polymer Chemistry*, vol. 39, pp. 343–356, 2001.
- [DAD 14a] DADASHI-SILAB S., TASDELEN M.A., ASIRI A.M. *et al.*, “Photoinduced atom transfer radical polymerization using semiconductor nanoparticles”, *Macromolecular Rapid Communications*, vol. 35, pp. 454–459, 2014.
- [DAD 14b] DADASHI-SILAB S., TASDELEN M.A., KISKAN B. *et al.*, “Photochemically mediated atom transfer radical polymerization using polymeric semiconductor mesoporous graphitic carbon nitride”, *Macromolecular Chemistry and Physics*, vol. 215, pp. 675–681, 2014.
- [DEB 05] DEBUIGNE A., CAILLE J.-R., JÉRÔME R., “Highly efficient cobalt-mediated radical polymerization of vinyl acetate”, *Angewandte Chemie International Edition*, vol. 44, pp. 1101–1104, 2005.
- [DEC 98] DECKER C., “Highly efficient cobalt-mediated radical polymerization of vinyl acetate”, *Polymer International*, vol. 45, pp. 133–141, 1998. The use of UV irradiation in polymerization.
- [DEC 02] DECKER C., “Kinetic study and new applications of uv radiation curing”, *Macromolecular Rapid Communications*, vol. 23, pp. 1067–1093, 2002.
- [DEN 95] DENIZLIGIL S., YAĞCI Y., MCARDLE C., “Photochemically and thermally induced radical promoted cationic polymerization using an allylic sulfonium salt”, *Polymer*, vol. 36, pp. 3093–3098, 1995.

- [DEV 97] DEVONPORT W., MICHALAK L., MALMSTROM E. *et al.*, ““Living” free-radical polymerizations in the absence of initiators: controlled autopolymerization”, *Macromolecules*, vol. 30, pp. 1929–1934, 1997.
- [DIN 03] DING W., SANDERSON C.T., CONOVER R.C. *et al.*, “Characterization of the low-energy electronic excited states of benzoyl-substituted ferrocenes”, *Inorganic Chemistry*, vol. 42, pp. 1532–1537, 2003.
- [DIZ 11] DIZMAN C., ATEŞ S., UYAR T. *et al.*, “Polysulfone/clay nanocomposites by in situ photoinduced crosslinking polymerization”, *Macromolecular Materials and Engineering*, vol. 296, pp. 1101–1106, 2011.
- [DIZ 13] DIZMAN C., UYAR T., TASDELEN M.A. *et al.*, “Synthesis and characterization of polysulfone/POSS hybrid networks by photoinduced crosslinking polymerization”, *Macromolecular Materials and Engineering*, vol. 298, pp. 1117–1123, 2013.
- [DON 08] DONG H., MATYJASZEWSKI K., “ARGET ATRP of 2-(Dimethylamino)ethyl Methacrylate as an intrinsic reducing agent”. *Macromolecules*, vol. 41, pp. 6868–6870, 2008.
- [DOS 96] DOSSOW D., ZHU Q.Q., HIZAL G. *et al.*, “Photosensitized cationic polymerization of cyclohexene oxide: A mechanistic study concerning the use of pyridinium-type salts”, *Polymer*, vol. 37, pp. 2821–2826, 1996.
- [DUA 05] DUAN G.L., ZHU Y.G., TONG Y.P. *et al.*, “Characterization of arsenate reductase in the extract of roots and fronds of chinese brake fern, an arsenic hyperaccumulator”, *Plant Physiology*, vol. 138, pp. 461–469, 2005.
- [FAL 05] FALK B., ZONCA M.R., CRIVELLO J.V., “Modification of photoinitiated cationic epoxide polymerizations by sulfides”, *Journal of Polymer Science Part A: Polymer Chemistry*, vol. 43, pp. 2504–2519, 2005.
- [FAU 87] FAUST R., KENNEDY J.P., “Living carbocationic polymerization. IV. Living polymerization of isobutylene”, *Journal of Polymer Science Part A: Polymer Chemistry*, vol. 25, pp. 1847–1869, 1987.
- [FOR 12] FORS B.P., HAWKER C.J., “Control of a living radical polymerization of methacrylates by light”, *Angewandte Chemie International Edition*, vol. 51, pp. 8850–8853, 2012.
- [FOR 13] FORS B.P., POELMA J.E., MENYO M.S. *et al.*, “Fabrication of unique chemical patterns and concentration gradients with visible light”, *Journal of American Chemical Society*, vol. 135, pp. 14106–14109, 2013.

- [FOU 94] FOUASSIER J.P., BURR D., CRIVELLO J.V., “Photochemistry and photopolymerization activity of diaryliodonium salts”, *Journal of Macromolecular Science*, Part A. Pure and Applied Chemistry, vol. A31, pp. 677–701, 1994.
- [FUK 87] FUKUCHI Y., TAKAHASHI T., NOGUCHI H. *et al.*, “Photoinitiated anionic coordination polymerization of epoxides, a novel polymerization process”, *Macromolecules*, vol. 20, pp. 2316–2317, 1987.
- [GEB 97] GEBEL T., “Arsenic and antimony: comparative approach on mechanistic toxicology”, *Chemico-Biological Interactions*, vol. 107, pp. 131–144, 1997.
- [GOM 01] GOMURASHVILI Z., CRIVELLO J.V., “Phenothiazine photosensitizers for onium salt photoinitiated cationic polymerization”, *Journal of Polymer Science Part A: Polymer Chemistry*, vol. 39, pp. 1187–1197, 2001.
- [GOT 07] GOTO A., SCAIANO J.C., MARETTI L., “Photolysis of an alkoxyamine using intramolecular energy transfer from a quinoline antenna-towards photo-induced living radical polymerization”, *Photochemical & Photobiological Sciences*, vol. 6, pp. 833–835, 2007.
- [GRA 98] GRANEL C., JEROME R., TEYSSIE P. *et al.*, “Investigation of methyl methacrylate and vinyl acetate polymerization promoted by Al(iBu)<sub>3</sub>/2,2′-Bipyridine and Al(iBu)<sub>3</sub>/2,2′-Bipyridine/TEMPO Complexes”, *Macromolecules*, vol. 31, pp. 7133–7141, 1998.
- [GUA 00] GUAN Z.B., SMART B., “A remarkable visible light effect on atom-transfer radical polymerization”, *Macromolecules*, vol. 33, pp. 6904–6906, 2000.
- [GUI 10] GUILLANEUF Y., BERTIN D., GIGMES D. *et al.*, “Toward nitroxide-mediated photopolymerization”, *Macromolecules*, vol. 43, pp. 2204–2212, 2010.
- [HAY 91] HAYASE K., ZEPP R.G., “Photolysis of copper(II)-amino acid complexes in water”, *Environmental Science & Technology*, vol. 25, pp. 1273–1279, 1991.
- [HER 09a] HERBERT D.E., GILROY J.B., CHAN W.Y. *et al.*, “Redox-active metallomacrocycles and cyclic metallopolymers: photocontrolled ring-opening oligomerization and polymerization of silicon-bridged [1]ferrocenophanes using substitutionally-labile lewis bases as initiators”, *Journal of American Chemical Society*, vol. 131, pp. 14958–14968, 2009.
- [HER 09b] HERBERT D.E., MAYER U.F.J., GILROY J.B. *et al.*, “Photocontrolled ring-opening polymerization of strained dicarba[2]ferrocenophanes: a route to well-defined polyferrocenylethylene homopolymers and block copolymers”, *Chem. Eur. J.*, vol. 15, pp. 12234–12246, 2009.

- [HIZ 94] HIZAL G., YAĞCI Y., SCHNABEL W., “Charge-transfer complexes of pyridinium ions and methyl- and methoxy-substituted benzenes as photoinitiators for the cationic polymerization of cyclohexene oxide and related compounds”, *Polymer*, vol. 35, pp. 2428–2431, 1994.
- [IOV 03] IOVU M.C., MATYJASZEWSKI K., “Controlled/living radical polymerization of vinyl acetate by degenerative transfer with alkyl iodides”, *Macromolecules*, vol. 36, pp. 9346–9354, 2003.
- [JOH 81] JOHNSTON D.S., PEPPER D.C., “Polymerisation via macrozwitterions, 3. Ethyl and butyl cyanoacrylates polymerised by benzyldimethyl, triethyl and tribenzylamines”, *Macromolecular Chemistry and Physics*, vol. 182, pp. 421–435, 1981.
- [KAH 07] KAHVECI M.U., TASDELEN M.A., YAĞCI Y., “Photochemically initiated free radical promoted living cationic polymerization of isobutyl vinyl ether”, *Polymer*, vol. 48, pp. 2199–2202, 2007.
- [KAH 08a] KAHVECI M.U., TASDELEN M.A., COOK W.D. *et al.*, “Photoinitiated cationic polymerization of mono and divinyl ethers in aqueous medium using ytterbium triflate as lewis acid”, *Macromolecular Chemistry and Physics*, vol. 209, pp. 1881–1886, 2008.
- [KAH 08b] KAHVECI M.U., TASDELEN M.A., YAĞCI Y., “Photo-induced cross-linking of divinyl ethers by using diphenyliodonium salts with highly nucleophilic counter anions in the presence of zinc halides”, *Macromolecular Rapid Communications*, vol. 29, pp. 202–206, 2008.
- [KAH 09] KAHVECI M.U., UYGUN M., TASDELEN M.A. *et al.*, “Photoinitiated cationic polymerization of vinyl ethers using substituted vinyl halides”, *Macromolecules*, vol. 42, pp. 4443–4448, 2009.
- [KAM 91] KAMIGAITO M., SAWAMOTO M., HIGASHIMURA T., “Living cationic polymerization of isobutyl vinyl ether by RCOOH/Lewis acid initiating systems: effects of carboxylate ions and Lewis acid activators”, *Macromolecules*, vol. 24, pp. 3988–3992, 1991.
- [KAM 92a] KAMIGAITO M., SAWAMOTO M., HIGASHIMURA T., “Living cationic polymerization of isobutyl vinyl ether by protonic acid/zinc halide initiating systems: evidence for the halogen exchange with zinc halide in the growing species”, *Macromolecules*, vol. 25, pp. 2587–2591, 1992.
- [KAM 92b] KAMIGAITO M., YAMAOKA K., SAWAMOTO M. *et al.*, “Living cationic polymerization of isobutyl vinyl ether by benzoic acid derivatives/zinc chloride initiating systems: slow interconversion between dormant and activated growing species”, *Macromolecules*, vol. 25, pp. 6400–6406, 1992.

- [KAS 03a] KASAPOGLU F., AYDIN M., ARSU N. *et al.*, “Photoinitiated polymerization of methyl methacrylate by phenacyl type salts”, *Journal of Photochemistry and Photobiology A*, vol. 159, pp. 151–159, 2003.
- [KAS 03b] KASAPOGLU F., CIANGA I., YAĞCI Y. *et al.*, “Photoinitiated cationic polymerization of monofunctional benzoxazine”, *Journal of Polymer Science Part A: Polymer Chemistry*, vol. 41, pp. 3320–3328, 2003.
- [KAT 95] KATO M., KAMIGAITO M., SAWAMOTO M. *et al.*, “Polymerization of Methyl Methacrylate with the Carbon Tetrachloride/Dichlorotrakis(triphenylphosphine)ruthenium(II)/Methylaluminum Bis(2,6-di-tert-butylphenoxide) Initiating System: Possibility of Living Radical Polymerization”, *Macromolecules*, vol. 28, pp. 1721–1723, 1995.
- [KOL 96] KOLCZAK U., RIST G., DIETLIKER K. *et al.*, “Reaction mechanism of monoacyl- and bisacylphosphine oxide photoinitiators studied by  $^{31}\text{P}$ -,  $^{13}\text{C}$ -, and  $^1\text{H}$ -CIDNP and ESR”, *Journal of American Chemical Society*, vol. 118, pp. 6477–6489, 1996.
- [KON 12] KONKOLEWICZ D., SCHROEDER K., BUBACK J. *et al.*, “Visible light and sunlight photoinduced ATRP with ppm of Cu Catalyst”, *ACS Macro Letters*, vol. 1, pp. 1219–1223, 2012.
- [KOU 08] KOUMURA K., SATOH K., KAMIGAITO M., “Manganese-Based controlled/living radical polymerization of vinyl acetate, methyl acrylate, and styrene: Highly active, versatile, and photoresponsive systems”, *Macromolecules*, vol. 41, pp. 7359–7367, 2008.
- [KOU 09] KOUMURA K., SATOH K., KAMIGAITO M., “ $\text{Mn}_2(\text{CO})_{10}$ -induced controlled/living radical copolymerization of vinyl acetate and methyl acrylate: Spontaneous formation of block copolymers consisting of gradient and homopolymer segments”, *Journal of Polymer Science Part A: Polymer Chemistry*, vol. 47, pp. 1343–1353, 2009.
- [KWA 10] KWAK Y., MATYJASZEWSKI K., “Photoirradiated atom transfer radical polymerization with an alkyl dithiocarbamate at ambient temperature”, *Macromolecules*, vol. 43, pp. 5180–5183, 2010.
- [KWA 11] KWAK Y., MAGENAU A.J.D., MATYJASZEWSKI K., “ARGET ATRP of methyl acrylate with inexpensive ligands and ppm concentrations of catalyst”, *Macromolecules*, vol. 44, pp. 811–819, 2011.
- [KWO 04] KWON S., CHUN H., MAH S., “Photo-induced living cationic polymerization of isobutyl vinyl ether in the presence of various combinations of halides of diphenyliodonium and zinc salts in methylene chloride”, *Fibers and Polymers*, vol. 5, pp. 253–258, 2004.

- [KWO 06] KWON S., LEE Y., JEON H. *et al.*, “Living cationic polymerization of isobutyl vinyl ether (II): Photoinduced living cationic polymerization in a mixed solvent of toluene and diethyl ether”, *Journal of Applied Polymer Science*, vol. 101, pp. 3581–3586, 2006.
- [LAL 07] LALEVÉE J., EL-ROZ M., ALLONAS X. *et al.*, “Controlled photopolymerization reactions: The reactivity of new photoiniferters”, *Journal of Polymer Science Part A: Polymer Chemistry*, vol. 45, pp. 2436–2442, 2007.
- [LEE 08] LEE K.-S., KIM R.H., YANG D.-Y. *et al.*, “Advances in 3D nano/microfabrication using two-photon initiated polymerization”, *Progress in Polymer Science*, vol. 33, pp. 631–681, 2008.
- [LU 05] LU L., YANG N., CAI Y., “Well-controlled reversible addition-fragmentation chain transfer radical polymerisation under ultraviolet radiation at ambient temperature”, *Chemical Communications*, vol. 52, pp. 5287–5288, 2005.
- [MAR 94] MARDARE D., MATYJASZEWSKI K., “‘Living’ radical polymerization of vinyl acetate”, *Macromolecules*, vol. 27, pp. 645–649, 1994.
- [MAT 95] MATYJASZEWSKI K., GAYNOR S., GRESZTA D. *et al.*, “‘Living’ and controlled radical polymerization”, *Journal of Physical Organic Chemistry*, vol. 8, pp. 306–315, 1995.
- [MAT 07] MATYJASZEWSKI K., TSAREVSKY N.V., BRAUNECKER W.A. *et al.*, “Role of Cu<sup>0</sup> in Controlled/‘Living’ Radical Polymerization”, *Macromolecules*, vol. 40, pp. 7795–7806, 2007.
- [MAY 00] MAYADUNNE R.T.A., RIZZARDO E., CHIEFARI J. *et al.*, “Living polymers by the use of trithiocarbonates as reversible addition–fragmentation chain transfer (RAFT) Agents: ABA triblock copolymers by radical polymerization in two steps”, *Macromolecules*, vol. 33, pp. 243–245, 2000.
- [MIY 84] MIYAMOTO M., SAWAMOTO M., HIGASHIMURA T., “Living polymerization of isobutyl vinyl ether with hydrogen iodide/iodine initiating system”, *Macromolecules*, vol. 17, pp. 265–268, 1984.
- [MOR 15] MORRIS J., TELITEL S., FAIRFULL-SMITH K.E. *et al.*, “Novel polymer synthesis methodologies using combinations of thermally- and photochemically-induced nitroxide mediated polymerization”, *Polymer Chemistry*, 2015.
- [MOS 12] MOSNACEK J., ILCIKOVA M., “Photochemically mediated atom transfer radical polymerization of methyl methacrylate using ppm amounts of catalyst”, *Macromolecules*, vol. 45, pp. 5859–5865, 2012.
- [MUS 13] MUSGRAVE R.A., RUSSELL A.D., MANNERS I., “Strained ferrocenophanes”, *Organometallics*, vol. 32, pp. 5654–5667, 2013.

- [MUT 07] MUTHUKRISHNAN S., PAN E.H., STENZEL M.H. *et al.*, “Ambient temperature RAFT polymerization of acrylic acid initiated with ultraviolet radiation in aqueous solution”, *Macromolecules*, vol. 40, pp. 2978–2980, 2007.
- [ONE 99] ONEN A., ARSU N., YAĞCI Y., “Photoinitiated polymerization of ethyl cyanoacrylate by phosphonium salts”, *Angewandte Makromolekulare Chemie*, vol. 264, pp. 56–59, 1999.
- [ORA 09] ORAL A., TASDELEN M.A., DEMIREL A.L. *et al.*, “Poly(cyclohexene oxide)/clay nanocomposites by photoinitiated cationic polymerization via activated monomer mechanism”, *Journal of Polymer Science Part A: Polymer Chemistry*, vol. 47, pp. 5328–5335, 2009.
- [OTS 82] OTSU T., YOSHIDA M., TAZAKI T., “A model for living radical polymerization”, *Macromolecular Rapid Communications*, vol. 3, pp. 133–140, 1982.
- [PAL 95] PALMER B.J., KUTAL C., BILLING R. *et al.*, “A model for living radical polymerization”, *Macromolecules*, vol. 28, pp. 1328–1329, 1995.
- [PER 87] PERCEC V., TOMAZOS D., “Liquid crystalline copoly(vinylether)s containing 4(4′)-methoxy-4′ (4)-hydroxy- $\alpha$ -methylstilbene constitutional isomers as side groups”, *Polymer Bulletin*, vol. 18, pp. 239–246, 1987.
- [PER 95] PERCEC V., BARBOIU B., ““Living” radical polymerization of styrene initiated by arenesulfonyl chlorides and CuI(bpy) $_n$ Cl”, *Macromolecules*, vol. 28, pp. 7970–7972, 1995.
- [POE 13] POELMA J.E., FORS B.P., Meyers G.F. *et al.*, “Fabrication of complex three-dimensional polymer brush nanostructures through light-mediated living radical polymerization”, *Angewandte Chemie International Edition*, vol. 52, pp. 6844–6848, 2013.
- [QIN 01] QIN S.H., QIN D.Q., QIU K.Y., “A novel photo atom transfer radical polymerization of methyl methacrylate”, *New Journal of Chemistry*, vol. 25, pp. 893–895, 2001.
- [QUI 02] QUINN J.F., BARNER L., BARNER-KOWOLLIK C. *et al.*, “Reversible addition–fragmentation chain transfer polymerization initiated with ultraviolet radiation”, *Macromolecules*, vol. 35, pp. 7620–7627, 2002.
- [RAN 07] RAN R., YU Y., WAN T., “Photoinitiated RAFT polymerization in the presence of trithiocarbonate”, *Journal of Applied Polymer Science*, vol. 105, pp. 398–404, 2007.
- [RIB 14a] RIBELLI T.G., KONKOLEWICZ D., BERNHARD S. *et al.*, “How are Radicals (Re)Generated in Photochemical ATRP?”, *Journal of American Chemical Society*, vol. 136, pp. 13303–13312, 2014.

- [RIB 14b] RIBELLI T.G., KONKOLEWICZ D., PAN X. *et al.*, “Contribution of Photochemistry to Activator Regeneration in ATRP”, *Macromolecules*, vol. 47, pp. 6316–6321, 2014.
- [SAN 02] SANDERSON C.T., PALMER B.J., MORGAN A. *et al.*, “Classical metallocenes as photoinitiators for the anionic polymerization of an alkyl 2-cyanoacrylate”, *Macromolecules*, vol. 35, pp. 9648–9652, 2002.
- [SAN 05] SANDERSON C.T., QUINLAN J.A., CONOVER R.C. *et al.*, “Characterization of the low-energy electronic excited states of benzoyl-substituted ruthenocenes”, *Inorganic Chemistry*, vol. 44, pp. 3283–3289, 2005.
- [SAN 07] SANGERMANO M., TASDELEN M.A., YAĞCI Y., “Photoinitiated curing of mono- and bifunctional epoxides by combination of active chain end and activated monomer cationic polymerization methods”, *Journal of Polymer Science Part A: Polymer Chemistry*, vol. 45, pp. 4914–4920, 2007.
- [SHI 96] SHIRAI M., TSUNOOKA M., “Photoacid and photobase generators: Chemistry and applications to polymeric materials”, *Progress in Polymer Science*, vol. 21, pp. 1–45, 1996.
- [SLU 96] SLUGGETT G.W., MCGARRY P.F., KOPTYUG I.V. *et al.*, “Laser flash photolysis and time-resolved esr study of phosphinoyl radical structure and reactivity”, *Journal of American Chemical Society*, vol. 118, pp. 7367–7372, 1996.
- [SUY 09] SUYAMA K., SHIRAI M., “Photobase generators: Recent progress and application trend in polymer systems”, *Progress in Polymer Science*, vol. 34, pp. 194–209, 2009.
- [TAN 04] TANABE M., MANNERS I., “photolytic living anionic ring-opening polymerization (ROP) of silicon-bridged [1]ferrocenophanes via an iron-cyclopentadienyl bond cleavage mechanism”, *Journal of American Chemical Society*, vol. 126, pp. 11434–11435, 2004.
- [TAN 06] TANABE M., VANDERMEULEN G.W.M., CHAN W.Y. *et al.*, “Photocontrolled living polymerizations”, *Nature Materials*, vol. 5, pp. 467–470, 2006.
- [TAS 06a] TASDELEN M.A., KISKAN B., YAĞCI Y., “Photoinitiated free radical polymerization using benzoxazines as hydrogen donors”, *Macromolecular Rapid Communications*, vol. 27, pp. 1539–1544, 2006.
- [TAS 06b] TASDELEN M.A., KUMBARACI V., TALINLI N. *et al.*, “Photochemically masked benzophenone: Photoinitiated free radical polymerization by using benzodioxinone”, *Polymer*, vol. 47, pp. 7611–7614, 2006.

- [TAS 07a] TASDELEN M.A., DEMIREL A.L., YAĞCI Y., “Poly(propylene imine) dendrimers as hydrogen donor in Type II photoinitiated free radical polymerization”, *European Polymer Journal*, vol. 43, pp. 4423–4430, 2007.
- [TAS 07b] TASDELEN M.A., KUMBARACI V., TALINLI N. *et al.*, “Photoinduced cross-linking polymerization of monofunctional vinyl monomer without conventional photoinitiator and cross-linker”, *Macromolecules*, vol. 40, pp. 4406–4408, 2007.
- [TAS 08a] TASDELEN M.A., KUMBARACI V., JOCKUSCH S. *et al.*, “Photoacid generation by stepwise two-photon absorption: photoinitiated cationic polymerization of cyclohexene oxide by using benzodioxinone in the presence of iodonium salt”, *Macromolecules*, vol. 41, pp. 295–297, 2008.
- [TAS 08b] TASDELEN M.A., DURMAZ Y.Y., KARAGOZ B. *et al.*, “A new photoiniferter/RAFT agent for ambient temperature rapid and well-controlled radical polymerization”, *Journal of Polymer Science Part A: Polymer Chemistry*, vol. 46, pp. 3387–3395, 2008.
- [TAS 09] TASDELEN M.A., MOSZNER N., YAĞCI Y., “The use of poly(ethylene oxide) as hydrogen donor in type II photoinitiated free radical polymerization”, *Polymer Bulletin*, 2009, 63,173–183.
- [TAS 10a] TASDELEN M.A., UYGUN M., YAĞCI Y., “Photoinduced controlled radical polymerization in methanol”, *Macromolecular Chemistry and Physics*, vol. 211, pp. 2271–2275, 2010.
- [TAS 10b] TASDELEN M.A., YAĞCI Y., “Light-induced copper(I)-catalyzed click chemistry”, *Tetrahedron Letters*, vol. 51, pp. 6945–6947, 2010.
- [TAS 11a] TASDELEN M.A., UYGUN M., YAĞCI Y., “Studies on photoinduced ATRP in the presence of photoinitiator”, *Macromolecular Chemistry and Physics*, vol. 212, pp. 2036–2042, 2011.
- [TAS 11b] TASDELEN M.A., UYGUN M., YAĞCI Y., “Photoinduced controlled radical polymerization”, *Macromolecular Rapid Communications*, vol. 32, pp. 58–62, 2011.
- [TAS 11c] TASDELEN M.A., YAĞCI Y., “Photochemical methods for the preparation of complex linear and cross-linked macromolecular structures”, *Australian Journal of Chemistry*, vol. 64, pp. 982–991, 2011.
- [TAS 12a] TASDELEN M.A., CIFTCI M., UYGUN M. *et al.*, in MATYJASZEWSKI K., SUMERLIN B.S., TSAREVSKY N.V. (eds), “Possibilities for photoinduced controlled radical polymerizations”, *Progress in Controlled Radical Polymerization: Mechanisms and Techniques*, vol. 1100, pp. 59–72, 2012.

- [TAS 12b] TASDELEN M.A., YILMAZ G., ISKIN B. *et al.*, “Photoinduced free radical promoted copper(i)-catalyzed click chemistry for macromolecular syntheses”, *Macromolecules*, vol. 45, pp. 56–61, 2012.
- [TAS 13] TASDELEN M.A., YAĞCI Y., “Light-induced click reactions”, *Angewandte Chemie International Edition*, vol. 52, pp. 5930–5938, 2013.
- [TAS 14] TASKIN O.S., YILMAZ G., TASDELEN M.A. *et al.*, “Photoinduced reverse atom transfer radical polymerization of methyl methacrylate using camphorquinone/benzhydryl system”, *Polymer International*, vol. 63, pp. 902–907, 2014.
- [TRE 14] TREAT N.J., FORS B.P., KRAMER J.W. *et al.*, “Controlled radical polymerization of acrylates regulated by visible light”, *ACS Macro Letters*, vol. 3, pp. 580–584, 2014.
- [VEE 11] VEETIL A.T., SOLOMEK T., NGOY B.P. *et al.*, “Photochemistry of S-phenacyl xanthates”, *Journal of Organic Chemistry*, vol. 76, pp. 8232–8242, 2011.
- [WAK 01] WAKIOKA M., BAEK K.-Y., ANDO T. *et al.*, “Possibility of living radical polymerization of vinyl acetate catalyzed by iron(I) complex”, *Macromolecules*, vol. 35, pp. 330–333, 2002.
- [WAN 95a] WANG J.S., MATYJASZEWSKI K., “Controlled/“living” radical polymerization. atom transfer radical polymerization in the presence of transition-metal complexes”, *Journal of American Chemical Society*, vol. 117, pp. 5614–5615, 1995.
- [WAN 95b] WANG J.S., MATYJASZEWSKI K., “Controlled/“living” radical polymerization. halogen atom transfer radical polymerization promoted by a Cu(I)/Cu(II) redox process”, *Macromolecules*, vol. 28, pp. 7901–7910, 1995.
- [WEN 14] WENNA B., CONRADI M., CARREIRAS A.D. *et al.*, “Photo-induced copper-mediated polymerization of methyl acrylate in continuous flow reactors”, *Polymer Chemistry*, vol. 5, pp. 3053–3060, 2014.
- [WU 03] WU D.C., HONG C.Y., PAN C.Y. *et al.*, “Study on controlled radical alternating copolymerization of styrene with maleic anhydride under UV irradiation”, *Polymer International*, vol. 52, pp. 98–103, 2003.
- [XI 14] XI W.X., SCOTT T.F., KLOXIN C.J. *et al.*, “Click chemistry in materials science”, *Advanced Functional Materials*, vol. 24, pp. 2572–2590, 2014.
- [YAĞ 88a] YAĞCI Y., LEDWITH A., “Mechanistic and kinetic studies on the photoinitiated polymerization of tetrahydrofuran”, *Journal of Polymer Science Part A: Polymer Chemistry*, vol. 26, pp. 1911–1918, 1988.

- [YAĜ 88b] YAĜCI Y., SCHNABEL W., "Light-induced cationic polymerization", *Makromolekulare Chemie, Macromolecular Symposia*, vol. 13–4, pp. 161–174, 1988.
- [YAĜ 90] YAĜCI Y., SCHNABEL W., "Light-induced synthesis of block and graft copolymers", *Progress in Polymer Science*, vol. 15, pp. 551–601, 1990.
- [YAĜ 92a] YAĜCI Y., KORNOWSKI A., Schnabel W., "N-alkoxy-pyridinium and N-alkoxy-quinolinium salts as initiators for cationic photopolymerizations", *Journal of Polymer Science Part A: Polymer Chemistry*, vol. 30, pp. 1987–1991, 1992.
- [YAĜ 92b] YAĜCI Y., SCHNABEL W., "New aspects on the photoinitiated free radical promoted cationic polymerization", *Makromolekulare Chemie, Macromolecular Symposia*, vol. 60, pp. 133–143, 1992.
- [YAĜ 93] YAĜCI Y., LUKÁČ I., SCHNABEL W., "Photosensitized cationic polymerization using N-ethoxy-2-methylpyridinium hexafluorophosphate", *Polymer*, vol. 34, pp. 1130–1133, 1993.
- [YAĜ 97] YAĜCI Y., ENDO T., "N-benzyl and N-alkoxy pyridinium salts as thermal and photochemical initiators for cationic polymerization", *Polymer Synthesis/Polymer Catalysis*, Springer, Berlin Heidelberg, vol. 127, pp. 59–86, 1997.
- [YAĜ 98] YAĜCI Y., REETZ I., "Externally stimulated initiator systems for cationic polymerization", *Progress in Polymer Science*, vol. 23, pp. 1485–1538, 1998.
- [YAĜ 99] YAĜCI Y., HEPUZER Y., "A novel visible light initiating system for cationic polymerization", *Macromolecules*, vol. 32, pp. 6367–6370, 1999.
- [YAĜ 10] YAĜCI Y., JOCKUSCH S., TURRO N.J., "Photoinitiated polymerization: advances, challenges, and opportunities", *Macromolecules*, vol. 43, pp. 6245–6260, 2010.
- [YAĜ 14] YAĜCI Y., TASDELEN M.A., JOCKUSCH S., "Reduction of Cu(II) by photochemically generated phosphonyl radicals to generate Cu(I) as catalyst for atom transfer radical polymerization and azide-alkyne cycloaddition click reactions", *Polymer*, vol. 55, pp. 3468–3474, 2014.
- [YAM 98] YAMAGUCHI Y., PALMER B.J., KUTAL C. *et al.*, "Ferrocenes as anionic photoinitiators", *Macromolecules*, vol. 31, pp. 5155–5157, 1998.
- [YAM 99] YAMAGUCHI Y., KUTAL C., "Efficient photodissociation of anions from benzoyl-functionalized ferrocene complexes", *Inorganic Chemistry*, vol. 38, pp. 4861–4867, 1999.

- [YAM 00] YAMAGUCHI Y., KUTAL C., “Benzoyl-substituted ferrocenes: an attractive new class of anionic photoinitiators”, *Macromolecules*, vol. 33, pp. 1152–1156, 2000.
- [YAM 04] YAMAGO S., RAY B., IIDA K. *et al.*, “Highly versatile organostibine mediators for living radical polymerization”, *Journal of American Chemical Society*, vol. 126, pp. 13908–13909, 2004.
- [YAM 07] YAMAGUCHI Y., DING W., SANDERSON C.T. *et al.*, “Electronic structure, spectroscopy, and photochemistry of group 8 metallocenes”, *Coordination Chemistry Reviews*, vol. 251, pp. 515–524, 2007.
- [YAN 10] YAN Y., ZHANG W., QIU Y. *et al.*, “Universal xanthate-mediated controlled free radical polymerizations of the “less activated” vinyl monomers”, *Journal of Polymer Science Part A: Polymer Chemistry*, vol. 48, pp. 5206–5214, 2010.
- [YOS 10a] YOSHIDA E., “Photo-living radical polymerization of methyl methacrylate using alkoxyamine as an initiator”, *Colloid and Polymer Science*, vol. 288, pp. 7–13, 2010.
- [YOS 10b] YOSHIDA E., “Nitroxide-mediated photo-living radical polymerization of methyl methacrylate using (4-tert-butylphenyl)diphenylsulfonium triflate as a photo-acid generator”, *Colloid and Polymer Science*, vol. 288, pp. 239–243, 2010.
- [YOS 12] YOSHIDA E., “Controlled photoradical polymerization mediated by 2,2,6,6-Tetramethylpiperidine-1-Oxyl”, *Polymers*, vol. 4, pp. 1125–1156, 2012.
- [YOU 00] YOUSU Z., JIAN L., RONGCHUAN Z. *et al.*, “Synthesis of block copolymer from dissimilar vinyl monomer by stable free radical polymerization”, *Macromolecules*, vol. 33, pp. 4745–4749, 2000.
- [YOU 02] YOU Y.Z., HONG C.Y., BAI R.K. *et al.*, “Photo-initiated living free radical polymerization in the presence of dibenzyl trithiocarbonate”, *Macromolecular Chemistry and Physics*, vol. 203, pp. 477–483, 2002.
- [ZHU 11] ZHU G.H., ZHANG L.F., ZHANG Z.B. *et al.*, “Iron-Mediated ICAR ATRP of Methyl Methacrylate”, *Macromolecules*, vol. 44, pp. 3233–3239, 2011.



---

# Applied Photochemistry in Dental Materials: From Beginnings to State of the Art

---

## 4.1. Photoinitiated free radical polymerization

### 4.1.1. *Introduction: from ultraviolet to visible light curing*

The development of the first ultraviolet (UV) light-cured dental composites in the early 1960s marked a milestone in dentistry that facilitated further discoveries in dental restorative and adhesive technology [COO 92]. Light-cured composites were superior to the preceding two-component, self-cured restoratives due to improved physical as well as handling properties. As the final compounding was moved to the manufacturer, the risk of incomplete mixing was avoided and highly filled materials with less polymerization shrinkage and better marginal adaption to tooth cavities could be produced. Optimized mixing processes resulted in less air inclusion and hence improved esthetics, while a higher degree of double-bond conversion afforded durable materials with lower amounts of leachable monomers. Decomposition was not as pronounced compared to conventional redox initiators so that the shelf lives of sufficiently light-protected composites could be improved [MAH 13]. Also, the fast curing on demand

---

Chapter written by Joachim E. KLEE, Maximilian MAIER and Christoph P. FIK.

allowed for the safer and more efficient treatment of patients. Typical classes of UV photoinitiators comprised benzophenones [LEE 74], benzoin ether [WAL 70], benzilketals [SCH 77] and mercaptophenones [ZHA 11]. Activation was usually carried out by rustic devices emitting light of wavelengths up to 380 nm.

While light curing as such was generally considered favorable, UV curing, as a classical transition technology, soon exhibited critical constraints and side effects. In this sense, UV wavelengths limited the depth of cure to 1–2 mm, impairing the physical properties of cured composites to an intolerable extent or making durable fillings tedious to prepare [STA 00]. Even more severely, high energy levels of the curing devices led to adverse effects on human tissue, causing eye damage in dentists and patients alike [WAT 04]. Alternatives were found by the 1970s, when photoinitiators absorbing in the spectral region of blue light (460–480 nm) were introduced. This progress was based on the discovery of D,L-camphorquinone (CQ)/tertiary amine systems as potent photoinitiators [DAR 71]. Until today, CQ, paired with different cointiators, is applied in almost every commercially available blue light-cured dental product (Figure 4.1).

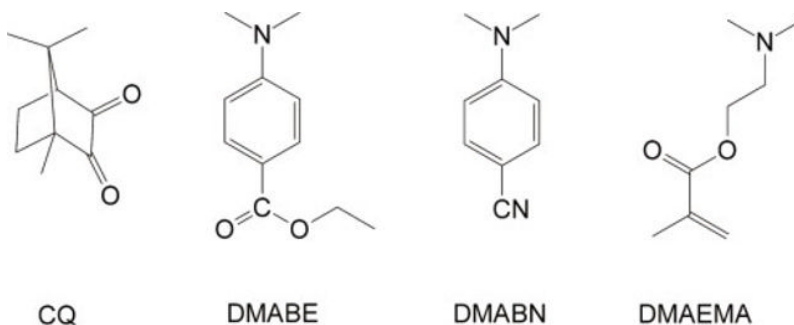


**Figure 4.1.** *D, L-camphorquinone (CQ) and typical amino cointiators*

#### 4.1.2. The camphorquinone/amine system

Besides mild conditions for photocleaving ( $\lambda_{\max} = 468$  nm,  $\phi = 6.61 \times 10^3$  mol/E), CQs ubiquitousness in dentistry is based upon its excellent solubility in a wide range of (meth-)acrylate resins, its temperature/storage

stability and toxicological safety as well as near complete photobleaching at relevant levels of concentration [LEP 13, MOS 07]. CQ belongs to the Norrish type II class of initiators, forming active species after excitation and complexation of coinitiator, usually tertiary amine, followed by sequential intermolecular electron–proton transfer (Figure 4.2). Out of the emerging radicals, only the  $\alpha$ -amino alkyl radical is able to start the polymerization as the ketyl radicals tend to recombine or disproportionate. Preferred coinitiators include ethyl-4-dimethylaminobenzoate (DMABE), 4-(dimethylamino) benzonitril (DMABN) or the polymerizable 2-(N,N-dimethylamino)ethyl methacrylate (DMAEMA) (Figure 4.1), with the latter being able to reduce the amount of potentially leachable amine by incorporation in emerging network structures [NIE 02]. In acidic dental adhesives, the amount of amine needs to be precisely adjusted to the equilibrium of free amine and protonated inactive species. Alternatively, 1,3-diethyl-2-thiobarbituric acid was also found to improve the polymerization kinetics and degree of conversion in some cases of acidic resins [MUE 13]. For all types of filled and unfilled dental materials, the literature provides extensive studies on the optimal ratios of CQ to amine [MUS 06, VIL 05]. Ultimately, the balance of mechanical strength, initiator leaching/biocompatibility and discoloration has to be considered carefully.

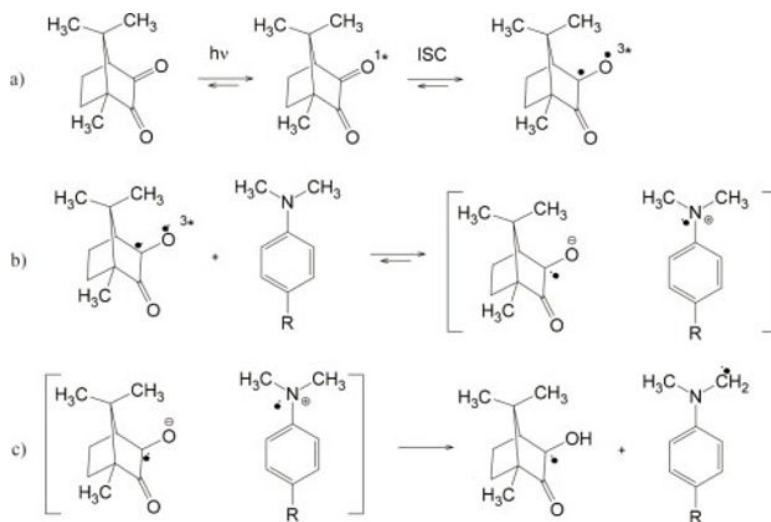


**Figure 4.2.** Reaction scheme for the formation of starting radicals from CQ and aromatic N,N-dimethyl amine: a) excitation and intersystem crossing (ISC) of CQ, b) formation of CQ/amine exciplex and electron transfer and c) proton transfer to ketyl and  $\alpha$ -amino alkyl radical [COO 11]

While the general concept of combining CQ and amine coinitiator has remained the same throughout the years, several refinements have been attempted. The shortcomings addressed comprise reduced leaching of initiator, e.g. via polymer-tethered CQ [HUS 12], a higher biocompatibility of amines [LIU 07, SHI 07] or a lower discoloration of the cured materials by reducing the impurities of amines. In order to improve the diffusion-limited, binary system in high-viscosity media, initiator and coinitiator were combined in one molecule and thus enabled higher polymerization rates [ULL 04]. However, the characteristic oxygen inhibition layer remains present in most systems [MOS 08].

To further optimize the conversion of monomers, the CQ/amine system was enhanced with additional components. Ternary systems with 1-phenyl-1,2-propanedione (PPD) or diphenyliodonium (DPI) salts were most promisingly following this approach. PPD was found to synergize well with CQ in conventional resin mixtures with regard to monomer conversion and reduced discoloration at certain levels of concentration [PAR 99]. Mixtures with DPI performed better than CQ/amine alone, while the proposed mechanism suggests the formation of benzene derivatives, which has yet to be proven for actual materials [COO 11, GON 13]. The absorption spectrum of PPD fits to the commonly used dental lights (quartz tungsten halogen (QTH):  $\lambda_{\text{emission}} = 380\text{--}510$  nm, light-emitting diode (LED):  $\lambda_{\text{emission}} = 420\text{--}480$  nm), while DPI is dependent on CQ as a photosensitizer (Figure 4.3).

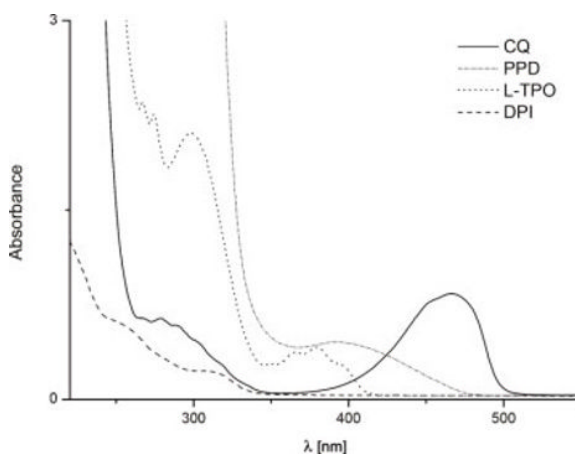


**Figure 4.3.** UV-VIS spectra of relevant photoinitiators for dental composites; concentrations in methanol: CQ: 3.86 g/L, PPD: 3.70 g/L, Lucirin® TPO: 0.22 g/L, DPI: 0.11 g/L

Commercially available, i.e. already marketed, LED-curing lights are mostly fixed to the emission of blue light. This is one of the reasons why CQ is still predominant in dentistry.

#### 4.1.3. Acyl phosphine oxides

Besides CQ, monoacylphosphine oxides, i.e. 2,4,6-trimethylbenzoyldiphenyl phosphine oxide (Lucirin® TPO), with an absorption maximum of  $\lambda_{\max}=390$  nm (see Figure 4.3), and the bis(2,4,6-trimethylbenzoyl)-phenylphosphine oxide (Irgacure® 819), a variation of TPO with an absorption maxima of  $\lambda_{\max}=370/400$  nm, are used in dental materials (Figure 4.4) [IKE 08].

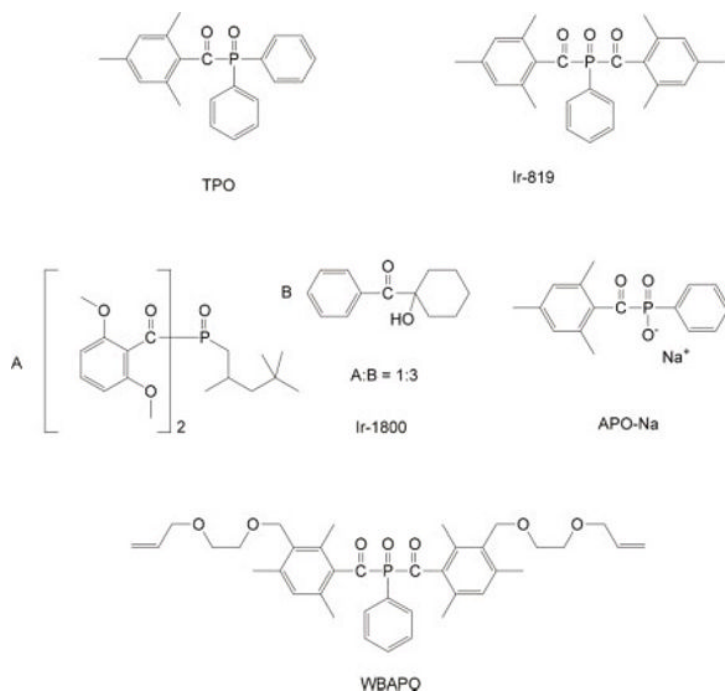


**Figure 4.4.** Chemical structures of selected acyl phosphine oxide initiators: 2,4,6-trimethylbenzoyldiphenyl phosphine oxide (TPO), bis(2,4,6-trimethylbenzoyl)-phenylphosphine oxide (Ir-819), sodium 2,4,6-trimethylbenzoylphenyl phosphine oxide (APO-Na), A: bis(2,6-dimethoxybenzoyl)-2,4,4-trimethyl-pentyl phosphine oxide, B: 1-hydroxycyclohexylphenylketone and A:B = 1:3 (Ir-1800) and bis(3-((2-allyloxy)ethoxy)methyl)-2,4,6-trimethylbenzoyl(phenyl) phosphine oxide (WBAPO)

Solubilities in methyl methacrylate are  $0.99 \times 10^{-3}$  mol/L (TPO) and  $1.03 \times 10^{-3}$  mol/L (Ir-819), respectively, and thus eightfold lower than the one of the CQs ( $8.31 \times 10^{-3}$  mol/L). Nevertheless, both TPO and Ir-819 strongly profit from quantum yields significantly higher than those of CQ ( $\phi = 6.61 \times 10^3$  mol/E vs. TPO:  $\phi = 31.64 \times 10^3$  mol/E and Ir-819:  $\phi = 9.62 \times 10^3$  mol/E). Because TPO reveals a high quantum yield and a good overlap of absorption spectrum with emission spectra of QTH light sources in the near UV region (350–410 nm), it is suited to be used in this particular combination. However, when using modern single-wavelength LED light sources, photopolymerization efficiencies of common phosphine oxide initiators are lower than those of CQs [NEU 06]. Although TPO-based resins exhibited very high conversion rates in filled and unfilled materials [PON 14], depths of cure were typically lower than those with CQ/amine systems [LEP 11]. Nevertheless, the commercially available derivative Ir-1800 exhibited a reactivity higher than the CQ/amine system, when it is used in unfilled resin matrix containing bisGMA, HEMA and an acidic monomer [IKE 08]. With respect to reaction speed, TPO and TPO/amine combinations seem to have an advantage over the CQ/amine system [SCH 12]. Although the residual color of the initiated materials after light curing is strongly concentration-dependent, it may compromise the final dental material esthetics, and thus, has to be taken into considerations when using TPO [ARI 09, LEP 11].

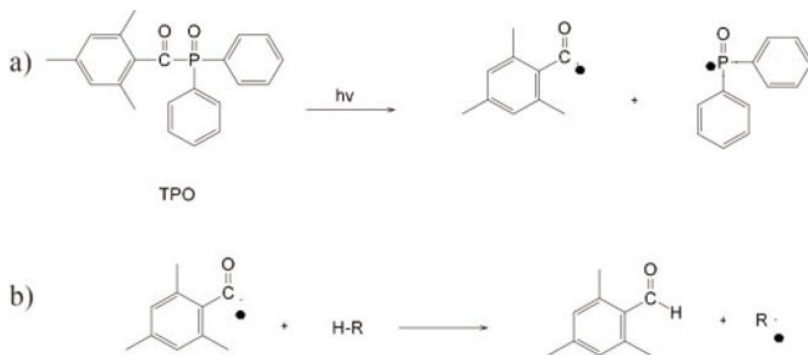


**Figure 4.5.** Reaction scheme for the formation of starting radicals from TPO: a)  $\alpha$ -cleavage of the C-P bond forming C-centered acyl and P-centered phosphinoyl radicals and b) possible H-atom abstraction and radical shift from the C-centered acyl radical [NEU 06]

When used in dental adhesive formulations, the water-soluble sodium 2,4,6-trimethylbenzoylphenyl phosphine oxide (APO-Na) [IKE 09] or the double-bond bearing derivative with improved solubility in polar solvents such as bis(3-((2-(allyloxy)ethoxy)methyl)-2,4,6-trimethylbenzoyl)(phenyl) phosphine oxide (WBAPO) [MOS 10] may be beneficial.

In a light-excited process from singlet to triplet state, acyl phosphine oxides such as TPO undergo a Norrish type I photoreaction, the so-called C-P  $\alpha$ -cleavage (Figure 4.5). Although both radicals are able to initiate, P-centered phosphinoyl radicals exhibit a significantly higher reactivity than the C-centered acyl radicals – typically by a factor of 2–6 [IKE 08, IKE 10]. In general, TPO reveals its advantages over the CQ/amine system especially when used at very low concentrations [PON 14].

#### 4.1.4. Various other photoinitiator systems

Leaving CQ and acyl phosphine oxides, several other photoinitiators have been suggested for dental materials, from which only a few were considered for actual dental products.

Although the laser photolysis of acyl germanium compounds was described in the 1980s [MOC 85], their use as photoinitiators, especially for dental materials, has found little attention. Only recently, have mono- and bisbenzoyl germanium compounds been described as photoinitiators for composites [MOS 08, MOS 07] (Figure 4.6).

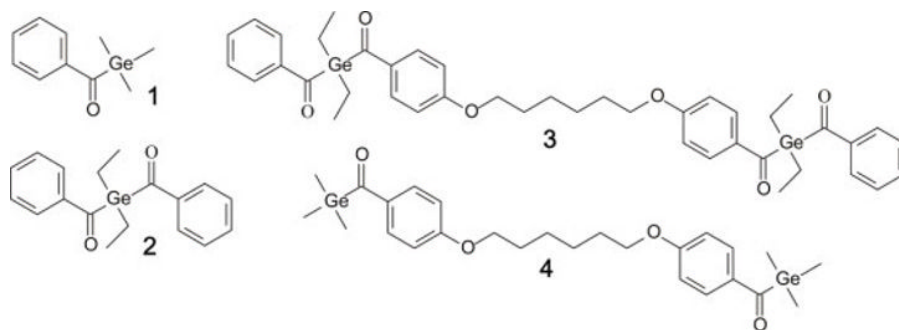


**Figure 4.6.** Selected examples of acyl and bisacyl germanium compounds [MOS 07]

Like acyl phosphine oxides, mono- and bisbenzoyl germanium compounds are promising Norrish type I photoinitiators. They show a distinct absorption in the visible light region and decompose, when irradiated with the right wavelength, into geryml and benzoyl radicals (Figure 4.7).

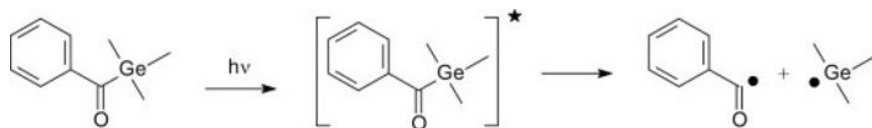


**Figure 4.7.** Reaction scheme for the formation of C-centered acyl and Ge-centered geryml starting radicals by decomposition of benzoyl trimethyl germanium [MOS 08, MOS 07]

The compounds 1 ( $\lambda_{\max} = 411 \text{ nm}$ ,  $\epsilon = 1,460 \text{ dm}^2 \text{ mol}^{-1}$ ) and 2 ( $\lambda_{\max} = 418 \text{ nm}$ ,  $\epsilon = 5,470 \text{ dm}^2 \text{ mol}^{-1}$ ) show an even stronger absorption at their maximum than CQ (Figure 4.6) [MOS 08]. However, the absorption spectra of acyl germanium initiators only slightly overlap with emission spectra of common dental polymerization lamps. In this sense, the efficiency of 1 is rather limited compared to CQ/amine systems [GAN 08]. Also, it has been shown that increasing concentrations of these types of initiators decreases the depth of cure compared to CQ-/amine-based restorative materials [MOS 08, MOS 07].

Recently, other types of photoinitiators based on various hexaaryl bisimidazole derivatives (HABI) have been described for the use in dental materials [BLA 09] (Figure 4.8). These initiators exhibit an improved curing performance and have absorption maxima well above 530 nm, rendering them compatible with modern visible light curing devices.

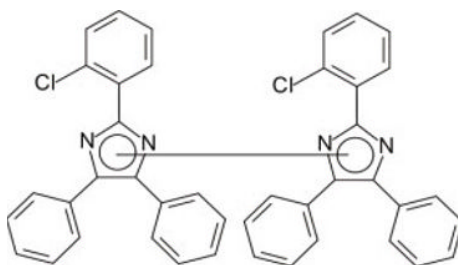


**Figure 4.8.** Selected example of a hexaaryl bisimidazole derivative [BLA 09]

After irradiation, the HABI molecules decompose into lophyl radicals which subsequently abstract protons from a donor, e.g. thiols [BER 14] (Figure 4.9), heteroaromatic thiols, benzothiazoles, benzoxazoles, tertiary amines, alcohols, thiocarboxylic acids [BLA 09] or dyes [BEN 02]. If used in a dental composite, they lead to improved compressive, yield and flexural strengths compared to conventional composites with CQ/DMABE. Furthermore, the sensitivity to ambient light could be decreased [BLA 09].

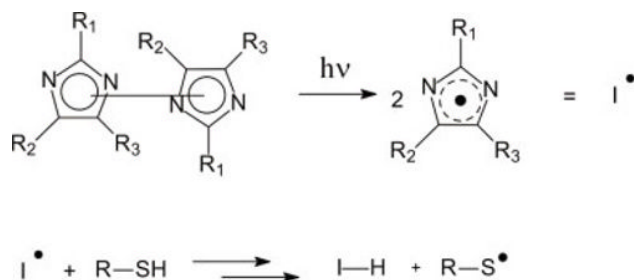


**Figure 4.9.** Reaction scheme for the formation of lophyl radicals followed by the abstraction of protons from a thiol [BER 14]

Cunningham suggested borate photoinitiators for dental compositions [CUN 96, CUN 99]. The boron atom can be substituted by aliphatic or aromatic moieties (Figure 4.10). Preferably, the cation  $G^+$  is an ammonium or tetraalkylammonium moiety, a substituted aromatic compound or a transition metal complex. Depending on the composition of the borate photoinitiators, the photosensitivity extends from approximately 200 nm to the infrared region.

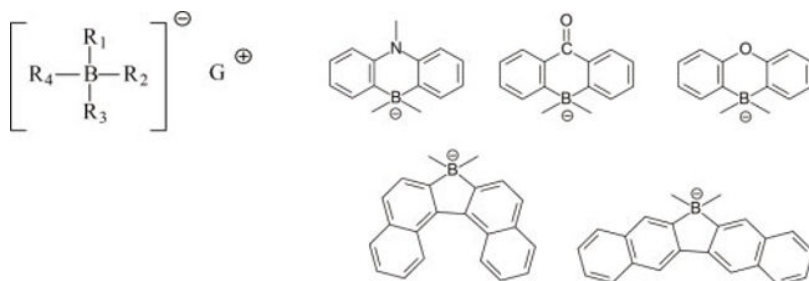


**Figure 4.10.** Selected examples of borate photoinitiators;  $R_1$  to  $R_3$  are aromatic hydrocarbons and  $R_4$  are aliphatic radicals.  $G^+$  is a metal ion, ammonium or tetraalkylammonium [CUN 96, CUN 99]

Titanate initiators of various structures were discovered by Ciba-Geigy AG [RHO 88, STE 90] (Figure 4.11). Among these structures were methacrylated molecules with the ability to be embedded in forming polymer structures. The titanate initiators are reported to be temperature and humidity stable, but readily decompose when irradiated with light in the wavelength region from 200 to 600 nm.

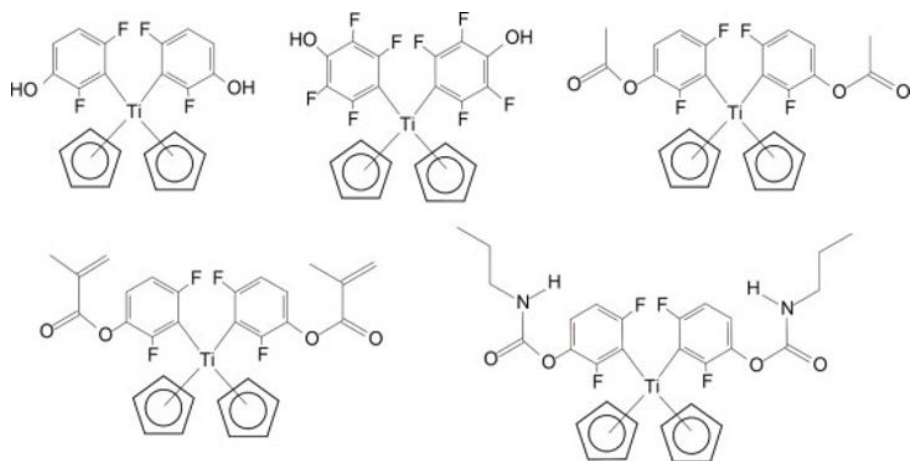


**Figure 4.11.** Selected examples of titanate initiators [RHO 88, STE 90]

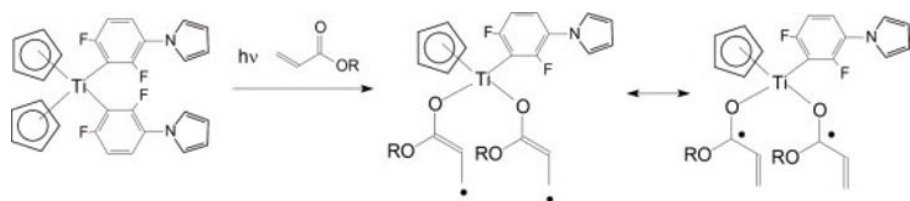


**Figure 4.12.** Reaction scheme for the formation of starting diradical by exchange of two of the ligands in the presence of unsaturated monomers [FIN 89]

In 1988, effective titanate initiators were claimed for light and dual cured dental materials by Dentsply [WHI 89]. In particular, the initiator shown in

Figure 4.12 has interesting properties, as it displays two distinct  $\lambda_{\max}$  at 405 and 480 nm [DIE 91]. In the presence of  $\alpha,\beta$ -unsaturated compounds and subsequent to irradiation, an exchange of ligands is followed by isomerization to a coordinative unsaturated complex. The complex is a biradical that is capable to initiate the polymerization of unsaturated monomers [FIN 89].

## 4.2. Cationic photopolymerization

Up to now, to the best knowledge of the authors, there is no application of the classic cationic photopolymerization for dental materials. However, by combining classical CQ-/amine-initiated radical photopolymerization of (meth)acrylates and cationic ring opening polymerization (CROP) of epoxides, the class of *Silorane* dental materials was recently introduced to the market. Here, an iodonium salt such as phenyl-(para-(2-hydroxytetradecyloxy)phenyl)iodonium hexafluoroantimonate is added as a third initiator component. In contrast to free radically cured materials (see section 4.1), the concentration of the iodonium salt in *Silorane* systems is higher than the concentration of CQ, for instance, CQ/iodonium salt/DMABE: 1.0/3.0/0.1 wt.% [EIC 07]. In a redox process, the light-activated amine decomposes the iodonium salt forming a highly reactive acidic carbocation, which finally starts the CROP of the oxirane monomer species in the resin mixture [OGL 07, WEI 05] (Figure 4.13).

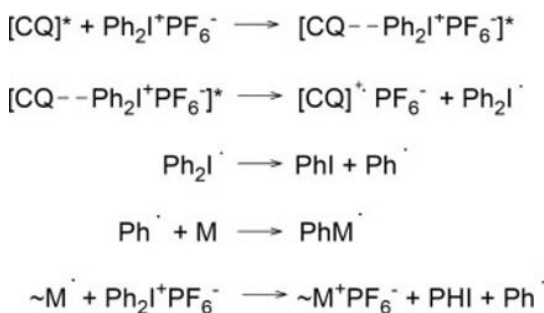


**Figure 4.13.** Reaction scheme for the cationic ring opening polymerization [OGL 07]

In comparison to the radical polymerization mechanism of (meth)acrylates, the CROP process is not influenced by oxygen and thus does not suffer from the typical oxygen inhibition layer [ILE 09]. Advantages of this material class are low shrinkage and shrinkage stress, while the kinetics of the curing reaction is slower than that of purely methacrylate-based materials and the polymerization enthalpy is higher.

### 4.3. Conclusion

Modern, light-cured dental materials are generally accepted to be state of the art by clinicians and researchers alike. They are characterized by superior mechanical, esthetical and handling properties, while intrinsic challenges such as shrinkage, shrinkage stress and resistance to abrasion have been addressed in recent years. Concerning the absorption spectra of photoinitiators and emission spectra of corresponding curing lights, an efficient match was found and established in the market – CQ remains the foundation for most products in this context. Future developments should be directed toward overcoming the limitations in depth of cure, e.g. by the development of novel photoinitiators with improved quantum yields, bathochromic shifts or additives for indirect excitation. Furthermore, shorter curing times of dental materials are demanded by dentists and need to be addressed by an appropriate design of the initiating system and its components in coming generations of dental products.

### 4.4. Bibliography

- [ARI 09] ARIKAWA H., TAKAHASHI H., KANIE T. *et al.*, “Effect of various visible light photoinitiators on the polymerization and color of light-activated resins”, *Dental Materials Journal*, vol. 28, no. 4, pp. 454–460, 2009.
- [BEN 02] BENDYK M., JEDRZEJEWSKA B., PACZKOWSKI J. *et al.*, “Hexaarylbisimidazoles and ketocyanine dyes as effective electron transfer photoinitiating systems”, *Polimery*, vol. 47, pp. 654–656, 2002.
- [BER 14] BERDZINSKI S., STREHMEL N., LINDAUER H. *et al.*, “Extended mechanistic aspects on photoinitiated polymerization of 1,6-hexanediol diacrylate by hexaarylbisimidazoles and heterocyclic mercapto compounds”, *Photochemical & Photobiological Sciences*, vol. 13, pp. 789–798, 2014.
- [BLA 09] BLACKWELL G., Radical polymerization initiators for light-curable dental materials, Patent EP 2,276,446 B1, 2009.

- [COO 92] COOK W.D., "Photopolymerization kinetics of dimethacrylates using the camphorquinone amine initiator system", *Polymer*, vol. 33, no. 3, pp. 600–609, 1992.
- [COO 11] COOK W.D., CHEN F., "Enhanced Photopolymerization of Dimethacrylates with Ketones, Amines, and Iodonium Salts: The CQ System", *Journal of Polymer Science Part A: Polymer Chemistry*, vol. 49, no. 23, pp. 5030–5041, 2011.
- [CUN 96] CUNNINGHAM A.F., KUNZ M., KURA H., Borate photoinitiators from polyboranes, US Patent 5,807,905, 1996.
- [CUN 99] CUNNINGHAM A.F., KUNZ M., KURA H., Borate photoinitiators from monoboranes, US Patent 6,045,974, 1999.
- [DAR 71] DART E.C., NEMCEK J., Photopolymerisable composition, Patent GB 1,408,265, JP 54-10986, 1971.
- [DIE 91] DIETLIKER K., "Photoinitiators for free radical and cationic polymerization", *Chemistry and Technology of UV and EB Formulations for Coatings, Inks and Paints*, volume III, ed. PKT Oldring SITA Technology, 1991.
- [EIC 07] EICK J.D., KOTHA S.P., CHAPPELOW C.C. *et al.*, "Properties of silorane-based dental resins and composites containing a stress-reducing monomer", *Dental Materials*, vol. 23, no. 8, pp. 1011–1017, 2007.
- [FIN 89] FINTER J., RIEDICKER M., ROHDE O. *et al.*, *Makromolekulare Chemie, Macromolecular Symposia*, vol. 24, pp. 177–181, 1989.
- [GAN 08] GANSTER B., FISCHER U.K., MOSZNER N. *et al.*, "New photocleavable structures. IV. Acylgerman based photoinitiator for visible light curing", *Macromolecular Rapid Communications*, vol. 29, pp. 57–62, 2008.
- [GON 13] GONCALVES L.S., MORAES R.R., OGLIARI F.A. *et al.*, "Improved polymerization efficiency of methacrylate-based cements containing an iodonium salt", *Dental Materials*, vol. 29, no. 12, pp. 1251–1255, 2013.
- [HUS 12] HUSAR B., MOSZNER N., LUKAC I., "Synthesis and photooxidation of styrene copolymer bearing camphorquinone pendant groups", *Beilstein Journal of Organic Chemistry*, vol. 8, pp. 337–343, 2012.
- [IKE 08] IKEMURA K., ICHIZAWA K., YOSHIDA M. *et al.*, "UV-VIS spectra and photoinitiation behaviors of acylphosphine oxide and bisacylphosphine oxide derivatives in unfilled, light-cured dental resins", *Dental Materials Journal*, vol. 27, no. 6, pp. 765–774, 2008.

- [IKE 09] IKEMURA K., ICHIZAWA K., FUCHIGAMI K. *et al.*, “Design of a new dental adhesive – Effect of a water-soluble sodium acylphosphine oxide with crown ether on adhesion to dental hard tissues”, *Dental Materials Journal*, vol. 28, no. 3, pp. 267–276, 2009.
- [IKE 10] IKEMURA K., ENDO T., “A review of the development of radical photopolymerization initiators used for designing light-curing dental adhesives and resin composites”, *Dental Materials Journal*, vol. 29, no. 5, pp. 481–501, 2010.
- [ILE 09] ILIE N., HICKEL R., “Macro-, micro- and nano-mechanical investigations on silorane and methacrylate-based composites”, *Dental Materials*, vol. 25, no. 6, pp. 810–819, 2009.
- [LEE 74] LEE H.L., ORLOWSKI A., Dentalglasurmasse, Patent DE 2,437,978, 1974.
- [LEP 11] LEPRINCE J.G., HADIS M., SHORTALL A.C. *et al.*, “Photoinitiator type and applicability of exposure reciprocity law in filled and unfilled photoactive resins”, *Dental Materials*, vol. 27, no. 2, pp. 157–164, 2011.
- [LEP 13] LEPRINCE J.G., PALIN W.M., HADIS M.A. *et al.*, “Progress in dimethacrylate-based dental composite technology and curing efficiency”, *Dental Materials*, vol. 29, no. 2, pp. 139–156, 2013.
- [LIU 07] LIU S.J., “Benzodioxole derivate as coinitiator for dental resin”, *Acta Odontologica Scandinavica*, vol. 65, pp. 313–318, 2007.
- [MAH 13] MAHN E., “Clinical criteria for the successful curing of composite materials”, *Revista Clínica de Periodoncia, Implantología y Rehabilitación Oral*, vol. 6, no. 3, pp. 148–153, 2013.
- [MOC 85] MOCHIDA K., ICHIKAWA K., OKUI S. *et al.*, “Direct observation of germlyl radicals by a laser-photolysis of germlyl ketones”, *Chemistry Letters*, vol. 14, no. 19, pp. 1433–1436, 1985.
- [MOS 07a] MOSZNER N., SALZ U., “Recent Developments of New Components for Dental Adhesives and Composites”, *Macromolecular Materials and Engineering*, vol. 292, pp. 245–271, 2007.
- [MOS 07b] MOSZNER N., ZEUNER F., LISKA R. *et al.*, Polymerisable compositions comprising acyl-germanium as initiators, Patent EP 1,905,415 B1, 2007.
- [MOS 08] MOSZNER N., FISCHER U.K., GANSTER B. *et al.*, “Benzoyl germanium derivatives as novel visible light photoinitiators for dental materials”, *Dental Materials*, vol. 24, no. 7, pp. 901–907, 2008.

- [MOS 10] MOSZNER N., LAMPARTH I., ANGERMANN J. *et al.*, “Synthesis of bis(3-(2-(allyloxy)ethoxy methyl)-2,4,6-trimethylbenzoyl)(phenyl)phosphine oxide – a tailor-made photoinitiator for dental adhesives”, *Beilstein Journal of Organic Chemistry*, vol. 6, no. 26, 2010.
- [MUE 13] MUENCHOW E.A., VALENTE L.L., PERALTA S.L. *et al.*, “1,3-Diethyl-2-thiobarbituric acid as an alternative coinitiator for acidic photopolymerizable dental materials”, *Journal of Biomedical Material Research Part B: Applied Biomaterials*, vol. 101, no. 7, pp. 1217–1221, 2013.
- [MUS 06] MUSANJE L., FERRACANE J.L., FERRACANE L.L., “Effects of resin formulation and nanofiller surface treatment on in vitro wear of experimental hybrid resin composite”, *Journal of Biomedical Materials Research Part B: Applied Biomaterials*, vol. 77, no. 1, pp. 120–125, 2006.
- [NEU 06] NEUMANN M.G., SCHMITT C.C., FERREIRA G.C. *et al.*, “The initiating radical yields and the efficiency of polymerization for various dental photoinitiators excited by different light curing units”, *Dental Materials*, vol. 22, no. 6, pp. 576–584, 2006.
- [NIE 02] NIE J., BOWMAN C.N., “Synthesis and photopolymerization of N,N'-dimethyl-N,N'-di(methacryloxy ethyl)-1,6-hexanediamine as a polymerizable amine coinitiator for dental restorations”, *Biomaterials*, vol. 23, no. 4, pp. 1221–1226, 2002.
- [OGL 07] OGLIARI F.A., ELY C., PETZOLD C.L. *et al.*, “Onium salt improves the polymerization kinetics in an experimental dental adhesive resin”, *Journal of Dentistry*, vol. 35, no. 7, pp. 583–587, 2007.
- [PAR 99] PARK Y.J., CHAE K.H., RAWLS H.R., “Development of a new photoinitiation system for dental light-cure composite resins”, *Dental Materials*, vol. 15, no. 2, pp. 120–127, 1999.
- [PON 14] PONGPRUEKSA P., MILETIC V., JANSSENS H. *et al.*, “Degree of conversion and monomer elution of CQ/amine and TPO adhesives”, *Dental Materials*, vol. 30, no. 6, pp. 695–701, 2014.
- [RHO 88] RHODE O., SCHAFFNER A., RIEDIKER M. *et al.*, Photoinitiator mixture comprising a titanocen and a 3-keto coumarin, Patent EP 277,915 B1, 1988.
- [SCH 77] SCHMITT W., PURRMANN R., Durch UV-Licht polymerisierbare Massen auf Basis von Acrylsäureestern, Patent DE 2,811,039, 1977.
- [SCH 12] SCHNEIDER L.F.J., CAVALCANTE L.M., PRAHL S.A. *et al.*, “Curing efficiency of dental resin composites formulated with camphorquinone or trimethylbenzoyl-diphenyl-phosphine oxide”, *Dental Materials*, vol. 28, no. 4, pp. 392–397, 2012.

- [SHI 07] SHI S.Q., NIE J., “A natural component as coinitiator for unfilled dental resin composite”, *Journal of Biomedical Material Research Part B: Applied Biomaterials*, vol. 82, pp. 44–50, 2007.
- [STA 00] STANSBURY J.W., “Curing dental resins and composites by photopolymerization”, *Journal of Esthetic Dentistry*, vol. 12, no. 6, pp. 300–308, 2000.
- [STE 90] STEINER E., BEYELER H., RIEDIKER M. *et al.*, New oxygen containing titanocens and their application, Patent EP 0,401,165 B1, 1990.
- [ULL 04] ULLRICH G., HERZOG D., LISKA R. *et al.*, “Photoinitiators with functional groups VII. Covalently bonded camphorquinone-amines”, *Journal of Polymer Science Part A: Polymer Chemistry*, vol. 42, pp. 4948–4952, 2004.
- [VIL 05] VILJANEN E.K., LASSILA L.V., SKRIFVARIS M. *et al.*, “Degree of conversion and flexural properties of a dendrimer/methyl methacrylate copolymer: design of experiments and statistical screening”, *Dental Materials*, vol. 21, no. 2, pp. 172–177, 2005.
- [WAL 70] WALLER D.E., Photopolymerisierbare Dentalprodukte, Patent DE 2,126,419, 1970.
- [WAT 04] WATAHA J.C., LOCKWOOD P.E., LEWIS J.B. *et al.*, “Biological effects of blue light from dental curing units”, *Dental Materials Journal*, vol. 20, pp. 150–157, 2004.
- [WEI 05] WEINMANN W., THALACKER C., GUGGENBERGER R., “Siloranes in dental composites”, *Dental Materials*, vol. 21, no. 1, pp. 68–74, 2005.
- [WHI 89] WHITTEN D., VENZ S., Titanate initiators for light cured compositions, Patent EP 0,334,338 A2, 1989.
- [ZHA 11] ZHAO W., MA Z., LI J. *et al.*, Mercapto benzophenone compounds, compositions and preparation method thereof, US Patent 20,130,150,479, 2011.

---

## Photoinitiated Cross-linking in OLEDs: An Efficient Tool for Addressing the Solution-Processed Devices Elaboration and Stability Issues

---

### 5.1. Introduction

Energy saving has become a major concern of the modern world, and electricity saving through phasing out traditional incandescent light bulbs is a priority. For the purposes of general lighting, this issue can clearly be discussed with organic light-emitting devices (OLEDs) [KAP 08, THE 12]. Research on this emerging technology is notably sustained by the numerous advantages of OLEDs over inorganic LEDs: these devices are easier to produce and can be made to larger sizes, and OLEDs can be fabricated on flexible and lightweight thin sheets instead of the heavy and rigid glass substrates used for inorganic LEDs. Organic materials and especially polymers are amenable to solution-based fabrication methods, severely simplifying the device production and cutting manufacturing costs. The molar mass of the materials used is not limited. Conversely, the manufacturing of inorganic LEDs today is still limited to vacuum evaporation techniques and these latter routes are severely limited in terms of molar weight and thermal stability of the materials used. With the aim of

---

Chapter written by Frédéric DUMUR and Didier GIGMES.

developing an energy-saving lighting technology, the much thinner layers used in OLEDs also allow a reduction of the operating voltage in addition to bringing flexibility to devices. Organic electroluminescent (EL) devices are thus looking real breakthroughs in energy-saving research.

If the development of devices using a solution process appears to be an appealing approach by reducing the material consumption and lowering the equipment costs compared to the incumbent technology, the fabrication of multilayered devices remains a challenge if orthogonal solvents are not found for the successive deposition of the different layers [AHM 12, EAR 12, GON 05, HUA 04, WU 04]. Indeed, the main problem facing solution-processed OLEDs is undoubtedly the undesired dissolution between layers, the former layers being dissolved by the solvent of the upper layer. Avoiding an unwanted interfacial mixing between different layers and circumventing the formation of pinholes that can give rise to short circuits [OOS 14] are also other difficulties to overcome. For devices made up of a 5–10 multilayer stack, the selection of solvents that do not dissolve or adversely damage the previous organic layers cannot reasonably be envisioned. The development of methodologies enabling the preparation of solution-processed devices free of layer dissolution problems is thus actively being researched. To address this issue, several approaches have been tested. Notably, the use of a buffer interlayer intercalated between each layer during the device fabrication and finally removed by baking the multilayer stack has been proposed [TSE 06, TSE 08]. However, such an approach can be detrimental for interfacial contacts and phase segregation or delamination can occur during solvent removal. Blade coating of layers was proposed as another possible alternative to spin-coating [KO 10, YOU 09]. Finally, cross-linking of layers appears to be the most promising strategy. Using this approach, soluble material can be deposited by spin-coating and subsequently converted to a totally insoluble cross-linked layer possessing a very good solvent resistance, an enhanced thermal stability greatly facilitating the fabrication process. Preparation of these insoluble polymer networks has been investigated from the chemical [HUY 08, KOH 09], thermal [BOZ 03, LIM 11, LIN 09, LIU 08, MA 07, MA 09, ZHO 11], electrochemical [BAB 04, GU 11, PAR 11a] and photochemical point of view [YER 11]. Notably, the autocatalyzed cross-linking proved to be a major breakthrough in the level of sophistication that can be developed for designing OLEDs

[VOL 12]. Indeed, the photoluminescent copper (I) complex C1 further used as the emitter in these devices itself acted as the catalyst for its own click-chemistry-based polymerization (see Figure 5.1). In this concept, the copper complex had the dual role of catalyst of its own polymerization and emitters. In order for the copper (I) complex to be tough enough, a dinuclear copper (I) halide complex comprising bridging chelate ligands was used, as these complexes are reported as being the most stable copper (I) complexes. As an other specificity, these complexes also meet the demands of high stability and solution processability [FIF 84, VOL 13]. OLED measurements confirmed the suitability of this approach in device application. In this chapter, we will focus on the photoinitiated cross-linking applied to OLED design. In particular, for efficiently immobilizing layers, enhancing the thermal stability or increasing the device lifetime, photo-cross-linking of small molecules, metal complexes or polymers has been investigated.

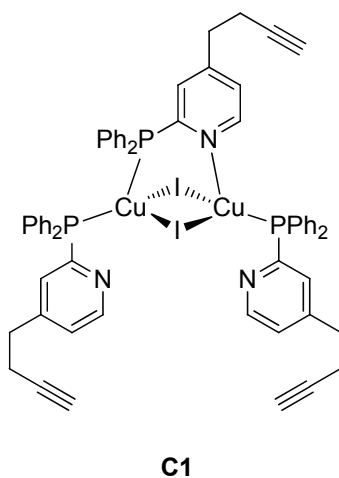


**Figure 5.1.** Copper (I) complex C1 used as autocatalyst of cross-linking and emitter of OLED

## 5.2. Cross-linking of light-emitting materials

### 5.2.1. Polymer-based light-emitting materials

#### 5.2.1.1. Conjugated polymers

The fabrication of advanced (multilayer) device architectures is commonly realized by vacuum sublimation as the device efficiency is

intimately related to a stepped progression of the energy levels of the different materials used for each layer of the device. To reduce the driving voltage and to overcome the mismatch between the energy levels of the emitter with those of the electrodes, the emissive layer (EML) is typically sandwiched between a hole-transport layer (HTL) and an electron-transport layer (ETL). To facilitate charge injection, a hole-injection layer (HIL) and an electron-injection layer (EIL) are typically introduced as adjacent layers of HTL and ETL, respectively (see Figure 5.2). Ideally, the driving voltage of an OLED can be reduced to the photon energy of the emitted light if the charge-injection barrier from the charge-transport layer to the EML becomes negligible so that no energy barrier exists. Fabrication of these ideal OLEDs with an energy barrier-free structure can result in a significant reduction of the driving voltage [JEO 11]. Until now, most of these developed structures have been fabricated by high-vacuum sequential vapor deposition of small molecules. Unfortunately, this thermal evaporation process severely limits the OLED device size to relatively small areas. Transposition of this vacuum-based approach to solution-processed devices without sacrificing device efficiency is challenging, especially for solution processing multilayer structures.

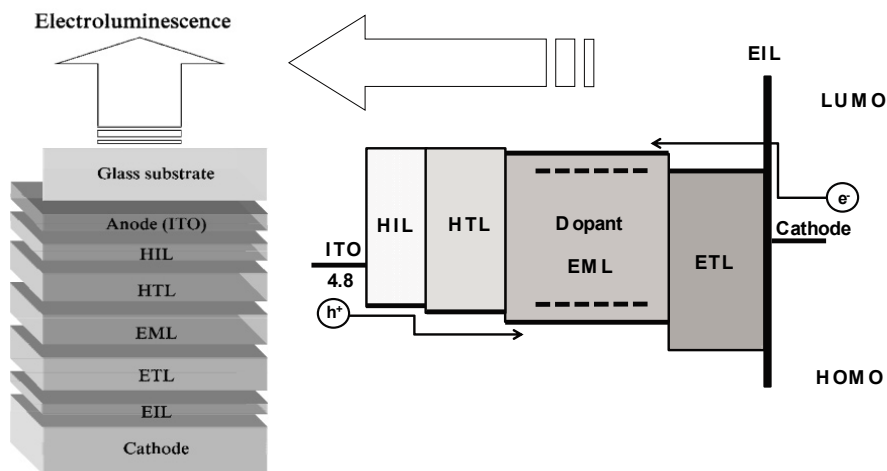


**Figure 5.2.** Typical device structure used for preparing highly emissive OLEDs:  
*HIL: hole-injection layer, HTL: hole-transporting layer, EML: emissive layer,*  
*ETL: electron-transport layer, EIL: electron injection layer*

Cross-linkable EML materials have been demonstrated successfully in multilayer structured OLEDs. However, there are only a few reports of photo-cross-linkable emitting materials based on fluorescent emitters. The first EL polymer was reported in 2001 and contained polymerizable oxetane groups attached through flexible chains to the phenylene units of the polymer backbone [FAB 01]. If only cross-linked thin films of the blue photoluminescent polymers were examined, the concept was established. Examination of this concept in devices was brilliantly realized in 2003 [MUL 03]. Here again, reactive side-groups attached to cross-linkable spirobifluorene-*co*-fluorene polymers were oxetane groups. Use of oxetane units as cross-linkable groups is motivated by the numerous advantages of these groups: first, oxetanes were identified as the only group that does not affect the electrical and optical functionalities of OLEDs [MUE 00]. Second, to initiate the cross-linking reaction, the oxetane-functionalized cross-linkable EL polymers are simply blended with a small amount of photoacid that donates a proton upon exposure to UV light. Cross-linking is thus achieved by cationic ring opening polymerization (CROP) without deterioration of the (electro)-optical properties of the emitters. Third, the volume shrinkage of the functional photoresist is very small and formation of microcracks upon curing is thus efficiently avoided. This last point is a crucial parameter for OLED design as the leakage current should be as low as possible to achieve high efficiencies [CHA 12]. The presence of pinholes in films as well as the strong crystallization tendency of small organic molecules constitutes the main leakage pathways in solution-processed OLEDs. With the general structure: indium tin oxide (ITO)/poly(3,4-ethylene-dioxythiophene) (PEDOT) (20 nm)/electroluminescence (EL) polymer (80 nm)/Ca (20 nm)/Ag (200 nm), the blue cross-linked copolymer P1 exhibited a maximum current efficiency (CE) of 2.9 cd/A, close to that obtained with the reference devices using the corresponding copolymer P4 without cross-link (3.0 cd/A). Slightly reduced efficiencies were obtained with the red and green emitting cross-linkable polymers P2 and P3 (1 and 7 cd/A instead of 2 and 10 cd/A for the corresponding non-cross-linkable copolymers), and the lower performances were assigned to an unfavorable change of the charge-carrier balance in the polymers (see Figure 5.3). In 2007, the same authors designed a display prototype with a pixel size of  $200\ \mu\text{m} \times 600\ \mu\text{m}$  and a display resolution of 1,000 pixels per inch [GAT 07]. Pixilation of the EML was achieved via ultraviolet (UV) illumination through an ultrafine shadow mask.

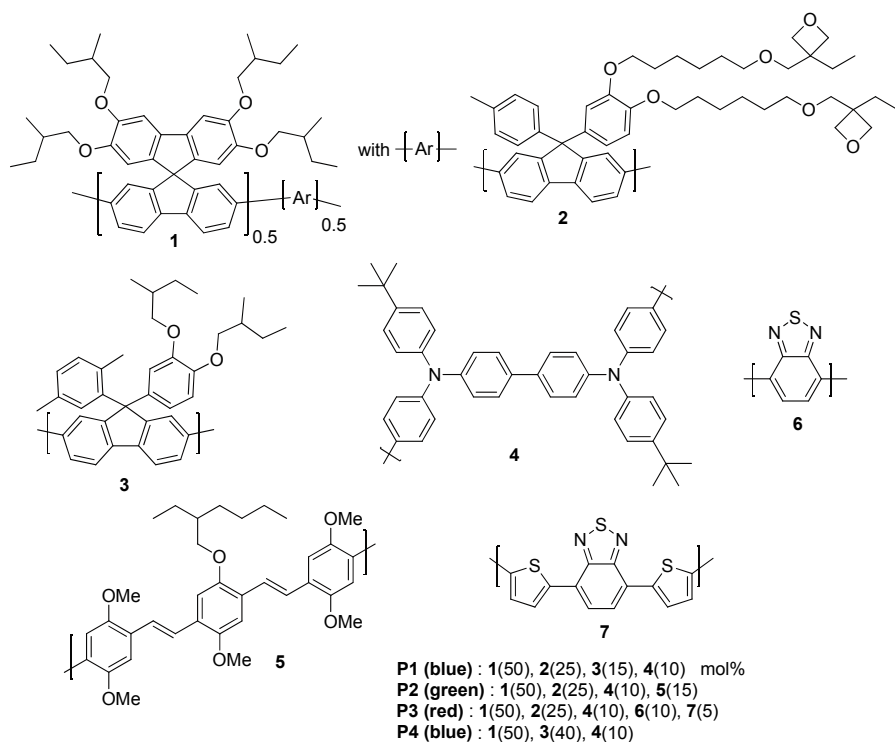


**Figure 5.3.** Electroluminescent copolymers P1–P4

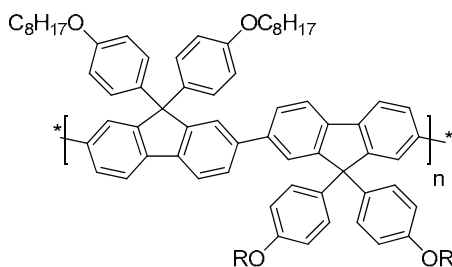
Pure white OLEDs (WOLEDs) with *Commission Internationale de l'Eclairage* (CIE) values of (0.33, 0.33) and color rendering index (CRI) of 76 were obtained. To enhance the device efficiency, a photo-cross-linkable HTL (triphenylamine-dimer (TPD)) was introduced [BAY 99, MUE 00, YAN 06]. In the following device configuration, ITO/PEDOT:PSS (35 nm)/HTL (40 nm)/EL polymer (60 nm)/Ba (4 nm)/Ag (150 nm), the red, green and blue OLEDs achieved a maximum CE of 2.5, 7.9 and 6.5 cd/A, respectively. Finally, in a third study, the same copolymers were studied as EL materials suitable for organic lasing applications [WAL 09].

Design of solution-processed devices is often associated with simplification of the device structure. An ideal OLED is reduced to a unique

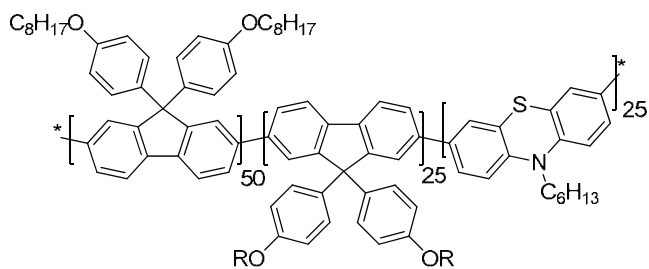
monolayer sandwiched between the two electrodes. To reach such a simple structure, the EML should also exhibit charge injection/transport properties. However, it is difficult to synthesize ideal emitting material that meets the request for the balanced charge injection and transportation [SUN 04]. To circumvent this problem, balanced electron and hole transportation of the EML is often provided by blending two different materials where the first material possesses good hole-transport properties and the second material exhibits good electron-transport properties. Devices approaching these requirements were prepared with an alternating copolymer composed of *bis*(4-octyl-oxyphenyl)fluorene and *bis*((3-hexyloxy-3'-ethyl)oxetane)fluorene [poly(PF-*alt*-OXTF)], and a terpolymer composed of the above two monomers with *N*-hexylphenotiazine [poly(PF-*co*-OXTF-*co*-PTZ)] (see the diagram below) [PAR 09]. To implement the photoresist properties, the required photosensitivity was introduced by attaching oxetane side groups to the polymer backbone via an alkyl spacer. To promote the cross-linking, a proper photoacid generator, i.e. (4-[(2-hydroxytetradecyl)-oxyl]-phenyl)-phenyliodonium hexafluorantimonate, was used. Photo-cross-link reaction was performed upon UV light exposure at 100°C for 10 min. EL performances were evaluated in double-layer devices with ITO/PEDOT:PSS (50 nm)/polymer (80 nm)/LiF (1 nm)/Al (100 nm) configuration and reference devices with polymers without cross-link were also fabricated for comparison. Interestingly, devices based on photo-cross-linked polymers exhibited lower operating voltages than the corresponding reference devices. Lower operating voltages with the two cross-linked polymers were assigned to the presence of the ionic photoacid generator in the EML, lowering the charge injection barrier at the two interfaces.

The effect of the presence of ionic species in EML resulting in charge separation and migration upon application of a driving voltage is well known for devices called light-emitting electrochemical cells (LECs) [COS 12, DUM 11, HU 12]. Poly(PF-*co*-OXTF-*co*-PTZ) furnished the best devices with a maximum brightness of 4,750 cd/m<sup>2</sup> and a maximum CE of 0.68 cd/A. Numerous polyfluorene derivatives were investigated and red-, green- and blue-emitting copolymers (PFR, PFG and PFB) were obtained by simply changing the copolymerizing unit (see the diagram below) [WAN 10]. For all devices, the active layer was photochemically cross-linked at room temperature under inert atmosphere by using diphenyliodonium hexafluoroarsenate as the photoinitiator. The resulting network was subsequently annealed at 120°C for 30 min. Incorporation of

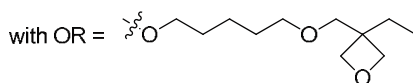
the phenyl group at the C-9 position of fluorenes had several uses. First, because of the strong tendency of polyfluorene to undergo interchain aggregation, phenyl groups attached at the C-9 position efficiently inhibit the aggregation of the polymer chains. Second, the presence of the phenyl groups at the C-9 position can effectively suppress the keto formation. Indeed, the keto defects are responsible for the green contribution detectable in the photoluminescence and electroluminescence spectra of polyfluorenes-based devices [BLI 99, GAA 03, PEI 99, YU 99]. The thermal stability is a crucial parameter as an elevation of temperature can occur during device operation. In particular, color stability and device performances of devices fabricated with alkyl-substituted polyfluorenes were reported as being strongly affected for operating temperatures higher than 86°C [ZHO 00].

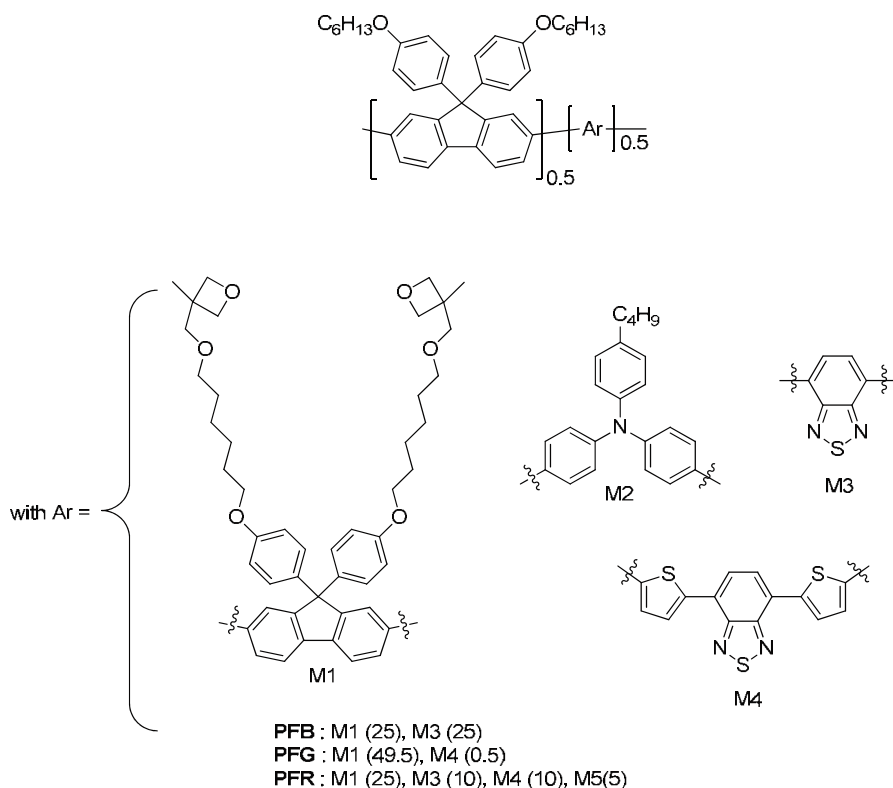


**poly(PF-*alt*-OXTF)**



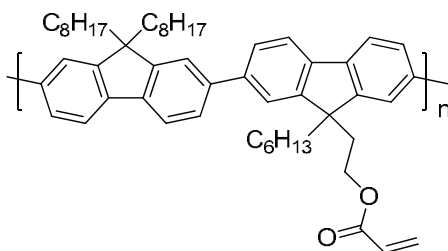
**poly(PF-*co*-OXTF-*co*-PTZ)**



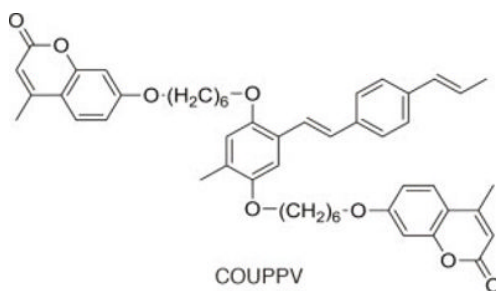


In this study, best performances were achieved with the double-layer devices comprising PFG as the EML. A maximum brightness of 6,447 cd/m<sup>2</sup> and a maximum CE of 1.27 cd/m<sup>2</sup> were obtained. Other cross-linkable side groups were also attached to polyfluorenes. To illustrate this point, acrylate side chains can be cited as examples [WU 06]. To synthesize the cross-linkable EL polymer (poly[2,7-(9,9-dioctylfluorene)-*co*-2,7-(9-hexyl-9-(2-acrylate ethyl)-9H-fluorene)]) as a functional photoresist, a specific synthetic procedure was developed (see the diagram below). Notably, the cross-linkable acrylate groups were introduced into the side chains of the polyfluorene derivative only after polymerization of the polymer backbone. A main point of merit is that no additional reagent such as a photoinitiator was necessary. Upon exposure to UV light under nitrogen atmosphere, the

copolymer could be cross-linked via its acrylate groups. While examining the EL spectrum before and after UV exposure, a redshift of the EL maximum could be clearly evidenced. Notably, before the UV exposure, the EL spectra showed two main emission peaks at 422 and 447 nm, respectively. After irradiation, the appearance of a new 517 nm peak was observed. As the exposition time increases, intensity of the 517 nm peak increased.

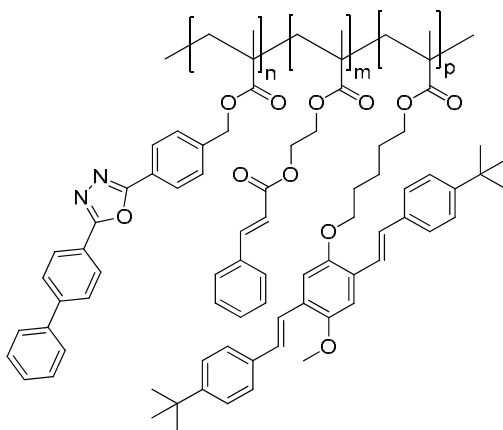


Redshift of the emission was assigned to the cross-linking that inhibited chain mobility and led to the suppression of intermolecular-excited state interactions, as previously reported by Klärner *et al.* [KLA 99a]. Formation of keto defects was also evoked to support the appearance of the new emission peak in the 500–600 nm region. To circumvent the disadvantages of an additional reagent to initiate the cross-linkage, coumarins were studied as a photo-cross-linkable group also capable to act as a sensitizer (see the diagram below) [TSA 06]. Photo-cross-linking behavior of coumarin-based polyphenylenevinylene (COUPPV) was only investigated in thin films even if the electroluminescence properties of this polymer (without performing the cross-linking step) were studied in double-layer devices. As the main drawback of the cross-linking, gradual dimerization of the double bonds of the PPV backbone to cyclobutane derivatives led to the interruption of conjugation and thus to a strong modification of the photoluminescence (PL) spectrum [BUC 04]. Additional dimerization of 7-oxy-4-methylcoumarin chromophores to cyclobutane derivatives were also suggested as another factor contributing to the fast photobleaching of the COUPPV films. Cross-linking of coumarin side groups is thus not suitable for designing OLEDs as it strongly impacts the PL spectrum of the polymer upon cross-linkage and thus alters the EL wavelength.

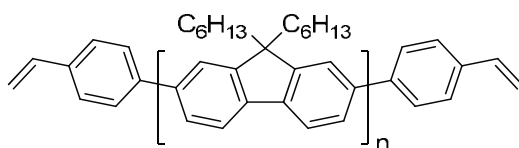
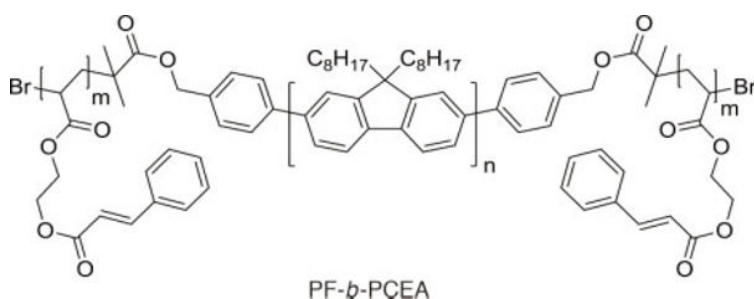


### 5.2.1.2. Non-conjugated polymers

As part of ongoing efforts to design EL materials, OLEDs were also fabricated with non-conjugated polymers. In this last case, the polymer backbone is an insulator [DUM 11] and the charge transport properties of the polymer must be provided by introducing hole and electron-transport pendant groups. The first copolymer bearing charge transport and photo-cross-linking functional groups was reported in 1997 (see the diagram below) [LI 97]. To promote the cross-linking, UV-sensitive cinnamoyl groups were copolymerized with the blue-emitting distyryl benzene and the electron-transporting 1,3,4-oxadiazole. The copolymerization reaction was simply carried out by using Azobisisobutyronitrile (AIBN) as the radical initiator and a copolymer comprising the different elements in the following ratio (n,m,p:0.28, 0.53, 0.19) was obtained.

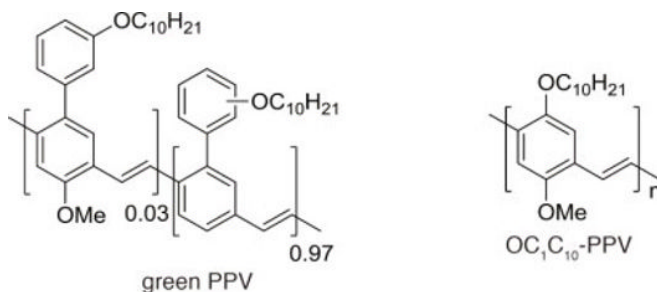


As an interesting feature, the UV-cured film does not exhibit any modification of its emissive properties. When tested as a single layer between two electrodes, the resulting devices emitted a blue light. Synthesis of the copolymer can also be achieved by atom transfer radical polymerization (ATRP). In the same spirit as the former copolymer, cross-linkable cinnamoyl groups were introduced at both ends of a rod-coil triblock copolymer associating a rigid segment (rod block, i.e. conjugated part) with two flexible fragments (coil block, i.e. non-conjugated part) issued from the subsequent polymerization of methyl methacrylate (see the diagram below) [QIA 06]. In terms of thermal stability, superiority of the rod-coil PF-*b*-PCEA copolymer compared to the corresponding fluorescent homopolymer was clearly evidenced. Notably, thermal annealing at 120°C of the homopolymer thin films showed a redshifted emission maximum with the appearance of new emission peaks assigned to aggregates of the polymer and the paralleled arrangement of the polymer chains [ARI 03, CHE 05, GRE 98, GRE 99]. On the opposite, no modification of the emission of the triblock PF-*b*-PCEA was observed, showing greater stability than the homopolymer under thermal stress in the solid state. Changes of the photoluminescence spectra of PF-*b*-PCEA and the corresponding PF homopolymer after UV-cross-linkage and thermal annealing at 160°C for 24 h under air were tracked by fluorescence spectroscopy. When annealed in air, the homopolymer showed an intense emission band at 530 nm assigned to aggregates, excimers or fluorenone defects [CRA 03, GAA 03, LEE 99, SIM 04]. In comparison, the triblock copolymer gave to a lesser extent than that observed for the homopolymer a green emission assigned to fluorenone defects. Photooxidation of the rod-coil copolymer was also strongly limited and the antioxidative properties of this polymer were assigned to the self-assembly of the polymer that spaces the polyfluorene fragments and prevented the appearance of defects and interchain cross-linking [CHO 04, KLA 99a, KON 04, LU 02, LU 03, MAR 99]. If the triblock copolymer was not examined as an emitter for OLEDs, this photoluminescent copolymer exhibited appealing features such as thermal responsiveness and antioxidative properties. EL polymer networks were also prepared by mean of the photoassisted thiol-ene “click” chemistry [DAV 11]. Only one example is reported for demonstrating the suitability of this method to cross-link thin films of 4-phenylethenyl end-capped poly(fluorenes) (see the diagram below).



A main point of merit is that the cross-linking could be realized by a brief UV curing step at moderate temperature and does not require an oxygen-free environment. While the requirement of an additional photoinitiator and the use of high-energy UV to cross-link might be a concern with regard to material stability and device lifetime, this report establishes the concept of cross-linkable emissive materials by “click” chemistry. In particular, thiol-ene photoresist was found to preserve the emissive color integrity, contrarily to the cinnamoyl and coumarin-based cross-linkers previously detailed in this review. Thiol-ene “click” chemistry definitely addresses the two issues of photocuring at low temperature and short reaction times that are two detrimental parameters for photodegradable and thermally unstable EL materials. When tested in double-layer devices, OLEDs exhibited a relatively high turn-on voltage (15 V), far from the turn-on voltage commonly observed for usual vacuum-processed devices for which the turn-on voltage is classically observed approximately 2.5–3.0 V. In a related fashion, photocured devices exhibited similar performances to that obtained for thermally cured OLEDs. However, UV-cured OLEDs showed a lower stability at high voltages and could only be operated at lower voltages than that used for thermally cured OLEDs. Device performances remained limited as the maximum brightness only reached 40–60 cd/m<sup>2</sup> at 18 V.

Notably, prior to this study, the same styryl-functionalized oligomer was thermally cross-linked by an autopolymerization mechanism of styrene [KLA 99b]. Similarly, no modification of the electrical and optical properties of the photoresist was evidenced. Recently, a new cross-linker, namely, ethylene *bis*(4-azido-2,3,5-trifluoro-6-isopropylbenzoate), which does not degrade the semiconductor properties of the cross-linked polymers, was developed (see the diagram below) [PNG 10]. This methodology proved to be versatile as its applicability could be extended to organic field effect transistors and organic solar cells. As specificity, the photolysis of azides generated singlet nitrenes and the predominant reaction of the singlet nitrenes turned out to be the insertion of this group into alkyl CH bonds. However, several potential side reactions were identified for this non-specific methodology such as reactions with ketenimine, attacks on the double bonds of the aromatic rings, on the classical double bonds of the conjugated polymer backbone or on heteroatom sites [BRA 05, MAR 94, POE 92]. These last reactions could be efficiently suppressed by sterically hindering the conjugated polymers, allowing the cross-links to form more favorably at the alkyl side chains. Due to the non-specificity of the cross-linking mechanism, an extremely high photo-cross-linking rate could be achieved at very low cross-linker concentration. Cross-linked devices achieved the remarkable CE of 13 cd/A at 4.0 V, with a maximum external quantum efficiency (EQE) of 4.5%. While examining the device lifetime with green PPV as the EL polymer, cross-linked devices exhibited a lifetime at 100 cd/m<sup>2</sup> of more than 10,000 h, and these values were similar to that obtained for the reference non-cross-linked devices. Likewise, LED characteristics of devices fabricated with OC<sub>1</sub>C<sub>10</sub>-PPV were not degraded by cross-linking.



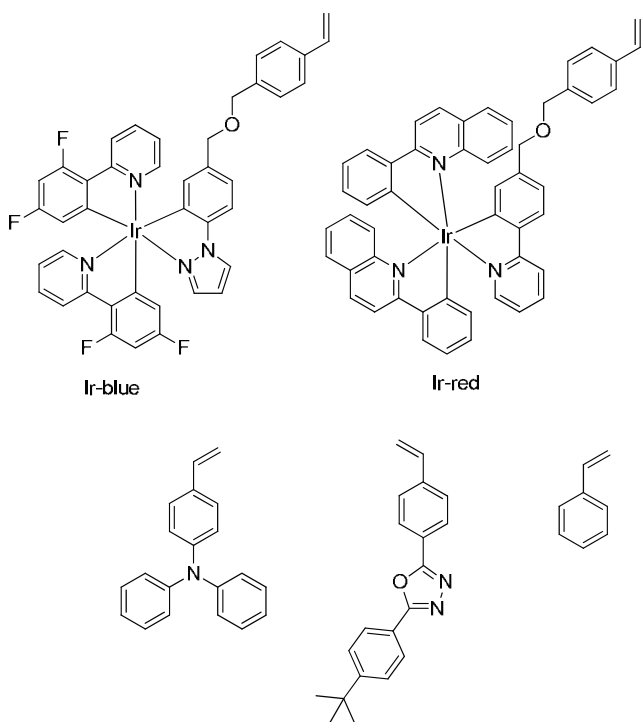


**Figure 5.4.** Monomers used for the preparation of the red- and blue-emitting nanoparticles

Finally, the cross-linking of polymers was extended to the synthesis of polymer nanoparticles with the aim of isolating the emitter molecules from each other (see Figure 5.4) [GAO 10]. Separation of emitters is a general requirement for OLEDs based on phosphorescent emitters. Indeed, triplet-triplet annihilation (TTA), which is a bimolecular interaction between two triplet states, is a key adverse factor for OLEDs [LUO 10, ZHA 10]. TTA is favored by the long triplet exciton lifetime that allows their diffusion over a long distance and their bimolecular interaction. TTA is detrimental for OLEDs as it directly competes with the radiative relaxation of triplet excitons and therefore considerably reduces the device efficiency and is responsible for the efficiency roll-off, i.e. the decline of the efficiency with increasing the current density. TTA can also negatively affect color quality and device stability. To overcome this problem, dilution of the emitter in an

ambipolar host matrix such that the distance between two dopant molecules exceeds the diffusion length of triplet excitons was developed and this method, commonly used in OLEDs, is known as the host-guest strategy (see Figure 5.4) [JEO 09, KAP 08, SAL 13]. In this chapter, polymer domains were appropriately sized such that all dopant molecules were isolated from each other by generating polymer nanoparticles around emitters. If this strategy is applied to a red and a blue emitter and if the corresponding nanoparticles are mixed together within the same emitting layer in an appropriate ratio (3:1, blue:red), a WOLED was fabricated.

To generate the nanoparticles, the polymerization process was initiated in water by adding  $K_2S_2O_8$  as an initiator into the emulsion. Device performance remained limited as only a maximum brightness of 260 cd/m<sup>2</sup> at 25 V and a maximum quantum efficiency (EQE) hardly reaching 1% were obtained.

### 5.2.2. Small-molecule-based light-emitting materials

More generally, cross-linking was investigated with small molecules, and a great deal of effort has been devoted to modifying the emitters such that their covalent linkage to the host could be possible. This approach saves several synthetic steps compared to the cross-linking of polymers by avoiding the synthesis of the polymers prior to photopolymerization. The polymer is directly formed "*in-situ*" with the formation of the polymer network. Numerous phosphorescent dopants were developed with this aim but several drawbacks have also been identified. Notably, the covalent linkage of two cross-linkable dopants to a cross-linkable host *N,N'*-bis(4-(6-((3-ethyloxetane-3-yl)methoxy)hexyl-oxy)phenyl)-*N,N'*-bis(4-methoxy)phenyl benzidine (QUPD)) was achieved by photochemical CROP using 4-octyloxydiphenyliodonium hexa-fluoroantimonate (OPPI) as the photoinitiator [ULB 07, ULB 09]. The necessity of using a higher concentration of photoinitiator to cross-link the host in the presence of the dopant was clearly evidenced with the two cross-linkable iridium complexes Ir\_1 and Ir\_2 (see Figure 5.5). If the pure host matrix can be cross-linked with an initiator concentration of 0.5 wt%, a concentration 10 times higher was required to cross-link both emitter and dopants. The cross-linking step is still followed by thermal annealing (150°C for 15 min) and a decomposition

of emitters approaching 40% was also observed. Apparently, the cross-linking process had a positive impact on the devices' performances. Comparison with the parent non-cross-linking complex Ir\_3 evidenced that Ir\_3-based devices required a higher operating voltage to achieve the same luminance than Ir\_1-based devices. At 10 wt% dopant concentration, a maximum CE and power efficiency of 0.56 cd/A and 0.25 lm/W were only achieved for these orange PhOLEDs, far from the performances achieved with vacuum-processed devices. The second complex investigated in this study Ir\_2 even showed more limited performances, with a maximum CE lower than 0.1 cd/A.

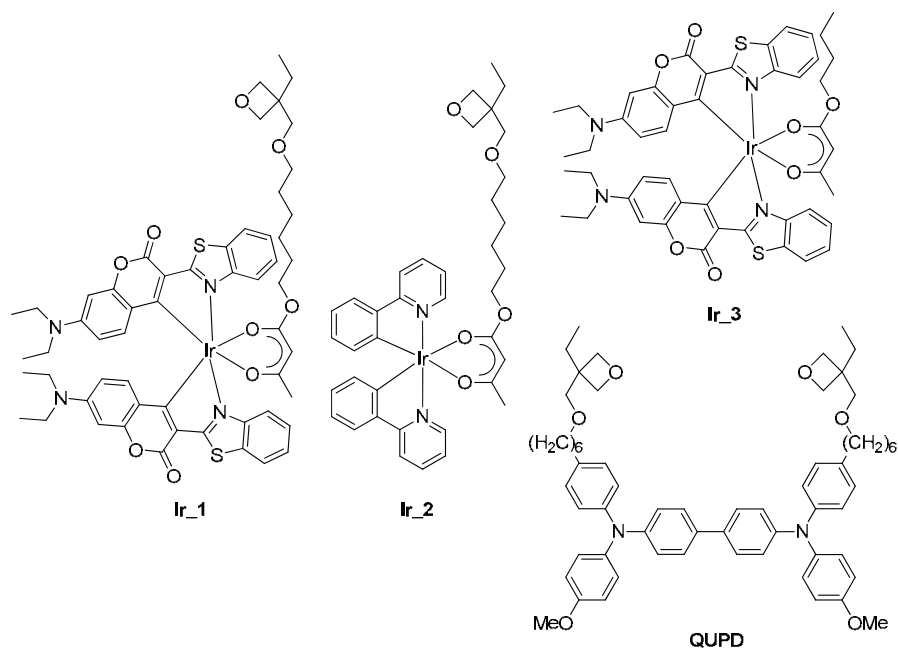


**Figure 5.5.** Chemical structure of Ir\_1-Ir\_3 and the commercial available QUPD

While slightly modifying the former stacking (ITO/PEDOT (35 nm)/QUPD (20 nm)/*N,N'*-bis(4-(6-((3-ethyloxetane-3-yl) methoxy) hexylphenyl))-*N,N'*-diphenylbenzidine OTPD (10 nm)/OTPD:Ir\_1 (10 wt.%),

70 nm)/CsF (2 nm)/Al (100 nm)) by introducing an additional electron-transporting layer between the EML and EIL, luminescence quenching at the cathode could be efficiently suppressed and highly efficient phosphorescent devices were obtained [REH 08]. To be solution processable and to avoid the crystallization of 2-(4-biphenyl)-5-(4-*tert*-butylphenyl)-1,3,4-oxadiazole (PBD) upon drying, the ETL was mixed with 25% poly(methyl methacrylate) (PMMA) to provide a sufficient film-forming ability to the ETL layer. An improvement of the device performance by a factor of 30 was achieved. After optimization of the layers thickness, a maximum CE of 18.4 cd/A and a maximum PE of 15.4 lm/W were obtained with this new device structure.

The cross-linkable emitter can also simply be a fluorescent molecule and blue-emitting devices were fabricated with 3,3'-((((((2,3-diphenyltriphenylene-1,4-diyl)bis(4,1-phenylene))bis(oxy))bis(hexane-6,1-diyl))bis(oxy))bis(methylene))bis(3-ethyloxetane) (PCTP) which can be cross-linked cationically upon UV illumination (see Figure 5.6) [WET 10]. Comparison with reference devices comprising the non-polymerizable 1,4-diphenyl-2,3-bis(4-(trifluoromethyl)phenyl)triphenylene (BFTP) clearly evidenced a moderate enhancement of the device performance as the maximum CE only increased from 0.20 to 0.28 cd/A for PCTP. However, these results have to be relativized with regard to the low luminances obtained with these two devices that do not exceed 40 cd/m<sup>2</sup> at 18–20 V. Improvement of the device performance for the photocured devices is nevertheless evidenced.

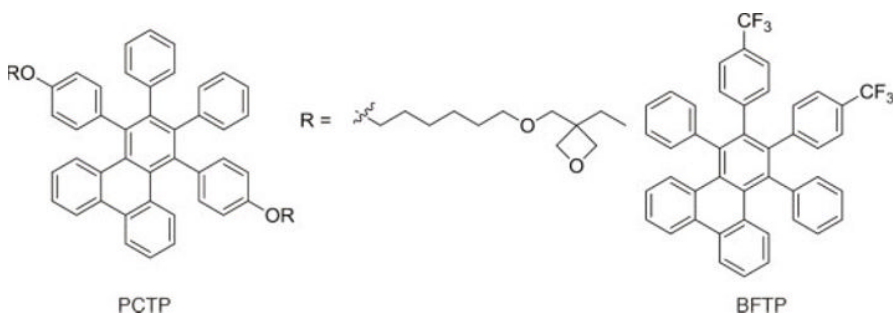


**Figure 5.6.** Cross-linkable fluorescent emitters PCTP and BFTP

Fluorescent organometallic emitters were also cross-linked and one interesting example has been furnished with *tris*-8-hydroxyquinoline aluminum  $\text{Alq}_3$  [DU 06]. Early works on OLEDs were done with  $\text{Alq}_3$  due to its high thermal stability, high quantum yield of fluorescence and high electron-transport ability [TAN 87, TAN 89]. To make the photoresist feasible,  $\text{Alq}_3$  was substituted with methacrylate groups on each ligand (see Figure 5.7). Photopolymerization of methacrylate-based  $\text{Alq}_3$  was achieved using Irgacure 184 as the photoinitiator (0.025 wt%) upon irradiation at 365 nm. When tested in two-layer devices (ITO/PEDOT/ $\text{Alq}_3$  polymer (80 nm)/LiF (1 nm)/Al), device performance of the photoresist was compared with those of the  $\text{Alq}_3$ -homopolymer prepared by classical thermal polymerization. The first observation concerned the electroluminescence spectra obtained with the two polymers that were significantly red-shifted (29 nm) relative to their respective PL spectra. For the two polymers, the threshold voltage was relatively high, approximately 17 V. Brightness of the  $\text{Alq}_3$ -homopolymer and  $\text{Alq}_3$ -photoresist remained extremely limited since only a luminance of 54 and 50  $\text{cd/m}^2$  at 28 V was achieved.

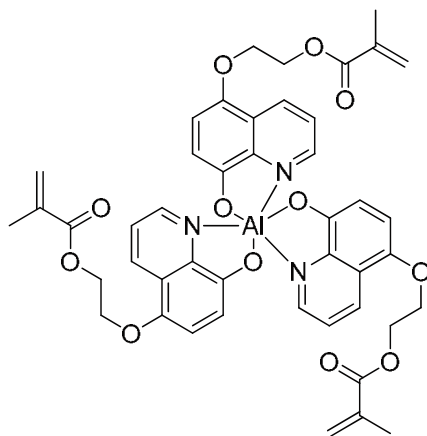


Figure 5.7.  $\text{Alq}_3$ -monomers used to prepare the photoresist

### 5.3. Cross-linking of charge-transport materials

#### 5.3.1. Polymer-based hole-transport materials

To fabricate multilayer polymer light-emitting diodes using solution processes, extensive efforts have been invested in developing new

cross-linkable hole-transporting materials. A recent review has been devoted to providing a general overview of all cross-linkable small molecules and polymers hole-transporting materials that have been developed to date [HUA 08]. Only the new development concerning the photo-cross-linkable HTLs will be discussed in this chapter. Notably, green PhOLEDs were prepared with a new TPD-based copolymer P-TPD-F bearing cross-linkable cinnamoyl side groups attached via an alkyl spacer. The cross-linkable copolymer P-TPD-F was synthesized by radical initiation polymerization as previously reported (see Figure 5.8) [HRE 02]. Surprising results were obtained with these devices comprising as the EML a blend composed of an electron-transporting polymer OP2 and a hole transporting polymer PVK mixed together, and by doping the resulting blend with  $\text{Ir}(\text{ppy})_3$  as the phosphorescent dopant.

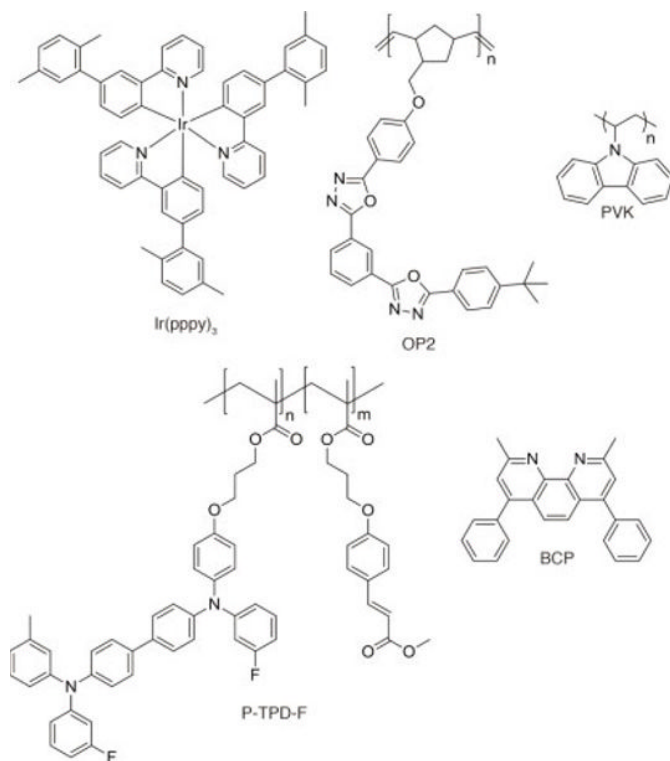


**Figure 5.8.** Cross-linkable copolymer P-TPD-F and materials used to fabricate OLEDs

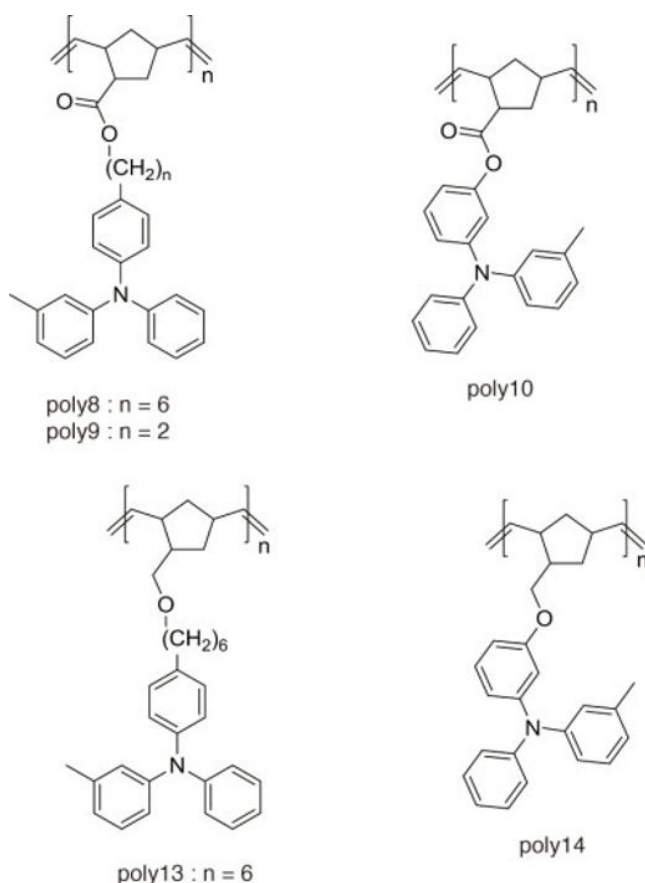


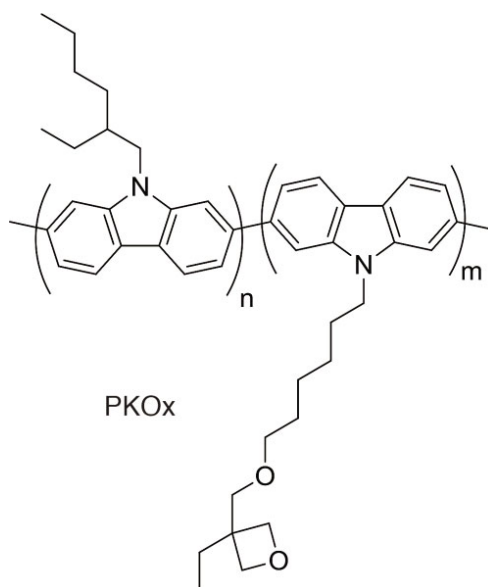
**Figure 5.9.** Structure of the cross-linkable polymers poly8-10, poly13 and poly14

Phase segregation could be expected for a blend comprising three different components. While studying the device characteristics in the following configuration: ITO/ P-TPD-F (35 nm)/PVK:OP2:Ir(pppy)<sub>3</sub> (20 nm)/2,9-dimethyl-4,7-diphenyl-1,10-phenanthroline (BCP) (40 nm)/LiF (2.5 nm)/Al, an EQE of 13.6% at a luminance of 1,000 cd/m<sup>2</sup> and a peak CE of 44.6 cd/A were obtained. A low turn-on voltage of 5.9 V was also determined, far from the values commonly observed for the other polymeric electrophosphorescent devices. An appealing feature is that the high device performances clearly proved the ambipolar character of the cross-linked polymer blend and that no phase segregation between the two polymers occurred, the phase segregation being responsible for a decrease in the

device efficiency and lifetime [HAL 00, XIA 06]. This initial report inspired the design of other cross-linkable hole-transporting copolymers based on polystyrene-based copolymers that were, however, never tested in devices [BAC 05]. Conversely, the next series of poly(norbornenes) with pendant triarylamine (TPA) groups (poly8-poly10, poly13, poly14) was synthesized and was also evaluated as hole-transporting materials in OLEDs [BEL 98]. These polymers were prepared by ring-opening metathesis polymerization (ROMP) and influence on the length as well as the polarity of the linker used between the triarylamine functionality and the polymer backbone was examined (see Figure 5.9). Notably, replacement of the ester linker by the less polar ether function significantly enhanced the device performances, lowered the overall operating voltage and was also beneficial in terms of device stability. Notably, a maximum EQE of 0.2% and a maximum luminance of 240 cd/m<sup>2</sup> at 11 V were only achieved with poly8 in bilayer devices (ITO/poly(norbornene)-TPA (20 nm)/Alq<sub>3</sub> (50 nm)/Mg). On the other hand, a maximum brightness of 2,540 cd/m<sup>2</sup> at 8 V and a maximum EQE of 0.77% were achieved with poly14. All polymers could easily be cross-linked upon exposure to UV light, without addition of other reagents or removal of by-products, simply by cycloaddition between polymer chains.

Surprisingly, cross-linked devices showed poorer performance relative to the non-cross-linked devices and this decrease in performances was assigned to a partial decomposition of the polymers upon irradiation (cross-linking achieved upon irradiation for 1 h). Slight volume changes of the HTL layer were also observed upon cross-linking, affecting the hole-transporting ability of the layers. Carbazole-based hole-transport materials have been widely studied and the most common material is undoubtedly poly(*N*-vinyl)carbazole (PVK). This polymer is widely used for hole injection/transport materials because of its good solubility in common organic solvents, excellent film-forming properties, high glass-transition temperature (200°C) and high triplet energy (3.0 eV) [PIN 04]. If poly(carbazoles) can be designed by tethering the carbazole units via their nitrogen atoms (PVK), covalent linkage between carbazole units can also be envisioned by mean of the aromatic rings (see the diagram below). In this example, the cross-linkable poly(3,6-carbazole) was synthesized by an Ni(0)-catalyzed Yamamoto-type aryl-aryl coupling that linked all carbazole units by their 3,6-positions [GRI 11]. The required photosensitivity is introduced by attaching oxetane side groups to the poly(3,6-carbazole). For device development, cross-linking of the polymer was

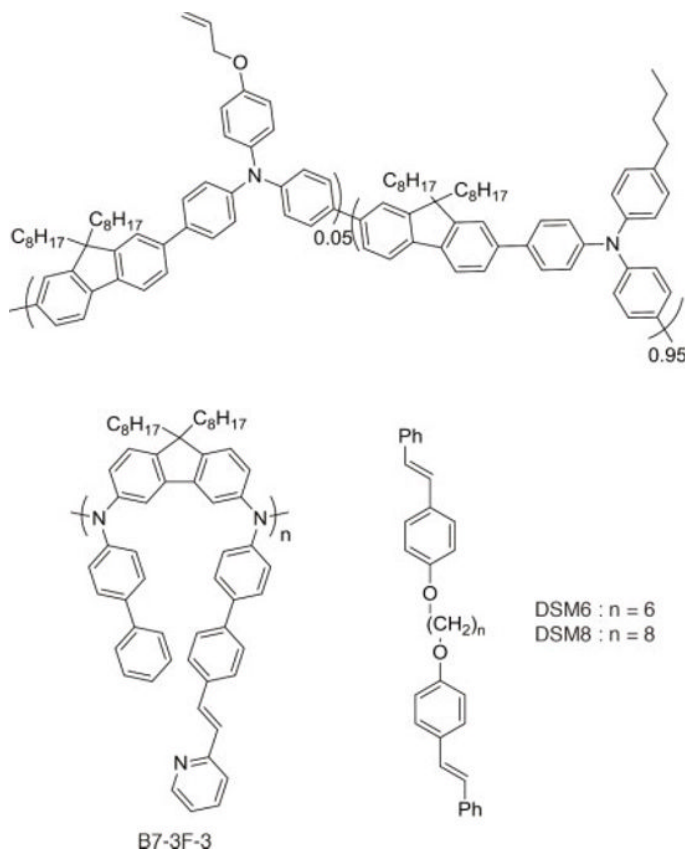
achieved photochemically by cationic ring-opening polymerization, at room temperature, during a short irradiation time (2 min) and in the presence of a cationic photoinitiator. After cross-linking, the presence of residual initiator and/or troublesome side products may result in several deleterious effects and to get rid of these side products, the resulting polymer network was thoroughly rinsed with toluene. In solution-processed double-layer devices (ITO/PKOx (15–100 nm)/poly(9,9-dioctylfluorene)-*co*-(2,5-dioctyloxyphenylene-cobenzothiadiazole) (GEP) (100 nm)/Ca/Al), the maximum brightness of ca. 15,000 cd/m<sup>2</sup>, a turn-on voltage of 3.5 V and the relatively low operational voltage suggested PKOx to act as an efficient hole-transporting layer.



Device characteristics evidenced the hole-transporting PKOx network to significantly improve both device efficiency and operational stability at high operational voltages while comparing with reference devices that do not comprise the PKOx layer. This year, thiol-ene chemistry was used for the first time to cross-link an HTL [LEE 14]. Thiol-ene chemistry exhibits a major advantage compared to the oxetane-based chemistry, namely, its insensitivity to oxygen and moisture that allows the reaction to be performed under air [KAD 10]. No complicated facilities are thus required for

cross-linking. For the thiol-ene reaction, the HTL polymer was substituted with allyl ether moieties acting as the “ene” part, the “thiol” part being brought by the photoinitiating pentaerythritol tetrakis-(3-mercaptopropionate) (see the diagram below). To create the polymer network, a mixture of 100:0.94:0.056 by weight of cross-linkable polymer: pentaerythritol tetrakis(3-mercaptopropionate) and Irgacure 369 were used. To ascertain the usefulness of the new HTL, phosphorescent OLEDs were fabricated using the following configuration: ITO/PEDOT:PSS/HTL (10 nm)/2,6-*bis*(3-(9*H*-carbazol-9-yl)phenyl)pyridine (26DCzPPy):Ir(mppy)<sub>3</sub> (7 wt%, 40 nm)/TPBI (57 nm)/CsF (1 nm)/Al. Interestingly, UV irradiation time for generating the cross-linked polymer network strongly impacted the device performances. Notably, elongation of the irradiation time increased the turn-on voltage of OLEDs and decreased the efficiencies. Hence, after 30 s of irradiation, OLEDs exhibited a CE of 31.4 cd/A and a PE of 21.8 lm/W and a turn-on voltage of 3.1 V. Conversely, after 180 s irradiation, device characteristics decreased to 27.6 cd/A and 15.6 lm/W for the maximum CE and maximum PE, respectively, with a turn-on voltage increasing to 3.7 V. To determine the origin of this difference, surface morphology was examined and no notable difference in surface roughness was detected. Investigation of the hole-transporting properties of the HTL with the irradiation time evidenced that more current passed through the HTL film at the same applied voltage with the increase in the irradiation time, explaining the decrease in device performances. Here again, the benefits of the cross-linked network were clearly demonstrated by comparing the device characteristics of OLEDs with and without cross-linkable HTL. Generation of a polymer network by the convenient substitution of a hole-injection material that can only react with a specific cross-linker was recently reported [YOO 14]. In this aim, the HIL polymer B7-3F-3 was substituted with pendant phenylstyrylpyridine groups. As cross-linking agents, distyrylpyridyl alkyl monomers (DSM6-DSM8) that can react with the pendant phenylstyrylpyridine of the polymer via a  $[2\pi + 2\pi]$  cycloaddition were used (see the diagram below). Photoreactivity of the cross-linkable conjugated polymers with the cross-linkers was clearly evidenced by the decrease in the absorption bands at high energy from the UV-visible absorption spectra upon cross-linkage. To evaluate the benefits of the cross-linkage, devices with the uncross-linked B7-3F-3 copolymer were fabricated. Devices using the well-known PEDOT:PSS were also prepared. As anticipated, in the following device configuration (ITO/HIL

(60 nm)/Alq<sub>3</sub>:NPB (3:1 wt:wt%)/LiF (1 nm)/Al where Alq<sub>3</sub> stands for *tris* (8-hydroxyquinoline)aluminum and NPB for *bis*[*N*-(1-naphthyl)-*N*-phenyl]benzidine, a higher luminance was obtained upon cross-linkage with DMS6 (2,241 cd/m<sup>2</sup> for the photoresist instead of 1,852 cd/m<sup>2</sup> for the uncross-linked B7-3F-3 copolymer). These results clearly evidenced the higher HIL ability of B7-3F-3 relative to PEDOT:PSS since B7-3F-3-based devices exhibited a higher luminance than commercially available HIL polymer PEDOT:PSS in the same device configuration (1,581 cd/m<sup>2</sup>). On the other hand, elongation of the alkyl spacer in DSM8 was detrimental to device performances that were reduced to 1,280 cd/m<sup>2</sup> as a result of the surface roughness of the photoresist. The ability of devices to withstand higher driving voltage than uncross-linked OLEDs was also noted.



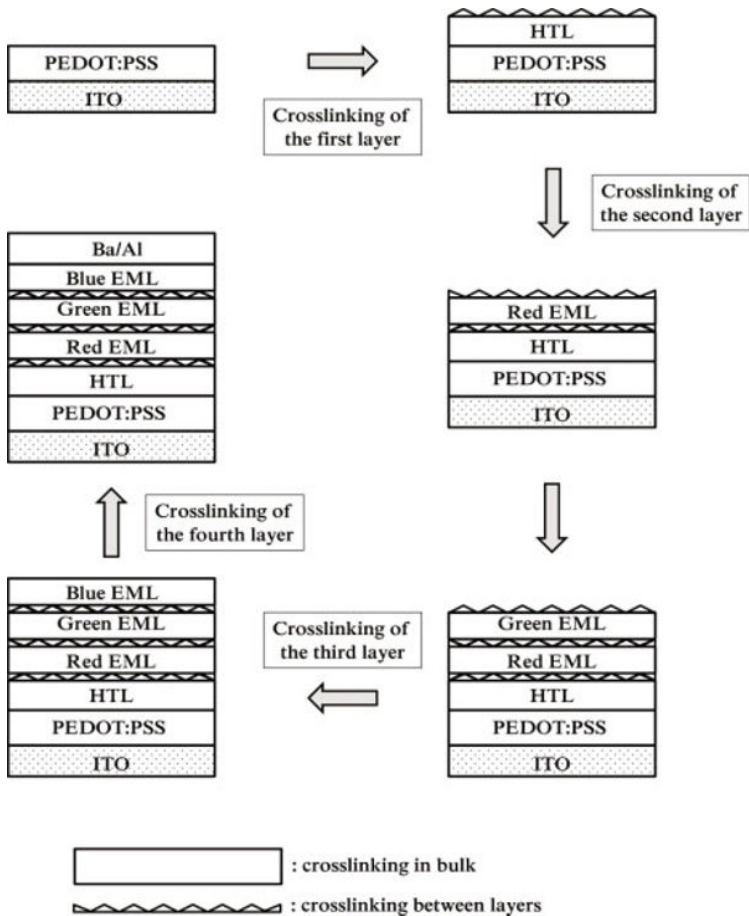


**Figure 5.10.** A multilayer device comprising four cross-linked layers

An achievement of the cross-linking strategy consists not only of cross-linking one layer of the device, as previously exemplified, but also cross-linking several layers and generating a fully cross-linked device. This goal was achieved by Meerholz and coworkers [KOH 09]. In this study, nonetheless, the oxetane-functionalized HTL was cross-linked, but the three different polymers used to produce the three complementary red/green/blue primary colors were subsequently cross-linked on top of each other, resulting in layered block-copolymer networks by living cationic polymerization (see Figure 5.10). Blend systems or copolymers containing several

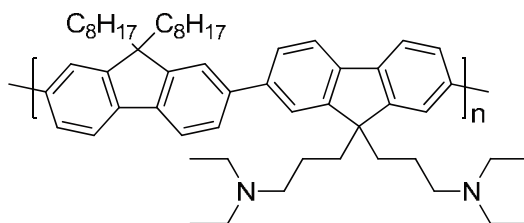
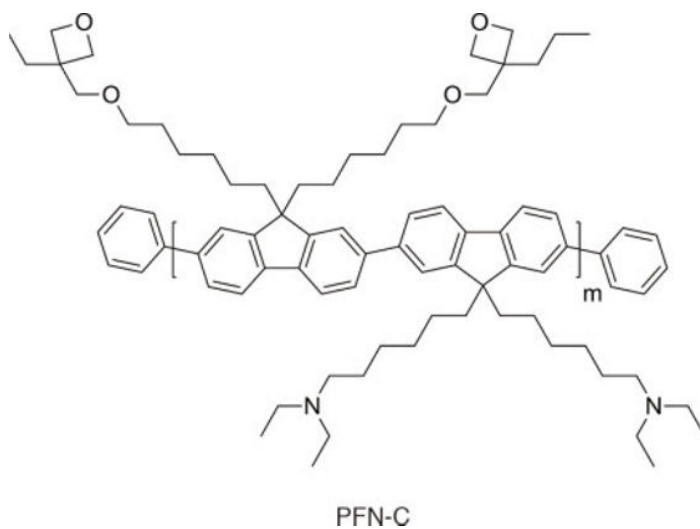
chromophores emitting in different regions of the visible spectrum are frequently used to obtain emission profiles that closely match the white point and this work continues along the same path of previous works devoted to WOLEDs. To establish the validity of this conceptually new route for processing multilayer OLEDs from solution, 20 different cross-linkable emitting polymers and cross-linkable hole-transporting polymers were tested, thus multiplying the variety of combinations. This study clearly represented a proof-of-concept as pointed out by the authors. A main point of merit is that device lifetime could be multiplied by a factor of 3, assigned to the exceptional thermal stability of the cross-linked network and a suppression of the delamination effects, commonly observed for conventional devices. In particular, the cross-linking was highly efficient as it concerned both the photopolymerization in bulk of the layers but also the cross-linkage between layers. By the presence of reactive groups exposed at the surface of the underlayer, these groups could be cross-linked with the functional groups of the upperlayer, reinforcing the strength of the cross-linking between layers.

Regarding the number of layers, this work brilliantly demonstrated that no limit exists and that up to four layers can be cross-linked. As last appealing feature, authors demonstrated that the whole process could even work in air, which dramatically simplifies OLED fabrication from the manufacturing point of view.

### **5.3.2. Polymer-based electron-transport/injection materials**

To the best of our knowledge, the first example of cross-linkable ETL was reported in 2011 [JIA 11]. Green OLEDs were prepared with this novel cross-linkable ETL material poly[9,9-*bis*(6'-(*N,N*-diethylamino)hexyl)-fluorene-*alt*-9,9-*bis*(3-ethyl(oxetane-3-ethyloxy)-hexyl)-fluorene] (PFN-C) (see the diagram below). To promote the cross-linking in bulk, soft irradiation conditions were used since exposure of the ETL to UV light was limited to 10 s, followed by thermal annealing at 120°C for 15 min. Clearly, devices showed significantly improved performances with the cross-linked ETL, compared to the non-cross-linked ETL. Thus, a maximum CE of 13.53 cd/A and a maximum EQE of 4.01% were obtained contrarily to 11.22 cd/A and 3.31% for the comparable non-cross-linked devices. Lower turn-on voltages were also obtained after cross-linking (3.7 V instead of

3.9 V). Recently, a photocurable buffer layer (BL) consisting of a blend of an epoxide adhesive (ELC 2500CL from Electro-Lite Corp.) with a well-known EIL (poly[(9,9-*bis*(3'-(*N,N*-dimethylamino) propyl)-2,7-fluorene)-*alt*-2,7-(9,9-dioctylfluorene)] (PFNR2) was developed for ink-jetting the silver cathode (see the diagram below) [ZHE 13]. Comparison with a control device fabricated with PFNR2 and an evaporated Ag cathode showed that devices fabricated with the BL and the ink-jetted nanosilver cathode exhibited higher performances than the reference devices.



Notably, devices comprising the functional EIL photoresists reached a maximum CE of 7.87 cd/A, far from the 3.60 cd/A obtained with the

vacuum processed devices. These remarkable results obtained for a fully solution-processed device, including the cathode, pave the way to industrial roll-to-roll manufacturing of OLEDs.

### 5.3.3. *Small-molecule-based hole-transport materials*

Cross-linking of hole-transport materials has been widely studied and several reviews have been published on this topic [DUA 10, NUY 02, NUY 06, PIS 09]. Among all cross-linkable HTLs that have been studied, triphenylamine dimers have been a constant model for different researchers and various derivatives of this basic structure have been designed and synthesized (see Figure 5.11) [BAC 04, BAY 99, KOE 07, KOE 10, MEE 05, PAR 11b, PAR 11c, RUD 11, RUD 12, ZAC 07]. Triphenylamine dimer comprising a dicarbazole spacer was also synthesized and tested as HTL in OLEDs [LEN 10]. To promote the cross-linking in bulk, oxetane is the most common cross-linkable functionality. The work developed by Park and coworkers constitute an elegant strategy to generate a frozen junction in double-layered ionic *p-i-n* OLEDs by combining simultaneously a thermal and an electrical treatment [PAR 11b, PAR 11c]. After spin-coating the HTL, a soft photocuring step was carried out to promote the cross-linking. To dope the interfaces and accumulate ions at both interfaces, the emitter in the EML was blended with a salt that separated upon application of an electric field and the simultaneous thermal annealing applied to the device favored the charge migration/separation (see Figure 5.12). Ion mobility is facilitated by heating the EML and positive charges accumulate at the cathode, the negative charge accumulating in the cross-linked HTL close to the anode.

After terminating the electric field and cooling, ions remained immobilized near the electrodes, facilitating hole and electron injection through the tunneling barriers from the electrodes. A frozen junction is thus formed. This work is really similar to that reported by Gao and coworkers the same year [WAN 12]. As salt that could separate under an electric field, tetrabutylammonium tetrafluoroborate  $\text{Bu}_4\text{NBF}_4$  was used. Using this strategy, a peak brightness of approximately  $38,000 \text{ cd/m}^2$  and a peak CE of ca.  $35 \text{ cd/A}$  were achieved, which constitute among the best results ever reported for solution-processed devices.

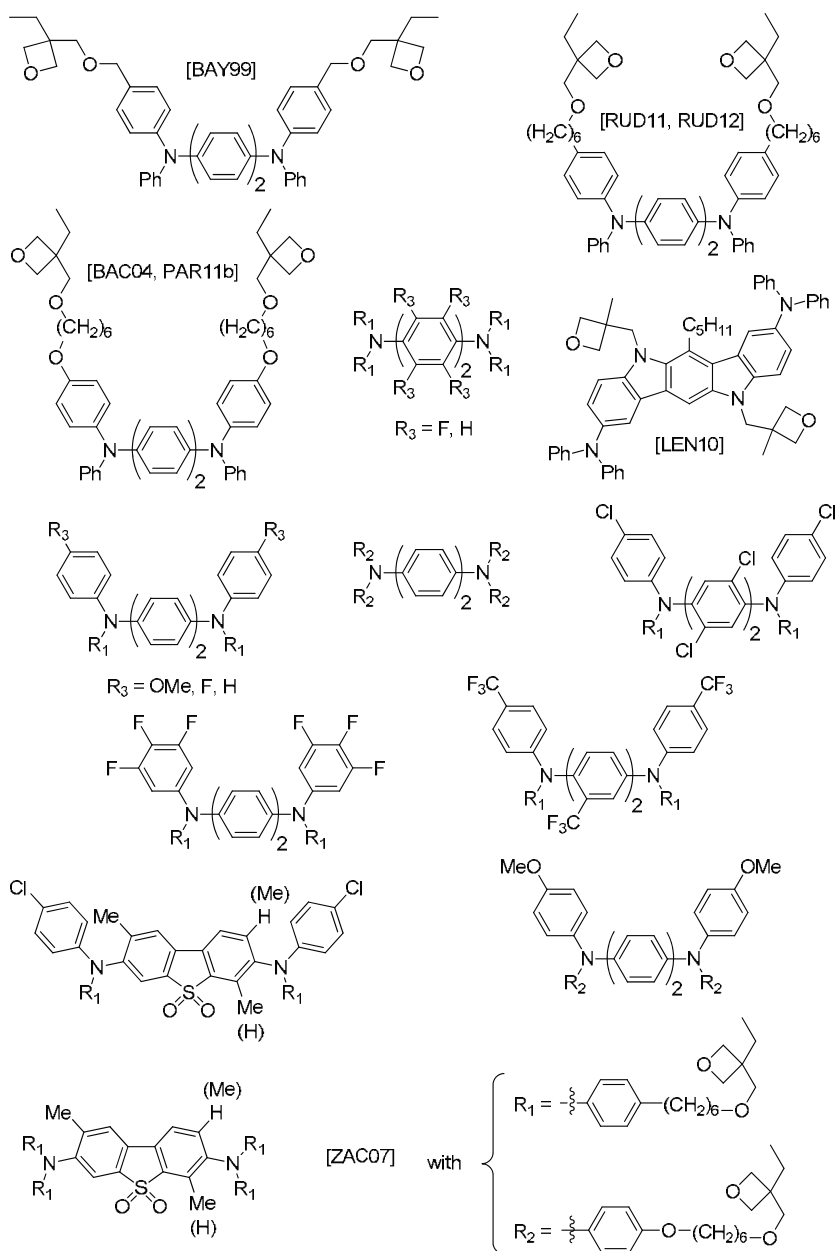
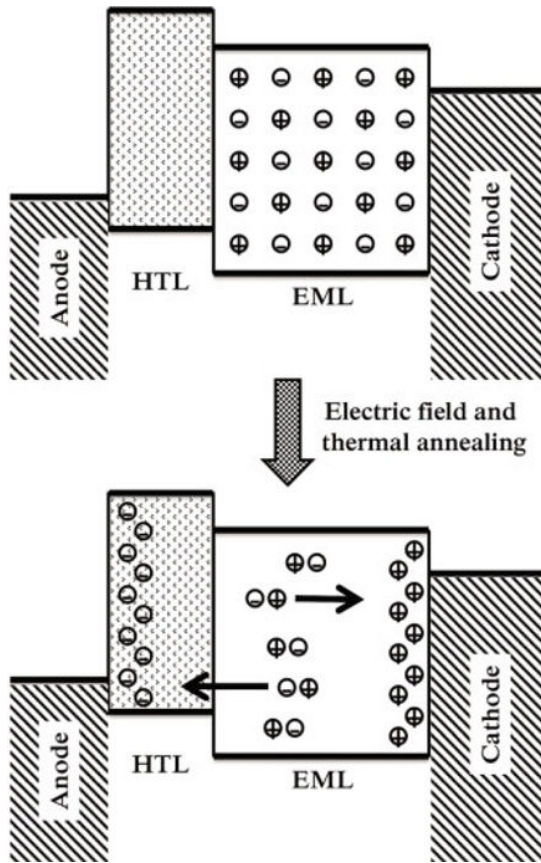


Figure 5.11. Examples of cross-linkable triphenylamine dimers



**Figure 5.12.** Principle developed by Park and coworkers to dope the two interfaces

## 5.4. Conclusion

Cross-linking in LEDs clearly addresses the device development issue. By generating chemical bonds between polymer chains, the former layer can no longer be dissolved by the solvent of the subsequent layer. Devices comprising up to four cross-linked layers have been fabricated. Cross-linking is also going beyond the unique simplification of the device fabrication. Benefits in terms of device performance, device lifetime and thermal stability have also been evidenced. Photocuring is often combined to

thermal annealing that allows direct structuring of the EL layer and/or HTL of OLEDs during exposure to UV light. Use of oxetane-functionalized cross-linkable materials for functional photoresists is undoubtedly the most common strategy as this cross-linkable group does not affect the electrical and optical properties of OLEDs even though some limitations have been identified. Notably, the presence of the cationic photoinitiator required during cross-linking can constitute a major drawback as the presence of residual initiator and/or undesired side products may result in several deleterious effects for device performances. This chapter has clearly evidenced that the hole transport and the EML have been the focus of numerous studies. One field has only been scarcely studied, i.e. the development of cross-linkable ETL/EIL. The future of this research definitely concerns the synthesis of cross-linkable ETL/EIL as a stepped progression of the LUMO energy levels from the cathode is determinant for reducing of the driving voltage and favoring electron transport/injection in the EML.

## 5.5. Bibliography

- [AHM 12] AHMED E., EARMME T., JENEKHE S.A., “High-performance multilayered phosphorescent OLEDs by solution-processed commercial electron-transport materials”, *Journal of Materials Chemistry*, vol. 22, no. 11, pp. 4660–4668, 2012.
- [ARI 03] ARIU M., SIMS M., RAHN M.D. *et al.*, “Exciton migration in  $\beta$ -phase poly(9,9-dioctylfluorene)”, *Physical Review B*, vol. 67, no. 195333, 2003.
- [BAB 04] BABA A., ONISHI K., KNOLL W. *et al.*, “Investigating work function tunable hole-injection/transport layers of electrodeposited polycarbazole network thin films”, *Journal of Physical Chemistry B*, vol. 108, no. 49, pp. 18949–18955, 2004.
- [BAC 04] BACHER E., JUNGERMANN S., ROJAHN M. *et al.*, “Photopatterning of crosslinkable hole-conducting materials for application in organic light-emitting devices”, *Macromolecular Rapid Communications*, vol. 25, no. 12, pp. 1191–1196, 2004.
- [BAC 05] BACHER E., BAYERL M., RUDATI P. *et al.*, “Synthesis and characterization of photo-crosslinkable hole-conducting polymers”, *Macromolecules*, vol. 38, no. 5, pp. 1640–1647, 2005.

- [BAY 99] BAYERL M., BRAIG T., NUYKEN O. *et al.*, “Crosslinkable hole-transport materials for preparation of multilayer organic light emitting devices by spin-coating”, *Macromolecular Rapid Communications*, vol. 20, no. 4, pp. 224–228, 1999.
- [BEL 98] BELLMANN E., SHAHEEN S.E., THAYUMANAVAN S. *et al.*, “New triarylamine-containing polymers as hole transport materials in organic light-emitting diodes: effect of polymer structure and cross-linking on device characteristics”, *Chemistry of Materials*, vol. 10, no. 6, pp. 1668–1676, 1998.
- [BLI 99] BLIZNYUK V.N., CARTER S.A., SCOTT J.C. *et al.*, “Electrical and photoinduced degradation of polyfluorene based films and light-emitting devices”, *Macromolecules*, vol. 32, no. 2, pp. 361–369, 1999.
- [BRA 05] BRAESE S., GIL C., KNEPPER K. *et al.*, “Organic azides: an exploding diversity of a unique class of compounds”, *Angewandte der Chemie International Edition*, vol. 44, no. 33, pp. 5188–5240, 2005.
- [BOZ 03] BOZANO L.D., CARTER K.R., LEE V.Y. *et al.*, “Electroluminescent devices based on cross-linked polymer blends”, *Journal of Applied Physics*, vol. 94, no. 5, pp. 3061–3068, 2003.
- [BUC 04] BUCHGRABER C., SPANRING J., POGANTSCH A. *et al.*, “Organosilanes as new reagents for the photopatterning of PPV type polymers”, *Synthetic Metals*, vol. 147, nos. 1–3, pp. 91–95, 2004.
- [CHA 12] CHARAS A., MORGADO J., “Oxetane-functionalized conjugated polymers in organic (opto)electronic devices”, *Current Physical Chemistry*, vol. 2, no. 3, pp. 241–264, 2012.
- [CHE 05] CHEN S.H., SU A.C., SU C.H., “Crystalline forms and emission behavior of poly(9,9-di-n-octyl-2,7-fluorene)”, *Macromolecules*, vol. 38, no. 2, pp. 379–385, 2005.
- [CHO 04] CHOCHOS C.L., TSOLAKIS P.K., GREGORIOU V.G. *et al.*, “Influence of the coil block on the properties of rod-coil diblock copolymers with oligofluorene as the rigid segment”, *Macromolecules*, vol. 37, no. 7, pp. 2502–2510, 2004.
- [COS 12] COSTA R.D., ORTI E., BOLINK H.J. *et al.*, “Luminescent ionic transition-metal complexes for light-emitting electrochemical cells”, *Angewandte der Chemie International Edition*, vol. 51, no. 33, pp. 8178–8211, 2012.
- [CRA 03] CRAIG M.R., DE KOH M.M., HOSFTRAAT J.W. *et al.*, “Improving color purity and stability in a blue emitting polyfluorene by monomer purification”, *Journal of Material Chemistry*, vol. 13, no. 12, pp. 2861–2862, 2003.

- [DAV 11] DAVIS A.R., MAEGERLEIN J.A., CARTER K.R., “Electroluminescent networks via photo ‘Click’ chemistry”, *Journal of the American Chemical Society*, vol. 133, no. 24, pp. 20546–20551, 2011.
- [DU 06] DU N., TIAN R., PENG J. *et al.*, “Cross-linked Alq<sub>3</sub>-containing polymers with improved electroluminescence efficiency used for OLEDs”, *Macromolecular Rapid Communications*, vol. 27, no. 6, pp. 412–417, 2006.
- [DUA 10] DUAN L., HOU L., LEE T.-W. *et al.*, “Solution processable small molecules for organic light-emitting diodes”, *Journal of Material Chemistry*, vol. 20, no. 31, pp. 6392–6407, 2010.
- [DUM 11] DUMUR F., GUILLANEUF Y., GUERLIN A. *et al.*, “Random copolymers with pendant cationic mixed-ligand terpyridine-based iridium (III) complexes: synthesis and application in light-emitting devices”, *Macromolecular Chemistry and Physics*, vol. 212, no. 15, pp. 1616–1628, 2011.
- [DUM 12] DUMUR F., BERTIN D., GIGMES D., “Iridium (III) complexes as promising emitters for solid-state light-emitting electrochemical cells (LECs)”, *International Journal of Nanotechnology*, vol. 9, no. 3/4/5/6/7, pp. 377–395, 2012.
- [EAR 12] EARMME T., JENEKHE S.A., “Solution-processed, alkali metal-salt-doped, electron-transport layers for high-performance phosphorescent organic light-emitting diodes”, *Advanced Functional Materials*, vol. 22, no. 24, pp. 5126–5136, 2012.
- [FAB 01] FABER R., STASKO A., NUYKEN O., “New blue crosslinkable polymers for organic light emitting devices”, *Journal of Macromolecular Science: Pure and Applied Chemistry*, vol. A38, no. 4, pp. 353–364, 2001.
- [FIF 84] FIFE D.J., MOORE W.M., MORSE K.W., “Solution equilibria of tertiary phosphine complexes of copper (I) halides”, *Inorganic Chemistry*, vol. 23, no. 12, pp. 1684–1691, 1984.
- [GAA 03] GAAL M., LIST E.J.W., SCHERF U., “Excimers or emissive on-chain defects?”, *Macromolecules*, vol. 36, no. 11, pp. 4236–4237, 2003.
- [GAO 10] GAO H., POULSEN D.A., MA B. *et al.*, “Site isolation of emitters within cross-linked polymer nanoparticles for white electroluminescence”, *Nano Letters*, vol. 10, no. 4, pp. 1440–1444, 2010.

- [GAT 07] GATHER M.C., KOEHNEN A., FALCOU A. *et al.*, “Solution-processed full-color polymer organic light-emitting diode displays fabricated by direct photolithography”, *Advanced Functional Materials*, vol. 17, no. 2, pp. 191–200, 2007.
- [GON 05] GONG X., WANG S., MOSES D. *et al.*, “Multilayer polymer light-emitting diodes: white-light emission with high efficiency”, *Advanced Materials*, vol. 17, no. 17, pp. 2053–2058, 2005.
- [GRE 98] GRELL M., BRADLEY D.D.C., LONG X. *et al.*, “Chain geometry, solution aggregation and enhanced dichroism in the liquidcrystalline conjugated polymer poly(9,9-dioctylfluorene)”, *Acta Polymerica*, vol. 49, no. 8, pp. 439–444, 1998.
- [GRE 99] GRELL M., BRADLEY D.D.C., UNGAR G. *et al.*, “Interplay of physical structure and photophysics for a liquid crystalline polyfluorene”, *Macromolecules*, vol. 32, no. 18, pp. 5810–5817, 1999.
- [GRI 11] GRIGALEVICIUS S., ZHANG B., XIE Z. *et al.*, “Polycarbazole-based networks made by photo-crosslinking for hole transporting layers of OLED devices”, *Organic Electronics*, vol. 12, no. 12, pp. 2253–2257, 2011.
- [GU 11] GU C., FEI T., YAO L. *et al.*, “Multilayer polymer stacking by *in situ* electrochemical polymerization for color-stable white electroluminescence”, *Advanced Materials*, vol. 23, no. 4, pp. 527–530, 2011.
- [HAL 00] HALLS J.J.M., ARIAS A.C., MACKENZIE J.D. *et al.*, “Photodiodes based on polyfluorene composites: influence of morphology”, *Advanced Materials*, vol. 12, no. 7, pp. 498–502, 2000.
- [HRE 02] HREHA R.D., ZHANG Y.D., DOMERCQ B. *et al.*, “Synthesis of photo-crosslinkable hole-transport polymers with tunable oxidation potentials and their use in organic light-emitting diodes”, *Synthesis*, vol. 9, no. 9, pp. 1201–1212, 2002.
- [HU 12] HU T., HE L., DUAN L. *et al.*, “Solid-state light-emitting electrochemical cells based on ionic iridium(III) complexes”, *Journal of Material Chemistry*, vol. 22, no. 10, pp. 4206–4215, 2012.
- [HUA 04] HUANG F., HOU L.T., WU H.B. *et al.*, “High-efficiency, environment-friendly electroluminescent polymers with stable high work function metal as a cathode: green- and yellow-emitting conjugated polyfluorene polyelectrolytes and their neutral precursors”, *Journal of the American Chemical Society*, vol. 126, no. 31, pp. 9845–9853, 2004.

- [HUA 08] HUANG F., CHENG Y.-J., ZHANG Y. *et al.*, “Crosslinkable hole-transporting materials for solution processed polymer light-emitting diodes”, *Journal of Materials Chemistry*, vol. 18, no. 38, pp. 4495–4509, 2008.
- [HUY 08] HUYAL I.O., KOLDEMIR U., OZEL T. *et al.*, “On the origin of high quality white light emission from a hybrid organic/inorganic light emitting diode using azide functionalized polyfluorene”, *Journal of Material Chemistry*, vol. 18, no. 30, pp. 3568–3574, 2008.
- [JEO 09] JEON W.S., PARK T.J., KIM S.Y. *et al.*, “Ideal host and guest system in phosphorescent OLEDs”, *Organic Electronics*, vol. 10, no. 2, pp. 240–246, 2009.
- [JEO 11] JEON S.O., JANG S.E., SON H.S. *et al.*, “External quantum efficiency above 20% in deep blue phosphorescent organic light-emitting diodes”, *Advanced Materials*, vol. 23, no. 12, pp. 1436–1441, 2011.
- [JIA 11] JIAN L.S., MEI Z.C., JIE Z. *et al.*, “A novel crosslinkable electron/injection transporting material for solution processed polymer light-emitting diodes”, *Science China Chemistry*, vol. 54, no. 11, pp. 1745–1749, 2011.
- [KAD 10] KADE M.J., BURKE D.J., HAWKER C.J., “The power of thiol-ene chemistry”, *Journal of Polymer Science Part A: Polymer Chemistry*, vol. 48, no. 4, pp. 743–750, 2010.
- [KAP 08] KAPPAUN S., SLUGOCV C., LIST E.J.W., “Phosphorescent organic light-emitting devices: working principle and iridium based emitter materials”, *International Journal of Molecular Sciences*, vol. 9, no. 8, pp. 1527–1547, 2008.
- [KLA 99a] KLAERNER G., LEE J.I., LEE V.Y. *et al.*, “Cross-linkable polymers based on dialkylfluorenes”, *Chemistry of Materials*, vol. 11, no. 7, pp. 1800–1805, 1999.
- [KLA 99b] KLAENER G., TROLLSAS M., HEISE A. *et al.*, “Concurrent chain and stepwise polymerizations for the preparation of block copolymers in one step”, *Macromolecules*, vol. 32, no. 24, pp. 8227–8229, 1999.
- [KO 10] KO L.-C., LIU T.-Y., CHEN C.-Y. *et al.*, “Multi-layer organic light-emitting diodes processed from solution using phosphorescent dendrimers in a polymer host”, *Organic Electronics*, vol. 11, no. 6, pp. 1005–1009, 2010.
- [KOE 07] KOEHNEN A., GATHER M.C., RIEGEL N. *et al.*, “Enhanced efficiency of multilayer organic light-emitting diodes with a low-refractive index hole-transport layer: an effect of improved outcoupling?”, *Applied Physics Letters*, vol. 91, no. 11, no. 113501, 2007.

- [KOE 10] KOEHNEN A., IRION M., GATHER M.C. *et al.*, “Highly color-stable solution-processed multilayer WOLEDs for lighting application”, *Journal of Materials Chemistry*, vol. 20, no. 16, pp. 3301–3306, 2010.
- [KOH 09] KOHNEN A., RIEGEL N., KREMER J.H.-W.M. *et al.*, “The simple way to solution-processed multilayer OLEDs – layered block-copolymer networks by living cationic polymerization”, *Advanced Materials*, vol. 21, no. 8, pp. 879–884, 2009.
- [KON 04] KONG X.X., JENEKHE S.A., “Block copolymers containing conjugated polymer and polypeptide sequences: synthesis and self-assembly of electroactive and photoactive nanostructures”, *Macromolecules*, vol. 37, no. 22, pp. 8180–8183, 2004.
- [LEE 14] LEE J., HAN H., LEE J. *et al.*, “Utilization of ‘thiol–ene’ photo cross-linkable hole-transporting polymers for solution-processed multilayer organic light-emitting diodes”, *Journal of Material Chemistry C*, vol. 2, no. 8, pp. 1474–1481, 2014.
- [LEE 99] LEE J.K., KLAERNER G., MILLER R.D., “Oxidative Stability and Its Effect on the Photoluminescence of Poly(Fluorene) Derivatives: End Group Effects”, *Chemistry of Materials*, vol. 11, no. 4, pp. 1083–1088, 1999.
- [LEN 10] LENGVINAITE S., GRAZULEVICIUS J.V., GRIGALEVICIUS S. *et al.*, “Indolo[3,2-b]carbazole-based functional derivatives as materials for light emitting diodes”, *Dye and Pigments*, vol. 85, no. 3, pp. 183–188, 2010.
- [LI 97] LI X.-C., YONG T.-M., GRUENER J. *et al.*, “A blue light emitting copolymer with charge transporting and photo-crosslinkable functional units”, *Synthetic Metals*, vol. 84, nos. 1–3, pp. 437–438, 1997.
- [LIM 11] LIM Y., PARK Y.-S., KANG Y. *et al.*, “Hole injection/transport materials derived from Heck and sol–gel chemistry for application in solution-processed organic electronic devices”, *Journal of the American Chemical Society*, vol. 133, no. 5, pp. 1375–1382, 2011.
- [LIN 09] LIN C.-Y., LIN Y.-C., HUNG W.-Y. *et al.*, “A thermally cured 9,9-diarylfuorene-based triaryldiamine polymer displaying high hole mobility and remarkable ambient stability”, *Journal of Materials Chemistry*, vol. 19, no. 22, pp. 3618–3623, 2009.
- [LIU 08] LIU M.S., NIU Y.-H., KA J.-W. *et al.*, “Thermally cross-linkable hole-transporting materials for improving hole injection in multilayer blue-emitting phosphorescent polymer light-emitting diodes”, *Macromolecules*, vol. 41, no. 24, pp. 9570–9580, 2008.

- [LU 02] LU S., FAN Q.L., LIU S.Y. *et al.*, “Synthesis of conjugated–acidic block copolymers by atom transfer radical polymerization”, *Macromolecules*, vol. 35, no. 27, pp. 9875–9881, 2002.
- [LU 03] LU S., FAN Q.L., CHUA S.J. *et al.*, “Synthesis of conjugated–ionic block copolymers by controlled radical polymerization”, *Macromolecules*, vol. 36, no. 2, pp. 304–310, 2003.
- [LUO 10] LUO Y., AZIZ H., “Correlation between triplet–triplet annihilation and electroluminescence efficiency in doped fluorescent organic light-emitting devices”, *Advanced Functional Materials*, vol. 20, no. 8, pp. 1285–1293, 2010.
- [MA 07] MA B., LAUTERWASSER F., DENG L. *et al.*, “New thermally cross-linkable polymer and its application as a hole-transporting layer for solution processed multilayer organic light emitting diodes”, *Chemistry of Materials*, vol. 19, no. 19, pp. 4827–4832, 2007.
- [MA 09] MA B., KIM B.J., POULSEN D.A. *et al.*, “Multifunctional crosslinkable iridium complexes as hole transporting/electron blocking and emitting materials for solution-processed multilayer organic light-emitting diodes”, *Advanced Functional Materials*, vol. 19, no. 7, pp. 1024–1031, 2009.
- [MAR 94] MARCINEK A., PLATZ M.S., CHAN S.Y. *et al.*, “Unusually long lifetimes of the singlet nitrenes derived from 4-azido-2,3,5,6-tetrafluorobenzamides”, *Journal of Physical Chemistry*, vol. 98, no. 2, pp. 412–419, 1994.
- [MAR 99] MARSITZKY D., KLAPPER M., MUELLEN K., “End-functionalization of poly(2,7-fluorene): a key step toward novel luminescent rod–coil block copolymers”, *Macromolecules*, vol. 32, no. 25, pp. 8685–8688, 1999.
- [MEE 05] MEERHOLZ K., MUELLER C.D., NUYKEN O., *Organic Light-Emitting Devices: Synthesis, Properties and Applications*, MÜLLEN K., SCHERF U. (eds), Wiley-VCH, Weinheim, p. 426, 2005.
- [MUE 00] MUELLER D.C., BRAIG T., NOTHOFER H.-G. *et al.*, “Efficient blue organic light-emitting diodes with graded hole-transport layers”, *ChemPhysChem*, vol. 1, no. 4, pp. 207–211, 2000.
- [MUL 03] MULLER C.D., FALCOU A., RECKEFUSS N. *et al.*, “Multi-colour organic light-emitting displays by solution processing”, *Nature*, vol. 421, pp. 829–833, 2003.

- [NUY 02] NUYKEN O., BACHER E., BRAIG T. *et al.*, “Crosslinkable hole- and electron-transport materials for application in organic light emitting devices (OLEDs)”, *Designed Monomers and Polymers*, vol. 5, nos. 2–3, pp. 195–210, 2002.
- [NUY 06] NUYKEN O., JUNGERMANN S., WIEDERHIRN V. *et al.*, “Modern trends in organic light-emitting devices (OLEDs)”, *Monatshefte für Chemie*, vol. 137, no. 7, pp. 811–824, 2006.
- [OOS 14] OOSTRA A.J., BLOM P.W.M., MICHELS J.J., “Prevention of short circuits in solution-processed OLED devices”, *Organic Electronics*, vol. 15, no. 6, pp. 1166–1172, 2014.
- [PAR 09] PARK M.-J., LEE J.-I., CHU H.-Y. *et al.*, “Light-emitting properties of photo-curable polyfluorene derivatives”, *Synthetic Metals*, vol. 159, no. 14, pp. 1393–1397, 2009.
- [PAR 11a] PARK J.Y., KIM D.-E., PONNAPATI R. *et al.*, “Electroluminescent properties of an electrochemically cross-linkable carbazole peripheral poly(benzyl ether)dendrimer”, *ChemPhysChem*, vol. 12, no. 5, pp. 1010–1015, 2011.
- [PAR 11b] PARK B., JEON H.G., HUH Y.H. *et al.*, “Solution-processable double-layered ionic p-i-n organic light-emitting diodes”, *Current Applied Physics*, vol. 11, no. 3, pp. 673–676, 2011.
- [PAR 11c] PARK B., HUH Y.H., PARK J. *et al.*, “Solution-processable double-layered ionic p-i-n organic light-emitting diodes”, *Journal of the Society for Information Display*, vol. 19, no. 4, pp. 342–345, 2011.
- [PEI 99] PEI J., YU W.L., HUANG W. *et al.*, “The synthesis and characterization of an efficient green electroluminescent conjugated polymer: poly[2,7-bis(4-hexylthienyl)-9,9-dihexyl-fluorene]”, *In Chem. Commun.*, no. 17, pp. 1631–1632, 2000.
- [PIN 04] PINA J., SEIXAS DE MELO J., BURROWS H.D. *et al.*, “On the triplet state of poly(N-vinylcarbazole)”, *Chemical Physics Letters*, vol. 400, nos. 4–6, pp. 441–445, 2004.
- [PIS 09] PISULA W., ZORN M., CHANG J.Y. *et al.*, “Liquid crystalline ordering and charge transport in semiconducting materials”, *Macromolecular Rapid Communications*, vol. 30, no. 14, pp. 1179–1202, 2009.

- [PNG 10] PNG R.-Q., CHIA P.-J., TANG J.-C. *et al.*, “High-performance polymer semiconducting heterostructure devices by nitrene-mediated photocrosslinking of alkyl side chains”, *Nature Materials*, vol. 9, no. 2, pp. 152–158, 2010.
- [POE 92] POE R., SCHNAPP K.A., YOUNG M.J.T. *et al.*, “Chemistry and kinetics of singlet (pentafluorophenyl)nitrene”, *Journal of the American Chemical Society*, vol. 114, no. 13, pp. 5054–5067, 1992.
- [QIA 06] QIANG Z., MA Z., ZHENG Z. *et al.*, “Novel Photo-crosslinkable light-emitting rod/coil copolymers: underlying facile material for fabricating pixelated displays”, *Macromolecular Rapid Communications*, vol. 27, no. 20, pp. 1779–1786, 2006.
- [REH 08] REHMANN N., ULBRICHT C., KOEHNEN A. *et al.*, “Advanced device architecture for highly efficient organic light-emitting diodes with an orange-emitting crosslinkable iridium(III) complex”, *Advanced Materials*, vol. 20, no. 1, pp. 129–133, 2008.
- [RUD 11] RUDATI P.S., “The preparation of insoluble hole-transport layer via cationic induced ring-opening polymerization of oxetan-derivatized materials by poly(3,4-ethylenedioxythiophene)”, *Journal Material dan Energi Indonesia*, vol. 01, no. 03, pp. 148–153, 2011.
- [RUD 12] RUDATI P.S., MUELLER D.C., MEERHOLZ K., “Preparation of insoluble hole-injection layers by cationic ring-opening polymerisation of oxetane-derivatized triphenylamine dimer for organic electronics devices”, *Procedia Chemistry*, vol. 4, pp. 216–223, 2012.
- [SAL 13] SALERT B.C.D., KRUEGER H., BAGHICH S.A. *et al.*, “New polymer matrix system for phosphorescent organic light-emitting diodes and the role of the small molecular co-host”, *Journal of Polymer Science A: Polymer Chemistry*, vol. 51, no. 3, pp. 601–613, 2013.
- [SIM 04] SIMS M., BRADLEY D.D.C., ARIU M. *et al.*, “Understanding the origin of the 535-nm emission band in oxidized poly(9,9-dioctylfluorene): the essential role of inter-chain/inter-segment interactions”, *Advanced Functional Materials*, vol. 14, no. 8, pp. 765–781, 2004.
- [SUN 04] SUNG H.H., LIN H.C., “Novel alternating fluorene-based conjugated polymers containing oxadiazole pendants with various terminal groups”, *Macromolecules*, vol. 37, no. 21, pp. 7945–7954, 2004.
- [TAN 87] TANG C.W., VANSLYKE S.A., “Organic electroluminescent diodes”, *Applied Physics Letters*, vol. 51, no. 12, pp. 913–915, 1987.

- [TAN 89] TANG C.W., VANSLYKE S.A., CHEN C.H., “Electroluminescence of doped organic thin films”, *Journal of Applied Physics*, vol. 65, no. 9, pp. 3610–3616, 1989.
- [THE 12] THEJO KALYANIA N., DHOBLE S.J., “Organic light emitting diodes: energy saving lighting technology – a review”, *Renewable & Sustainable Energy Reviews*, vol. 16, no. 5, pp. 2696–2723, 2012.
- [TSA 06] TSAI C.-J., CHEN Y., “Luminescent poly(p-phenylenevinylene) with 4-methylcoumarin side groups: synthesis, optical properties and photo-crosslinking behaviors”, *Reactive & Functional Polymers*, vol. 66, no. 11, pp. 1327–1335, 2006.
- [TSE 06] TSENG S.-R., LIN S.-C., MENG H.-F. *et al.*, “General method to solution-process multilayer polymer light-emitting diodes”, *Applied Physics Letters*, vol. 88, no. 163501, 2006.
- [TSE 08] TSENG S.-R., MENG H.-F., YEH C.-H. *et al.*, “High-efficiency blue multilayer polymer light-emitting diode fabricated by a general liquid buffer method”, *Synthetic Metals*, vol. 158, nos. 3–4, pp. 130–134, 2008.
- [ULB 07] ULBRICHT C., REHMANN N., HOLDER E. *et al.*, “Design of polymerizable phosphorescent iridium(III) complexes”, *Polymer Preprints*, vol. 48, pp. 703–704, 2007.
- [ULB 09] ULBRICHT C., REHMANN N., HOLDER E. *et al.*, “Synthesis and characterization of oxetane-functionalized phosphorescent Ir(III)-complexes”, *Macromolecular Chemistry and Physics*, vol. 210, no. 7, pp. 531–541, 2009.
- [VOL 12] VOLZ D., BAUMANN T., FLUEGGE H. *et al.*, “Auto-catalysed crosslinking for next-generation OLED-design”, *Journal of Materials Chemistry*, vol. 22, no. 38, pp. 20786–20790, 2012.
- [VOL 13] VOLZ D., ZINK D.M., BOCKROCKER T. *et al.*, “Molecular construction kit for tuning solubility, stability and luminescence properties: heteroleptic MePyrPHOS-copper iodide-complexes and their application in organic light-emitting diodes”, *Chemistry of Materials*, vol. 25, no. 17, pp. 3414–3426, 2013.
- [WAL 09] WALLIKEWITZ B.H., HERTEL D., MERRHOLZ K., “Cross-linkable polyspirobifluorenes: a material class featuring good OLED performance and low amplified spontaneous emission thresholds”, *Chemistry of Materials*, vol. 21, no. 21, pp. 2912–2919, 2009.

- [WAN 10] WANG P.-H., HO M.-S., YANG S.-H. *et al.*, “Synthesis of thermal-stable and photo-crosslinkable polyfluorenes for the applications of polymer light-emitting diodes”, *Journal of Polymer Science Part A: Polymer Chemistry*, vol. 48, no. 3, pp. 516–524, 2010.
- [WAN 12] WANTZ G., GAUTIER B., DUMUR F. *et al.*, “Towards frozen organic PN junctions at room temperature using high-Tg polymeric electrolytes”, *Organic Electronics*, vol. 13, no. 10, pp. 1859–1864, 2012.
- [WET 10] WETTACH H., JESTER S.S., COLSMANN A. *et al.*, “Deep blue organic light-emitting diodes based on triphenylenes”, *Synthetic Metals*, vol. 160, nos. 7–8, pp. 691–700, 2010.
- [WU 04] WU H., HUANG F., MO Y.Q. *et al.*, “Efficient electron injection from a bilayer cathode consisting of aluminum and alcohol-/water-soluble conjugated polymers”, *Advanced Materials*, vol. 16, no. 20, pp. 1826–1830, 2004.
- [WU 06] WU G., YANG C., FAN B. *et al.*, “Synthesis and characterization of photo-crosslinkable polyfluorene with acrylate side-chains”, *Journal of Applied Polymer Science*, vol. 100, no. 3, pp. 2336–2342, 2006.
- [XIA 06] XIA Y., FRIEND R.H., “Phase separation of polyfluorene-based blend films and its influence on device operations”, *Advanced Materials*, vol. 18, no. 11, pp. 1371–1376, 2006.
- [YAN 06] YANG X.H., MULLER D.C., NEHER D. *et al.*, “Highly efficient polymeric electrophosphorescent diodes”, *Advanced Materials*, vol. 18, no. 7, pp. 948–954, 2006.
- [YER 11] YERSIN H., RAUSCH A.F., CZERWIENIEC R. *et al.*, “The triplet state of organo-transition metal compounds. Triplet harvesting and singlet harvesting for efficient OLEDs”, *Coordination Chemistry Review*, vol. 255, nos. 21–22, pp. 2622–2652, 2011.
- [YOO 14] YOO T.W., PARK C., MAI N.T. *et al.*, “Synthesis of new conjugated polymers as hole injection layer and performance of OLED devices”, *Molecular Crystals and Liquid Crystals*, vol. 551, no. 1, pp. 69–77, 2014.
- [YOU 09] YOU J.-D., TSENG S.-R., MENG H.-F. *et al.*, “All-solution-processed blue small molecular organic light-emitting diodes with multilayer device structure”, *Organic Electronics*, vol. 10, no. 8, pp. 1610–1614, 2009.
- [YU 99] YU W.L., PEI J., CAO Y. *et al.*, “New efficient blue light emitting polymer for light emitting diodes”, *in chem. Commun.*, no. 18, pp. 1837–1838, 1999.

- [ZAC 07] ZACHARIAS P., GATHER M.C., ROJAHN M. *et al.*, “New crosslinkable hole conductors for blue-phosphorescent organic light-emitting diodes”, *Angewandte der Chemie International Edition*, vol. 46, no. 23, pp. 4388–4392, 2007.
- [ZHA 04] ZHAO W., CAO T., WHITE J.M., “On the origin of green emission in polyfluorene polymers: the roles of thermal oxidation degradation and crosslinking”, *Advanced Functional Materials*, vol. 14, no. 8, pp. 783–790, 2004.
- [ZHA 10] ZHANG Y., FORREST S.R., “Triplet diffusion leads to triplet–triplet annihilation in organic phosphorescent emitters”, *Chemical Physics Letters*, vol. 590, pp. 106–110, 2013.
- [ZHE 13] ZHENG H., ZHENG Y., LIU N. *et al.*, “All-solution processed polymer light-emitting diode displays”, *Nature Communications*, vol. 4, no. 1971, 2013.
- [ZHO 00] ZHOU X., HE J., LIAO L.S. *et al.*, “Real-time observation of temperature rise and thermal breakdown processes in organic LEDs using an IR imaging and analysis system”, *Advanced Materials*, vol. 12, no. 4, pp. 265–269, 2000.
- [ZHO 11] ZHONG C., LIU S., HUANG F. *et al.*, “Highly efficient electron injection from indium tin oxide/cross-linkable amino-functionalized polyfluorene interface in inverted organic light emitting devices”, *Chemistry of Materials*, vol. 23, no. 21, pp. 4870–4876, 2011.



---

# Polymers as Light-Harvesting Dyes in Dye-Sensitized Solar Cells

---

## 6.1. Introduction

After relying on fossil fuels and nuclear power as primary sources of energy for centuries, humanity is now facing some major problems. Fossil fuels add greenhouse gases to the atmosphere and the foreseeable depletion of fossil sources is fast approaching. Meanwhile, cheap nuclear energy is associated with troubling environmental issues, including the problem of radioactive waste disposal. Humanity has to turn to clean, renewable sources of powers, and notably toward the potentiality of solar energy. In an hour, the Earth receives from the Sun the equivalent of the world's energy consumption for 1 year. Photovoltaics (PV) is a promising renewable energy technology that converts sunlight into electricity, with broad potential to contribute significantly to solving the future energy problem that humanity faces. In 1954, researchers at Bell Laboratories created the first silicon-based solar cells with significant power conversion efficiency (6%) [CHA 54]. To date, inorganic semiconductor solar cells dominate commercial markets, with crystalline Si having an 80% share; the remaining 20% is mostly inorganic thin-film solar technology (CdTe, CuInGaSe, etc.) [BIS 11]. There are four important aspects of solar cells: cost, efficiency, lifetime and productivity. Efficiency has been thought of as the key factor, indicating the advancements of solar cells. However, the cells with the best efficiency may

---

Chapter written by Thanh-Tuân BUI, Xavier SALLENAVE and Fabrice GOUBARD.

not become popular for practical applications because of their high production cost. Thus, cost is the core issue of solar cells. In addition, the technology of solar cells has to be compatible with mass-production techniques for the cost and deployment of solar panels to be practical. However, the use of conventional *silicon materials* involves a non-negligible production cost, in particular because of the *silicon's purification* process to reach the solar-grade silicon (i.e. with a purity of 99.9999%). This cost considerably reduces the competitiveness of these silicon cells compared with the traditional sources of energy for the ground applications. Low-cost solutions have emerged mainly using thin-film solar PV technologies. Over the last two decades, a new type of cell, referred to as dye-sensitized solar cells (DSSCs) [HAG 10], has been studied to develop low-cost PV. This technology can be compared to artificial photosynthesis artificial photosynthesis because it imitates natural absorption and transformation of light energy. DSSC can be used to produce electricity in a wide range of light conditions, indoors and outdoors, enabling the user to convert both artificial and natural light into energy to power a broad range of electronic devices.

In essence, a DSSC device is composed of a transparent photoactive anode and a photo-inert counter electrode (cathode) sandwiching an electrolyte-containing redox mediator (Figure 6.1(a)). Conceptually, the device is based on the superposition of active layers whose thicknesses are 10- to 20-fold less than that of crystalline silicon wafers. Moreover, the requested purity of materials is 10–100 times less than for a silicon device.

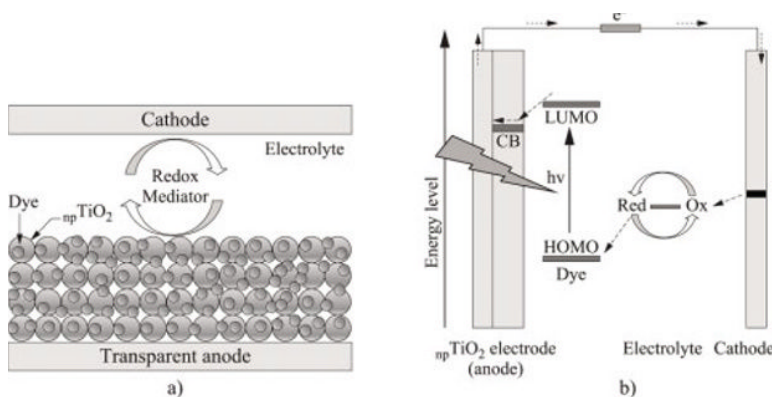


**Figure 6.1.** Schematic presentation of a) liquid electrolyte-based DSSC and b) its operation principle

A schematic presentation of the operating principles of DSSCs is shown in Figure 6.1(b) [GRÄ 05]. In this type of cell, a *light-harvesting* material (commonly called dye or photosensitizer) chemically anchored onto the TiO<sub>2</sub> surface absorbs sunlight photons. Upon absorption of photons, dye molecules are excited and an electron passes from the highest occupied molecular orbital (HOMO) to the lowest unoccupied molecular orbital (LUMO). The excited dyes inject electrons from their LUMOs into the conduction band of the oxide. The photogenerated electrons and holes from the dye are quickly separated and transferred into two different transporting media (metallic oxide and electrolyte) strongly reducing the electron-hole recombination in the absorber material. The oxidized dyes are then regenerated by electron donation from the redox mediator, such as the iodide/triiodide couple. The iodide is regenerated, in turn, by the reduction of triiodide at the counter electrode, with the circuit being completed via electron migration through the external load.

## 6.2. Characterization of DSSC devices

The electrical characterization of DSSC consists of connecting the device to an external power source, sweeping a direct current voltage (V) and measuring the electrical current density (J). The measurement of each device is done in the dark and under light illumination. Typical J–V responses of DSSC devices are shown in Figure 6.2. In the dark, the solar cell behaves as a diode. Its electrical response (current density vs. applied voltage plot) is represented by the dashed curve on the graph. The other solid curve beneath the dark curve shows what happens under light illumination. Under illumination, photons are absorbed in the dye layer. These molecules will be excited forming excitons (electron-hole pairs). If these excitons disassociate at the interface dye/<sub>np</sub>TiO<sub>2</sub> due to the built in potential, the electron will go toward the anode and the hole will go toward the cathode. In this case, we will have a reverse current, also called a photocurrent. Although an external voltage is not applied, a photocurrent can result under illumination. Three important characteristics of a DSSC can be extracted from the J–V curve: short-circuit current ( $J_{SC}$ ), open voltage circuit ( $V_{OC}$ ) and fill factor (FF).  $J_{SC}$  is the photocurrent when the applied voltage equals 0 V.  $V_{OC}$  is the required applied voltage to shut off the current in the device under light illumination. FF is a quantity for comparing the maximum output power ( $P = J \cdot V$ ) relative

to the photocurrent and photovoltage produced by any particular device, given by  $FF = P_{\max}/(J_{SC} \cdot V_{OC}) = (J_{\max} \cdot V_{\max}) / (J_{SC} \cdot V_{OC})$ . Finally, the power conversion efficiency ( $\eta$ ) is calculated by  $\eta = P_{\max}/P_{\text{incident}}$  or  $\eta = (J_{SC} \cdot V_{OC} \cdot FF) / P_{\text{incident}}$ .

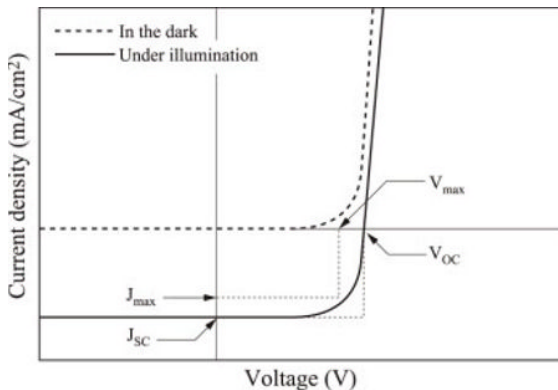


**Figure 6.2.** Typical  $J$ - $V$  responses of DSSC device in the dark (dashed line) and under illumination (solid line)

Another important optical characteristic of a DSSC is incident-photon-to-charge-carrier efficiency (IPCE) which is a measure of how efficiently the device converts the incident light into electrical energy at a given wavelength. It indicates the ratio between the number of collected carriers and the number of all the incident photons on the device active area at a given wavelength. The principle of IPCE measurement is based on illuminating the DSSC device by a monochromatic light and recording the device electrical current (number of generated carriers). By varying the frequency of the light, the entire curve of the current as a function of wavelength can be established. The area under the curve will then represent the total number of carriers created by the device under full spectrum white light illumination. In other words, the integration of the curve will give the electrical current density.

The first seminal work on DSSC was reported in 1991 by O'Regan and Grätzel [O'RE 91]. The originality and the device performances of DSSC are mainly governed by (i) the high surface area and the controlled nanoporosity of the oxide materials and (ii) the high efficiency regeneration of the photo-oxidized dye molecules induced with a redox mediator in electrolyte.

There are a lot of factors that affect the conversion efficiency of the solar cells, and the photosensitizer is the heart of the DSSC structure because it determines the device's light absorption properties. The first efficient light-harvesting dyes are ruthenium coordination complexes. Since then, a large amount of research has been focused on the development of ruthenium dyes, and device efficiency of up to 12% has been achieved [GRÄ 09]. However, the rarity and high cost of the ruthenium metal limits development for large-scale applications. Therefore, due to their low cost, metal complex sensitizers containing common metal instead of ruthenium have attracted great interest. A typical example is zinc porphyrin dye associated with cobalt-based redox mediator, which has led to a power conversion efficiency (PCE) exceeding 13% [MAT 14]. This demonstrates that common metal dyes can also achieve as high an efficiency as the Ru-complex. On the other hand, small molecular organic dyes have received considerable attention because of their high-incident solar light-to-electricity conversion efficiency, unlimited molecular conception and low production cost. Thousands of organic dyes have thus far been developed and investigated in DSSC [KIM 13, OOO 09]. The relationship between the chemical structures and the PV performances of dyes has also been examined. To create high-performance DSSCs, it is important to develop effective photosensitizers possessing good light-harvesting features, providing good electron communication between the dyes and nanoporous  $\text{TiO}_2$  electrode, and to control the molecular arrangements on the  $\text{TiO}_2$  electrode [OOO 12]. Chemical molecular engineering coupled with theoretical calculations are expected to provide efficient dyes with the following desired properties:

- the dye needs to have maximum possible width electronic absorption bands with high extinction molar coefficients being able to collect photons of the visible and near infrared (NIR) spectral domains;
- the molecule must have favorable HOMO and LUMO energy levels for having good energy alignments at nanoporous  $\text{TiO}_2$ /dye/electrolyte interfaces for efficient charge transfer;
- fast rate constant of electron injection and slow rate constant of charge recombination are required;
- good carrier transport bridges are needed to enhance the carrier transport;
- good solubility of dye molecule with strong anchoring on  $\text{TiO}_2$  surface is required;

– high light stability, chemical stability and thermal stability for durable devices.

The panchromatic dyes processing high molecular absorption coefficients could be effectively synthesized by introducing donor–acceptor push-pull substituents, enlarging the  $\pi$ -conjugated systems, transition from aromatic to quinodal structure or polymerization. Degradation of dye under illumination is one of the hurdles that must be overcome in DSSCs. The organic dyes have poor chemical and light stability, where the thermal stability is especially affected due to a small molecular weight [TAN 13].

Recently, substantial progress has been made in the development of PV devices from thin films of conjugated polymers due to the following advantageous points: sufficient photo charge generation under illumination, relatively easy deposition on various substrates, wide absorption band and high absorption coefficient leading to efficient light-harvesting properties [BUJ 13, RIV 13]. A high density of anchoring groups of a polymer chain, which can offer better thermal stability than low weight molecules, may be another advantage of polymeric photosensitizers. Taking into account lessons learned, one of the strategies to obtain high PV performance for DSSC is to design a polymeric dye. Many successful examples of  $\pi$ -conjugated polymeric dyes have been reported. Recently, new types of solar cells using polymeric sensitizers, namely polymer-sensitized solar cells (PSSCs), have been developed. Hybrid polymers, which contain both inorganic and organic segments with encouraging PV efficiencies, have also been investigated. Efficient photoinduced charge transfer and well-matched energy levels among the polymer and other components in PSSCs are essential requirements to produce efficient solar-to-electric energy conversion efficiencies. In the next section, polymeric dyes classified by family of  $\pi$ -conjugated (co)polymer are presented and discussed in detail.

### **6.3. Poly(3-thiophenylacetic acid)-based polymers**

Toward high efficiency, PSSCs have the potential for high durability because of the stability of conjugated polymers. To design these conjugated polymers, a vast number of potential building blocks have been explored over the years. Of the various conjugated polymers, polythiophene (PT) is one of the most important families and most widely studied polymers

because of their ability to be processed, their environmental and thermal stability and their good electronic properties. They have been used in a variety of electronic applications, such as organic field-effect transistors, polymer light-emitting diodes, organic solar cells and chemical sensors. PT has shown good light absorption properties when used as donor materials in organic PV devices. The introduction of carboxylic acid groups, which can act as anchoring moieties onto the surface of the nanoporous  $\text{TiO}_2$  layers, onto PT backbone could make these functionalized PTs being interesting light absorber in DSSCs. The first carboxylic acid functionalized PT designed for DSSC applications was reported in 2003 by Senadeera *et al.* who synthesized two interesting materials (PTA1-PTA2) [SEN 03]. These materials were tested as dyes in multilayered PSSCs with  $\text{I}_3^-/\text{I}^-$  as redox mediator. In this pioneering work, coating of poly(3-thiophenylacetic acid) PTA1 onto mesoporous  $\text{TiO}_2$  or  $\text{SnO}_2$ -ZnO electrodes was found to be highly beneficial for the injection of electrons into the acceptor materials. In particular, adding 1-methyl-3-*n*-hexylimidazolium iodide ionic liquid into the electrolyte was found to drastically enhance the cell performance (2.4 and 1.5% for  $\text{TiO}_2$  or  $\text{SnO}_2$ -ZnO electrodes, respectively). Such additive is expected to reduce charge recombination at the polymer–electrolyte interface and also to the increase of the surface contacts between them in these cells. Otherwise, incorporation of mixture of large and small  $\text{TiO}_2$  nanoparticles as n-type materials increased PV efficiency (2.4%). Moreover, due to pore filling, the lower the molecular weight average of the  $\pi$ -type polymer PTA1 is, the better is the efficiency (2.92%,  $M_w$ : 4,500) [CHO 11]. PTA1 had also been characterized in volatile solvent-free solid-state DSSC with poly(3,4-ethylenedioxythiophene) (PEDOT) as the hole-conducting material. PTA1 has led to solid-state cells with modest PV efficiency (0.5%) [SEN 05b]. As a continuation of this work, Senadeera *et al.* have synthesized poly(3-thiophenemalonic acid) PTA2 bearing two carboxylic groups attached to the monomer [SEN 05a]. This polymer had been designed in order to have better surface contacts with inorganic semiconductors and higher spectral responses in the solar devices. Unexpectedly, DSSC devices employing PTA2 dye showed slightly lower efficiencies than that of PTA1. This unsatisfying performance might be explained by the lower degree of attachments of two carboxylate groups located on the same thiophene ring on the  $\text{TiO}_2$  surfaces due to the steric reasons causing inefficient electrons injection.

Apart from the examples of PTs with carboxylic acid groups, a wide range of copolymers with poly(thiophene) and poly(3-thiophenylacetic acid)

moieties were developed to sensitize the mesoporous TiO<sub>2</sub> electrodes in solar cell devices [AKI 12, KIM 06, LEE 11, YAN 04]. Importantly, a progressive red-shifted absorption band, desirable for light harvesting of solar energy, is observed in these polymers due to the increase in the  $\pi$ -conjugation system according to the increase in the molecular weights. As first examples of combinations, the simplest ones consisted of the linkage of a poly(3-thiophenylacetic acid) with poly(3-alkylthiophene) as exemplified with the molecules PTA3-5. The influence of the nature of alkyl chains on the optical property and on the device performance was investigated. The position of the maximum absorption peak of the different copolymers has been proved to be strongly affected by the alkyl chain lengths. Notably, hexylthiophene copolymer PTA3 displays an unexpected absorption band in 385 nm in DMSO which is blue-shifted compared to that obtained with the 3-dodecyl (PTA4) or without alkyl chain (PTA5) analogs and remained in the range of 460–485 nm (see Table 6.1). Consequently, copolymer PTA3 could not absorb the light in the longer wavelengths than the poly(3-thiophenylacetic acid). This detrimental result impacts in charge injection in mesoporous TiO<sub>2</sub> inducing a relatively lower PV efficiency (1.6%) compared to that of PTA4 and PTA5 (2.4 and 3.8%, respectively). Another example of poly(thiophene)/poly(3-thiophenylacetic acid) copolymers as dyes for DSSC is PTA6. It was synthesized using two kinds of thiophene monomers (N-(3-thienylmethylene)-2-amino-fluorene and 3-thiophene acetic acid) [LEE 20]. The synthesis temperature seems to have an influence on the optical properties of the copolymer. Effectively, polymers synthesized at 0°C give broader absorption and higher overall PCE (1.53%) compared to that of the devices using copolymer synthesized at room temperature (0.9%).

While extending this concept to more polymer structures, Saji *et al.* synthesized PTA7 [SAJ 10]. This consists of the synthesis of a poly(thieno[3,4-b]thiophene-2-carboxylic acid), PTA7, with thienothiophene blocks in order to decrease the band gap polymers allowing an NIR absorption ( $\lambda_{\text{max}} = 820$  nm). The PTA7-sensitized DSSC showed a cell efficiency of 1.2%, suggesting that PTA7 was involved in the NIR solar energy conversion process. Co-adsorption of PTA7 with ruthenium reference dye (N3) resulted in an efficiency of 4.3%, which was lower than 5.8% of N3-sensitized DSSC control device. This is certainly because polymer aggregation hampers the dye regeneration by accepting electrons from iodide electrolytes.

Another strategy is to introduce carboxylic groups as end-capping groups to poly(3-alkylthiophenes) as compound PTA8 [LOH 09]. Lohwasser *et al.* showed its potential to anchor onto mesoporous TiO<sub>2</sub> and prepared a solid-state solar cell with PTA8 as sensitizer and spiro-OMeTAD as solid hole conductor with a PCE equal to 0.9%. This is promising because the absorption of P3HT can be tuned by introducing different side chain substituents.

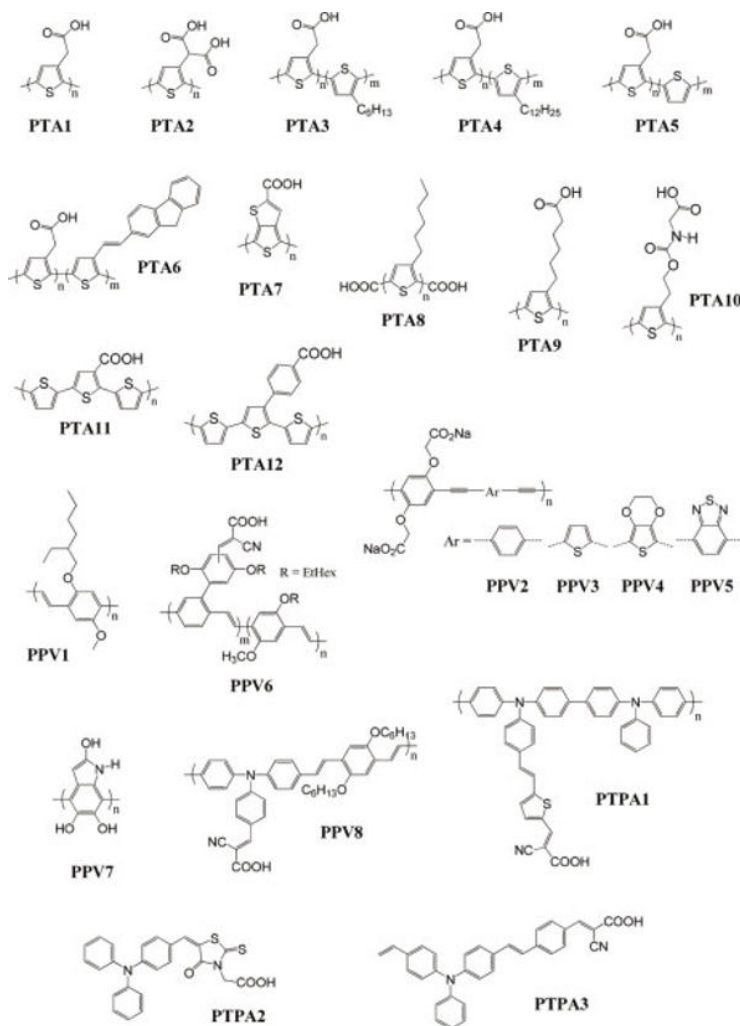


**Figure 6.3.** Chemical structures of  $\pi$ -conjugated polymer PTA1-12, PPV1-8 and PTPA1-3

The previous results showed that the mono (or di)carboxylated P3HT derivative dyes induce a relatively low value of  $V_{oc}$  (0.3–0.5V). This was attributed to a shift in the position of the surface conduction band of  $TiO_2$  due to protonation of the surface by the carboxylic groups. Also, a high density of carboxylic groups anchored to the surface of the n-type semiconductor was found to decrease the  $V_{oc}$  due to the creation of interface dipoles at the  $TiO_2$ -polymer interface. Thus, different studies were carried out with carboxylated P3HT derivative with an alkyl chain of a larger number of  $CH_2$ -groups separating the  $\pi$ -conjugated structure from the carboxylate moiety. Shankar *et al.* [SHA 07] incorporated the carboxylated polymer poly[3-(5-carboxypentyl)thiophene-2,5-diyl] (PTA9) as dye function into the  $TiO_2$  nanotubes. They observed relatively higher photovoltages of up to 0.7 V involving a PCE equal to 2.1%. Thelakkat *et al.* [BHO 10] used the same carboxylated P3HT derivative into solid-state hybrid PV cell with P3HT as hole transporter materials and obtained an interesting 0.9% as PCE. Moreover, a poly[2-(3-thienyl) ethanol hydroxyl carbonyl-methyl-urethane] (PTA10) that bears carboxylic acid and urethane groups has been synthesized and employed in solar cells with a PCE of 1.5% [KIM 03]. It is important to note that this latter polymer has the band gap and HOMO levels quite similar to that of N3 which could explain a better electron injection into mesoporous  $TiO_2$  compared to P3HT.

Recently, a series of carboxylated PT comprising a terthiophene backbone moiety acting as an electron donor and carboxylic acid moiety acting as an acceptor with or without a phenyl ring as  $\pi$ -conjugated bridge (PTA11 and PTA12) was developed [KIM 12, YOO 11]. The PTA12-sensitized solar cell shows a short-circuit current of  $10.47 \text{ mA cm}^{-2}$  with an energy conversion efficiency of 3.97% which is, up to now, the best result for carboxylated PT as polymer dye. Moreover, the stability of PTA12-sensitized solar cell showed almost no decrease in energy conversion efficiency after 2,000 h at  $40^\circ\text{C}$ . Otherwise, PTA11 without phenyl ring exhibited much smaller energy conversion efficiency (2.32%) with short-circuit current of  $6.78 \text{ mA cm}^{-2}$  [YOO 11]. In the case of PTA12, the carboxylate group of the polymer film can effectively anchor on the surface of the nanocrystalline  $TiO_2$ . Moreover, a conjugated phenyl moiety can help to enhance the intermolecular charge transfer between the  $TiO_2$  surface and the polymer backbone. Beyond that, the originality of PTA11 and PTA12 compared to the others is their coating methods: electrochemically polymerized films of the precursor monomers of PTA11 and PTA12 on a

nanocrystalline TiO<sub>2</sub> layer are developed as photo sensitizers. Consequently, the insertion of small molecules (as monomers) could increase the pore filling and the interface with TiO<sub>2</sub> surface which in turn enhances the overall device performance (see Table 6.1).

Polymer	M <sub>w</sub> (g.mol <sup>-1</sup> )	λ <sub>max</sub> (nm)	HOMO	LUMO	Acceptor	Donor	V <sub>OC</sub> (mV)	J <sub>SC</sub> (mA.cm <sup>-2</sup> )	FF	η (%)	Ref
PTA1	17000	418			TiO <sub>2</sub>	I <sub>3</sub> <sup>-</sup> /T	400	9.76	0.61	2.4	[SEN 03]
PTA1	17000	418			SnO <sub>2</sub> -ZnO	I <sub>3</sub> <sup>-</sup> /T	500	5.37	0.55	1.5	[SEN 03]
PTA1	18000	418			TiO <sub>2</sub>	I <sub>3</sub> <sup>-</sup> /T	510	7.4	0.62	2.4	[CHO 11]
					mixture						
PTA1	4500	418			TiO <sub>2</sub>	I <sub>3</sub> <sup>-</sup> /T	520	8.6	0.64	2.92	[CHO 11]
					mixture						
PTA1	17000	418	-5.27	-2.95	TiO <sub>2</sub>	PEDOT	365	2.5	0.54	0.5	[SEN 05a]
PTA2	56000	440	-5.49	-3.34	TiO <sub>2</sub>	I <sub>3</sub> <sup>-</sup> /T	355	7.65	0.65	1.8	[SEN 05b]
PTA3	36000	385	-5.34	-3.01	TiO <sub>2</sub>	I <sub>3</sub> <sup>-</sup> /T	375	7.00	0.62	1.6	[YAN 04]
PTA4		495			TiO <sub>2</sub>	I <sub>3</sub> <sup>-</sup> /T	380	1.03	0.45	0.18	[KIM 06]
PTA5	2300	460			TiO <sub>2</sub>	I <sub>3</sub> <sup>-</sup> /T	640	11.3	0.54	3.8	[AKI 12]
PTA6	18400	490			TiO <sub>2</sub>	I <sub>3</sub> <sup>-</sup> /T	600	4.5	0.56	1.5	[LEE 11]
PTA7		820	-4.7	-3.7	TiO <sub>2</sub>	I <sub>3</sub> <sup>-</sup> /T	420	4.5	0.62	1.2	[SAJ 10]
PTA8	4700	446			TiO <sub>2</sub>	Spiro-OMETAD	540	3.7	0.46	0.9	[LOH 09]
					Nanotubes						
PTA9					TiO <sub>2</sub>	I <sub>3</sub> <sup>-</sup> /T	700	5.5	0.55	2.1	[SHA 07]
					TiO <sub>2</sub>						
PTA9		455			TiO <sub>2</sub>	P3HT	473	4.5	0.37	0.79	[BHO 10]
PTA10			-6.52	-1.53	TiO <sub>2</sub>	I <sub>3</sub> <sup>-</sup> /T	460	5.7		1.5	[KIM 03]
PTA11		448	-5.6	-3.5	TiO <sub>2</sub>	I <sub>3</sub> <sup>-</sup> /T	540	6.78	0.64	2.32	[YOO 11]
PTA12		472	-5.53	-3.55	TiO <sub>2</sub>	I <sub>3</sub> <sup>-</sup> /T	590	10.47	0.64	3.97	[KIM 12]
PPV1		500			TiO <sub>2</sub>	CuI	400	0.3	0.3	0.05	[SIR 03]
PPV2		404			TiO <sub>2</sub>	I <sub>3</sub> <sup>-</sup> /T	470	1.46	0.49	0.34	[JIA 09]
PPV3		435			TiO <sub>2</sub>	I <sub>3</sub> <sup>-</sup> /T	470	2.6	0.43	0.53	[JIA 09]
PPV4		457			TiO <sub>2</sub>	I <sub>3</sub> <sup>-</sup> /T	500	3.12	0.37	0.58	[JIA 09]
PPV5		495			TiO <sub>2</sub>	I <sub>3</sub> <sup>-</sup> /T	430	2.52	0.3	0.33	[JIA 09]
PPV6		450	-4.84	-2.26	TiO <sub>2</sub>	I <sub>3</sub> <sup>-</sup> /T	690	6.7	0.65	3	[CHH 12]
PPV7		420			TiO <sub>2</sub>	I <sub>3</sub> <sup>-</sup> /T	330	3.63	0.34	0.41	[MOZ 14]
PPV8	19800	430	-5.45	-3.45	TiO <sub>2</sub>	I <sub>3</sub> <sup>-</sup> /T	740	9.45	0.54	3.78	[MIK 11]
PTPA1	9000	444	-5.31	-3.16	TiO <sub>2</sub>	I <sub>3</sub> <sup>-</sup> /T	717	9.2	0.51	3.39	[ZHA 09a]
PTPA2		480	-5.08	-2.98	TiO <sub>2</sub>	I <sub>3</sub> <sup>-</sup> /T	540	11	0.51	3.04	[YAN 09]
PTPA3		459	-5.18	-2.9	TiO <sub>2</sub>	I <sub>3</sub> <sup>-</sup> /T	760	10.2	0.74	5.74	[SU 12]
PF1	19800	444	-5.6	-3.26	TiO <sub>2</sub>	I <sub>3</sub> <sup>-</sup> /T	523	4.03	0.66	1.39	[LIU 08]
PF1		444			Nanofiber s TiO <sub>2</sub>	I <sub>3</sub> <sup>-</sup> /T	700	1.73	0.52	0.63	[ZHA 09b]
PF2	4200	407	-5.76	-1.29	TiO <sub>2</sub>	I <sub>3</sub> <sup>-</sup> /T	539	0.55	0.63	0.19	[GRI 10]
PF3			-5.74	-1.56	TiO <sub>2</sub>	I <sub>3</sub> <sup>-</sup> /T	627	1.93	0.73	0.88	[GRI 10]
PF4	10000	372	-5.75	-3.68	TiO <sub>2</sub>	I <sub>3</sub> <sup>-</sup> /T	550	7.02	0.44	1.68	[FAN 11]
PF5	4800	378	-5.62	-3.72	TiO <sub>2</sub>	I <sub>3</sub> <sup>-</sup> /T	540	12.58	0.45	2.99	[FAN 11]
PF6		470	-5.5		TiO <sub>2</sub>	PF6	920	0.4	0.44	1.4	[RAV 04]
PAD1	4600	380	-5.27	-3.74	TiO <sub>2</sub>	I <sub>3</sub> <sup>-</sup> /T	670	8.43	0.73	4.11	[CHA 11]
PAD2	3950	330/372			TiO <sub>2</sub>	I <sub>3</sub> <sup>-</sup> /T	742	5.3	0.77	3.0	[TAN 13]
PAD3	3000	329/370			TiO <sub>2</sub>	I <sub>3</sub> <sup>-</sup> /T	775	6.06	0.75	3.5	[TAN 13]
PAD4	3360	372/455			TiO <sub>2</sub>	I <sub>3</sub> <sup>-</sup> /T	769	8.12	0.71	4.4	[TAN 13]
PAD5		655			TiO <sub>2</sub>	I <sub>3</sub> <sup>-</sup> /T	660	6.3	0.58	2.41	[KAN 10]
PAD6		563			TiO <sub>2</sub>	I <sub>3</sub> <sup>-</sup> /T	590	4.5	0.54	1.43	[KAN 10]

**Table 6.1.** Physical, optical and photovoltaic characteristics of PTA1-12, PPV1-8, PTPA 1-3, PF1-6 and PAD1-6

#### 6.4. Phenylenevinylene-based polymers

Several dye polymers in addition to poly(3-thiophenylacetic acid) have been used with varying success in DSSCs, and there is much ongoing research in pursuit of new polymers with the appropriate energy levels, absorption and stability properties. Another family frequently employed in DSSC with  $\text{TiO}_2$  as an acceptor is poly(2-methoxy-5(2-ethyl-hexyloxy)-p-phenylene vinylene) derivatives (MEH-PPV). With both a strong absorption visible light and a good electron injection to the conduction band of  $\text{TiO}_2$ , first results with MEH-PPV, in solid-state cell with  $\text{TiO}_2$ |MEH-PPV (PPV1)|CuI configuration, involved a low PCE of the cell equal to 0.05% [SIR 03]. Another series of poly(phenylene ethynylene) (PPE) derivatives was investigated by Schanze *et al.* [JIA 09] with ambipolar alternating copolymers PPE as donor with a second arylene ethynylene moiety, which has a different electron demand 1,4-phenyl (PPV2), 2,5-thienyl (PPV3), 2,5-(3,4-ethylenedioxy)thienyl (PPV4) and 1,4-benzo[2,1,3]thiadiazole (PPV5). Each of the polymers effectively adsorbs onto nanocrystalline  $\text{TiO}_2$  electrodes, presumably via an interaction of the carboxyl group with the  $\text{TiO}_2$  interface. The wavelength maxima of the absorption and fluorescence spectra are systematically red-shifted across the series in the order  $\text{PPV2} < \text{PPV3} < \text{PPV4} < \text{PPV5}$ , with the absorption maxima ranging from 404 nm (PPV2) to 495 nm (PPV5). In the case of PPV3 and PPV4, the band gap narrowing likely arises mainly because of an increase in the HOMO level caused by incorporation of the thienylene and ethylene dioxythienylene repeat units. However, for PPV5, which has the lowest band gap of the series, the HOMO-LUMO gap narrowing likely arises because the 1,4-benzo[2,1,3]thiadiazole moiety is a strong electron acceptor, leading to lowering of the LUMO level. The photocurrent and power conversion efficiency in a solar cell configuration, using an  $\text{I}_3^-/\text{I}^-$  propylene carbonate electrolyte, increase slightly in the order  $\text{PPV2} < \text{PPV3} < \text{PPV4}$ , consistent with an observed red shift in absorption. Interestingly, the PCE for the  $\text{TiO}_2$ /PPV5 system is substantially less than that for the other PPE derivatives, and the decreased efficiency is attributed to exciton trapping in polymer aggregates that are present in the film.

Indeed, a significant enhancement of PCE was obtained by Wadgaonkar *et al.* [CHH 12] with a copolymer, PPV6, with alternating poly[2-[2',5'-bis(2''-ethylhexyloxy)phenyl]-1,4-phenylenevinylene] unit with MEH-PPV. The performance of the polymer showed a 10-fold increase in the device performance with PCE equal to 3% compared to the base polymer without

carboxyl functionality. Once again, the anchoring group effect of carboxylic acid is a crucial factor in the device performance. Concerning stability of devices based on such compound, the PV efficiency with PPV6 decreases slower compared to N719 reference ruthenium complex dye until 200°C.

Another alternative to improve the stability of the dye attached to the surface of TiO<sub>2</sub> is to introduce dye-polymer with several anchor functions. As a result, epinephrine, composed of three OH groups in the epinephrine structure, preferably enhances the linkage of poly epinephrine (PPV7) to the TiO<sub>2</sub> and then facilitates electron injection from dye to the semiconductor compared to polydopamine as reference polymer [MOZ 14]. Binding the catechol amines onto a TiO<sub>2</sub> surface through OH groups is a very promising method for creating stable interfaces for use in solar cells that can form strong tri- and bi-dentate complexes with unsaturated Ti atom derivatives. An efficient electronic coupling between the pi orbital of the excited state of PPV7 and the conduction band of TiO<sub>2</sub> causes an increase in short-circuit photocurrent. Finally, the best result (PCE = 3.78%) with phenylenevinylene derivatives was obtained from an alternating phenylenevinylene copolymer PPV8, which contains substituted triphenylamine (TPA) units along the backbone, cyanoacrylic acid anchoring groups and solubilizing hexyloxy side chains [MIK 11]. TPA is a unique molecule possessing 3D propeller-like geometry, glass-forming property, and relatively high oxidation potential as well as an excellent hole-transporting property. A literature survey revealed that various TPA-based materials have been used for solid-state DSSC recently [BUI 13a, BUI 13b, DIA 13, MET 12]. Moreover, the presence of TPA unit both increases the conjugation of such molecule and suppresses the dye aggregation for its non-planar structure.

## 6.5. Triphenylamine-based polymer

The presence of donor TPA in dye polymer is largely employed in donor (D)- $\pi$ -acceptor (A) configuration. Effectively, such structures revealed the intramolecular charge transfer characters of these molecules in the excited state [MOO 98]. This property is essential for dye sensitizers in DSSCs, since the light-induced intramolecular electron transfer could easily occur from the electron donor to the electron acceptor through the  $\pi$ -bridge, which favors photocurrent generation. A conjugated polymer PTPA1 containing TPA and cyanoacetic acid as the acceptor with conjugated thiophene units as

the linkers has been synthesized and found suitable by Zhang *et al.* [ZHA 09a]. A high and promising efficiency (3.39%) for DSSCs based on PTPA1 was obtained with few optimizations (absence of dense film and scattering layer). At the same time, as other acceptor units in D- $\pi$ -A structure, rhodanine-3-acetic acid was employed by Yang *et al.* [YAN 09] to synthesize TPA-based indoline dye and its polymer-type dye (PTPA2) via electropolymerization. The resulting polymer dye (PTPA2) exhibits a network structure of  $\pi$ -conjugation polymer chains that cause a significant blue shift in the absorption spectrum. Nevertheless, stabilizing the  $\pi$ -conjugated network decreases the IPCE. PTPA2 is less efficient (3.04%) than monomer-sensitized DSSCs (4.57%), but this network polymer might provide a stable dye to combine other conducting polymers (hole conductor) forming a solid-state solar cell. Finally, Su *et al.* [SU 12] prepared a simple yet effective method to reduce the electron recombination in DSSCs by functionalizing organic dyes with a thermally cross-linkable styryl group, which can be conveniently polymerized into polystyrene during the annealing step of the device fabrication. The used polymer dye PTPA3, first developed as monomer by Park and Kim in 2007 [HWA 07], utilized stilbene as a  $\pi$ -bridge of the electron-donating diphenylamino group and the electron-withdrawing 2-cyanoacrylic acid. The new dye molecule can undergo polymerization during the annealing step of device fabrication to generate an electrolyte blocking shell, which can impede undesirable electron recombination with the electrolyte. The PV measurements yield an overall conversion efficiency of 5.31%. In addition, with the incorporation of co-adsorbent chenodeoxycholic acid and cross-linkable repair additive 4,4'-divinyltriphenylamine, the optimized device with a robust shell shows a PCE equal to 5.74%.

## 6.6. Fluorene-based polymers

Relative to conventional donors, the high electron-donating character of fluorene could be a good candidate for the purpose of designing dye. Surprisingly, few studies were initiated with such moiety. However, through the D- $\pi$ -A structure, the used functionalities will induce a red shift in absorption toward visible range. With TiO<sub>2</sub> as an acceptor and I<sub>3</sub><sup>-</sup>/I<sup>-</sup> as a redox couple, Liu *et al.* obtained promising results (PCE = 1.4%) with anionic conjugated polymer PF1 as donor material including fluorene and [2,1,3]-benzothiadiazole (BTD) units [LIU 08]. In order to increase the pore filling in TiO<sub>2</sub> which could be poor with conjugated polymer, the same

author developed a novel photoanode composed of electrospun  $\text{TiO}_2$  nanofibers with an energy conversion efficiency of 0.63% [ZHA 09b]. By modifying the polymer backbone by incorporating an appropriate amount (25% mol/mol) of carboxy-2,5-phenylene moieties [GRI 11] between the two units (PF2), an absorption spectrum becomes broader but PCE decreases. Otherwise, substitution of electron-deficient BTB units, which probably inhibits the electron-transfer to the photoelectrode, by thiophene moieties (PF3) induces moderate efficiencies (0.88%) not better than those reported for other polymeric sensitizers. The strong absorption ability of D- $\pi$ -A structure has been revisited with  $\pi$ -conjugated backbone consisting of an electron-poor BTB unit as an acceptor, alternating with either a thiophene-fluorene-thiophene triad (PF4) or a terthiophene (PF5) segment as the donor [FAN 11]. These species combination leads to charge separation in the excited state, and this may facilitate charge injection into  $\text{TiO}_2$ . Moreover, the long alkyl side chains that are linked to the fluorene or thiophene units facilitate the polymers' solubility but may impede interchain interactions between the conjugated polymer backbones, decreasing the probability of exciton trapping/quenching by aggregate states. Importantly, for the set of polymer sensitizers PF5 with varying  $M_n$ , the DSSC efficiency varies inversely with  $M_n$ , a result that reflects the difference in adsorption efficiency observed in the film absorption experiments. The best DSSC cell tested is based on a sample of PF5 with  $M_n = 4,000$ , and it exhibits an overall PCE of 3% (see Figure 6.4). Fluorene is also associated with bithiophene units to form a poly(9,9-dioctylfluorene-co-bithiophene). In this article, the oligothiophene-functionalized fluorene PF6 was directly acted as both dye and hole transporter material inducing a significant increase the PCE in reduced  $\text{TiO}_2$  thickness [RAV 04] (see Figure 6.4).

## 6.7. Dye polymers with acceptor–donor structure

In 2011, Baek *et al.* synthesized PAD1, which comprises an electron-donating backbone (carbazole) and an electron-accepting side chain (cyanoacetic acid) connected through conjugated vinylene and terthiophene, and tested it as a photosensitizer. The well-defined donor (D)–acceptor (A) structure of PAD1 has made it possible, for the first time, to reach a PCE of over 4% in DSSCs with an organic polymer sensitizer [CHA 11]. Based on the research mentioned above, combining the outstanding properties of electron-rich donor and pendent acceptor conjugated polymers may lead to

the development of a series of promising dyes for high-performance polymer DSSCs. With the same goal, by increasing the effective conjugation length of backbone polymer chain with 9,9-dioctylcarbazole, Tan *et al.* have successfully synthesized different D- $\pi$ -A organic molecules (PAD2-4) with different donor units in the backbone [TAN 13a]. Their presence influences the polymer molecule's energy level and PV characteristics. PAD2 is a basic structure, and contains a phenothiazine (PTZ) chromophore and has a 9,9-dioctylfluorene (F) group as the donor unit in the main chain and a cyanoacrylic acid acceptor in the side chain, linked by a thiophene unit. Two different kinds of structural modification to the backbone of PAD2 have been selected to examine their effect on the performance of the polymer. 9,9-dioctylcarbazole and TPA were selected to replace F and PTZ, respectively, to get another two polymers: PAD3 and PAD4.

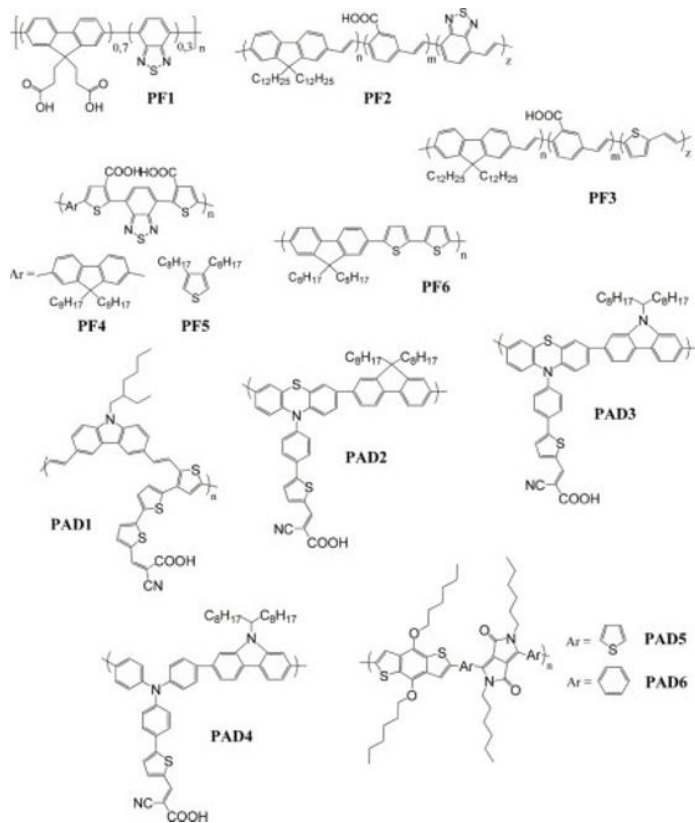


**Figure 6.4.** Fluorene-based polymers and dye polymers with acceptor–donor structure PF1-6 and PAD1-6

A red shift in absorption is observed in the order PAD2, PAD3 and PAD4. Similarly, the onsets of the IPCE spectra increase in the same order. In particular, the PAD4-based cell has a much broader and higher IPCE peak, which is in good agreement with the absorption spectra of these dyes. The result showed that the PAD4 dye exhibited excellent PV performance with a relatively high PCE of 4.4% for DSSCs. Finally, it ought to be pointed out that the two diketopyrrolopyrrole (DPP)-based copolymers with different donor (phenyl, PAD5 and thiophene, and PAD6 in DPP core) segments as organic polymer sensitizers for the quasi-solid state DSSCs (Figure 6.3) [KAN 10] have been synthesized. Without a COOH group, the polymers used in this study exhibit C=O groups in their backbone; hence, the polymers can adsorb onto the TiO<sub>2</sub> surface, and as a result electrons can be injected from the excited state of polymers into the conduction band of TiO<sub>2</sub> as observed in the case of a carboxylated PT. The PCE of the solar cells with PAD5 as sensitizer is higher than that of PAD6. It has been attributed to the improved light harvesting ability of PAD5 as sensitizer due to an excellent overlap with the solar spectrum and low band gap.

## 6.8. Polymer containing metal complexes

The application of polymers containing metal complexes as dye sensitizer in DSSCs is an area of increasing interest. Most researchers have tried to construct sensitizers with rare earth metal ions, such as Os, Re, Pt and Ru. Among the metal complexes, Ru complexes dyes have shown the best PV properties due to having a broad absorption spectrum, ground state energy levels, and suitable excited and long excited-state lifetime. Several Ru complexes dyes used in DSSCs have reached more than 11% solar cell efficiency under standard measurement conditions. Recently, more common metal ions have been introduced in DSSCs, such as Cu (I) ions and Zn (II) ions. Consequently, polymeric metal complexes (PMCs) have received considerable attention because these hybrid materials provide outstanding physical and chemical properties of both the organic and inorganic components, for example, unique process ability, good solubility and easy film forming ability of polymer, prominent luminescence efficiency and good thermal stability of metal. We can find many research papers about main or side chain PMCs. Most of these hybrid polymer dyes have the D- $\pi$ -A structure as the common motif because of its intramolecular charge transfer characteristics [BRY 99].

On the basis of the concept of donor- $\pi$  conjugation bridge acceptor structure, many papers have been published about main chain PMCs. Among the electron-donating units, phenylethyl, phenylenevinylene, fluorenevinylene and carbazole units are very attractive: they not only have low band gap, but are also the  $\pi$ -conjugated ring moieties. On the other hand, as acceptor units, 8-hydroxyquinoline (8-HQ), benzimidazole, diaminomaleonitrile (DAMN) or 1,10 phenanthroline metal complex in the polymeric main chain might expand the  $\pi$ -conjugation system, sustain the stability of the dye molecule and have the ability to be donors and acceptors simultaneously. Xiao *et al.* have synthesized 8-HQ europium complexes and phenylethyl (PMC1) or fluorine (PMC2) units in the main chain with resulting device efficiencies of around 2–3% [XIA 10]. The two materials have showed moderate stabilities with thermal decomposition temperatures of 280 and 225°C, respectively. Still using 8-HQ as ligand, but with Zn(II) or Ni(II) as metal, PMC3 and PMC4 complexes were chosen as the monomers with carbazole units for their interesting charge properties, low toxicity and low cost [DEN 12a]. The two materials have high thermal stability (320–330°C) and exhibit good open-circuit voltages, FFs but moderate PCE (1.11 and 0.45%, respectively). Replacing zinc metal by cadmium metal and in the same way, carbazole derivatives by thiophene derivatives, Jin *et al.* synthesized two phenylenevinylene copolymers (namely, PMC5 and PMC6) with octyloxy and methoxy side groups [JIN 13a]. Surprisingly, although the maximal absorption is blue-shifted compared to the previous ones,  $J_{SC}$  is better and consequently so is PCE. The presence of alkoxy moieties in side groups must certainly increase affinities with TiO<sub>2</sub> surface. Otherwise, the length of the alkyl chain in alkoxy moiety did not really impact the obtained PCE. To complete this study, the same authors have synthesized a new series of D- $\pi$ -A main chain polymeric cadmium complexes with carbazole-alkyl fluorine (PMC7) or carbazole-alkoxy phenylene (PMC8), donor unit, C=N  $\pi$ -conjugation linkage and 8-HQ Zn(II) or Cd(II) complex acceptor portion [JIN 13b]. The presence of electron-rich alkoxy benzene moiety in PMC8 explains the improved optical and PV properties. As PMC with new acceptor unit, it is well known that metal chelates of DAMN derivatives are one of the most widely used materials as an electron transporter. Moreover, increasing the number of thiophene units in poly(phenylenevinylene) can further extend the  $\pi$ -conjugation, which can also increase the short-circuit photocurrent, as the result of the red-shifted absorption of the sensitizer loaded TiO<sub>2</sub> film [LI 10]. Recently, Zhang *et al.* elaborated two D- $\pi$ -A dyes possessing a metal

(Cd or Ni)-DAMN as an acceptor (A), ethylene bond as a  $\pi$ -conjugation linkage and bithiophene phenylenevinylene as donor group (D) [ZHA 14]. Optical properties indicate that polymers containing metal-Cd (PMC9) show better light absorption than polymers containing metal-Ni (PMC10). Moreover, the increase in glass transition temperature from 120 to 144°C suggests that PMC containing metal-Cd has higher rigidity than that containing metal-Ni. Finally, the best result of PCE is obtained with PMC9. As an important ligand, 1,10-phenanthroline has been extensively used in functional metal complexes. This molecule, with a rigid structure and high electron transfer capability, can provide two aromatic nitrogens that make it possible to coordinate with many transition metal ions easily. Considering the distinctive physical and chemical properties of phenanthroline, many researchers have used metal phenanthroline derivative complexes in DSSCs. For instance, [Ru(dcbpy)(otip)(NCS<sub>2</sub>)] [YIN 09] containing thiophene-substituted spacer has achieved the energy efficiency of 8.3%. For this reason, D-A-type main chain PMCs (PMC11 and PMC12) containing phenanthroline metal derivatives by heck coupling reaction have been synthesized [ZHO 14]. The results indicate that the introduction of 1,4-divinyl-2-methoxyl-5-octyloxybenzene and 2,7-divinyl-9,9-dioctylfluorene could lengthen  $\pi$ -conjugation system effectively, as well as help improve the solubility of the PMCs. TGA measurements demonstrate that PMC11 and PMC12 have good thermal stability and get the  $T_d$  at 392 and 436°C, respectively. Nevertheless, PV results are quite low with a PCE equal to 1.05 and 1.15%, respectively. Finally, with benzimidazole and its derivatives, ubiquitous in biology, the larger  $\pi$ -conjugated system is obtained. Their presence in main chain PMC comprising thiophene and 2-(2'-pyridyl)benzimidazole ligand based on Zn (II) (PMC13) involved a PCE of DSSCs equal to 1.88% [XIU 11]. For each previous case, the lack of an anchoring group explains the limited results in  $J_{SC}$  and IPCE. Effectively, the introduction of carboxylic acid or sulfonic acid groups as anchoring groups in the structure mainly impacts light absorption, electron injection efficiency and adsorption affinities on the TiO<sub>2</sub>. The anchor group can bind the molecules on the surface and inject the electrons from the excited dye molecule into the conducting band of the semiconductor. So, 3,3'-dicarboxy-2,2'-bipyridine is an excellent polydentate ligand, and was used in four PMCs (PMC14-17) based on 1,10-phenanthroline metal complexes and alkylfluorene or alkoxybenzene [YU 13]. Zn(II) or Co(II) was chosen as the metal. The dyes containing alkoxybenzenes (PMC16 and PMC17) exhibited higher PCE values than the corresponding target polymers containing

alkylfluorenes (PMC14 and PMC15). The PMC16 dye showed a maximal PCE of 2.12%. In addition, the four polymers possessed excellent stabilities, and their thermal decomposition temperatures all exceeded 300°C. The same trend is observed with PMCs based on 8-hydroxyquinoline metal complexes using alkoxy benzene or alkyl fluorene as the electron donor.

Polymer	$M_n$ (g.mol <sup>-1</sup> )	$\lambda_{max}$ (nm)	HOMO	LUMO	Acceptor	Donor	$V_{oc}$ (mV)	$J_{sc}$ (mA.cm <sup>-2</sup> )	FF	$\eta$ (%)	Ref
PMC1	25900	436	-5.3	-3.28	TiO <sub>2</sub>	I <sub>3</sub> /T	630	4.77	0.75	2.25	[XIA 10]
PMC2	27800	448	-5.3	-3.4	TiO <sub>2</sub>	I <sub>3</sub> /T	640	6.33	0.75	3.04	[XIA 10]
PMC3	5780	427	-5.77	-3.69	TiO <sub>2</sub>	I <sub>3</sub> /T	745	2.52	0.586	1.11	[DEN 12a]
PMC4	6350	447	-5.73	-3.59	TiO <sub>2</sub>	I <sub>3</sub> /T	650	1.27	0.55	0.45	[DEN 12a]
PMC5	48000	404	-5.64	-3.4	TiO <sub>2</sub>	I <sub>3</sub> /T	710	3.34	0.66	1.57	[JIN 13a]
PMC6	43200	401	-5.66	-3.36	TiO <sub>2</sub>	I <sub>3</sub> /T	670	3.8	0.69	1.77	[JIN 13a]
PMC7	12400	423	-5.78	-3.35	TiO <sub>2</sub>	I <sub>3</sub> /T	632	4.67	0.74	2.18	[JIN 13b]
PMC8	22600	448	-5.73	-3.42	TiO <sub>2</sub>	I <sub>3</sub> /T	745	5.35	0.61	2.45	[JIN 13b]
PMC9	17870	451	-5.57	-3.58	TiO <sub>2</sub>	I <sub>3</sub> /T	720	4.75	0.658	2.25	[ZHA 14]
PMC10	14500	422	-5.52	-3.51	TiO <sub>2</sub>	I <sub>3</sub> /T	710	4.52	0.653	2.1	[ZHA 14]
PMC11	17400	398	-5.67	-3.15	TiO <sub>2</sub>	I <sub>3</sub> /T	670	2.5	0.63	1.05	[ZHO 14]
PMC12	20000	420	-5.73	-3.3	TiO <sub>2</sub>	I <sub>3</sub> /T	649	2.71	0.65	1.15	[ZHO 14]
PMC13	2900	383	-4.98	-3.16	TiO <sub>2</sub>	I <sub>3</sub> /T	650	4.09	0.71	1.88	XIU 11
PMC14	18000	411	-5.66	-3.28	TiO <sub>2</sub>	I <sub>3</sub> /T	650	4.26	0.64	1.76	[YU 13]
PMC15	13500	396	-5.72	-3.36	TiO <sub>2</sub>	I <sub>3</sub> /T	600	4.37	0.65	1.71	[YU 13]
PMC16	16900	442	-5.55	-3.42	TiO <sub>2</sub>	I <sub>3</sub> /T	690	4.91	0.625	2.12	[YU 13]
PMC17	14300	424	-5.58	-3.35	TiO <sub>2</sub>	I <sub>3</sub> /T	640	4.59	0.61	1.81	[YU 13]
PMC18	22500	329/483	-5.7	-3.54	TiO <sub>2</sub>	I <sub>3</sub> /T	625	2.32	0.66	0.96	[DEN 12b]
PMC19	17600	353/468	-5.78	-3.57	TiO <sub>2</sub>	I <sub>3</sub> /T	615	2.35	0.69	1.0	[DEN 12b]
PMC20	26500	353/492	-5.73	-3.47	TiO <sub>2</sub>	I <sub>3</sub> /T	645	2.29	0.68	1.01	[DEN 12b]
PMC21	22600	380/462	-5.85	-3.55	TiO <sub>2</sub>	I <sub>3</sub> /T	695	2.49	0.59	1.21	[DEN 12b]
PMC22	4100	381	-4.89	-3.1	TiO <sub>2</sub>	I <sub>3</sub> /T	720	6.1	0.69	3.01	[LIU 10a]
PMC23	3960	390	-4.87	-3.07	TiO <sub>2</sub>	I <sub>3</sub> /T	670	7.27	0.69	3.37	[LIU 10a]
PMC24		520	-5.37	-3.57	TiO <sub>2</sub>	I <sub>3</sub> /T	680	11.1	0.67	5.1	[LIU 10b]
PMC25		520			TiO <sub>2</sub>	I <sub>3</sub> /T	740	18.24	0.56	7.53	[LIU 11]

**Table 6.2.** Physical, optical and photovoltaic characteristics of PMC1-25

Another possibility is to prepare PMCs with metal complexes in the branched chain. As a general rule, the obtained products have showed good solubility, outstanding stabilities and good open-circuit voltages but moderate power conversion. For instance, Deng *et al.* synthesized four PMCs as dyes containing thiophene–fluorene (PMC18 and PMC19) or thiophene–phenylene (PMC20 and PMC21) with Co(II) or Ni(II) metal complexes in the branched chain. It is seen that these PMCs have glass transition temperature ( $T_g$ ) ranging from 123 to 161°C and follow the order PMC18 > PMC19 > PMC21 > PMC20. This suggests that a fluorenevinylene unit embedded in the polymer backbones renders higher rigidity compared with the phenylenevinylene units [DEN 12b]. Moreover, another PMCs comprising also thiophene fluorene in main chain and 1,10-phenanthroline, 8-HQ, based on Zn(II) (PMC 22) and Cd(II) (PMC23) in branched chain exhibited the best results with PCE equal to 3.01 and 3.37%

[LIU 11]. Such results could be explained by the presence of cadmium metal, which indeed induces a red-shifted absorption by about 10 nm relative to that of PMC22. Cd(II) has more electrons than Zn(II) ion and the radius of Cd(II) is bigger than that of Zn(II) inducing an easy  $\pi-\pi^*$  transition. Therefore,  $\pi-\pi^*$  transition takes place easily.

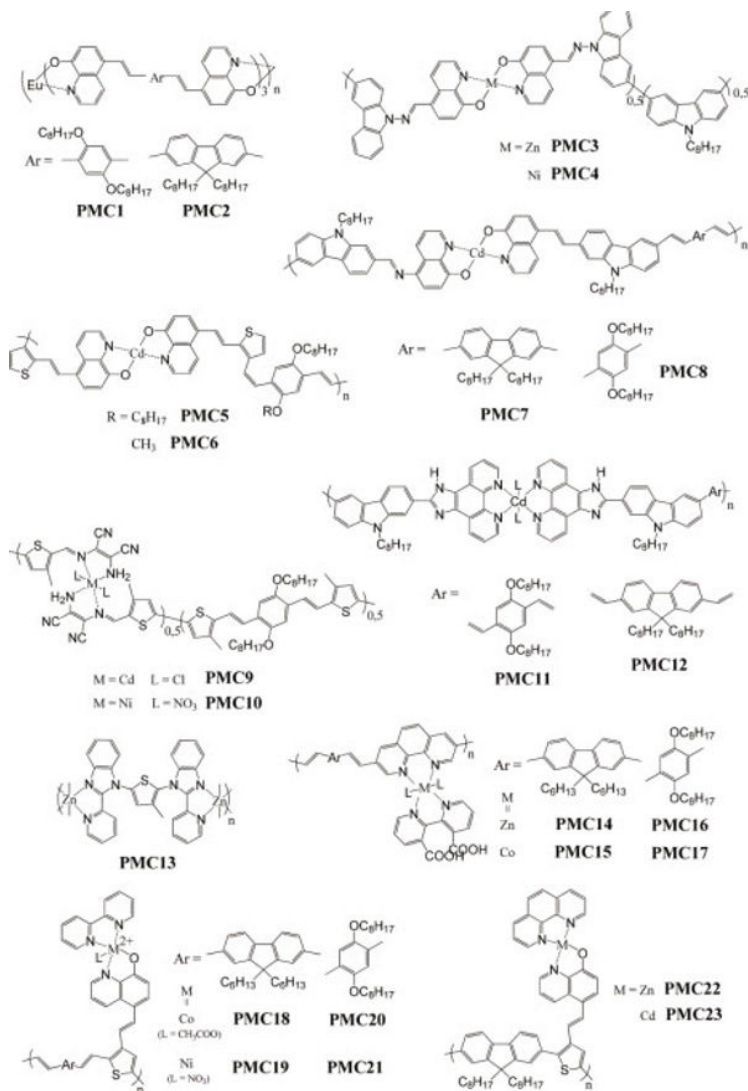
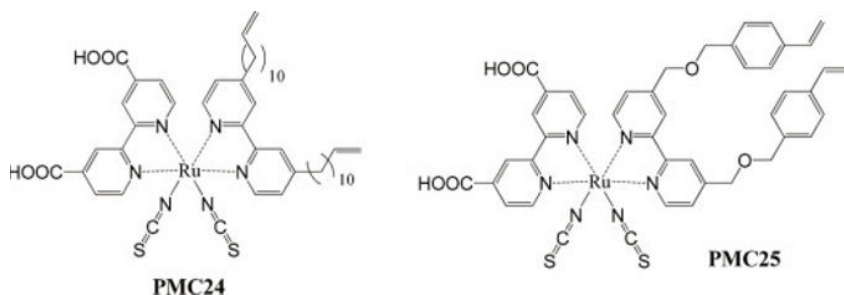


Figure 6.5. Polymer containing metal complexes PMC1-23

Finally, another way to increase the stability of PSSCs could be to directly cross-link metal complexes by tethering aliphatic side chains carrying allyl groups on one of the bipyridine ligands after applying onto a  $\text{TiO}_2$  layer. The synthesized PMC24 and PMC25 were cross-linked with methylacrylic acid (MAA) monomers through its allyl groups or glycerol propoxylate triacrylate (GPTA), respectively. The DSSC with cross-linked PMC24-co-MAA acquired  $J_{sc} = 12.52 \text{ mA/cm}^2$ ,  $V_{oc} = 0.67 \text{ V}$ ,  $ff = 0.63$  and  $\eta = 5.18\%$  [LIU 10], whereas that with cross-linked PMC25-co-GPTA attained

$J_{sc} = 18.73 \text{ mA/cm}^2$ ,  $V_{oc} = 0.72 \text{ V}$ ,  $ff = 0.58$  and  $\eta = 7.88\%$  [LIU 11]). Because the polymerized MAA or GPTA units which contain carboxylic acid or acrylic groups were able to attract  $\text{I}_3^-/\text{I}^-$  redox couples in the gelled electrolyte system, it enhanced the dye regeneration so as to increase the photocurrent.



**Figure 6.6.** Polymer containing metal complexes PMC24-25

For the time-course change test of power efficiency in storage, both DSSCs showed an initial increase in power efficiencies and then stayed almost unchanged for 1 month, whereas that with well-known N3 dye showed a rapid decrease in efficiency in 2 weeks. Effectively, the typical ruthenium dyes contain carboxylate groups which were designed to adsorb onto the nanoporous  $\text{TiO}_2$  layer rendering the excited electrons straightforwardly injected into the conduction band of the  $\text{TiO}_2$ . However, during service, these ruthenium dyes are prone to desorb from  $\text{TiO}_2$  surface due to the fact that they are surrounded by the electrolytes. This higher stability of the DSSCs with cross-linked PMC24-co-MAA or PMC25-co-GPTA, respectively, has shed lights on their potential application for outdoor usage.

From the analysis of PV properties of different PSSCs cited in the chapter, it seems that the rational design of a new polymeric dye has some requirements. However, some criteria are more relevant than others:

– a broad band and high-level absorption of the visible and NIR region of the electromagnetic spectrum is required. Moreover, the energy level of the LUMO of the dye must be slightly higher than that of the  $\text{TiO}_2$ . A difference of 0.3–0.4 eV is requested in order to ensure good electron injection from excited photosensitizer toward electron transporter;

– a polymeric dye faithfully chelating to the semiconductor oxide surface and injecting electrons into the conduction band with a quantum yield of unity is needed. The introduction, for instance, of carboxylic acid groups, which can act as anchoring moieties onto the surface of the nanoporous  $\text{TiO}_2$  layers, drastically increases the PCE while promoting the charge injection;

– a good solubility of the polymeric dye in order to facilitate penetration of such macromolecular molecules inside the porosity of nanoporous  $\text{TiO}_2$ . A original strategy is to use electrochemically polymerized films of precursor monomers in the porosity of a nanocrystalline  $\text{TiO}_2$  layer. Consequently, the insertion of small molecules (as monomers) could increase the pore filling and the interface with  $\text{TiO}_2$  surface, which, in turn, enhances the PCE.

Finally, PSSC must exhibit thermal and photochemical stability. For this to happen, a high density of anchoring groups of a polymer chain, which can offer better thermal stability than low weight molecules, is the main advantage of polymeric photosensitizers.

## 6.9. Conclusion

In this chapter, we reviewed current progress in the use of  $\pi$ -conjugated polymer as dye polymeric materials in DSSCs. Contrary to the metal complexes or small organic molecule-based dyes, interfacial issues of mesoporous  $\text{TiO}_2$ /sensitizer are more critical and strongly influence the PV performance of devices as well as their stability. The conception of new polymeric dyes and their chemical molecular engineering primarily focuses on the delicate balance of HOMO-LUMO energy levels/interface effect in absorption with photosensitizer/infiltration into the mesoporous metal oxide

network. Many organic polymeric dyes have been reported in the literature. Structurally, these compounds are mainly composed of  $\pi$ -conjugated polymers (as PT, polyphenylenevinylene, TPA-based polymer or polyfluorene) or metal complexes-based polymers. The introduction of anchoring group units onto  $\text{TiO}_2$  surface in the molecular structure seems to be primordial. These groups help both to increase the electron injection and to offer better thermal stability. On the other hand, the insertion of conjugated monomer into porous networks before their electrochemical polymerization is favored leading to more efficient devices.

## 6.10. Bibliography

- [AKI 12] AKITSU K., KUBO T., UCHIDA S. *et al.*, “Polymer-sensitized solar cells using polythiophene derivatives with directly attached carboxylic acid groups”, *Japanese Journal of Applied Physics*, vol. 51, p. 10NE04, 2012.
- [BHO 10] BHONGALE C.J., THELAKKAT M., “Efficient hybrid polymer/titania solar cells sensitized with carboxylated polymer dye”, *Solar Energy Materials and Solar Cells*, vol. 94, no. 5, pp. 817–822, 2010.
- [BIS 11] BISQUERT J., “Dilemmas of dye-sensitized solar cells”, *ChemPhysChem*, vol. 12, no. 9, pp. 1633–1636, 2011.
- [BRY 99] BRYCE M.R., “Tetrathiafulvalenes as  $\pi$ -electron donors for intramolecular charge-transfer materials”, *Advanced Materials*, vol. 11, no. 1, pp. 11–23, 1999.
- [BUI 13a] BUI T.-T., BEOUCH L., SALLENAVE X. *et al.*, “Carbazol-N-yl and diphenylamino end-capped triphenylamine-based molecular glasses: synthesis, thermal, and optical properties”, *Tetrahedron Letters*, vol. 54, pp. 4277–4280, 2013.
- [BUI 13b] BUI T.-T., GOUBARD F., “Recent advances in small molecular, non-polymeric organic hole transporting materials for solid-state DSSC”, *EPJ Photovoltaics*, vol. 4, p. 40402, 2013.
- [BUJ 13] BUJAK P., KULSZEWICZ-BAJER I., ZAGORSKA M. *et al.*, “Polymers for electronics and spintronics”, *Chemical Society Reviews*, vol. 42, no. 23, pp. 8895–8999, 2013.
- [CHA 54] CHAPIN D.M., FULLER C.S., PEARSON G.L., “A new silicon p-n junction photocell for converting solar radiation into electrical power”, *Journal of Applied Physics*, vol. 25, pp. 676–677, 1954.

- [CHA 11] CHANG D.W., KO S.-J., KIM J.Y. *et al.*, “Multifunctional conjugated polymers with main-chain donors and side-chain acceptors for dye sensitized solar cells (DSSCs) and organic photovoltaic cells (OPVs)”, *Macromolecular Rapid Communications*, vol. 32, no. 22, pp. 1809–1814, 2011.
- [CHH 12] CHHATRE S., AGARKAR S., DHAS V. *et al.*, “Carboxyl-modified conjugated polymer sensitizer for dye sensitized solar cells: significant efficiency enhancement”, *Journal of Materials Chemistry*, vol. 22, no. 43, pp. 23267–23271, 2012.
- [CHO 11] CHO Y., KIM H., OH M. *et al.*, “TiO<sub>2</sub> composites for efficient poly(3-thiophene acetic acid) sensitized solar cells”, *Journal of The Electrochemical Society*, vol. 158, no. 2, pp. B106–B111, 2011.
- [DEN 12a] DENG J., GUO L., XIU Q. *et al.*, “Two polymeric metal complexes based on polycarbazole containing complexes of 8-hydroxyquinoline with Zn(II) and Ni(II) in the backbone: synthesis, characterization and photovoltaic applications”, *Materials Chemistry and Physics*, vol. 133, no. 1, pp. 452–458, 2012.
- [DEN 12b] DENG J., XIU Q., GUO L. *et al.*, “Branched chain polymeric metal complexes containing Co(II) or Ni(II) complexes with a donor– $\pi$ –acceptor architecture: synthesis, characterization, and photovoltaic applications”, *Journal of Materials Science*, vol. 47, no. 7, pp. 3383–3390, 2012.
- [DIA 13] DIALLO A.K., METRI N., BRUNEL F. *et al.*, “A star-shaped molecule as hole transporting material in solution-processed thin-film transistors”, *Synthetic Metals*, vol. 184, pp. 35–40, 2013.
- [FAN 11] FANG Z., ESHBAUGH A.A., SCHANZE K.S., “Low-bandgap donor-acceptor conjugated polymer sensitizers for dye-sensitized solar cells”, *Journal of the American Chemical Society*, vol. 133, no. 9, pp. 3063–3069, 2011.
- [GRÄ 05] GRÄTZEL M., “Solar energy conversion by dye-sensitized photovoltaic cells”, *Inorganic Chemistry*, vol. 44, no. 20, pp. 6841–6851, 2005.
- [GRÄ 09] GRÄTZEL M., “Recent advances in sensitized mesoscopic solar cells”, *Accounts of Chemical Research*, vol. 42, no. 11, pp. 1788–1798, 2009.
- [GRI 11] GRISORIO R., MASTRORILLI P., SURANNA G.P. *et al.*, “The suzuki–heck polymerization as a tool for the straightforward obtainment of poly(fluorenylene-vinylene) sensitizers for dye-sensitized solar cells”, *Journal of Polymer Science Part A: Polymer Chemistry*, vol. 49, no. 4, pp. 842–847, 2011.
- [HAG 10] HAGFELDT A., BOSCHLOO G., SUN L. *et al.*, “Dye-sensitized solar cells”, *Chemical Reviews*, vol. 110, pp. 6595–6663, 2010.

- [HWA 07] HWANG S., LEE J.H., PARK C. *et al.*, “A highly efficient organic sensitizer for dye-sensitized solar cells”, *Chemical Communications*, vol. 46, pp. 4887–4889, 2007.
- [JIA 09] JIANG H., ZHAO X., SHELTON A.H. *et al.*, “Variable-band-gap poly(arylene ethynylene) conjugated polyelectrolytes adsorbed on nanocrystalline TiO<sub>2</sub>: photocurrent efficiency as a function of the band gap”, *ACS Applied Materials & Interfaces*, vol. 1, no. 2, pp. 381–387, 2009.
- [JIN 13a] JIN X., YU X., ZHANG W. *et al.*, “Main chain polymeric metal complexes based on linkage fluorenevinylene or phenylenevinylene with thienyl(8-hydroxyquinoline)–cadmium (II) complexes as dye sensitizer for dye-sensitized solar cells”, *Journal of Applied Polymer Science*, vol. 129, no. 6, pp. 3104–3112, 2013.
- [JIN 13b] JIN X., YU X., ZHANG W. *et al.*, “Synthesis and photovoltaic properties of main chain polymeric metal complexes containing 8-hydroxyquinoline metal complexes conjugating alkyl fluorene or alkoxy benzene by C=N bridge for dye-sensitized solar cells”, *Polymer Composites*, vol. 34, no. 10, pp. 1629–1639, 2013.
- [KAN 10] KANIMOSHI C., BALRAJU P., SHARMA G.D. *et al.*, “Diketopyrrolopyrrole-based donor-acceptor copolymers as organic sensitizers for dye sensitized solar cells”, *Journal of Physical Chemistry C*, vol. 114, no. 7, pp. 3287–3291, 2010.
- [KIM 03] KIM Y.-G., WALKER J., SAMUELSON L.A. *et al.*, “Efficient light harvesting polymers for nanocrystalline TiO<sub>2</sub> photovoltaic cells”, *Nano Letters*, vol. 3, no. 4, pp. 523–525, 2003.
- [KIM 06] KIM M.-R., SHIN W.S., KIM W.-S. *et al.*, “Polymer-sensitized solar cells using thiophene copolymers”, *Molecular Crystals and Liquid Crystals*, vol. 462, no. 1, pp. 91–99, 2006.
- [KIM 12] KIM D.-M., YOON J.-H., WON M.-S. *et al.*, “Electrochemical characterization of newly synthesized polyterthiophene benzoate and its applications to an electrochromic device and a photovoltaic cell”, *Electrochimica Acta*, vol. 67, no. 0, pp. 201–207, 2012.
- [KIM 13] KIM B.-G., CHUNG K., KIM J., “Molecular design principle of all-organic dyes for dye-sensitized solar cells”, *Chemistry – A European Journal*, vol. 19, no. 17, pp. 5220–5230, 2013.
- [LEE 11] LEE S.-M., LEE S.-B., KIM K.-H. *et al.*, “Syntheses and photovoltaic properties of polymeric sensitizers using thiophene-based copolymer derivatives for dye-sensitized solar cells”, *Solar Energy Materials and Solar Cells*, vol. 95, no. 1, pp. 306–309, 2011.

- [LI 10] LI C., LIU M., PSCHIRER N.G. *et al.*, “Polyphenylene-based materials for organic photovoltaics”, *Chemical Reviews*, vol. 110, no. 11, pp. 6817–6855, 2010.
- [LIU 08] LIU X., ZHU R., ZHANG Y. *et al.*, “Anionic benzothiadiazole containing polyfluorene and oligofluorene as organic sensitizers for dye-sensitized solar cells”, *Chemical Communications*, vol. 32, pp. 3789–3791, 2008.
- [LIU 10] LIU Y., GUO X., XIANG N. *et al.*, “Synthesis and photovoltaic properties of polythiophene stars with porphyrin core”, *Journal of Materials Chemistry*, vol. 20, no. 6, pp. 1140–1146, 2010.
- [LIU 11] LIU Y., XIU Q., XIAO L. *et al.*, “Two novel branched chain polymeric metal complexes based on Cd(II), Zn(II) with fluorene, thiophene, 8-hydroxyquinoline, and 1,10-phenanthroline ligand: synthesis, characterization, photovoltaic properties, and their application in DSSCs”, *Polymers for Advanced Technologies*, vol. 22, no. 12, pp. 2583–2591, 2011.
- [LOH 09] LOHWASSER R.H., BANDARA J., THELAKKAT M., “Tailor-made synthesis of poly(3-hexylthiophene) with carboxylic end groups and its application as a polymer sensitizer in solid-state dye-sensitized solar cells”, *Journal of Materials Chemistry*, vol. 19, no. 24, pp. 4126–4130, 2009.
- [MAT 14] MATHEW S., YELLA A., GAO P. *et al.*, “Dye-sensitized solar cells with 13% efficiency achieved through the molecular engineering of porphyrin sensitizers”, *Nature Chemistry*, vol. 6, no. 3, pp. 242–247, 2014.
- [MET 12] METRI N., SALLENAVE X., PLESSE C. *et al.*, “Processable star-shaped molecules with triphenylamine core as hole-transporting materials: experimental and theoretical approach”, *Journal of Physical Chemistry C*, vol. 116, no. 5, pp. 3765–3772, 2012.
- [MIK 11] MIKROYANNIDIS J.A., TSAGKOURNOS D.V., BALRAJU P. *et al.*, “Synthesis and photovoltaic properties of an alternating phenylenevinylene copolymer with substituted-triphenylamine units along the backbone for bulk heterojunction and dye-sensitized solar cells”, *Journal of Power Sources*, vol. 196, no. 4, pp. 2364–2372, 2011.
- [MOO 98] MOORE A.J., BRYCE M.R., BATSANOV A.S. *et al.*, “New 1,3-dithiol-2-ylidene donor-[small pi]-acceptor chromophores with intramolecular charge-transfer properties, and related donor-[small pi]-donor molecules: synthesis, electrochemistry, X-ray crystal structures, non-linear optical properties and theoretical calculations”, *Journal of Materials Chemistry*, vol. 8, no. 5, pp. 1173–1184, 1998.

- [MOZ 14] MOZAFFARI S., NATEGHI M.R., ZARANDI M.B., “Effects of multi anchoring groups of catecholamine polymer dyes on the electrical characteristics of metal free dye-sensitized solar cells: a comparison study”, *Solar Energy*, vol. 106, pp. 63–71, 2014.
- [OOY 09] OOOYAMA Y., HARIMA Y., “Molecular designs and syntheses of organic dyes for dye-sensitized solar cells”, *European Journal of Organic Chemistry*, vol. 18, pp. 2903–2934, 2009.
- [OOY 12] OOOYAMA Y., OHSHITA J., HARIMA Y., “Control of molecular arrangement and/or orientation of D- $\pi$ -A fluorescent dyes for dye-sensitized solar cells”, *Chemistry Letters*, vol. 41, no. 11, pp. 1384–1396, 2012.
- [O'RE 91] O'REGAN B., GRÄTZEL M., “A low-cost, high-efficiency solar cell based on dye-sensitized colloidal TiO<sub>2</sub> films”, *Nature*, vol. 353, no. 6346, pp. 737–740, 1991.
- [RAV 04] RAVIRAJAN P., HAQUE S.A., DURRANT J.R. *et al.*, “Hybrid nanocrystalline TiO<sub>2</sub> solar cells with a fluorene–thiophene copolymer as a sensitizer and hole conductor”, *Journal of Applied Physics*, vol. 95, p. 1473, 2004.
- [RIV 13] RIVATON A., TOURNEBIZE A., GAUME J. *et al.*, “Photostability of organic materials used in polymer solar cells”, *Polymer International*, vol. 63, no. 8, pp. 1335–1345, 2013.
- [SAJ 10] SAJI V.S., ZONG K., PYO M., “NIR-absorbing poly(thieno[3,4-b]thiophene-2-carboxylic acid) as a polymer dye for dye-sensitized solar cells”, *Journal of Photochemistry and Photobiology A: Chemistry*, vol. 212, nos. 2–3, pp. 81–87, 2010.
- [SEN 03] SENADEERA G.K.R., NAKAMURA K., KITAMURA T. *et al.*, “Fabrication of highly efficient polythiophene-sensitized metal oxide photovoltaic cells”, *Applied Physics Letters*, vol. 83, pp. 5470–5472, 2003.
- [SEN 05a] SENADEERA G.K.R., KITAMURA T., WADA Y. *et al.*, “Photosensitization of nanocrystalline TiO<sub>2</sub> films by a polymer with two carboxylic groups, poly(3-thiophenemalonic acid)”, *Solar Energy Materials and Solar Cells*, vol. 88, pp. 315–322, 2005.
- [SEN 05b] SENADEERA R., FUKURI N., SAITO Y. *et al.*, “Volatile solvent-free solid-state polymer-sensitized TiO<sub>2</sub> solar cells with poly(3,4-ethylenedioxythiophene) as a hole-transporting medium”, *Chemical Communications*, pp. 2259–2261, 2005.
- [SHA 07] SHANKAR K., MOR G.K., PRAKASAM H.E. *et al.*, “Self-assembled hybrid polymer-TiO<sub>2</sub> nanotube array heterojunction solar cells”, *Langmuir*, vol. 23, no. 24, pp. 12445–12449, 2007.

- [SIR 03] SIRIMANNE P.M., SHIRATA T., DAMODARE L. *et al.*, “An approach for utilization of organic polymer as a sensitizer in solid-state cells”, *Solar Energy Materials and Solar Cells*, vol. 77, no. 1, pp. 15–24, 2003.
- [SU 12] SU J.-Y., TSAI C.-H., WANG S.-A. *et al.*, “Functionalizing organic dye with cross-linked electrolyte-blocking shell as a new strategy for improving DSSC efficiency”, *RSC Advances*, vol. 2, no. 9, pp. 3722–3728, 2012.
- [TAN 13a] TAN H., PAN C., WANG G. *et al.*, “Synthesis and characterization of conjugated polymers with main-chain donors and pendent acceptors for dye-sensitized solar cells”, *RSC Advances*, vol. 3, no. 37, pp. 16612–16618, 2013.
- [TAN 13b] TANAKA H., TAKECHI A., SHIOZAWA M. *et al.*, “Chemical stability of sensitizer molecules for dye sensitized solar cells”, *R&D Review of Toyota CRDL*, vol. 44, no. 1, pp. 17–26, 2013.
- [XIA 10] XIAO L., LIU Y., XIU Q. *et al.*, “Two main chain polymeric metal complexes as dye sensitizers for dye-sensitized solar cells based on the coordination of the ligand containing 8-hydroxyquinoline and phenylethyl or fluorene units with Eu(III)”, *Journal of Polymer Science Part A: Polymer Chemistry*, vol. 48, no. 9, pp. 1943–1951, 2010.
- [XIU 11] XIU Q., HUANG H., LIU Y. *et al.*, “A novel main chain polymeric metal complex based on Zn(II) with thiophene and 2-(2'-pyridyl)benzimidazole ligand: synthesis, characterization, photovoltaic property and application in DSSCs”, *Synthetic Metals*, vol. 161, nos. 5–6, pp. 455–459, 2011.
- [YAN 04] YANAGIDA S., SENADEERA G.K.R., NAKAMURA K. *et al.*, “Polythiophene-sensitized TiO<sub>2</sub> solar cells”, *Journal of Photochemistry and Photobiology A: Chemistry*, vol. 166, pp. 75–80, 2004.
- [YAN 09] YANG C.-H., CHEN H.-L., CHEN C.-P. *et al.*, “Electrochemical polymerization effects of triphenylamine-based dye on TiO<sub>2</sub> photoelectrodes in dye-sensitized solar cells”, *Journal of Electroanalytical Chemistry*, vol. 631, nos. 1–2, pp. 43–51, 2009.
- [YIN 09] YIN J.-F., BHATTACHARYA D., HSU Y.-C. *et al.*, “Enhanced photovoltaic performance by synergism of light-cultivation and electronic localization for highly efficient dye-sensitized solar cells”, *Journal of Materials Chemistry*, vol. 19, no. 38, pp. 7036–7042, 2009.
- [YOO 11] YOON J.-H., KIM D.-M., YOON S.-S. *et al.*, “Comparison of solar cell performance of conducting polymer dyes with different functional groups”, *Journal of Power Sources*, vol. 196, no. 20, pp. 8874–8880, 2011.

- [YU 13] YU X., JIN X., TANG G. *et al.*, “D- $\pi$ -A dye sensitizers made of polymeric metal complexes containing 1,10-phenanthroline and alkylfluorene or alkoxybenzene: synthesis, characterization and photovoltaic performance for dye-sensitized solar cells”, *European Journal of Organic Chemistry*, vol. 2013, no. 26, pp. 5893–5901, 2013.
- [ZHA 09a] ZHANG W., FANG Z., SU M. *et al.*, “A triphenylamine-based conjugated polymer with donor- $\pi$ -acceptor architecture as organic sensitizer for dye-sensitized solar cells”, *Macromolecular Rapid Communications*, vol. 30, no. 18, pp. 1533–1537, 2009.
- [ZHA 09b] ZHANG W.E.I., ZHU R.U.I., LIU X.-Z. *et al.*, “Conjugated polymer-sensitized solar cells based on electrospun TiO<sub>2</sub> nanofiber electrode”, *International Journal of Nanoscience*, vol. 08, no. 1–2, pp. 227–230, 2009.
- [ZHA 14] ZHANG W., JIN X., YU X. *et al.*, “Novel dye sensitizers of main chain polymeric metal complexes based on complexes of diaminomaleonitrile with Cd(II), Ni(II): synthesis, characterization, and photovoltaic performance for dye-sensitized solar cells”, *Journal of Organometallic Chemistry*, vol. 749, pp. 26–33, 2014.
- [ZHO 14] ZHOU J., YU X., JIN X. *et al.*, “Novel carbazole-based main chain polymeric metal complexes containing complexes of phenanthroline with Zn(II) or Cd(II): synthesis, characterization and photovoltaic application in DSSCs”, *Journal of Molecular Structure*, vol. 1058, pp. 14–21, 2014.

---

# NIR-Dyes for Photopolymers and Laser Drying in the Graphic Industry

---

## 7.1. Introduction

After the release of the first *Tablet Computers* in 2010, many people forecasted the early end of printed materials. This also included printed matter made by offset printing that uses a lithographic plate for image generation and a press machine to print the image with many impressions. Today, offset printing technology still exists despite the newly reorganized market. Particularly, the use of digital media has resulted in a reduction in the costs needed for printing and logistics/storage. Internet-printing businesses have been established that can print as many as 100k files in one night with fast delivery to many global destinations worldwide. Flyers represent one main target of internet-printing shops. Other printing applications relate to packaging or commercial printing to name a few examples. Nevertheless, the amount of printed newspapers has decreased presumably as a result of more intense use of mobile devices to obtain news from all over the world. Lithographic plates represent one prerequisite for modern offset printing comprising of dyes as sensitizers.

Digital exposure has been used to transfer a lithographic pattern in offset printing [BAU 15, STR 14, VOL 80, BAU 94, TIM 88, BAU 93, TIM 01, FRA 83, TIM 87, KAR 05, HAT 00, STR 09]. Such light-sensitive materials are made of a roughed aluminum substrate oxidized at the surface. This is

---

Chapter written by Bernd STREHMEL, Thomas BRÖMME, Christian SCHMITZ, Knut REINER, Steffen ERNST and Dietmar KEIL.

coated with a light sensitive material. Furthermore, offset printing uses a water-in-oil (W/O) emulsion of oleophilic printing ink and water that is generated *in situ* in the press machine. The hydrophilic  $\text{Al}_2\text{O}_3$ -layer functions as the water accepting (non-printing) part while the hydrophobic coating accepts the oleophilic ink (printing parts). Thus, exposure differentiates between printing (image) and non-printing (non-image) areas after exposing and processing. Printing plates based on photopolymers work as negative materials (unexposed parts dissolve during processing). They exhibit a thickness between 1 and 2  $\mu\text{m}$ . The processed lithographic photopolymer plates can print several 100,000 impressions without thermal post-treatment (baking) depending on the press conditions. Sometimes, dusty paper and aggressive printing chemicals result in an undesired early coating wear-off during the printing job<sup>1</sup>. Nevertheless, there exists a certain demand to create lithographic plates with increased robustness on press. From this point of view, photopolymer materials are the matter of choice.

Photopolymers for imaging exhibit a high photosensitivity. This gives access to digital laser exposure techniques first shown at the IPEX in 1993<sup>2</sup>. Moreover, lithographic plate manufacturers started to study NIR-photopolymers at the beginning of this century. A first commercial product was offered by Kodak-Polychrome [HAU 00a]. Nevertheless, the idea to use a laser as an exposure source for printing plates was published much earlier in the 1970s [WEG 74]. During that time, common UV-lasers were disclosed in the patent literature. Today's commercialized CtP systems based on photoinduced polymerization exhibit a resolution of  $\geq 10 \mu\text{m}$  depending on the exposure source [PHO 14]. Better resolution would be possible but this is not necessary because the resolution of the human eye is  $\geq 50 \mu\text{m}$  at a distance of about 50 cm between the object printed and the human eye [OGL 51, YAN 11].

The term "Computer to Plate (CtP)" has been mostly used to describe lithographic plate digital exposure by laser sources. Visible lasers emitting at 488 nm ( $\text{Ar}^+$ laser) were first used in the graphic industry. FD-Nd-YAG lasers emitting at 532 nm partially replaced these sources. The development of semiconductor lasers has resulted in a quantitative substitution of gas

---

1 Photopolymer printing plates are available from three big suppliers; see [AGF 14, FUJ 14, KOD 14].

2 CEP Technology was first introduced at the IPEX in 1993. For more details, see [KIP 00] and [LIM 96].

lasers by these sources emitting either in the near infrared (NIR) region (808 or 830 nm) or violet spectral part (405 nm). This change resulted in a huge saving of costs and has helped to eliminate the red safe light requirement. From this point of view, synthetic dyes possess a major function as sensitizers in these systems [BAU 15, MUS 00]. Moreover, dyes are also as important as colorants [MUS 00].

NIR imaging technology results in better resolution on press and it represents the more expensive option. Thus, NIR photopolymers can be found in all types of applications whereas the 405 nm CtP systems are limited more or less to the less-demanding newspaper printing. Many NIR exposure machines, which have been called platesetters, use as light valve modulators [BAU 15, MOU 00, MOU 04], the so-called square spot technology. It offers a higher resolution compared to those with Gaussian beam profile. Nevertheless, exposure machines based on flat-bed scanning technique have been available as well [BAU 15].

Modern photopolymer printing plates must exhibit a long shelf life ( $\geq 12$  months) where the sensitivity exhibits only small changes within the specifications in this time frame. This requires the design of systems exhibiting a high stability even under tropic storage conditions. Thus, the components of the initiator system as well as the monomers must be stable in the coating over a long period of time. Many initiator systems comprising of an NIR dye as sensitizer and radical initiator shown in this contribution fulfill these requirements.

Physical drying has often been applied to remove water/solvents in the paper of the printed material. Physical drying requires conditions where the printed stuff does not require long storage periods after it releases the press machine. This is important particularly for printing businesses working according to lean-manufacturing conditions where the material should be delivered to the customer immediately with no additional storage time. Thus, a shortening of the drying time is necessary. Recently, the laser-drying method was introduced as a new physical drying technique in offset printing where an NIR-absorber dye absorbs NIR radiation that is immediately released as heat in the printed layer resulting in the removal of water/solvents with no thermal destruction of the substrate (paper) [ERN 13, PIT 03, SCH 08, SCH 12, ERN 13]. This also significantly reduces the drying time. Laser drying can be considered

a new ecological technique in offset printing that was first developed in the industry.

## 7.2. Computer to plate systems

### 7.2.1. *Technical remarks*

1) *Digital exposure and imaging-CtP*. This requires the generation of a digital file in a page description language (vector graphics, i.e. PostScript or PCL) in the first step. Then, a raster image processor (RIP), which is a software as part of a machine, generates a raster image (bitmap) from this file format. This is sent to the digital exposing device – the platesetter – for exposure. In other words, the RIP transforms a vector graphics into a raster image; that is a raw binary of dot patterns. Thus, the RIP transfers the information where the platesetter must expose the photopolymer layer (*one* in terms of logic thinking, i.e. there is a pixel in the image) or not (*zero* in terms of logic thinking, i.e. there is no pixel in the image) the lithographic plate. This occurs step by step over the entire image/plate. Both, laser power and scan speed control the exposure time of each dot that locates in the  $\mu$ s-time frame.

2) *Image generation and processing*. After completion of exposure, the material requires processing to wash-out the non-exposed parts of a negative imaging material. This may include after completion of: (i) exposing the preheat to complete photopolymerization in the image layer (1–3  $\mu$ m thickness), (ii) the prewash to remove the water soluble oxygen barrier layer (0.5–3  $\mu$ m thickness), (iii) the developing to wash out the non-exposed parts resulting in the lithographic pattern, (iv) the post-rinse to remove residual processing liquid on the substrate and (v) the finishing that keeps the substrate of the printing plate precursor hydrophilic in the non-image areas by applying a hydrophilic water-soluble polymer layer. References [KOD 13, FUJ 14, AGF 14] provide more technical details. The oxygen barrier layer comprises polyvinyl alcohol (PVA), which has been known as a material with a low capability of oxygen permeability [BAU 15, STR 09]. The higher the thickness of PVA and the higher the degree of saponification, the better works the barrier function of the PVA. Thus, we need to find a reasonable compromise between shelf-life and sensitivity. This can be achieved by variation of PVA-thickness (0.5–3  $\mu$ m) and/or saponification degree (85–99.5%). Stabilization of such imaging materials in which oxygen

can penetrate into the imaging layer through the PVA oxygen barrier has been achieved by the addition of aerobic inhibitors (steric hindered phenols) into the coating. In case that diffusion of oxygen into the imaging layer would be avoided, we need to stabilize the lithographic plate with anaerobic inhibitors. This can be stable radicals such as (2,2,6,6-tetramethyl-piperidin-1-yl) oxyl (TEMPO) [BAU 15, STR 09]. References [BAU 15, STR 14, VOL 80, BAU 94, TIM 88, BAU 93, TIM 01, FRA 83, TIM 87, KAR 05, HAT 00, STR 09, PHO 14] summarize more technical details.

Modern printing plate development also addresses environmental questions to the plate design. Today's research focuses to reduce the amount of processing chemicals needed per m<sup>2</sup> plate by simplifying the number of necessary processing steps. This requires creation of plates allowing to omit some steps (i–v) described above resulting in a system being as simple as possible for the user with the goal to save processing time, resources (electrical energy and water) and to keep the amount of waste generated (loaded processing liquid) as low as possible. Furthermore, the omission of preheat requires, in contrast to a preheat system, an immediate completion of photopolymerization after exposure because no latent image exists. However, a preheat system requires only generation of a latent image. These are immobilized radicals exhibiting a stability of at least 30 min at room temperature. Application of preheat requires a temperature greater than 100°C resulting in an increase of the radical mobility in the latent image and finally completes polymerization and cross-linking of the multifunctional monomers. This occurs above the glass transition temperature of the imaging layer.

The developer capacity has become one of the most important parameters for new lithographic plate systems. Today, more than 30 m<sup>2</sup> can be developed in 1 L developer, which requires sufficient solubility or dispersibility of all plate components in the processing liquid. Furthermore, the combination of developing and finishing would result in a lithographic plate which only needs one bath for processing. It combines more steps just in one bath. The challenge of simple processing can be seen in the fact that we need to find processing chemicals showing no attack to the cross-linked plate coating during storage between processing and printing (up to one week in some cases). In addition, a simple processing solution also contains finishing chemicals to avoid “drying-out” of the substrate. Thus, it additionally functions as a gum.

A test image has often been used to image lines on the lithographic plate. They exhibit a different line width and different distance between them, which is the image-free part. This treatment of imaging is necessary to prove the resolution of the imaging material. The thinner the line in the image reproduced, the better the resolution. The imaging material loses its resolution if lines and image-free parts merge. This depends on the condition of the laser head [BAU 15, STR 14] and the composition of the coating. Furthermore, NIR-photopolymers can differentiate between a line having a thickness of  $\geq 20 \mu\text{m}$ . This brought the idea to image source-drain electrode structures on the roughened surface of a negative offset printing plate. These structures can be applied to print conductive inks for printed electronics [STR 09]. Even for this purpose photopolymer materials would be the matter of choice because some of these functional inks comprise metallic nanoparticles. This requires the usage of a robust cross-linked coating to avoid a fast plate wearing on press [BAU 15].

There also exist lithographic plates that do not even need a processing bath after exposure because the press machine washes out the non-exposed parts resulting in the lithographic pattern on the plate. In other words, such a plate develops on press and consequently those materials have been introduced as process free plates [MUN 09, YAM 05, MUN 10]. This technique is already available on the market using NIR lasers [BAU 15, TIM 01, MUN 09, YAM 05, MUN 10] and can be seen as the future in this industrial application. The light sensitivity of *on-press developable* plates is about  $50\text{--}100 \text{ mJ/cm}^2$  with no need to preheat and any other processing equipment [BAU 15, TIM 01, KOD 14, FUJ 14]. Such a plate can be called a true “green plate” meaning that no additional waste, such as a loaded processing solution, would be generated.

### 7.2.2. Photochemical aspects of photoinitiation using NIR lasers

The photoinitiator system, embedded in a thin film comprising polymeric binder, functionalized monomers, colorants/color on demand materials and additives, mostly influences light sensitivity of the coating. The reaction scheme as shown in Figure 7.1 generally describes the mechanism for photonic generation of initiating radicals. This electron transfer between the excited singlet state of a sensitizer (**Sens**<sup>\*</sup>) and an acceptor (**A**) results in the generation of a radical pair **Sens**<sup>+•</sup> and **A**<sup>•-</sup>, respectively, whose spin multiplicity does not change. **Sens**<sup>+•</sup> can either disproportionate or

decompose [BRÖ 15b, BRÖ 15c]. This must occur very fast to avoid electron back-transfer. Typical NIR-dyes following the reaction path, as shown in Figure 7.1, exhibit a neutral structure with no counter ion. Nevertheless, such sensitizers have not disclosed for NIR-photopolymers yet. From our best knowledge, the most common sensitizer used for these applications have been chosen from polymethine dyes showing photochemistry from the singlet state. From our best knowledge, there are no triplet sensitizers available in the NIR.

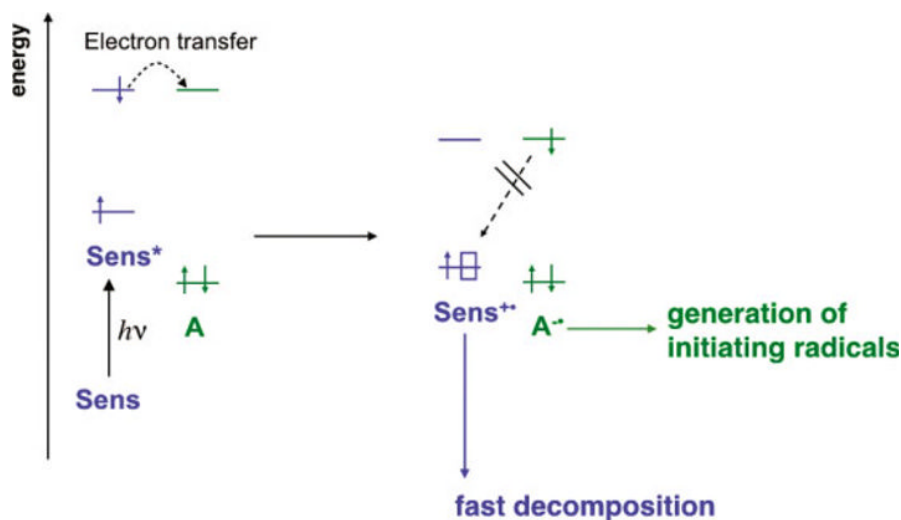


**Figure 7.1.** Reaction scheme for generation of initiating radicals using a photoinitiator system comprising a sensitizer (*Sens*) and an electron acceptor *A*. Excitation results in generation of the excited state of the sensitizer *Sens*\* donating an electron in the **LUMO** of *A* resulting in the formation of *Sens*<sup>+</sup> and *A*<sup>·</sup>, which is a singlet radical pair. Fast decomposition of *Sens*<sup>+</sup> reduces probability of electron back transfer from *Sens*<sup>+</sup>→*A*<sup>·</sup>. The positive charge of *Sens*<sup>+</sup> in the **SOMO** interacts with the electrons of its lower filled orbitals resulting in a decrease of the **SOMO** energy compared to the **HOMO** energy of *Sens*

Neutral dyes form photoproducts exhibiting huge hypsochromic-shifted absorption, which can be seen by a change of the coating color from green to deep yellow. Thus, the bleaching of the sensitizer at the excitation wavelength leads to the scenario that the excitation light can penetrate through the entire coating. The UV–VIS–NIR spectrum of the coating, taken after exposure, shows almost complete disappearance of sensitizer absorption at 800 nm.

Furthermore, some patent applications disclose the addition of a third component **D** exhibiting electron donating properties. Thus, the donor **D** can promote an electron into the hole of **Sens<sup>+</sup>**, if its HOMO-energy is higher compared to the SOMO of **Sens<sup>+</sup>** resulting in the back-formation of **Sens** while **D<sup>+</sup>** may additionally decompose to initiating radicals. Absorption of **Sens** should not change according to this mechanism because electron transfer from **D** to **Sens<sup>+</sup>** would completely reverse the sensitizer. Because no bleaching would occur at the excitation wavelength, it requires choosing an absorption that guarantees an almost unique exposure of the entire coating. This is an optical density (OD) of 0.43. Figure 7.2 explains the scenario in more detail.

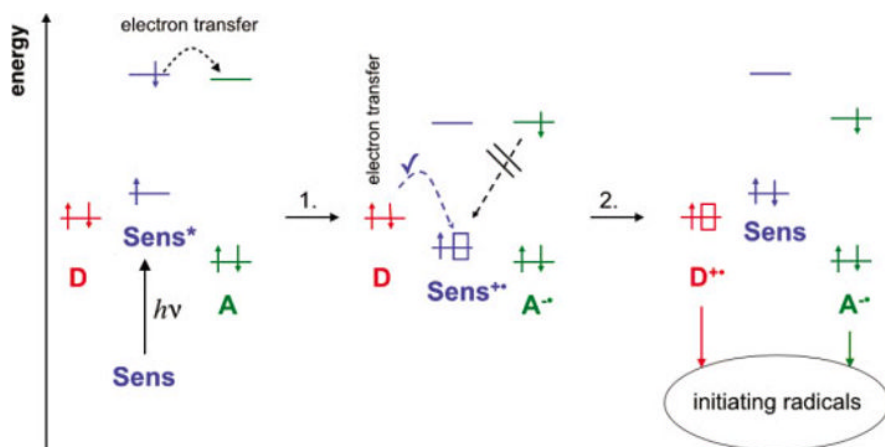
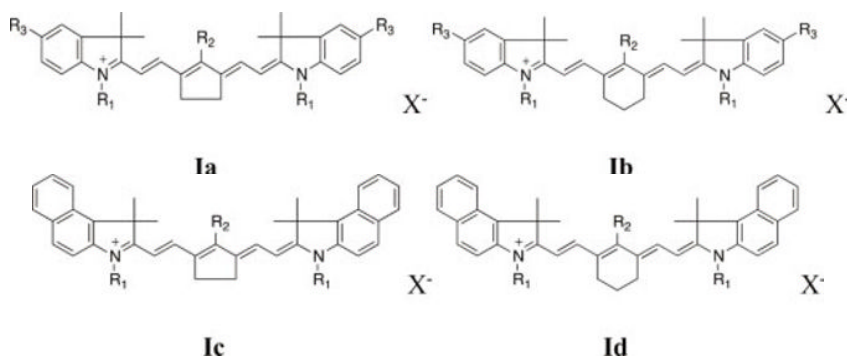


**Figure 7.2.** Reaction scheme for generation of initiating radicals using a photoinitiator system **Sens**, **A**, and electron donating component **D**. Excitation results first in generation of **Sens<sup>\*</sup>** donating an electron in the **LUMO** of **A**. This yields **Sens<sup>+</sup>** and **A<sup>-</sup>**. The positive charge of **Sens<sup>+</sup>** in the **SOMO** interacts with the electrons of its lower filled orbitals resulting in a decrease of the **SOMO** energy compared to the **HOMO** energy of **Sens**. This opens the possibility to donate an electron from **D**→**Sens<sup>+</sup>** resulting in back formation of **Sens** and **D<sup>+</sup>**. The latter additionally decomposes and releases additional initiating radicals

However, our spectroscopic investigations also indicated a decrease of the sensitizer absorption in the system comprising **Sens**, **A** and **D** as described in Figure 7.2. Thus, we believe the occurrence of additional processes relates to thermal events. The laser used for exposure transfers a huge amount of energy into the coating resulting in a temperature increase of the coating to  $\gg 130^\circ\text{C}$ . The NIR sensitizer additionally functions as absorber promoting thermal events because it releases most of the absorbed

energy as heat based on internal conversion [BRÖ 15b, BRÖ 15c]. This is concluded from the fluorescence quantum yield measured [BRÖ 15b]. Furthermore, photochemical studies confirm the proposed pathways as shown in Figures 7.1 and 7.2 [BRÖ 15c]. The sensitizer therefore possesses a dual function; that is the description of the photonic pathways as disclosed in Figure 7.2 and as NIR-absorber resulting in release of heat. The latter also leads thermally to the generation of radicals as found in coatings comprising NIR-dyes and radical initiators [SCH 15]. Thus, the onset of polymerization started at temperatures below 100°C considering an NIR-photoinitiator system embedded in a model coating [SCH 15]. Typical NIR sensitizers following the scheme, as shown in Figure 7.2, have been cationic polymethine dyes. They may bear as counter ion  $X^-$  with a negative charge. The fast decomposition of  $Sens^{+}$ ,  $A^*$ , and  $D^*$  favors to direct the reaction particular in one direction with low probability of electron back transfer.

The structures **Ia-d** represent sensitizers following the mechanism depicted either in Figure 7.1 or 7.2. They differ in the *meso*-position of the polymethine dye in which either a five- (**Ia** and **Ic**) or six-membered ring (**Ib** and **Id**) controls either the methine chain, which is almost planar (**Ia** and **Ic**) or disturbed in geometry (**Ib** and **Id**). This has an impact on the solubility as well. The more distorted the geometry, the better soluble the NIR-dye. Furthermore, the squaraine structure **II** [NAG 89] and structure **III** [SAV 12] have also attracted the attention as sensitizer in lithographic printing plate materials. Both belong to the group of polymethine dyes.



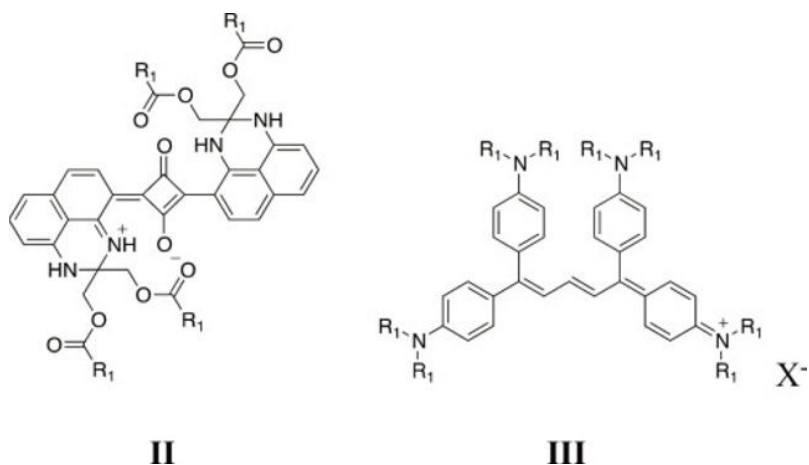
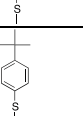
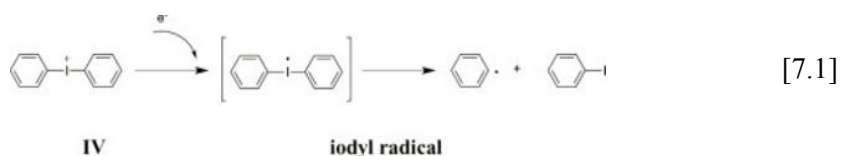


Table 7.1 summarizes some examples of the structures **Ia-d** compiling the location of the absorption maximum  $\lambda_{\max}$  and molar extinction coefficient  $\epsilon_{\max}$  [WWW 14]. This bathochromically shifts if  $R_3$  changes from H to Cl in both structures **Ia** and **Ib**. Furthermore, a bathochromic shift of absorption occurs as expected by switching from **Ia** to **Ic** and **Ib** to **Id**, respectively, by changing the terminal groups from indolium to benzindolium. Moreover, geometry changes in the methine chain from an almost flat structure (**Ia** and **Ic**) to a molecular framework in which not all  $sp^2$ -carbons of the methine chain are kept in one plane (**Ib** and **Id**) results in a hypsochromic shift of the absorption. Squaraines (**II**) and branched polymethines (**III**) exhibit absorption maximum at around 800 nm while the extinction coefficient is lower as compared to structure I.

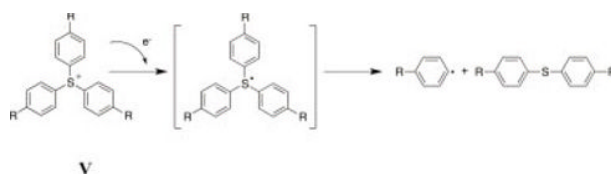
The mechanisms shown in Figures 7.1 and 7.2 require the addition of an electron acceptor compound (**A**). Diaryliodonium salts (**IV**) have been very popular in this field [CRI 84, HAU 00b, STR 03]. Electron transfer results in reduction of this compound are shown in equation [7.1]. The iodyl radical formed decomposes quickly and releases highly reactive initiating aryl radicals. The iodyl radical must possess a very short lifetime indicating the fast decomposition into the iodine atom and phenyl radical. Further onium salts (i.e. triarylsulfonium salts **V**) alternatively decompose after acceptance of an electron resulting in formation of the phenyl radical and diaryl thioether as shown in equation [7.2].

Structure	R <sub>1</sub>	R <sub>2</sub>	R <sub>3</sub>	X <sup>-</sup>	λ <sub>max</sub> (nm)	ε <sub>max</sub> (M <sup>-1</sup> cm <sup>-1</sup> )
<b>Ia1</b>	CH <sub>3</sub>	Cl	H	Cl <sup>-</sup>	797	280,000
<b>Ia2</b>	C <sub>2</sub> H <sub>5</sub>		Cl	Cl <sup>-</sup>	792	308,000
<b>Ia3</b>	CH <sub>3</sub>		H	Cl <sup>-</sup>	784	270,000
<b>Ia4</b>	C <sub>4</sub> H <sub>9</sub>		Cl	ClO <sub>4</sub> <sup>-</sup>	797	266,000
<b>Ia5</b>	C <sub>4</sub> H <sub>9</sub>		H	ClO <sub>4</sub> <sup>-</sup>	794	250,000
<b>Ia6</b>	C <sub>2</sub> H <sub>5</sub>		Cl	none	785	308,000
<b>Ia7</b>	CH <sub>3</sub>		H	none	780	295,000
<b>Ib1</b>	C <sub>2</sub> H <sub>5</sub>	Cl	Cl	Tosylate	785	290,000
<b>Ib2</b>	CH <sub>3</sub>		H	Cl <sup>-</sup>	798	224,000
<b>Ib3</b>	CH <sub>3</sub>	Cl	H	Cl <sup>-</sup>	775	252,000
<b>Ib4</b>	CH <sub>3</sub>		Cl	Cl <sup>-</sup>	795	206,000
<b>Ib5</b>	CH <sub>3</sub>		H	Cl <sup>-</sup>	787	249,000
<b>Ib6</b>	CH <sub>3</sub>		H	Cl <sup>-</sup>	787	228,000
<b>Ic1</b>	C <sub>4</sub> H <sub>9</sub>		-	ClO <sub>4</sub> <sup>-</sup>	831	264,000
<b>Ic2</b>	CH <sub>3</sub>		-	Cl <sup>-</sup>	821	291,000
<b>Ic3</b>	CH <sub>3</sub>		-	none	813	264,000
<b>Id1</b>	CH <sub>3</sub>	Cl	-	Cl <sup>-</sup>	813	245,000
<b>Id2</b>	CH <sub>3</sub>	CH <sub>3</sub>	-	Cl <sup>-</sup>	800	247,000
<b>Id3</b>	CH <sub>3</sub>		-	Cl <sup>-</sup>	790	260,000
<b>Id4</b>	C <sub>2</sub> H <sub>5</sub>		-	none	791	306,000
<b>II</b>	C <sub>5</sub> H <sub>11</sub>	-	-	none	800	156,000
<b>III</b>	C <sub>2</sub> H <sub>5</sub>	-	-	Tosylate	817	133,000 [DAT 14]

**Table 7.1.** Compilation of spectral data (absorption maximum λ<sub>max</sub> and molar extinction coefficient ε<sub>max</sub>) of several NIR dyes studied as sensitizer for CtP applications (taken in MeOH), data were taken from [STR 14]

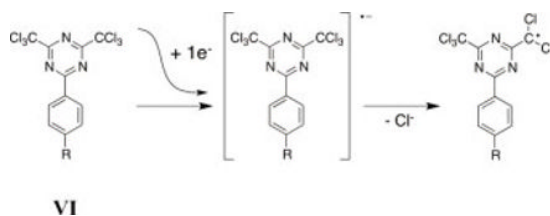


[7.1]



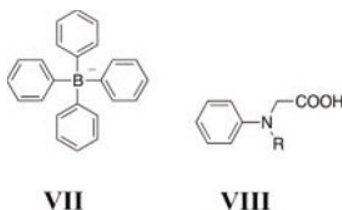
[7.2]

Triazines (VI) are alternative electron acceptor materials [HAU 00a] with comparable electron affinity as compared to iodonium salts (IV). Electron transfer reduces VI while the anion radical formed fast decomposes into the highly reactive halogenated radical derived from VI that efficiently initiates radical polymerization. Structure VI possesses the possibility to initiate polymerization in two positions, which makes them attractive as bivalent radical initiators.

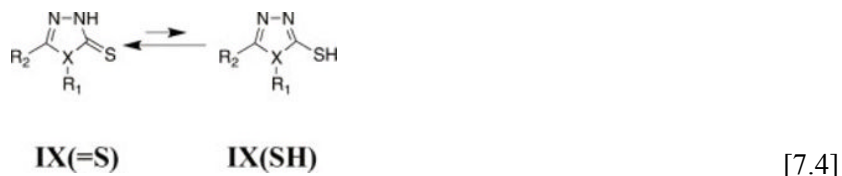


[7.3]

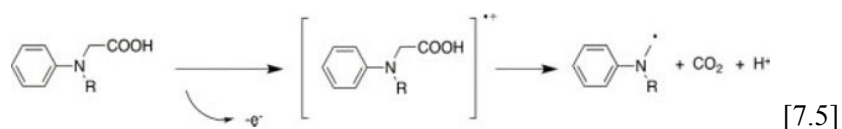
The mechanism shown in Figure 7.2 requires adding of a donor **D** to avoid electron back-transfer from  $A^{\cdot-}$  to  $Sens^{+}$ , which would be applicable in case of positively charged cyanine dyes. Tetraarylborates **VII** [YU 08], (aniline)acetic acids **VIII** [PHO 14] or heterocyclic sulfur compounds **IX** [WIT 04] represent some representative materials with electron donating properties that can be added as donor.



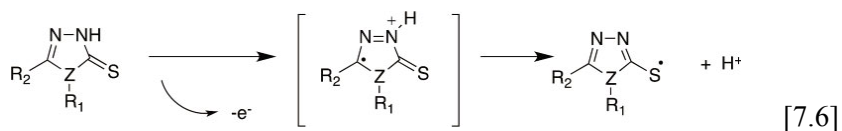
Structure **IX** exists in a tautomeric equilibrium with the mercapto **IX(SH)** and thione **IX(=S)** structure as shown in equation [7.4]. NMR experiments demonstrated a major contribution of the thione (**IX**) in this equilibrium in model coatings [BER 14] proving that particularly the thione responsibly contributes to initiator radical formation. Nevertheless, the thiol tautomer **IX(SH)** possesses some stabilizing functions.



Dye-borate systems were disclosed to initiate radical polymerization [PAC 08, PAC 01, KAB 98] but the sensitivity significantly increases by addition of iodonium borates to a dye-borate system [SIM 09]. This combination avoids ion exchange in systems comprising a cationic polymethine dye and an iodonium ion because both comprise the same counter ion. Ion exchange can lead to undesired events (i.e. crystallization) affecting sensitivity of the lithographic material. Further studies on dye-borate systems discuss the efficiency of electron transfer from the borate to the acceptor excited [SCH 90]. Moreover, oxidation of the (anilino)acetic acid results in fast generation of the aminyl radical and the release of  $\text{CO}_2$  as shown in equation [7.5].



Moreover, the thione should also play a major role in the oxidation mechanism of the heterocycle resulting in generation of thiyl radicals as shown in equation [7.6].



Equation [7.7] shows how the redox potentials of **Sens**, **A** and the excitation energy  $E_{00}$  relate to the free energy of electron transfer  $\Delta G_{el}$ . This quantity is necessary to get a rough estimate regarding the rate constant of electron transfer  $k_{et}$  according to the relation shown in equation [7.8] known as the Marcus-Equation [KAV 86, KAV 93]. It contains as further adjustable parameter, the total reorganization energy combining the inner (vibrational components) and outer sphere (dielectric constant of the surroundings) reorganization energy [KAV 86, KAV 93]. In case  $\Delta G_{el} \approx 0$ , the reorganization energy mainly influences the rate constant of electron transfer.

$$\Delta G_{el} = F \cdot (E^{1/2}_{ox}[\text{Sens}/\text{Sens}^{++}] - E^{1/2}_{red}[\text{A}^{\bullet}/\text{A}]) + E_{coul} - E_{00} \quad [7.7]$$

where  $F$  is the Faraday constant,  $E^{1/2}_{ox}[\text{Sens}/\text{Sens}^{++}]$  represent the half wave oxidation potential of the sensitizer,  $E^{1/2}_{red}[\text{A}^{\bullet}/\text{A}]$  is the half wave reduction potential of the acceptor,  $E_{coul}$  is coulomb energy and  $E_{00}$  is the excitation energy of the sensitizer.

$$k_{et} = 2\pi/\hbar \times |H_{el}|^2 / 4\lambda k_B T \times \exp(-(\Delta G_{el} - \lambda)^2 / 4\lambda k_B T) \quad [7.8]$$

where  $\lambda$  is the total reorganization energy,  $k_B$  is the Boltzmann constant,  $T$  is the temperature and  $H_{el}$  is the interaction energy describing the splitting of the two reaction coordinates of participating reactants.

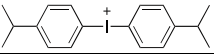
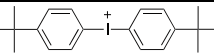
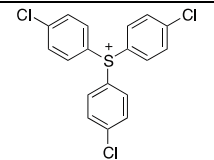
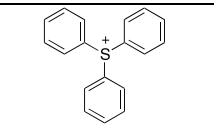
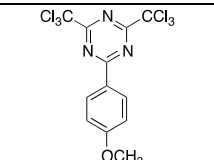
Table 7.2 shows the HOMO and LUMO energies of the dyes **1a-d** determined from the redox potentials ( $E^{1/2}_{ox}[\text{Sens}/\text{Sens}^{++}]$ ) and ( $E^{1/2}_{red}[\text{Sens}^{\bullet}/\text{Sens}]$ ) of the sensitizer [STR 14]. Ferrocene was used as reference electrode [POM 95]. Sensitizers with a barbituric acid substituent in the *meso*-position exhibit the highest HOMO energy. Thus, these materials possess the best capability for oxidation by an acceptor. Other substituents such as -Ph, -SPh, Cl, and -N(Ph)<sub>2</sub> result in slight decrease of the HOMO energy. Furthermore, incorporation of chlorine in R<sub>3</sub> results in a decrease of the HOMO energy while the LUMO energy shows no response on this structural change. No significant change was found by changing the substitution at the terminal polymethine chain from indolium (**1a**, **1b**) to benzindolium (**1c**, **1d**).

Structure	R <sub>1</sub>	R <sub>2</sub>	R <sub>3</sub>	X <sup>-</sup>	HOMO (eV)	$E^{1/2}_{ox}[\text{Sens}/\text{Sens}^+]$ (V)	LUMO (eV)	$E^{1/2}_{red}[\text{Sens}/\text{Sens}^-]$ (V)
<b>Ia1</b>	CH <sub>3</sub>	Cl	H	Cl <sup>-</sup>	-4.91	0.62	-3.89	-0.40
<b>Ia2</b>	C <sub>2</sub> H <sub>5</sub>		Cl	Cl <sup>-</sup>	-4.90	0.61	-3.79	-0.50
<b>Ia3</b>	CH <sub>3</sub>		H	Cl <sup>-</sup>	-4.86	0.57	-3.75	-0.54
<b>Ia4</b>	C <sub>4</sub> H <sub>9</sub>		Cl	ClO <sub>4</sub> <sup>-</sup>	-4.94	0.65	-3.78	-0.51
<b>Ia5</b>	C <sub>4</sub> H <sub>9</sub>		H	ClO <sub>4</sub> <sup>-</sup>	-4.88	0.59	-3.71	-0.58
<b>Ia6</b>	C <sub>2</sub> H <sub>5</sub>		Cl	-	-4.74	0.45	-3.54	-0.75
<b>Ia7</b>	CH <sub>3</sub>		H	-	-4.68	0.39	-3.49	-0.80
<b>Ib1</b>	C <sub>2</sub> H <sub>5</sub>	Cl	Cl	Tos <sup>-</sup>	-5.02	0.73	-3.86	-0.43
<b>Ib2</b>	CH <sub>3</sub>		H	Cl <sup>-</sup>	-4.98	0.69	-3.95	-0.34
<b>Ib3</b>	CH <sub>3</sub>	Cl	H	Cl <sup>-</sup>	-4.97	0.68	-3.84	-0.45
<b>Ib4</b>	CH <sub>3</sub>		Cl	Cl <sup>-</sup>	-4.96	0.67	-3.86	-0.43
<b>Ib5</b>	CH <sub>3</sub>		H	Cl <sup>-</sup>	-4.96	0.67	-3.85	-0.44
<b>Ib6</b>	CH <sub>3</sub>		H	Cl <sup>-</sup>	-4.95	0.66	-3.83	-0.46
<b>Ic1</b>	C <sub>4</sub> H <sub>9</sub>		-	ClO <sub>4</sub> <sup>-</sup>	-4.83	0.54	-3.70	-0.59
<b>Ic2</b>	CH <sub>3</sub>		-	Cl <sup>-</sup>	-4.80	0.51	-3.73	-0.56
<b>Ic3</b>	CH <sub>3</sub>		-	-	-4.64	0.35	-3.51	-0.78
<b>Id1</b>	CH <sub>3</sub>	Cl	-	Cl <sup>-</sup>	-4.94	0.65	-3.81	-0.48
<b>Id2</b>	CH <sub>3</sub>	CH <sub>3</sub>	-	Cl <sup>-</sup>	-4.96	0.57	-3.72	-0.57
<b>Id3</b>	CH <sub>3</sub>		-	Cl <sup>-</sup>	-4.88	0.59	-3.70	-0.61
<b>II</b>	C <sub>5</sub> H <sub>11</sub>	-	-	-	-5.00	0.70	-3.77	-0.53
<b>III</b>	C <sub>2</sub> H <sub>5</sub>	-	-	Tos <sup>-</sup>	-5.07	0.78	-3.94	-0.34

**Table 7.2.** Redox potentials for half wave oxidation  $E^{1/2}_{ox}[\text{Sens}/\text{Sens}^+]$  and half wave reduction  $E^{1/2}_{red}[\text{Sens}^-/\text{Sens}]$  of NIR-sensitizers (taken in CH<sub>3</sub>CN) determined by cyclic voltammetry (taken in CH<sub>3</sub>CN) using a three-electrode setup with platinum disks as working respectively auxiliary electrode and Ag/AgCl electrodes as reference. Ferrocene was used as an internal standard and 0.1 M tetrabutylammonium hexafluorophosphate (Bu<sub>4</sub>N<sup>+</sup>PF<sub>6</sub><sup>-</sup>) as supporting electrolyte. Data taken from [STR 14]

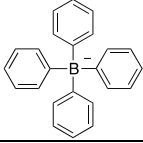
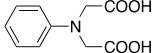
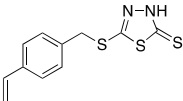
Table 7.3 summarizes some acceptors often used as radical generator in lithographic plates. Triazines (**VI**) exhibit a similar LUMO energy in comparison with iodonium salts (**IV**). Electrochemical data obtained for the iodonium salt agree well with literature data [KUN 97]. Accordingly, both acceptors **IV** and **VI** should exhibit similar sensitivity if the electron transfer rate mainly controls the formation of radicals as shown in equation [7.8]. Nevertheless, our experiments resulted in a higher sensitivity of systems using iodonium salts as radical initiator considering conditions with similar molar ratio of either **IV** or **VI** with respect to Sens.

Furthermore, sensitizers shown in Table 7.2 result in a  $\Delta G_{el} \approx 0$  ( $\pm 0.4$ ) eV using structure **IV** as acceptor. Moreover, sulfonium salts (**V**) were also reported in the patent literature [AOS 99] as acceptors though  $\Delta G_{el} > 0$ . In such cases, the residual energy must be provided by the laser to generate initiating radicals.

Acceptor (A)	structure	LUMO (eV)	$E_{red}^{1/2}[A^*/A]$ (V)
	<b>IVa</b>	-3.72	-0.57
	<b>IVb</b>	-3.66	-0.63
	<b>Va</b>	-3.24	-1.05
	<b>Vb</b>	-3.05	-1.24
	<b>VI</b>	-3.82	-0.47

**Table 7.3.** Half wave reduction  $E_{red}^{1/2}[A^*/A]$  and corresponding LUMO energies of several acceptors determined by cyclic voltammetry (taken in  $CH_3CN$ ) using a three-electrode setup with platinum disks as working respectively auxiliary electrode and  $Ag/AgCl$  electrodes as reference. Ferrocene was used as an internal standard and 0.1 M tetrabutylammonium hexafluorophosphate ( $Bu_4NPF_6$ ) as supporting electrolyte. Data taken from [STR 14]

All cationic sensitizers require the addition of a donor (**D**) selected from Table 7.4 to accomplish a reasonable sensitivity of the lithographic plate. Table 7.4 summarizes some donor components (**VII- IX(SH)a/ IX(=S)b**) mentioned in patent applications that are needed to obtain the desired sensitivity. The mechanism occurs according to Figure 7.2. Electron transfer occurs from the excited singlet state [BAU 15, STR 14] of **Sens\***→**A** resulting in a decrease of the SOMO energy of **Sens<sup>+</sup>** because the semi-filled orbital interacts with the lower-filled orbitals. In case that the SOMO energy is lower as compared to the HOMO of **D**, electron transfer from **D**→**Sens<sup>+</sup>** can occur from a thermodynamic point of view resulting in irreversible formation of additional initiating species by oxidation of **D**→**D<sup>+</sup>** according to Figure 7.2. This reduces the probability of electron back transfer in such singlet systems.

Donor (D)	General structure	HOMO (eV)	$E^{1/2}_{ox}[Sens/Sens^{+}](V)$
	<b>VII</b>	-5.15	0.86
	<b>VIII</b>	-5.48	1.19
	<b>IXa(SH)</b>	-5.27	0.98
	<b>IXb(=S)</b>	-5.06	0.77

**Table 7.4.** Redox potentials for half wave oxidation ( $E^{1/2}_{ox}[Sens/Sens^{+}]$ ) of several donors determined by cyclic voltametry (taken in  $CH_3CN$ ) using a three-electrode setup with platinum disks as working respectively auxiliary electrode and  $Ag/AgCl$  electrodes as reference. Ferrocene was used as an internal standard and 0.1 M tetrabutylammonium hexafluorophosphate ( $Bu_4NPF_6$ ) as supporting electrolyte. Data taken from [STR 14]

Borates (**VII**) function well as donors in systems needing the same counter ion for both the cationic sensitizer and iodonium salt [SIM 09]. This avoids ion exchange between **Sens** and **IV** because both components bear the same counter ion. Initiator systems with different counter ions may

exhibit under certain circumstances ion exchange leading to a decrease of sensitivity. Furthermore, all cationic dyes as shown in Table 7.2 require to add a donor selected from Table 7.4 to obtain the necessary plate sensitivity. At the moment, there exists no universal recipe for which donor or acceptor can be combined with **Sens** to obtain a high sensitivity. All electron donors shown in Table 7.4 have been successfully applied in commercialized CtP systems to obtain the desired high sensitivity [BAU 15, STR 14].

### 7.2.3. Importance of thermal deactivation

Some patent application mention the use of radical generators in lithographic plates resulting in conditions where  $\Delta G_{el} > 0$  in NIR-initiating photopolymer systems. These are, for example, sulfonium salts, which also result in a high sensitivity of the lithographic plate. In general, the NIR sensitizer nonradiatively releases more than 85% of the energy absorbed promoting occurrence of thermal events in the coating. This is concluded from the fluorescence quantum yield of the NIR-dye, which can reach values up to 15% [BRÖ 15b]. The  $S_1$  of the polymethine dye possess a fluorescence decay time depending on structure between 200 and 500 ps [BRÖ 15b]. Therefore, the fluorescence decay is the slowest deactivation event of the  $S_1$  and electron transfer between **Sens\*** and **A** can compete with fluorescence. Nevertheless, high amounts on thermal energy released by internal conversion can thermally lead to formation of initiating radicals. Recent investigations showed thermal decomposition of NIR photoinitiator systems between 110 and 120°C in a model coating comprising the sensitizer selected from Table 7.1 and the radical initiator **IV** [SIM 09]. However, the neat coating was thermally stable up to 190°C [SCH 15]. This means that no initiator component was available in the coating.

The small energy difference between the ground state ( $S_0$ ) and the excited state ( $S_1$ ) of the NIR dye leads to the scenario shown in Figure 7.3 explaining where heat is available to generate thermally initiating radicals ( $k_{ic} \gg k_f$ ). Thus, excitation results in population of a higher vibrational mode of the  $S_1$ . This relaxes fast to the lowest vibrational level of the excited state resulting in the release of heat to the environment. Nevertheless, coupling of the lowest vibrational mode of the  $S_1$  with a higher vibrational mode of the  $S_0$  also results in thermal deactivation, which is internal conversion in this

case. This event releases the major part of heat to the surrounding as competition to electron transfer resulting in formation of initiating radicals. An excellent contribution published in 1976 supports our discussion explaining how electronic coupling affects the rate constant of internal conversion between two different electronic states [CAL 76].

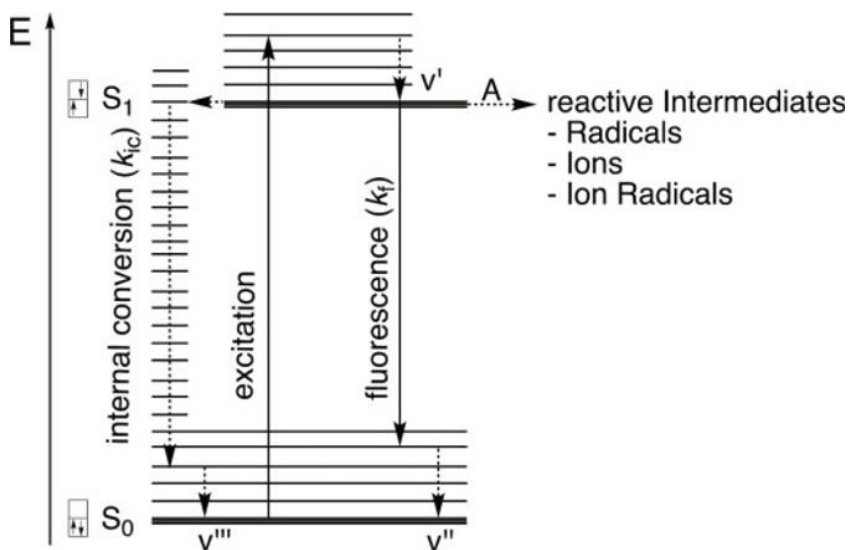


**Figure 7.3.** Explanation for heat release in NIR sensitizers. Excitation from the lowest vibrational level of the  $S_0$  into a higher vibrational level of the of the  $S_1$  results in fast vibrational relaxation ( $v'$ ) into the lowest vibrational level of the same excited state. The lowest vibrational mode of the  $S_1$  couples in NIR sensitizers very efficient with higher vibrational modes of the ground state  $S_0$  resulting in the release of heat. This occurs fast in NIR dyes and additional heat can be generated by internal vibrational relaxation of higher modes of the ground state to the lowest vibrational mode of the  $S_0$  ( $v''$ ,  $v'''$ ). Electron transfer of the  $S_1$  with A and fluorescence occur as competing processes

Thus, the rate constant for internal conversion between two electronic states ( $k_{ic}$ ) depends on the Franck-Condon factors  $\chi_{0j}$  and  $\chi_{1j}$  of the  $S_0$  and  $S_1$ , respectively. Equation [7.9] shows how these quantities relate to  $k_{ic}$ . Further parameters are an electronic coupling term  $C_e$  and a density of state function  $\rho_e$  describing how much vibrational modes of the ground state contribute to the coupling.

$$k_{ic} \propto C_e \cdot \rho_e \times \int \chi_{0j} \chi_{1j} d\xi \quad [7.9]$$

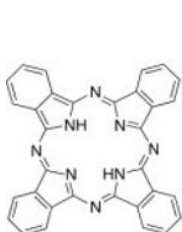
Therefore, such lithographic plates can be considered as dual operating materials because both photonic (electron transfer between **Sens\*** and **A**) and thermal events determine the desired sensitivity. Certain fluorescence would be necessary to obtain circumstances where the electron transfer may compete with the faster internal conversion. The latter releases heat that additionally accelerates chemical reactions during cross-linking. Thus, NIR-photopolymers benefit from both photonic events and thermal processes. Heat release can also contribute to a faster electron transfer and therefore more efficient formation of initiating species particular in case when  $\Delta G_{el}$  becomes slightly positive (equation [7.7]).

#### 7.2.4. Contrast materials and color on demand

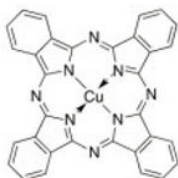
Contrast dyes, sometimes also called colorants, are necessary to give the processed plate a certain color on those parts where the coating remains on the plate. Thus, the operator in the pressroom obtains the impression that plate processing as disclosed in section 7.2.1 was successful. Nevertheless, systems developing on press do not require a colorant but the addition of a color on demand material is desirable for the operator to obtain the impression that imaging was successful either. Colorants used can be embedded in the coating as heterogeneous materials, i.e. either pigments or soluble dyes. The latter mostly belong to triphenylmethane dyes or polymethine dyes absorbing in the visible part.

The phthalocyanines (Pc) **X-XII** have been mostly applied as contrast materials in CtP-plates. The Pc **X** does not contain any heavy metal but is almost insoluble in common organic solvents, and can be therefore considered as a pigment. From this point of view, it requires a similar dispersing procedure to transfer it into the coating solution in comparison with the insoluble copper phthalocyanines **XI** (blue appearance) and **XII** (green appearance). These pigments function additionally as dissolution inhibitors and therefore improve the resistance against aggressive printing chemicals in the press machine. Furthermore, organic pigments were also tested as alternatives in R&D trials but these materials have not been established as colorants in commercialized products yet. Thus, the blue (**X**, **XI**) and green Pc **XII** have been widely accepted in today's printing rooms by the operators. A further benefit using such insoluble materials can

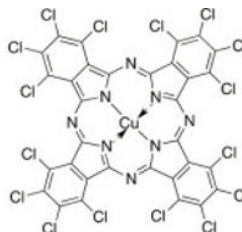
be seen in the fact that those cannot sensitize any photoreaction even under yellow safe light conditions.



X

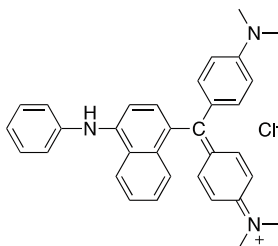


XI



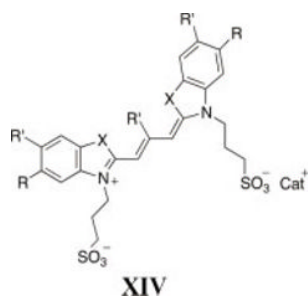
XII

Triphenyl methane dyes have been used for a long time. Victoria Blue (**XIII**) represents one dye used in CtP applications in the past. Sensitization under room light (yellow safe light) conditions might become an issue using soluble dyes because the redox potentials of those colorants allow photoinduced electron transfer to radical initiators **IV** ( $\Delta G < 0$ , equation [7.7]) resulting in the formation of initiating radicals.



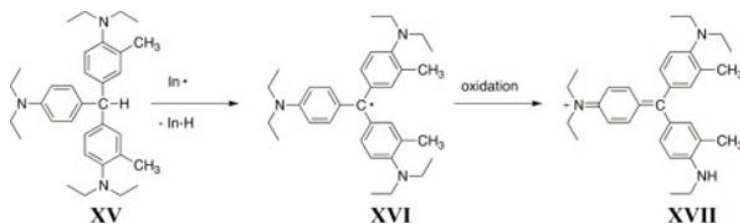
XIII

However, the use of soluble dyes aggregating in the light sensitive coating prevents the undesired event of sensitization by room light. Dye structure **XIV** represents one possibility of a polymethine dye forming H-aggregates in the light sensitive layer [STR 11]. These H-aggregates are not light sensitive and therefore do not sensitize any radical formation by reaction with a radical initiator under yellow safe light conditions. The counter ion in structure **XIV** comprises either an inorganic ion derived either from the first or second main group, a crown ether complex obtained by complexation between these cations using the appropriate ligand or a dye cation which may be an NIR dye as well [STR 11].

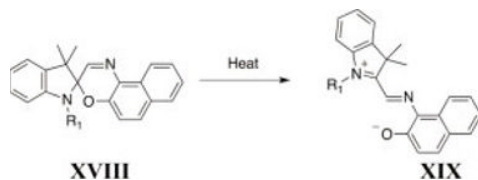


Nevertheless, on-press developable systems do not require a colorant. These materials prefer the addition of a color-on-demand material showing photochromic behavior on those parts where the laser shines on the plate. Patent literature mentions:

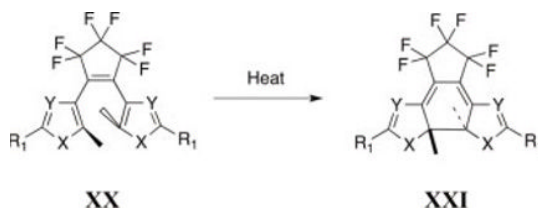
– color formation with leuco dyes [TIM 05];



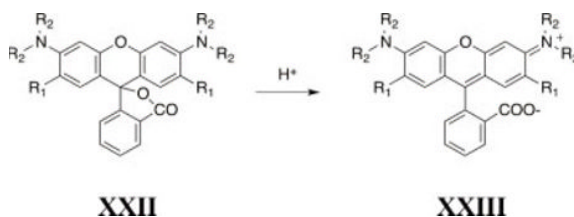
– color formation with photochromic spiro-compounds [KAK 07];



– color formation by isomerization of diarylethenes [FIG 12];



– color formation by ring opening of inner lactones [KAW 05] by protons formed according to the mechanism shown in Figure 7.1.



The addition of these color-on-demand systems may have an impact on the sensitivity if it interferes the initiation mechanism. Particular reactive initiator radicals (In) can easily abstract a hydrogen from leuco-dyes (XV). This results in the formation of a less reactive triaryl methane radical XVI. Oxidation of this intermediate yields the stable deeply colored cationic structure XVII. Thus, the reactivity/sensitivity of the initiator system reduces requiring to find an agreement between plate sensitivity and color formed. XVI can easily oxidize resulting in formation of the intensively blue-colored triaryl methane cation XVII.

Both, the spiro compound XVIII and the diarylethene XX exhibit nearly no color. Exposure with UV light converts XVIII and XX into the deep blue colored materials XIX and XXI [DÜR 03], respectively. This isomerization presumably occurs with the heat provided by the laser. Otherwise, the addition of both these chromophores would not be explainable.

Furthermore, the ring opening of XXII with photolytically generated protons results in the formation deeply colored structures XXIII. Formation of protons occurs to the mechanism disclosed in Figure 7.1 using a radical initiator with a weak nucleophilic anion; that is in most cases an iodonium salt with either PF<sub>6</sub><sup>-</sup> or SbF<sub>6</sub><sup>-</sup> anion. Electron transfer of the excited NIR dye to the iodonium salt results in the formation of aryl radicals as shown in equation [7.1], while the oxidized dye decomposes resulting in the formation of protons. The use of XXII requires to have conditions in the coating that are not acidic to prevent ring opening in the dark. However, nucleophilic reagents such as alkaline materials react with iodonium cations [ZHD 96, STA 96, BAN 66] resulting in a diminished shelf-life.

### 7.2.5. Sensitivity

The amount of energy density (in  $\text{mJ}/\text{cm}^2$ ) needed to build up an image determines the sensitivity. This includes the necessary processing steps (see section 7.2.1) and is in the simplest case a 100% screening exhibiting a fully imaged area. Experimentally, we observe an increase of the plate's optical density ( $OD_{\text{plate}}$ ) with increasing laser energy density after exposure and processing resulting in the curve shown in Figure 7.4. The plate's optical density was polychromatically measured using a SpectroPlate from TechKon in the visible region after exposure and processing in SP500 processing solution. Thus,  $OD_{\text{plate}}$  is a sum of both substrate and coating absorptivity. A blue colorant (XI) was added to obtain a better contrast of  $OD_{\text{plate}}$  changes. Thus, increase of exposure energy density results in an increase of the thickness of the crosslinked layer. This can be measured by the  $OD_{\text{plate}}$  changes because an increase of coating thickness associates with a higher content of embedded colorant dye either.

The energy density necessary to obtain the maximum of the first derivation of  $OD_{\text{plate}}$  with respect to the energy density exposed on the lithographic plate ( $dOD_{\text{plate}}/dE$ ) can be defined as the sensitivity (a) as shown in Figure 7.4. The lower this number the higher the sensitivity of the material because less energy density is necessary to obtain the image. Furthermore, the maximum of  $dOD_{\text{plate}}/dE$  (b) depicts a further interesting point to describe the material; that is  $(dOD_{\text{plate}}/dE)_{\text{max}}$ . The higher this quantity, the more digital works the photopolymer layer because it quickly switches from the non-image to the image area. In this example, we obtained  $31 \text{ mJ}/\text{cm}^2$  and  $27 \times 10^{-3} \text{ cm}^2/\text{mJ}$  for the sensitivity and  $(dOD_{\text{plate}}/dE)_{\text{max}}$ , respectively. The system investigated in Figure 7.4 comprises as initiator system, the NIR-Dye **Id4**, and as radical initiator, the iodonium salt  $[(p\text{-C}_4\text{H}_9\text{PhI})_2]^+[(\text{CF}_3\text{SO}_2)_2\text{N}]^-$ .

We additionally found an influence of the anion of the iodonium salt on the plate sensitivity using the same NIR-sensitizer disclosed in Figure 7.4 for evaluation of sensitivity [BRÖ 15a]. Thus, the same cation was used for all evaluations; that was  $[(p\text{-C}_4\text{H}_9\text{PhI})_2]^+$ . Table 7.5 shows the anion influence on both sensitivity and  $(dOD_{\text{plate}}/dE)_{\text{max}}$ . There is no clear tendency between anion structure and reactive radicals in the coating. Surprisingly, the redox inactive weakly coordinating anions  $[(\text{CF}_3\text{SO}_2)_2\text{N}]^-$  and  $[\text{B}(\text{CN})_4]^-$  result in a

similar sensitivity compared to the redox active  $[\text{BPh}_4]^-$  [BRÖ 15a]. Furthermore, alkyl borates have not been established in the graphic industry yet although they possess better oxidation potentials compared to tetraarylborates [SCH 90]. Radical formation occurs according to Figure 7.1 because both the  $[(\text{CF}_3\text{SO}_2)_2\text{N}]^-$  and  $[\text{B}(\text{CN})_4]^-$  anions are weak electron donors whose HOMO energy is below the HOMO energy of **Sens**.

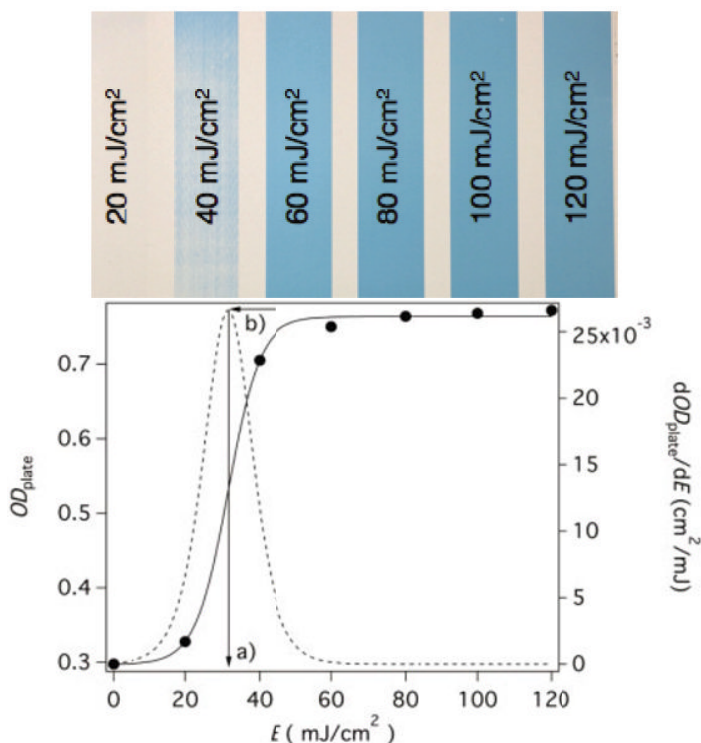


**Figure 7.4.** Optical density of the plate ( $OD_{\text{plate}}$ , full line) of an NIR photopolymer comprising the NIR sensitizer **Id4**, the radical initiator  $[(p\text{-C}_4\text{H}_9\text{PhI})_2]^+ [(\text{CF}_3\text{SO}_2)_2\text{N}]^-$ , a polymeric binder with 0.0015–0.0016 meq/g of COOH-groups, SR399 as monomer, SR 9053 as adhesion promoter, and copper phthalocyanine as colorant. The photopolymer was overcoated with poly(vinyl alcohol) as oxygen barrier. The imaging layer and oxygen barrier layer exhibited a coating weight of 1.2 g/m<sup>2</sup> and 0.6 g/m<sup>2</sup>, respectively. Exposure was carried out using a Kodak Trendssetter 800 as a function of exposure energy density ( $E$ ) resulting in the markers (●) connected through the full line after processing in the Kodak developer SP500.  $OD_{\text{plate}}$  was measured in reflection mode using the SpectroPlate from TechKon. The dashed line exhibits the first derivate of the plate's optical density with respect to the exposure energy density ( $dOD_{\text{plate}}/dE$ ) from where the sensitivity a) and the maximum of the first derivative b) were obtained

X <sup>-</sup>	Sensitivity (mJ/cm <sup>2</sup> )	(dOD <sub>plate</sub> /dE) <sub>max</sub> (10 <sup>-2</sup> cm <sup>2</sup> /mJ)
[BPh <sub>4</sub> ] <sup>-</sup>	31	2.7
[(CF <sub>3</sub> SO <sub>2</sub> ) <sub>2</sub> N] <sup>-</sup>	33	2.6
[BCN <sub>4</sub> ] <sup>-</sup>	33	1.6
[B(PhF <sub>5</sub> ) <sub>4</sub> ] <sup>-</sup>	41	1.3
SbF <sub>6</sub> <sup>-</sup>	42	1.2
PF <sub>6</sub> <sup>-</sup>	49	1.5
CF <sub>3</sub> SO <sub>3</sub> <sup>-</sup>	51	1.4
C <sub>4</sub> F <sub>9</sub> SO <sub>3</sub> <sup>-</sup>	53	1.9
Ph <sub>2</sub> (OH)COO <sup>-</sup>	55	2.1
[p-CH <sub>2</sub> =CH-Ph-SO <sub>3</sub> ] <sup>-</sup>	70	2.0
NO <sub>3</sub> <sup>-</sup>	75	1.7
[CN-N-CN] <sup>-</sup>	80	1.3
[p-C <sub>12</sub> H <sub>25</sub> -Ph-SO <sub>3</sub> ] <sup>-</sup>	86	1.6
CH <sub>3</sub> -CH(OH)-COO <sup>-</sup>	104	1.6

**Table 7.5.** Change of sensitivity and maximum of (dOD<sub>plate</sub>/dE)<sub>max</sub> of a NIR photopolymer comprising the NIR sensitizer Id4, the radical initiator [(p-C<sub>4</sub>H<sub>9</sub>Ph)<sub>2</sub>]<sup>+</sup> with different anions X<sup>-</sup>, a polymeric binder with 0.0015-0.0016 meq/g of COOH-groups, SR399 as monomer, SR 9053 as adhesion promoter, and copper phthalocyanine as colorant. The photopolymer was overcoated with poly(vinyl alcohol) as oxygen barrier. The imaging layer and oxygen barrier layer exhibited a coating weight of 1.2 g/m<sup>2</sup> and 0.6 g/m<sup>2</sup>, respectively. Exposure was carried out using a Kodak Trendsetter 800 as a function of exposure energy density (E) and processed in the Kodak developer SP500

Many NIR dyes and radical initiators compiled in the Tables 7.2–7.4 were evaluated regarding plate sensitivity. Most of them exhibit a similar characteristic curve as shown in Figure 7.4 covering one energy range. For sake of simplicity, we avoided to compiling this data. Small changes of polymer and monomer structure, change of contrast material, overcoat, and different processing solutions (developer) may have a deep impact on the sensitivity of the NIR photoinitiator system embedded in the photopolymer layer.

Furthermore, aggregation of the NIR-sensitizer must be avoided because it can contribute to a decrease of initiator radical formation resulting in a decrease of sensitivity. H-aggregation of the sensitizer would

hypsochromically shift the absorption while formation of *J*-aggregates results in bathochromic shift of the sensitizer absorption [KAS 65, KAS 63, MCR 58]. This decreases the absorption of the monomeric NIR-dye being unavailable for laser excitation at either 808 or 830 nm.

### **7.3. Laser-drying and offset-printing**

#### **7.3.1. Principle of laser-drying**

NIR-dyes can be additionally used in offset printing inks where they accelerate physical drying [ERN 13, PIT 03]. A common printing ink comprises the ink stuff (pigments) and the solvents (mostly mineral oils). An emulsion spontaneously forms in the press machine consisting of water and the ink. During the press procedure, all liquid quickly goes into the printed substrate – the paper. This contains the ink solvent in the image part and water in the non-image part. Long storage has been often necessary before such printed stuff further processed (cut, folding, shipping, etc). Therefore, shortening of the drying time can be considered as a huge demand to reduce the time between printing and delivery to the customer. Big energy consuming heaters have often been applied for drying. This drying technique is not an economical procedure because only a small energy fraction would be used for the drying process while most of the inserted energy blows unused into the surrounding space. This can be accelerated and improved by an NIR semiconductor laser emitting at 980 nm in combination with NIR-absorber dye [ERN 13, PIT 03, SCH 08, SCH 12, ERN 07]. The hardware used (Figure 7.5) focuses the laser light on the substrate in a short time frame resulting in a temperature increase of several 100°C degree with no damage of the printed paper. The dye absorbing at 980 nm absorbs nearly all the NIR light emitted resulting in a significantly better drying efficiency because nearly all emitted light by the laser would be quantitatively absorbed and converted to thermal energy by thermal/nonradiative deactivation, as shown in Figure 7.3. Nearly no fluorescence or other competitive pathways occur in comparison to thermal deactivation. The dye transfers the heat generated by this deactivation process to the surrounding. This leads to selective and fast drying of the printed substrate resulting in a significant shortening of the drying time. This physical drying technique – the laser drying of offset printing inks – was developed industry and strongly financially

supported by the German Federal Ministry of Education and Research [ERN 13].

Figure 7.5(a) shows the schematic drawing of offset printing integrating a radiation source – the semiconductor laser – (10) for drying [PIT 03]. Number 14 stands for the printed substrate running through the press machine on which radiation (12) shines on 14. The numbers 110 and 112 represent the press cylinders. Integration of many radiation sources with a combined optics opens the possibility to expose continuously a large area with an array. Figure 7.5(b) shows the radiation generation of this array, which is composed of many emitter chips (Figure 7.5(c)). Furthermore, this technique can be used to generate a line that continuously shines on the printed substrate resulting in physical drying as shown in Figure 7.5(d). Figure 7.5(e) depicts a complete setup of laser-drying in a press machine. Nevertheless, there also exist other alternatives to generate a continuous laser line with an almost homogeneous intensity profile over a length greater than 50 cm on a line width of a few millimeters [MEI 09, FOR 08, WOO 06].

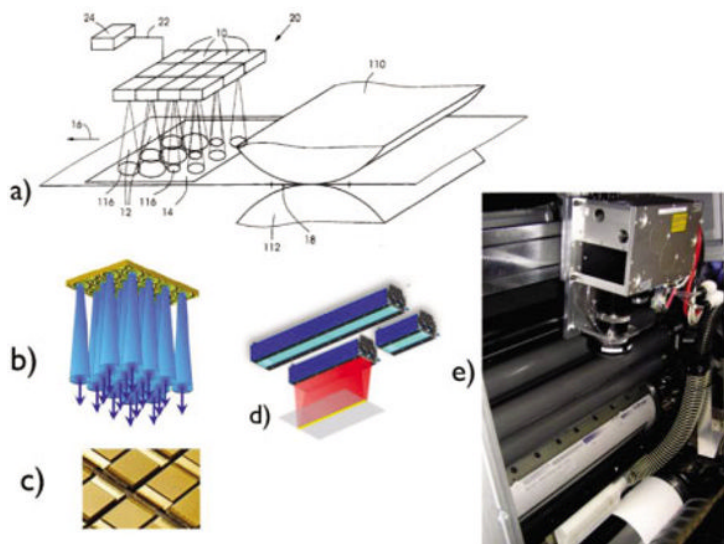
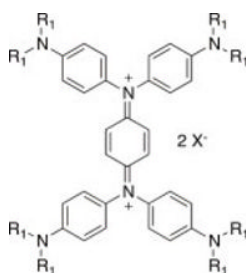


**Figure 7.5.** Schematic sketch of the printing process integrating a light source a). Furthermore, the inset shows the generation of the laser light b) by the diode laser chips c). Integration of many diode laser chips and optical components results in a line shape laser continuously emitting a homogeneous laser line d) shining on the printed substrate in a press machine e) (source: a) [PIT 03], b)–d): Philips Photonics, [www.philips.com/photronics](http://www.philips.com/photronics), e) [HTT 14])

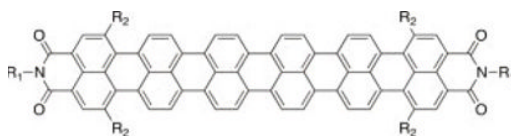
### 7.3.2. Chemical systems

The NIR-absorber dye plays the major role in offset printing inks working together with a semiconductor laser. The use of dyes absorbing at around 1,000 nm opens the possibility to use dyes exhibiting a yellow color which does not strongly interfere the appearance of colorants added either. Nevertheless, the ionic dye must dissolve in the nonpolar ink, which is a huge challenge. Chromophore **XXIV** depicts two structural features where changes affect solubility. This is the anion ( $X^-$ ) and the substituent  $R_1$  at the cationic dye skeleton [SCH 12].



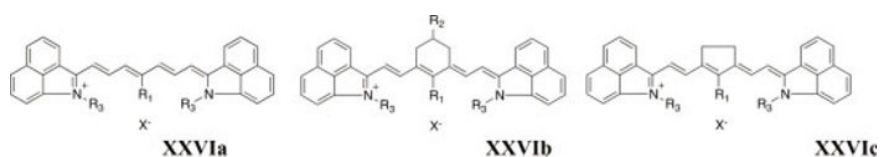
**XXIV**

Rylenes **XXV** represent a further interesting class of NIR-dyes [YUA 13, SCH 08]. The substituents  $R_1$  and  $R_2$  influence the solubility of these neutral compounds. Nevertheless, these chromophores sensitively change their absorption spectra upon change of the surrounding, which was discussed as a result of H-aggregation [YUA 13].



**XXV**

Polymethine dyes exhibiting the general structures **XXVIa-c** were extensively studied as NIR-absorber dyes [ERN 07]. They possess a reasonable absorption at 980 nm and the solubility varies by change of the substituents at the dye cation and the nature of the anion. Anions derived from sulfonic acids, i.e.  $C_{12}H_{25}-Ph-SO_3^-$ , have brought the best success in these studies [ERN 13, ERN 07]. Table 7.6 summarizes some spectral data of the dyes **XXIV-XXVI**.



Structure	R <sub>1</sub>	R <sub>2</sub>	R <sub>3</sub>	X <sup>-</sup>	λ <sub>max</sub> (nm)	ε <sub>max</sub> (M <sup>-1</sup> cm <sup>-1</sup> )	Solvent	Source
<b>XXIV</b>	C <sub>4</sub> H <sub>9</sub>			SbF <sub>6</sub> <sup>-</sup>	1065	100,000	CH <sub>3</sub> CN	[WWW 14]
<b>XXV</b>	CH- (C <sub>11</sub> H <sub>23</sub> ) <sub>2</sub>	-(CH <sub>2</sub> ) <sub>2</sub> - C(CH <sub>3</sub> ) <sub>3</sub>			908	256,000	THF	[YUA 13]
<b>XXVIa</b>	H		C <sub>4</sub> H <sub>9</sub>	[(CF <sub>3</sub> SO <sub>2</sub> ) <sub>2</sub> N] <sup>-</sup>	994	320,000	CH <sub>2</sub> Cl <sub>2</sub>	[WWW 14]
<b>XXVIb1</b>	Ph	H	C <sub>4</sub> H <sub>9</sub>	BF <sub>4</sub> <sup>-</sup>	997	230,000	MeOH	[WWW 14]
<b>XXVIb2</b>	Ph	H	C <sub>4</sub> H <sub>9</sub>	C <sub>12</sub> H <sub>25</sub> SO <sub>3</sub> <sup>-</sup>	1012	220,000	CHCl <sub>3</sub>	[ERN 07]
<b>XXVIb3</b>	Ph	H	C <sub>4</sub> H <sub>9</sub>	C <sub>12</sub> H <sub>25</sub> -Ph-SO <sub>3</sub> <sup>-</sup>	1012	275,000	CHCl <sub>3</sub>	[ERN 07]
<b>XXVIb4</b>	Ph	H	C <sub>12</sub> H <sub>25</sub>	C <sub>12</sub> H <sub>25</sub> SO <sub>3</sub> <sup>-</sup>	1013	264,000	CHCl <sub>3</sub>	[ERN 07]
<b>XXVIb5</b>	Ph	H	C <sub>12</sub> H <sub>25</sub>	C <sub>12</sub> H <sub>25</sub> -Ph-SO <sub>3</sub> <sup>-</sup>	1013	262,000	CHCl <sub>3</sub>	[ERN 07]
<b>XXVIb6</b>	Ph	<i>t</i> -C <sub>4</sub> H <sub>9</sub>	C <sub>4</sub> H <sub>9</sub>	C <sub>12</sub> H <sub>25</sub> -Ph-SO <sub>3</sub> <sup>-</sup>	1011	271,000	CHCl <sub>3</sub>	[ERN 07]
<b>XXVIb7</b>	Cl	H	C <sub>4</sub> H <sub>9</sub>	BF <sub>4</sub> <sup>-</sup>	1014	180,000	MeOH	[WWW 14]
<b>XXVIc1</b>	N(Ph) <sub>2</sub>		C <sub>4</sub> H <sub>9</sub>	BF <sub>4</sub> <sup>-</sup>	996	180,000	MeOH	[WWW 14]
<b>XXVIc2</b>	N(Ph) <sub>2</sub>		C <sub>4</sub> H <sub>9</sub>	C <sub>12</sub> H <sub>25</sub> SO <sub>3</sub> <sup>-</sup>	996	189,000	MeOH	[ERN 07]
<b>XXVIc3</b>	N(Ph) <sub>2</sub>		C <sub>4</sub> H <sub>9</sub>	C <sub>12</sub> H <sub>25</sub> -Ph-SO <sub>3</sub> <sup>-</sup>	996	183,000	MeOH	[ERN 07]
<b>XXVIc4</b>	Ph		C <sub>4</sub> H <sub>9</sub>	BF <sub>4</sub> <sup>-</sup>	1024	240,000	MeOH	[WWW 14]

**Table 7.6.** Summary of spectral data of some selected NIR-absorber dyes applied for laser drying with diode lasers emitting at 980 nm

## 7.4. Conclusions and outlook

Our contribution discusses both thermal and photonic events contributing to the formation of initiator radicals in NIR photopolymer materials with a focus on CtP technology. This often requires multiple processing steps (preheat, prewash, post-rinse and gumming) after exposure to obtain the printing image. Nowadays, research focuses on the development of lithographic plates working either “processless”, i.e. without the need of any processing hardware (on-press development), or with only one processing step that washes out the image in just one bath. These plates are called “green” materials because their use saves valuable resources. This meets the requirements of the European Community requiring the introduction of environmentally friendly and energy-saving processes. In the coming years, this would be mandatory.

Future lithographic plates require the development of special binders and monomers operating well under either processless or simple processing conditions. This requires the use of initiator components comprising sensitizer and coinitiators (radical initiator) compatible with the entire plate chemistry of the chemistry. Therefore, the sensitizing dye should exhibit a low aggregation tendency to accomplish a high sensitivity in the coating. In other words, a good solubility of both the sensitizer and coinitiator results in a high sensitivity of the coating as long as the free energy of electron transfer between **Sens\*** and the coinitiator is  $\lesssim 0$ . This addresses challenges the chemists who design plate components face because they must introduce both solubility promoting groups/moieties and appropriate unsaturated functions enhancing the electron transfer between **Sens\*** and the coinitiator. Furthermore, an improvement of white light stability on press would be a further demand on future plates operating in the NIR without loss of press performance. This gives the operator in the pressroom more confidence because such materials exhibit a better tolerance by maintaining all benefits. Such white light stable systems possess a certain threshold, which can be chemically adjusted as well.

The laser drying of offset printing plates has received some attention in printing market. This new drying technique was already successfully tested in the market. There exist enough possibilities to expand this technique particular for chemical drying. Furthermore, the extensive R&D work in the

graphic industry may also give new impetus in the coating industry wherever it will bring advantages compared to the traditional UV technology using mercury lamps for excitation [BRÖ 12]. Thus, larger depth curing profiles, embedding of UV-protecting additives or yellow pigments would be some substantial benefits for NIR-initiated photopolymerization. Combining this technology with semiconductor light sources such as LEDs or semiconductor lasers will presumably address this kind of photopolymerization to a broader diversity of the coating industry.

## 7.5. Acknowledgments

The authors would like to acknowledge Dr. H. Baumann Kodak Graphic Communications GmbH for their experimental support of this work. Furthermore we thank Dr. M. Schlörholz from Heidelberger Druckmaschinen AG for fruitful discussions regarding the laser drying.

## 7.6. Bibliography

- [AGF 14] AGFA (<http://www.agfagraphics.com>). More technical Parameters are available on these internet sources, 30 September 2014.
- [AND 01] ANDRZEJEWSKA E., “Photopolymerization kinetics of multifunctional monomers”, *Progress in Polymer Science*, vol. 26, p. 605, 2001.
- [AOS 99] AOSHIMA K., Negative-type image recording material and precursor for negative-type lithographic printing plate, EP 1096315 B1, 1999.
- [BAN 66] BANKS D.F., “Organic polyvalent iodine compounds”, *Chemical Reviews*, vol. 66, pp. 243–266, 1966.
- [BAU 15] BAUMANN H., “Lithographische Druckplatten für Laserbelichtung”, *Chemie in unserer Zeit*, no. 49, pp. 14–29, 2015.
- [BAU 93] BAUMANN H., HERTING H.P., TIMPE H.-J., “Modern plates for offset printing”, *Journal of Information Recording Materials*, vol. 20, pp. 301–323, 1993.
- [BAU 94] BAUMANN H., TIMPE H.-J., “Chemical aspects of offset printing”, *J. Prakt. Chem*, vol. 336, pp. 377–389, 1994.
- [BER 14] BERDZINSKI S., STREHMEL N., LINDAUER H. *et al.*, “Photoinitiated polymerization by hexarylbisimidazoles and heterocyclic mercapto compounds: revised mechanistic aspects”, *Photochemical and Photobiological Sciences*, vol. 13, pp. 789–798, 2014.

- [BRÖ 12] BRÖMME T., MOEBIUS J., SCHÄFER S. *et al.*, “Photocuring in a different light crosslinking can be achieved by near infrared (NIR) radiation”, *European Coatings Journal*, vol. 9, pp. 20–27, 2012.
- [BRÖ 15a] BRÖMME T., BAUMANN H., STREHMEL B., “Influence of Different Iodonium Ions on the Sensitivity of CtP NIR-Photopolymers”, *Photochemical and Photobiological Sciences*, in preparation, 2015.
- [BRÖ 15b] BRÖMME T., GRABOLLE M., RESCH-GENGER U. *et al.*, “Fluorescence of polymethine dyes”, *Photochemical & Photobiological Sciences*, in preparation, 2015.
- [BRÖ 15c] BRÖMME T., STREHMEL N., STREHMEL B., “Photochemistry of Polymethine Dyes in NIR-Photopolymers”, *Photochemical and Photobiological Sciences*, 2015.
- [CAL 76] CALZAFERRI G., GUGGER H., LEUTWYLER S., “Einfluss intramolekularer Bewegungen auf die Fluoreszenzquantenausbeute”, *Helvetica Chimica Acta*, vol. 58, pp. 1969–1987, 1976.
- [CRI 84] CRIVELLO J.V., “Cationic polymerization – iodonium and sulfonium salt photoinitiators”, *Advances in Polymer Sciences*, vol. 62, pp. 1–48, 1984; CRIVELLO J.V., “Photoinitiated cationic polymerization”, *The Annual Review of Materials Research*, vol. 13, pp. 173–190, 1983.
- [DAT 14] Data were taken in CH<sub>3</sub>CN. More details can be found at: <http://www.karenz.jp/en/shikiso/nir/>, 30 September 2014.
- [DÜR 03] DÜRR H., BOUS-LAURENT H., *Photochromism: Molecules and Systems*, Elsevier, 2003.
- [ERN 07] ERNST S., PEITER G.D., PITZ H. *et al.*, Verfahren zum Behandeln eines mit Druckfarbe bedruckten Bedruckstoff, DE 10 2008 013312 A1, 2007.
- [ERN 13] ERNST U., Final report of the BMBF project “Trock-o-dil”, FKZ 13N10011, available at: <http://www.ot-mabrilas.de/wp-content/uploads/2013/06/Abschlussbericht-Trockodil.pdf>.
- [FIG 12] FIGOV M., WANG R., MAROM M. *et al.*, Developer and method of coloring lithographic printing members, US 2012/0045720 A1, 2012.
- [FOR 08] FORBES A., BAYER A., MEINSCHIEN J. *et al.*, “Beam shaping of line generators based on high power diode lasers to achieve high intensity and uniformity levels”, *Proceedings of SPIE*, vol. 7062, 70620X-1-7, 2008.
- [FRA 83] FRAB W., “Reproduction techniques with radiation-sensitive systems”, *Chemie in unserer Zeit*, vol. 17, pp. 10–20 (part 1) and 33–40 (part 2), 1983.
- [FUJ 14] FUJI (<http://graphics.fujifilm.co.uk/products/plates>), 30 September 2014.

- [HAT 00] HATANO T., FUKUI K., KARATSU T. *et al.*, “Sensitization mechanisms of photopolymer coating layer using infrared dye”, *Journal of Photopolymer Science and Technology*, vol. 13, pp. 697–701, 2000.
- [HAU 00a] HAUCK G., SAVARIAR-HAUCK C., TIMPE H.-J., IR-Empfindliche Zusammensetzung und deren Verwendung zur Herstellung von Druckplatten, DE 19906823 A1, 2000.
- [HAU 00b] HAUCK G., SAVARIAR-HAUCK C., TIMPE H.-J. *et al.*, IR-sensitive composition for the preparation of printing plate precursors (Kodak Polychrome Graphics GmbH), Patent, WO 00/48836, 2000.
- [HTT 14] <http://www.photonics.philips.com>, 30 September 2014.
- [KAB 98] KABATC J., PIETRZAK M., PĄCZKOWSKI J., “Cyanine borates revisited. Application of the Marcus equation for the description of the kinetics of photoinitiated free radical polymerization”, *Macromolecules*, vol. 31, pp. 4651–4654, 1998.
- [KAB 99] KABATC J., KUCYBALA Z., PIETRZAK M. *et al.*, “Free radical polymerization initiated via photoinduced intermolecular electron transfer process: kinetic study”, *Polymer*, vol. 40, p. 735, 1999.
- [KAK 07] KAKINO R., KUNITA K., OOHASHI H. *et al.*, Lithographic plate precursor and lithographic printing method, Patent, US 2007/0082291, 2007.
- [KAR 05] KARATSU T., YANAI M., YAGAI S. *et al.*, “Evaluation of sensitizing ability of barbiturate-functionalized non-ionic cyanine dyes; application for photoinduced radical generation system initiated by near IR light”, *Journal of Photochemistry and Photobiology A*, vol. 170, pp. 123–129, 2005.
- [KAS 63] KASHA M., “Energy transfer mechanisms and the molecular exciton model for molecular aggregates”, *Radiation Research*, vol. 20, pp. 55–71, 1963.
- [KAS 65] KASHA M., RAWLS H.R., ASHRAF EL-BAYOUMI M., “The exciton model in molecular spectroscopy”, *Pure and Applied Chemistry*, vol. 11, pp. 371–392, 1965.
- [KAV 86] KAVARNOS G.J., TURRO N.J., “Photosensitization by reversible electron transfer: theories, experimental evidence, and examples”, *Chemical Reviews*, vol. 86, pp. 401–449, 1986.
- [KAV 93] KAVARNOS G.E., *Fundamentals of Photoinduced Electron Transfer*, VCH Publishers, Weinheim, 1993.
- [KAW 05] KAWUCHI I., Planographic printing plate precursor, Patent EP 1627735 A2, 2005.
- [KIP 00] KIPPHAN H., *Handbuch der Printmedien*, Springer, 2000.

- [KOD 14] Photopolymer printing plates are available from three big suppliers: Kodak (<http://graphics.kodak.com>), 30 September 2014.
- [KUN 97] KUNZE A., MÜLLER U., TITTES K. *et al.*, “Triplet quenching by onium salts in polar and nonpolar solvents”, *Journal of Photochemistry and Photobiology*, vol. A 110, pp. 115–122, 1997.
- [LIM 96] LIMBURG M., *Der digitale Gutenberg*, Springer, 1996.
- [MCR 58] MCRAE E.G., KASHA M., “Enhancement of phosphorescence ability upon aggregation of dye molecules”, *Journal of Chemical Physics*, vol. 28 pp. 721–722, 1958.
- [MEI 09] MEINSCHEN J., BAYER A., BRUNS P. *et al.*, “Improvements of high power diode laser line generators open up new application fields”, *Proceedings of SPIE*, vol. 7198, 71980N-1-9, 2009.
- [MOU 00] MOULIN M., Imaging device and method for eliminating edge effects in spatial modulators WO 2000054096, 2000.
- [MOU 13] MOULIN M., Electro-optic spatial modulator for high energy density, US 2004023198, 2004; [http://graphics.kodak.com/US/en/Product/computer\\_to\\_plate/SQUARESPOT\\_Technology/default.htm](http://graphics.kodak.com/US/en/Product/computer_to_plate/SQUARESPOT_Technology/default.htm), 30 September 2013.
- [MUN 09] MUNNELLY H.M., WANG R., STEGMAN D.A. *et al.*, On-press developable elements for lithographic printing plates and methods of use, US 20090269699 A1, 2009.
- [MUN 10] MUNNELLY H.M., WANG R., On-press developable imageable elements, WO 2010033182 A1, 2010.
- [MUS 00] MUSTROPH H., “Dyes: general survey”, *Ullmann's Encyclopedia of Industrial Chemistry*, Wiley-VCH Verlag GmbH & Co. KGaA, pp. 1–38, 2000.
- [NAG 89] NAGASAKA H., OHTA K., Photopolymerizable composition, EP397200 (Mitsubishi Kasei Corporation), 1989.
- [OGLE 51] OGLE K.N., “On the resolving power of the human eye”, *Journal of Optical Society of America*, vol. 41, pp. 517–520, 1951.
- [PAC 01] PAČKOWSKI J., NECKERS D.C., “Photoinduced electron transfer initiating systems for free-radical polymerization”, *Electron Transfer in Chemistry*, BALZANI V. (ed.), chapter 4, Wiley-VCH, pp. 516–585, 2001.
- [PAČ 08] PAČKOWSKI J., KABATC J., JĘDRZEJEWSKA B., “Polymethine dyes as fluorescent probes and visible light photoinitiators for free radical polymerization”, *Topics in Heterocyclic Chemistry*, vol. 14, *Heterocyclic Polymethine Dyes*, Springer, pp. 183–220, 2008.

- [PIT 03] PITZ H., Vorrichtung und Verfahren zur Zuführung von Strahlungsenergie auf einen Bedruckstoff in einer Flachdruckmaschine, EP 1302735 A2, Heidelberger Druckmaschinen AG, 2003.
- [POM 95] POMMEREHNE J., VESTWEBER H., GUSS W. *et al.*, “Efficient two layer leds on a polymer blend basis”, *Advanced Materials*, vol. 7, pp. 551–554, 1995.
- [SAV 12] SAVARIAR-HAUCK C., HAUCK G., On press developable lithographic printing plate precursors, US 2012/0094233, 2012.
- [SCH 07] SCHLÖRHOLZ M., Immonium-Absorber für Druckfarben und Lacke, DE 10 2012 017 010 A1, Heidelberger Druckmaschinen AG, 2012; ERNST S., PEITER G.D., PITZ H. *et al.*, Verfahren zum Behandeln eines mit Druckfarbe bedruckten Bedruckstoff, DE 10 2008 013312 A1, 2007.
- [SCH 08] SCHLÖRHOLZ M., KEIL D., PITZ H., Verfahren zum Trocknen von Druckfarbe auf einem Bedruckstoff (Rylene), DE 10 2008 028 533 A1, Heidelberger Druckmaschinen AG, 2008.
- [SCH 15] SCHMITZ C., HALBHUBER A., STREHMEL B., “Mechanistic aspects of photoinitiated radical polymerization in the near infrared applying LED und laser exposure”, *Macromolecules*, inpress, 2015.
- [SCH 90] SCHUSTER G.B., “Photochemistry of organoborates: intra-ion pair electron transfer to cyanines”, *Pure & Applied Chemistry*, vol. 62, pp. 1565–1572, 1990.
- [SIM 09] SIMPSON C., BAUMANN H., STREHMEL B., Negative working thermally sensitive compositions for production of lithographic plates, WO 2009109579 A1, 2009.
- [STA 96] STANG P.J., ZHDANKIN V.V., “Organic polyvalent iodine compounds”, *Chemical Reviews*, vol. 96, pp. 1123–1178, 1996.
- [STR 03] STREHMEL V., “Epoxyes: structures, photoinduced crosslinking, network properties, and applications”, *Handbook of Photochemistry and Photobiology*, in NALWA H.S. (ed.), American Scientific Publishers, vol. 2, pp. 1–110, 2003.
- [STR 09] STREHMEL B., Neue Materialien und Wirkprinzipien für Mikrostrukturierung durch Druckprozesse, final report of grant number FKZ 03X4502, German National Library of Science and Technology, Hannover, 2009.
- [STR 11] STREHMEL B., BAUMANN H., LUMMEL D., Negative-working imageable element, US 8034538 B2, 2011.
- [STR 14] STREHMEL B., ERNST S., REINER K. *et al.*, “Application of NIR-photopolymers in the graphic industry: from physical chemistry to lithographic applications”, *Zeitschrift für Physikalische Chemie*, vol. 228, pp. 129–153, 2014.

- [TIM 01] TIMPE H.-J., "IR sensitive layers for manufacturing of offset printing plates" *Materialwissenschaft und Werkstofftechnik*, vol. 32, pp. 785–788, 2001.
- [TIM 05] TIMPE H.-J., VON GYLDEFELD F., On press developable sensitive printing plates, US 6846614 B2, 2005.
- [TIM 87] TIMPE H.-J., BAUMANN H., "Photopolymere. Prinzipien und Anwendung", Deutscher Verlag für Grundstoffindustrie, Leipzig, 1987.
- [TIM 88] TIMPE H.-J., BAUMANN H., RAUTSCHEK H. *et al.*, "Photopolymers for printing plates", *Chem. Tech-Leipzig*, vol. 40, pp. 327–333, 1988.
- [VOL 80] VOLLMANN H.W., "New Technologies for the Filmless Manufacture of Printing Forms", *Angewandte Chemie International Edition*, vol. 92, pp. 95–106, 1980; *Angewandte Chemie International Edition*, vol. 45, pp. 99–110, 1980.
- [WEG 74] WEGNER U., Printing on polymeric printing plates using laser irradiation, DE 2302398 A1, 1974.
- [WIT 04] WITTIG T., TIMPE H.-J., KLIE A., Stabilized infrared-sensitive elements (Kodak Polychrome Graphics GmbH), WO 2004/022337 A1, 2004.
- [WOO 06] WOOD G.L., HOMBURG O., HAUSCHILD D. *et al.*, "Efficient beam shaping for high-power laser applications", *Proceedings of SPIE*, vol. 6219, 621608-1-8, 2006.
- [WWW 14] A huge compilation of absorption maxima can be found at [www.few.de](http://www.few.de), 30 September 2014.
- [YAM 05] YAMASAKI S., MAKINO N., INNO T., Lithographic printing plate precursor for direct imaging from a digital data and developing in a printing machine without passing through a development step, US 20050048398 A1, 2005.
- [YAN 11] YANG Y., JEONG Y.S., HU L. *et al.*, "Transparent lithium-ion batteries", *Proceedings of the National Academy of Sciences USA*, vol. 108, pp. 13013–13018, 2011.
- [YU 08] YU J., RAY K.B., SARAIYA S. *et al.*, Negative-working radiation sensitive compositions and imageable elements (Eastman Kodak Company), US7452638, 2008.
- [YUA 13] YUAN Z., LEE S.-L., CHEN L. *et al.*, "Processable rylene diimide dyes up to 4 nm in length: synthesis and STM visualization", *Chemistry – A European Journal*, vol. 19, pp. 11842–11846, 2013.
- [ZHD 96] ZHDANKIN V.V., STANG P.J., "Chemistry of polyvalent iodine", *Chemical Reviews*, vol. 108, pp. 5299–5358, 2008.



---

## Dyes and Photopolymers

---

Photosensitized photopolymer materials have received much attention for their use as fabrication or recording media [CUR 10, FOU 12, CAP 88, COU 88, GLE 08a] for applications such as holography [MAH 06, MAH 08], data storage [LIN 00, HSU 03], solar concentrators [CAS 10], hybrid optoelectronics [SUL 07, YE 08] and in self-trapping studies [TOL 11]. Their versatility, ease of use and self-processing ability give them many advantages over more traditional latent materials such as silver halide and dichromated gelatin (DCG) [MAN 94, LAW 01a].

### 8.1. Photopolymer

While the discussion of dyes is central in this chapter, we will begin with a brief review of some recent achievements made regarding the study of photopolymer materials.

Sheridan and Lawrence [SHE 00] introduced a non-local material response function into the photopolymerization-driven diffusion (PDD) model [ZHA 94], and referred to the resulting model as the non-local photopolymerization-driven diffusion (NPDD) model. The proposition was that during the photopolymerization process, the material response at point  $x$  and at time  $t$  depends on what happened at a point  $x'$  and time  $t'$ . In other words, during holographic exposure in a free radical polymer system, the

---

Chapter written by Yue QI and John T. SHERIDAN.

active tips of the polymer chains propagate by using locally available monomers and thus grow away from the starting point of initiation. It was originally assumed that the non-local temporal effects took place rapidly, on a short time scale, i.e. polymer chain growth was considered to be fast compared to other temporal effects present, such as monomer diffusion, diffusion constant  $D$ . Thus, the material response was assumed to include an instantaneous non-local time response. A one-dimensional (1D) diffusion equation governing the rate of monomer concentration,  $M$ , was then derived by:

$$\frac{\partial [M(x,t)]}{\partial t} = \frac{\partial}{\partial x} \left[ D(x,t) \frac{\partial [M(x,t)]}{\partial x} \right] - \int_{-\infty}^{+\infty} R(x,x') F(x',t') [M(x',t')] dx' \quad [8.1]$$

where  $F(x',t')$  describes the rate of polymerization (conversion) and  $R(x,x')$  is the non-local spatial response function, which is given by:

$$R(x,x') = \frac{1}{\sqrt{2\pi\sigma}} \exp \left[ \frac{-(x-x')^2}{2\sigma} \right] \quad [8.2]$$

where  $\sigma$  represents the non-local response parameter. The equation governing the polymer concentration,  $P$ , becomes:

$$[P(x,t)] = \int_0^t \int_{-\infty}^{+\infty} R(x,x') F(x,t') [M(x,t')] dx' dt' \quad [8.3]$$

It was assumed that the refractive index modulation induced during holographic grating formation was linearly related to the polymer concentration. It was noted that as  $\sigma \rightarrow 0$ , equations [8.1] and [8.3] were reduced to the equivalent localized PDD forms.

A number of different non-local response functions were examined by Sheridan *et al.* [SHE 01] including Chernov/Debye and super- and sub-Gaussian non-local material responses generalized to include a power-law response. The effects of these responses were examined for various material parameters. It was found that, in general, assuming an isotropic, or even

area-normalized, response function, qualitatively acceptable growth curve and spatial frequency response behavior were observed.

Experimental verification of the high spatial frequency cutoff was required to validate the model and was carried out by Lawrence *et al.* [LAW 01a]. This included fitting experimental data using the new model, and a number of significant material parameters were estimated including the rate of monomer diffusion.

Following previous work [ZHA 95, KWO 99], Lawrence *et al.* [LAW 01b] further developed the NPDD model to take into account the nonlinear response of the photopolymer materials for steady-state exposure irradiance [KWO 99].

In 2001, O'Neill *et al.* [O'NE 01] examined the use of an aerosol sealant (varnish) to seal the photopolymer holographic recording material from the environment. Application of the sealant was found to produce some deterioration in the optical quality of the resulting holographic optical elements (HOEs). It was also shown to produce an increased lifetime of the active material (pre-recording), an increase in the diffraction efficiency from the resulting diffraction gratings recorded and improved HOE shelf life. While some of the material characteristics were improved by the introduction of the varnish layer, an increase in diffuse optical scatter was observed during replay. This technique was examined in order to replace coverplating as it was found to be a cheaper and simpler method to seal the photopolymer recording material from the environment. The coverplating of material layers, in general, leads to better humidity stability, reduced inhibition effects and more stable long-term diffraction efficiency.

In 2004, Sheridan *et al.* [SHE 04] presented a work on a generalized non-local model with higher harmonic retention. Numerical methods of solution for the first-order coupled differential equations had up to this point involved retaining four harmonics, or less, of the Fourier series of monomer concentration in the calculations. Here, a general set of coupled first-order differential equations was derived and presented, allowing for the inclusion of higher harmonics and different material spatial response functions. The effect of the number of retained harmonics on the values of the monomer harmonic amplitudes predicted was examined and the effects of varying  $R$ ,

the normalized parameter not the response in equation [8.2], and general material response parameters  $\kappa$  (power law parameter) [SHE 04] and  $\sigma$  (non-local parameter) were explored. Retaining different numbers of harmonics, i.e. 4, 8 and 12, numerical comparisons were carried out and the resulting simulations were presented in terms of percentage difference versus the exposure. A number of results were presented, including: (i) as  $R$  decreases, the each harmonic amplitude value increases by a larger percentage, (ii) as  $\kappa$  increases, the percentage difference in each harmonic increases and (iii) as  $\sigma$  increases, the percentage difference in each harmonic increases slightly. Nonlinear effects in the material (e.g. if  $F$  is proportional to  $I^n$ ) between the rate of polymerization and the exposure irradiance were also examined, however, time variations were omitted.

Kelly *et al.* [KEL 05a] proposed an extension to the NPDD model [SHE 00, LAW 02] to account for the temporal response associated with polymer chain growth in acrylamide (AA)/polyvinyl alcohol (PVA) material. This was achieved by including an exponential temporal material response along with the non-local spatial material response function. Previously, all temporal effects were assumed to be instantaneous, and were neglected. Using rigorous coupled wave analysis (RCWA) and the Lorentz–Lorenz expression, the temporal evolution of refractive index modulation was determined during and after illumination. Comparisons were then made between the theory and experiment for two models. In the first model, the dominant termination mechanism was assumed to be bimolecular, while in the second model, primary termination was assumed to be dominant. Material parameters were then extracted based on best fits to the experimental data for both models. For the two models examined, values for the diffusion coefficient were found to be of the order,  $D \sim 10^{-11} \text{ cm}^2 \text{ s}^{-1}$ , the non-local spatial response parameter was found to be  $\sqrt{\sigma} \approx 60 \text{ nm}$  and the non-local temporal response parameter was found to be  $\tau_n \sim 0.1 \text{ s}$ . The best fits, i.e. higher correlation, to the experimental data were achieved assuming the primary termination model.

In the same year, Kelly *et al.* [KEL 05b] extended the photochemical analysis of Kwon *et al.* [KWO 99], and a rate,  $R_r$ , associated with the generation of primary radicals,  $R^*$ , was introduced. Primary radicals, assumed to interact with a monomer  $M$ , produce the chain initiation

species,  $M_1^\cdot$  (where  $M_{n \geq 1}^\cdot$  is denoted by  $M^\cdot$ ). This reaction takes place at the rate  $R_i$ .

O'Neill *et al.* [O'NE 05] examined the temporal evolution of the optically induced surface relief pattern in AA/PVA-based holographic recording materials during and after exposure to intense light. In this work, they examined the effects of coherent exposure energy and mask pattern on the final surface relief pattern. The temporal evolution of the exposed spot was estimated. The 44  $\mu\text{m}$ -thick photopolymer layer was exposed using a 24  $\text{mJ}/\text{cm}^2$  beam. It clearly showed that there is rapid initial shrinkage,  $\sim 0.34 \mu\text{m}$ , followed by a longer period during which swelling occurs. The resulting profile was a pedestal  $\sim 1.2 \mu\text{m}$  in height. The effects of varying the exposure energy on the resulting temporal behavior of the central height were also examined. The height parameter was defined as the difference between the heights at the edge and the centre of the exposure. The material variation increases with increasing intensity as was expected. From an examination of the effects of exposing the layer with both single-beam and double-beam (holographic) illumination, it was found that although the swelling is less for the two beam recording, it is still appreciable. The examined layers were 47 and 50  $\mu\text{m}$  thick for the double-beam and single-beam exposures, respectively. The exposure energy in both cases was  $\sim 240 \text{mJ}/\text{cm}^2$ . This result has implications for holographic recording in this material as shrinkage/swelling of the material can result in Bragg detuning effects, which are important for slanted gratings recording. This study also demonstrated that it is possible to use the volume change in holographic recording materials to produce patterned surfaces.

In 2006, Kelly *et al.* [KEL 06] further generalized the NPDD model to include the effects of volume shrinkage of the polymer layer due to exposure.

In 2007, Gleeson *et al.* [GLE 07] developed the NPDD model to more exactly include the effects of both temporally varying photosensitive dye absorption and oxygen-based inhibition. A detailed examination of photoinitiation processes taking place during illumination was presented. Particular attention was paid to the photosensitive dye kinetics and inhibition effects that dominate at the start of exposure.

One of the key predictions of the NPDD model [SHE 00, LAW 02] is that a reduction in the extent of the non-local effects within a material will improve its high spatial frequency response. In the work presented in 2008 by Gleeson *et al.* [GLE 08a], the spatial frequency response of an AA/PVA-based photopolymer was improved through the addition of a chain transfer agent (CTA), sodium formate. The CTA has the effect of decreasing the average length of the polyacrylamide (PA) chains formed, thus reducing the non-local response parameter  $\sigma$  while maintaining a high rate of polymerization. In addition, this work indicated that the chain transfer kinetic effects introduced by the CTA, which contribute to the increased localization of the polymerization, include: (i) an increase in the concentration of the monomer radicals available for bimolecular termination, and/or (ii) the effects of less than 100% efficiency in the reinitiation process. A significant reduction in the non-local parameter from 63 to 50 nm was obtained.

Kelly *et al.* [KEL 08] proposed an algorithm, using a more rigorous NPDD formulation, to determine an appropriate holographic data storage recording schedule based on the physical properties of the AA/PVA recording medium's properties. The predictions of the algorithm and the inverse-square scaling law of holographic diffraction were examined experimentally for a peristrophic multiplexing scheme. The scaling law was shown to significantly break down for low numbers of high diffraction efficiency gratings. Using the algorithm, a good correlation between the theoretically predicted and experimentally achieved exposure schedules was found. The largest discrepancy in all cases occurs for the final exposure, where the reduced monomer concentration available, and possible grating non-uniformities, strongly affects the exposure schedule time. The examinations showed that for multiple high diffraction efficiency gratings, the scaling relationship between the diffraction efficiency of each grating and the numbers of gratings recorded broke down, but that this could be explained using Kogelnik's model.

Further generalizations of the 1D NPDD model were then presented by Gleeson *et al.* [GLE 08a, GLE 09]. These included:

- 1) the time varying photoabsorption [GLE 08b, LIU 11] is included more physically;

2) inclusion of the multiple inhibition effects [GLE 06, GLE 07] during the early stages of the exposure;

3) removal of the necessity for the steady-state approximation [KEL 05a, KWO 99, KEL 05b, GLE 06], including the simultaneous effects of both the *primary* (i.e.  $R^*-M'$ ) and *bimolecular* (i.e.  $M'-M'$ ) termination mechanisms, results in a more accurate physical representation of the initial transient behavior at the start of holographic grating formation in photopolymers.

In 2010, Gleeson *et al.* [GLE 10] further developed the NPDD model applied to AA/PVA systems to more accurately model the effects of (i) time varying primary radical production, (ii) the rate of removal of photosensitizer and (iii) inhibition. For the first time, the spatial and temporal variations in primary radical generation were included. These extensions provide a more physically comprehensive theoretical representation of the processes, which occur during free radical photopolymerization. The model was also extended to incorporate the effect of oxygen diffusion from outside the material layer by including a rate of oxygen replenishment from the surrounding environment. This allowed accurate modeling of the inhibition effects, which dominate the start of grating growth. Thus, a comprehensive approach to analyze and optimize the photopolymer materials under low-intensity condition was provided.

Guo *et al.* [GUO 11a] examined the effects of photosensitizer diffusion, i.e. erythrosine B (EB), in AA/PVA material. This was achieved using simple experimental techniques and by using a 2D diffusion model. The rate of EB diffusion,  $D \approx 6.27 \times 10^{-12} \text{ cm}^2/\text{s}$ , was estimated. In the literature [LOU 97, CLO 11a, CLO 11b], the rate of diffusion of the AA monomer in such photopolymer layers has been reported to be of the order of  $\sim 10^{-10} \text{ cm}^2/\text{s}$ . The molecular weight of EB is 879.86 g/mol, while that of AA is 71.08 g/mol. While molecular weight alone does not determine the rate of diffusion, it would be reasonable to expect EB to diffuse more slowly than AA. The results indicated that the EB dye molecules diffuse at a rate at least an order of magnitude slower than the AA monomer.

Sabol *et al.* [SAB 10] then reported a detailed study on the photoinitiation process of the photosensitizer, Irgacure 784, used in the epoxy

resin-based photopolymer [TRE 00]. Irgacure 784 is a type of the titanocene photoinitiator which has the property that it does not require a coinitiator to produce the free radical. In this work, the photochemical reactions of Irgacure 784 involved are thoroughly discussed. Importantly, the experimental results reported verify that multiple different absorbers are simultaneously present in the layer at different stages during the exposure.

In 2011, Gleeson *et al.* [GLE 11a] demonstrated how NPDD-based modeling of the mechanisms, which occur in AA/PVA photopolymers during and postexposure, can lead to the development of analysis tools, which can be used to predict the behavior of many distinct types of material for a wide range of recording conditions. They reported on work to the extended their NPDD model, in order to clearly quantify some of the trends, in which the model predicts and thus be able to analyze their implications for attempts to improve the photopolymer material performance. The results are of practical importance when attempting to optimize the performance of a photopolymer material. As the many types of monomer have diverse chemical and structural characteristics, knowledge of these characteristics is necessary. For example, while choosing a monomer, an informed choice can yield specific improvements in material performance. One of the implications of the predictions of the NPDD model is that utilizing a monomer with a large propagation rate constant and low bimolecular termination rate will produce a higher refractive index modulation,  $\Delta n_{\text{sat}}$ . However, it is also desirable to have a monomer with high mobility, i.e. a fast diffusion rate, in order to increase the dynamic range of the photopolymer and to maximize the index modulation achievable. One of the results highlighted in this work is that if the propagation rate is too large, or the bimolecular termination rate is too small, the optimum refractive index modulation will not be obtained. These deleterious effects are compounded further by increased material viscosity as a result of polymerization. In this work, a qualitative understanding of trends is given quantitative predictability.

Liu *et al.* [LIU 11] have revised the NPDD model to characterize the behavior of the PQ/PMMA photopolymer material. Based on a detailed analysis of the photochemical mechanisms present in phenanthrenequinone (PQ)/poly(methyl methacrylate) (PMMA) photopolymer during holographic grating formation, a set of rate equations have been derived, which govern

the temporal and spatial variations of each associated chemical species concentration. Experimental results are presented, which are then fit using this model.

Gleeson *et al.* [GLE 11b] reported results for an impressive new acrylate-based photopolymer material developed by Bayer Material Science (BMS) [RÖL 10]. The material was examined using various optical techniques and then characterized using the NPDD model. Refractive index modulation up to  $\Delta n_{\text{sat}} = 8 \times 10^{-3}$  and a very low non-local parameter value of 9.2 nm were estimated. A comparison between AA/PVA-based and BMS materials shows that the BMS material has: (i) a substantially faster response of the refractive index modulation with respect to the recording dosage, especially at lower power densities; (ii) three times higher refractive index modulation achievable; (iii) six times smaller non-local response parameter (representing the spatial spread of the reactive chain ends of the formed polymer coils during photopolymerization), indicating a much higher resolution, i.e. little drop-off in material response up to 5,000 lines/mm; and (iv) an improved performance at high spatial frequencies permitting high diffraction efficiency reflection holograms to be recorded. This material demonstrated the capabilities of a new class of photopolymer, which, importantly, can be produced on an industrial scale as large-area plastic films, offering high index modulation, full color recording, high light sensitivity and environmental stability.

The NPDD model has been extended to include the kinetics of chain transfer and reinitiation, in order to analyze the effects of various CTAs on the system kinetics and to study their use in reducing the average polymer chain length [GLE 08a], in free-radical-based photopolymer materials. Guo *et al.* [GUO 11b, GUO 11c] studied AA/PVA-based photopolymer material containing CTAs. The effects of two different types of CTA, i.e. sodium formate (HCOONa) and 1-mercapto-2-propanol ( $\text{CH}_3\text{CH}(\text{OH})\text{CH}_2\text{SH}$ ), were compared. The validity of the extended NPDD model [GUO 11b, GUO 11c] was examined by applying it to fit the resulting experimental data. It is confirmed that the average polymer chain length formed is reduced by the addition of the CTAs, as they reduce the non-local response of the materials. The most effective material combination used resulted in a reduction in the non-local parameter, from 61 to 41 nm. Comparing the two types of transfer agents, the results achieved using 1-mercapto-2-propanol were shown to be better than those using sodium formate. These CTAs produced improved

high spatial frequency material response, giving up to ~28% increase in the refractive index modulation achieved at 3,000 lines/mm.

## 8.2. Dye study of the photopolymer materials

Photopolymers are highly researched in diverse areas such as data storage and metrology. They offer significant advantages as holographic recording media as they are inexpensive, self-processing materials with the ability to capture low loss and high-fidelity volume recordings of 3D illuminating patterns. As a result, the study of the dye behavior in the material has become more crucial and necessary.

In [QI 12], an NPDD model is proposed to study the initiation process during photopolymerization. Three primary mechanisms are studied: (i) the dye absorption, (ii) recovery and (iii) bleaching. In order to avoid the complexities involved in estimating the rate constant of intersystem crossing  $k_{st}$  in going from the excited singlet state dye to the excited triplet state dye, we are introducing two rates,  $k_{aS}$  and  $k_{aT}$ , which are the proposed rate constants of photon absorption in going from the ground state to the singlet and triplet states, respectively. Four kinds of xanthene dyes (EB, eosin Y (EY), phloxine B (PB) and rose bengal (RB)) and one thiazine dye (methylene blue (MB)) are experimentally characterized for use in the AA/PVA photopolymer.

Figures 8.1–8.3 show the transmission, recovery and bleaching of the five dyes in an AA/PVA photopolymer. By fitting the experimental data with the theoretical model, the values of some key material parameters, i.e. molar absorption, quantum efficiency, recovery and bleaching rate of the dyes, can be estimated.

In [QI 14b], more studies of the AA/PVA material, involving examining the kinetics involved within photopolymer materials during holographic recording, are presented. The behavior of four different photosensitizers in an AA/PVA photopolymer material is examined in detail using the developed 1D NPDD model. In order to characterize the photosensitizers precisely, holographic illuminations with different spatial frequencies and exposing intensities are applied. The experimental results are fit using the developed NPDD model.

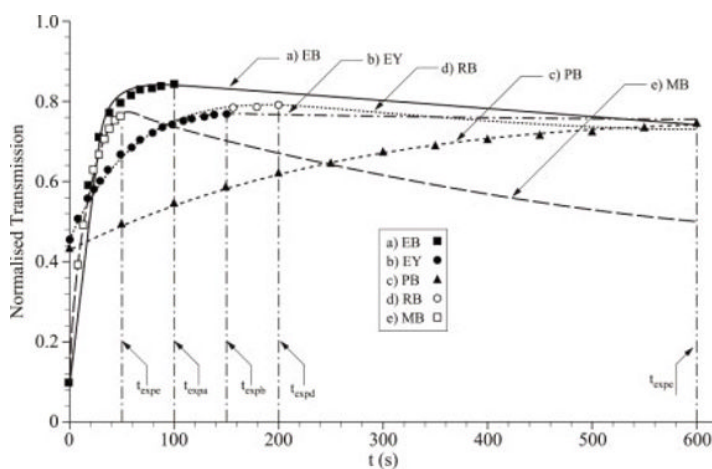


**Figure 8.1.** The normalised transmission characteristics of five different photosensitizers a) EB (solid line and filled square), b) EY (dot-dash line and filled circle), c) PB (short dashed line and filled triangle), d) RB (dotted line and empty circle) and e) MB (long dashed line and empty square) in AA/PVA photopolymer material. Both the experimental data points and theoretical fits for exposure intensities of  $10\text{mW/cm}^2$  for a), b), c) and d) and  $4.03\text{mW/cm}^2$  for e) are shown

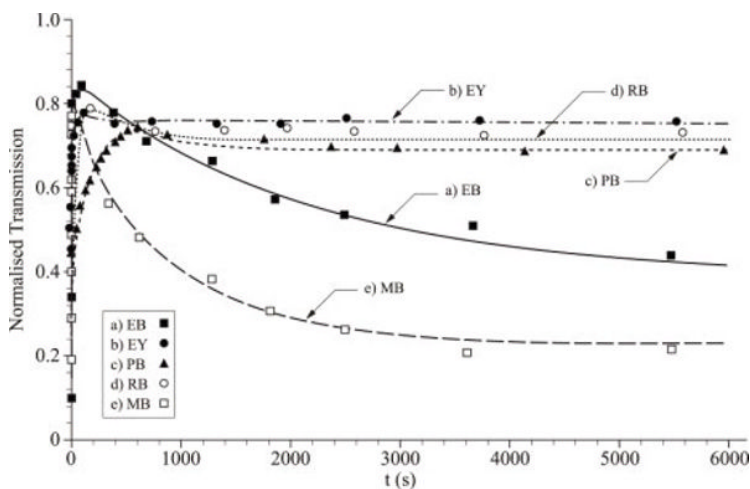


**Figure 8.2.** The recovery process for five different photo sensitizers: a) EB (solid line and filled square), b) EY (dot-dash line and filled circle), c) PB (short dashed line and filled triangle), d) RB (dotted line and empty circle) and e) MB (long dashed line and empty square) in AA/PVA photopolymer material. Both the experimental data points and theoretical fits for the exposure intensity of  $10\text{mW/cm}^2$  for a), b), c) and d) and  $4.03\text{mW/cm}^2$  for e) are shown

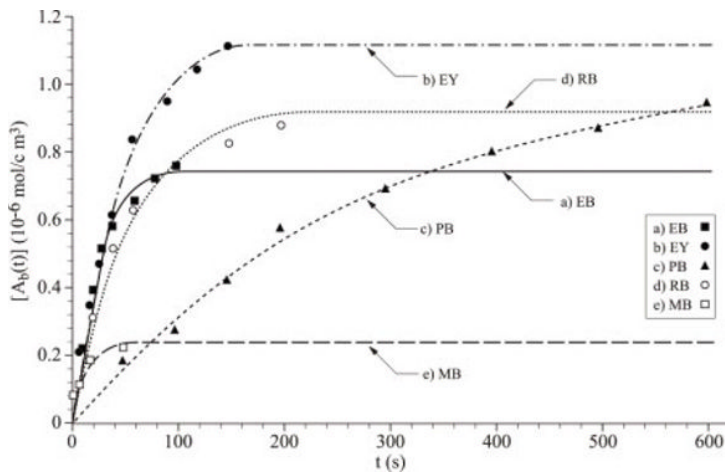


**Figure 8.3.** The bleaching process for five different photosensitizers: a) EB (solid line and filled square), b) EY (dot-dash line and filled circle), c) PB (short dashed line and filled triangle), d) RB (dotted line and empty circle) and e) MB (long dashed line and empty square) in AA/PVA photopolymer material. All the experimental data points and theoretical fits for the exposure intensity of  $10 \text{ mW/cm}^2$  for a), b), c) and d) and  $4.03 \text{ mW/cm}^2$  for e) are shown. In all the cases, the illuminated area was  $0.25 \text{ cm}^2$

Figure 8.4 presents the five experimental growth curves obtained, exposing with  $I_0 = 10 \text{ mW/cm}^2$  for each of the spatial frequencies examined, using material layers containing the photosensitizer EB. The corresponding theoretical fits are also presented. As can be seen in Figure 8.4, the gratings formed are weaker in the high spatial frequency cases due to the fact that the non-local effect plays a more significant role for high spatial frequency cases.

Similarly, Figure 8.5 presents the first harmonic refractive index modulation of a material containing EY dye recorded at a spatial frequency of 2,500 lines/mm, when three different exposing intensities are used. The experimental behavior observed in Figure 8.5 shows that the gratings formed will be weaker for higher exposing intensities. We note that in Figure 8.5(b) (inset), there is a dead band at the beginning of the exposure. This is due to the inhibition process [QI 12, GLE 10] involving rapid reaction of the photosensitizer with inhibiting radicals (oxygen) dissolved in the layer. This effect becomes more pronounced and significant for low-intensity exposures. By coverplating the material layer [GLE 10], less inhibitor (oxygen) can

diffuse during exposure from the air above the layer, and thus the effect of inhibition can be reduced [GLE 10, CLO 11a, CLO 11b].

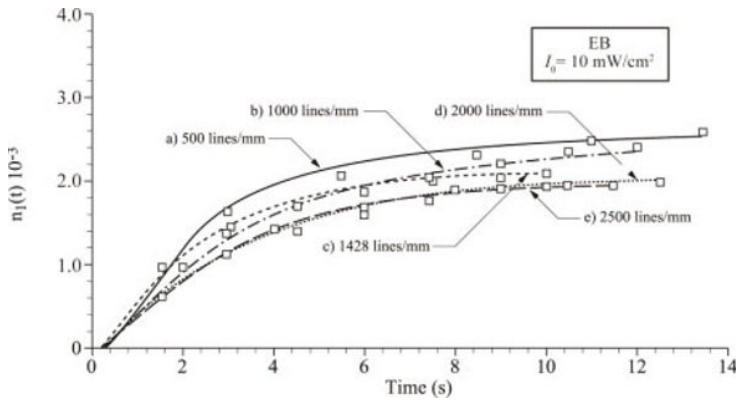


**Figure 8.4.** Growth curves at different spatial frequencies for the material layers containing EB: a) 500 lines/mm (solid line and filled circle), b) 1,000 lines/mm (dot-dash line and filled square), c) 1,428 lines/mm (short dashed line and filled triangle), d) 2,000 lines/mm (dotted line and empty circle) and e) 2,500 lines/mm (long dashed line and empty square)

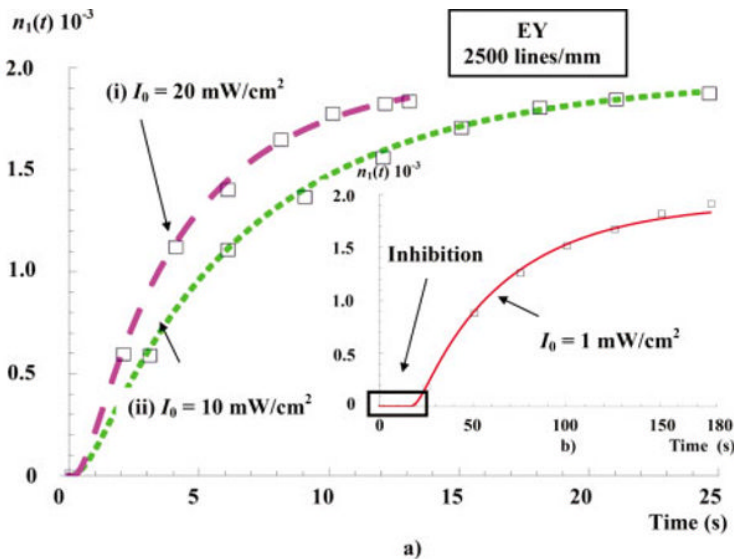


**Figure 8.5.** Growth curves for material layers containing EY: a) (1)  $I_0 = 20 \text{ mW/cm}^2$  (long dashed line and filled triangle) and (2)  $I_0 = 10 \text{ mW/cm}^2$  (short dashed line and filled square, and inset b)  $I_0 = 1 \text{ mW/cm}^2$  (solid line and filled circle)

In this study, it is found that for low spatial frequency cases, the size of the saturation value refractive index modulation strongly depends on the absorptivity of the photosensitizer. The mobility of the photosensitizer appears to become more important for the mid-range spatial frequencies examined. In the high spatial frequency cases, the results for the different dyes become more comparable than one another due to the greater significance of the material non-local response.

In [QI 14a], a newly synthesized photosensitizer, 2-(4-(N,N-dimethylamino)benzylidene)-1H-indene-1,3(2H)-dione, also referred to as D\_1, is used in an AA/PVA-based photopolymer material and is examined and characterized using an extended NPDD model. The experimental results obtained are compared to the corresponding results with a commonly used xanthene dye, i.e. EB, under the same experiment condition.

Electron spin resonance (ESR) spin trapping (ST) is carried out for the identification and the quantification of free radicals produced for both EB and D\_1 cases. The hyperfine coupling constants values were estimated from the simulations of the spectrum using WINSIM, as shown in Figures 8.6 and 8.7. The values of the hyperfine coupling constants, i.e.  $a_N$  and  $a_H$  (where  $a_N$  and  $a_H$  stand for the hyperfine coupling constants in Phenyl-N-tertbutylnitron (PBN) radical adducts for nitrogen and hydrogen, respectively), depend on the radical generated from EB or D\_1. The obtained results show that the values  $a_N$  and  $a_H$  extracted for D\_1 case are the same as those estimated for EB case. Thus, the same radical, i.e.  $R^{\bullet}$ , is generated from D\_1 and EB, respectively.

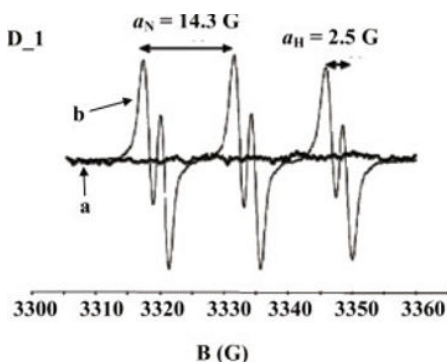


**Figure 8.6.** ESR spin trapping spectrum recorded upon irradiation of a D\_1/triethanolamine solution in tert-butylbenzene (irradiation diode laser 532 nm; under  $N_2$ ); a) before and b) after irradiation

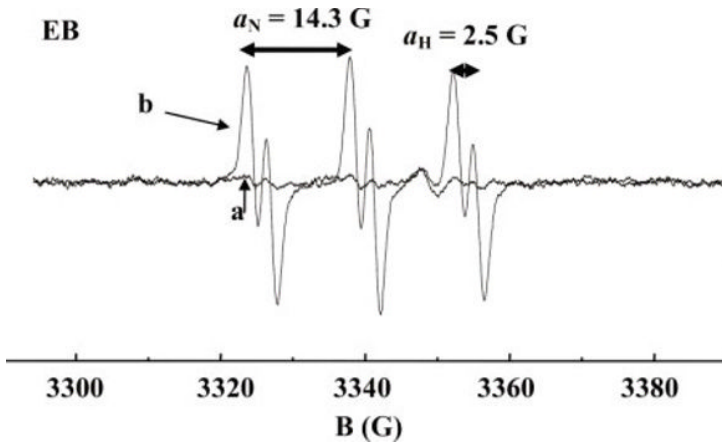


**Figure 8.7.** ESR spin trapping spectrum recorded upon irradiation of an EB/ triethanolamine solution in tert-butylbenzene (irradiation diode laser 532 nm; under  $N_2$ ); a) before and b) after irradiation

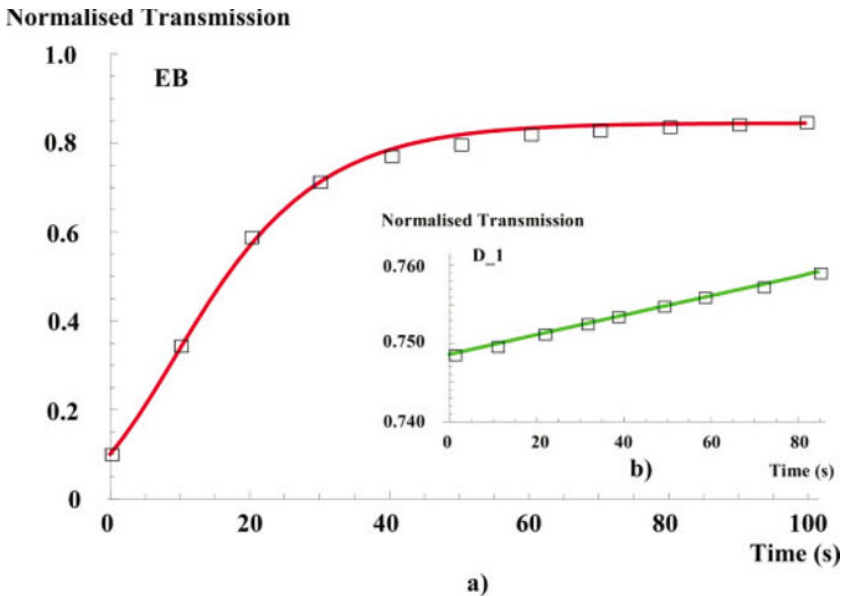


**Figure 8.8.** The normalized transmission characteristics of a) EB and inset b) D\_1 in AA/PVA photopolymer material with the presence of amine. The concentration of photosensitizer used in both cases is  $1.22 \times 10^{-6}$  mol/cm<sup>3</sup>. Both the experimental data points (circles and triangles) and theoretical fits (solid lines) for exposure intensities of 10 mW/cm<sup>2</sup> are shown

Normalized transmittance curves (verses time) for identical EB and D\_1 photosensitizer concentrations are given in Figure 8.8. Due to the weak absorptivity of D\_1 (see Figure 8.8(b)), the transmission curve, which, when  $t = 0$ , has a large value  $T_0 = T(t = 0) = 0.75$ , only increases by approximately 0.01.

Experimental measurements are also made to examine the evolution of the index modulation,  $n_1(t)$ , in the material layer during exposure, see Figure 8.9.

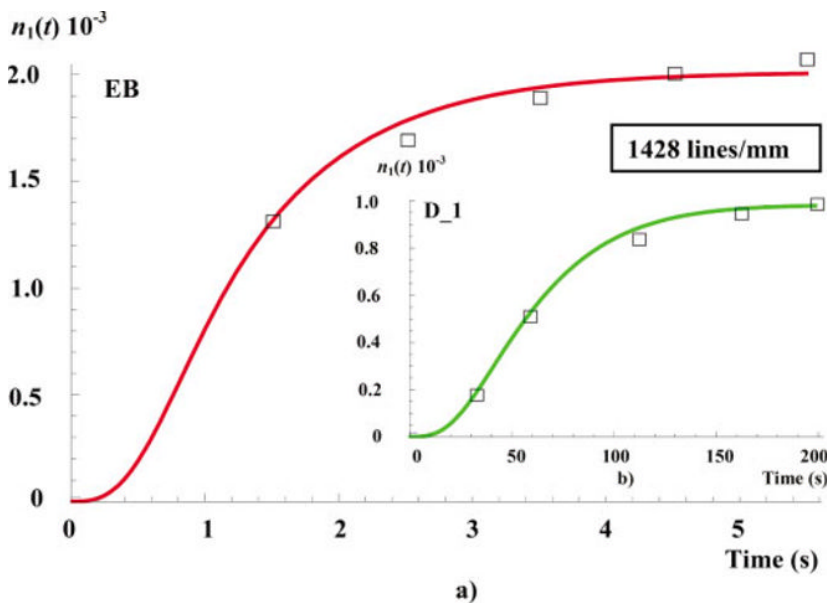


**Figure 8.9.** The refractive index modulation for the material layer containing a) EB and inset, b) D\_1, for  $I_0 = 20 \text{ mW/cm}^2$  and  $\lambda = 532 \text{ nm}$ . In both cases, the experimental data points (circles and triangles) and theoretical fits (solid lines) for a spatial frequency of 1,428 lines/mm are shown

Inspecting Figure 8.9, we see that in the case of D\_1, the maximum saturated first harmonic refractive index modulation value,  $n_{\text{sat}}$ , is smaller (half) than that found in the EB case. This is mainly due to: (i) the weak absorptivity of D\_1, (ii) the slow constant rate of primary radical production

identified and (iii) the larger non-local effect in the D\_1 case. It is, in fact, reasonable that non-locality will play a more significant role in materials with photosensitizers that have weaker absorptivity. In the case of D\_1, weaker absorptivity means that fewer D\_1 molecules become excited and the lower rate  $k_d$  results in fewer radicals,  $R^*$ , being produced. This, in turn, leads to fewer  $M_1^*$  molecules being available to initiate polymer chains. As a result, fewer photopolymer chains are created, and more monomers molecules remain available to become attached (polymerized) in the volume surrounding the growing active polymer chains tips during the propagation process. Since the chains have greater opportunities to grow and fewer opportunities to terminate, they grow longer. Therefore, it is reasonable that the non-local effect becomes stronger for D\_1, as longer chains result in more smearing of the recorded pattern.

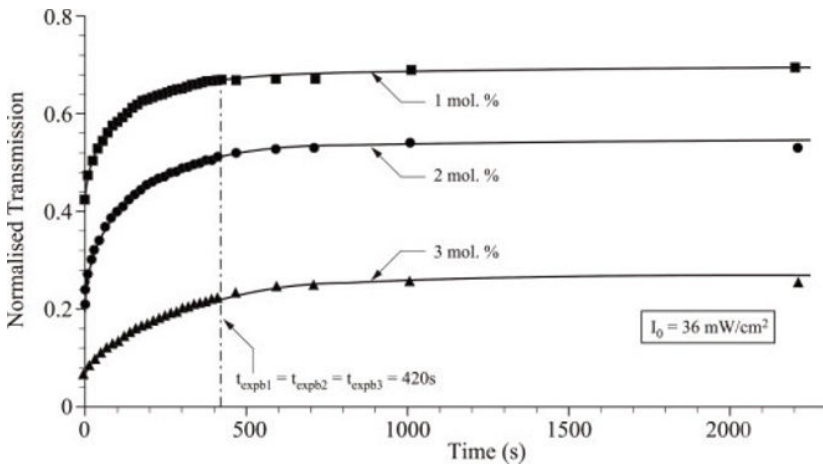
In [QI 13a], a very different photopolymer, *PQ*-doped *PMMA* photopolymer material, is studied. A suitably modified kinetic NPDD model is developed, and the various assumptions made are discussed. These include: (i) the inclusion of time varying photon absorption, including the absorptivity of a second absorber, i.e. the singlet excited state of *PQ*, (ii) the recovery/regeneration and the bleaching of the excited state *PQ*, (iii) the non-local effect and (iv) the diffusion effects of both the ground and excited state *PQ* molecules and of the *MMA*. A set of coupled rate equations are derived, governing the temporal and spatial variations of each chemical component concentration. Based on this analysis, simulations describing the normalized transmission of the material are presented and the predicted effects of the non-local material response and the diffusion of both the ground state *PQ* and excited state *PQ* molecules during and postexposure are also examined.

In [QI 13b], employing the extended 1D NPDD model developed in [QI 13a], the temporal and spatial variations of each chemical component concentration within a *PQ/PMMA* material layer are analyzed. The resulting simulations are used to predict the material-normalized transmission, non-local effect and the diffusion of ground and excited states of *PQ*. The validity of the proposed model is examined by applying it to fit experimental data captured when using *PQ/PMMA* layers containing three different initial *PQ* concentrations, i.e. 1, 2 and 3 mol.%. The effect of different exposure intensities is also examined. Material parameter values are estimated by numerically fitting experimental normalized transmission

curves and the refractive index modulation growth curves, using the developed model.

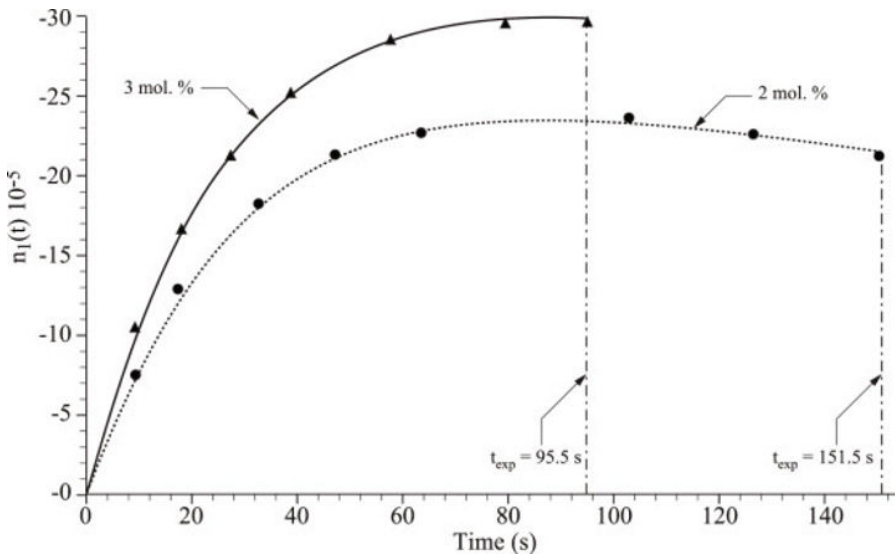
Figure 8.10 shows the normalized transmission characteristics for samples with different  $PQ$  concentrations. We note that the transmittance curves continue to increase postexposure. This takes place due to the absorptivity of the  ${}^1PQ^*$  and the slow intercrossing rate  $k_{st}$ . Once the exposure ends, an amount of  ${}^1PQ^*$  still remains in the exposing area and this continues to be converted postexposure into  ${}^3PQ^*$  at the intercrossing rate of  $k_{st}$ . Therefore, an increase in the transmitted intensity is detected.

Figure 8.11 shows the experimental measurements made to examine the evolution of the index modulations,  $n_1(t)$ , in the  $PQ/PMMA$  photopolymer layer during exposure. It can be observed from Figure 8.11 that in both cases,  $n_1(t)$  gradually increases to a maximum value. For the 3 mol.% case, due to the higher initial  $PQ$  concentration,  $n_1$  grows more quickly [VEN 05], and the value of  $n_1$  is larger than that for the 2 mol.% case. If the exposure continues after  $n_1$  reaches its maximum saturation value, a decrease in the rate of growth is observed, which is due to the degradation of the purity (fidelity) of the sinusoidal shape of the grating formed [VEN 05].



**Figure 8.10.** The normalized transmission characteristics for samples with three different  $PQ$  concentrations: a) 1 mol.% (solid line and filled square), b) 2 mol.% (solid line and filled circle) and c) 3 mol.% (solid line and filled triangle). Both the experimental data points and theoretical fits for the exposure intensity of  $36 \text{ mW/cm}^2$  are shown

In [QI 15], based on the theoretical and experimental work presented in [QI 13a] and [QI 13b], the simulated prediction of the behavior of the *PQ/PMMA* photopolymer post-exposure was studied. The resulting predicted evolution of the first harmonic refractive index modulation is examined for both a long time post-exposure and in the case of thermal treatment post-exposure. Several physical processes are studied, including the non-local material response and the effects of the diffusion of both the ground state and excited states *PQ* molecules (during and post exposure). The effects of the use of different exposing intensities on the final grating formed are studied. The size of the higher grating harmonic concentration amplitudes in this final distribution is also discussed.



**Figure 8.11.** The refractive index modulation characteristics for samples with two different *PQ* concentrations: a) 2 mol.% (dotted line and filled circle) and b) 3 mol.% (solid line and filled triangle). Both the experimental data points and theoretical fits for a spatial frequency of 1,428 lines/mm are shown

Figure 8.12 shows the predicted evolution of the spatial distribution of *PQ* (two periods) over a long time interval postexposure, i.e.  $t_{\text{exp}} \leq t \leq 7 \times 10^6$  s. It is therefore  $180^\circ$  out of phase with the exposing pattern and, as

can be seen, the  $PQ$  concentration has maxima at the locations of the dark parts of the illumination fringes. Although the  $PQ$  (and  ${}^1PQ^*$ ) molecules diffuse at a very slow rate, after an extended time postexposure, the fixed distribution becomes uniform. The refractive index modulation then only depends on the fixed distribution of  $PQ$ - $PMMA$  and this distribution is in phase with the original exposing pattern.

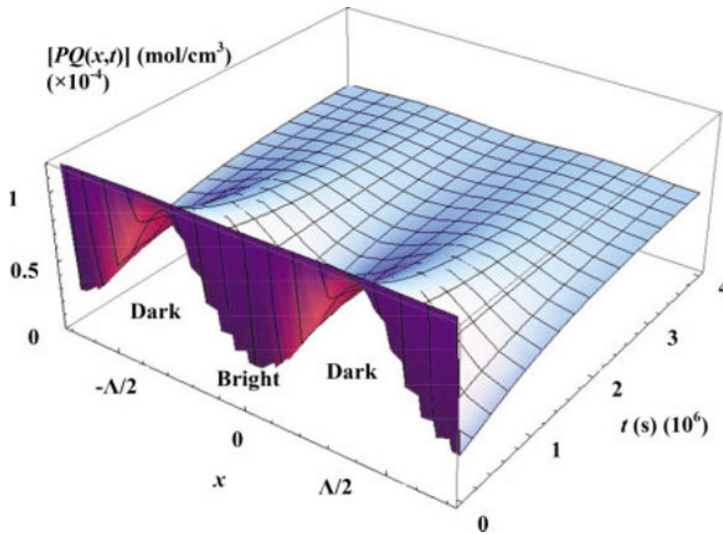


**Figure 8.12.** Evolution of the  $PQ$  concentration during and post-exposure with time shown across two grating periods.  $-A \leq x \leq A$  and  $0 \leq t \leq 7 \times 10^6 \text{ s}$ ,  $\sqrt{\sigma} = 0$  and  $D_{PQ} = D_{1PQ^*} = D_{3PQ^*} = 1.09 \times 10^{-16} \text{ cm}^2/\text{s}$ ,  $t_{\text{exp}} = 60 \text{ s}$ ,  $I_0 = 1.152 \times 10^{-3} \text{ mW/cm}^2$

In Figure 8.13, the resulting predicted first harmonic refractive index changes with time, during and post-exposure (when simulated thermal treatment is applied), are presented.

The initial negative values indicate the  $180^\circ$  phase shift of the resulting modulation. As noted due to the diffusion of  $PQ$  (see Figure 8.12) (and both the diffusion and consumption of the  ${}^1PQ^*$  molecules), the distribution post-exposure eventually becomes uniform (i.e. the associated modulations disappear). As can be seen in Figure 8.13, the index modulation eventually becomes positive and depends only on the fixed  $PQ$ - $PMMA$  distribution. We recall that a negative modulation amplitude indicates a

grating  $180^\circ$  ( $\pi$  radian) shifted out of phase with the exposing interference pattern.

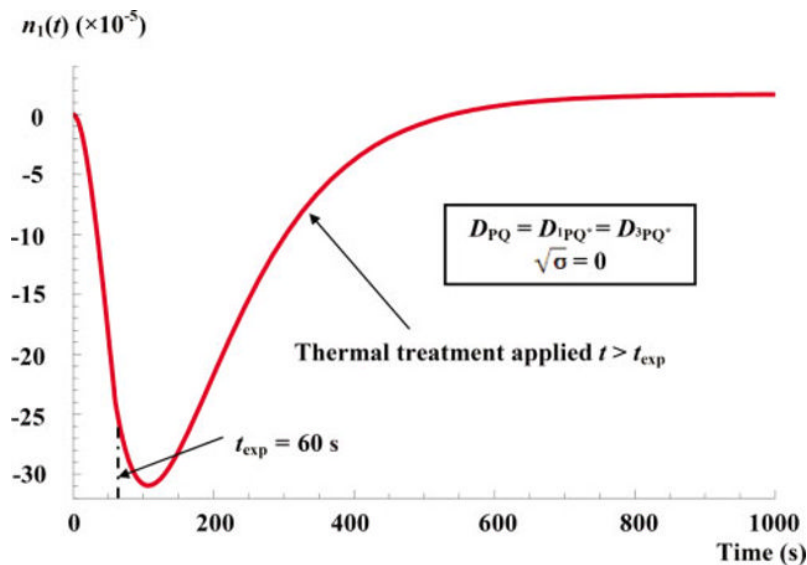


**Figure 8.13.** Refractive index modulation during and post-exposure. Simulated thermal treatment is applied post-exposure. The total exposing intensity used is  $I_0 = 1.152 \times 10^{-3} \text{ mW/cm}^2$

### 8.3. Conclusion

We believe that the work presented in this chapter represents a significant contribution to the area of holographic recording material and photopolymer research. The results increase the understanding of the photochemical and photophysical kinetics, which take place in photopolymers during and postexposure. The development of the NPDD model reported involves several significant contributions. The most recent NPDD model has been demonstrated to more accurately and physically describe and predict the measured experimental behavior. The model has also been successfully applied and adapted to explain the behaviors of several different photopolymer materials. The availability of this model is of practical value as it permits the study of the further optimizations of material performance. This is not only true for AA/PVA- and PQ/PMMA-based photopolymer materials, but many other holographic recording materials.

Work is ongoing, with several papers recently being published examining the fundamental nature and modeling of dye absorption in thick layers [LI 15a, LI 15b]. A 3D NPDD for use in the 3D modeling of the recording and replay of thick holograms has also recently been published [LI 14a, LI 14b]. Related work describing the use of AA/PVA to record self-written waveguides has also recently been presented [LI 14c].

#### 8.4. Bibliography

- [CAP 88] CAPOLLA N., LESSARD R.A., “Processing of holograms recorded in methylene blue sensitized gelatin”, *Applied Optics*, vol. 27, pp. 3008–3012, 1988.
- [CAS 10] CASTRO J.M., ZHANG D., MYER B. *et al.*, “Energy collection efficiency of holographic planar solar concentrators”, *Applied Optics*, vol. 49, pp. 858–870, 2010.
- [CLO 11a] CLOSE C.E., GLEESON M.R., SHERIDAN J.T., “Monomer diffusion rates in photopolymer material. Part I. Low spatial frequency holographic gratings”, *Journal of the Optical Society of America B*, vol. 28, no. 4, pp. 658–666, 2011.
- [CLO 11b] CLOSE C.E., GLEESON M.R., MOONEY D.A. *et al.*, “Monomer diffusion rates in photopolymer material. Part II. High-frequency gratings and bulk diffusion”, *Journal of the Optical Society of America B*, vol. 28, no. 4, pp. 842–850, 2011.
- [COU 88] COUTURE J.J.A., LESSARD R.A., “Modulation transfer function measurements for thin layers of azo dyes in PVA matrix used as an optical recording material”, *Applied Optics*, vol. 27, pp. 3368–3374, 1988.
- [CUR 10] CURTIS K., DHAR L., MURPHY L. *et al.*, *Future Developments, in Holographic Data Storage: From Theory to Practical Systems*, Wiley, Chichester, UK, 2010.
- [FOU 12] FOUASSIER J.P., LALEVÉE J., *Photoinitiators for Polymer Synthesis*, Wiley, New York, NY, 2012.
- [GLE 06] GLEESON M.R., KELLY J.V., CLOSE C.E. *et al.*, “The effects of absorption and inhibition during grating formation in photopolymer materials”, *Journal of the Optical Society of America B*, vol. 23, no. 10, pp. 2079–2088, 2006.
- [GLE 07] GLEESON M.R., KELLY J.V., SABOL D. *et al.*, “Modeling the photochemical effects present during holographic grating formation in photopolymer materials”, *Journal of Applied Physics*, vol. 102, no. 2, no. 023108, 2007.

- [GLE 08a] GLEESON M.R., SABOL D., LIU S. *et al.*, “Improvement of the spatial frequency response of photopolymer materials by modifying polymer chain length”, *Journal of the Optical Society of America B*, vol. 25, no. 3, pp. 396–406, 2008.
- [GLE 08b] GLEESON M.R., LIU S., O’DUILL S. *et al.*, “Examination of the photoinitiation processes in photopolymer materials”, *Journal of Applied Physics*, vol. 104, no. 064917, 2008.
- [GLE 09] GLEESON M.R., SHERIDAN J.T., “Non-local photo-polymerization kinetics including multiple termination mechanisms and dark reactions. Part I. Modeling”, *Journal of the Optical Society of America B*, vol. 26, no. 9, pp. 1736–1745, 2009.
- [GLE 10] GLEESON M.R., LIU S., GUO J. *et al.*, “Non-Local photo-polymerization kinetics including multiple termination mechanisms and dark reactions. Part III. Primary radical generation and inhibition”, *Journal of the Optical Society of America B*, vol. 27, pp. 1804–1812, 2010.
- [GLE 11a] GLEESON M.R., GUO J., SHERIDAN J.T., “Optimisation of photopolymers for holographic applications using the non-local photo-polymerization driven diffusion model”, *Optics Express*, vol. 19, no. 23, pp. 22423–22436, 2011.
- [GLE 11b] GLEESON M.R., SHERIDAN J.T., BRUDER F.K. *et al.*, “Comparison of a new self developing photopolymer with AA/PVA based photopolymer utilizing the NPDD model”, *Optics Express*, vol. 19, no. 27, pp. 26325–26342, 2011.
- [GUO 11a] GUO J., LIU S., GLEESON M.R. *et al.*, “Study of photosensitizer diffusion in a photopolymer material for holographic applications”, *Optical Engineering*, vol. 50, no. 1, no. 015801, 2011.
- [GUO 11b] GUO J., GLEESON M.R., LIU S. *et al.*, “Non-local spatial frequency response of photopolymer materials containing chain transfer agents. Part I. Theoretical modeling”, *Journal of Optics*, vol. 13, no. 9, no. 095601, 2011.
- [GUO 11c] GUO J., GLEESON M.R., LIU S. *et al.*, “Non-local spatial frequency response of photopolymer materials containing chain transfer agents. Part II. Experimental results”, *Journal of Optics*, vol. 13, no. 9, no. 095602, 2011.
- [HSU 03] HSU K.Y., LIN S.H., HSIAO Y. *et al.*, “Experimental characterization of phenanthrenequinone-doped poly(methylmethacrylate) photopolymer for volume holographic storage”, *Optical Engineering*, vol. 42, pp. 1390–1396, 2003.
- [KEL 05a] KELLY J.V., GLEESON M.R., CLOSE C.E. *et al.*, “Temporal analysis of grating formation in photopolymer using the nonlocal polymerization-driven diffusion model”, *Optics Express*, vol. 13, no. 18, pp. 6690–7004, 2005.

- [KEL 05b] KELLY J.V., O'NEILL F.T., SHERIDAN J.T. *et al.*, "Holographic photopolymer materials: nonlocal polymerization-driven diffusion under nonideal kinetic conditions", *Journal of the Optical Society of America B*, vol. 22, pp. 407–416, 2005.
- [KEL 06] KELLY J.V., GLEESON M.R., CLOSE C.E. *et al.*, "Temporal response and first order volume changes during grating formation in photopolymers", *Journal of Applied Physics*, vol. 99, no. 113105, 2006.
- [KEL 08] KELLY J.V., GLEESON M.R., CLOSE C.E. *et al.*, "Optimized scheduling for holographic data storage", *Journal of Optics A: Pure and Applied Optics*, vol. 10, no. 115203, 2008.
- [KWO 99] KWON J.H., HWANG H.C., WOO K.C., "Analysis of temporal behaviour of beams diffracted by volume gratings formed in photopolymers", *Journal of the Optical Society of America B*, vol. 16, no. 10, pp. 1651–1657, 1999.
- [LAW 01a] LAWRENCE J.R., O'NEILL F.T., SHERIDAN J.T., "Photopolymer holographic recording material", *Optik*, vol. 112, pp. 449–463, 2001.
- [LAW 01b] LAWRENCE J.R., O'NEIL F.T., SHERIDAN J.T., "Photopolymer holographic recording material parameter estimation using a nonlocal diffusion based model", *Journal of Applied Physics*, vol. 90, pp. 3142–3148, 2001.
- [LAW 02] LAWRENCE J.R., O'NEILL F.T., SHERIDAN J.T., "Adjusted intensity nonlocal diffusion model of photopolymer grating formation", *Journal of the Optical Society of America B*, vol. 19, no. 4, pp. 621–629, 2002.
- [LI 14a] LI H., QI Y., SHERIDAN J.T., "Three-dimensional extended nonlocal photo-polymerization driven diffusion model. Part I. Absorption", *Journal of the Optical Society of America B*, vol. 31, no. 11, pp. 2638–2647, 2014.
- [LI 14b] LI H., QI Y., SHERIDAN J.T., "Three-dimensional extended nonlocal photo-polymerization driven diffusion model. Part II: Photo-polymerization and model development", *Journal of the Optical Society of America B*, vol. 31, no. 11, pp. 2648–2656, 2014.
- [LI 14c] LI H., QI Y., RYLE J.P. *et al.*, "Self-trapping of optical beams in a selfwrittenchannel in a solid bulk photopolymer material", *Applied Optics*, vol. 53, no. 34, pp. 8086–8094, 2014.
- [LI 15a] LI H., QI Y., SHERIDAN J.T., "Analysis of the absorptive behaviour of photopolymer materials. Part I. Theoretical modelling", *Journal of Modern Optics*, vol. 62, no. 2, pp. 145–156, 2015.
- [LI 15b] LI H., QI Y., SHERIDAN J.T., "Analysis of the absorptive behaviour of photopolymer materials. Part II. Experimental validation", *Journal of Modern Optics*, vol. 62, no. 2, pp. 157–167, 2015.

- [LIN 00] LIN S.H., HSU K.Y., CHEN W. *et al.*, “Phenanthrenequinone-doped poly(methyl methacrylate) photopolymer bulk for volume holographic data storage”, *Optics Letters*, vol. 25, pp. 451–453, 2000.
- [LIU 11] LIU S., GLEESON M.R., GUO J. *et al.*, “Modeling the photochemical kinetics induced by holographic exposures in PQ/PMMA photopolymer material”, *Journal of the Optical Society of America B*, vol. 28, pp. 2833–2843, 2011.
- [LOU 97] LOUGNOT D.J., JOST P., LAVIELLE L., “Polymers for holographic recording. VI. Some basic ideas for modeling the kinetics of the recording process”, *Pure Applied Optics*, vol. 6, pp. 225–245, 1997.
- [MAH 06] MAHILNY U.V., MARMYSH D.N., STANKEVICH A.I. *et al.*, “Holographic volume gratings in a glass-like polymer material”, *Applied Physics B*, vol. 82, pp. 299–302, 2006.
- [MAH 08] MAHILNY U.V., MARMYSH D.N., TOLSTIK A.L. *et al.*, “Phase hologram formation in highly concentrated phenanthrenequinone-PMMA media”, *Journal of Optics A: Pure and Applied Optics*, vol. 10, no. 085302, 2008.
- [MAN 94] MANIVANNAN G., LESSARD R.A., “Trends in holographic recording materials”, *Trends Polymer Science*, vol. 2, pp. 282–290, 1994.
- [O’NE 01] O’NEILL F.T., LAWRENCE J.R., SHERIDAN J.T., “Improvement of holographic recording material using aerosol sealant”, *Journal of Optics A: Pure and Applied Optics*, vol. 3, pp. 20–25, 2001.
- [O’NE 05] O’NEILL F.T., CARR A.J., DANIELS S.M. *et al.*, “Refractive elements produced in photopolymer layers”, *Journal of Materials Science*, vol. 40, pp. 4129–4132, 2005.
- [QI 12] QI Y., GLEESON M.R., GUO J. *et al.*, “Quantitative comparison of five different photosensitizers for use in a photopolymer”, *Physics Research International*, vol. 2012, article ID 975948, 2012.
- [QI 13a] QI Y., LI H., TOLSTIK E. *et al.*, “Study of PQ/PMMA photopolymer. Part 1: theoretical”, *Journal of the Optical Society of America B*, vol. 30, pp. 3298–3307, 2013.
- [QI 13b] QI Y., TOLSTIK E., LI H. *et al.*, “Study of PQ/PMMA photopolymer. Part 2: experimental results”, *Journal of the Optical Society of America B*, vol. 30, pp. 3308–3315, 2013.
- [QI 14a] QI Y., LI H., FOUASSIER J.P. *et al.*, “Comparison of a new photosensitizer with erythrosin B in an AA/PVA-based photopolymer material”, *Applied Optics*, vol. 53, pp. 1052–1062, 2014.

- [QI 14b] QI Y., LI H., GUO J. *et al.*, “Material response of photopolymer containing four different photosensitizers”, *Optics Communications*, vol. 320, pp. 114–124, 2014.
- [QI 15] QI Y., LI H., TOLSTIK E. *et al.*, “PQ/PMMA photopolymer: modeling post-exposure”, *Optics Communications*, vol. 338, pp. 406–415, 2015.
- [RÖL 10] RÖLLE T., BRUDER F.-K., FÄCKE T. *et al.*, Photopolymerzusammensetzungen für optische Elemente und visuelle Darstellungen, Patent EP2 172 505 A1, 2010.
- [SAB 10] SABOL D., GLEESON M.R., LIU S. *et al.*, “Photoinitiation study of Irgacure 784 in an epoxy resin photopolymer”, *Journal of Applied Physics*, vol. 107, no. 8, article no. 053113, 2010.
- [SHE 00] SHERIDAN J.T., LAWRENCE J.R., “Nonlocal-response diffusion model of holographic recording in photopolymer”, *Journal of the Optical Society of America A*, vol. 17, no. 6, pp. 1108–1114, 2000.
- [SHE 01] SHERIDAN J.T., DOWNEY M., O’NEIL F.T., “Diffusion-based model of holographic grating formation in photopolymers: generalized non-local material responses”, *Journal of Optics A: Pure and Applied Optics*, vol. 3, pp. 477–488, 2001.
- [SHE 04] SHERIDAN J.T., KELLY J.V., O’BRIEN G. *et al.*, “Generalized non-local responses and higher harmonic retention in non-local polymerization driven diffusion model based simulations”, *Journal of Optics A: Pure and Applied Optics*, vol. 6, no. 12, pp. 1089–1096, 2004.
- [SUL 07] SULLIVAN A.C., GRABOWSKI M.W., MCLEOD R.R., “Three-dimensional direct-write lithography into photopolymer”, *Applied Optics*, vol. 46, pp. 295–301, 2007.
- [TOL 11] TOLSTIK E., KASHIN O., MATUSEVICH V. *et al.*, “Broadening of the light self-trapping due to thermal defocusing in PQ-PMMA polymeric layers”, *Optics Express*, vol. 19, pp. 2739–2747, 2011.
- [TRE 00] TRENTLER T., BOYD J., COLVIN V., “Epoxy resin photopolymer composites for volume holography”, *Chemistry of Materials*, vol. 12, pp. 1431–1438, 2000.
- [VEN 05] VENIAMINOV A., BARTSCH E., POPOV A., “Postexposure evolution of a photoinduced grating in a polymer material with phenanthrenequinone”, *Optics and Spectroscopy*, vol. 99, pp. 744–750, 2005.
- [YE 08] YE C., MCLEOD R.R., “GRIN lens and lens array fabrication with diffusion-driven photopolymer”, *Optics Letters*, vol. 33, no. 22, pp. 2575–2577, 2008.

- [ZHA 94] ZHAO G.H., MOUROULIS P., “Diffusion-model of hologram formation in dry photopolymer materials”, *Journal of Modern Optics*, vol. 41, no. 10, pp. 1929–1939, 1994.
- [ZHA 95] ZHAO G.H., MOUROULIS P., “Extension of a diffusion-model for holographic photopolymers”, *Journal of Modern Optics*, vol. 42, pp. 2571–2573, 1995.



---

# Advanced Strategies for Spatially Resolved Surface Design via Photochemical Methods

---

## 9.1. Introduction

Encoding chemical information onto surfaces in defined positions is of key importance for a wide range of applications including cell patterning and other biomedical, as well as sensor and optoelectronic, devices. In recent years, a wide range of photopatterning systems have been developed, relying on a diverse set of chemistries that can be triggered by light [TAS 13, HOF 08, FOR 12, TRE 14], including systems that allow for a spatially controlled photopolymerization [POE 13, MUE 14]. Many of the employed chemistries are triggered by variable wavelength ultraviolet (UV) light, with only a few examples exist that allow for triggering with visible light [AN 13, FUK 14, YAM 06]. The ideal light-triggered reaction for surface patterning should fulfill certain criteria. These should include a facile synthetic access route to the light-sensitive compounds, rapid reaction rates (several seconds to minutes) at low photon fluxes at a wavelength preferably in the visible light or at least low energetic UV regime, a quantitative conversion at equimolarity of the reactants, and bio-orthogonality. Yet, there is arguably no single reaction that fulfills all of the above criteria, although some possess many of them. The most employed reaction class is arguably

---

Chapter written by Anja S. GOLDMANN, Guillaume DELAITTRE, Jan O. MUELLER and Christopher BARNER-KOWOLLIK.

cycloadditions – often triggered indirectly, as in the case of [4 + 2] cycloadditions such as Diels–Alder (DA) or 1,3-dipolar cycloadditions, where one active species is produced upon irradiation, or less frequently directly triggered as for [2 + 2] or [4 + 4] additions. The light-triggered provision of electrophiles (such as (thio)aldehydes) with ensuing nucleophilic attack can also be an attractive route, but lacks the key criterion of (bio-)orthogonality. The light-induced release of electrophiles will thus also be discussed herein when they offer specific advantages.

Thus, in this chapter, we will concisely summarize our latest advances in developing effective light-triggered protocols for spatially resolved surface modification embedded in the context of current literature examples, focusing on those where the light-reactive species are attached to the surface. In addition to surface modification via covalent attachment, we also discuss an example of polymer patterning onto surfaces without any covalent attachment of the material to the surface but rather a cross-linked layer is deposited in a spatially resolved fashion. Moreover, not only the type of the employed ligation reaction is of key importance, but also the type of surface that is to be modified, as often the chosen ligation has to be adjusted to a specific surface. Arguably, the most frequently modified surfaces are (activated) silicon wafers as well as glass slides. While such surfaces can be useful for some applications (e.g. cell guiding) and often serve as model substrates, particular progress has been made in the realm of biosurface modification, most notably in cellulose and paper. In this chapter we won't be considering polymer surfaces. We will discuss the spatially resolved surface modifications using the nature of the employed substrate as a guiding principle: inorganic substrates, biosubstrates/biomimetic surfaces and processes where no direct covalent attachment to the surface is used will be treated in this order. The reason for the noted structuring of the chapter is associated with the level of difficulty experienced in the surface modification. A very uniform and flat silicon wafer is less challenging to functionalize (and characterize) than a fibrillar cellulose substrate, for instance. Surface modifications can be challenging to evidence and the considered ligation chemistry is typically initially evidenced in solution. A particularly useful approach in this context is the attachment of the studied photoreactive group to the terminus of a polymer strand which is able to readily ionize during soft ionization mass spectrometry (e.g. electrospray

ionization (ESI-MS)) and the ligation of a small molecule by irradiation. The effectiveness of the end group transformation can then be readily evidenced via mass spectrometry and the reaction conditions (e.g. solvent, irradiation time, stoichiometry and concentration) can be established.

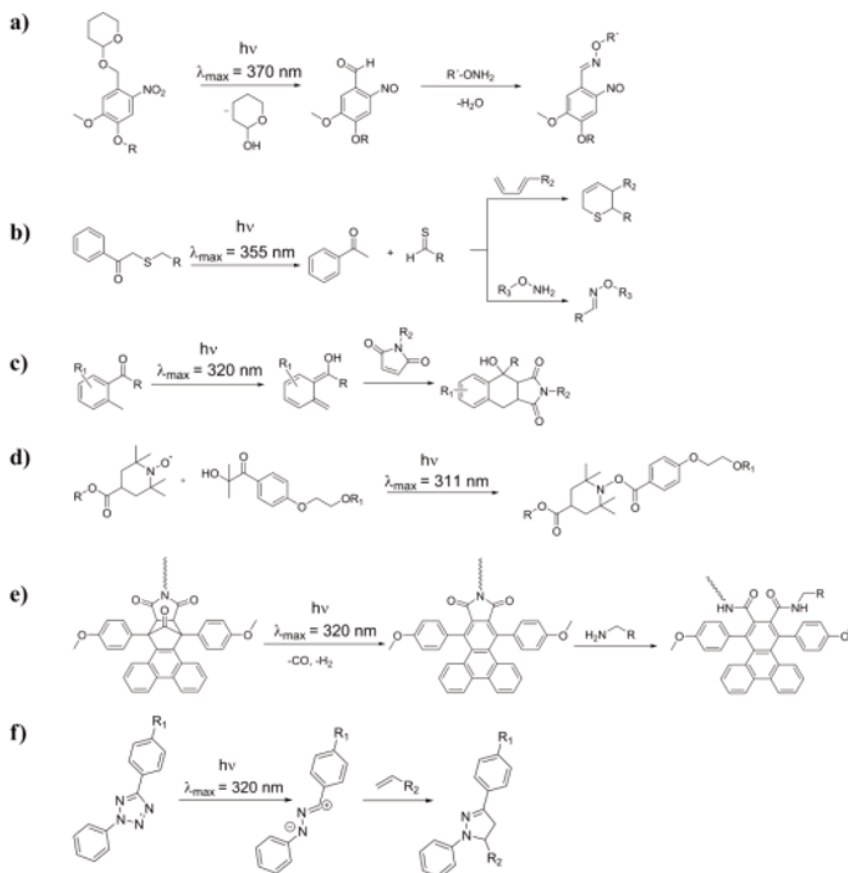


**Figure 9.1.** General chemical pathways involved in the light-triggered chemistries applied in our group for surface modifications: a) oxime ligation of a photogenerated aldehyde with a hydroxylamine, b) phenacyl sulfide ligation: nucleophilic attachment or Diels–Alder reaction of a photogenerated thioaldehyde with a hydroxylamine or a diene, c) photoenol chemistry: Diels–Alder reaction of a photogenerated diene with a dienophile, d) UV-induced nitroxide spin-trapping, e) phencyclone ligation: ring-opening reaction of a photogenerated triphenylene imide derivative with an amine and f) tetrazole-ene ligation: 1,3-dipolar cycloaddition of a photogenerated nitrile imine with a dipolarophile

## 9.2. Inorganic surfaces

In this first section, we will describe efficient avenues to modify the surface of inorganic substrates employing phototriggered chemistries. The main substrate we have investigated is silicon, in particular silicon wafers. These are, in fact, often employed as the first substrate when we investigate a new – at least in our study – surface modification method. There are several reasons for such a procedure, the primary reason being that the first modification step necessary to attach the photoreactive moieties is straightforward, i.e. silanization yielding either a self-assembled monolayer or a thicker cross-linked polysiloxane layer. This type of substrate also offers a high reproducibility since wafers are products designed for high-technology applications such as semiconductors. Furthermore, it is relatively simple to obtain – with constant quality – a very clean reactive substrate using media such as plasma or the so-called “Piranha solution”, while not harming the underlying bulk material. In addition, modifications of Si wafers with organic molecules are readily evidenced with surface characterization methods such as X-ray photoelectron spectroscopy (XPS) or time-of-flight secondary-ion mass spectrometry (ToF-SIMS) since the wafers are topographically highly regular. Although – as mentioned above – Si wafers are our substrate of choice to explore new chemistries, driven by applications, we have investigated the modification of other inorganic materials such as silicon–acrylic hybrid three-dimensional (3D) microstructures and silver nanoparticles. In the following, we will detail our work based on five photochemistries relying on either a cleavage step or an isomerization event following irradiation, as well as some closely related systems employed by other groups.

One of the most studied photoreactions in organic chemistry is the cleavage of *o*-nitrobenzyl (ONB) derivatives, for instance (thio)ethers, esters or carbamates [KLA 12]. Generally, an ONB group, or its often used dimethoxy-substituted counterpart (i.e. nitroveratryl, designed for longer wavelengths), is introduced in order to protect a chemical group during a multistep synthesis. Upon UV irradiation, ONB ethers, thioethers, esters and carbamates release alcohols [RUS 12], thiols [DEL 12b, PAU 12], carboxylic acids [KOT 09] and amines [YOU 06], respectively, along with a nitrosobenzaldehyde molecule which is usually considered as a by-product to be eliminated. However, we took a reverse approach that exploits the

released aldehyde by-product and turned it into our intermediate of interest. Indeed, aldehydes can react in a very efficient bio-orthogonal reaction with aminoxy compounds in the so-called oxime ligation. Consequently, we introduced the concept of *phototriggered oxime ligation* (Figure 9.1(a)) [PAU 12a]. For this purpose, we synthesized a silane derivative possessing a nitroveratryl thioether-type module connected to the silane part of the molecule – the envisaged anchoring point to the Si wafers – through the nitroveratryl side so that the nitrobenzaldehyde fragment would remain on the surface after irradiation, as opposed to all previous methods involving similar compounds where it is released from the surface. Here, an alcohol fragment is cleaved off the cross-linked polysiloxane layer. Indeed, for our system, we aimed at finding a structure with fast kinetics, reducing the irradiation time as much as possible. We therefore selected (tetrahydropyran-2-yl)alcohol as the released fragment since it had previously been demonstrated that ethers possess an overall quantum yield one order of magnitude higher than most other ONB derivatives [KAM 10]. In addition, its incorporation onto the ONB-type scaffold can be readily achieved using dihydropyran.

In order to characterize the photocleavage event and the subsequent oxime ligation step at the molecular level, we first performed a solution study, attaching the 2-[(4,5-dimethoxy-2-nitrobenzyl)oxy]tetrahydro-2H-pyran module (NOTP) to a low molar mass poly(ethylene glycol) (PEG) as it allows reaction product analysis by mass spectrometry, in particular with a mild ionization method such as ESI-MS [BAR 11a, GRU 10]. It is important to note that the NOTP-functionalized molecules exhibit a maximum of absorption at 346 nm, yet also show significant absorption until at least 400 nm, making them interesting for applications where UV-sensitive compounds are involved. Particularly, we demonstrated the quantitative formation of a nitrosobenzaldehyde-capped PEG within 3 min of irradiation at room temperature using a low-cost compact fluorescent lamp with an emission wavelength of  $\lambda_{\text{max}} = 370$  nm ( $14 \text{ mW}\cdot\text{cm}^{-2}$ , 18 W). We subsequently showed that quantitative oxime ligation was achieved by stirring the PEG aldehyde overnight at room temperature in a solution of hydroxylamine hydrochloride, a model aminoxy compound. Despite the presence of by-products originating from side reactions of the nitroso substituent on the aromatic ring (dimerization, 2- and 4-electron reduction and condensation), all molecules possessed the desired aldoxime group, revealing the power of this methodology for surface functionalization along with a slightly reduced applicability for solution-based coupling. Upon

successful assessment of the newly designed methodology, we carried out subsequent surface functionalization using the aforementioned silane derivative. XPS analysis confirmed the attachment of an NOTP-functionalized layer onto the wafers without destruction of the nitro moiety and also evidenced complete disappearance of the signals corresponding to  $\text{NO}_2$  after 3 min of irradiation employing the previously described conditions. ToF-SIMS imaging of wafers having undergone a partial irradiation (using a photomask) further proved that  $\text{NO}_2$  and tetrahydro-2*H*-pyranyl fragments were not present – or at least in negligible amounts – in the irradiated zones. Finally, oxime-ligation-based photopatterning was performed by placing partially irradiated wafers for 16 h into solutions of both a perfluorinated aminoxy molecule, well suitable for easy detection by XPS and ToF-SIMS – as all halides – and an aminoxy-GRGSGR peptide sequence to demonstrate the suitability of our approach for biofunctionalization of substrates. The coupling step was in each case followed by careful rinsing to remove any physisorbed material. In both cases, ToF-SIMS analysis showed clear patterns of fragments originating from each molecule and XPS revealed a large increase in fluorine content in the previously irradiated areas. The phototriggered oxime ligation methodology is certainly interesting in the context of biofunctionalization as ONB-based photocaging has widely been employed in biomaterials science as well as in peptide-based applications.

A further light-based chemical method, which we have applied to pattern silicon wafers and can be applied in life sciences application due to its demonstrated biocompatibility *in vitro* and *in vivo*, is the NITEC approach. NITEC stands for *nitrile-imine-mediated tetrazole-ene cycloaddition* (Figure 9.1(f)). Here, the mechanism is also based on a photocleavage event after irradiation of a diaryl tetrazole moiety releasing a molecule of gaseous nitrogen and a very reactive nitrile imine dipole [CLO 67]. The generated dipole is able to react efficiently with an exceptionally broad spectrum of dipolarophiles ranging from significantly electron-deficient alkenes such as maleimides to non-activated alkenes, in particular strained ones such as norbornenes and cyclopropenes [BER 94, WAN 07, WAN 08]. In addition to its bioorthogonal reactivity, the main interesting feature of NITEC lies in the formation of a cycloadduct exhibiting intense fluorescence, which makes it interesting for labeling, yet also for direct visual assessment of the success of the reaction, which is a clear asset in surface patterning applications. Following our strategy of preassessing surface-photoinduced structuring, we initially assessed the power of the NITEC methodology on silicon wafers

before progressing to highly challenging cellulose modification (*vide infra*) [DIE 12]. As in the case of phototriggered oxime ligation, we carried out a primary investigation of this chemistry in solution, employing size-exclusion chromatography (SEC) and ESI-MS. We synthesized a diaryl tetrazole-capped PEG (Tet-PEG) by classic  $N,N'$ -dicyclohexylcarbodiimide (DCC) coupling and several maleimide end-functionalized polymers such as PEG and poly(methyl methacrylate) (PMMA) by either DCC coupling for the former or atom-transfer radical polymerization for the latter. Placed under a lamp classically employed for thin-layer chromatography (TLC) and irradiating at 254 nm, an equimolar mixture of Tet-PEG and maleimido-PEG underwent rapid coupling: after 5 min of irradiation, 50% had reacted and after 15 min, close to quantitative conversion was achieved. A similar outcome was observed when the maleimide-functionalized polymer was PMMA, producing an amphiphilic copolymer with a fluorescent moiety at the block junction.

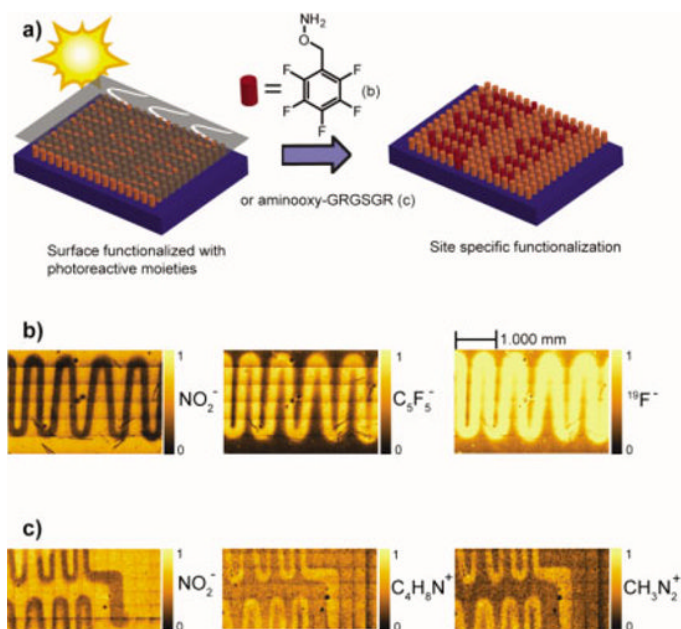


**Figure 9.2.** Schematic representation of the oxime-driven photopatterning of fluorine and peptide containing aminoxy species onto silicon wafers a) and ToF-SIMS ion maps of the fluorine b) and peptide c) species. The disappearance of the original  $\text{NO}_2$  species is also shown. The reaction sequence can be found in Figure 9.1(a). Reproduced with kind permission from Wiley-VCH from [PAU 12a]. For a color version of this figure, see [www.iste.co.uk/lalevee/dye.zip](http://www.iste.co.uk/lalevee/dye.zip)

As for the oxime ligation route, we subsequently went onto coating silicon wafers with a functionalized silane, in that case possessing a diaryl tetrazole group. XPS clearly showed the presence of the tetrazole moiety on the surface of the wafers and evidenced the loss of nitrogen after irradiation. When irradiation was carried out in the presence of maleimido-PMMA, a clear increase in carbonyl and saturated carbon contents was witnessed as well as a significant decrease in the silicon signal, revealing the effective attachment of the polymer.

We later extended the NITEC method to produce patterned photoresponsive surfaces that possess switchable wettability [BLA 13]. For this purpose, tetrazole-functionalized Si wafers prepared in the same way as before were patterned with maleimide derivatives containing either one or two azobenzene motifs through masked irradiation. Due to the absorption characteristics of the azobenzene group, irradiation at 254 nm with the aforementioned TLC lamp was unsuccessful in solution – low conversion at low power and decomposition at higher powers – and a more suitable lamp with a maximum of emission around 290–315 nm (out of the azobenzene absorption range) was employed. We initially carried out the full irradiation of the tetrazole-coated wafers in the presence of the azobenzene maleimide derivatives in order to confirm the occurrence of the reaction by XPS. Indeed, we found that the top layer of the irradiated wafers exhibited a lower content in nitrogen relative to carbon-based fragments due to the photoinduced formation of the nitrile imine accompanied by the loss of gaseous nitrogen and the grafting of the azobenzene derivatives. The attachment of the molecule containing two azobenzene motifs yielded a lower density as compared to the monofunctionalized counterpart, certainly due to the higher steric hindrance arising from the dendron-like structure of the former. Nevertheless, in both cases, the reaction was successful and was further employed for patterning using a photomask, as conclusively evidenced by ToF-SIMS imaging. Finally, the presence of the azobenzene derivatives could be simply demonstrated by exploiting the photoresponsive behavior of this motif. Indeed, azobenzene motifs can be isomerized by irradiating with UV light at appropriate wavelengths. The *trans* isomer is thermodynamically more stable but can be converted to the *cis* isomer by shining light in the 360 nm region. The *cis* isomer has a significantly higher dipole moment and therefore it is more hydrophilic. The system can be reverted back to the *trans* isomer through thermal isomerization – already effective at common laboratory room temperature – or subsequent irradiation, this time in the visible range. Therefore, we performed a

masked irradiation of the azobenzene-modified wafers at 355 nm and simply examined the behavior of water droplets. When a drop was deposited onto an area which was irradiated, it was not possible to move it using the tip of a glass pipette. However, on an area exposed to conditions supposed to lead to the presence of *trans* isomer, it was possible to easily drag the drop around. Interestingly, we did not measure any difference in the advancing water contact angle but found a significant difference of 10°–15° in the receding contact angle. This demonstrates that it is possible to use NITEC chemistry for patterning of photoreactive groups without harming their photophysical properties.

In the area of phototriggered 1,3-dipolar cycloadditions on surfaces, the work of Locklin and Popik on cyclopropanone-masked dibenzocyclooctynes is highly interesting. Indeed, Popik showed in 2003 that UV irradiation of a range of cyclopropanones yielded alkynes by decarbonylation [POL 03]. In the last decade, alkynes have been extensively used in organic chemistry and materials science in the framework of the popular conjugation method termed as “click chemistry”, i.e. copper-catalyzed azide-alkyne cycloaddition (CuAAC). Nevertheless, the necessity for copper has slightly tempered the excitement of the life science community until a copper-free approach was developed by Bertozzi (strain-promoted AAC, i.e. SPAAC), where a strained alkyne readily reacts with an azide derivative [AGA 04]. In this context, one of the most commonly encountered strained alkyne motifs is dibenzocyclooctyne, a diarylcyclooctyne, as it is rather straightforward to prepare [NIN 08]. Interestingly, the photolysis of diarylcyclopropanones – which produces diarylcyclooctynes – exhibits high quantum yields ( $\Phi$  up to 0.7) in solution and even higher in solid state through chemical amplification ( $\Phi > 1$ ) [KUZ 09]. Therefore, Locklin and Popik developed the idea of a phototriggered SPAAC and applied it for surface modification [ORS 10]. In order to bring the cyclopropanone moieties to the surface of silicon wafers, the authors chose to employ an approach different from direct silanization: activated ester polymer brushes were grown by surface-initiated ATRP and subsequently reacted with a cyclopropanone derivative bearing an amine group. As in the case of most deprotection-based methods, such as our oxime ligation work (see above), one of the advantages of the method is that the irradiation step can be decoupled from the coupling step in case the aim is to pattern-photosensitive (bio)molecules. Irradiating with a handheld UV lamp at 350 nm ( $3.5 \text{ mW}\cdot\text{cm}^{-2}$ ), 90% of the cyclopropanone moieties were decarbonylated in only 90 s. Full conversion could be reached in 150 s. A subsequent sequential procedure (masked irradiation, click, flood irradiation

and click) demonstrated the ability of this method for multicomponent patterning.

In addition to the NITEC method, we have explored the opportunity of employing another cycloaddition-based photochemistry for the grafting of (macro)molecules onto solid inorganic substrates: the so-called *photoenol* chemistry (Figure 9.1(c)). This methodology relies on *o*-methylbenzaldehyde or *o*-methylbenzylketone derivatives that can enter an isomerization equilibrium under UVA–UVC irradiation [SAM 76]. In that case, a diene is formed – one of the double bonds being actually an enol, hence the term photoenol – and in the presence of a suitable dienophile can undergo a DA cycloaddition. Particularly in the framework of polymer functionalization in solution, we have already evidenced that 2-methylbenzophenone worked well [GRU 11]. The reaction proceeds under mild conditions: neither heat nor a catalyst is required. In contrast to NITEC, the photoenol chemistry has the slight disadvantage of being not as fast in aqueous media as it is in organic ones – as far as it concerns the photoenol precursors we have tested – yet, it presents different features that can be advantageous depending on the context. For instance, the selectivity of the photoenol moiety can be adjusted by choosing the appropriate photoenol precursor: it either exclusively reacts with maleimide species or the more reactive version can also undergo efficient cycloaddition with acrylates and dithiobenzoates [WIN 12, OEH 13], while nitrile imines react with a very large range of enes, from maleimides and fumarates to non-activated enes such as 1-decene [WAN 07]. In addition, NITEC yields fluorescent products, which is a very interesting feature but may sometimes be undesirable.

In the study involving surface functionalization by photoenol chemistry, we introduced a novel 2-formyl-3-methylphenoxy (FMP) motif which we found more efficient than the 2-methylbenzophenone (at least in the conditions we used) [PAU 12b]. In particular, we demonstrated that complete cycloaddition could take place in minutes. Therefore, we aimed at bringing an FMP derivative onto surfaces in order to carry out patterning experiments. Again, we synthesized a silane derivative which we coated onto silicon wafers and assessed the success of the reaction by XPS and ToF-SIMS. The former confirmed the presence of the FMP moiety and the success of the photoinduced functionalization of a bromine-containing maleimide which can act as a polymerization initiator as we will describe below. We also showed by ToF-SIMS that it is possible to use the photoenol method in the framework of peptide immobilization.

Probably the most impressive example of the power of photoenol chemistry was its translation to 3D substrates [RIC 13]. In order to carry out photochemical reactions with full control in the three dimensions of space, the considered chemistry should be amenable to a two-photon activation with a low-energy irradiation, i.e. in the infrared (IR). In that case, generating a high density of photons in only a little volume – via a femtosecond pulsed laser – will only trigger the transition to the excited state in that volume and not outside of the focus where the photon density is too low for a molecule to absorb simultaneously two IR photons [FIS 13]. This implies that we first had to demonstrate the possibility of inducing the photoenol isomerization using a femtosecond pulsed IR laser. For this purpose, we immobilized the FMP silane onto glass slides to perform patterned irradiation with a direct laser writing (DLW) setup [DEU 04, KAW 01, LAF 07] at various scanning speeds and laser powers. To assess the success of the genuine 3D patterning, it was not possible to use XPS and ToF-SIMS anymore but confocal fluorescence microscopy could be employed and we therefore proceeded to pattern fluorescent molecules. We chose an indirect method and initially wrote patterns of protein ligands which could further form complexes with fluorescent proteins (as with the biotin–(strept)avidin couple, typically). We observed that the highest fluorescence (i.e. the most effective surface grafting) was obtained with an irradiation wavelength between 640 and 660 nm, which is precisely double the maximum of absorption of the FMP moiety. Laser powers as low as 5 mW yielded the maximal grafting efficiency. Therefore, we concluded that it was possible to transfer the methodology to 3D substrates. Notably, we managed to immobilize the FMP moiety onto organic–inorganic hybrid 3D microstructures possessing submicrometer features by a simple silanization step, as the original photoresist (Ormocomp) contains silane-functionalized methacrylates as well as orthosilicates. We demonstrated that precise patterning of discrete domains functionalized with two distinct proteins (rhodamine-labeled streptavidin and green fluorescent protein (GFP)) surrounded by passivated PEG areas was possible. A multi-step procedure was developed:

- 1) IR point irradiation of the FMP-functionalized 3D structures in the presence of a biotin maleimide solution;
- 2) IR point irradiation with a benzylguanine–maleimide solution (benzylguanine is the substrate for SNAP-tagged proteins [ENG 10, KEP 03, KIN 03]);
- 3) flood irradiation with a maleimide-functionalized PEG;

4) incubation in solutions of rhodamine-labeled streptavidin and SNAP-tagged GFP.

This sequence allowed us to produce well-defined 3D polymeric microstructures with arbitrary binary protein patterns (Figure 9.3). Such materials can find applications in the area of cell biology, in particular to manipulate the fate of cells as it is known that their behavior depends on geometrical, mechanical and chemical external cues.

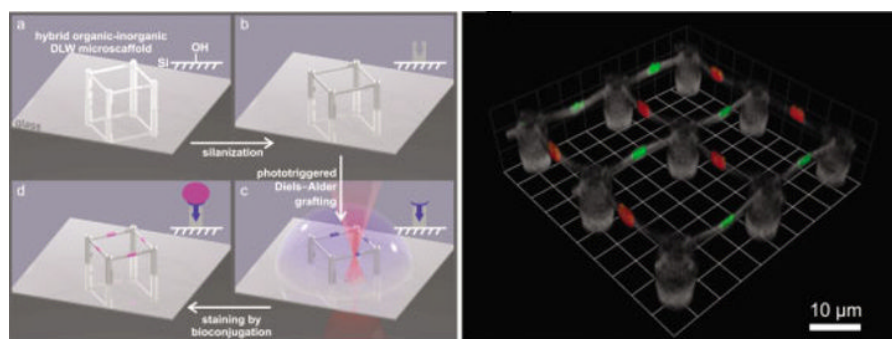


**Figure 9.3.** (Left) General strategy toward the spatially controlled photochemical functionalization of 3D organic–inorganic scaffolds. A 3D microcylinder scaffold made using Ormocomp is activated by plasma cleaning under argon a) and covalently coated with photoenol precursors by silanization b). The silanized microcylinder scaffold is covered with a solution of maleimide derivative (maleimide-biotin or maleimide-benzylguanine). Maleimides are locally covalently attached to the scaffold by laser-triggered Diels–Alder cycloaddition c). Finally, the molecular 3D patterns are stained by non-covalent or covalent bioconjugation with fluorescent proteins (rhodamine-labeled streptavidin, SA<sub>v</sub>–Cy3 or SNAP-tagged green fluorescent protein) d). (Right) Biotin (stained with SA<sub>v</sub>–Cy3, red) and benzylguanine (stained with GFP, green) patterned on separate beams, highlighting the ability to precisely position multiple functional groups by photoenol chemistry without altering the entire microcylinder surface. Reproduced with kind permission from Wiley-VCH from [RIC 13]. For a color version of this figure, see [www.iste.co.uk/lalevee/dye.zip](http://www.iste.co.uk/lalevee/dye.zip)

Photoenol chemistry was additionally employed to modify silver nanoparticles [STO 14]. The FMP moiety was installed at the surface by a ligand exchange method. Thus, a bifunctional molecule possessing a benzotriazole group at one end – able to displace the citrate capping agent stabilizing the Ag nanoparticle surface – and an FMP moiety at the other end was synthesized. The success of this introduction method could be assessed by a change in the zeta potential of the nanoparticles as well as by XPS characterization showing a clear decrease in carbonyl content (originally from the citrate). Subsequently, two maleimide-functionalized polymers,

namely PEG and poly(carboxybetaine methacrylate) (PCBMA), were grafted by irradiating the nanoparticles in their presence at 320 nm for 15 and 60 min, respectively. XPS analysis once more evidenced the success of the reaction, while zeta potential measurements clearly showed the presence of the zwitterionic polymer PCBMA at the surface of the nanoaggregates. Furthermore, high-resolution transmission electron microscopy coupled to energy-dispersive X-ray spectroscopy demonstrated that a thin polymer layer coated the Ag nanoparticle surface.

Simultaneously with our first report on surface-borne photoenol-based patterning [PAU 12b], Popik and Locklin reported a similar approach for surface functionalization where a diene (2-naphthoquinone-3-methide (*o*NQM)) is formed after UV irradiation of 3-(hydroxymethyl)naphthalene-2-ol (NQMP) [ARU 11a]. Strictly speaking, it is not an isomerization process (no direct equilibrium) but in the presence of water molecules, the unreacted *o*NQM is able to regenerate NQMP. From a structural point of view, *o*NQM resembles the *o*-quinodimethane produced by irradiation of FMP but exhibits a very different reactivity. Indeed, *o*NQM reacts only with electron-rich enes such as vinyl ethers and enamines in aqueous solution [ARU 11B]. As they did in their work on photoSPAAC (vide supra), the authors introduced the *o*NQM moieties in reactive polymer brushes grown onto Si wafers. Using a handheld UV lamp (300 nm, 3.5 mW·cm<sup>-2</sup>), it was possible to obtain patterns of fluorescent dyes (rhodamine and fluorescein) and reactive groups (azide and alkyne), as well as to immobilize biotin. This chemistry can be considered as complementary to the photoenol method as these two methods are efficient in distinct solvents and with different dienophiles.

Photoligation chemistries based on cycloadditions (e.g. photoenol and NITEC chemistries) have the key advantage of featuring a high (bio-)orthogonality. However, these techniques are beset with the challenge that ene moieties have to artificially be introduced into substrates. This aspect can sometimes be a significant challenge, specifically if the ligation point is to be introduced in a site-specific fashion. Thus, patterning methodologies are of importance that make use of inherently present functionalities such as those present in biomolecules or peptides. However, we have to keep in mind that such an approach will inherently lower the orthogonality of the employed process. The first process with this feature we introduced into the realm of surface patterning is based on *phenacyl sulfides* (Figure 9.1(b)), which represent photocaged thioaldehydes, which, in turn,

are highly reactive species able to undergo hetero DA reactions [VED 82, VED 86] as well as nucleophilic attacks by amines, thiols and aminoxy species, for instance [DUC 93]. The first reactivity of the thioaldehydes which we exploited is toward (open chain) dienes, including cyclopentadiene (Cp) as well as sorbic acid and sorbic alcohol [GLA 11]. Following our assessment strategy, the phenacyl-sulfide-based photochemical ligation strategy in its DA variant was initially tested in solution. For this purpose, a phenacyl sulfide terminal PEG was prepared from its OH terminal precursor and subjected to irradiation ( $\lambda_{\text{max}} = 355 \text{ nm}$ , 36 W, revolving sample vials with a single lamp) for 30 min at room temperature in the presence of an excess of variable dienes in dichloromethane. Under these conditions, quantitative conversion was achieved for all studied dienes (refer to Figure 9.4). Importantly, the generated thioaldehyde is orthogonal to carboxylic acid and alcohol functions.

Subsequently, a silanized variant of the phenacyl sulfide was generated and employed to cover an activated silicon wafer for the subsequent irradiation in the presence of a shadow mask with a Cp-capped PEG for 60 min in differently unchanged conditions from the corresponding solution experiments. The surface attachment of the initial phenacyl sulfide silane onto the surface and the subsequent patterning of PEG-Cp was evidenced via XPS for fully irradiated samples and ToF-SIMS for spatially resolved attachment (see Figure 9.4).

While the DA-driven trapping of the photolytically generated thioaldehydes is an attractive method for photochemical patterning of ene-containing substrates, these species can also be trapped in solution by variable nucleophiles under similar conditions as were required for the trapping of the dienes (see Figure 9.1(b), bottom reaction). In each case (amine, thiol and aminoxy), quantitative conversions were reached. Again, the surface patterning was evidenced by employing a phenacyl sulfide functional silicon wafer, which was photopatterned in the presence of various nucleophiles which carried atoms that can be readily identified via ToF-SIMS, i.e. bromine and fluorine (see Figure 9.5) [PAU 13a]. Interestingly, when using a thiol as nucleophile, the thioaldehyde trapping leads (in the presence of a base) to the formation of a disulfide connecting the grafted species to the surface, offering the possibility to using a reducing agent to remove the substrates from the surface.

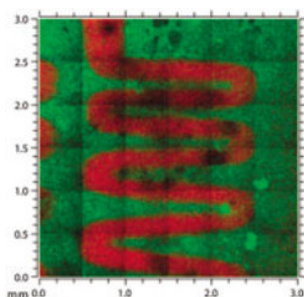
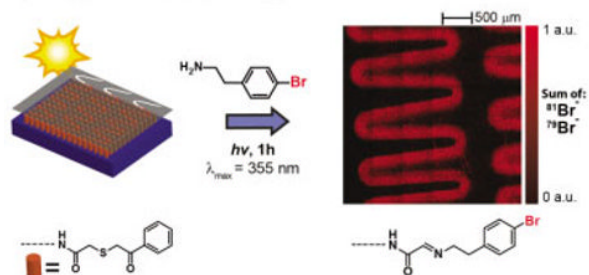


**Figure 9.4.** ToF-SIMS image resulting from the photolithographic patterning of PEGs onto phenacyl sulfide functional silicon wafers via a hetero Diels–Alder ligation. The red areas correspond to fragments associated with PEG, i.e.  $C_2H_4O^+$ ,  $C_3H_7O^+$ ,  $C_2H_3O^+$  and  $CH_3O^+$ . The underpinning phenacyl sulfide ligation reaction can be found in Figure 9.1(b) (top reaction pathway). Reproduced with kind permission from the Royal Chemical Society from [GLA 11]. For a color version of this figure, see [www.iste.co.uk/lalevee/dye.zip](http://www.iste.co.uk/lalevee/dye.zip)

**a) Locally constrained patterning of an amine**



**b) Locally constrained patterning of a polymer**

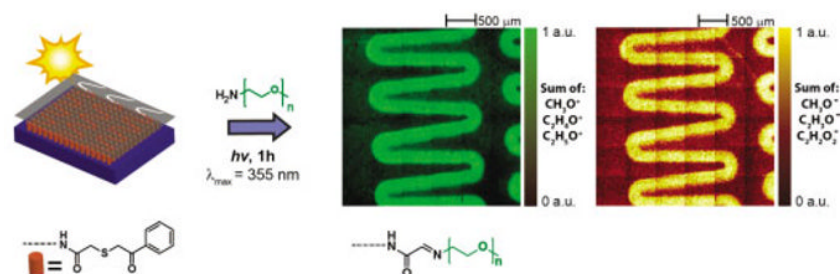


**Figure 9.5.** Trapping of nucleophiles, here amines, with photogenerated thioaldehydes and selected examples of ToF-SIMS images evidencing the successful spatially resolved surface grafting. The underpinning phenacyl sulfide ligation reaction can be found in Figure 9.1 b) (bottom reaction pathway). Reproduced with kind permission from the Royal Society of Chemistry from [PAU 13a]. For a color version of this figure, see [www.iste.co.uk/lalevee/dye.zip](http://www.iste.co.uk/lalevee/dye.zip)

<i>Phototriggered chemistry</i>	<i>Surfaces</i>	<i>Grafted species</i>	<i>Irradiation conditions</i>	<i>Patterning</i>	<i>Surface characterization</i>	<i>Reference</i>
<i>Oxime ligation</i>	Si wafers	Pentafluorophenylmethyl derivative GRGSGR peptide	$\lambda_{\text{max}} = 370 \text{ nm}$ , 14 mW cm <sup>-2</sup> , 18 W; 3 min, RT, dichloromethane	yes	XPS, ToF-SIMS	[PAU 12a]
<i>NITEC</i>	Si wafers	PMMA ( $M_n = 2,500 \text{ g mol}^{-1}$ , $D = 1.3$ )	$\lambda_{\text{max}} = 254 \text{ nm}$ ; 1.5 min, RT, ethanol	no	XPS	[DIE 12]
		Azobenzene	$\lambda_{\text{max}} = 290\text{--}315 \text{ nm}$ , 9 W; 2–6 h, RT, dichloromethane	yes	Contact angle, XPS, ToF-SIMS	[BLA 13]
<i>PhotoSPAAC</i>	Si wafers + polymer brushes	Rhodamine B, fluorescein	$\lambda_{\text{max}} = 350 \text{ nm}$ , 3.5 mW cm <sup>-2</sup> , 150 s, RT, neat	yes	UV-Vis spectroscopy, GATR-FTIR, fluorescence microscopy	[ORS 10]
<i>Photoenol-mediated Diels-Alder cycloaddition</i>	Si wafers	ATRP initiator PEG ( $M_n = 2,000 \text{ g mol}^{-1}$ )	$\lambda_{\text{max}} = 320 \text{ nm}$ , 36 W; 2 h, RT, dichloromethane	yes	XPS, ToF-SIMS	[PAU 12b]
		GRGSGR peptide	$\lambda_{\text{max}} = 320 \text{ nm}$ , 36 W; 2 h, RT, acetonitrile/PBS (3:1 v/v)	yes	ToF-SIMS	[PAU 12b]
	Glass slides	Biotin	$\lambda_{\text{max}} = 560\text{--}700 \text{ nm}$ Scanning femtosecond pulsed laser, 0–19.75 mW; 100 m s <sup>-1</sup> , RT, <i>N,N</i> -dimethyl formamide	yes	Confocal fluorescence microscopy	[RIC 13]
		PEG (600 g mol <sup>-1</sup> )	UVA, 250 mW cm <sup>-2</sup> , 250 W; 2 h, RT, <i>N,N</i> -dimethyl formamide	no	Confocal fluorescence microscopy	[RIC 13]
	3D organic-inorganic microscavolds	Biotin Benzylguanane	$\lambda_{\text{max}} = 560\text{--}700 \text{ nm}$ Scanning femtosecond pulsed laser, 0–19.75 mW; 100 m s <sup>-1</sup> , RT, <i>N,N</i> -dimethyl formamide	yes	Confocal fluorescence microscopy	[RIC 13]
		POEGMA (6,500 g mol <sup>-1</sup> , $D = 1.29$ )	UVA, 250 mW cm <sup>-2</sup> , 250 W; 2 h, RT, <i>N,N</i> -dimethyl formamide	no	Confocal fluorescence microscopy	[RIC 13]
	Ag nanoparticles	PEG (1,300 g mol <sup>-1</sup> ) PCBMA (21,700 g mol <sup>-1</sup> )	$\lambda_{\text{max}} = 320 \text{ nm}$ , 36 W; 15–60 min, RT, dimethyl sulfoxide	no	XPS, HRTEM, EDXS	[STO 14]

<i>o</i> NQM-mediated hetero-Diels-Alder cycloaddition	Si wafers or glass slides + polymer brushes	2-(vinylloxy)ethyl rhodamine B, propargyl vinyl diethylene glycol, azido(ethoxy)ethyl biotin	acetate, fluorescein, either of (2-azidoethoxy)ethyl vinyl ether, biotin	$\lambda_{\text{max}} = 300$ or $350$ nm, $3.5 \text{ W cm}^{-2}$ , 2 min and longer, RT, aqueous solution	yes	Ellipsometry, contact angle, GATR-FTIR, fluorescence microscopy	[ARU 11A]
Thioaldehyde-mediated hetero Diels-Alder cycloaddition	Si wafers	(1) Phenacyl sulfide capped PEG solution studies of phenacyl sulfide capped PEG with (2) 2,3-dimethyl-1,3-butadiene (3) <i>trans,trans</i> -2,4-hexadien-1-ol (4) cyclohexadiene (5) cyclopentadiene (6) <i>trans,trans</i> -2,4-hexadienoic acid (1) 2-(4-bromophenyl)ethanamine (2) monofunctional amino end capped poly(ethylene glycol) methyl ether (3) (4-bromophenyl) methanethiol with DIPEA (4) <i>o</i> -(2,3,4,5,6-pentafluorobenzyl)hydroxylamine hydrochloride	(1) Phenacyl sulfide capped PEG solution studies of phenacyl sulfide capped PEG with (2) 2,3-dimethyl-1,3-butadiene (3) <i>trans,trans</i> -2,4-hexadien-1-ol (4) cyclohexadiene (5) cyclopentadiene (6) <i>trans,trans</i> -2,4-hexadienoic acid	(1) $\lambda_{\text{max}} = 355$ nm; 2 h, RT, dichloromethane	yes	XPS, ToF-SIMS	[GLA 11]
Thioaldehyde-mediated nucleophilic addition	Si wafers	(1) 2-(4-bromophenyl)ethanamine (2) monofunctional amino end capped poly(ethylene glycol) methyl ether (3) (4-bromophenyl) methanethiol with DIPEA (4) <i>o</i> -(2,3,4,5,6-pentafluorobenzyl)hydroxylamine hydrochloride	(1) 2-(4-bromophenyl)ethanamine (2) monofunctional amino end capped poly(ethylene glycol) methyl ether (3) (4-bromophenyl) methanethiol with DIPEA (4) <i>o</i> -(2,3,4,5,6-pentafluorobenzyl)hydroxylamine hydrochloride	$\lambda_{\text{max}} = 355$ nm; 1 h, RT, (1)-(3) dichloromethane, (4) acetonitrile	yes	ToF-SIMS	[PAU 13a]
Phenylcane-based nucleophilic addition	Si wafers	(1) 2-(4-bromophenyl)ethanamine (2) c(RGDfK) (3) statherin peptide sequence	(1) 2-(4-bromophenyl)ethanamine (2) c(RGDfK) (3) statherin peptide sequence	$\lambda_{\text{max}} = 320$ nm; 40–60 h, 45 °C, (1) methanol, (2) dimethyl formamide, (3) dimethyl formamide/H <sub>2</sub> O (3:2 v/v)	yes	ToF-SIMS	[PAU 13b]

**Table 9.1.** Overview of the conjugation methods used for inorganic substrate modification including the reaction conditions and the grafted species involved

Nucleophile trapping via photochemically generated species is – as mentioned – an attractive route for the spatially resolved surface immobilization of species containing naturally occurring amine residues. In our experiments, a strategy based on phencyclone derivatives revealed to be particularly interesting, as it allows the decoupling of the irradiation step from the grafting process, since the photochemically generated species is shelf-stable [PAU 13b]. The *phencyclone* encoding sequence is schematically shown in Figure 9.1(e). The initial step is the reaction of the phencyclone derivative with a maleimide species leading to the photoreactive species. The subsequent photoactivation using a 36 W ( $\lambda_{\max} = 355$  nm) light source in a revolving reactor setup leads to decarbonylation and subsequent dehydrogenation, affording a species (see Figure 9.1(e), middle species) which is now open for nucleophilic attack in the carbonyl position, in analogy to the well-known phthalimide system. Following this, a silanized version of the photoreactive maleimide-phencyclone DA adduct was prepared and surface tethered onto an activated silicon wafer, which was subsequently photopatterned with a arginylglycylaspartic acid (RGD) as a model peptide system.

### 9.3. Bio and bioinspired surfaces

Our team has employed four of the above introduced and assessed phototriggered ligation techniques (i.e. nitroxide spin trapping modification [DEL 12a], phenacyl sulfide ligation in its DA variant [TIS 14a], photoenol and tetrazole chemistry [DIE 12, ROD 13, TIS 14b]) for the modification of cellulose in the form of fibrillar filter paper and/or spin-coated hyaluronan (HA), in a mild and efficient fashion, building on our experiences gained – in some cases – when employing them on inorganic substrates. These strategies represent an ideal platform for biosurface modifications as the mild reaction conditions ensure that the fibers of the cellulose are kept intact since harsh pretreatment or reaction conditions are excluded. Moreover, we employed other surfaces such as gold, polyethylene terephthalate and graphite as scaffolds for bioinspired coatings such as polydopamines (PDAs) and the aforementioned HA in order to develop interfaces allowing, for instance, the spatially resolved control of cell adhesion. These systems will also be covered in this section.

Cellulose, considered as a natural biosurface, is a remarkable biopolymer. It is the most widely generated organic polymer with an annual

bioproduction of more than  $10^{12}$  tons, and thus an important renewable resource [KLE 05] which is primarily used to produce cardboard or paper. Paper itself is a highly attractive candidate for modification as it is cheap, readily accessible and can often be easily disposed without harming the environment [KLE 05, MAR 07, PEL 09]. Innovative applications include paper-based biosensing devices, as liquids can simply be driven by capillary forces without the need of a pump. Currently, materials from paper sources meet new challenges, as low cost, fast, portable, sensitive and easy to use sensing devices are required in point of care diagnostics, for instance. Additionally, we chose HA as an appropriate scaffold for biomodification as in modern research, HA is of a high importance, e.g. in the lubrication and viscosity of joints [BUC 04]. The material has also a vital role in tissue repair and wound healing [CHE 99], embryonic development (by possibly creating hydrated channels for cell movement) [TOO 00], and interacts with cell receptors [BUR 11], yet is also associated with the generation of cancer metastasis [BHA 09]. Thus, HA is a highly interesting material for the application in tissue engineering in clinical usage [BUR 11, ALL 06, BAL 86, BEL 06].

As previously mentioned in the chapter, several approaches toward fast and efficient modifications of biosurfaces have been developed in our team. As mentioned in section 9.1, we only focus on modification strategies where the photoactive group is immobilized covalently onto the surface as this is the safest way to guarantee a high patterning resolution. To the best of our knowledge, there are only limited examples in the literature where the photoactive group is immobilized covalently to biosurfaces. Therefore, we only briefly present selected examples where photochemistry is related to biosurfaces in a broader context. For example, Biesalski and coworkers demonstrated a photochemical approach for the preparation of microstructured paper having millimeter-scale channels [BÖH 13]. Therefore, PMMA copolymers carrying photoreactive benzophenone functional groups are absorbed to the substrate by a dip-coating process. Subsequent UV irradiation with a photomask allowed covalent attachment of the PMMA copolymers. König and coworkers used the photo-Meerwein arylation reaction for the modification of coumarin-functionalized cellulose sheets [SCH 13b]. This catalytic process generates aryl radicals from diazonium salts in the presence of the photocatalyst  $[\text{Ru}(\text{bpy})_3]^{2+}$  upon irradiation with visible light that allows for the preparation of spatially resolved pattern. A different application was published by Huang and

coworkers [JIN 11]. The team prepared cellulose with a photoreversible wettability by self-assembly of 7-[(trifluoromethoxyphenylazo)-phenoxy] pentanoic acid monolayer onto titania ultrathin film precoated filter paper. Photoinduced patterning of hydrogels was described by Suri and Schmidt [SUR 09]. Here, photo-cross-linkable interpenetrating polymeric networks of collagen and HA were prepared featuring controlled biomechanical properties. Photoinduced spatially resolved grafting of caged thioaldehyde end-functionalized polystyrenes (PSs) on silicon wafers and glass slides via a two-photon DLW process was reported by Kaupp *et al.* [KAU 13]. Here, the spatially resolved grafting with a thioaldehyde ligation enables the preparation of any pattern with a submicrometer resolution.

The first approach for cellulose modification followed in the Barner-Kowollik team employs the photoinduced functionalization of photoinitiator-modified substrates with preformed *nitroxide*-functionalized macromolecules, which are derived from commercially available photoinitiators and nitroxides [DEL 12a]. The approach is based on the generation of radicals at the cellulose surface by mild UV irradiation ( $\lambda_{\max} \sim 311$  nm) of an immobilized photoinitiator, followed by radical trapping with a nitroxide species. To evaluate the new photochemical grafting method, preliminary studies were carried out based on the nitroxide end functionalization of PEG in solution. Moreover, the light-induced radical technique was used to couple two synthetic macromolecular strands.

The macromolecular covalent coating of cellulose filter paper was generated by irradiation of the sample placed in a solution of (2,2,6,6-tetramethylpiperidin-1-yl)oxyl (TEMPO) functionalized PS in toluene and irradiated 10 min on each side under ambient conditions. The samples, thoroughly rinsed with organic solvents, were analyzed by XPS and displayed a significantly different spectrum compared to the precursor materials. The main peak can clearly be associated with hydrocarbons (285.0 eV), revealing an efficient coverage of the surface with PS. Furthermore, a new low-intensity signal appearing close to 291.8 eV can unambiguously be assigned to a  $\pi-\pi^*$  transition arising from the presence of an aromatic system. Control experiments were conducted where virgin or photoinitiator-functionalized cellulose is incubated in a solution of nitroxide functional PS without irradiation. In both cases, the XPS spectrum remained unchanged. A further proof of the macroscopic modification of the cellulosic

substrate with PS was obtained by water contact angle measurement. While it was impossible to measure any contact angle for the virgin or photoinitiator-functionalized cellulose – the latter showed a slightly slower rate of water droplet absorption though – the PS-functionalized cellulose exhibited a contact angle of  $86^\circ$ , revealing a dramatic increase in hydrophobicity of the surface.

To achieve the aim of developing interesting and innovative (bio)materials, the highly efficient phototriggered *phenacyl sulfide chemistry*, *NITEC chemistry* and *photoenol chemistry* were selected as appropriate linkage methods to spatially encode different solid substrates such as gold, poly(ethylene terephthalate) (PET) and graphite as well as cellulose substrates and HA. The photoligation reactions proceed rapidly under very mild reaction conditions, do not require a catalyst and are thus very attractive for (spatially controlled) biosubstrate modifications. *Phenacyl sulfide chemistry*, for instance, was applied to cellulose modification [TIS 14a]. The characteristics of this chemistry are described above and will therefore not be reiterated here. The generated photoactive cellulose is able to react with both open chain and ring-strained dienes. To demonstrate the high photochemical reactivity of the phenacyl-sulfide-decorated cellulose, two routes have been followed, in particular the conjugation of a Cp-capped poly(trifluoroethyl methacrylate) (Cp-PTFEMA;  $M_n = 4,400 \text{ g mol}^{-1}$ ,  $D = 1.18$ ), which was employed as an easy to track chemical marker for XPS and ToF-SIMS analysis, and an open-chain diene-functionalized RGD containing peptide. After the successful preparation of the photoreactive cellulose via carbodiimide-mediated esterification with the phenacyl sulfide moiety, irradiation ( $\lambda_{\text{max}} = 355 \text{ nm}$ ) was performed to ligate the fluorinated polymer. To underpin the versatility of the phenacyl sulfide approach, an open chain diene functional RGD containing peptide was ligated photochemically to the cellulose. Both spatially resolved functionalization approaches give a convincing patterning in the ToF-SIMS images which depicts the characteristic fragments of both the immobilized PTFEMA and the RGD containing peptide. The ToF-SIMS results were supported by XPS analysis before and after functionalization, giving the expected binding energies for the coated surfaces with the fluorinated polymer as well as the peptide.

As for silicon-based surfaces, the profluorescent character of the *NITEC reaction* is a highly attractive tool for the functionalization of biosubstrates

such as fibrillar cellulose materials as the success of the reaction can easily be tracked due to the fluorescent character of the formed pyrazoline linkage. In 2012, the first NITEC-based report in the context of surface modification was published by our group, exploring the tetrazole ligation on polymeric substrates in solution as a prestudy and the application of tetrazole ligation for surface modification on silicon wafers (*vide supra*) [DIE 12]. After the successful grafting onto silicon wafers, the functionalization of a more complex system – cellulose – was investigated. The same carboxy containing diaryl tetrazole was covalently bounded to the cellulose by esterification of the primary alcohol present in the sugar repeating unit. The tetrazole-functionalized cellulose was subsequently immersed in a solution of  $\alpha$ -maleimido PMMA in ethanol and irradiated at 254 nm at room temperature for 10 min on each side and left to stand in the polymer solution for a further 50 min before being washed with different solvents and dried under vacuum. XPS data support the formation of a grafted methacrylic polymer layer. Indeed, in comparison to the cellulose characteristic peaks, a clear increase in the C–C/C–H signal (285.0 eV) is observed on the one hand and in the O = C–O signal (289.2 eV) on the other hand. Within the experimental uncertainties, all measured binding energies are similar to those found for the Si-based system.

As a complementary surface characterization technique, Fourier transform IR microscopy (FT-IRM) was additionally employed. FT-IRM functionality mapping is ideally suited for the investigation of microspheres [KAU 13, KAU 12, KAU 14a] or cellulose substrates [GOL 11, HAN 12a, HAN 12b, TIS 12] having a fibrillar nature in the micrometer dimension, as shown in several studies of the Barner–Kowollik team. The integration range corresponding to the characteristic cellulose signals of the C–O stretching vibration ( $950\text{--}1,200\text{ cm}^{-1}$ ) can readily be detected. The carbonyl spectral region ( $1,675\text{--}1,765\text{ cm}^{-1}$ ), corresponding to PMMA lateral ester groups, can also be visualized. Although a carbonyl bond is introduced onto the cellulose after the tetrazole functionalization, it is not visible as its amount is too low to be detected with the focal plane array detector. The sample obtained from the reaction of PMMA with the tetrazole-functionalized cellulose is clearly much richer in carbonyl groups than the control sample (non-photoreactive cellulose was employed), where no distinguishable peak is visible. This result corroborates the attribution of the carbonyl to the presence of the polymer on the surface of the cellulose fibers and proves that no polymer is physically adsorbed to the surface. In direct support of the

macromolecular conjugation experiments, the appearance of fluorescence provides a direct visualization method to assess the success of the grafting reaction. Indeed, all the samples that proved to have been functionalized when analyzed by XPS or FT-IRM exhibited fluorescence. An additional proof that polymer grafting only occurred on the non-masked part is provided by the change of physical properties due to the presence of a hydrophobic polymer such as PMMA on the surface. While a water droplet can be observed on an irradiated sample for several tens of minutes without any drastic morphological change, a similar experiment with a control sample led to instantaneous absorption of the droplet. Consequently, water-based contact angle measurements were carried out. Due to the inherent roughness and absorbing nature of the cellulose surface, such a measurement is not straightforward. Indeed, it is generally very difficult to obtain a value for the pristine cellulose due to the aforementioned fast absorption. However, in the present case, the control sample is not native cellulose but a tetrazole-functionalized cellulose. The unaltered wetting behavior when going from the virgin cellulose to the tetrazole-functionalized cellulose is rather interesting, since it shows that before polymer grafting, the sample properties are not drastically altered by the presence of the tetrazole. On the contrary, the part that was irradiated became very hydrophobic exhibiting a water contact angle of  $126^\circ$ . In addition to the grafting of a hydrophobic polymer and to evidence the power of the combination of modern polymer chemistry and NITEC to yield functional materials, the covalent coating of a thermo- and pH-sensitive polymer as well as an antibacterial polymer was carried out as evidenced by FT-IRM. Similarly, simple fluorescence observation revealed the presence of the pyrazoline linkage.

The photopatterning of various substrates was later achieved for different applications, e.g. paper with non-fouling bioactive properties [TIS 14b] or surfaces for cell guiding [ROD 13]. Facing the challenge of translating bioactive paper to real applications, a new strategy for the spatially resolved patterning of non-fouling brushes on cellulose and the immobilization of key biomolecules as new platforms for biosensing was developed. The approach represents the first spatially resolved functionalization of paper with non-fouling polymer brushes as well as functional protein entities. In this example, NITEC chemistry was combined with the excellent resistance to fouling of poly(carboxybetaine acrylamide) (PCBAAM) brushes and the versatility of streptavidin for subsequent conjugation with biotin containing

biomacromolecules. Streptavidin – a protein with a molecular weight of close to 53 kDa – can indeed bind up to four biotinylated molecules, having one of the highest affinities found in biology ( $K_D \sim 10^{-14}$  mol L<sup>-1</sup>), close in strength to a covalent bond. The convenient modification of our previously reported tetrazole [DIE 12] by addition of a methoxy group in the *para* position of the 2-N-phenyl ring allowed the photoexcitation wavelength to be shifted from the UVC to UVA region ( $\lambda \approx 320$  nm). The modification resulted in considerably milder reaction conditions than our previous report [DIE 12], allowing for the functionalization of more sensitive (bio)systems. The tetrazole acid chloride derivative was esterified with the hydroxyl moieties of cellulose. Two pronounced signals in the N1s orbital X-ray photoelectron spectra appear at 400.4 and 402.7 eV that can be attributed to the tetrazole species ( $-\text{N}=\text{N}-$ ) and to the probably positively charged nitrogen, respectively. Subsequently, the tetrazole-functionalized surface was subjected to the phototriggered NITEC reaction with a maleimide-functionalized tertiary bromide in order to grow non-fouling brushes of PCBAAm by surface-initiated single-electron transfer living radical polymerization (SET-LRP). The PCBAAm brushes fully prevented the fouling of fetal calf serum, one of the most strongly fouling biofluids [ROD 12], evidencing the non-fouling property of the paper. The spatial control of the immobilized PCBAAm brushes was evidenced by ToF-SIMS imaging. Here, the composition analysis was based on the presence of the  $\text{CNO}^-$  fragment (41.99 u, assigned to the maleimide moiety, where the nitrogen is adjacent to the carbonyl group) and the  $\text{C}_3\text{H}_2\text{N}_2^-$  fragment (65.99 u, assigned to the pyrazoline ring, which is formed in the photoconjugation reaction). The presence of the  $\text{C}_7\text{H}_5\text{N}^-$  fragment originating from the tetrazole moiety represents the remaining non-reacted tetrazole. Additional evidence for the successful grafting was obtained by FT-IRM. Two integration regions are displayed in Figure 9.6: (left images) 950–1,200 cm<sup>-1</sup>, associated with the fingerprint region of cellulose and (right images) 1,500–1,700 cm<sup>-1</sup>, associated with the two carbonyl signals of the PCBAAm brushes. The initiator-functionalized cellulose exhibits a strong absorbance in the cellulose signal region (Figure 9.6(a)), whereas no significant carbonyl signal is visible in the carbonyl region (Figure 9.6(b)). In contrast, the PCBAAm-grafted cellulose displays pronounced signals in the carbonyl region (Figure 9.6(d)), evidencing that the fibers are fully coated with PCBAAm brushes, which is corroborated by the weak absorption in the corresponding cellulose region (Figure 9.6(c)).

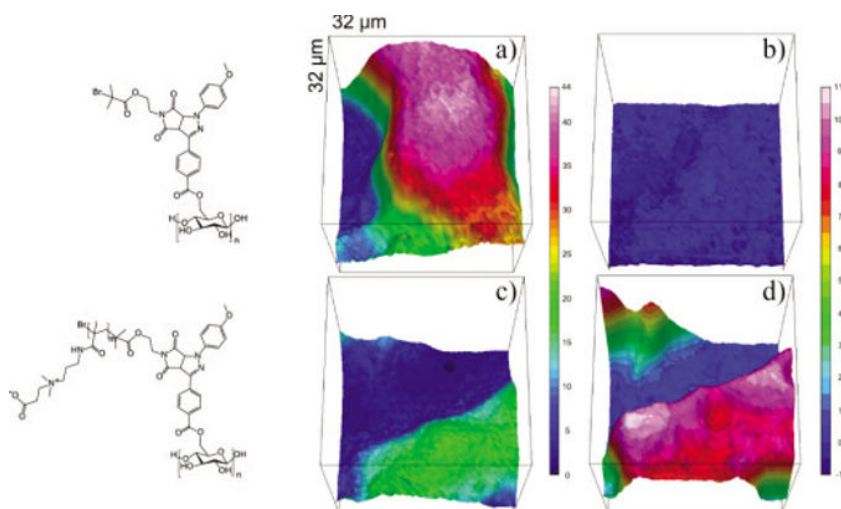


**Figure 9.6.** High-resolution FT-IR microscopy images of an initiator-functionalized cellulose fiber (top a) and b)) and PCBAAM-grafted cellulose fibers (bottom c) and d)). Comparison of the integration values of the cellulose fingerprint vibrations ( $950\text{--}1,200\text{ cm}^{-1}$ ) of a) and c) and the polymer signal ( $1,500\text{--}1,700\text{ cm}^{-1}$ ) of b) and d). Intensity increases from blue to red displayed in the scales on the right side indicating the successful grafting of PCBAAM from the functional cellulose substrate. Reproduced with kind permission from Wiley from [TIS 14b]. For a color version of this figure, see [www.iste.co.uk/lalevee/dye.zip](http://www.iste.co.uk/lalevee/dye.zip)

To modify the surfaces entirely (and not spatially resolved as shown with PCBAAM in the previous example) with streptavidin, the tetrazole-functionalized cellulose filter papers were immersed in a solution of maleimide-functionalized streptavidin in phosphate-buffered saline and irradiated. The success of the streptavidin immobilization was ascertained by XPS analysis. A significant increase in the C-C/C-H compared to the tetrazole-functionalized surfaces is in agreement with the presence of the protein on the cellulose fibers. Additionally, a significant increase from 6.0 at % to approximately 11.6 at% is observed in the N1s spectrum. The visual proof can be depicted by the remarkably bright fluorescence (excitation wavelength  $\lambda_{\text{max}} = 366\text{ nm}$ ), whereas the control sample shows, as expected, no fluorescence. It is envisioned that the strategy can be translated to the development of novel bioactive papers and microfluidic paper-based analytical devices necessary for forthcoming developments in medicine.

For the fabrication of interfaces with precise control of cell adhesion, the NITEC conjugation protocol was combined with the resistance of poly(oligoethylene glycol methyl ether methacrylate) (poly(MeOEGMA)) brushes and the versatility of bioinspired PDA surfaces (see Figure 9.7).

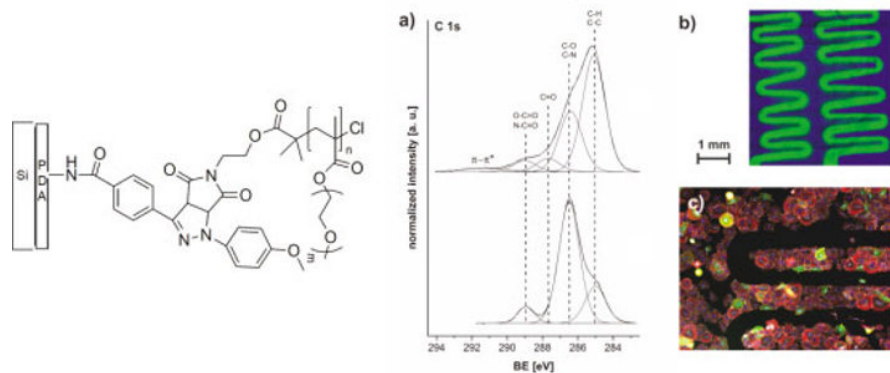


**Figure 9.7.** Preparation of photopatterned poly(MeOEGMA) brushes from polydopamine-coated silicon wafers via surface-initiated ATRP having cell adhesion resistance. a) XPS characterization and comparison of the C 1s spectra of the ATRP initiator surface and the surface after surface-initiated polymerization of MeOEGMA via ATRP; b) ToF-SIMS overlay image constructed from ion maps of the OEG fragments  $C_2HO^-$ ,  $C_2H_3O^-$  and  $C_2H_2O_2^-$  (meander structure) and the CN<sup>-</sup> fragment for the non-patterned polydopamine (PDA) area image; c) cell pattern after 7 h culture, fixation and staining of the cells. Reproduced with kind permission from Wiley-VCH from [ROD 13]. For a color version of this figure, see [www.iste.co.uk/lalevee/dye.zip](http://www.iste.co.uk/lalevee/dye.zip)

In the present example, the combination of NITEC chemistry with PDA surfaces and non-fouling polymer brushes (poly(MeOEGMA)) could raise light-triggered chemistries to a new level. PDA coatings were prepared by the spontaneous polymerization of dopamine in TRIS buffer at pH = 8. PDA films not only adhere to virtually any surface but also have shown to enhance attachment, proliferation and phenotypic maintenance of cells as well have shown strong resistance to proteolytic enzymes [HAL 12, KU 10, WAN 13]. The universal character of dopamine-driven adhesion to any surface combined with the spatial and temporal control and the bioorthogonality of the photoinduced techniques opens a platform to a range of functional materials. A tetrazole moiety was attached to the PDA-coated substrates as confirmed by XPS, ellipsometry and water contact angle measurements followed by subjection to the NITEC reaction with a maleimide-functionalized ATRP initiator evidenced by XPS as well as

wettability studies. The thickness increases 1.4 nm as confirmed by ellipsometry. The poly(MeOEGMA) brushes were grown by surface-initiated ATRP employing a shadow mask. Within 30 min, ellipsometry analysis confirmed the growth of 15 nm-thick brushes of a dry sample.

The investigated system could provide resistance toward cell adhesion of rat embryonic fibroblasts by precisely patterning poly(MeOEGMA) brushes. Only the areas that were covered by the photomask (where no polymerization of poly(MeOEGMA) was initiated) are covered with the cells. The image in the lower right corner of Figure 9.7 shows the merged image of the attached cells on the photopatterned surface. The surfaces were exposed with transfected rat embryonic fibroblasts at 1 h intervals on the vasodilator-stimulated phosphoprotein (VASP) allowing for the facile identification of focal contacts and cell matrix adhesion. Here, the cells were fixed and stained for the nuclei with 4',6-diamidino-2-phenylindole (DAPI, blue), the actin cytoskeleton and the VASP with a GFP and paxilin (green) to visualize the cells that precisely follow the photochemically generated pattern. It was shown that the rat embryonic fibroblasts have multiple focal contact points in the non-irradiated areas. The study clearly reveals the applicability of the NITEC reaction in cellular-sensitive environments as well as the application in biomedical devices.

Further access to spatially resolved functional interfaces is achieved via *photoenol chemistry* by introducing a novel photoreactive molecule onto a 3,4-dihydroxy-L-phenylalanine (DOPA) scaffold [PRE 14]. Thus, a photoenol-functionalized molecule bearing a DOPA moiety was prepared that can polymerize under alkaline conditions in a similar fashion as PDA and DOPA groups [BAL 77, DIS 09, SWA 70] forming ultrathin films on virtually any surface. Consequently, the photoenol moiety is available on the entire surface, regardless of the topography or shape of the substrate, attributed to the covalent binding of the photoenol moiety. The system allows the modification of several materials of different topographies and surface energy (Au, PET and graphite) modified with different polymers and peptides. Gold substrates are relevant for biomedical and biosensing applications, and thus were chosen as substrate of choice. PET was especially employed to demonstrate photoligation of peptide sequences on a flexible substrate which is commonly employed in biomedical devices. The photoreactive surface was irradiated with an Arimed B6 UV lamp ( $\lambda_{\max} = 320$  nm) to form an *o*-xylylene intermediate which further reacts in a DA reaction with maleimide end capped polymers or a

maleimide-functionalized peptide sequence that contains the amino acid sequence Gly-Arg-Gly-Asp-Ser. All surfaces were characterized by XPS. In order to evidence the spatial control of the photoreactive biomimetic system, the ligation of a maleimide-functionalized PTFEMA was studied by employing a shadow mask during irradiation as the fluorinated polymer provides fragments ( $F^-$ ,  $CF_3^-$ ) in ToF-SIMS which unambiguously evidence the patterning structure. After 12 h of incubation in the aqueous solution of photoenol DOPA, the substrates exhibited a visible change in color ascribed to the oxidation of catechol followed by polymerization. Importantly, after coating, it was found that the contact angle of surfaces with initially very different surface energy – the advancing water contact angle of Au is  $53^\circ$  and of PET  $79^\circ$  – becomes identical ( $87^\circ$ ), thus demonstrating that the current approach shares the substrate-independent film-forming nature of PDOPA and DOPA melanine. The chemical composition, assessed by XPS, further supports the presence of the DOPA-based coating.

Spatially resolved functionalization via photoenol chemistry cannot only be applied on planar surfaces as described above, but also on cellulose and HA for the spatially controlled conjugation of synthetic polymers and peptides [BAL 77, DIS 09, SWA 70, TIS 13]. The general strategy is depicted in Figure 9.8.

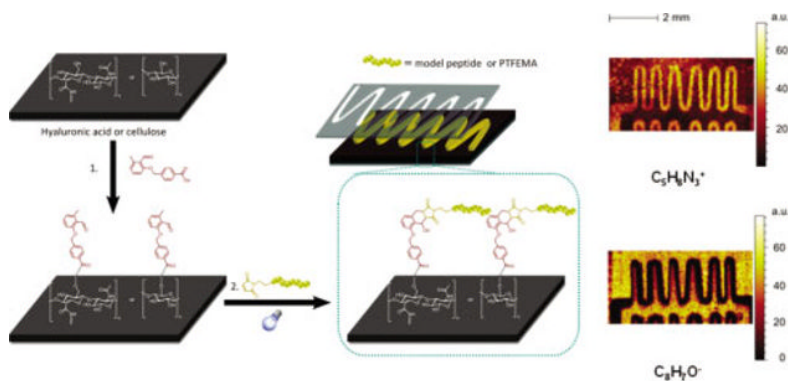


**Figure 9.8.** Modification of hyaluronan or cellulose via photoenol chemistry. When the FMP moiety is tethered to a surface, spatially controlled surface modification can be achieved with either a peptide sequence or a polymer strand. Right: ToF-SIMS images of GIGKFLHS-grafted HA with mapping of  $C_3H_8N_3^+$  corresponding to the peptide sequence (top) and  $C_8H_7O^-$  corresponding to a fragment of the photoenol moiety (bottom) on the non-peptide functional areas of the hyaluronan surface, where the photoenol moieties persist. Reproduced with kind permission from ACS from [TIS 13]. For a color version of this figure, see [www.iste.co.uk/lalevee/dye.zip](http://www.iste.co.uk/lalevee/dye.zip)

To demonstrate the broad field of application of the photoenol approach, synthetic polymers and a peptide (GIGKFLHS, part of the sequence of Magainin I) were used. The surfaces were functionalized with 4-((2-formyl-3-methylphenoxy)methyl)benzoic acid via carbodiimide-mediated coupling. PTFEMA ( $M_n = 3,700 \text{ g mol}^{-1}$ ,  $D = 1.27$ ) and the peptide GIGKFLHS were grafted onto thin HA films and cellulose (filter paper) surfaces. The tethering of both the peptide and the polymer strand onto the surfaces was characterized in detail via ellipsometry, surface plasmon resonance (SPR) spectroscopy and atomic force microscopy (AFM). The success of the spatially resolved surface functionalization is evidenced by XPS as well as ToF-SIMS. To generate the bioactive surfaces, HA was tethered covalently on amine-functionalized surfaces, thus resulting in a higher stability of the layer and allows for a reproducible analysis such as SPR, XPS and ToF-SIMS. In contrast, simple absorption would favor desorption from the surface. Grafting of HA on the silicon wafers resulted in a homogeneous layer with a thickness of 7 nm determined by spectroscopic ellipsometry. To estimate the mass of HA that can be attached to the surface, SPR spectroscopy was used allowing the determination of the kinetics of the covalent immobilization of HA on amine-functionalized SAMs resulting in a fast immobilization within 30 min and reaching a plateau after 1 h. The grafting density of tethered HA was estimated, suggesting a grafting density of  $7.9 \times 10^7$  to  $9.5 \times 10^7$  chains  $\text{cm}^{-2}$ . The homogeneity of the HA films was monitored via AFM. The cellulose-based photoenol surfaces were generated using a carbodiimide-mediated esterification approach. In a subsequent step, the photoreactive surfaces were photopatterned utilizing a photomask (as described in the previous examples) to pattern the maleimide-functionalized PTFEMA by placing the wafer in a sample holder and irradiating with UV light. To monitor and image the spatial resolution, ToF-SIMS mapping of the functionalized surface evidences the clear spatially controlled patterning. Similarly, the peptide pattern was imaged by mapping the expected fragments of the photoenol moiety ( $\text{C}_8\text{H}_7\text{O}^-$ ) and the peptide ( $\text{C}_5\text{H}_8\text{N}_3^+$ ). For the peptide-functionalized cellulose, the characteristic peptide fragments  $\text{CNO}^-$  and  $\text{CN}^-$  were detected showing the typical meander structure. The fibrous structure of the cellulose makes the precise spatial control challenging; however, the images evidence a clear photopatterning.

Photo-triggered chemistry	Surfaces	(Bio)Polymers grafted	Irradiation conditions	Patterning	Surface characterization	Reference
Nitroxide spin trapping	Cellulose	PEG ( $M_n = 2,000 \text{ g mol}^{-1}$ ) PS ( $M_n = 2,000 \text{ g mol}^{-1}$ , $\bar{D} = 1.09$ )	$\lambda_{\text{max}} = 311 \text{ nm}$ ; $2 \times 10 \text{ min}$ , RT, toluene	no	XPS	[DEL 12a]
Thioaldehyde-mediated Diels-Alder cycloaddition	Cellulose	PTFEMA ( $M_n = 4,400 \text{ g mol}^{-1}$ , $\bar{D} = 1.18$ ) Arg-Gly-Asp (RGD) containing peptide sequence	$\lambda_{\text{max}} = 355 \text{ nm}$ ; 2 h, RT in DCM (PTFEMA DMF (peptide sequence))	yes	XPS, ToF-SIMS	[TIS 14a]
NITEC	1) Cellulose	PMMA ( $M_n = 2,500 \text{ g mol}^{-1}$ , $\bar{D} = 1.30$ ) PDMAEMA ( $M_n = 6,120 \text{ g mol}^{-1}$ , $\bar{D} = 1.37$ ) Quaternized PDMAEMA	$\lambda_{\text{max}} = 254 \text{ nm}$ ; 2 h, RT, DMF	yes	XPS, FT-IR microscopy imaging, UV/VIS, contact angle	[DIE 12]
	2) Cellulose	Poly(carboxybetaine acrylamide) Streptavidin	$\lambda_{\text{max}} = 320 \text{ nm}$ ; 2 h, RT, DCM	yes (PCBAAM) no (Streptavidin)	For PCBAAM: XPS, ToF-SIMS, FT-IR microscopy imaging For Streptavidin: XPS, UV/VIS, fouling studies	[TIS 14b]
	3) Polydopamine on SiO <sub>2</sub>	Poly(oligoethylene glycol methyl ether methacrylate)	$\lambda_{\text{max}} = 320 \text{ nm}$ ; 1 h, RT, DCM	yes	XPS, ToF-SIMS, cell adhesion studies	[ROD 13]
Photoenol-mediated Diels-Alder cycloaddition	1) Polydopamine coating	PTFEMA ( $M_n = 4,400 \text{ g mol}^{-1}$ , $\bar{D} = 1.18$ ) PEG ( $M_n = 900 \text{ g mol}^{-1}$ , $\bar{D} = 1.09$ ) Arg-Gly-Asp (RGD) containing peptide sequence	$\lambda_{\text{max}} = 320 \text{ nm}$ ; overnight, RT, Tris buffer, ethanol	yes	XPS, ToF-SIMS, contact angle	[PRE 14]
	2) Cellulose, Hyaluronan	PTFEMA ( $M_n = 4,400 \text{ g mol}^{-1}$ , $\bar{D} = 1.18$ ) Peptide (GIGKFLHS)	$\lambda_{\text{max}} = 320 \text{ nm}$ ; 2 h, RT, DMF	yes	XPS, ToF-SIMS, contact angle, SPR, ellipsometry, AFM	[TIS 13]

**Table 9.2.** Overview of the conjugation methods used for biosurface modification including the reaction conditions and (bio)polymers involved

## 9.4. Cross-linking

In contrast to the previous two sections where the common procedure was based on covalently linking the surface material with the photosensitive compounds, an entirely different approach will be discussed in this section. Although covalent binding of particular compounds that are capable of undergoing photoligation reactions to the substrate is a powerful tool, an early established straightforward method for surface modifications is realized via network formation of the desired material on the substrate. Cross-linking polymeric species usually yields insoluble material which cannot be removed by washing procedures and only mechanical force can break the adhesive interaction between network and surface. Another advantageous aspect of the cross-linking approach for surface modification is the fact that it is applicable to a large variety of substrates since the cross-linking chemistry itself does not necessarily depend on the surface properties of the substrate.

Photochemical techniques play a vital role in the context of cross-linking polymeric materials. A variety of light-triggered approaches has been explored to gain spatial control over the cross-linking process. In this chapter, the most common techniques for forming networks in a light-induced fashion will be discussed, starting with typical radical cross-linking polymerization. A similar approach is based on multifunctional acrylate photoresists, whereas epoxide-based photoresists are more related to the cross-linking polymerization of oxetane-functionalized polymer backbones. Photochemical dimerization reactions are also suitable techniques to achieve efficient cross-linking, e.g. through coumarin, anthracene, thymine or cinnamate moieties [KAU 14b]. Finally, modern light-induced conjugation methods, such as thiol-ene, photoenol or NITEC, have entered the stage of cross-linking chemistry, which significantly increases the available chemical toolbox. All the chemical approaches listed above have been applied to a large variety of applications, ranging from dental care [PAR 99, RUE 97, YOS 94] over simple two-dimensional (2D) patterning [KHI 06] to the generation of light emissive patterns [MUL 03] and 3D structures with attached fluorescent dyes [QUI 13]. A selection of publication highlights will be introduced for each cross-linking method, thereby demonstrating the current state of the art in light-triggered surface modifications via cross-linking.

The first and most feasible route for photochemical cross-linking is based on a radical mechanism connecting double bond containing molecules via a polymerization procedure. Therefore, typical photoinitiators such as benzophenone are suitable for generating radicals to either cross-link polymer chains by hydrogen abstraction [OST 59] or initiate the polymerization of mixtures of multifunctional monomers, so-called photoresins [REI 89]. These photoresins found their first application in the field of dental care, where UV-initiated curing of viscous material is supposed to yield a robust surface coating [RUE 97]. In further studies on the mechanical properties of cross-linked polymer blends [TAN 04], polyethylene surfaces [FAL 03] and melts [RÅN 98], as well as multiphase systems [HAR 97], the phototriggered process was explored and established. Sophisticated applications were generated by incorporating functional materials into the cross-linked films, such as the modification with azide compounds enabling the immobilization of biomolecules on the polymer surface [YAN 94]. Later, radical-based cross-linking systems were employed for producing pattern of cross-linked material, making use of the spatial control which is the unique advantage of light-induced processes. Patterning, as mentioned previously, can be realized by employing a shadow mask which allows the cross-linking reaction to proceed only in the illuminated regions. Thus, a variety of applications were explored, including the patterning of Langmuir–Blodgett films by cross-linking monolayers of amphiphilic block copolymers [MIY 98] and the incorporation of fluorescent species producing light emissive pattern at a micrometer scale [PAR 99, YUA 07]. Other fields of application with constantly increasing impact include optoelectronics. For example, hole transporting materials were produced by radically photo-cross-linking triphenylenes [BEC 99], modulated optical diffraction gratings were generated *via* photolithographic patterning of electroactive polymer films [SCH 96], and the photo-cross-linking of conjugated polymers could be used for realizing three color polymer light emitting diodes [DEN 09].

An alternative type of cross-linking mechanism is based on epoxy resins. A large field of research depends on this type of chemistry, which proceeds via polymerization of multifunctional epoxide moieties in combination with a photoinitiator. The applicability of such a system led to the production of a commercially available photoresist – SU-8 – developed by IBM in 1989 [GEL 89]. Furthermore, SU-8 is involved in hundreds of patents and thousands of journal articles about photolithography in general or micro-electromechanical systems (MEMS). A detailed overview concerning the

applications of SU-8 photo-cross-linking would exceed the scope of this chapter; therefore, the reader is referred to the corresponding literature [DEU 04, JAM 11, TOE 05]. Nevertheless, in this section, we would like to introduce a related type of cross-linking technique which is less popular than the SU-8 chemistry, yet at least as efficient with regard to applications in the field of optoelectronics. The cationic ring opening polymerization of oxetane compounds can readily be employed for producing networks by using multifunctional oxetane moieties, or attaching oxetane units to the backbone of preexisting polymer chains – a method that has been proven to work efficiently for a large variety of conjugated polymer backbones [CHA 12]. Thus, for example, blue-light-emitting diodes could be produced from a monomer containing two oxetane units [MÜL 00]. Moreover, oxetane-functionalized polymers luminescent in red, green and blue could be consecutively photo-cross-linked in desired areas fabricating a pixelated RGB matrix display [MUL 03].

From a chemical point of view, the cross-linking techniques discussed above are basically cross-polymerization reactions yielding hardly characterized linking points. In contrast to the cross-polymerization approach, dimerization reactions are well understood, in depth analyzed processes, which can also be used for generating networks [KAU 14b]. In the following, selected examples of photochemical dimerization reactions will be discussed. Each of them proved to be an advanced tool for producing surface modifications via interconnecting polymer chains. In addition, the photochemical dimerization reactions of species such as coumarin, anthracene, thymine and cinnamate can be reversed, which adds another feature to the set of surface chemistry methodologies. The photoreaction of coumarin-based polyesters, for instance, provides the opportunity of generating complementary surface patterns, based on the different irradiation wavelengths necessary for cross-linking (350 nm) or de-cross-linking and polymer chain scission (254 nm) [MAD 13]. Employing the anthracene approach, honeycomb-structured films were produced, which can be photochemically cross-linked and patterned on an additional level by reversing the dimerization reaction [CON 08]. Incorporating thymine-pendant groups into polymers enables entering water-based media. Thus, surface coating via photo-cross-linking of environmentally benign copolymers in an aqueous medium could be achieved [BAR 10], as well as patterning from water-based photoresists of copolymers [TRA 06] and terpolymers [BIA 07]. To date, the cinnamate approach is the most widely applied photochemical dimerization reaction for surface modifications.

Originally, cinnamate cross-linking of polymers was used for incorporation of fluorescent acidic dyes [M'BO 84], whereas most efforts are directed into the development of optoelectronics, e.g. blue-light-emitting copolymers [LI 97], optical writing in liquid crystal cells [YAM 08], electrochromic-conjugated films [KUM 08], pattern of hole-transport material for light-emitting diodes [DOM 03] and organic transistors [QIU 11].

A modern and rapidly growing field of chemical research concerns the discovery of efficient conjugation reactions, which are termed as “click” reactions [KOL 01]. Ten years after the definition of “click” chemistry, the “click” criteria for chemical reactions were adapted to polymer science by Barner-Kowollik *et al.* [BAR 11b]. Also, numerous photochemical methods that fulfill these criteria were developed [TAS 13]. Since efficient light-triggered reactions are a valuable tool for surface cross-linking, the photoinitiated thiol–ene reaction was employed for designing novel photoresists, which were, for instance, applied for surface patterning of ultrathin films [KHI 06] or rapid prototyping of multilayer thiol–ene fluidic chips [NAT 08]. Moreover, by cross-linking polyfluorenes via thiol–ene chemistry, electroluminescent networks could be photopatterned [DAV 11], and additionally, the cross-linking of conjugated polymers with tunable band gaps could be realized [BAY 12]. Furthermore, hole transporting surface coatings were produced for solution-processed multilayer light-emitting diodes [LEE 14]. DLW represents another advanced application for light-triggered thiol–ene chemistry. Subsequent to the introduction of thiol–ene chemistry to DLW via 3D photo fixation of DA networks [ADZ 12], the light-induced reaction itself was used to form processable 3D microstructures (i.e. woodpile photonic crystals). Since the surface of the cross-linked material still contains residual photoreactive groups, precise patterning of those surfaces with fluorescent dyes could be demonstrated [QUI 13]. In addition to thiol–ene reactions, there are other efficient light-induced ligation methods conforming with the concept of “click” chemistry which have been introduced above, e.g. photoenol chemistry [OEH 13] and NITEC [WIL 14]. DLW was again the first application for a photosensitive mixture of multifunctional photoenol and polymeric maleimide species forming a photoresist – a combination that had already attracted industrial attention [SCH 13a]. In the DLW study, woodpile photonic crystals with a rod distance of less than 500 nm were fabricated and the residual-surface-exposed photoenol moieties were subsequently employed for patterning a bromine bearing compound with high spatial resolution [QUI 14].

The final section of this chapter will give a detailed example for an in-depth study exploring a novel cross-linking technique and its application for surface patterning [MUE 14]. We reported a fusion of the concepts of NITEC photoligation with cross-linking of unsaturated commercial polybutadienes (PBs) to establish a methodology for patterning fluorescent material on arbitrary surfaces in a sunlight-induced process (Figure 9.9).

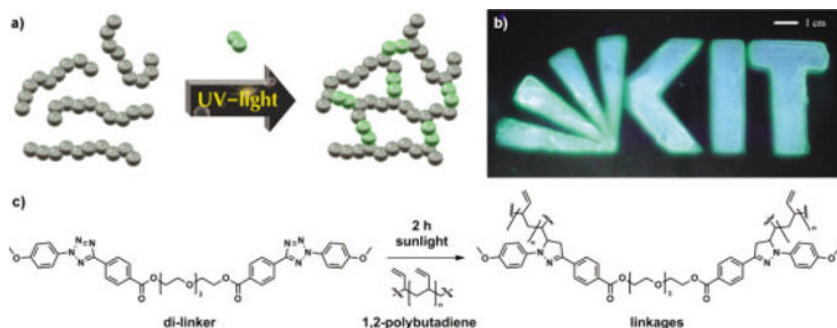


**Figure 9.9.** a) General scheme for the light-induced cross-linking process; b) fluorescent gel pattern of the Karlsruhe Institute of Technology (KIT) logo obtained by NITEC on a glass substrate; c) structures of the dilinker (left), 1,2-polybutadiene (middle) and the fluorescent linkages (right) produced by irradiation in sunlight. Reproduced with kind permission from the Royal Society of Chemistry from [MUE 14]. For a color version of this figure, see [www.iste.co.uk/lalevee/dye.zip](http://www.iste.co.uk/lalevee/dye.zip)

First, a newly designed linker compound consisting of two photosensitive diaryl-substituted tetrazoles – similar to those already described above – joined by a tetra(ethylene glycol) spacer was designed in order to provide (i) a polar basis for good solubility in polar photoreaction media and ionization properties in ESI-MS, (ii) high reactivity toward non-activated carbon-carbon double bonds and (iii) absorption of light in the near UV region. A small-molecule study with 1-pentene was conducted to investigate the proposed photochemical process. Therefore, detailed characterization of the small-molecule model study was performed by SEC, UV-Vis and fluorescence spectroscopies, as well as ESI-MS, which was also the analytical tool for monitoring the progress of the reaction (100% conversion in 20 min). The cross-linking process itself was subsequently investigated using two PBs of disparate molar masses, which were each photo-cross-linked with the dilinker. In order to optimize the cross-linking process, the

reaction parameters such as concentration, dilinker fraction and reaction time were adjusted. The monitoring was carried out by SEC analysis of the reaction with low molecular weight PB and gravimetric determination of gel fractions resulting from the reaction with high molar mass PB. The applicability of the novel cross-linking technology for generating spatially controlled highly fluorescent gel patterns was finally demonstrated in a very feasible approach. The solvent-casted mixture of linker and PB was covered with a shadow mask and irradiated for 2 h with sunlight. After washing away the soluble non-irradiated material, the remaining fluorescent material in shape of the Karlsruhe Institute of Technology (KIT) logo (see Figure 9.9) proves the successful introduction of a low-cost light-triggered technology platform for surface modifications via photopatterning polymers carrying non-activated double bonds.

## 9.5. Conclusion

Light-driven chemistries should ideally fulfill a series of requirements to be attractive for encoding highly defined polymer strands or biomolecules onto surfaces. These requirements include operation at room temperature, the absence of any catalyst, fast reaction times, simple synthetic preparation and chemical as well as bio-orthogonality. Herein, we have surveyed our most recent advances in the field of spatially resolved surface functionalization on inorganic 2D and 3D substrates as well as biomaterial surfaces, using techniques where the light-reactive functionality is tethered onto the surface to be modified. These approaches include photoenol chemistry, tetrazole-based approaches as well those relying on phenacyl sulfides, phencyclones, photoinitiators and ONB derivatives. Each technique has its particular advantages ranging from the formation of fluorescent linkages (tetrazoles) to being particularly versatile (phenacyl sulfides). Figure 9.10 compiles a critical evaluation of the chemistries we have employed so far for the functionalization, and in most cases, the patterning of surfaces and which were presented in Figure 9.1. While the starting materials involved in the phencyclone, phenacyl sulfide, and the nitroxide trapping methods are rather readily obtainable, these methods suffer from weaker features such as either a low product yield or a particular sensitivity to air or the solvent type. However, the most effective ligation strategies in terms of reaction rate or product yield (oxime ligation and photoenol) require more synthetic steps. All these criteria should serve as guidelines to select the appropriate chemistry by considering the experimental effort that can be

dedicated to setting up the photoreactive system, the type of molecules to be grafted and the context (orthogonality issue).

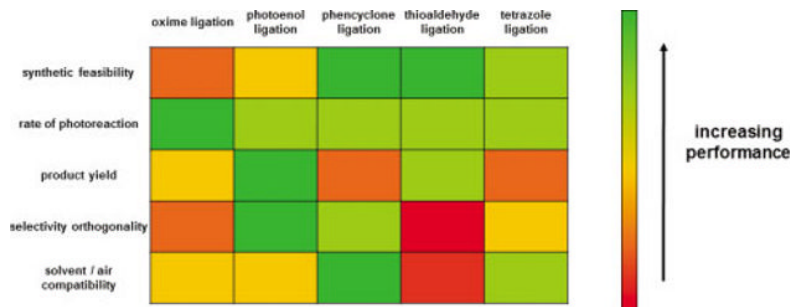


**Figure 9.10.** A user guide for the critical evaluation of the various photochemistries employed in our lab for the phototriggered functionalization of surfaces. See Figure 9.1 for the chemical details of the involved reaction pathways. For a color version of this figure, see [www.iste.co.uk/lalevee/dye.zip](http://www.iste.co.uk/lalevee/dye.zip)

## 9.6. Bibliography

- [ADZ 12] ADZIMA B.J., KLOXIN C.J., DEFOREST C.A. *et al.*, “3D Photofixation Lithography in Diels–Alder Networks”, *Macromolecular Rapid Communications*, vol. 33, pp. 2092–2096, 2012.
- [AGA 04] AGARD N.J., PRESCHER J.A., BERTOZZI C.R., “A Strain-Promoted [3 + 2] Azide–Alkyne Cycloaddition for Covalent Modification of Biomolecules in Living Systems”, *Journal of the American Chemical Society*, vol. 126, pp. 15046–15047, 2004.
- [ALL 06] ALLISON D.D., GRANDE-ALLEN K.J., *Tissue Engineering*, vol. 12, pp. 2131–2140, 2006.
- [AN 13] AN P., YU Z., LIN Q., “Design of oligothiophene-based tetrazoles for laser-triggered photoclick chemistry in living cells”, *Chemical Communications*, vol. 49, pp. 9920–9922, 2013.
- [ARU 11a] ARUMUGAM S., ORSKI S.V., LOCKLIN J. *et al.*, “Photoreactive Polymer Brushes for High-Density Patterned Surface Derivatization Using a Diels–Alder Photoclick Reaction”, *Journal of the American Chemical Society*, vol. 134, pp. 179–182, 2011.
- [ARU 11b] ARUMUGAM S., POPIK V.V., “Light-Induced Hetero-Diels–Alder Cycloaddition: A Facile and Selective Photoclick Reaction”, *Journal of the American Chemical Society*, vol. 133, pp. 5573–5579, 2011.

- [BAL 77] BALDRY P.A., SWAN G.A., “Studies related to the chemistry of melanins. Part 15. The electron transfer and free radical properties of dopa-melanin”, *Journal of the Chemical Society, Perkin Transactions*, vol. 2, pp. 1346–1350, 1977.
- [BAL 86] BALAZS E.A., LAURENT T.C., JEANLOZ R.W., *Biochemical Journal*, vol. 235, pp. 903, 1986.
- [BAR 10] BARBARINI A.L., REYNA D.L., MARTINO D.M., “The effect of light intensity, film thickness, and monomer composition in styrene-based bioinspired polymers”, *Green Chemistry Letters and Reviews*, vol. 3, pp. 231–237, 2010.
- [BAR 11a] BARNER-KOWOLLIK C., DELAITTRE G., GRUENDLING T. *et al.*, “Elucidation of Reaction Mechanisms and Polymer Structure: Living/Controlled Radical Polymerization”, *Mass Spectrometry in Polymer Chemistry*, Wiley-VCH Verlag GmbH & Co. KGaA, pp. 373–403, 2011.
- [BAR 11b] BARNER-KOWOLLIK C., DU PREZ F.E., ESPEEL P. *et al.*, “Polymers or Just Efficient Linking: What Is the Difference?”, *Angewandte Chemie International Edition*, vol. 50, pp. 60–62, 2011.
- [BAY 12] BAYCAN KOYUNCU F., DAVIS A.R., CARTER K.R., “Emissive Conjugated Polymer Networks with Tunable Band-Gaps via Thiol–Ene Click Chemistry”, *Chemistry of Materials*, vol. 24, pp. 4410–4416, 2012, 2012.
- [BEC 99] BACHER A., ERDELEN C.H., PAULUS W. *et al.*, “Photo-Cross-Linked Triphenylenes as Novel Insoluble Hole Transport Materials in Organic”, *Macromolecules*, vol. 32, pp. 4551–4557, 1999.
- [BEL 06] BELLAMY N., CAMPBELL J., ROBINSON V. *et al.*, *Cochrane Database Systematic Reviews*, CD005321, 2006.
- [BER 94] BERTRAND G., WENTRUP C., “Nitrile Imines: From Matrix Characterization to Stable Compounds”, *Angewandte Chemie International Edition*, vol. 33, pp. 527–545, 1994.
- [BHA 09] BHARADWAJ A.G., KOVAR J.L., LOUGHMAN E. *et al.*, “Spontaneous Metastasis of Prostate Cancer Is Promoted by Excess Hyaluronan Synthesis and Processing”, *American Journal of Pathology*, vol. 174, pp. 1027–1036, 2009.
- [BIA 07] BIANCHINI J.R., SAITO K., BALIN T.B. *et al.*, “Thymine-based, Water-soluble Phototerpolymers: Their Preparation and Synthesis”, *Journal of Polymer Science Part A: Polymer Chemistry*, vol. 45, pp. 1296–1303, 2007.
- [BLA 13] BLASCO E., PIÑOL M., ORIOL L. *et al.*, “Photochemical Generation of Light Responsive Surfaces”, *Advanced Functional Materials*, vol. 23, pp. 4011–4019, 2013.

- [BÖH 13] BÖHM A., GATTERMAYER M., TRIEB C. *et al.*, “Photo-attaching functional polymers to cellulose fibers for the design of chemically modified paper”, *Cellulose*, vol. 20, pp. 467–483, 2013.
- [BUC 04] BUCCI L. R., PH D., TURPIN A.A., *Journal of Applied Nutrition*, vol. 54, pp. 10–33, 2004.
- [BUR 11] BURDICK J.A., PRESTWICH G.D., “Hyaluronic Acid Hydrogels for Biomedical Applications”, *Advanced Materials*, vol. 23, pp. H41–H56, 2011.
- [CHA 12] CHARAS A., MORGADO J., “Oxetane-functionalized Conjugated Polymers in Organic (Opto)Electronic Devices”, *Current Physical Chemistry*, vol. 2, pp. 241–264, 2012.
- [CHE 99] CHEN W.Y.J., ABATANGELO G., “Functions of hyaluronan in wound repair”, *Wound Repair and Regeneration*, vol. 7, pp. 79–89, 1999.
- [CLO 67] CLOVIS J.S., ECKELL A., HUISGEN R. *et al.*, “1.3-Dipolare Cycloadditionen, XXV. Der Nachweis des freien Diphenylnitrilimins als Zwischenstufe bei Cycloadditionen”, *Chemische Berichte*, vol. 100, pp. 60–70, 1967.
- [CON 08] CONNALL L.A., VESTBERG R., HAWKER C.J. *et al.*, “Fabrication of Reversibly Crosslinkable, 3-Dimensionally Conformal Polymeric Microstructures”, *Advanced Functional Materials*, vol. 18, pp. 3315–3322, 2008.
- [D’IS 09] D’ISCHIA M., NAPOLITANO A., PEZZELLA A. *et al.*, “Chemical and Structural Diversity in Eumelanins: Unexplored Bio-Optoelectronic Materials”. *Angewandte Chemie International Edition*, vol. 48, pp. 3914–3921, 2009.
- [DAV 11] DAVIS A.R., MAEGERLEIN J.A., CARTER K.R., “Electroluminescent Networks via Photo “Click” Chemistry”, *Journal of the American Chemical Society*, vol. 133, pp. 20546–20551, 2011.
- [DEL 12a] DELAITTRE G., DIETRICH M., BLINCO J.P. *et al.*, “Photo-Induced Macromolecular Functionalization of Cellulose via Nitroxide Spin Trapping”, *Biomacromolecules*, vol. 13, pp. 1700–1705, 2012.
- [DEL 12b] DELAITTRE G., PAULOEHRL T., BASTMEYER M. *et al.*, “Acrylamide-Based Copolymers Bearing Photoreleasable Thiols for Subsequent Thiol–Ene Functionalization”, *Macromolecules*, vol. 45, pp. 1792–1802, 2012.
- [DEN 09] DENG X., WONG K.Y., “Cross-Linked Conjugated Polymers for Achieving Patterned Three-Color and Blue Polymer Light-Emitting Diodes with Multi-Layer Structures”, *Macromolecular Rapid Communications*, vol. 30, pp. 1570–1576, 2009.

- [DEU 04] DEUBEL M., VON FREYMAN G., WEGENER M. *et al.*, “Direct laser writing of three-dimensional photonic-crystal templates for telecommunications”, *Nature Materials*, vol. 3, pp. 444–447, 2004.
- [DIE 12] DIETRICH M., DELAITRE G., BLINCO J.P. *et al.*, “Photoclickable Surfaces for Profluorescent Covalent Polymer Coatings”, *Advanced Functional Materials*, vol. 22, pp. 304–312, 2012.
- [DOM 03] DOMERCQ B., HREHA R.D., ZHANG Y.-D. *et al.*, “Photo-Patternable Hole-Transport Polymers for Organic Light-Emitting Diodes”, *Chemistry of Materials*, vol. 15, pp. 1491–1496, 2003.
- [DUC 93] DUCHENET V., VALLEE Y., “The reaction of thiols with electron-deficient thioaldehydes. A new synthesis of unsymmetrical disulfides”, *Journal of the Chemical Society, Chemical Communications*, pp. 806–807, 1993.
- [ENG 10] ENGIN S., TROUILLET V., FRANZ C.M. *et al.*, “BenzylguanineThiol Self-Assembled Monolayers for the Immobilization of SNAP-tag Proteins on Microcontact-Printed Surface Structures”, *Langmuir*, vol. 26, pp. 6097–6101, 2010.
- [FAL 03] FALLANI F., RUGGERI G., BRONCO S. *et al.*, “Modification of surface and mechanical properties of polyethylene by photo-initiated reactions”, *Polymer Degradation and Stability*, vol. 82, pp. 257–261, 2003.
- [FIS 13] FISCHER J., WEGENER M., “Three-dimensional optical laser lithography beyond the diffraction limit”, *Laser & Photonics Reviews*, vol. 7, pp. 22–44, 2013.
- [FOR 12] FORS B.P., HAWKER C.J., “Inside Back Cover: Control of a Living Radical Polymerization of Methacrylates by Light”, *Angewandte Chemie International Edition*, vol. 51, pp. 8901–8901, 2012.
- [FUK 14] FUKAMINATO T., HIROSE T., DOI T. *et al.*, “Molecular Design Strategy toward Diarylethenes That Photoswitch with Visible Light”, *Journal of the American Chemical Society*, 2014.
- [GEL 89] GELORME J.D., COX R.J., GUTIERREZ S.A.R., Photoresist composition and printed circuit boards and packages made therewith, US Patent 4882245 A, IBM Corporation, 1989.
- [GLA 11] GLASSNER M., OEHLenschlaeger K.K., GRUENDLING T. *et al.*, “Ambient Temperature Synthesis of Triblock Copolymers via Orthogonal Photochemically and Thermally Induced Modular Conjugation”, *Macromolecules*, vol. 44, pp. 4681–4689, 2011.

- [GOL 11] GOLDMANN A.S., TISCHER T., BARNER L. *et al.*, “Mild and Modular Surface Modification of Cellulose via Hetero Diels–Alder (HDA) Cycloaddition”, *Biomacromolecules*, vol. 12, pp. 1137–1145, 2011.
- [GRU 10] GRUENDLING T., WEIDNER S., FALKENHAGEN J. *et al.*, *Polymer Chemistry*, vol. 1, pp. 599–617, 2010.
- [GRU 11] GRUENDLING T., OEHELENSCHLAEGER K.K., FRICK E. *et al.*, “Rapid UV Light-Triggered Macromolecular Click Conjugations via the Use of o-Quinodimethanes”, *Macromolecular Rapid Communications*, vol. 32, pp. 807–812, 2011.
- [HAL 12] HALLER C.M., BUERZLE W., KIVELIO A. *et al.*, “Mussel-mimetic tissue adhesive for fetal membrane repair: An ex vivo evaluation”, *Acta Biomaterialia*, vol. 8, pp. 4365–4370, 2012.
- [HAN 12a] HANSSON S., TISCHER T., GOLDMANN A.S. *et al.*, “Visualization of poly(methyl methacrylate) (PMMA) grafts on cellulose via high-resolution FT-IR microscopy imaging”, *Polymer Chemistry*, vol. 3, pp. 307–309, 2012.
- [HAN 12b] HANSSON S., TROUILLET V., TISCHER T. *et al.*, “Grafting Efficiency of Synthetic Polymers onto Biomaterials: A Comparative Study of Grafting-from versus Grafting-to”, *Biomacromolecules*, vol. 14, pp. 64–74, 2012.
- [HAR 97] HARADA A., TRAN-CONG Q., “Modulated Phases Observed in Reacting Polymer Mixtures with Competing Interactions”, *Macromolecules*, vol. 30, pp. 1643–1650, 1997.
- [HOF 08] HOFFMANN N., “Photochemical Reactions as Key Steps in Organic Synthesis”, *Chemical Reviews*, vol. 108, pp. 1052–1103, 2008.
- [JAM 11] JAMAL M., ZARAFSHAR A.M., GRACIAS D.H., “Differentially photocrosslinked polymers enable self-assembling microfluidics”, *Nature Communications*, vol. 2, pp. 527, 2011.
- [JIN 11] JIN C., YAN R., HUANG J., “Cellulose substance with reversible photo-responsive wettability by surface modification”, *Journal of Materials Chemistry*, vol. 21, pp. 17519–17525, 2011.
- [KAM 10] KAMMARI L., ŠOLOMEK T., NGOY B.P. *et al.*, “Orthogonal Photocleavage of a Monochromophoric Linker”, *Journal of the American Chemical Society*, vol. 132, pp. 11431–11433, 2010.
- [KAU 12] KAUPP M., VOGT A.P., NATTERODT J.C. *et al.*, “Modular design of glyco-microspheres via mild pericyclic reactions and their quantitative analysis”, *Polymer Chemistry*, vol. 3, pp. 2605–2614, 2012.

- [KAU 13] KAUPP M., TISCHER T., HIRSCHBIEL A.F. *et al.*, “Photo-Sensitive RAFT-Agents for Advanced Microparticle Design”, *Macromolecules*, vol. 46, pp. 6858–6872, 2013.
- [KAU 14a] KAUPP M., QUICK A.S., RODRIGUEZ-EMMENEGGER C. *et al.*, “Photo-Induced Functionalization of Spherical and Planar Surfaces via Caged Thioaldehyde End-Functional Polymers”, *Advanced Functional Materials*, vol. 24, pp. 5649–5661, 2014.
- [KAU 14b] KAUR G., JOHNSTON P., SAITO K., “Photo-reversible dimerisation reactions and their applications in polymeric systems”, *Polymer Chemistry*, vol. 5, pp. 2171–2186, 2014.
- [KAW 01] KAWATA S., SUN H.-B., TANAKA T. *et al.*, “Finer features for functional microdevices”, *Nature*, vol. 412, pp. 697–698, 2001
- [KEP 03] KEPPLER A., GENDREIZIG S., GRONEMEYER T. *et al.*, “A general method for the covalent labeling of fusion proteins with small molecules *in vivo*”, *Nature Biotechnology*, vol. 21, pp. 86–89, 2003.
- [KHI 06] KHIRE V.S., HARANT A.W., WATKINS A.W. *et al.*, “Ultrathin Patterned Polymer Films on Surfaces Using Thiol–Ene Polymerizations”, *Macromolecules*, vol. 39, pp. 5081–5086, 2006.
- [KIN 03] KINDERMANN M., GEORGE N., JOHNSON N. *et al.*, “Covalent and Selective Immobilization of Fusion Proteins”, *Journal of the American Chemical Society*, vol. 125, pp. 7810–7811, 2003.
- [KLA 12] KLÁN P., ŠOLOMEK T., BOCHET C.G. *et al.*, “Photoremovable Protecting Groups in Chemistry and Biology: Reaction Mechanisms and Efficacy”, *Chemical Reviews*, vol. 113, pp. 119–191, 2012.
- [KLE 05] KLEMM D., HEUBLEIN B., FINK H.-P. *et al.*, “Cellulose: Fascinating Biopolymer and Sustainable Raw Material”, *Angewandte Chemie International Edition*, vol. 44, pp. 3358–3393, 2005.
- [KOL 01] KOLB H.C., FINN M.G., SHARPLESS K.B., “Click Chemistry: Diverse Chemical Function from a Few Good Reactions”, *Angewandte Chemie International Edition*, vol. 40, pp. 2004–2021, 2001.
- [KOT 09] KOTZUR N., BRIAND B., BEYERMANN M. *et al.*, “Competition between cleavage and decarboxylation in photolysis of [small alpha]-carboxy-2-nitrobenzyl protected cysteine derivatives”, *Chemical Communications*, 3255–3257, 2009.
- [KU 10] KU S.H., PARK C.B., “Human endothelial cell growth on mussel-inspired nanofiber scaffold for vascular tissue engineering”, *Biomaterials*, vol. 31, pp. 9431–9437, 2010.

- [KUM 08] KUMAR A., JANG S.-Y., PADILLA J. *et al.*, “Photopatterned electrochromic conjugated polymer films via precursor approach”, *Polymer*, vol. 49, pp. 3686–3692, 2008.
- [KUZ 09] KUZMANICH G., GARD M.N., GARCIA-GARIBAY M.A., “Photonic Amplification by a Singlet-State Quantum Chain Reaction in the Photodecarbonylation of Crystalline Diarylcyclopropenones”, *Journal of the American Chemical Society*, vol. 131, pp. 11606–11614, 2009.
- [LAF 07] LAFRATTA C.N., FOURKAS J.T., BALDACCHINI T. *et al.*, “Multiphoton Fabrication”, *Angewandte Chemie International Edition*, vol. 46, pp. 6238–6258, 2007.
- [LEE 14] LEE J., HAN H., LEE J. *et al.*, “Utilization of “thiol-ene” photo cross-linkable hole-transporting polymers for solution-processed multilayer organic light-emitting diodes”, *Journal of Materials Chemistry*, vol. 2, pp. 1474–1481, 2014.
- [LI 97] LI X.-C., YONG T.-M., GRÜNER J. *et al.*, “A blue light emitting copolymer with charge transporting and photo-crosslinkable functional units”, *Synthetic Metals*, vol. 84, pp. 437–438, 1997.
- [M'BO 84] M'BON G., ROUCOUX C., LABLACHE-COMBIER A. *et al.*, “Photochemistry of polymeric systems. VI. Photocrosslinking of basic polymers and copolymers dyeing”, *Journal of Applied Polymer Science*, vol. 29, pp. 651–660, 1984.
- [MAD 13] MADDIPATLA M.V.S.N., WEHRUNG D., TANG C. *et al.*, “Photoresponsive Coumarin Polyesters That Exhibit Cross-Linking and Chain Scission Properties”, *Macromolecules*, vol. 46, pp. 5133–5140, 2013.
- [MAR 07] MARTINEZ A.W., PHILLIPS S.T., BUTTE M.J. *et al.*, “Patterned Paper as a Platform for Inexpensive, Low-Volume, Portable Bioassays”, *Angewandte Chemie International Edition*, vol. 46, pp. 1318–1320, 2007.
- [MIY 98] MIYASHITA T., NAKAYA M., AOKI A., “Molecular photopatterning with a two-dimensional network of polymer LB films”, *Thin Solid Films*, vol. 327–329, pp. 833–836, 1998.
- [MUE 14] MUELLER J.O., GUIMARD N.K., OEHLenschlaeger K.K. *et al.*, “Sunlight-induced crosslinking of 1,2-polybutadienes: access to fluorescent polymer networks”, *Polymer Chemistry*, vol. 5, pp. 1447–1456, 2014.
- [MÜL 00] MÜLLER D.C., BRAIG T., NOTHOFER H.-G. *et al.*, “Efficient Blue Organic Light-Emitting Diodes with Graded Hole-Transport Layers”, *ChemPhysChem*, vol. 1, pp. 207–211, 2000.

- [MUL 03] MULLER C.D., FALCOU A., RECKEFUSS N. *et al.*, “Multi-colour organic light-emitting displays by solution processing”, *Nature*, vol. 421, pp. 829–833, 2003.
- [NAT 08] NATALI M., BEGOLO S., CAROFIGLIO T. *et al.*, “Rapid prototyping of multilayer thiolene microfluidic chips by photopolymerization and transfer lamination”, *Lab on a Chip*, vol. 8, pp. 492–494, 2008.
- [NIN 08] NING X., GUO J., WOLFERT M.A. *et al.*, “Visualizing Metabolically Labeled Glycoconjugates of Living Cells by Copper-Free and Fast HuisgenCycloadditions”, *Angewandte Chemie International Edition*, vol. 47, pp. 2253–2255, 2008.
- [OEH 13] OEHLenschlaeger K.K., MUELLER J.O., HEINE N.B. *et al.*, “Light-Induced Modular Ligation of Conventional RAFT Polymers”, *Angewandte Chemie International Edition*, vol. 52, pp. 762–766, 2013.
- [ORS 10] ORSKI S.V., POLOUKHTINE A.A., ARUMUGAM S. *et al.*, “High Density Orthogonal Surface Immobilization via Photoactivated Copper-Free Click Chemistry”, *Journal of the American Chemical Society*, vol. 132, pp. 11024–11026, 2010.
- [OST 59] OSTER G., OSTER G.K., MOROSON H., “Ultraviolet induced crosslinking and grafting of solid high polymers”, *Journal of Polymer Science Part A: Polymer Chemistry*, vol. 34, pp. 671–684, 1959.
- [PAR 99] PARK Y.J., CHAE K.H., RAWLS H.R., “Development of a new photoinitiation system for dental light-cure composite resins”, *Dental Materials*, vol. 15, pp. 120–127, 1999.
- [PAU 12] PAULOEHRL T., DELAITTRE G., BASTMEYER M. *et al.*, “Ambient temperature polymer modification by in situ phototriggered deprotection and thiol-ene chemistry”, *Polymer Chemistry*, vol. 3, pp. 1740–1749, 2012.
- [PAU 12a] PAULOEHRL T., DELAITTRE G., BRUNS M. *et al.*, “(Bio)Molecular Surface Patterning by Phototriggered Oxime Ligation”, *Angewandte Chemie International Edition*, vol. 51, pp. 9181–9184, 2012.
- [PAU 12b] PAULOEHRL T., DELAITTRE G., WINKLER V. *et al.*, “Adding Spatial Control to Click Chemistry: Phototriggered Diels–Alder Surface (Bio)functionalization at Ambient Temperature”, *Angewandte Chemie International Edition*, vol. 51, pp. 1071–1074, 2012.
- [PAU 13a] PAULOEHRL T., WELLE A., OEHLenschlaeger K.K. *et al.*, “Spatially controlled surface immobilization of nucleophiles via trapping of photo-generated thioaldehydes”, *Chemical Science*, vol. 4, pp. 3503–3507, 2013.

- [PAU 13b] PAULOEHL T., WELLE A., BRUNS M. *et al.*, “Spatially Controlled Surface Immobilization of Nonmodified Peptides”, *Angewandte Chemie International Edition*, vol. 52, pp. 9714–9718, 2013.
- [PEL 09] PELTON R., “Bioactive paper provides a low-cost platform for diagnostics”, *TrAC Trends in Analytical Chemistry*, vol. 28, pp. 925–942, 2009.
- [POE 13] POELMA J.E., FORS B.P., MEYERS G.F. *et al.*, “Fabrication of Complex Three-Dimensional Polymer Brush Nanostructures through Light-Mediated Living Radical Polymerization”, *Angewandte Chemie International Edition*, vol. 52, pp. 6844–6848, 2013.
- [POL 03] POLOUKHTINE A., POPIK V.V., “Highly Efficient Photochemical Generation of a Triple Bond: Synthesis, Properties, and Photodecarbonylation of Cyclopropenones”, *Journal of Organic Chemistry*, vol. 68, pp. 7833–7840, 2003.
- [PRE 14] PREUSS C.M., ZIEGER M.M., RODRIGUEZ-EMMENEGGER C. *et al.*, “Fusing Catechol-Driven Surface Anchoring with Rapid Hetero Diels–Alder Ligation”, *ACS Macro Letters*, vol. 3, pp. 1169–1173, 2014.
- [QIU 11] QIU L., XU Q., LEE W.H. *et al.*, “Organic thin-film transistors with a photo-patternable semiconducting polymer blend”, *Journal of Materials Chemistry*, vol. 21, pp. 15637–15642, 2011.
- [QUI 13] QUICK A.S., FISCHER J., RICHTER B. *et al.*, “Preparation of Reactive Three-Dimensional Microstructures via Direct Laser Writing and Thiol-ene Chemistry”, *Macromolecular Rapid Communications*, vol. 34, pp. 335–340, 2013.
- [QUI 14] QUICK A.S., ROTHFUSS H., WELLE A. *et al.*, “Fabrication and Spatially Resolved Functionalization of 3D Microstructures via Multiphoton-Induced Diels–Alder Chemistry”, *Advanced Functional Materials*, vol. 24, pp. 3571–3580, 2014.
- [RÅN 98] RÅNBY B., “Photoinitiated modifications of polymers: photocrosslinking, surface photografting and photolamination”, *Materials Research Innovations*, vol. 2, pp. 64–71, 1998.
- [REI 89] REICHMANIS E., THOMPSON L.F., “Polymer materials for microlithography”, *Chemical Reviews*, vol. 89, pp. 1273–1289, 1989.
- [RIC 13] RICHTER B., PAULOEHL T., KASCHKE J. *et al.*, “Three-Dimensional Microscaffolds Exhibiting Spatially Resolved Surface Chemistry”, *Advanced Materials*, vol. 25, pp. 6117–6122, 2013.

- [ROD 12] RODRIGUEZ-EMMENEGGER C., HOUSKA M., ALLES A.B. *et al.*, “Surfaces Resistant to Fouling from Biological Fluids: Towards Bioactive Surfaces for Real Applications”, *Macromolecular Bioscience*, vol. 12, pp. 1413–1422, 2012.
- [ROD 13] RODRIGUEZ-EMMENEGGER C., PREUSS C.M., YAMEEN B. *et al.*, “Controlled Cell Adhesion on Poly(dopamine) Interfaces Photopatterned with Non-Fouling Brushes”, *Advanced Materials*, vol. 25, pp. 6123–6127, 2013.
- [RUE 97] RUEGGERBERG F.A., ERGLE J.W., LOCKWOOD P.E., “Effect of photoinitiator level on properties of a light-cured and post-cure heated model resin system”, *Dental Materials*, vol. 13, pp. 360–364, 1997.
- [RUS 12] RUSSELL A.G., SADLER M.J., LAIDLAW H.J. *et al.*, “Photorelease of tyrosine from [small alpha]-carboxy-6-nitroveratryl ( $\alpha$ CNV) derivatives”, *Photochemical & Photobiological Sciences*, vol. 11, pp. 556–563, 2012.
- [SAM 76] SAMMES P.G., “Photoenolisation”, *Tetrahedron*, vol. 32, pp. 405–422, 1976.
- [SCH 13a] SCHMIDT F.G., HILF S., BARNER-KOWOLLIK C. *et al.*, Photoinduzierte Vernetzung von Doppelbindungen-enthaltenden Polymeren mittels pericyclischer Reaktionen, Patent WO2013104486 A1, 2013.
- [SCH 13b] SCHROLL P., FEHL C., DANKESREITER S. *et al.*, “Photocatalytic surface patterning of cellulose using diazonium salts and visible light”, *Organic and Biomolecular Chemistry*, vol. 11, pp. 6510–6514, 2013.
- [SCH 96] SCHANZE K.S., BERGSTEDT T.S., HAUSER B.T., “Photolithographic patterning of electroactive polymer films and electrochemically modulated optical diffraction gratings”, *Advanced Materials*, vol. 8, pp. 531–534, 1996.
- [STO 14] STOLZER L., AHMED I., RODRIGUEZ-EMMENEGGER C. *et al.*, “Light-induced modification of silver nanoparticles with functional polymers”, *Chemical Communications*, vol. 50, pp. 4430–4433, 2014.
- [SUR 09] SURI S., SCHMIDT C.E., “Photopatterned collagen–hyaluronic acid interpenetrating polymer network hydrogels”, *Acta Biomaterials*, vol. 5, pp. 2385–2397, 2009.
- [SWA 70] SWAN G.A., WAGGOTT A., “Studies related to the chemistry of melanins. Part X. Quantitative assessment of different types of units present in dopa-melanin”, *Journal of the Chemical Society C: Organic*, pp. 1409–1418, 1970.
- [TAN 04] TANG L., QU B., SHEN X., “Mechanical properties, morphological structure, and thermal behavior of dynamically photocrosslinked PP/EPDM blends”, *Journal of Applied Polymer Science*, vol. 92, pp. 3371–3380, 2004.

- [TAS 13] TASDELEN M.A., YAĞCI Y., “Light-Induced Click Reactions”, *Angewandte Chemie International Edition*, vol. 52, pp. 5930–5938, 2013.
- [TIS 12] TISCHER T., GOLDMANN A.S., LINKERT K. *et al.*, “Modular Ligation of Thioamide Functional Peptides onto Solid Cellulose Substrates”, *Advanced Functional Materials*, vol. 22, pp. 3853–3864, 2012.
- [TIS 13] TISCHER T., CLAUS T.K., BRUNS M. *et al.*, “Spatially Controlled Photochemical Peptide and Polymer Conjugation on Biosurfaces”, *Biomacromolecules*, vol. 14, pp. 4340–4350, 2013.
- [TIS 14a] TISCHER T., CLAUS T.K., OEHLENSCHLAEGER K.K. *et al.*, “Ambient Temperature Ligation of Diene Functional Polymer and Peptide Strands onto Cellulose via Photochemical and Thermal Protocols”, *Macromolecular Rapid Communications*, vol. 35, pp. 1121–1127, 2014.
- [TIS 14b] TISCHER T., RODRIGUEZ-EMMENEGGER C., TROUILLET V. *et al.*, “Photo-Patterning of Non-Fouling Polymers and Biomolecules on Paper”, *Advanced Materials*, vol. 26, pp. 4087–4092, 2014.
- [TOE 05] TOEPKE M.W., KENIS J.A., Multilevel Microfluidics via Single-Exposure Photolithography, *Journal of the American Chemical Society*, vol. 127, pp. 7674–7675, 2005.
- [TOO 00] TOOLE B.P., “Hyaluronan is not just a goo!”, *The Journal of Clinical Investigation*, vol. 106, pp. 335–336, 2000.
- [TRA 06] TRAKHTENBERG S., WARNER J.C., NAGARAJAN R. *et al.*, “Spectroscopic and Microscopic Analysis of Photo-cross-linked Vinylbenzylthymine Copolymers for Photoresist Applications”, *Chemistry of Materials*, vol. 18, pp. 2873–2878, 2006.
- [TRE 14] TREAT N.J., FORS B.P., KRAMER J.W. *et al.*, “Controlled Radical Polymerization of Acrylates Regulated by Visible Light”, *ACS Macro Letters*, vol. 3, pp. 580–584, 2014.
- [VED 82] VEDEJS E., EBERLEIN T.H., VARIE D.L., “Dienophilicthioaldehydes”, *Journal of the American Chemical Society*, vol. 104, pp. 1445–1447, 1982.
- [VED 86] VEDEJS E., EBERLEIN T.H., MAZUR D.J. *et al.*, “Thioaldehyde Diels-Alder reactions”, *Journal of Organic Chemistry*, vol. 51, pp. 1556–1562, 1986.
- [WAN 07] WANG Y., RIVERA VERA C.I., LIN Q., “Convenient Synthesis of Highly Functionalized Pyrazolines via Mild, Photoactivated 1,3-Dipolar Cycloaddition”, *Organic Letters*, vol. 9, pp. 4155–4158, 2007.
- [WAN 08] WANG Y., HU W.J., SONG W. *et al.*, “Discovery of Long-Wavelength Photo activatable Diaryltetrazoles for Bioorthogonal 1,3-Dipolar Cycloaddition Reactions”, *Organic Letters*, vol. 10, pp. 3725–3728, 2008.

- [WAN 13] WANG J.-L., REN K.-F., CHANG H. *et al.*, Poly(dopamine) Coating Through Endogenous “Fibronectin and Integrin  $\alpha_5\beta_1$ ”, *Macromolecular Bioscience*, vol. 13, pp. 483–493, 2013.
- [WIL 14] WILLENBACHER J., WUEST K.N.R., MUELLER J.O. *et al.*, “Photochemical Design of Functional Fluorescent Single-Chain Nanoparticles”, *ACS Macro Letters*, vol. 3, pp. 574–579, 2014.
- [WIN 12] WINKLER M., MUELLER J.O., OEHELENSCHLAEGER K.K., “Highly Orthogonal Functionalization of ADMET Polymers via Photo-Induced Diels–Alder Reactions”, *et al.*, *Macromolecules*, vol. 45, pp. 5012–5019, 2012.
- [YAM 06] YAMADA H., KAWAMURA E., SAKAMOTO S. *et al.*, “Effective photochemical synthesis of an air-stable anthracene-based organic semiconductor from its diketone precursor” *Tetrahedron Letters*, vol. 47, pp. 7501–7504, 2006.
- [YAM 08] YAMAGUCHI R., SATO S., “Double-Faced Optical Writing in Guest-Host Mode Liquid Crystal Cell Using Crosslinkable Polymer Alignment Film”, *Journal of Photopolymer Science and Technology*, vol. 21, pp. 203–206, 2008.
- [YAN 94] YAN M., CAI S.X., WYBOURNE M.N. *et al.*, “N-Hydroxysuccinimide Ester Functionalized Perfluorophenyl Azides as Novel Photoactive Heterobifunctional Crosslinking Reagents. The Covalent Immobilization of Biomolecules to Polymer Surfaces”, *Bioconjugate Chemistry*, vol. 5, pp. 151–157, 1994.
- [YOS 94] YOSHIDA K., GREENER E.H., *Journal of Dentistry*, vol. 22, pp. 296–299, 1994.
- [YOU 06] YOUNG D.D., DEITERS A., “Photochemical hammerhead ribozyme activation”, *Bioorganic & Medicinal Chemistry Letters*, vol. 16, pp. 2658–2661, 2006.
- [YUA 07] YUAN W.Z., QIN A., LAM J.W.Y. *et al.*, “Disubstituted Polyacetylenes Containing Photopolymerizable Vinyl Groups and Polar Ester Functionality: Polymer Synthesis, Aggregation-Enhanced Emission, and Fluorescent Pattern Formation”, *Macromolecules*, vol. 40, pp. 3159–3166, 2007.

---

# Photosynthesized High-Performance Biomaterials

---

## 10.1. Introduction

The performance of polymeric materials largely relies on the nature of the functionalities and groups present on their surfaces for many applications. It is widely known that the surface chemistry of polymeric substrates directly affects their behavior for many applications, such as adhesion, coatings, printing paintings, lamination or packaging. The fact that most of the polymeric materials are hydrophobic rather than hydrophilic leads to the main drawback when used as biomaterials: hydrophobic surfaces have a limitation for many biological applications because this property enhances non-specific adsorption of proteins, resulting in the so-called “bio-fouling” (deposition and growth of microorganisms on surface) and limits cell attachment. To tackle these problems, numerous studies have been conducted on the surface modifications of polymeric materials. Thus, the control of the chemical nature of the polymer surfaces has rapidly become an area of interest, and has been used to introduce surface functionalities onto substrates to enhance properties such as wettability, antifouling and biocompatibility.

---

Chapter written by Julien BABINOT, Estelle RENARD, Valérie LANGLOIS and Davy-Louis VERSACE.

To date, many innovative surface modification routes have been developed to introduce graft chains onto the surface of polymeric substrates depending on the system of interest, including chemical, plasma, corona and flame treatments or photochemical modification. These grafting methods are generally divided into two groups: “grafting-from” and “grafting-to” processes. In the latter case, preformed polymer chains containing reactive groups are covalently grafted onto activated surfaces. Some limitations such as incomplete surface coverage and irregular distribution of the target reactive sites are addressed by the steric repulsion of the polymer chains. According to the “grafting-from” method, the active species generated on the polymer surfaces can initiate the polymerization of monomers from the surface toward the bulk phase. However, most of the previous cited “grafting-from” methods would substantially degrade the bulk properties of the synthesized materials. In light of these insights, photoinduced grafting method appears as a useful technique for the modification and functionalization of polymeric materials due to its significant advantages, e.g. low cost of operation, mild reaction conditions, fast reaction rate, simple equipment and easy industrialization. Thus, surface photografting polymerization offers the unique ability to tune and manipulate surface properties without affecting the bulk polymer substrate.

Photografting of polymers has been extensively studied since the 1950s up until the 1980s; most of the investigations concerning surface graft polymerizations relied on initiation by high energy irradiation. Studies related to this technique have rapidly grown in the past few decades, and despite the increasing popularity of this promising technique for the development of biomaterials, only a handful of review articles have been published so far. Thus, it is of interest to have an overview of the advances in this key research area.

This chapter first reviews the various techniques to perform the surface photografting modifications (according to the “grafting-from” and “grafting-to” methods) and all the photoinduced mechanisms involved in these processes. Finally the achievements of the photoinduced modified materials are summarized, wherein the enhancement of wettability, adhesion and some useful applications are reported. Examples are mainly focused on polyester substrates.

## 10.2. Surface photografting methodology

### 10.2.1. Photoinduced “grafting-from” method

Numerous investigations have described the photoinduced modification of polymeric substrates with the use of commonly used benzophenone (BP) and derivatives, ketones or aldehydes, hydrogen peroxide, photoiniferters and, more recently, triarylsulfonium salts (TAS).

### 10.2.2. Benzophenone and derivatives

Ultraviolet (UV) light is largely used to perform the modification of polymer surfaces with either photoinitiator or photosensitizer. Norrish type I photoinitiators are less frequently used because of their higher polymerization yield and rate and lower grafting efficiency in comparison to the used Norrish type II photoinitiators [DWO 88, ANG 80]. Among the most commonly used Norrish type II photoinitiators, BP and its derivatives [DEC 98, KON 98, MA 99] have shown a high efficiency. In the first step (Figure 10.1), when UV irradiated, BP goes to its singlet excited state ( $^1\text{BP}^*$ ), passes through its triplet state ( $^3\text{BP}^*$ ) by intersystem crossing and then abstracts a hydrogen atom from the substrate, thus generating surface radicals ( $\text{R}\cdot$ ) and semi-pinacol radicals. As there is no monomer present in this step, the recombination of  $\text{R}\cdot$  and semi-pinacol radicals takes place and generates the surface initiators. In the second step, the substrate containing the surface initiators is exposed to the monomer solution (which should be grafted) and UV light. The latter cleaves the carbon-carbon bond between the semi-pinacol and the substrate, thus generating surface radicals capable of initiating the monomer polymerization. The benzopinacol radical ( $\text{BP-OH}\cdot$ ) tends to participate in the termination reaction due to its weak reactivity. The overall mechanism with BP is described in Figure 10.1.

This novel sequential photoinduced graft polymerization was tested by Bowman *et al.* [MA 99] on hydrophobic porous polypropylene (PP) membrane in the presence of acrylic acid. Experimental results showed that the grafting density and the graft polymer chain length could be controlled by choosing the suitable reaction conditions in both steps. In addition, the method substantially eliminates the formation of undesired homopolymer

and cross-linked or branched polymers. According to this procedure, Lao *et al.* [LAO 10] described the covalent photografting of 2-hydroxyethyl methacrylate onto polyhydroxyalkanoate films for promoting the cell colonizing and developing biocompatible materials. Such a method was also applied by Chen *et al.* [KE 07] for the surface modification of poly(3-hydroxybutyrate-co-3-hydroxyvalerate) (PHBHV) films by the photografting polymerization of polyacrylamide to enhance mesenchymal stromal cells (MSCs) cell affinity and cell compatibility.

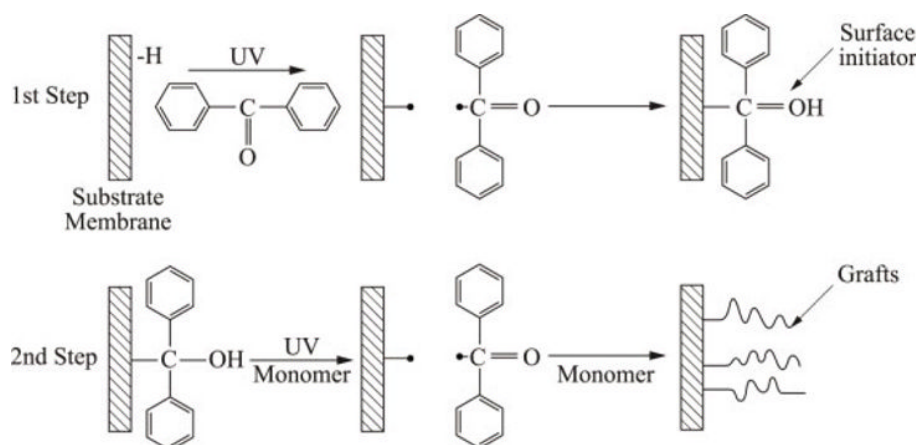


**Figure 10.1.** Photografting mechanisms involving benzophenone.  
Reprinted (adapted) with permission from [MA 00]

The performance of a series of BP derivatives including xanthone, anthraquinone or 9-fluorenone has been tested by Yang *et al.* [YAN 99], with low-density polyethylene (LDPE) as the film substrate and acrylic acid as the monomer. The polymerization rate, the grafting conversion and the grafting efficiency were compared and the results indicated that BP, xanthone and 9-fluorenone have high grafting efficiency and could be used as photoinitiators for depth photografting applications. On the contrary, anthraquinone, 4-chlorobenzophenone and 4-benzylbenzophenone all preferentially underwent photoreduction, but the active fragment radicals

formed made it difficult to achieve depth photografting polymerization. In addition to BP, Geuskens *et al.* [GEU 00] used anthraquinone-2-sulfonate sodium (AQS) and (4-benzoyl benzyl) trimethylammonium chloride (BTC) as photoinitiator to perform the surface graft polymerization of an aqueous solution of acrylamide. First, the photoinitiators were adsorbed onto the polyethylene substrate, and then irradiated the substrate with UV light. According to this method, the homopolymerization of acrylamide was not avoided, but it was demonstrated that AQS was more efficient than BTC to allow the grafting of acrylamide monomer due to its higher absorption properties. In some cases, the efficiency of BP has been increased with the introduction of co-photoinitiators. The latter acts as photosensitizer and transfers electrons or energy to BP by forming excited-state complex, thus improving the efficiency of the photoinitiator to generate more reactive radical species. For example, Xu *et al.* [HU 06] demonstrated that the combination BP/ferric chloride ( $\text{FeCl}_3$ ) appears as a remarkable photoinitiating system in comparison with BP alone for enhancing the surface photografting of 2-hydroxyethyl methacrylate monomer onto PP microporous membranes. In this sense, Hong *et al.* [CHO 06] underlined this “photosensibilization effect” with the use of BP/isopropylthioxanthone (ITX) as photografting initiator.

A particularly interesting example with BP/maleic anhydride (MAH) described by Hoyle and coworkers [PAN 04] pointed out that BP could also be used as an efficient photosensitizer for the photografting of MAH onto PP. The occurrence of the MAH grafting could be ascribed via the formation of excited triplet state of MAH sensitized by BP.

### 10.2.3. Ketones and derivatives

Some ketones and aldehydes have been studied and have demonstrated an efficient ability for hydrogen abstraction reactions from the polymeric substrate upon light activation. A series of alkyl ketones and diketones has been experimentally tested by Yang and Rånby [YAN 99]. Their investigations demonstrated that high triplet state energy, strong UV absorption properties, stable molecular structure and low initiating reactivity of the resulting ketyl radicals are the key factors that make ketones efficient enough for being used in photografting applications on LDPE. Similar results have also been reported with some aliphatic ketones (heptan-3-one, butan-2-one and pentan-3-one) when solubilized in water, ethanol or

water/ethanol mixture for the photografting of methacrylic acid (MAA) onto high-density polyethylene (HDPE) [WAN 04, WAN 07]. Recently, we used butan-2-one and heptan-3-one to tailor the surface properties of PHBHV films [MAN 14] upon UV light. The electron spin resonance spin-trapping (ESR-ST) experiments have highlighted the possible mechanisms involved in the grafting-from process. Figure 10.2 outlines the photografting of an acrylate-derived monomer onto PHBHV films using a ketone system. The photolysis ((1), Figure 10.2) of the ketone generates both a carbon-centered radical (A) and an alkoxy adduct radical (B), which are capable of hydrogen abstraction. Both photoinduced radicals may diffuse to the aqueous monomer solution to abstract a hydrogen atom from the PHBHV surface ((2), Figure 10.2). The latter reaction generates free radicals onto the PHBHV surface which initiate the polymerization of acrylate-derived monomer, thus producing surface-grafted acrylate chains ((3), Figure 10.2). According to the same procedure, methacrylic acid (MAAH) was photografted onto PHBHV, and the tethered MAAH chains allowed the adsorption of silver nanoparticles for antibacterial applications.

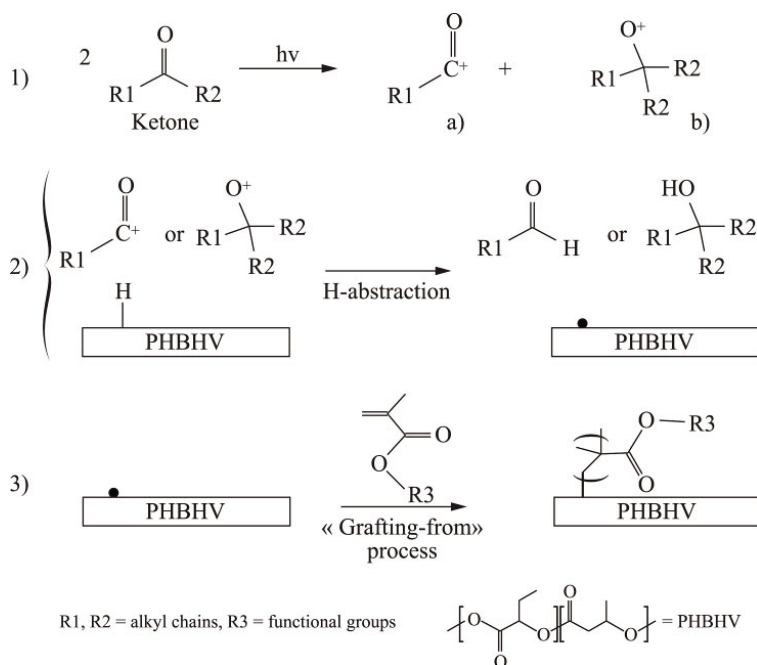


**Figure 10.2.** Mechanisms of acrylate photografting process from the surface of PHBHV films, according to the "grafting-from" process. Reprinted (adapted) with permission from [MAN 14]

The performance of alkyl phenyl ketones including acetophenone, benzyl dimethoxy-ketal and hydroxycyclohexyl acetophenone for the hydrogen abstraction reaction on LDPE has been described by Yang and Rånby [YAN 99]. They demonstrated that a subsequent photografting of acrylic acid or acrylonitrile monomers could be performed onto the surface of LDPE in a reduced time. Tomovska *et al.* [DAN 10] have also provided additional evidence of the photografting process involving acetophenone and tentatively explained their results of UV-induced HDPE surface modification as follows: the bond dissociation energy of carbon–carbon single bonds ( $\Phi\text{-C(=O)-CH}_3$ ) is so high (86 kcal/mol) that the absorbed UV light excites acetophenone (AcP) to singlet state, which is quickly transformed by the process of intersystem crossing into excited triplet state (step 1), thus generating radicals by H abstraction from HDPE films. In the presence of benzocaine (BC), the formation of excited BC triplet state (sensitizing by AcP triplet) is expected. The latter may react with HDPE to create carbon-centered radical and modify the properties of the HDPE surface.

#### 10.2.4. Photo-oxidation process

According to this process, peroxide groups can be introduced onto polymer surfaces [GUA 00, MA 02] by soaking the materials in hydrogen peroxide solution under UV irradiation. Compared with other methods, the photo-oxidation process does not need special instrument and is easily performed. The peroxide groups can then be used to initiate the grafting polymerization under UV light activation. Hydrophilic polymers, such as poly(2-hydroxyethyl methacrylate) (PHEMA) and poly(acrylamide), have been grafted onto polycaprolactone [ZHU 02], poly(L-lactic acid) (PLLA) [MA 03] or PHBHV surfaces [LAO 10]. In the later investigation, Lao *et al.* [LAO 10] used a two-step procedure to modulate the hydrophilicity of the PHBHV surface. In the first step, hydroperoxide functions were generated directly on the PHBHV film via the UV treatment in the presence of oxygen. The photolysis of  $\text{H}_2\text{O}_2$  enables the formation of hydroxyl radicals that are able to abstract hydrogen atom both from the PHBHV backbone (thus forming reactive carbon radicals on PHBHV surface) and  $\text{H}_2\text{O}_2$  to form OOH radicals (Figure 10.3), and thus creating hydroperoxide linkages. In the second step, oxygen-centered radicals are generated from the UV irradiation

of PHBHV-modified OOH functions by a homolytic photocleavage of the O–O bonds. The oxygen radical species initiated the polymerization of 2-hydroxyethyl methacrylate (HEMA) monomer from the modified PHBHV surface.

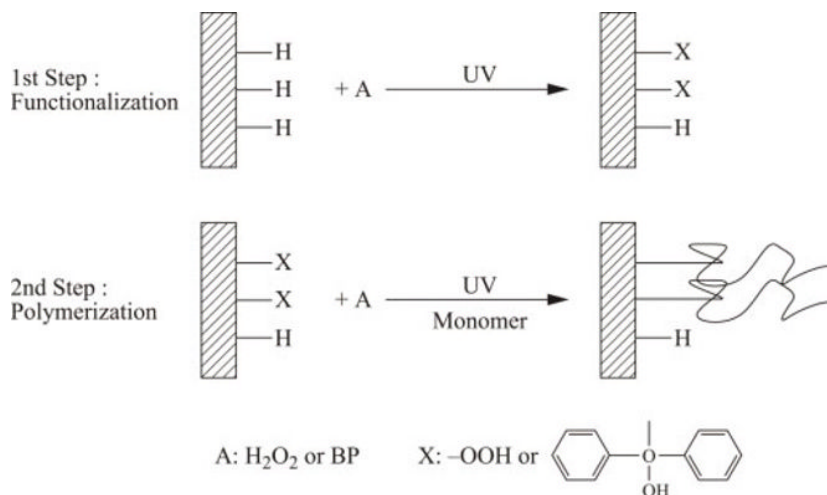


**Figure 10.3.** Mechanisms of the photografting procedure with  $\text{H}_2\text{O}_2$  [LAO 10]

### 10.2.5. Photoiniferters for living/controlled surface photografting

Conventional graft polymerization techniques mediated by plasma, corona discharge or ozone oxidation treatments have been developed over the years. However, the use of these techniques, which facilitate radical polymerization, cannot provide precise graft architectures due to the extremely high reactivity of free radicals. Therefore, the regiospecificity of graft-polymerized surfaces and precise graft-chain architectures cannot be controlled. To tackle these problems, another effective route to realize living/controlled surface photografting was developed through the use of “photoiniferters”, as reported by Otsu *et al.* [OTS 98, OTS 82a, OTS 82b]. Based on numerous studies by Otsu’s group, which dealt with solution polymerization, investigations [LUO 02a, LUO 02b, DEB 99, MAT 03, KID 01] have focused on surface graft architectures using photoiniferter-modified polymer films as the substrate. Using the characteristic features of iniferter-based photopolymerization, graft-chain architectures can be easily tuned in the growing, branching and endcapping stages. Under light

activation, iniferter polymerization utilizing dithiocarbamate photolysis chemistry generates a radical pair: one radical (alkyl radical) is capable of initiating vinyl polymerization, and the other (dithiocarbamyl radical) rarely initiates such polymerization. The inherent high reactivity of these radicals leads to a recombination for producing “dormant” species; however, upon light activation, a pair of radical is again regenerated. This enables the realization of the quasi-livingness by which polymerization repeatedly reinitiates during photopolymerization.

### 10.2.6. *Triarylsulfonium salts*

Triarylsulfonium hexafluoroantimonate salts (TAS) are usually used in the cationic photopolymerization of vinyl ether or epoxidized derived monomers; however, some studies have demonstrated its ability to provide radicals for UV-induced photografting [VER 12, WAN 06]. A first investigation showed a simple route to covalently modify the surface of SU-8 with acrylic acid. The described polymeric coatings enhance the attractiveness and enlarge the use of SU-8 as a substrate material for the elaboration of bioanalytical devices [WAN 06]. Recently, Versace *et al.* [VER 12] provided details of the mechanisms involved in the H abstraction reaction with the triarylsulfonium hexafluoroantimonate salts from PHBHV surface. TAS was used for activating PHBHV surface according to the “grafting-from” technique. Figure 10.4 outlines the photografting of a monomer HEMA or MAA onto PHBHV using TAS. The photolysis ((1), Figure 10.4) of the latter generates both diphenylsulfonium radical cation (A) and benzyl radical ((B), Ph• radical). Only Ph• radical is able to be active in hydrogen abstraction while diphenylsulfonium radical cation exhibits high reactivity toward nucleophilic species including water and alcohol molecules. The free radicals (Ph• radical) diffuse to the aqueous monomer solution to abstract a hydrogen atom on the PHBHV surface ((2), Figure 10.4). The latter reaction generates free radicals onto PHBHV surface, which initiate the polymerization of HEMA or MAA, producing surface-grafted PHEMA or poly(methacrylic acid) (PMAA), respectively ((3), Figure 10.4). Micropatterning of PHBHV films (Figure 10.5) provides the opportunity to develop microdevices for allowing cells to grow at specific locations. Such a procedure can be applied to other monomer-containing chemical functions, for example, to improve their surface ability for cellular interactions.

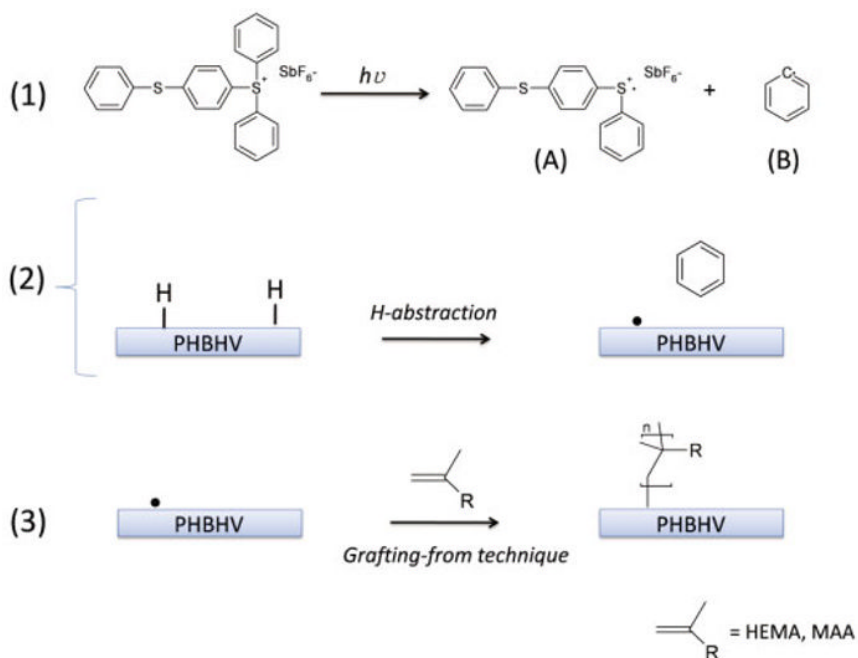


**Figure 10.4.** Photografting mechanisms of HEMA or MAA on the surface of PHBHV film according to the grafting-from technique. (1) Photolysis of TAS and production of both thiyls and phenyl radicals. (2) Hydrogen abstraction from PHBHV film and generation of free radicals on the surface of the PHBHV film. (3) Free radicals initiate covalent attachment of HEMA or MAA on the surface, followed by polymerization of the monomer. Reproduced with permission from The Royal Society of Chemistry [VER 12]

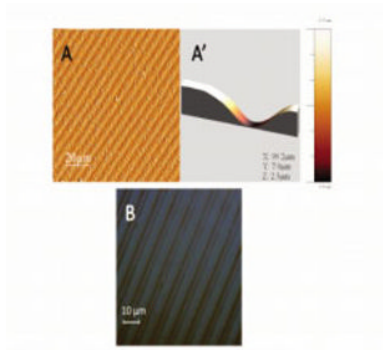


**Figure 10.5.** Characterization of the micropatterned structure: AFM image (A), profile of the patterned A') and optical microscopy image (B) after 400 s of irradiation and development in ethanol solution. Reproduced with permission from The Royal Society of Chemistry [VER 12]

### 10.3. Photoinduced “grafting-to” procedure

Few investigations have described the photoinduced modification of substrates with the employment of azido- or anthraquinone-derived polymers.

#### 10.3.1. *Aryl azides chemistry*

Azido photochemistry was frequently used to introduce functional groups onto polymeric substrates. It is also the main so-called “grafting-to” technique usually used to efficiently modify or functionalize surfaces [HAR 91, THO 98, ZIA 99]. This method was employed to covalently graft carbohydrates [KNA 01] or polysaccharides [BAR 01, BHA 08] containing azide groups to polymer substrates and was successfully used to modify a wide range of other substrates such as glass, tin oxide, silicon and aluminum.

Under UV light activation, the highly generated reactive nitrene radicals can undergo a multitude of reactions as the insertion into C–H, N–H and O–H bonds, the addition to olefins, proton abstraction reactions giving the corresponding amine, and in the case of aryl azides a number of ring expansion reactions have been demonstrated [SCR 88]. In light of these results, a new approach based on the photochemistry of aryldiazonium and aryldiazo groups has been developed [LEW 10]. These two photoreactive groups generate, respectively, under UV light irradiation an arylcarbene and arylation that are able to covalently bond to a wide range of surfaces (Figure 10.6).

#### 10.3.2. *Anthraquinone-derived monomers*

A new route for immobilizing polysaccharides on the surface of PHBHV electrospun fibers has been developed with the objective to design a new functional biomaterial having a significant increase in cell proliferation [VER 13a]. The approach consists of a one-step procedure involving the UV grafting of a photosensitive dextran (AQ-Dext) on the surface of PHBHV fibers according to the “grafting-to” method, with the use of a dextran-grafted anthraquinone. The photografting process is conducted through a

photoinduced free radical process employing an anthraquinone-based photosensitizer in aqueous medium. Figure 10.7 outlines the photografting of dextran onto PHBHV fibers using anthraquinone derivative (AQ-Dext). Under UV irradiation, AQ-Dext reacts with C–H  $\sigma$ -bonds of the polymer substrate (PHBHV and RH) to produce a semi-quinone radical (Figure 10.7, (A) or (B)) according to an H-abstraction reaction. The latter can recombine together with the alkylradical ( $R\cdot$ ) formed on the surface of PHBHV fibers. Therefore, dextran is covalently attached to PHBHV surface *via* the oxygen atom of the anthraquinone linker.

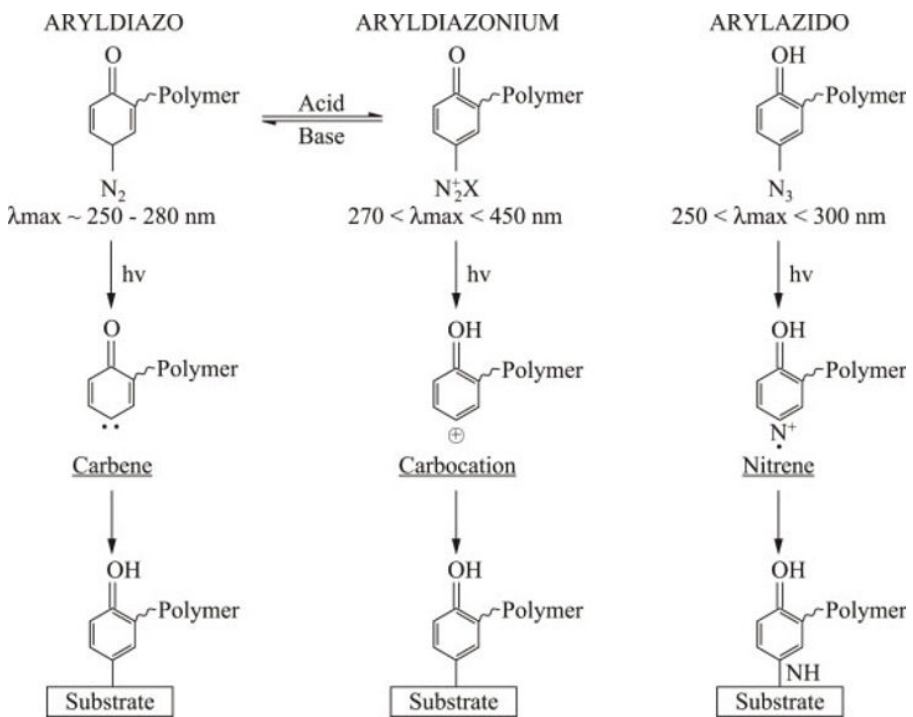


**Figure 10.6.** Representation of the photochemical processes involved in the surface modification of polymer substrate. Reprinted (adapted) with permission from [ZIA 99]

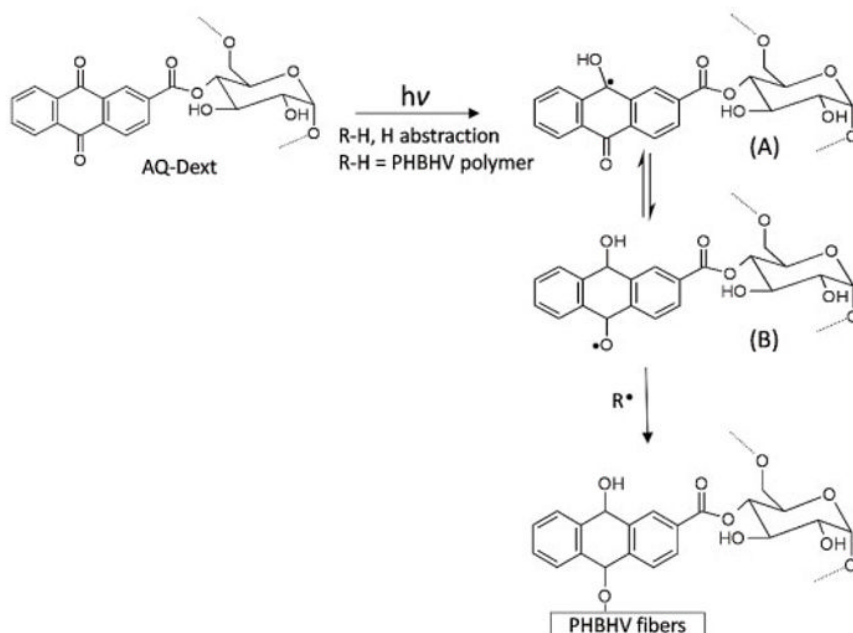


**Figure 10.7.** Photografting mechanisms of AQ-Dext on the surface of PHBHV microfibrinous scaffolds according to the “grafting-to” technique. (1) Hydrogen abstraction from PHBHV surface and generation of free radicals on the surface of PHBHV microfibrinous scaffolds. (2) Covalent grafting of AQ-Dext on PHBHV fibers. Reproduced with permission from. The Royal Society of Chemistry [VER 13a]

## 10.4. Achievements and biomedical applications of the photosynthesized materials

### 10.4.1. Achievements

#### 10.4.1.1. Wettability

The main objective is to tailor the hydrophilicity of the hydrophobic polymer surfaces (PHBHV, poly(l-lactide)) by a photografting process to extend their applications. Therefore, grafting hydrophilic monomers onto the targeted polymer drastically improved the wettability of the polymer surfaces [WAV 02, SUN 10, LEE 96, GUP 02]. Using the surface-confined photopolymerization procedure with BP under light activation, the graft-copolymer composition of the film surface was manipulated by changing the feed composition of the monomer solution [JAN 06]. These results showed

that the wettability of the PLA film surface could be tailored to a desired value from a hydrophobic surface (contact angle =  $82^\circ$  for neat PLA) to a hydrophilic surface (contact angle =  $12^\circ$  for PLA-g-PAAm) using a single monomer or a combination of monomers (acrylic acid or acrylamide monomer). Recently, Versace *et al.* [MAN 14] used the “grafting-from” process with butan-2-one to modify the hydrophilicity of PHBHV with three types of polymers: 2-hydroxyethyl methacrylate (HEMA), 2-(methacryloyloxy)-ethyl trimethylammonium (META) and 2-(methacryloylethyl)-dimethyl-(3-sulfopropyl) ammonium (MESA). The water contact angle dropped significantly when PHBHV films were treated with the three types of monomers due to the hydrophilic nature of the hydroxyl, ammonium and sulfopropyl ammonium groups which were grafted onto the PHBHV surface. Figure 10.8 illustrates the evolution of the measured contact angle as a function of irradiation time. For each grafted monomer, the water contact angle decreases as the exposure time is increased. After 300 s of irradiation, the water contact angle falls down until  $30^\circ$ ,  $50^\circ$  and  $75^\circ$  for PHBHV-g-PMETA film, PHBHV-g-PHEMA film and PHBHV-g-PMESA film, respectively. The same trend was observed (Figure 10.9) with the grafting of MAA and HEMA onto PHBHV with the use of TAS.

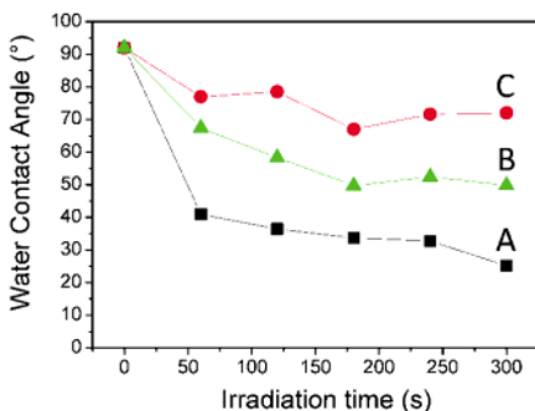


**Figure 10.8.** Evolution of the water contact angle of the modified PHBHV films for different irradiation times. a) PHBHV-g-PMETA film ( $[META]=3M$ , butan-2-one/water/ethanol volume ratio: 10/10/10), b) PHBHV-g-PHEMA film ( $[HEMA]=4M$ , butan-2-one/water/ethanol volume ratio: 10/80/10) and c) PHBHV-g-PMESA film ( $[MESA] = 1M$  with butan-2-one/water/ethanol volume ratio: 10/10/10). Reprinted (adapted) with permission from [MAN 14]

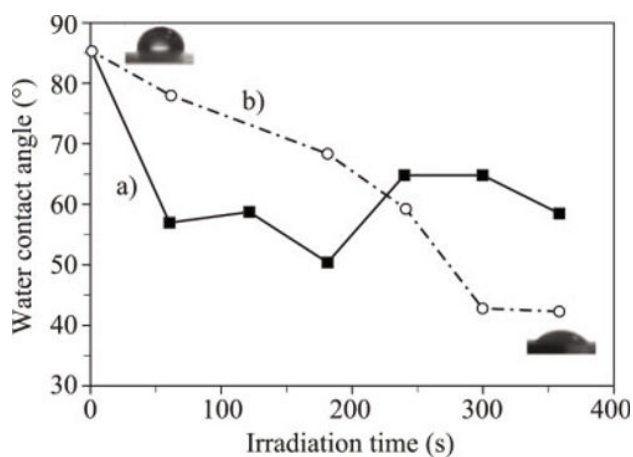


**Figure 10.9.** Dependence of the water contact angle of a) HEMA and b) MAA grafted PHBHV films surface on exposure time ( $180 \text{ mW/cm}^2$ , Hg-Xe lamp,  $50 \mu\text{l}$  of TAS/ $300 \mu\text{l}$  aqueous solution of monomer (4M)). Water contact angles correspond to a mean of three sample. Reproduced with permission from The Royal Society of Chemistry [VER 12]

#### 10.4.2. Stimuli-responsive materials

Temperature [SCH 92], pH [KAT 95], electricity [TAN 82] and light [SUZ 90] responsive polymers are of interest to researchers for a long time.

As poly(N-isopropylacrylamide) (PNIPAAm) exhibits thermally reversible soluble/insoluble changes in response to temperature change across a lower critical solution temperature (LCST) at  $32^\circ\text{C}$  in an aqueous system [HES 68], many researchers have attempted to develop intelligent materials by grafting PNIPAAm [SUZ 90, FEI 91]. The surfaces modified by PNIPAAm can be altered from hydrophilicity to hydrophobicity by external stimuli [TAK 94]. This unique characteristic enables the materials to be modified by using PNIPAAm as an intelligent biomaterial [SHI 95], a molecular separation system [IWA 91, LIA 99] and substrate for cell incubation [OKA 95]. Some researchers have grafted NIPAAm on porous polymer films such as LDPE, PP or polyamide films in order to prepare novel films used for pervaporation of liquid mixtures or separation membranes [KON 98, LIA 99]. The photografting of NIPAAm on PP film was also described by Wang [LI 02] according to two kinds of novel

methods: predipping photografting and dormant radical photografting. The water absorbency of the grafted films was also measured to investigate their temperature-sensitive characteristics. Liang *et al.* [LIA 98] reported the modification of glass plates with UV light activation for grafting NIPAAm in the presence of a cross-linking agent, N, N'-methylenebis-(acrylamide). The surface properties of the glass plates as a function of temperature have also been described. Although the surface shows the hydrophilic/hydrophobic change with a change of external temperature, the thick grafting layer (1,800 Å) shows a wider transition-temperature range that corresponds to a slower change of surface properties by thermal stimuli. The cross-linked network restricts the mobile rate of the polymer chain and, therefore, reduces the sensitivity of the polymer chain to temperature change. In the same trend, the surface of a silicon wafer coated by a photosensitizer has been modified by UV polymerization of NIPAAm by Liang *et al.* [LIA 00] to generate a thin grafting layer with a single terminal PNIPAAm. Single terminal PNIPAAm chains attached on the surface turn the surface to a thermal-sensitive surface. Dramatic changes of the hydrophilic/hydrophobic surface were observed by investigating the variation of the advancing contact angles. Kubota and Shiobara [KUB 98] grafted PNIPAAm chains on cellulose by photografting polymerization, and the resulting grafted cellulose exhibited a remarkable temperature-responsive characteristic.

pH-responsive surfaces can be synthesized through surface photografting polymerization with appropriate monomers. Luo *et al.* [LUO 03] demonstrated the use of living radical photopolymerization (LRP) surface chemistry as a means to covalently anchor a pH-sensitive, cross-linked, sodium methacrylic acid-containing hydrogel. These anchored hydrogels were used to monitor the pH, determined by the degree of hydrogel swelling, which was dependent on the pH of fluid placed in contact with modified regions. According to the same facilities, Bowman *et al.* [SEB 06] demonstrated the ability to use LRP chemistry as a surface modification platform for grafting optically responsive, pH-sensitive functionalities, as a means for integrating pH sensors onto polymeric microfluidic devices. Fluorescent, poly(ethylene glycol) acrylate succinyl fluorescein was specifically synthesized and photografted from device substrates. Switching between the fluorescent and non-fluorescent states was demonstrated when

sensing basic and acidic solutions, respectively. The dependence of graft exposure time and length on fluorescence intensity and function was also investigated. Finally, pH-sensitive grafts were easily produced and readily integrated onto a microfluidic device.

### **10.4.3. Modification of membranes**

A major part of the commercially available synthetic membranes is made up of hydrophobic polymeric materials. The latter have inert surface, thus resulting in high biofouling and decrease in flux. Surface photografting technique appears as a viable solution to overcome these disadvantages. In the following, some examples of photosynthesized membranes are summarized and concern the selective permeation and the molecular imprinting technique.

Since the late 1980s, the removal of carbon dioxide, chlorofluorocarbons, methane, etc., from industrial waste gas streams has been a major subject in view of global warming prevention. The development of environmentally friendly and energy-saving technologies for the recovery of CO<sub>2</sub> from the flue gas has become a special research interest. The development of membranes with high permeation rate and selectivity, as well as with thermal stability, still remains a challenging issue. For example, Kim *et al.* [KIM 01] developed a highly performing and selective membrane through CO<sub>2</sub>: asymmetric polyacrylonitrile (PAN) membrane was used for a substrate and methoxy poly(ethylene glycol) acrylate (MePEGA) was used for a photoinitiated graft polymer. The high permselectivity of the present membrane is attributed to high solubility selectivity due to the affinity of CO<sub>2</sub> to PEO segments. Recently, Svec *et al.* [BLI 12] demonstrated that separation performance of supported polyaniline membranes is significantly enhanced by the chemical modification and the presence of water. The modification of the supported membrane by photografting with a poly(2-hydroxyethylmethacrylate-glycidylmethacrylate) chains renders it both hydrophilic and reactive. Subsequent reaction of the epoxide group with diamines increases the basicity of the membrane and introduces functionalities serving as fixed carriers. These membranes can accommodate

significant amount of water that reacts with CO<sub>2</sub> and promotes CO<sub>2</sub> transport.

Photografting methods have been widely applied in molecular imprinted membranes also. Molecular imprinting is a straightforward method for the synthesis of materials with receptor properties similar to that of natural receptors, such as polyclonal antibodies [WUL 95, CHE 97].

The first preparation of a molecularly imprinted polymer (MIP) membrane [WAN 97] by a surface modification was accomplished with laboratory-made membranes from a special photoreactive polymer [poly(acrylonitrile-co-(diethylamino)dithiocarbamoyl-methylstyrene)]: UV-initiated graft copolymerization of acrylic acid and N,N-methylenebis(acrylamide) (MBA) in the presence of theophylline yielded membranes with theophylline specificity. Laterly, the development of a general method for molecular imprinting of a polymer surface was described by Ulbricht *et al.* [PIL 00]. PP membranes were functionalized via photograft copolymerization in water with an imprinted polymer, specific for desmetryn. Photoinitiation directly on the surface of the support polymer, PP, along with the cross-linking nature of the polymerization ensures the limitation of functionalization to a relatively thin and compact, moderately swollen layer. The method proposed could be adapted to other systems [SER 01], e.g. membranes and films, as well as to other templates. Some investigations indicated that different support materials, with larger specific surface area, can easily be applied when they can act as hydrogen donor coinitiator for the BP photoinitiator.

#### **10.4.4. Biomedical applications**

##### *10.4.4.1. Antibacterial properties*

Antibacterial materials have been employed in numerous applications, ranging from biomedical products to packing materials to air-filter systems. The first approach has focused on reducing the capacity of bacteria to attach onto a surface. Some methods to achieve this adhesion resistance rely on the modification of substrates by poly(ethylene glycol) [OST 01] or the use of diamond-like carbon films [ZHA 07]. Recently, superhydrophobic surfaces [PAR 05] created via a combination of chemical modifications, such as

addition of perfluorinated molecules [GEN 06] and zwitterionic polymers [CHE 07], have received particular interest. An alternative method for disinfecting surfaces consists of using a coating that produces reactive radical species which have no specific target within bacteria upon light activation. Two main coating types were developed: photosensitizer-immobilized [LIM 12] (as benzophenone, 4,4'-bis(dimethylamino) benzophenone or thioxanthen-9-one) and titanium dioxide-based photocatalyst coatings [PER 09, DEC 06]. A third approach has involved biocide leaching, namely antibiotics [RUC 12], cytotoxic organic [LU 01], inorganic compounds [KNE 11] or flavonoids [XIN 12] diffusing over time from a polymer material, thus inducing the death of either nearby bacteria or adhered bacteria. One of the most widely used organic antimicrobial agents in polymeric matrices is triclosan [CHU 03]. Zinc oxide [AMN 12], TiO<sub>2</sub> [PAN 11, KIM 03], montmorillonite clay derivatives [TAN 03] and metal nanoparticles [KNE 11] are the main inorganic antimicrobial compounds introduced in polymeric-based materials.

Because of the bactericidal compounds released from the matrix and the induced environmental pollution, antibacterial molecules which are chemically bonded onto the matrix appeared more desirable and have gained much more attention in the last decade. This approach is based on lethal contact which induces the biochemical death of bacteria. It generally includes positively charged molecules that aimed to penetrate cell membrane to disrupt the membrane integrity and provokes cell lysis. Several types of polymers [MUÑ 12] have been used, including polymers with quaternary ammonium groups, guanidine-containing polymers, polymers that mimic natural peptides, polymers containing phospho and sulfo derivatives, phenol and benzoic acid derivative polymers, organometallic polymers, and more recently polyelectrolyte multilayers. Concerning the photografting approach, a few studies could be cited. As an example, Yang *et al.* [XIN 05] used the sequential photografting process with BP for the covalent grafting of polyvinylpyrrolidone (PVP) onto PP film. The complexation of PVP with iodine demonstrated its efficient activity against *Escherichia coli*, *Staphylococcus aureus* and *Candida albicans*. Neoh and coworkers [SHI 05] successfully prepared modified commercial polyethylene terephthalate (PET) films with a viologen-derived monomer (HVV) by a UV photografting method. The antibacterial activity of the resulting films largely depends on the concentration of pyridinium groups tethered on the surface of

the material. The death of more than 99% of *E. coli* bacteria cells has even been demonstrated. A new straightforward and versatile method [VER 13b] for immobilizing both macromolecules and silver nanoparticles on the surface of PHBHV electrospun fibers was recently developed with the objective to design a new functional material having a significant antibacterial activity. The approach relies on a two-step procedure: UV photografting of PMAA on the surface of PHBHV fibers according to the “grafting-from” method and complexation of *in situ* photogenerated silver nanoparticles (Ag NPs) by carboxyl groups from tethered PMAA chains (Figure 10.10). Antibacterial tests confirmed that PHBHV microfibrillar scaffolds including silver nanoparticles led to a tremendous inhibition of the adhesion of *E. coli* and a reduction by 98% of the adherence of *S. aureus* (Figure 10.11). According to the same insights, ammonium, sulfopropyl ammonium and hydroxyl groups have been covalently grafted onto the PHBHV film surface [MAN 14] and the adhesion of *S. aureus* and *E. coli* decreased by 95 and 99%, respectively.

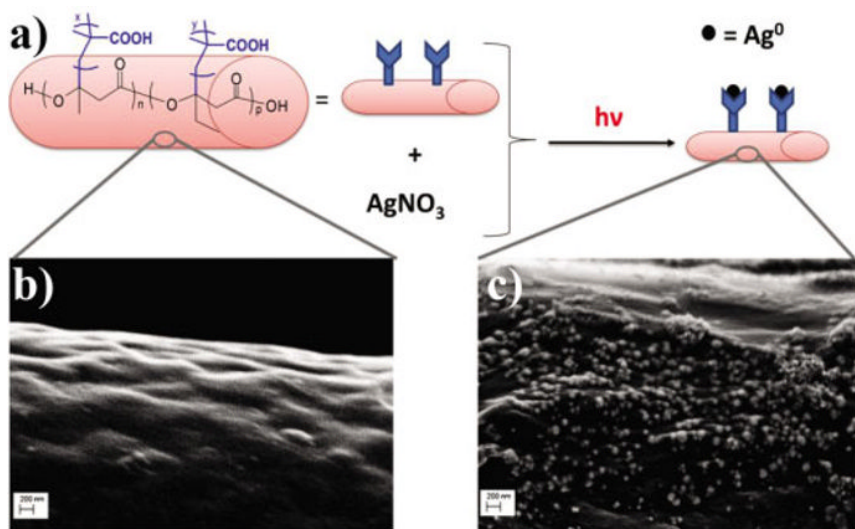


**Figure 10.10.** a) Diagram of the functionalized PHBHV-g-PMAA fibers by silver nanoparticles. Scanning electron microscopy (SEM) images of the surface of b) PHBHV-g-PMAA and c) PHBHV-g-PMAA/Ag microfibrillar materials [VER 13b]

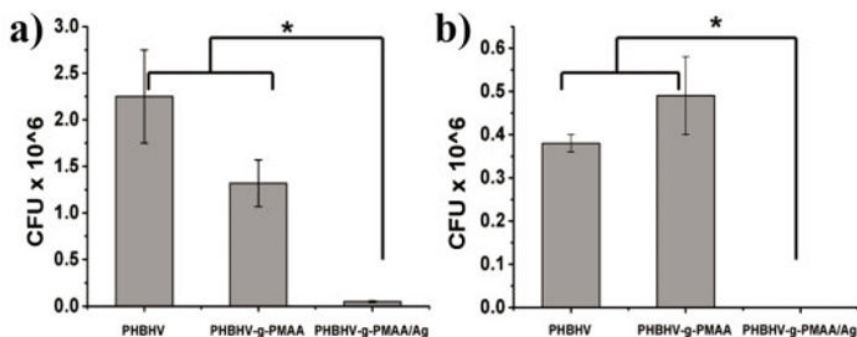


**Figure 10.11.** Comparison of anti-adherence activity against *Staphylococcus aureus* a) and *Escherichia coli* b) of PHBHV, PHBHV-g-PMAA and PHBHV-g-PMAA/Ag microfibrillar materials. Data are shown as mean plus standard deviation,  $n = 5$ . Asterisk indicates significant difference obtained by *t*-test ( $P < 0.05$ ) [VER 13b]

#### 10.4.5. Enzymes and proteins immobilization

Chemical approaches and the UV-induced grafting therein make possible the immobilization of enzymes or proteins on polymer surfaces. For instance, Akkaya [AKK 13] immobilized urease onto ethyl cellulose grafted with optimum amounts of MAA (according to the “grafting-from” method with BP). Similar results were obtained by Yamada *et al.* [YAM 06] with the use of expanded poly(tetrafluoroethylene) films grafted with 2-hydroxyethylmethacrylate and 2-hydroxyethyl acrylate. Under optimized conditions, the results revealed that the immobilized urease could be used repeatedly without highly influencing its reactivity. Albertsson and coworkers [EDL 11] successfully immobilized a vascular endothelial growth factor (VEGF)-type protein, a potent angiogenic effector molecule, onto the surfaces of resorbable polymers PLLA and poly( $\epsilon$ -caprolactone) through a three-step strategy including a UV grafting process. An enzyme sulfite oxidase has been successfully immobilized by Zhao *et al.* [NG 01] onto a UV-cured natural/synthetic copolymeric membrane chitosan-pHEMA through covalent bonding. Chitosan-pHEMA membranes, when activated with *p*-benzoquinone, have been shown to provide a suitable matrix for enzyme immobilization, applicable to biosensor fabrication. Another enzyme, trypsin [LOH 96], was also immobilized on UV-modified polytetrafluoroethylene (PTFE) films with acrylic acid (AAc), sodium salt of styrenesulfonic acid and N,N-dimethylacrylamide. Despite its

immobilization, trypsin could still retain 30% of its activity which increased with the increasing surface concentration of the grafted polymer and became saturated at a moderate AAc polymer concentration.

Generally, immobilizing enzymes on UV-modified substrates is expected to become an incredibly attractive field.

#### **10.4.6. Cell adhesion and compatibility**

Some biocompatible polymers intrinsically possess a hydrophobic surface, which is not always suitable for desired cellular response. Hence, hydrophilic surface modification has been extensively studied for hydrophobic polymers through, for example, graft polymerization [MA 05, WAN 08, LIU 04]. For instance, hydrophobic porous polyurethane (PU) scaffolds were modified by UV grafting of hydrophilic MAA monomers. From the results of human endothelial cell culture test, it was found that the PU scaffolds modified with hydrophilic PMAA had greater cell compatibility than the pure PU matrix [ZHU 03]. Surface graft polymerization has also been examined to introduce multifunctional groups on polymeric surface for the purpose of covalent immobilization of bioactive molecules for the enhancement of cell adhesion, cell proliferation and cell differentiation [MA 05]. For example, PET nanofiber mats were modified by the grafting polymerization of MAA initiated by Ce(IV), before gelatin was covalently attached to the PMAA-grafted PET nanofiber mats using water-soluble carbodiimide as coupling agent. The gelatin grafting method could obviously improve the spreading and the proliferation of endothelial cells on the PET nanofiber mats. The resulting hydrophilicity-controlled polymer surface could effectively be used for biomedical equipment such as antithrombogenic surfaces for guide wires, medical stents and artificial organs. Renard *et al.* [RAM 14] photografted glycidyl methacrylate (GMA) onto electrospun PHBHV fibers. The subsequent attachment of Arg-Gly-Asp (RGD) sequence was achieved by the epoxide opening of GMA, leading to a biomimetic scaffold. Human mesenchymal stromal cells (hMSCs) have finally exhibited a better adhesion on the latter scaffolds than that on non-functionalized Polyhydroxyalkanoates (PHAs) mats. Another efficient method is concerned with the immobilization of polysaccharides on the surface of PHBHV electrospun fibers with the use of a photosensitive anthraquinone-derived monomer [VER 13a] (AQ-Dext). The photografting is conducted through a

photoinduced free radical process employing an anthraquinone-based photosensitizer in aqueous medium. A primary investigation demonstrated that dextran-modified PHBHV fibers were favorable for optimized cell colonization and proliferation (Figure 10.12). The cell morphologies were described by Scanning Electron microscopy (SEM), revealing a significant affinity and favorable interactions for adherence of hMSCs on dextran-modified scaffolds. Moreover, the proliferation rate of hMSCs increased on this new functionalized biomaterial associated with a higher extra-cellular matrix production after 5 days of culture in comparison to native PHBHV fibers (Figure 10.13).

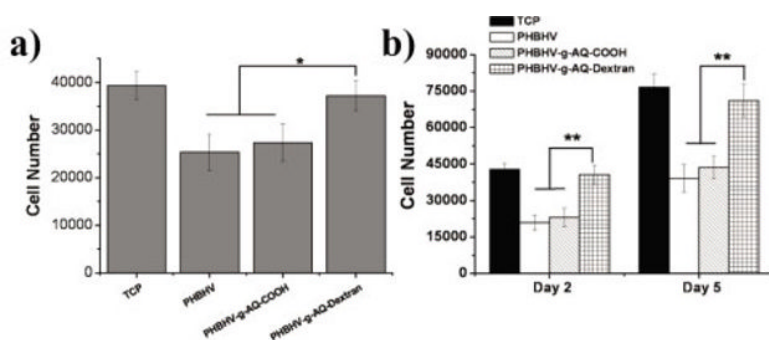


**Figure 10.12.** MTS assay of hMSC a) adhesion and b) proliferation on fibrous scaffolds of PHBHV, PHBHV-g-AQ-COOH, PHBHV-g-AQ-dextran and TCPs. Bars represent mean values  $\pm$  standard deviations ( $n = 4$ ). Asterisks indicate significant difference obtained by *t*-test. (\*) represents  $p < 0.05$  and (\*\*) represents  $p < 0.01$ . Reproduced with permission from The Royal Society of Chemistry [VER 13a]

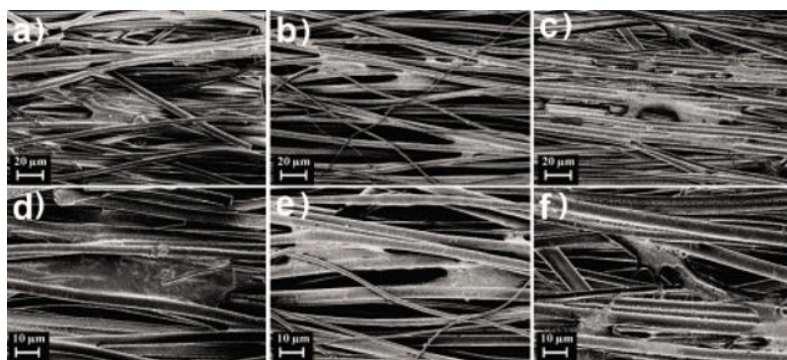


**Figure 10.13.** SEM micrographs of fibrous scaffolds after 5 days of hMSC culture on (a,d) PHBHV, (b,e) PHBHV-g-AQ-COOH and (c,f) PHBHV-g-AQ-dextran. Reproduced with permission from The Royal Society of Chemistry [VER 13a]

## 10.5. Conclusion

This chapter has addressed the main photochemical mechanisms, namely the “grafting-from” and the “grafting-to” techniques under light activation, and the principal photoinitiators that are involved in the UV-induced surface graft polymerization (BP, ketones and its derivatives, photoiniferters, TAS, aryl azide and anthraquinone-derived monomers). The discussion demonstrated, through the different examples of applications, that photografting process is a powerful and useful tool for tailoring the surface properties of polymer materials, particularly the hydrophobic polymers. The increasing investigations using the photografting process point out that it is becoming a rapidly growing and increasingly competitive research area. Photopolymerization method is a more environmentally friendly process than the traditional polymerizations, as it can advantageously be performed at room temperature and with a wide range of different monomers, including (meth)acrylates, and can lead to a large variety of final polymer properties. Another noteworthy point is that the UV-grafting polymerization of some special monomer systems might help us to rapidly design and develop novel high-performance materials. Finally, the photografting process appears to be the most valuable and promising technique in the future for both academic research and industrialization compared to usual polymerization techniques.

## 10.6. Bibliography

- [AKK 13] AKKAYA A., “Covalent immobilization of urease to modifiedethyl cellulose”, *Fibers and Polymers*, vol. 14, pp. 22–27, 2013.
- [AMN 12] AMNA T., HASSAN M.S., BARAKAT N.M. *et al.*, “Antibacterial activity and interaction mechanism of electrospun zinc-doped titania nanofibers”, *Applied Microbiology and Biotechnology*, vol. 93, pp. 743–751, 2012.
- [ANG 80] ANG C.H., GARNETT J.L., *et al.*, “Photosensitized grafting of styrene 4-vinylpyridine and methylmethacrylate to polypropylene”, *Journal of Polymer Science: Polymer Letter Edition*, vol. 18, pp. 471–475, 1980.
- [BAR 01] BARBE L.L., BOVAL B.M., WAUTIER M.-P.S. *et al.*, “An *in vitro* system for testing leucocyte and leukaemiccell line adhesion to synthetic fibres”, *British Journal of Haematology*, vol. 115, pp. 664–671, 2001.
- [BHA 08] BHAT V.T., JAMES N.R., JAYAKRISHNAN A., “A photochemical method for immobilization of azidated dextran onto aminated poly(ethyleneterephthalate) surfaces”, *Polymer International*, vol. 57, pp. 124–132, 2008.

- [BLI 12] BLINOVA N.V., SVEC F., “Functionalized polyaniline-based composite membranes with vastly improved performance for separation of carbondioxide from methane”, *Journal of Membrane Science*, vol. 423–424, pp. 514–521, 2012.
- [CHE 97] CHEONG S.H., MCNIVEN S., RACHKOV A. *et al.*, “Testosterone Receptor Binding Mimic Constructed Using Molecular Imprinting”, *Macromolecules*, vol. 30, pp. 1317–1322, 1997.
- [CHE 07] CHENG G., ZHANG Z., CHEN S. *et al.*, “Inhibition of bacterial adhesion and biofilm formation on zwitterionic surfaces”, *Biomaterials*, vol. 28, pp. 4192–4199, 2007.
- [CHO 06] CHO J.-D., KIM S.-G., HONG J.-W., “Surface modification of polypropylenesheets by UV-radiation grafting polymerization”, *Journal of Applied Polymer Science*, vol. 99, pp. 1446–1461, 2006.
- [CHU 03] CHUNG D., PAPADAKIS S.E., YAM K.L., “Evaluation of a polymer coating containing triclosan as the antimicrobial layer for packaging materials”, *International Journal of Food Science and Technology*, vol. 38, pp. 165–169, 2003.
- [DAN 10] DANILOSKA V., BLAZEVSKA-GILEV J., DIMOVA V. *et al.*, “UV light induced surface modification of HDPE films with bioactive compounds”, *Applied Surface Science*, vol. 256, pp. 2276–2283, 2010.
- [DEB 99] DE BOER B., SIMON H.K., “WERTS M.P.L. *et al.*, “Living” Free Radical Photopolymerization Initiated from Surface-Grafted Iniferter Monolayers”, *Macromolecules*, vol. 33, pp. 349–356, 1999.
- [DEC 98] DECKER C., ZAHOUILY K., “Light-stabilization of polymeric materials by grafted UV-cured coatings”, *Journal of Polymer Science Part A: Polymer Chemistry*, vol. 36, pp. 2571–2580, 1998.
- [DEC 06] DECRAENE V., PRATTEN J., WILSON M., “Cellulose Acetate Containing Toluidine Blue and Rose Bengal is an Effective Antimicrobial Coating when Exposed to White Light”, *Applied and Environmental Microbiology*, vol. 72, pp. 4436–4439, 2006.
- [DWO 88] DWORJANYN P.A., GARNETT J.L., “Synergistic effects of urea with polyfunctional acrylates for enhancing the photografting of styrene to polypropylene”, *Journal of Polymer Science Part C: Polymer Letter*, vol. 26, pp. 135–138, 1988.
- [EDL 11] EDLUND U., SAUTER T., ALBERTSSON A.C., “Covalent VEGF protein immobilization on resorbable polymeric surfaces”, *Polymers for Advanced Technologies*, vol. 22, pp. 166–171, 2011.

- [FEI 91] FEIL H., BAE Y.H., FEIJEN J. *et al.*, “Molecular separation by thermo sensitive hydrogel membranes”, *Journal of Membrane Science*, vol. 64, pp. 283–294, 1991.
- [GEN 06] GENZER J., EFIMENKO K., Recent developments in super hydrophobic surfaces and their relevance to marine fouling: are view Biofouling, *The Journal of Bioadhesion and Biofilm Research*, vol. 22, pp. 339–360, 2006.
- [GEU 00] GEUSKENS G., ETOC A., DI MICHELE P., “Surface modification of polymers VII.: Photo chemical grafting of acrylamide and N-isopropylacrylamide onto polyethylene initiated by anthraquinone-2-sulfonate adsorbed at the surface of the polymer”, *European Polymer Journal*, vol. 36, pp. 265–271, 2000.
- [GUA 00] GUAN J., GAO C., FENG L. *et al.*, “Functionalizing of polyurethane surfaces by photografting with hydrophilic monomers”, *Journal of Applied Polymer Science*, vol. 77, pp. 2505–2512, 2000.
- [GUP 02] GUPTA B., PLUMMER C., BISSON I. *et al.*, “Plasma-induced graft polymerization of acrylic acid onto poly(ethyleneterephthalate) films: characterization and human smooth muscle cell growth on grafted films”, *Biomaterials*, vol. 23, pp. 863–871, 2002.
- [HAR 91] HARMER M.A., “Photo modification of surfaces using heterocyclic azides”, *Langmuir*, vol. 7, pp. 2010–2012, 1991.
- [HES 68] HESKINS M., GUILLET J.E., “Solution Properties of Poly(N-isopropylacrylamide)”, *Journal of Macromolecular Science: Part A – Chemistry*, vol. 2, pp. 1441–1455, 1968.
- [HU 06] HU M.-X., YANG Q., XU Z.-K., “Enhancing the hydrophilicity of polypropylene microporous membranes by the grafting of 2-hydroxyethyl methacrylate via a synergistic effect of photoinitiators”, *Journal of Membrane Science*, vol. 285, pp. 196–205, 2006.
- [IWA 91] IWATA H., OODATE M., UYAMA Y. *et al.*, “Preparation of temperature-sensitive membranes by graft polymerization onto a porous membrane”, *Journal of Membrane Science*, vol. 55, pp. 119–130, 1991.
- [JAN 06] JANORKAR A.V., PROULX S.E., METTERS A.T. *et al.*, “Surface-confined photo polymerization of single- and mixed-monomer systems to tailor the wettability of poly(L-lactide) film”, *J. Polym. Sci. Part A: Polym. Chem.*, vol. 44, pp. 6534–6543, 2006.
- [KAT 95] KATAOKA K., KOYO H., TSURUTA T., “Novel pH-Sensitive Hydrogels of Segmented Poly(amine ureas) Having a Repetitive Array of Polar and Apolar Units in the Main Chain”, *Macromolecules*, vol. 28, pp. 3336–3341, 1995.

- [KE 07] KE Y., WANG Y., REN L. *et al.*, “Photografting polymerization of polyacrylamide on PHBV films (I)”, *Journal of Applied Polymer Science*, vol. 104, pp. 4088–4095, 2007.
- [KID 01] KIDOAKI S., OHYA S., NAKAYAMA Y. *et al.*, Thermoresponsive Structural Change of a Poly(*N*-isopropylacrylamide) Graft Layer Measured with an Atomic Force Microscope, *Langmuir*, vol. 17, pp. 2402–2407, 2001.
- [KIM 01] KIM J.H., HA S.Y., NAM S.Y. *et al.*, “Selective permeation of CO<sub>2</sub> through pore-filled polyacrylonitrile membrane with poly(ethylene glycol)”, *Journal of Membrane Science*, vol. 186, pp. 97–107, 2001.
- [KIM 03] KIM S.H., KWAK S.-Y., SOHN B.-H. *et al.*, “Design of TiO<sub>2</sub> nanoparticle self-assembled aromatic polyamide thin-film-composite (TFC) membrane as an approach to solve biofouling problem”, *Journal of Membrane Science*, vol. 211, pp. 157–165, 2003.
- [KNA 01] KNAUS S., NENNADAL A., FROSCHAUER B., “Surface and bulk modification of polyolefins by functional aryl nitrenes as highly reactive intermediates, *Macromolecular Symposia*”, vol. 176, pp. 223–232, 2001.
- [KNE 11] KNETSCH M.L.W., KOOLE L.H., “New Strategies in the Development of Antimicrobial Coatings: The Example of Increasing Usage of Silver and Silver Nanoparticles”, *Polymers*, vol. 3, pp. 340–366, 2011.
- [KON 98] KONDO T., KOYAMA M., KUBOTA H. *et al.*, Characteristics of acrylic acid and *N*-isopropylacrylamide binary monomers-grafted polyethylene film synthesized by photografting”, *Journal of Applied Polymer Science*, vol. 67, pp. 2057–2064, 1998.
- [KUB 98] KUBOTA H., SHIOBARA N., “Photografting of *N*-isopropylacrylamide on cellulose and temperature-responsive character of the resulting grafted celluloses”, *Reactive and Functional Polymers*, vol. 37, pp. 219–224, 1998.
- [LAO 10] LAO H.-K., RENARD E., LANGLOIS V. *et al.*, “Surface functionalization of PHBV by HEMA grafting via treatment: Comparison with Science”, *Journal of applied polymer*, vol. 116, no. 1, pp. 288–297, available at <http://nline.librar.wiley.com/doi/10.1002/app.31507/abstract>, 2010.
- [LEE 96] LEE S.-D., HSIUE G.-H., CHANG P.C.-T. *et al.*, “Plasma-induced grafted polymerization of acrylic acid and subsequent grafting of collagen onto polymer film as biomaterials”, *Biomaterials*, vol. 17, pp. 1599–1608, 1996.
- [LEW 10] LEWIS E.S., *Diazonium and Diazo Groups (1978)*, John Wiley & Sons Ltd., pp. 499–510, 2010.

- [LI 02] LI B., CHEN W., LIU X. *et al.*, "Preparation of temperature-sensitive polymer films by surface photografting techniques", *Polymers for Advanced Technologies*, vol. 13, pp. 239–241, 2002.
- [LIA 98] LIANG X., FENG J., LIU P.C. *et al.*, "Reversible Surface Properties of Glass Plate and Capillary Tube Grafted by Photopolymerization of N-Isopropylacrylamide", *Macromolecules*, vol. 31, pp. 7845–7850, 1998.
- [LIA 99a] LIANG L., FENG X., LIU J. *et al.*, "Preparation of composite-crosslinked poly(N-isopropylacrylamide) gel layer and characteristics of reverse hydrophilic–hydrophobic surface", *Journal of Applied Polymer Science*, vol. 72, pp. 1–11, 1999.
- [LIA 99b] LIANG L., FENG X., PEURUNG L. *et al.*, "Temperature-sensitive membranes prepared by UV photopolymerization of N-isopropylacrylamide on a surface of porous hydrophilic polypropylene membranes", *Journal of Membrane Science*, vol. 162, pp. 235–246, 1999.
- [LIA 00] LIANG P.C., RIEKE G.E., FRYXELL J. *et al.*, "Temperature-Sensitive Surfaces Prepared by UV Photografting Reaction of Photosensitizer and N-Isopropylacrylamide", *The Journal of Physical Chemistry B*, vol. 104, pp. 11667–11673, 2000.
- [LIM 12] LIM K.S., OH K.W., KIM S.H., "Antimicrobial activity of organic photo sensitizers embedded in electrospun nylon 6 nanofibers", *Polymer International*, vol. 61, pp. 1519–1524, 2012.
- [LIU 04] LIU M., XU Z.-K., WANG J.-Q. *et al.*, "Surface modification of polypropylene microfiltration membranes by graft polymerization of N-vinyl-2-pyrrolidone", *European Polymer Journal*, vol. 40, pp. 2077–2087, 2004.
- [LOH 96] LOH F.C., TAN K.L., KANG E.T. *et al.*, "XPS Characterization of Surface Functionalized Electroactive Polymers", *Surface and Interface Analysis*, vol. 24, pp. 597–604, 1996.
- [LU 01] LU J., HILL M.A., HOOD M. *et al.*, "Formation of antibiotic, biodegradable polymers by processing with Irgasan DP300R (triclosan) and its inclusion compound with  $\beta$ -cyclodextrin", *Journal of Applied Polymer Science*, vol. 82, pp. 300–309, 2001.
- [LUO 02a] LUO N., HUTCHISON J.B., ANSETH K.S. *et al.*, "Surface-Initiated Photopolymerization of Poly(ethylene glycol) Methyl Ether Methacrylate on a Diethyldithiocarbamate-Mediated Polymer Substrate", *Macromolecules*, vol. 35, pp. 2487–2493, 2002.

- [LUO 02b] LUO N., HUTCHISON J.B., ANSETH K.S. *et al.*, “Synthesis of a novel methacrylic monomer iniferter and its application in surface photo grafting on cross linked polymer substrates”, *Journal of Polymer Science Part A: Polymer Chemistry*, vol. 40, pp. 1885–1891, 2002.
- [LUO 03] LUO N., METTERS A.T., HUTCHISON J.B. *et al.*, “A Methacrylated Photo iniferter as a Chemical Basis for Microlithography: Micro patterning Based on Photo grafting Polymerization”, *Macromolecules*, vol. 36, pp. 6739–6745, 2003.
- [MA 02] MA Z., GAO C., YUAN J. *et al.*, “Surface modification of poly-L-lactide by photografting of hydrophilic polymers towards improving its hydrophilicity”, *Journal of Applied Polymer Science*, vol. 85, pp. 2163–2171, 2002.
- [MA 03] MA Z., GAO C., GONG Y. *et al.*, “Chondrocyte behaviors on poly-l-lactic acid (PLLA) membranes containing hydroxyl, amide or carboxyl groups”, *Biomaterials*, vol. 24, pp. 3725–3730, 2003.
- [MA 05] MA Z., KOTAKI M., YONG T. *et al.*, “Surface engineering of electrospun polyethylene terephthalate (PET) nano fibers towards development of a new material for blood vessel engineering”, *Biomaterials*, vol. 26, pp. 2527–2536, 2005.
- [MA 99] MA H., DAVIS R.H., BOWMAN C.N., “A Novel Sequential Photo induced Living Graft Polymerization”, *Macromolecules*, vol. 33, pp. 331–335, 2000.
- [MAN 14] MANECKA G.M., LABRASH J., ROUXEL O. *et al.*, “Green Photoinduced Modification of Natural Poly(3-hydroxybutyrate-co-3-hydroxyvalerate) Surface for Antibacterial Applications”, *ACS Sustainable Chemistry and Engineering*, vol. 2, pp. 996–1006, 2014.
- [MAT 03] MATSUDA T., NAGASE J., GHODA A. *et al.*, “Phosphorylcholine-endcapped oligomer and block co-oligomer and surface biological reactivity”, *Biomaterials*, vol. 24, pp. 4517–4527, 2003.
- [MUÑ 12] MUÑOZ-BONILLA A., FERNÁNDEZ-GARCÍA M., “Polymeric materials with antimicrobial activity”, *Progress in Polymer Science*, vol. 37, pp. 281–339, 2012.
- [NG 01] NG L.-T., GUTHRIE J.T., YUAN Y.J. *et al.*, “UV-cured natural polymer-based membrane for biosensor application”, *Journal of Applied Polymer Science*, vol. 79, pp. 466–472, 2001.
- [OKA 95] OKANO T., YAMADA N., OKUHARA M. *et al.*, “Mechanism of cell detachment from temperature-modulated, hydrophilic-hydrophobic polymer surfaces”, *Biomaterials*, vol. 16, pp. 297–303, 1995.

- [OST 01] OSTUNI E., CHAPMAN R.G., LIANG M.N. *et al.*, “Self-Assembled Monolayers That Resist the Adsorption of Proteins and the Adhesion of Bacterial and Mammalian Cells”, *Langmuir*, vol. 17, pp. 6336–6343, 2001.
- [OTS 82a] OTSU T., YOSHIDA M., “Role of initiator-transfer agent-terminator (iniferter) in radical polymerizations: Polymer design by organic disulfides as iniferters”, *Die Makromolekulare Chemie, Rapid Communications*, vol. 3, pp. 127–132, 1982.
- [OTS 82b] OTSU T., YOSHIDA M., TAZAKI T., “A model for living radical polymerization”, *Die Makromolekulare Chemie, Rapid Communications*, vol. 3, pp. 133–140, 1982.
- [OTS 98] OTSU T., MATSUMOTO A., “Controlled Synthesis of polymers using the iniferter technique : developments in living radical polymerization”, *Advances in Polymer Science*, vol. 136, pp. 75–137, 1998;
- [PAN 04] PAN B., VISWANATHAN K., HOYLE C.E. *et al.*, “Photo initiated grafting of maleic anhydride onto polypropylene”, *Journal of Polymer Science Part A: Polymer Chemistry*, vol. 42, pp. 1953–1962, 2004.
- [PAN 11] PANT H.R., PANDEYA D.R., NAM K.T. *et al.*, “Photocatalytic and antibacterial properties of a TiO<sub>2</sub>/nylon-6 electrospun nano composite mat containing silver nano particles”, *Journal of Hazardous Materials*, vol. 189, pp. 465–471, 2011.
- [PAR 05] PARKIN I.P., PALGRAVE R.G., “Self-cleaning coatings”, *Journal of Materials Chemistry*, vol. 15, pp. 1689–1695, 2005.
- [PER 09] PERNI S., PICCIRILLO C., PRATTEN J. *et al.*, “The anti microbial properties of light-activated polymers containing methylene blue and gold nanoparticles”, *Biomaterials*, vol. 30, pp. 89–93, 2009.
- [PIL 00] PILETSKY S.A., MATUSCHEWSKI H., SCHEDLER U. *et al.*, “Surface Functionalization of Porous Polypropylene Membranes with Molecularly Imprinted Polymers by Photo graft Copolymerization in Water”, *Macromolecules*, vol. 33, pp. 3092–3098, 2000.
- [RAM 14] RAMIER J., BOUBAKER M.B., GUERROUCHE M. *et al.*, “Novel routes to epoxy functionalization of PHA-based electrospun scaffolds as ways to improve cell adhesion”, *Journal of Polymer Science Part A: Polymer Chemistry*, vol. 52, pp. 816–824, 2014.
- [RUC 12] RUCKH T., OLDINSKI R., CARROLL D. *et al.*, “Antimicrobial effects of nano fiber poly(caprolactone) tissue scaffolds releasing rifampicin”, *Journal of Materials Science: Materials in Medicine*, vol. 23, pp. 1411–1420, 2012.

- [SCH 92] SCHILD H.G., "Poly(*N*-isopropylacrylamide): experiment, theory and application", *Progress in Polymer Science*, vol. 17, pp. 163–249, 1992.
- [SCR 88] SCRIVEN E.F.V., TURNBULL K., "Azides: their preparation and synthetic uses", *Chemical Reviews*, vol. 88, pp. 297–368, 1988.
- [SEB 06] SEBRA R.P., KASKO A.M., ANSETH K.S. *et al.*, "Synthesis and photografting of highly pH-responsive polymer chains", *Sensors and Actuators B: Chemical*, vol. 119, pp. 127–134, 2006.
- [SER 01] SERGEYEVA T.A., MATUSCHEWSKI H., PILETSKY S.A. *et al.*, "Molecularly imprinted polymer membranes for substance-selective solid-phase extraction from water by surface photo-grafting polymerization", *Journal of Chromatography A*, vol. 907, pp. 89–99, 2001.
- [SHI 05] SHI Z., NEOH K.G., KANG E.T., "Anti bacterial activity of polymeric substrate with surface graft edviologenmoieties", *Biomaterials*, vol. 26, pp. 501–508, 2005.
- [SHI 95] SHIROYA T., YASUI M., FUJIMOTO K. *et al.*, "Control of enzymatic activity using thermo sensitive polymers", *Colloids and Surfaces B: Biointer faces*, vol. 4, pp. 275–285, 1995.
- [SUN 10] SUN J., YAO L., GAO Z. *et al.*, "Surface modification of PET films by atmospheric pressure plasma-induced acrylic acid inverse emulsion graft polymerization", *Surface and Coatings Technology*, vol. 204, pp. 4101–4106, 2010.
- [SUZ 90] SUZUKI A., TANAKA T., "Phase transition in polymer gels induced by visible light", *Nature*, vol. 346, pp. 345–347, 1990.
- [TAK 94] TAKEI Y.G., AOKI T., SANUI K. *et al.*, "Dynamic Contact Angle Measurement of Temperature-Responsive Surface Properties for Poly(*N*-isopropylacrylamide) Grafted Surfaces", *Macromolecules*, vol. 27, pp. 6163–6166, 1994.
- [TAN 03] TANG Z., KOTOV N.A., MAGONOV S. *et al.*, "Nanostructured artificial nacre", *Nature Materials*, vol. 2, pp. 413–418, 2003.
- [TAN 82] TANAKA T., NISHIO I., SUN S.-T. *et al.*, "Collapse of Gels in an Electric Field", *Science*, vol. 218, pp. 467–469, 1982.
- [THO 98] THOM V., JANKOVA K., ULBRICHT M. *et al.*, "Synthesis of photoreactive  $\alpha$ -4-azidobenzoyl- $\omega$ -methoxy-poly(ethylene glycol)s and their end-on photografting onto polysulfone ultra filtration membranes", *Macromolecular Chemistry and Physics*, vol. 199, pp. 2723–2729, 1998.

- [VER 12] VERSACE D.-L., DUBOT P., CENEDESE P. *et al.*, “Natural biopolymer surface of poly(3-hydroxybutyrate-co-3-hydroxyvalerate)-photo induced modification with triarylsulfonium salts”, *Green Chemistry*, vol. 14, pp. 788–798, 2012.
- [VER 13a] VERSACE D.-L., RAMIER J., BABINOT J. *et al.*, “Photoinduced modification of the natural biopolymer poly(3-hydroxybutyrate-co-3-hydroxyvalerate) microfibrinous surface with anthraquinone-derived dextran for biological applications”, *Journal of Materials Chemistry B*, vol. 1, pp. 4834–4844, 2013.
- [VER 13b] VERSACE D.-L., RAMIER J., GRANDE D. *et al.*, “Versatile Photochemical Surface Modification of Biopolyester Microfibrinous Scaffolds with Photogenerated Silver Nanoparticles for Antibacterial Activity”, *Advanced Healthcare Materials*, vol. 2, pp. 1008–1018, 2013.
- [WAN 04] WANG H., BROWN H.R., “Aliphatic Ketones as Photoinitiators for Photografting”, *Macromolecular Rapid Communications*, vol. 25, pp. 1257–1262, 2004.
- [WAN 06] WANG Y., BACHMAN M., SIMS C.E. *et al.*, “Simple Photografting Method to Chemically Modify and Micropattern the Surface of SU-8 Photoresist”, *Langmuir*, vol. 22, pp. 2719–2725, 2006.
- [WAN 07] WANG H., BROWN H.R., LI Z., Aliphatic ketones/water/alcohol as a new photo initiating system for the photografting of methacrylic acid onto high-density polyethylene, *Polymer*, vol. 48, pp. 939–948, 2007.
- [WAN 08] WANG W., ZHANG Y., ZHU M. *et al.*, “Effect of graft modification with poly(*N*-vinylpyrrolidone) on thermal and mechanical properties of poly (3-hydroxybutyrate-co-3-hydroxyvalerate)”, *Journal of Applied Polymer Science*, vol. 109, pp. 1699–1707, 2008.
- [WAN 97] WANG H.Y., KOBAYASHI T., FUJII N., “Surface molecular imprinting on photo sensitive dithiocarbamoyl polyacrylonitrile membranes using photo graft polymerization”, *Journal of Chemical Technology and Biotechnology*, vol. 70, pp. 355–362, 1997.
- [WAV 02] WAVHAL D.S., FISHER E.R., “Membrane Surface Modification by Plasma-Induced Polymerization of Acrylamide for Improved Surface Properties and Reduced Protein Fouling”, *Langmuir*, vol. 19, pp. 79–85, 2003.
- [WUL 95] WULFF G., “Molecular Imprinting in Cross-Linked Materials with the Aid of Molecular Templates—A Way towards Artificial Antibodies”, *Angewandte Chemie International Edition in English*, vol. 34, pp. 1812–1832, 1995.

- [XIN 05] XING C.-M., DENG J.-P., YANG W.-T., “Synthesis of antibacterial polypropylene film with surface immobilized polyvinyl pyrrolidone-iodine complex”, *Journal of Applied Polymer Science*, vol. 97, pp. 2026–2031, 2005.
- [XIN 12] XING Z.-C., MENG W., YUAN J. *et al.*, “In Vitro Assessment of Antibacterial Activity and Cytocompatibility of Quercetin-Containing PLGA Nanofibrous Scaffolds for Tissue Engineering”, *Journal of Nanomaterials*, Article ID 202608, vol. 2012, p. 7, 2012.
- [YAM 06] YAMADA K., IIZAWA Y., YAMADA J.-I. *et al.*, “Retention of activity of urease immobilized on grafted polymer films”, *Journal of Applied Polymer Science*, vol. 102, pp. 4886–4896, 2006.
- [YAN 99] YANG W., RÅNBY B., “Photo initiation performance of some ketones in the LDPE–acrylic acid surface photografting system”, *European Polymer Journal*, vol. 35, pp. 1557–1568, 1999.
- [ZHA 07] ZHAO Q., LIU Y., WANG C. *et al.*, “Evaluation of bacterial adhesion on Si-doped diamond-like carbon films”, *Applied Surface Science*, vol. 253, pp. 7254–7259, 2007.
- [ZHU 02] ZHU H., JI J., LIN R. *et al.*, “Surface engineering of poly(dl-lactic acid) by entrapment of alginate-amino acid derivatives for promotion of chondrogenesis”, *Biomaterials*, vol. 23, pp. 3141–3148, 2002.
- [ZHU 03] ZHU Y., GAO C., GUAN J. *et al.*, “Engineering porous polyurethane scaffolds by photo grafting polymerization of methacrylic acid for improved endothelial cell compatibility”, *Journal of Biomedical Materials Research Part A*, vol. 67A, pp. 1367–1373, 2003.
- [ZIA 99] ZIANI-CHERIF H., IMACHI K., “Matsuda T., Preparation of Aryldiazonium-, Aryldiazo-, and Arylazido-Derivatized Copolymers and their Surface Photografting”, *Macromolecules*, vol. 32, pp. 3438–3447, 1999.



---

## Light-cured Luminescent Coatings for Photovoltaic Devices

---

### 11.1. Photovoltaics: technology, devices and spectral management

#### 11.1.1. *Energy demand and photovoltaic converters*

The current efforts that the scientific community is undertaking in the energy field can easily be exemplified by a few statements concerning the current planet energy situation. The world population exceeded 7 billion at the end of 2011 and now consumes a quantity of energy estimated in  $5.6 \times 10^{20}$  J per year, which corresponds to a continuous demand of 17.8 TW. At present, the world's primary energy consumption increases by 1.6% per year, and it has been recently estimated that this figure will increase up to around  $8.1 \times 10^{20}$  J per year (25.8 TW) in 2035 [RED 14]. The present energy economy is still highly dependent on three forms of fossil fuels (oil, natural gas and coal), which cover more than 85% of the total energy production. However, at the current reserves-to-production ratio, oil might run out in around 50 years (although the uncertainty of these data is very high), natural gases can last for about 70 years and coal for 150 years [RED 14]. Moreover, the periodic increases in oil price, the interruption in gases distribution and the unstable political situation in the Middle East region are leading to a continuous increase in the fossil energy cost. Last but

---

Chapter written by Federico BELLA, Gianmarco GRIFFINI, Roberta BONGIOVANNI and Stefano TURRI.

not least, we have to keep in mind the environmental impact of energy production from fossil fuels. Indeed, the measured concentration of carbon dioxide (CO<sub>2</sub>), the most important greenhouse gas, has significantly increased in the past few decades as a result of human activities, primarily due to fossil fuel use, and it is leading to an increase in the average global temperature, a phenomenon known as “global warming”.

As a result of this alarming situation, a strong interest in alternative energy resources has arisen over the past few years, at a political and social level. For example, the European Union decided that no later than 2020 the CO<sub>2</sub> emissions should decrease by 20% and the 20% of the energy produced should originate from renewable energy sources [EUR 15]. Alternative energy, as it is currently conceived, is a resource that does not lead to the undesirable consequences typical of fossil fuel use, such as the high CO<sub>2</sub> emissions [DRE 01].

Among alternative energy resources, renewable energies constitute and will represent the main solution to face the growing energy demand of world population [TUR 99]. Renewable energies come from sources that regenerate themselves at least at the same speed they are consumed, or are not exhaustible in human time scale, so that their usage does not compromise the natural resources for future generations [NEG 12]. Mainstream forms of renewable energy are wind power, solar energy, hydropower, geothermal energy, biomass and biofuel.

Among all, solar energy is considered the most promising renewable resource. Indeed, the Sun provides the Earth with approximately  $3 \times 10^{24}$  J a year, a figure that is about  $10^4$  times larger than the current global population demand [GRÄ 01]. In other words, the amount of solar energy reaching the surface of the planet is so vast that in 1 year it is about twice as much as will ever be obtained from all non-renewable resources currently exploited, i.e. coal, oil, natural gas and mined uranium [GLO 15]. Prompted by these numbers, the scientific community is working hard to propose and improve solar energy conversion technologies. To give an idea of the magnitude of this effort, a simple search on a commonly used scientific database such as Scopus will provide more than 10,000 publications about “solar energy” per year for the past 5–10 years.

Over the past few decades, various technologies have been proposed for the conversion of solar energy into electricity by the photovoltaic (PV) effect. All these technologies are classified into three main categories, which are distinguished by the nature of the materials used, the thickness of the devices, the mechanism of generation, separation and collection of the charge carriers. First-generation solar cells are the so-called “solid junction cells”, in which the constituent material is Si, both in mono- and polycrystalline forms. At present, the PV market for terrestrial applications is dominated by Si crystalline solar cells due to their high efficiency, long lifetime (over 20 years) and availability on the market. The main drawbacks of mono-Si devices are their high processing and manufacturing costs and their relatively long (~4 years) payback time, the latter being defined as the time interval in which a PV cell produces the amount of electricity necessary to cover the energy spent during its fabrication [KAT 97].

Second-generation solar cells are also called thin film (TF) technologies, because materials with high absorption coefficients are used, which allow a significant reduction of active layer thickness with respect to first-generation devices. Cadmium telluride (CdTe), gallium arsenide (GaAs) and copper indium (gallium) selenide (CIS/CIGS) are widely used as cell components. However, the environmental, health and safety aspects of these compounds should be taken into serious consideration if the TF technology is to expand on a large scale.

Third-generation approaches to PVs include devices developed following two main lines of thought. The first line of thought is that of achieving high-efficiency devices by using and improving TFs fabricated with second-generation deposition methods [CON 07]. The second and most popular research field is focused on the fabrication of devices based on organic or hybrid organic/inorganic materials which are widely available, non-toxic and of low cost [NUN 02]. In particular, the greatest expectations are focused on the so-called “hybrid solar cells”, which combine advantages of both organic and inorganic semiconductors. In a general setup, an organic material absorbs light and/or transports holes, while the inorganic material is used as the electron acceptor and transporter. Currently, two of the most relevant and representative devices belonging to this category are dye-sensitized solar cells (DSSCs) [BEL 13a) and perovskite solar cells (PSCs) [ZHO 14]). Even if PSCs have been able to provide higher efficiency than DSSCs, they

are composed of such materials (methylammonium tin and lead organohalide compounds) that still make them less suitable for a widespread and cheap diffusion on the market. Conversely, DSSCs are emerging as a leading third-generation technology. Among other things, the success of DSSC devices is also due to their ability to exploit the versatility of polymeric materials, which can act as templating agents, conductors of electrons and ions, sealants and waveguides of the incident solar radiation. The operating principles and application of DSSC devices are discussed in detail in the next sections, with particular focus on their use in combination with light management luminescent coatings to improve their device performance.

### ***11.1.2. Spectral management for photovoltaics: principles, materials and applications***

Despite the enormous potential offered by the PV technology and the progresses made by the PV industry in the past few decades, the use of solar electricity in modern society is still limited by the difficulties in achieving efficient devices at competitive costs. One of the major problems that limits the sunlight-to-electricity conversion efficiency of PV devices is their limited spectral response. Indeed, while the Air Mass 1.5 Global (AM 1.5G) solar spectrum extends over a wide range of usable wavelengths (from ultraviolet (UV) to infrared, 280–2,500 nm, 0.5–4.4 eV), current PV devices can only utilize a relatively small portion of such photons. This behavior arises from the ability of each PV material to respond optimally only to a narrow range of photons with energies ideally matching its characteristic band gap. As a result, the excess energy of photons with energy higher than the bandgap will be lost by thermalization processes, while photons with energies lower than the bandgap will not be absorbed and thus will be wasted. This behavior is well exemplified by the well-known Shockley–Queisser equation [SHO 61] that identifies the theoretical maximum efficiency of crystalline silicon (c-Si) solar cells with a band gap energy ( $E_g$ ) of 1.1 eV as approximately 30% for non-concentrated systems.

A very promising approach to minimize the intrinsic thermalization and non-absorption photon losses of existing solar cells makes use of luminescent materials as spectral converters embedded into passive transparent layers incorporated into the PV cell. The application of such

spectral management luminescent coatings does not involve any interference between the luminescent species and the solar cell active material, thus representing a viable and flexible strategy that can potentially be implemented on an industrial scale on complete PV devices.

Typically, the optimization of sunlight harvesting in PV devices by means of spectral managing coatings can be performed via three different luminescence processes: upconversion (UC), downconversion (DC) (or quantum-cutting (QC)) and downshifting (DS) (see Figure 11.1). As a rule of thumb, UC layers are placed at the rear of the PV cell so as to collect transmitted photons, while DC and DS layers are placed on the front surface.

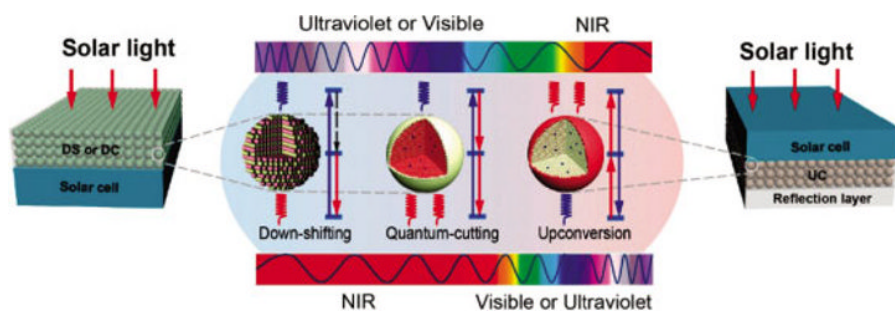


**Figure 11.1.** Spectral conversion design for PV applications involving downshifting (DS), quantum-cutting (QC) and upconversion (UC) luminescent materials. In a typical downshifting process, upon excitation with a high-energy photon, non-radiative relaxation takes place followed by radiative relaxation, thereby resulting in the emission of a lower energy photon. In contrast, two-step radiative relaxation occurs in the quantum-cutting process upon excitation with a high-energy photon, leading to the emission of two (or more) lower energy photons. The upconversion process can convert two (or more) incident low-energy photons into a single higher energy photon. Adapted and reprinted from [HUA 13]

In the UC process, two or more sub-band gap photons are converted into a single higher energy photon via nonlinear anti-Stokes optical processes [DE 11]. Considering that a major energy loss in conventional PV systems is represented by the transmission of sub-band gap photons, the use of UC layers may represent a promising strategy to limit such losses by converting sub-band gap photons into a photon with sufficient energy to be absorbed by the PV material. At present, two material classes are considered in

which low-energy photons are absorbed to yield a higher energy UC emission: lanthanides and organic chromophores with extended  $\pi$ -conjugated systems. Lanthanides (most commonly found in their ionized trivalent state  $\text{Ln}^{3+}$ ) are by far the most widely investigated materials. They are particularly interesting because of their ladder-like energy levels that facilitate photon absorption and the subsequent energy transfer steps and because they show luminescent properties covering a large portion of the solar spectrum from the UV to the near infrared (NIR) wavelengths. Typically, these materials are embedded in hosts such as fluorides, chlorides, iodides and bromides to impart the desired optical properties. The most efficient mechanisms responsible for the UC of photons to a higher energy level in lanthanides are ground state absorption/excited state absorption (GSA/ESA) and energy transfer upconversion (ETU). GSA/ESA is a two-step excitation process in which the sequential absorption of photons within a single ion (excitation to the ground state – the GSA process – followed by ESA) leads to its promotion to a higher energy state. In the ETU process, two (or more) neighboring ions are simultaneously excited by pump photons (one each) to a metastable energy level via GSA. The excited ions can then exchange energy between each other non-radiatively so that one ion (the “sensitizer”) transfers its energy to the neighboring ion (the “activator”). The “activator” is then promoted to an upper emitting state, while the “sensitizer” relaxes back to the ground state. Typically,  $\text{Er}^{3+}$ ,  $\text{Tm}^{3+}$  and  $\text{Ho}^{3+}$  ions are chosen as activators for efficient visible emissions under low pump power densities, and they are often codoped with  $\text{Yb}^{3+}$  as sensitizer, the latter being characterized by a large absorption cross-section in the NIR region (900–1,100 nm) [WAN 09]. In particular, one of the most efficient materials for NIR to visible UC is represented by the  $\text{Yb}^{3+}/\text{Er}^{3+}$  couple embedded in a host such as  $\text{NaYF}_4$ , in which  $\text{Yb}^{3+}$  serves as a sensitizer and  $\text{Er}^{3+}$  serves as an activator. Their interesting UC characteristics originate from the large spectral overlap between  $\text{Yb}^{3+}$  emission and  $\text{Er}^{3+}$  absorption and the efficient ETU process taking place in this system, and they have made the  $\text{Yb}^{3+}/\text{Er}^{3+}$  couple one of the most widely studied ion combinations. Another interesting class of materials for UC processes is organic and organometallic chromophores. In this case, the UC system consists of organic molecules with  $\pi$ -conjugated systems and high fluorescence quantum yield serving as acceptor, and organometallic complexes characterized by metal-to-ligand charge transfer transitions serving as sensitizer (examples are shown in Figure 11.2). The UC in organic molecules is based on the so-called triplet-triplet annihilation (TTA) process [SIN 10], which requires that the triplet

and singlet excited state of the sensitizer lie between the singlet and triplet excited state of the activator. This implies that the sensitizer has a much smaller singlet–triplet splitting than the activator (this is usually the case for metal-to-ligand transitions on the sensitizer compared to an aromatic hydrocarbon activator that has, in general, a large singlet–triplet splitting). In the TTA process, a sensitizer is excited to the lowest singlet state and relaxes through intersystem crossing to the triplet state. The long-lived triplet state of the sensitizer transfers the energy to the long-lived activator triplet state. Two activator molecules in the triplet state annihilate yielding one activator in the high-energy singlet state and one activator in the ground state. UC emission is observed from the singlet state of the activator. For organic systems, blue-shifts in the order of 100–200 nm can be typically obtained, which are shorter than those observed for Ln-based UC due to the energy relaxation processes taking place in these systems that lead to photon energy losses.

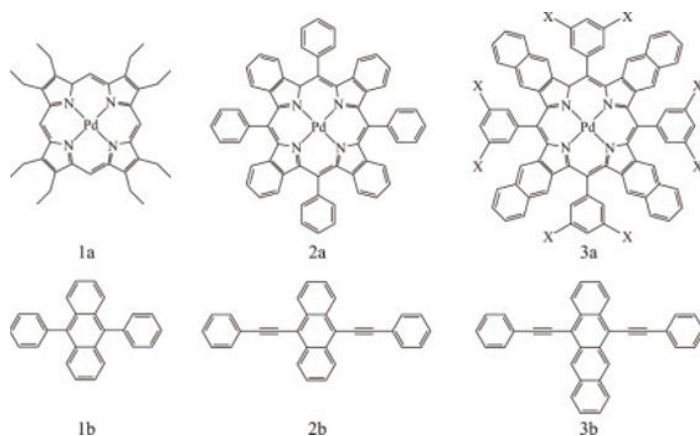


**Figure 11.2.** Examples of organic molecules used for upconversion. The metal complexes 1a (PdOEP), 2a (PdPh<sub>4</sub>TBP) and 3a (PdPh<sub>4</sub>OMe<sub>8</sub>TNP) serve as sensitizers, while the molecules 1b (DPA), 2b (BPEA) and 3b (BPEN) are activators. Adapted and reprinted from [BAL 08]

The concept of DC (or QC) involves the splitting of one absorbed high-energy photon into two (or more) emitted lower energy photons with a quantum efficiency higher than 100% [WEG 00]. Such a process may prove useful for limiting the photon energy losses due to thermalization of hot charge carriers after absorption of photons with energies higher than the band gap, in the cases where the DC photons can be absorbed by the PV

material. As a result, the photocurrent of the PV device can theoretically be doubled. For practical PV applications, the so-called NIR QC that involves the emission of two NIR photons after the absorption of a visible photon seems promising. The NIR QC system has been demonstrated in different  $\text{Ln}^{3+}$ - $\text{Yb}^{3+}$  donor-acceptor co-doped systems (with  $\text{Ln} = \text{Tb}, \text{Tm}, \text{Pr}, \text{Er}, \text{Nd}, \text{Ho}, \text{Dy}$ ) and in phosphors with a single luminescent center, such as  $\text{Ho}^{3+}$ ,  $\text{Tm}^{3+}$  and  $\text{Er}^{3+}$ . The mechanisms responsible for the NIR QC may be different, depending on the number of luminescent centers involved in the process (Figure 11.3). In the case of single luminescent centers, the formation of two sequential NIR photons may occur after transition of the optical center to the highest energy level by absorption of one UV or visible photon, with the optical center returning to its ground state after populating for a short time the intermediate level (Figure 11.3(a)). In co-doped systems, the NIR QC process may occur (i) via a two-step resonant energy transfer process between physically interacting lanthanide ion pairs followed by the emission of two NIR photons (Figure 11.3(b)), (ii) via a one-step resonant energy transfer between two different optical centers (Figure 11.3(c–d)) or (iii) via cooperative sensitization energy transfer, in which the simultaneous excitation of two acceptors occurs followed by the subsequent emission of two NIR photons (Figure 11.3(e)).

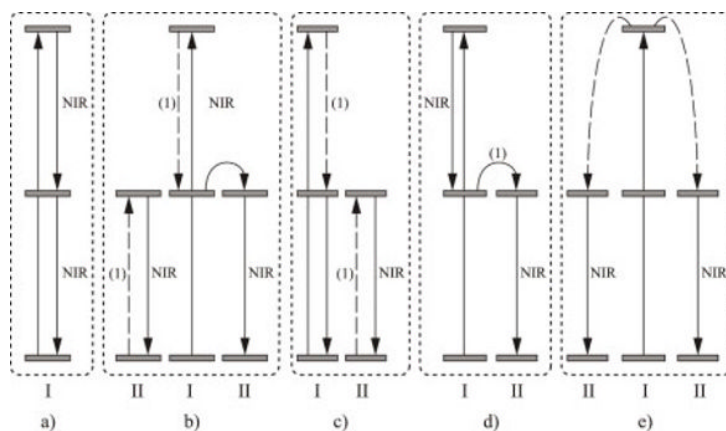


**Figure 11.3.** Summary of typical mechanisms of NIR quantum-cutting for PV applications. Simplified energy-level diagrams for ions (types I and II) are given to illustrate the concept of NIR quantum-cutting. a) NIR quantum-cutting on a single ion by the sequential emission of two NIR photons. b)–d) NIR quantum-cutting due to resonant ET from ion I to ion II. e) NIR quantum-cutting due to cooperative ET from ion I to ion II. Note that two type II ions simultaneously emit two photons in the NIR spectral region. Adapted and reprinted from [HUA 13]

In the DS process, absorbed high-energy (typically UV) photons are reemitted Stokes-shifted at lower energies. DS is a single photon process whose quantum efficiency is limited to 100%, as the absorption of one high-energy photon by the DS material can only result in the emission of one lower energy photon that can in turn generate only one electron-hole pair in the PV device. This implies that the use of DS systems coupled with PV devices does not allow us to overcome the Shockley–Queisser efficiency limit. Nevertheless, DS may represent an interesting approach for improving the spectral response in the UV region of the solar spectrum in PV systems that show poor external quantum efficiency at short wavelengths [KLA 09]. The ideal materials for use in DS systems should satisfy all the main optical requirements for a highly efficient DS process, namely a broad absorption spectrum (especially in the region where the solar cell exhibits poor spectral response), a large Stokes shift (to minimize self-absorption losses due to partial overlap between absorption and emission spectra), a high luminescence quantum yield (to ensure a large portion of absorbed photons to be reemitted downshifted), a high absorption coefficient (to maximize incident photon harvesting), optimal matching between the emission spectrum of the luminophore and the spectral response of the PV cell (to maximize PV cell performance), high solubility in the host matrix material (to avoid aggregation-induced luminescence quenching) and long-term outdoor stability (to ensure long device lifetime) [DEB 12]. At present, different classes of materials have been investigated as potential candidates for DS systems, including inorganic phosphors/rare-earth ions, quantum dots and organic dyes. Inorganic phosphors are interesting DS materials mainly because they are characterized by large Stokes shifts. Indeed, by means of photoluminescence, they allow the conversion of UV-photons into lower energy red and NIR photons. Examples of phosphors employed for DS applications combined with different PV technologies include the NIR-emitting  $\text{Nd}^{3+}$  and  $\text{Yb}^{3+}$ , often sensitized with higher absorption coefficient ions such as  $\text{Cr}^{3+}$ ,  $\text{Ce}^{3+}$  or  $\text{Bi}^{3+}$ ,  $\text{Sm}^{3+}$  and wide band gap semiconductor nanocrystals such as  $\text{LaVO}_4:\text{Dy}^{3+}$  [HUA 13, TEN 11, FU 12, LIU 11, ZHA 11]. Similar to inorganic phosphors and glasses, rare-earth organic complexes present large Stokes shifts that allow to completely avoid the problem of self-absorption losses. These systems are composed of a ligand serving as an antenna and a lanthanide ion that is responsible for the

photoluminescence emission. The mechanisms underlying the DS process in rare-earth complexes consist of light absorption by the ligand, singlet-to-triplet state intersystem crossing within the ligand and resonant energy transfer from the ligand triplet state to the excited state of the lanthanide ion. The most representative examples of rear-earth organic complexes investigated for DS application are those based on  $\text{Eu}^{3+}$ , which are characterized by a sharp emission at 613 nm that can be readily exploited in combination with Si-based, organic and hybrid organic-inorganic PV cells [LIM 13]. Quantum dots are nanostructured semiconducting crystals with tunable size-related spectral properties (absorption and emission). They can exhibit wide absorption bands and are expected to exhibit relatively good photostability due to their crystalline structure. Examples of these systems include CdSe, CdSe-ZnS, CdS and CdSe-CdTe for emission in the visible region of the spectrum and ZnTe-CdSe, CdTe-CdSe and PbS for emission in the NIR [PUR 12]. Recent concerns about the toxicity of some of these materials have pushed the research toward the development of quantum dots free from heavy metals, such as  $\text{CuInS}_2$ -ZnS and Cu-doped ZnInS-ZnS systems [FOD 14, DEN 12]. Organic dyes are  $\pi$ -conjugated systems characterized by high absorption coefficients, high luminescence quantum yields and relatively good solubility and easy processability in polymeric host matrices. These characteristics have made organic dyes extensively investigated for DS purposes. Several classes of organic dyes have been explored for DS applications, including rhodamines, coumarins, perylenes and naphthalimides derivatives. In this context, the Lumogen F<sup>®</sup> series commercialized by BASF is by all means one of the most popular families of dyes. The main drawbacks of organic dyes are their relatively narrow absorption bands and their limited Stokes shifts that determine significant self-absorption losses. In addition, their photostability remains an issue especially under prolonged exposure to harmful UV light, as photochemical decomposition of the dye molecule may lead to reduction of absorption and emission intensity as well as loss of conjugation with consequent blue-shifted optical response. A key issue for organic dyes is the need of achieving high levels of solubility of the luminescent species in the host matrix material during processing in order to obtain high device efficiencies. Indeed, poor dye solubility may lead to the formation of non-luminescent dimers and aggregates that cause drop of fluorescence quantum yield and device performance [COL 10]. For this reason, appropriate choice of the luminophore/host matrix combination is very important for optimal

operations [GRI 14a]. To date, different classes of host matrix materials have been considered for DS purposes, with polymers being one of the most widely investigated materials due to their high transparency over the entire visible spectrum, easy processability and relatively good compatibility with organic dyes. Among these, poly(methyl-methacrylate) (PMMA), polycarbonate (PC) and poly(ethylene-vinyl acetate) (EVA) are some of the most commonly employed systems. However, a common drawback of these polymeric materials is their limited photostability under prolonged outdoor light exposure, especially because of the interaction of UV photons with the polymer macromolecules [RAN 75, TOR 00]. It is therefore of interest to develop new polymeric systems that can ensure improved outdoor stability while maintaining the optical properties required for DS application. One way to do so is to employ cross-linkable fluorinated polymers, which are intrinsically more stable toward photooxidation because of the high strength of the C–F bonds, and may lead to lower permeability toward oxygen and moisture compared to non-cross-linked systems because of their lower free-volume. However, a major problem of this approach that needs to be overcome is the very limited thermodynamic miscibility of organic dyes in fluoropolymeric matrices that may cause worsening of the emission properties of the systems due to aggregation-induced quenching of the luminescence.

So far, two main types of DS systems for PV applications have been investigated: luminescent solar concentrators (LSCs) and luminescent DS (LDS) layers. Although they are based on the same physical principle, which is the emission of one lower energy photon upon absorption of one higher energy photon, these two approaches present specific technological differences that characterize their final use. In the following sections, both these DS strategies are thoroughly discussed, with practical examples specifically focusing on the use of photo-curable fluoropolymeric systems in different PV technologies.

## **11.2. Photocurable luminescent downshifting layers and dye-sensitized solar cells**

The DSSC is the most representative prototype of third-generation PV devices, in which a sensitizer (as light-absorbing material) and a wide band gap semiconductor (with nanocrystalline morphology) are coupled to

realize the optical absorption and the charge separation processes [GRÄ 03]. The DSSC was invented and first published in 1991 as a sensitized electrochemical PV device with a conversion efficiency of 7.1% under solar illumination [O'RE 91]. Device evolution has continued progressively since then: 13,000 research articles and 350 reviews in international journals, besides 4,000 patents, have led to certified efficiencies of over 11% [NAT 15] and academic values higher than 13% [MAT 14].

A schematic of the interior of a standard DSSC is shown in Figure 11.4. At the heart of the device is a mesoporous semiconducting oxide layer composed of a network of  $\text{TiO}_2$  nanoparticles (NPs) that have been sintered together to establish electronic conduction. The film thickness is typically around 10  $\mu\text{m}$ , the porosity being 50–60% and the NPs diameter 10–30 nm. The  $\text{TiO}_2$  layer is deposited on a transparent conducting oxide (TCO) on a glass (or plastic) substrate. The most commonly used substrate is glass coated with fluorine-doped tin oxide (FTO). A monolayer of a molecular sensitizer is chemisorbed on the surface of the nanocrystalline film. The set that includes conductive substrate, semiconductor NPs and adsorbed dye molecules is called “photoanode”. The cell architecture also includes the electrolyte, usually an organic solvent containing the iodide/triiodide ( $\text{I}^-/\text{I}_3^-$ ) redox system, and a counter electrode, which is usually an FTO glass coated with a thin layer of platinum (Pt) catalyst. The operating principle of the DSSC is relatively simple and is typical of a photoelectrochemical regenerative cell [BEL 13b, IMP 14]. It is based on the absorption of the sunlight by the sensitizer molecules and on the charge transfer at the interfaces between the electrolyte and the electrodes. In fact, electron-hole pairs, generated after the absorption of photons by the dye molecules, are separated at the interface with the semiconductor, so that the negative charges are injected into the conduction band of  $\text{TiO}_2$ . By hopping between adjacent NPs, electrons arrive at the front electrode, ready to travel through the external circuit. On the other hand, oxidized dye molecules are regenerated by electron donation from  $\text{I}^-$ , thus forming  $\text{I}_3^-$ . Then, triiodide ions diffuse toward the counter electrode where, in conjunction with electrons coming from the external circuit, they are reduced to iodide (this reaction is accelerated by the presence of the Pt deposited on the electrode).

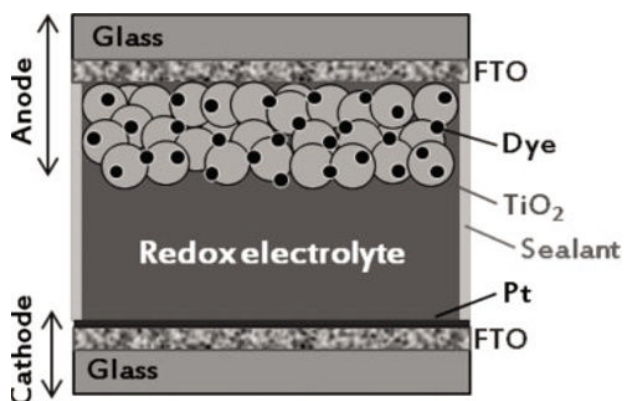
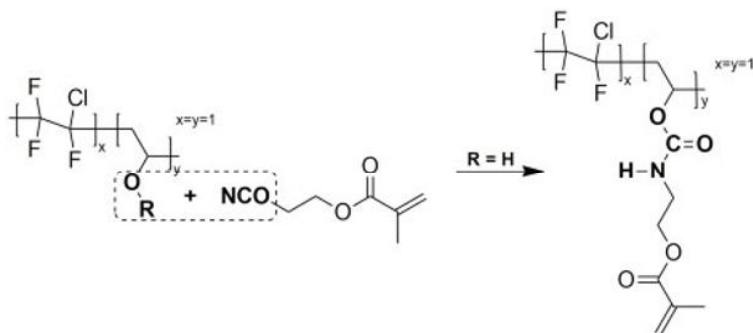


Figure 11.4. Schematic of a DSSC device

Spectral management technologies (see section 11.1.2) and DSSC devices are two hot topics in the PV field, and the very promising results obtained so far justify the great effort made by the scientific community toward their widespread use. In particular, the synergistic application of these two technologies can lead to further achievements in terms of device performance and may help to reduce the gap-to-market of DSSC devices. In this context, one major problem currently affecting top-performing DSSC devices is the use of ruthenium (Ru)-based organometallic compounds that still suffer from issues related to their high costs, toxicity and limited availability of the starting material. To this end, metal-free organic dyes are receiving increasing attention from the scientific community as potential alternative to Ru-based systems [AHM 13]. Because they do not contain any rare or noble metal, they generate fewer concerns about resource limits. In addition, they have recently demonstrated interesting device performance with efficiency values as high as 12.5% [KAK 14]. However, organic dyes often present a relatively narrow spectral breadth [LIN 14], which limits the photocurrent that can be generated by the device. Thus, a possible combination of a luminescent coating and an organic DSSC may allow to increase the portion of wavelengths of the solar spectrum useful for the PV device. In addition to device efficiency, the combination of LDS layers and DSSCs may also be exploited in view of a potential increase in device durability. In fact, when operating outdoor, these PV devices are required to withstand critical aggressive conditions such as the accumulation of dirt, as well as the permeation of water into the cell, which would lead to the degradation of the electrochemical system.

A great opportunity to synergistically exploit the interesting characteristics of LDS and DSSC technologies described above is offered by luminescent fluoropolymeric downshifters. These systems are based on multifunctional coatings which can simultaneously be easy-cleaning (because of their fluoropolymeric matrix) and light-shifter (due to the presence of an embedded fluorophore). Furthermore, fluoropolymeric downshifters can be prepared by means of fast (few seconds) UV-induced polymerization reactions, thus potentially enabling their use in large-scale production volumes. As already noted at the end of the previous section, the main limitation to their use is represented by the very low solubility parameter of fluoropolymers and by the poor miscibility of fluoropolymers in organic solvents and with organic dyes. However, among the various fluoropolymers currently available on the market, some copolymers of chlorotrifluoroethylene and vinyl ethers (CTFE-VEs) show a moderately higher polarity and are actually soluble in some common solvents such as aromatics (xylenes) and esters. Functional CTFE-VE low molecular weight copolymers with -OH functionalities are available as resins suitable to produce polyurethane coatings by combination with polyisocyanate cross-linkers [MUN 98]. In addition, the presence of hydroxyls in the CTFE-VE resin can be exploited to introduce UV-curable methacrylic groups by reaction of the CTFE-VE resin with isocyanato-ethyl-methacrylate (IEM), as shown in Diagram 11.1.



**Diagram 11.1.** Schematic representation of the mechanism of formation of photocrosslinkable CTFE-VE resins by the introduction of methacrylic functionalities as pendant groups through urethane bonds

Using this strategy, it is possible to obtain new UV-curable fluoropolymer resins showing good solubility with several types of organic

dyes, allowing the realization of different types of luminescent coatings as described in the next paragraphs.

Following this approach, a new LDS coating for DSSC application has recently been proposed by Griffini *et al.* [GRI XX]. The presence of methacrylic groups allowed an efficient photocrosslinking reaction under UV-light, leading to the formation of the polymeric solid film on the top of a DSSC device. To provide the light-shifting behavior to the coating, europium tetrakis dibenzoylmethide triethylammonium ( $\text{EuD}_4\text{TEA}$ , Figure 11.5(b)) was mixed in the UV-curable CTFE-VE resin due to its large Stokes shift and good spectral breadth in the UV region of the solar spectrum. In particular,  $\text{EuD}_4\text{TEA}$  showed a broad absorption band in the 300–400 nm spectral range ( $\lambda_{\text{max}} = 350$  nm) and a narrow emission band at 613 nm, due to the  $^5\text{D}_0 \rightarrow ^7\text{F}_{0-4}$  transitions. What makes this LDS system particularly interesting for DSSC application is its ability to screen the DSSC device from the harmful UV radiation present in sunlight ( $\approx 6\%$ ), which can photodegrade the organic components of the PV cell, thus leading to significant performance decrease over operation time. To further exploit the interesting optical properties of this new fluoropolymeric downshifter, an appropriate organic dye was selected for the fabrication of the solar cell. In particular, the Ru-free indoline-based organic dye D205 (Figure 11.5(c)) allowed to obtain a good match between the emission spectrum of the luminescent material and the absorption spectrum of the DSSC dye (Figure 11.5(d)). In principle, this means that UV photons absorbed by the polymeric coating are re-emitted in the visible range at a wavelength that can be exploited by the dye present in the DSSC. In this way, not only is the photodegradation of the photosensitive components of the cell avoided, but an increase in the photon flux at wavelengths useful for optimal DSSC device operation can also be achieved, as illustrated in Figure 11.5(a).

The performance of the fluoropolymeric downshifters illustrated in Figure 11.5(a) was assessed in actual DSSCs sensitized with the D205 dye and coated with the  $\text{EuD}_4\text{TEA}$ -laden fluoropolymeric cross-linked film. A remarkable 37% improvement of short-circuit current density ( $J_{\text{sc}}$ ) was achieved when a 1 wt%  $\text{EuD}_4\text{TEA}$  was introduced in the functional coating (inset of Figure 11.6), thus confirming that the luminescent material effectively converted the spectral region peaked at 350 nm into lower energy photons of wavelengths well matching the absorption spectrum of D205 (Figure 11.6).

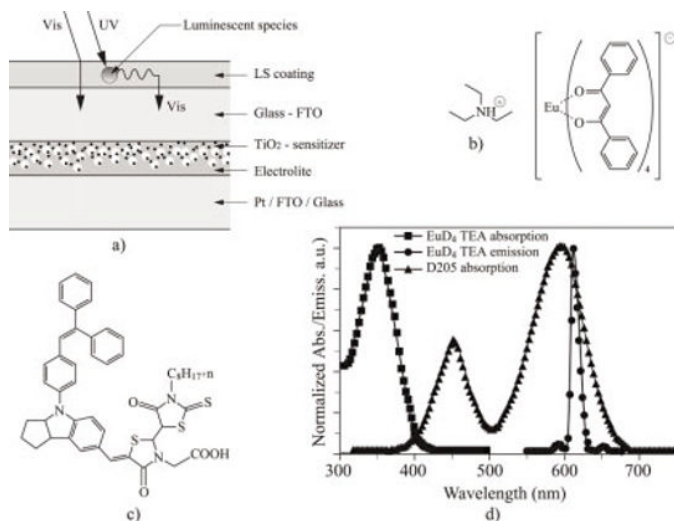


**Figure 11.5.** a) Operation of a fluoropolymeric downshifter applied on the top of a DSSC; b) molecular structure of EuD<sub>4</sub>TEA; c) molecular structure of D205 dye; d) and normalized UV-vis absorption and photoluminescence emission spectra of EuD<sub>4</sub>TEA-doped LDS coatings and absorption spectrum of D205 deposited on TiO<sub>2</sub>

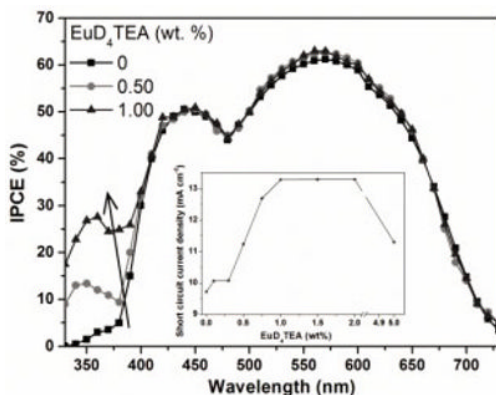


**Figure 11.6.** IPCE curves of LDS-coated DSSCs at increasing concentration of the EuD<sub>4</sub>TEA luminescent species. Inset: variation of generated photocurrent at increasing concentration of EuD<sub>4</sub>TEA luminescent species

With the aim of assessing the long-term stability of the functional coating and its easy-cleaning behavior, a long-term weathering study was conducted under real outdoor conditions for 3 months. DSSCs experimented outdoor

temperatures ranging from  $-2$  to  $32^{\circ}\text{C}$ , and experienced about 350 mm of rain onto the coated electrodes. This aging test showed that control uncoated DSSC devices (0 wt%  $\text{EuD}_4\text{TEA}$ ) lost about 30% of their initial efficiency, while LDS-coated systems (1 wt%  $\text{EuD}_4\text{TEA}$ ) fully preserved the starting performance (Figure 11.7(a)). The strong improvement of long-term stability under real outdoor conditions observed when the fluoropolymeric coating was applied to the DSSC device was ascribed to the action of three combined factors. First, the coating showed easy-cleaning properties due to its fluorinated surface. The remarkable increase in water contact angle ( $\theta_{\text{H}_2\text{O}}$ ) and the decrease in surface tension ( $\gamma$ ) compared to bare glass allowed to keep the external side of the photoelectrode clean, thus avoiding the decrease in device photocurrent caused by the formation of physical barriers (dust, dirt and water residues) that may prevent incident solar photons from reaching the D205-sensitized electrode for PV conversion (Figure 11.7(b–c)). Moreover, the hydrophobic nature of the functional coating hindered the permeation of water into the device, which is often found to alter the composition and the correct functionality of photoanode and electrolyte [LIU 98]. Finally, since the LDS coating can act as a light-shifter, its UV-filtering action reduced the light-induced degradation phenomena normally occurring to the photosensitive components of DSSC devices (dye, redox couple and electrolyte additives) during outdoor exposure [LIS 13].

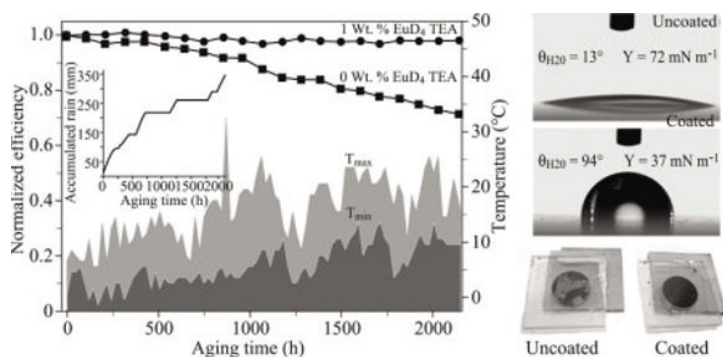


**Figure 11.7.** a) Stability test carried out on LDS-free (0 wt%  $\text{EuD}_4\text{TEA}$ ) and LDS-coated (1 wt%  $\text{EuD}_4\text{TEA}$ ) DSSCs in real outdoor conditions. The lower part of the graph shows the outdoor temperatures (minimum and maximum) registered during the testing period, while the inset shows the accumulated rainfall; b) static contact angles ( $\theta_{\text{H}_2\text{O}}$ ) and total surface tension values ( $\gamma$ ) for bare glass and glass coated with the LDS film; c) and photograph of control (uncoated) and LDS-coated DSSC devices after 2,140 h of exposure to real outdoor conditions. The control device shows the presence of dirty areas and water residues on the top surface, which are not detected on the LDS-coated device

In summary, it is clear that luminescent UV-curable fluoropolymeric coatings are not only able to produce a great improvement of PV cell efficiency, but they can also impart high long-term durability in real operating conditions, where the latter is seen as an aspect of paramount importance for practical exploitation of the DSSC technology. The use of light-shifting protective coatings will be soon extended to a large variety of sensitizer/luminophore combinations, as well as to the nascent world of PSCs, whose instability to humidity and near-UV radiation represents one of the major problems currently under intense investigation [GRE 14b].

### **11.3. Luminescent solar concentrators**

As briefly discussed in section 11.1, solar cells based on mono- and polycrystalline Si largely dominate the PV market nowadays. These devices have found applications mainly as small-scale devices in solar panels on building roofs, pocket calculators, water pumps and portable electronics, although some examples of the so-called solar parks have also been presented in the past decades. These conventional PV technologies allow for as much as 25% [GRE 14a] of the incoming solar energy to be harvested and converted into electricity, a value that is very close to the theoretically predicted upper limit of 30% [SHO 61] for single junction non-concentrated PV cells. One major drawback that characterizes the Si-based PV technology is associated with the high production costs of the actual solar cells that still require many energy-intensive processes at high temperatures (400–1400°C). This adds to the increasingly high cost of polycrystalline silicon, the starting material for solar cell production.

One strategy to meet the cost reduction challenge may be to reduce the amount of silicon necessary for solar cell fabrication by using concentrating systems to collect sunlight over a large area and redirect it onto small-area solar cells [ANT 03]. This approach would reduce material (Si) consumption while preserving and potentially improving the electrical power output from the PV device because of the increased illumination intensity experienced by the solar cells. To date, two main types of concentrating technologies have

been presented in the literature: imaging and non-imaging solar concentrators [SME 90].

The first category includes the conventional approach to solar concentration that makes use of Fresnel lenses, parabolic dish collectors, or a combination of both to collect sunlight and focus it onto very small units of high-cost high-efficiency solar cells [BAR 11]. Although very high concentration factors can be achieved with these devices (hundreds suns) resulting in improved solar cell performance, they have some significant drawbacks: high sunlight concentration may lead to excessive heating of the solar cell; therefore, cooling systems are needed to alleviate high temperature effects and prolong solar cell lifetime; these devices are only able to capture direct solar radiation. Therefore, precise solar tracking systems (typically two-axis systems) are required to keep the solar cell under constant illumination; finally, to avoid shadowing from neighbor collectors, large areas for installation are required. These characteristics add to the limited choice of colors and shapes of Si PVs that represents a further drawback to be overcome, especially for application in the urban environment where these problems may represent clear technological disadvantages.

In order to override some of these limitations, LSCs have been introduced as a promising technology to provide a rapid and cost-effective way to commercialization and widespread use of PV energy. In its typical configuration, an LSC system consists of a transparent host matrix containing luminescent species (typically organic dyes or quantum dots, see section 11.1.2) that absorb part of the incident solar spectrum and reemit it at a longer wavelength. Part of the light emitted by the luminescent species is guided (in a waveguide mode) toward the edges of the transparent matrix by total internal reflection (TIR), where high-efficiency solar cells can collect it. Two typical device configurations are commonly used in LSC technology: bulk-plate LSC and thin-film LSC. In both cases, a planar arrangement is normally employed, though cylindrical, bent or flexible configurations have recently appeared in the literature as promising LSC architectures [MCI 07, EL 07, YOO 11, YOO 08]. In the bulk-plate configuration (which is more conventional), a slab of transparent host matrix (a polymer such as PMMA or an inorganic material such as glass) that also

serves as the waveguide is lightly doped with one or more luminescent species, with solar cells optically matched to the plate edges (Figure 11.8(b)). Conversely, in the thin film design, a transparent carrier matrix (polymeric or inorganic) more heavily doped with one or more luminescent species is deposited as a thin film onto a transparent substrate (typically glass) at the edges of which solar cells are placed (Figure 11.8(a)).

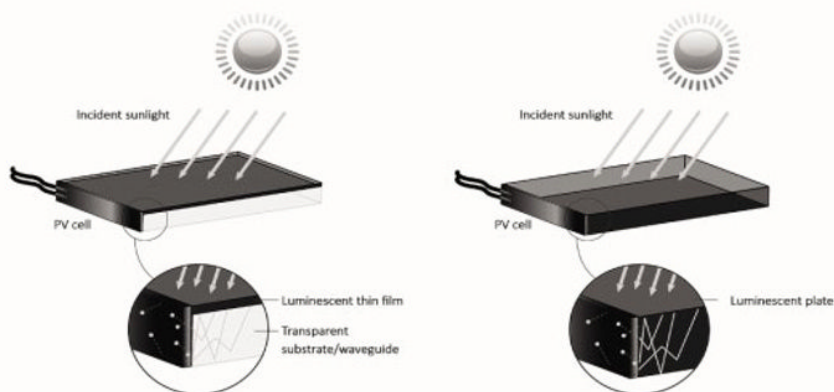


**Figure 11.8.** Schematic representation of thin film (left) and bulk (right) LSC configurations

Although no notable differences in performance have been observed between these two configurations, thin-film LSCs present some technological advantages compared to conventional bulk-plate LSCs, as they can be easily deposited as thin coatings on a wide range of substrates by means of deposition techniques typical of the coating industry [BOS 07, GRI 14b].

The host matrix should exhibit maximum transmission over a broad range of wavelengths and minimal scattering. Accordingly, polymers such as PMMA and PC have been used as host matrix materials because they are relatively inexpensive, transparent and have excellent optical properties (high refractive index,  $n \approx 1.49$  for PMMA). However, they have some limitations when it comes to weatherability. Indeed, prolonged exposure to outdoor light (especially UV light) may yield photodegradation of the

polymeric matrix (especially when deposited as a thin film) [RAN 75, KAC 00], leading to the formation of photon trapping sites that may decrease the photon transport efficiency [GOL 09] as well as the formation of radical species that may interact with the luminescent organic dye molecule. Such detrimental action of polymer degradation products on the luminescent species may result in degradation and decreased fluorescence quantum yield of the luminophore [BAU 01, GRI 13a].

A great deal of work has been carried out in the past few years to develop new LSC host matrix polymeric systems alternative to the most commonly used PMMA, mainly focusing on attempts to improve the optical efficiency of the LSC device. Among these, several examples including elastomeric matrices, copolymers as well as systems based on renewable materials have been presented [LIM 12, BUF 12, FAT 11]. However, none of these materials were shown to yield substantial improvements in LSC device lifetime compared to standard PMMA upon prolonged exposure to continuous illumination. In the attempt to address this issue, we recently demonstrated the use of fluoropolymers based on CTFE-VE copolymers thermally cross-linked with aliphatic poly-isocyanates as a promising class of host matrix materials alternative to PMMA for the fabrication of high-durability polymer-based LSC devices [GRI 13b]. It was shown that superior long-term operational stability with respect to PMMA-based devices was achieved with these systems upon continuous light exposure, and the effect of light stabilizers was also investigated. Furthermore, efficiency values comparable to those obtained with PMMA-based thin-film LSCs were reported, thus also demonstrating the good optical properties of the new fluoropolymeric host matrices. As introduced in previous sections, the excellent weatherability of these systems is attributed to the higher dissociation energy of the carbon-fluorine bond (105.4 kcal/mol) with respect to the carbon-hydrogen bond (98.8 kcal/mol) [O'HA 08] that imparts improved resistance to photodegradation. In addition, the presence of a cross-linked polymer network can guarantee lower permeability toward atmospheric oxygen and moisture compared to a non-cross-linked structure because of its lower free-volume, thus leading to a slower rate of photodegradation of the polymeric coating. On the other hand, the presence of both carbon-fluorine and carbon-chlorine bonds in the repeating unit (CTFE-VE) of the fluoropolymeric binder can guarantee sufficiently high

polarity and good solubility in most organic solvents (including aromatics), thus allowing relatively easy dissolution of the most commonly employed luminescent organic dyes used in the LSC field together with good device efficiencies.

Notwithstanding the excellent weatherability characteristics of the fluoropolymeric systems discussed so far, the use of two-component thermally cross-linked polymers as host matrix materials for LSC devices is not free from critical issues that may hamper their widespread use on a large industrial scale. Above all, this approach is limited by the need of a relatively long post-deposition treatment at high temperature ( $\sim 150^\circ\text{C}$ ) to form the final cross-linked films. In this context, light-mediated cross-linking is an interesting strategy to overcome this limitation, as it is typically characterized by low electrical power input and energy requirements, low temperature operation and short curing times [TEH 13].

The use of photocurable fluoropolymeric systems as host matrix materials for LSC devices may allow to combine the excellent durability of cross-linked fluoropolymers with the straightforward and rapid approach ensured by the photocrosslinking strategy. To this end, thin-film LSC devices were fabricated based on the photocurable fluoropolymeric system described in section 11.2 (characterized by the presence of reactive methacrylate pendant groups attached to the CTFE-VE-based fluoropolymeric backbone) as host matrix material. A solution of this UV-curable CTFE-VE resin containing a given amount of a commercial perylene-based fluorescent dye (Lumogen F<sup>®</sup> Red 305 from BASF, see Figure 11.9(a) for its molecular structure) was deposited by spin-coating onto transparent glass waveguides before exposure to UV light to form the final photocrosslinked LSC. Subsequently, a mc-Si solar cell was attached to one edge of the glass waveguide by means of an optically matched hotmelt polyurethane adhesive to produce the final LSC device. During the LSC device optimization, the concentration of the fluorescent dye in the fluoropolymeric matrix was varied progressively in order to find a maximum performance. As shown in Figure 11.9(b), the optical efficiency of the LSC device (also called optical collection probability [DES 12]), defined as the ratio between the power conversion efficiency of the LSC device illuminated through the top LSC area and the power conversion efficiency of the PV cell under

direct illumination, reaches a maximum for a dye concentration of about 4 wt%.

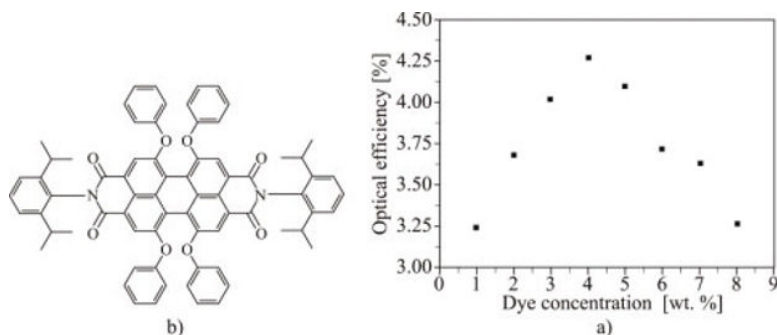


**Figure 11.9.** a) Molecular structure of Lumogen F<sup>®</sup> Red 305; b) and optical efficiency of photocrosslinked LSC devices at increasing fluorescent dye concentration

This trend may be explained by considering two counter-acting effects of dye concentration on LSC device operation. An increasing concentration of organic dye in the LSC thin film results in a progressively higher fraction of incident photons to be absorbed (increased optical density), reemitted by fluorescence and made available to the PV cell for light-to-electricity conversion. This results in progressively better LSC device performance (up to a dye concentration of 4 wt%). However, a higher concentration of dye molecules may increase the probability of reabsorption events occurring in the LSC thin film before fluorescence photons can reach the PV cell, due to the partial overlap between absorption and emission spectra of the fluorescent dye and because of the decreasing dye-to-dye intermolecular distance with increasing dye concentration. Additionally, an increased concentration of dye molecules may lead to the formation of dimers and aggregates, resulting in decreased fluorescence [COL 10]. Both these phenomena may be responsible for the decrease in optical efficiency observed at higher dye concentrations. Overall, the efficiency values obtained on this system are in line with those obtained on LSC devices based on different polymeric host matrices, demonstrating the good optical properties of this fluoropolymeric system.

In order to evaluate the potential of this photocrosslinked fluoropolymer as high-durability host matrix for LSC devices, a long-term durability test was conducted on photocrosslinked LSCs under accelerated weathering conditions. In particular, the LSC devices were subjected to continuous illumination in a weather-o-meter chamber (Xenon light) at constant temperature (40°C) and relative humidity (15%), and the PV performance of the LSC devices under test was periodically evaluated under AM1.5G simulated sunlight. For comparison, the weathering behavior of PMMA-based thin-film LSC devices was also monitored. Figure 11.10 shows the PV response (in terms of optical efficiency as previously defined) of both the photocrosslinked fluoropolymer LSCs and reference PMMA-based devices as a function of light exposure time. No photostabilizers were added in the experimental UV-curable CFTE-VE resin, while a commercially available PMMA grade proposed for outdoor application was used as a reference material.

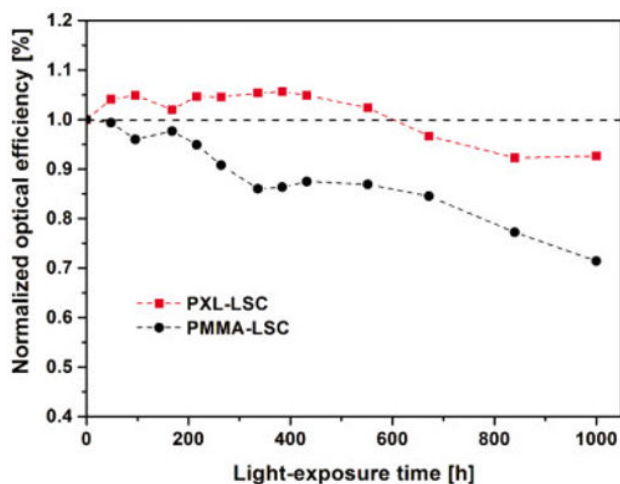


**Figure 11.10.** Normalized trends of optical efficiency at increasing exposure time for photocrosslinked (PXL-LSC) and reference PMMA-based (PMMA-LSC) LSC devices (each trend was normalized with respect to the corresponding value measured at 0 h)

As shown in the figure, after more than 1,000 h of continuous light exposure, photocrosslinked LSC devices (PXL-LSC) only lose about 7% of their initial efficiency, as opposed to PMMA-based LSCs that present a 30%

loss of optical efficiency. These trends are in agreement with recent reports on similar thermally cross-linked fluoropolymeric systems and further confirm the excellent durability properties of these materials, especially when compared to commonly employed host matrix materials such as PMMA.

To conclude, UV-curable fluoropolymeric systems are a very promising alternative to standard thermoplastic materials to easily obtain high-durability coatings to be successfully employed in LSC and light management applications.

#### 11.4. Bibliography

- [AHM 13] AHMAD S., GUILLÉN E., KAVAN L. *et al.*, “Metal free sensitizer and catalyst for dye sensitized solar cells”, *Energy & Environmental Science*, vol. 6, pp. 3439–3466, 2013.
- [ANT 03] ANTON I., PACHON D., SALA G., “Characterization of optical collectors for concentration photovoltaic applications”, *Progress in Photovoltaics: Research and Applications*, vol. 11, pp. 387–405, 2003.
- [BAL 08] BALUSCHEV S., YAKUTKIN V., MITEVA T. *et al.*, “A general approach for non-coherently excited annihilation up-conversion: transforming the solar-spectrum”, *New Journal of Physics*, vol. 10, p. 013007, 2008.
- [BAR 11] BARLEV D., VIDU R., STROEVE P., “Innovation in concentrated solar power”, *Solar Energy Materials and Solar Cells*, vol. 95, pp. 2703–2725, 2011.
- [BAU 01] BAUMBERG I., BEREZIN O., DRABKIN A. *et al.*, “Effect of polymer matrix on photo-stability of photo-luminescent dyes in multi-layer polymeric structures”, *Polymer Degradation and Stability*, vol. 73, pp. 403–410, 2001.
- [BEL 13a] BELLA F., BONGIOVANNI R., “Photoinduced polymerization: an innovative, powerful and environmentally friendly technique for the preparation of polymer electrolytes for dye-sensitized solar cells”, *Journal of Photochemistry and Photobiology C: Photochemistry Reviews*, vol. 16, pp. 1–21, 2013.
- [BEL 13b] BELLA F., SACCO A., SALVADOR G.P. *et al.*, “First pseudohalogen polymer electrolyte for dye-sensitized solar cells promising for *in situ* photopolymerization”, *The Journal of Physical Chemistry C*, vol. 117, pp. 20421–20430, 2013.

- [BOS 07] BOSE R., FARRELL D.J., CHATTEN A.J. *et al.*, *Proceedings of 22nd European Photovoltaic Solar Energy Conference (EUPVSEC)*, Milan, Italy, pp. 210–214, 2007.
- [BUF 12] BUFFA M., CARTURAN S., DEBIJE M.G. *et al.*, “Dye-doped polysiloxane rubbers for luminescent solar concentrator systems”, *Solar Energy Materials and Solar Cells*, vol. 103, pp. 114–118, 2012.
- [COL 10] COLBY K.A., BURDETT J.J., FRISBEE R.F. *et al.*, “Electronic energy migration on different time scales: concentration dependence of the time-resolved anisotropy and fluorescence quenching of Lumogen Red in poly(methyl methacrylate)”, *The Journal of Physical Chemistry A*, vol. 114, pp. 3471–3482, 2010.
- [CON 07] CONIBEER G., “Third-generation photovoltaics”, *Materials Today*, vol. 10, pp. 42–50, 2007.
- [DE 11] DE WILD J., MEIJERINK A., RATH J.K. *et al.*, “Upconverter solar cells: materials and applications”, *Energy & Environmental Science*, vol. 4, pp. 4835–4848, 2011.
- [DEB 12] DEBIJE M.G., VERBUNT P.P.C., “Thirty years of luminescent solar concentrator research: solar energy for the built environment”, *Advanced Energy Materials*, vol. 2, pp. 12–35, 2012.
- [DEN 12] DENG D., CHEN Y., CAO J. *et al.*, “High-quality CuInS<sub>2</sub>/ZnS quantum dots for *in vitro* and *in vivo* bioimaging”, *Chemistry of Materials*, vol. 24, pp. 3029–3037, 2012.
- [DES 12] DESMET L., RAS A.J.M., DE BOER D.K.G. *et al.*, “Monocrystalline silicon photovoltaic luminescent solar concentrator with 4.2% power conversion efficiency”, *Optics Letters*, vol. 37, pp. 3087–3089, 2012.
- [DRE 01] DRESSELHAUS M.S., THOMAS I.L., “Alternative energy technologies”, *Nature*, vol. 414, pp. 332–337, 2001.
- [EL 07] EL SHAARAWY M.G., EL BASHIR S.M., HAMMAM M. *et al.*, “Bent fluorescent solar concentrators (BFSCs): spectroscopy, stability and outdoor performance”, *Current Applied Physics*, vol. 7, pp. 643–649, 2007.
- [EUR 15] EUROPE, available at [http://ec.europa.eu/europe2020/index\\_en.htm](http://ec.europa.eu/europe2020/index_en.htm), 2015.
- [FAT 11] FATTORI V., MELUCCI M., FERRANTE L.M. *et al.*, “Poly(lactic acid) as a transparent matrix for luminescent solar concentrators: a renewable material for a renewable energy technology”, *Energy & Environmental Science*, vol. 4, pp. 2849–2853, 2011.

- [FOD 14] FODA M.F., HUANG L., SHAO F. *et al.*, “Biocompatible and highly luminescent near-infrared CuInS<sub>2</sub>/ZnS quantum dots embedded silica beads for cancer cell imaging”, *ACS Applied Materials & Interfaces*, vol. 6, pp. 2011–2017, 2014.
- [FU 12] FU H., CUI S., LUO Q. *et al.*, “Broadband downshifting luminescence of Cr<sup>3+</sup>/Yb<sup>3+</sup>-codoped fluorosilicate glass”, *Journal of Non-Crystalline Solids*, vol. 358, pp. 1217–1220, 2012.
- [GOL 09] GOLDSCHMIDT J.C., PETERS M., HERMLE M. *et al.*, “Characterizing the light guiding of fluorescent concentrators”, *Journal of Applied Physics*, vol. 105, p. 114911, 2009.
- [GLO 15] GLOBAL EXERGY RESOURCE CHART, Global climate and energy project, available at <http://gcep.stanford.edu/research/exergycharts.html>, 2015.
- [GRÄ 01] GRÄTZEL M., “Photoelectrochemical cells”, *Nature*, vol. 414, pp. 338–344, 2001.
- [GRÄ 03] GRÄTZEL M., “Dye-sensitized solar cells”, *Journal of Photochemistry and Photobiology C: Photochemistry Reviews*, vol. 4, pp. 145–153, 2003.
- [GRE 14a] GREEN M.A., EMERY K., HISHIKAWA Y. *et al.*, “Solar cell efficiency tables (version 44)”, *Progress in Photovoltaics: Research and Applications*, vol. 22, pp. 701–710, 2014.
- [GRE 14b] GREEN M.A., HO-BAILLIE A., SNAITH H.J., “The emergence of perovskite solar cells”, *Nature Photonics*, vol. 8, pp. 506–514, 2014.
- [GRI 13a] GRIFFINI G., BRAMBILLA L., LEVI M. *et al.*, “Photo-degradation of a perylene-based organic luminescent solar concentrator: molecular aspects and device implications”, *Solar Energy Materials and Solar Cells*, vol. 111, pp. 41–48, 2013.
- [GRI 13b] GRIFFINI G., LEVI M., TURRI S., “Novel crosslinked host matrices based on fluorinated polymers for long-term durability in thin-film luminescent solar concentrators”, *Solar Energy Materials and Solar Cells*, vol. 118, pp. 36–42, 2013.
- [GRI 14a] GRIFFINI G., BRAMBILLA L., LEVI M. *et al.*, “Anthracene/tetracene cocrystals as novel fluorophores in thin-film luminescent solar concentrators”, *RSC Advances*, vol. 4, pp. 9893–9897, 2014.
- [GRI 14b] GRIFFINI G., LEVI M., TURRI S., “Novel high-durability luminescent solar concentrators based on fluoropolymer coatings”, *Progress in Organic Coatings*, vol. 77, pp. 528–536, 2014.

- [GRI 15] GRIFFINI G., BELLA F., NISIC F. *et al.*, “Multifunctional luminescent down-shifting fluoropolymer coatings: a straightforward strategy to improve the UV-light harvesting ability and long-term outdoor stability of organic dye-sensitized solar cells”, *Advanced Energy Materials*, vol. 5, no. 1401312, 2015.
- [HUA 13] HUANG X., HAN S., HUANG W. *et al.*, “Enhancing solar cell efficiency: the search for luminescent materials as spectral converters”, *Chemical Society Reviews*, vol. 42, pp. 173–201, 2013.
- [IMP 14] IMPERIYKA M., AHMAD A., HANIFAH S.A. *et al.*, “A UV-prepared linear polymer electrolyte membrane for dye-sensitized solar cells”, *Physica B: Condensed Matter*, vol. 450, pp. 151–154, 2014.
- [KAC 00] KACZMAREK H., KAMINSKA A., VAN HERK A., “Photooxidative degradation of poly(alkyl methacrylate)s”, *European Polymer Journal*, vol. 36, pp. 767–777, 2000.
- [KAK 14] KAKIAGE K., AOYAMA Y., YANO T. *et al.*, “An achievement of over 12 percent efficiency in an organic dye-sensitized solar cell”, *Chemical Communications*, vol. 50, pp. 6379–6381, 2014.
- [KAT 97] KATO K., MURATA A., SAKUTA K., Energy payback time and life-cycle CO<sub>2</sub> emission of residential PV power system with silicon PV module, Appendix B-8 of the “Environmental Aspects of PV Power Systems”, Utrecht University, Utrecht, 1997.
- [KLA 09] KLAMPAFTIS E., ROSS D., MCINTOSH K.R. *et al.*, “Enhancing the performance of solar cells via luminescent down-shifting of the incident spectrum: a review”, *Solar Energy Materials and Solar Cells*, vol. 93, pp. 1182–1194, 2009.
- [LIM 12] LIM Y.S., LO C.K., TEH G.B., “Unsaturated polyester resin blended with MMA as potential host matrix for luminescent solar concentrator”, *Renewable Energy*, vol. 45, pp. 156–162, 2012.
- [LIM 13] LIMA N.B.D., GONÇALVES S.M.C., JUNIOR S.A. *et al.*, “A comprehensive strategy to boost the quantum yield of luminescence of europium complexes”, *Scientific Reports*, vol. 3, p. 2395, 2013.
- [LIN 14] LIN L.Y., YEH M.H., LEE C.P. *et al.*, “Insights into the co-sensitizer adsorption kinetics for complementary organic dye-sensitized solar cells”, *Journal of Power Sources*, vol. 247, pp. 906–914, 2014.

- [LIS 13] LISSAU J.S., NAUROOZI D., SANTONI M.P. *et al.*, “Anchoring energy acceptors to nanostructured  $\text{ZrO}_2$  enhances photon upconversion by sensitized triplet-triplet annihilation under simulated solar flux”, *The Journal of Physical Chemistry C*, vol. 117, pp. 14493–14501, 2013.
- [LIU 98] LIU Y., HAGFELDT A., XIAO X.R. *et al.*, “Investigation of influence of redox species on the interfacial energetics of a dye-sensitized nanoporous  $\text{TiO}_2$  solar cell”, *Solar Energy Materials and Solar Cells*, vol. 55, pp. 267–281, 1998.
- [LIU 11] LIU G.X., ZHANG R., XIAO Q.L. *et al.*, “Efficient  $\text{Bi}^{3+} \rightarrow \text{Nd}^{3+}$  energy transfer in  $\text{Gd}_2\text{O}_3:\text{Bi}^{3+}, \text{Nd}^{3+}$ ”, *Optical Materials*, vol. 34, pp. 313–316, 2011.
- [MAT 14] MATHEW S., YELLA A., GAO P. *et al.*, “Dye-sensitized solar cells with 13% efficiency achieved through the molecular engineering of porphyrin sensitizers”, *Nature Chemistry*, vol. 6, pp. 242–247, 2014.
- [MCI 07] MCINTOSH K.R., YAMADA N., RICHARDS B.S., “Theoretical comparison of cylindrical and square-planar luminescent solar concentrators”, *Applied Physics B: Lasers and Optics*, vol. 88, pp. 285–290, 2007.
- [MUN 98] MUNEKATA S., “Fluoropolymers as coating material”, *Progress in Organic Coatings*, vol. 16, pp. 113–134, 1998.
- [NAT 15] NATIONAL CENTER FOR PHOTOVOLTAICS, National renewable energy laboratory, available at <http://www.nrel.gov/ncpv>, 2015.
- [NEG 12] NEGRO S.O., ALKEMADE F., HEKKERT M.P., “Why does renewable energy diffuse so slowly? A review of innovation system problems”, *Renewable & Sustainable Energy Reviews*, vol. 16, pp. 3836–3846, 2012.
- [NUN 02] NUNZI J.M., “Organic photovoltaic materials and devices”, *Comptes Rendus Physique*, vol. 3, pp. 523–542, 2002.
- [O’HA 08] O’HAGAN D., “Understanding organofluorine chemistry, An introduction to the C–F bond”, *Chemical Society Reviews*, vol. 37, pp. 308–319, 2008.
- [O’RE 91] O’REGAN B., GRÄTZEL M., “A low-cost, high-efficiency solar cell based on dye-sensitized colloidal  $\text{TiO}_2$  films”, *Nature*, vol. 353, pp. 737–740, 1991.
- [PUR 12] PURCELL-MILTON F., GUN’KO Y.K., “Quantum dots for luminescent solar concentrators”, *Journal of Materials Chemistry*, vol. 22, pp. 16687–16697, 2012.
- [RAN 75] RANBY B., RABEK J.F., *Photodegradation, Photo-oxidation and Photostabilization of Polymers: Principles and Applications*, John Wiley & Sons Ltd, 1975.

- [RED 14] REDDY K.G., DEEPAK T.G., ANJUSREE G.S. *et al.*, “On global energy scenario, dye-sensitized solar cells and the promise of nanotechnology”, *Physical Chemistry Chemical Physics*, vol. 16, pp. 6838–6858, 2014.
- [SHO 61] SHOCKLEY W., QUEISSER H.J., “Detailed balance limit of efficiency of p–n junction solar cells”, *Journal of Applied Physics*, vol. 32, pp. 510–519, 1961.
- [SIN 10] SINGH-RACHFORD T.N., CASTELLANO F.N., “Photon upconversion based on sensitized triplet–triplet annihilation”, *Coordination Chemistry Reviews*, vol. 254, pp. 2560–2573, 2010.
- [SME 90] SMESTAD G., RIES H., WINSTON R. *et al.*, “The thermodynamic limits of light concentrators”, *Solar Energy Materials*, vol. 21, pp. 99–111, 1990.
- [TEH 13] TEHFE M.A., LOURADOUR F., LALEVÉE J. *et al.*, “Photopolymerization reactions: on the way to a green and sustainable chemistry”, *Applied Sciences*, vol. 3, pp. 490–514, 2013.
- [TEN 11] TEN KATE O.M., HINTZEN H.T., DORENBOSA P. *et al.*, “Yb<sup>3+</sup> doped LaSi<sub>3</sub>N<sub>5</sub> and YSi<sub>3</sub>N<sub>5</sub> with low energy charge transfer for near-infrared light-emitting diode and solar cell application”, *Journal of Materials Chemistry*, vol. 21, pp. 18289–18294, 2011.
- [TOR 00] TORIKAI A., “Wavelength selectivity of photodegradation of polymers”, in HAMID S.H. (ed.), *Handbook of Polymer Degradation*, Marcel Dekker, Inc., New York, pp. 573–603, 2000.
- [TUR 99] TURNER J.A., “A realizable renewable energy future”, *Science*, vol. 285, pp. 687–689, 1999.
- [WAN 09] WANG F., LIU X., “Recent advances in the chemistry of lanthanide-doped upconversion nanocrystals”, *Chemical Society Reviews*, vol. 38, pp. 976–989, 2009.
- [WEG 00] WEGH R.T., DONKER H., VAN LOEF E.V.D. *et al.*, “Quantum cutting through downconversion in rare-earth compounds”, *Journal of Luminescence*, vol. 87–89, pp. 1017–1019, 2000.
- [YOO 08] YOON J., BACA A.J., PARK S.I. *et al.*, “Ultrathin silicon solar microcells for semitransparent, mechanically flexible and microconcentrator module designs”, *Nature Materials*, vol. 7, pp. 907–915, 2008.
- [YOO 11] YOON J., LI L.F., SEMICHAEVSKY A.V. *et al.*, “Flexible concentrator photovoltaics based on microscale silicon solar cells embedded in luminescent waveguides”, *Nature Communications*, vol. 2, p. 343, 2011.

- [ZHA 11] ZHANG H., WANG Y., HAN L., “Photoluminescence properties and energy transfer between  $\text{Eu}^{3+}$  and  $\text{Nd}^{3+}$  in polyborate  $\text{BaGdB}_9\text{O}_{16}$ :  $\text{Eu}^{3+}$ ,  $\text{Nd}^{3+}$ ”, *Journal of Applied Physics*, vol. 109, p. 053109, 2011.
- [ZHO 14] ZHOU H., CHEN Q., LI G. *et al.*, “Interface engineering of highly efficient perovskite solar cells”, *Science*, vol. 345, pp. 542–546, 2014.



---

## Polymers with Photoinduced Self-healing Properties

---

### 12.1. Introduction

Current research topics in polymer science have until now never been directed very much toward sustainable development issues. Major global challenges have already emerged from the inevitable decreasing availability of petroleum, which is of course the source of most of the monomers and derived synthetic polymers. In parallel with the identification of renewable alternative resources, the development of new materials that would have a reduced environmental impact is especially important. Besides necessary improved recovery in terms of recyclability, another challenging objective is to increase significantly the lifetime of manufactured goods. Beyond the continuous development of polymers or composites with outstanding mechanical, thermal or chemical resistance, the observation of some fascinating natural processes has revealed self-healing behavior as a promising progress to be explored. When they undergo mechanical damage, self-healing materials can heal themselves, that is to say they can restore their original shape and recover their original properties. The interest in such materials appears immediately obvious in many fields such as protective coatings, biomedical applications, piping and electronics. In 2013, self-healing materials were even named among the top 10 emerging technologies by the World Economic Forum.

---

Chapter written by Julien POLY.

More specifically, the development of self-healing polymers has been a very active area of research over the last decade [BIL 13, BIN 13, GUI 12, HAY 13]. Among the numerous concepts that have been experimentally validated, two main classes can be distinguished: extrinsic or intrinsic self-healing polymers. In the former case, healing is permitted by a healing agent, such as an encapsulated polymerizable formulation which can be released when the polymer is mechanically damaged [WHI 01]. On the contrary, healing will directly imply the composition or functionality of the polymer in the case of an intrinsic healing process. A supplementary distinction is sometimes introduced, with the so-called autonomous healing consisting of processes that are directly triggered by the mechanical damage itself. This distinction is debatable and can be misleading: considering intrinsic self-healing polymers, an energy supply (heat, light, etc.) is needed in any case so as to temporarily give enough mobility to the chains to relax the stress resulting from the damage, whether the process occurs spontaneously after the damage or not. In the case of intrinsic self-healing polymers which would apparently heal autonomously, the energy stored by the sample as a stress due to the mechanical damage is necessarily lower than that needed for a complete healing, that is to say, for complete stress relaxation. Therefore, the occurrence of complete healing at room temperature or under ambient light does not mean that the process is autonomous, but only that the energy brought as heat or irradiation is enough for it in these conditions.

Focusing now on the design of polymers with intrinsic self-healing properties, two main strategies can be considered at first sight, depending on their topological nature: polymers cross-linked at the macroscopic scale or not. This distinction is equivalent, indeed, to the one existing between the two main classes of polymers that can be usually distinguished, namely thermosets or thermoplastics, respectively. The reprocessability of the latter immediately suggests the convenient strategy: heating thermoplastics over their melting ( $T_m$ ) or glass transition ( $T_g$ ) temperatures is expected to result in enough plasticity to enable their efficient healing. On the contrary, macroscopically cross-linked polymers cannot gain enough plasticity to contemplate their healing upon heating. While the network topology of thermosets results in excellent properties in terms of thermal, mechanical and chemical resistances, it will conversely imply a restricted mobility of chains which is unfavorable to efficient healing properties. Moreover, a

partial healing, for instance, due to dangling chains would remain limited to esthetic aspects only: properties inherent to the cross-linked structure would be definitely lost in the damaged area.

This apparent antagonism between cross-linked structure and healing behavior was successfully overcome with the concept of polymers with a network structure based on reversible bonds. The dissociation of these bonds, caused by an external stimulus such as heat or light, temporarily enhances the mobility of the polymer chains, enabling the occurrence of healing. New bonds will be then created, resulting in the recovery of the desired properties along with the reformation of the network structure. The concept was first applied by Wudl *et al.* for the preparation of polymers possessing self-healing properties, exploiting the reversibility of the Diels–Alder reaction upon heating [CHE 02]. Beyond the ensuing application of this reaction to the design of many other polymers exhibiting self-healing properties under heating [LIU 13], the general concept based on reversible bonds has been also successfully adapted since then to several other chemistries and external stimuli.

In this chapter, we will focus on the design of polymers that exhibit photo-triggered self-healing properties. In addition to systems based on reversible network structures, the original strategies developed to heal un-cross-linked polymers with light will also be presented.

## 12.2. Healing based on photo-reversible cycloadditions

The aforementioned contribution of Wudl *et al.*, who exploited the Diels–Alder reaction as a thermally mediated reversible cycloaddition, paved the way for the investigation of other types of reversible cycloadditions for the design of self-healing polymers. In particular, dimerizations consisting of photochemically allowed [2 + 2] or [4 + 4] cycloadditions naturally appeared especially promising in this context [KAU 14]. After Wudl *et al.*'s work, the very first example of a cross-linked polymer able to heal itself in the presence of light was described by Chung *et al.*, who exploited the reversible dimerization of cinnamates under irradiation, resulting in the formation of cyclobutane cycles [CHU 04] (Figure 12.1). For this purpose, they designed a trifunctional cinnamate monomer, namely 1,1,1-tris(cinnamoyloxymethyl)ethane (TCE) which was then implemented for the preparation of a cross-linked film by irradiation at wavelengths over 280 nm

(72 mW.cm<sup>-2</sup>). Cross-linking was confirmed qualitatively by the hardness and insolubility of the film. Fourier transform infrared (FT-IR) spectroscopy was used to quantify the consumption of the C=C bonds of the cinnamate groups, related to the formation of the cyclobutane junctions between monomer units. The cinnamate functions were almost totally consumed after 120 s of irradiation. It was assumed that the propagation of a crack into this polymer would consist predominantly of the cleavage of the weakest bonds of the structure that are the high ring strain cyclobutane junctions, resulting in the regeneration of the cinnamate chromophores. In order to demonstrate the possibility of this retrocycloaddition upon mechanical degradation, the film was ground and the resulting powder was subsequently analyzed by FT-IR spectroscopy. A regeneration of 16% of the cinnamate groups was observed. When the polymer was submitted to a new irradiation, the characteristic bands of the cinnamate chromophores disappeared again, showing the possibility to reform cyclobutanes. Interpenetrated networks were also prepared from the simultaneous photopolymerizations of TCE and dimethacrylic cross-linkers. After the creation of cracks in the samples, flexural strength measurements revealed a partial healing in terms of mechanical resistance for the samples which were irradiated. The flexural strength was all the more restored that the initial loading in TCE was high. However, it should be noted that the healing process is necessarily limited in terms of mechanical properties recovery, since only the poly(TCE) network is expected to be reversibly reformed under irradiation, while the interpenetrated methacrylic network remains definitively damaged. Better results were obtained when the sample was heated at 100°C while being irradiated, which was ascribed to the enhanced mobility of the chains.

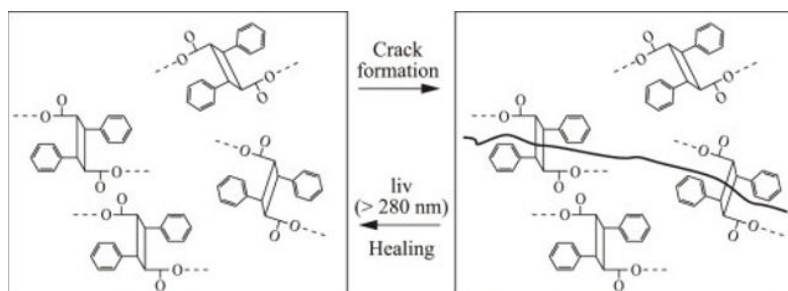


**Figure 12.1.** Mechanism proposed by Chung et al. for the photo-triggered healing process of polymers synthesized from multifunctional cinnamates. Reproduced with permission from [CHU 04]

Following the contribution by Chung *et al.*, photo-reversible [2 + 2] cycloadditions were also exploited by Zhang *et al.* to develop self-healing polymers [LIN 11, LIN 14]. In their case, coumarin derivatives were used as chromophores prone to dimerize under ultraviolet (UV) irradiation. In their first system, coumarins were used as pendant groups along polyurethane (PU) chains (Figure 12.2). Irradiation at 350 nm ( $14.4 \text{ mW}\cdot\text{cm}^{-2}$ ) led to cross-linking due to the formation of cyclobutanes from the reaction between two coumarin side groups. Conversely, irradiation at 254 nm ( $15.6 \text{ mW}\cdot\text{cm}^{-2}$ ) caused the cleavage of the cyclobutane cross-links, resulting in the regeneration of the coumarin pendant chromophores. It was possible to resort to several spectroscopies, namely UV-visible spectroscopy ( $\pi - \pi^*$  transitions), Raman spectroscopy (C=C and CH<sub>2</sub> bands) and FT-IR spectroscopy (C=C and C=O bands), so as to follow the extent of the cross-links formation or dissociation. The authors distinguished the respective expected effects of cracks and cuts: while the propagation of a crack, for instance, due to a tensile stress, should result predominantly in the cleavage of the weaker bonds of the cyclobutane cycles, a cut would damage the sample regardless of bond energies, which implies a need to aim at optimizing the fraction of cross-links that will be reformed in the damaged area during the healing process. Based on this remark, cut samples were first systematically irradiated at 254 nm so as to favor the maximal cleavage of the cyclobutane cross-links. This preliminary irradiation is expected to result in two complementary effects favorable to the healing process. The first effect is the enhanced mobility of the PU chains, enabling, in particular, stress relaxation in the damaged area. It is combined with the temporarily increased concentration of the regenerated coumarin side groups, which will ensure the efficient reformation of cross-links during the subsequent irradiation at 350 nm. Following this methodology, cut films healed efficiently, as observed by optical microscopy. Moreover, tensile stress-strain measurements demonstrated that this healing process under irradiation enables a significant recovery of the mechanical properties (up to 70.2% after the first healing). In a second contribution, the same group proposed another type of PU with healing properties under irradiation, still based on coumarin groups, which were incorporated along the chains [LIN 12]. Very efficient healing was observed here again with a possible total recovery of the mechanical properties tested after a first healing.



networks, Leblanc *et al.* reported earlier the functionalization of eight-armed star-shaped poly(ethylene glycol)s with terminal anthracene groups [ZHE 02]. In solution in water (10% w/v), these precursors led to the rapid formation of a hydrogel under irradiation at 365 nm. The cross-linking was reversed by irradiating the sample at 254 nm. It was possible to repeat the dimerization/retro-dimerization cycle many times while regenerating most of the anthracene functions at the end of each cycle. The self-healing properties of these hydrogels were not investigated, but the concept was then adapted in a contribution by Landfester *et al.*, who synthesized hyperbranched polyglycerols decorated with anthracene functions [FRO 11]. Hydrogels (10% w/v) and cross-linked films were formed under irradiation at 366 nm from these precursors. Here also and in both cases, an excellent reversibility of the junctions consisting of the anthracene-based dimers was observed when repetitive irradiations at 254 and 366 nm were performed. The total healing of a scratch at the scale of a few millimeters was also observed when the film was irradiated at 366 nm after a preliminary irradiation at 254 nm. The low  $T_g$  of the hyperbranched polyglycerol precursors ( $-46^\circ\text{C}$ ), which are temporarily regenerated when the cyclobutane junctions between them are cleaved, enables their mobility. This confirms once again the determining role of the temporary enhanced mobility of the chains in the healing process.

The efficiency of reversible cycloadditions for the design of self-healing polymers has been clearly demonstrated in the studies mentioned in this section. However, the application of this concept could be limited because of its intrinsic mechanism, which implies necessarily two different range of wavelengths: the first one to “unlock” the cross-links or junctions so as to enable the mobility of the chains which is necessary for the healing process, and the second to “re-lock” the network structure so as to restore the properties. This limitation is addressed in the following section, for which only one range of wavelengths is necessary for photodissociation, before new bonds can form when irradiation is stopped.

### **12.3. Healing based on photoinduced homolytic dissociations of covalent bonds**

Besides reversible cycloadditions, several other chemistries have been explored for the design of polymer covalent networks with self-healing

properties under irradiation. Another general concept relies on a network structure based on covalent bonds that can undergo homolytic dissociations, resulting either directly from their structure, such as chromophores at their vicinity, or from photoinduced radical transfer reactions. In the case of bond scissions resulting directly from light absorption, the concept will be similar to that of systems implying cycloadditions described previously: when enough covalent bonds are cleaved at the same time, a temporary enhanced mobility of the constitutive species can ensue, enabling the relaxation of the mechanical stress induced by the damage. The generated radical species can then recombine, progressively restoring a network structure. In the case of transfer reactions, the healing process does not imply to cleave simultaneously most of the bonds ensuring the network structure. On the contrary, only a few photo-generated radicals will initiate step-by-step transfer reactions, allowing a dynamic reorganization of the covalent network. Through this mechanism, the polymer will be able to progressively relax any mechanical stress, resulting, for instance, from a damage such as an impact or a crack, and thus to heal itself.

The second concept was first illustrated by Bowman *et al.*, who reported the preparation of cross-linked polymers exhibiting photoinduced plasticity that is the possibility to relax a mechanical stress or strain upon light irradiation [SCO 05, SCO 06]. For this purpose, they synthesized by photo-initiated thiol-ene polymerization a polymer network which incorporated allyl sulfide groups. Under irradiation (320–500 nm, 30mW.cm<sup>-2</sup>), radicals were generated from the residual photoinitiator which was used for the preparation of the network. Then, these radicals initiated transfer reactions involving allyl sulfide groups, based on an addition-fragmentation mechanism (Figure 12.3(a)). The low  $T_g$  of the network (from -34 to -25°C), implying a rubbery state at ambient temperature, is very probably a key parameter since it can contribute to the fastest reshuffling of the network. The strains which were observed when a stress was applied to the samples without irradiation were reversible, whatever the density in allyl sulfide groups. Conversely, the samples did not recover their initial length after having being submitted to a stress under irradiation. The irreversible strain was all the more important that the density of the allyl sulfide groups was important, consistently with more transfer reactions implying stress relaxation by reshuffling the network. Although the original behavior of these polymers was not investigated in terms of self-healing properties, strictly speaking, this study paved the way for the transposition of the concept in this field.

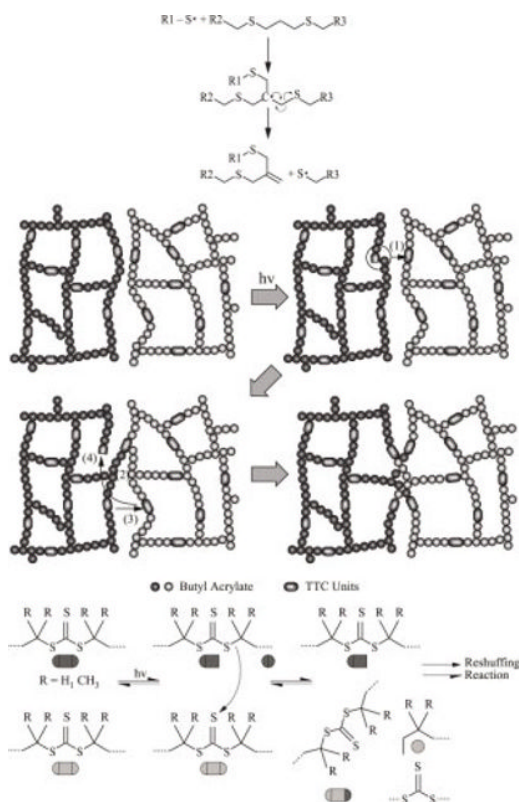


**Figure 12.3.** Addition-fragmentation chain transfer mechanisms based on: a) allyl sulfides and b) trithiocarbonates. Reproduced with permission from [SCO 06] and [AMA 11], respectively

On this subject, Matyjaszewski *et al.* reported the self-healing properties under UV irradiation of poly(butyl acrylate) networks including trithiocarbonate (TTC) functions along the chains [AMA 11]. These networks were synthesized by controlled radical polymerization by reversible addition-fragmentation chain transfer (RAFT). A difunctional methacrylate monomer including a TTC spacer was used, which acted both as a cross-linker and as a chain transfer agent. Contrary to the previous system based on allyl sulfides, no additional photoinitiator was needed for the occurrence of the transfer reactions under irradiation: the chromophores consisted of directly the TTC units since thiocarbonylthio compounds were already well-known photoinitiators and photoiniferters before having being commonly used as RAFT agents. This contribution exploited thus

simultaneously the two possible reactivities of TTC functions (Figure 12.3(b)). The healing procedure consisted of the UV irradiation (330 nm,  $0.9 \text{ mw.cm}^{-2}$ ) of a cut sample in a quartz tube under an inert atmosphere and under the pressure of a weight. A faster and more complete mending was observed when acetonitrile was added. The better healing obtained in the presence of this solvent is ascribable to the resulting swelling and plasticizing effects, enabling an intimate contact between the pieces of networks. In this case, the recovered tensile modulus after healing and drying was almost the same as the one of the sample before the damage. More recently, an elegant illustration of the original properties of these networks was proposed by demonstrating the possibility to modify their swelling ratio, depending on their affinity for the solvent in which their reshuffling under irradiation was previously performed [AMA 12a].

While the reshuffling process implied only transfer reactions in the case of the networks based on the allyl sulfide groups, the use of the TCC functions, being able both to undergo similar addition-fragmentation reactions and to generate primary radicals, necessarily implies the additional contribution of the direct photodissociation of C–S bonds. To this respect, other chemistries were proposed, which can lead to self-healing either through a photo-initiated chain transfer mechanism or through reversible photodissociations and subsequent recombinations.

The reactivity of disulfide bonds can be typically exploited in this way, as demonstrated by Klumperman *et al.*, who prepared and studied cross-linked polymers with self-healing properties upon heating, based on exchanges between disulfide bonds incorporated in the network structure [CAN 11]. Anseth *et al.* reported the synthesis of hydrogels with a network structure implying disulfide junctions, resulting from the oxidation of precursors consisting of four-armed poly(ethylene glycol) stars functionalized with thiol terminal groups [FAI 11]. The molded hydrogel samples were swollen in aqueous solutions containing a photoinitiator (lithium acylphosphinate). Under irradiation (365 nm,  $10 \text{ mW.cm}^{-2}$ ), radicals were generated from the photoinitiator. Similarly to the aforementioned contribution by Bowman *et al.* dealing with allyl sulfides, chain transfer reactions based on thiyl radicals were consequently initiated. Healing properties under irradiation were demonstrated by the annealing of two overlapped hydrogel disks (Figure 12.4). The corresponding initial conditions implied a low concentration in photoinitiator compared to that of the disulfide bonds. Conversely, an excess of photoinitiator was responsible for the

photo-degradation of the network structure, due to the recombination of thiyl radicals with those generated by the photoinitiator. This was turned to good account in this study for photo-patterning purposes. This scheme based on disulfide bonds could be advantageously exploited if no photoinitiator was needed, that is if these bonds would be the chromophores themselves, similarly to the network based on TTC described previously. In particular, the major contribution to the healing process could become in this case the direct photodissociation of covalent bonds followed by the recombination of radicals, instead of transfer reactions which could become a complementary mechanism only. Moreover, the possible sensitivity to oxygen, which was a limitation in the case of the systems based on TTC, is no longer an issue in the case of thiyl radicals.

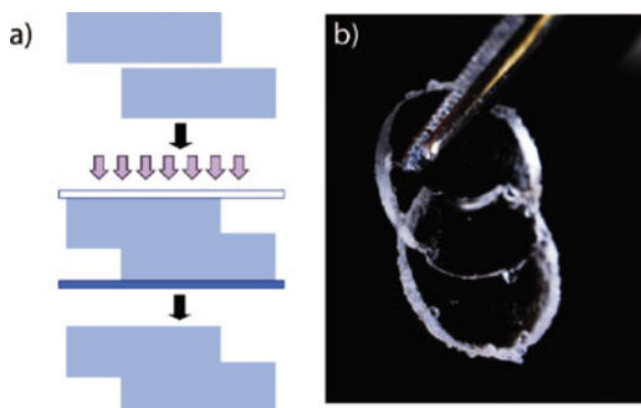


**Figure 12.4.** a) Scheme for photo-healing of disulfide hydrogel. Gels are pressed together to ensure adequate contact. Light exposure and accompanying disulfide rearrangement result in the annealing of the two hydrogels. b) Two hydrogels that have been covalently annealed by photo-initiated disulfide rearrangement. Reproduced with permission from [FAI 11]

Several studies have, indeed, suggested possible improvements in this regard. Otsuka *et al.* first demonstrated the possibility to reversibly photodissociate aliphatic disulfide bonds introduced along the main chain of polyesters under intense UV irradiation (400 W high-pressure mercury lamp, wavelengths between 312 and 577 nm), followed by recombination reactions, resulting in exchanges between chain fragments [OTS 10]. This reaction, the possible application of which was still limited at that stage due to the high intensity needed for the photodissociation, was then significantly improved in a follow-up study. In this second paper, Otsuka *et al.* reported

the synthesis of polyurethanes in which aromatic disulfide bonds were incorporated [OHI 13]. The aromatic cycles introduced as chromophores on both sides of the disulfide bonds facilitated the use of very softer irradiation conditions (9 W, 254 nm). Such disulfides with a stronger absorption constitute undoubtedly a very promising strategy for the design of new self-healing polymers.

Along the same lines and in collaboration with the same group, Matyjaszewski proposed new self-healing polyurethane networks based on thiuram disulfide (TDS) functions [AMA 12b]. The importance of this function lies in its well-known photoiniferter behavior. Under irradiation, its homolytic photodissociation will occur, generating two dithiocarbamyl radicals. Each radical can then either recombine with another one or initiate RAFT, enabling the reshuffling of the network. Similarly to the thiyl radicals generated from disulfide bonds, the dithiocarbamyl radicals generated from TDS functions are tolerant to oxygen. This enabled self-healing directly in the air, without requiring an inert atmosphere, contrary to the aforementioned system based on TTC cleavable functions. Besides this advantage, it was possible to use a simple tabletop lamp (14 W) as a visible light source and the reaction was performed at ambient temperature, due to the low  $T_g$  (from  $-50$  to  $-34^\circ\text{C}$ ) of this polyurethane network, ascribable to the constitutive aliphatic and oligo(ethylene glycol) segments. After qualitative preliminary tests on cylindrical samples, suggesting a total healing of the samples after 24 h of irradiation, quantitative tensile test were performed on thin samples (Figure 12.5). The effect of light was clearly demonstrated, with mechanical properties being almost totally recovered, in terms of elongation at break, after 12 h of irradiation.

Alternatively to the introduction of chromophores at the vicinity of the disulfide bonds in order to favor their photodissociation, a promising strategy could be the use of diselenides instead of disulfides. This idea emerged from a recent contribution by Xu *et al.*, who demonstrated the possibility to photodissociate diselenide bonds [JI 14]. Interestingly, diselenide bonds are weaker than disulfide bonds, which can suggest more dynamic exchanges due to easier dissociations and recombinations. This was evidenced in this study, in which relatively fast exchange reactions (typically one to a few hours) were observed in solution using very mild visible light irradiation conditions (one common lamp of 26–28 lux). This was notably the case for aliphatic diselenides, contrary to their disulfide counterparts, which implied intense UV irradiation, as described before.

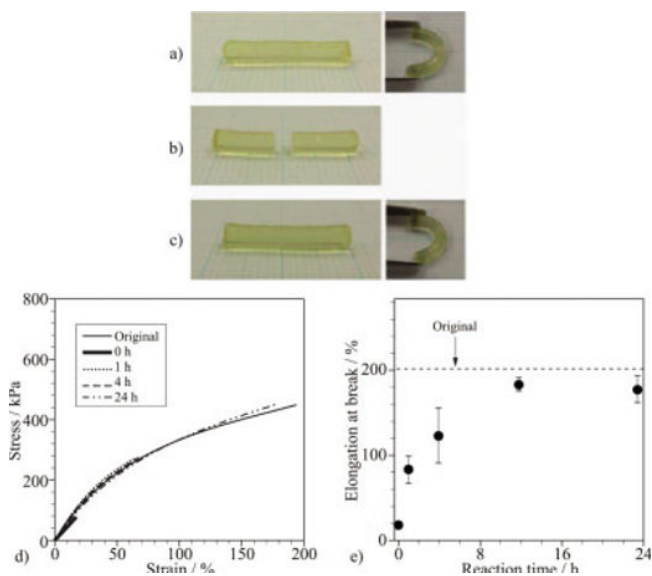


**Figure 12.5.** Photographs of TDS cross-linked polymer in self-healing reaction. a) Before self-healing reaction, b) after cutting cross-linked polymer and c) after self-healing reaction for 24 h. d) Stress–strain curve and e) elongation value at break (%) of cross-linked polymer after irradiation of visible light at room temperature over time. Reproduced with permission from [AMA 12b]

The homolytic dissociation of alkoxyamines is another reaction which has been successfully exploited for the preparation of reversible covalent networks with possible self-healing properties. Following previous studies for which their cleavage was triggered thermally [SU 11, YUA 11], we proposed the extension of this concept using the possible photodissociation of these compounds [TEL 14]. For this purpose, we designed polymer networks by click chemistry using two types of precursors: alkyne-difunctionalized alkoxyamine and azide-terminated poly(butyl acrylate) star-like oligomers synthesized by atom transfer radical polymerization (ATRP). Exploiting their absorption in the 250–300 nm wavelengths range, the efficient photodissociation of the alkoxyamine junctions under UV irradiation ( $100 \text{ mW}\cdot\text{cm}^{-2}$ ), resulting in the formation of nitroxides, was evidenced by electron spin resonance (ESR) spectroscopy (Figure 12.6). For a network prepared from the star precursors having four arms with a degree of polymerization of 15, the maximal concentration of nitroxides was reached after 3 h of irradiation. This was indicative of a maximal cleavage of the junctions, and thus a maximal mobility of the chains. The progressive

reformation of alkoxyamines was then observed with a recovery of 73%, the lost fraction being ascribable to the side reactions occurring in air due to the presence of oxygen. The photodissociation of the junctions was exploited for healing a scratch (depth: 0.6  $\mu\text{m}$ , width: 1.5  $\mu\text{m}$ ) on a 60  $\mu\text{m}$  thick film submitted to UV irradiation (100  $\text{mW}\cdot\text{cm}^{-2}$ ). A complete healing was observed by atomic force microscopy (AFM) after 24 h (Figure 12.7).

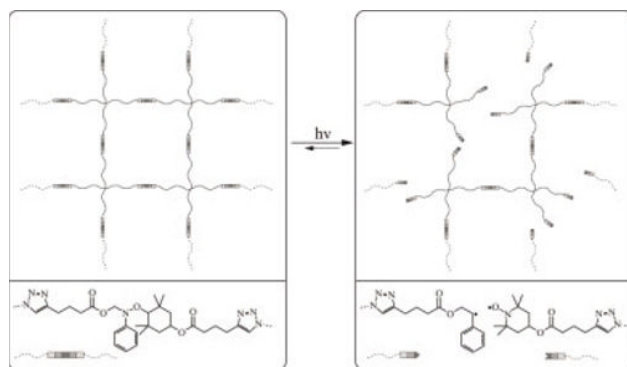


**Figure 12.6.** Representation of the photodissociation of the alkoxyamine junctions resulting in the cleavage of the network structure. Reproduced with permission from [TEL 14]

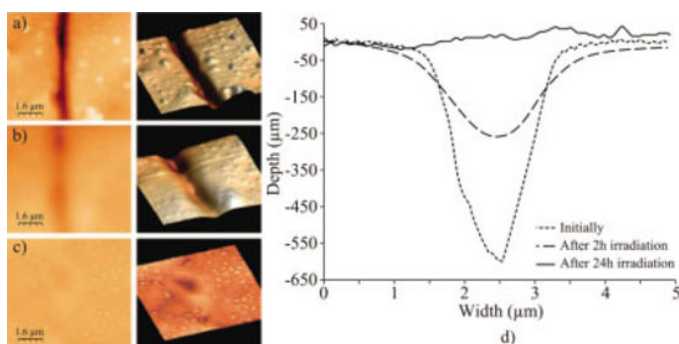


**Figure 12.7.** Observation of the surface of the sample by AFM after various irradiation times. a) Images before irradiation. b) Images after 2 h irradiation. c) Images after 24 h irradiation. d) Depth measurements. Reproduced with permission from reference [TEL 14]

In all the contributions mentioned in this section and as for self-healing polymers based on reversible cycloadditions, photodissociated cross-links or junctions can efficiently reform. However, and for both types of self-healing polymers, potential limitations to a subsequent healing could occur

depending on the nature of the mechanical damage. For instance, in the case of a slowly propagating crack, the preferential cleavage of the weakest covalent bonds can be expected, resulting in most cases in the same dissociation to the one which would have occurred under irradiation. On the contrary, a sudden scratch or cut will necessarily break some other covalent bonds, the dissociation of which is irreversible. A local weakening can thus ensue, despite a subsequent healing mechanism under irradiation that will involve the reversible covalent bonds. To this respect, the fragments resulting from the mechanically induced cleavage of the non-reversible covalent bonds could be advantageously considered for the photo-triggered formation of new bonds. Urban *et al.* proposed an original concept in this regard [GHO 09]. The detailed mechanism was deeply investigated and demonstrated in a follow-up study [GHO 11]. They synthesized polyurethane networks from diisocyanate oligomers, dihydroxyl terminated poly(ethylene glycol) and chitosan functionalized with oxetane groups, in the presence of a tin catalyst (Figure 12.8). A mechanical damage or a UV irradiation will result predominantly in the cleavage of the weaker bonds in the structure, which are localized in the chitosan segments: homolytic dissociation of C–O ether or C–N urea bonds or ring-opening of oxetane groups. An irradiation following a mechanical damage is thus expected to create more reactive fragments and favor self-healing due to a concomitant increase of the mobility of the chains. Depending on the formulation, this was observed experimentally with a fast healing (a few 10 min to a few hours) of 300  $\mu\text{m}$  thick films that were scratched (depth: 20  $\mu\text{m}$ , width: 30  $\mu\text{m}$ ) and subsequently irradiated using a UV lamp (120 W, 302 nm). The network structure can be partially recovered in the mechanically damaged area due to recombination reactions and, in particular, due to the formation of new urethane bonds, resulting from the recombination of a hydroxyl with a carbamyl radical. The concept was then extended to similar networks in which oxethane groups were replaced by oxolane ones [GHO 12]. Despite the healing efficiency which was observed, this chemistry is nevertheless not convenient for repetitive healing, due to the consumption of the reactive groups in the healed area.

Compared to the strategies based on cycloadditions, the schemes presented in this section exploiting radical chemistry have the advantage that only irradiation in one wavelength range is necessary to initiate the healing process. But these methods also have their own limitations. The first limitation is the possible occurrence of side reactions, for instance due to

oxygen, which could lead to the progressive decrease in the concentration of species implied in the reversible bonds dissociation, thus reducing the possibilities of repetitive healing. The second limitation consists of the necessary compatibility between the lifetime of the radicals and the time needed for the chains for complete stress relaxation. Other concepts avoiding radical chemistries could therefore constitute interesting alternatives.

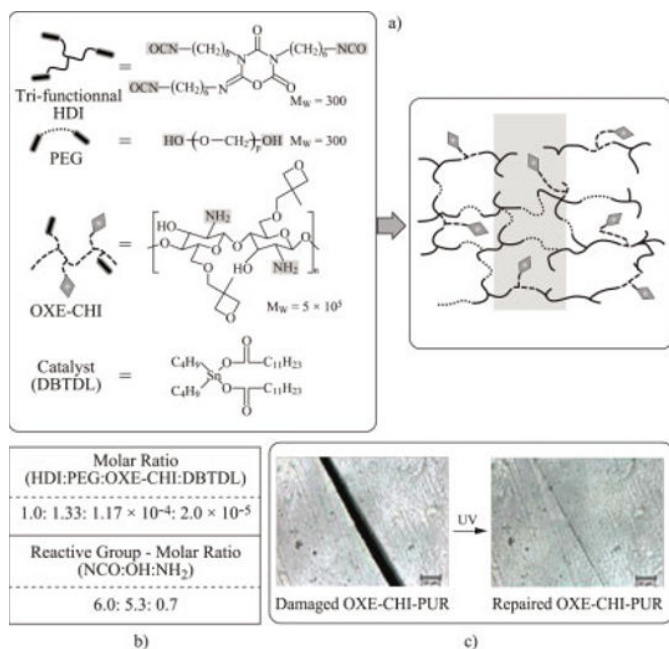


**Figure 12.8.** a) Synthesis of OXE-CHI-PUR networks, b) molar ratios of network components and reactive groups of the reagents and c) optical images of damaged and repaired networks. Reproduced with permission from reference [GHO 11]

#### 12.4. Photoinduced healing in supramolecular polymers and related systems

The strategies presented so far in this chapter rely on a common concept: polymers with a network structure based on reversible covalent bonds. Healing is permitted by a temporary transition from a thermoset state to a thermoplastic behavior with enough chains mobility at ambient temperature. Considering this, alternative routes based on the same concept could be

proposed. They consist of the use of supramolecular or related networks: instead of reversible ordinary covalent bonds (one electron pair shared by two atoms), the network structure can be based on either coordination covalent bonds (the two electrons derive from one atom) or physical bonds (hydrogen bonds,  $\pi$ -stacking, etc.). Following the seminal work by Leibler *et al.* [COR 08], the application of supramolecular chemistry for the development of self-healing polymers has already been extensively studied, but the use of light as the trigger for the healing process has remained very limited.

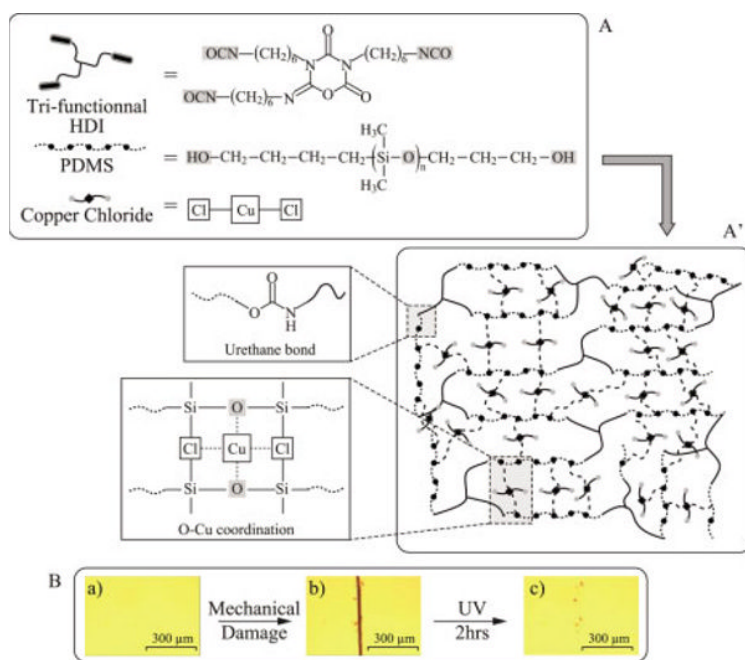


**Figure 12.9.** A) PDMS-PUR network components: tri-functional hexamethylene diisocyanate (HDI), OH-terminated polydimethylsiloxane (PDMS) and copper(II) chloride ( $\text{CuCl}_2$ ). A') Formation of polydimethylsiloxane-polyurethane (PDMS-PUR) networks: 6:3:1 molar ratios of PDMS:HDI: $\text{CuCl}_2$  correspond to 6:6:1 stoichiometry of OH:NCO:Cu reactive groups. B) Repair of PDMS-PUR networks upon UV exposure: a – before damage; b – after damage; c – repair after 2 h UV exposure. Reproduced with permission from [WAN 14]

Recently, and in the manner of their aforementioned work, Urban *et al.* proposed polyurethane networks implying flexible segments which were based on either polydimethylsiloxane (PDMS) or poly(ethylene glycol)

(PEG) [WAN 14].  $\text{CuCl}_2$  was also added in the network, which implied two types of cross-links: permanent covalent cross-links, resulting from the multifunctional isocyanate used, and reversible cross-links, resulting from the coordination of two oxygen atoms belonging to the flexible segments onto copper metallic centers (Figure 12.9). A complete healing of scratched films (width:  $\sim 30 \mu\text{m}$ ) was observed by optical microscopy after a few hours under UV irradiation (15W, 302 nm). Internal reflection infrared imaging revealed that the mechanical damage caused the dissociation of Cu–O bonds, while UV irradiation favored their reformation. The healing process was additionally ascribed to the change of symmetry of the copper complexes which occurs during the transition from their ground to their excited state, resulting in segmental mobility. The better healing properties observed in the case of the system based on PDMS were due to the complementary contribution of the siloxane bonds in the phenomenon, the self-healing behavior of PDMS being already well known [ZHE 12].

This study by Urban *et al.* followed an earlier contribution by Weder *et al.* who reported the light-triggered healing of the so-called metallosupramolecular polymers [BUR 11]. The structures that they described at that time did not exhibit a network topology, but simply a linear one. However, the healing process was directly governed by the reversibility of the supramolecular links along the chains. The structure was based on low molecular weight ( $4000 \text{ g}\cdot\text{mol}^{-1}$ ) poly(ethylene-*co*-butylene) (PEB), which was terminated on each side by 2,6-bis(1'-methylbenzimidazolyl)pyridine (Mebip) ligands. These polymers were associated by the coordination of two Mebip terminal groups by a metal cation, which was either  $\text{Zn}^{2+}$  or  $\text{La}^{3+}$ . Complete and very fast healing of scratched films (thickness: 350–400  $\mu\text{m}$ , depth: 50–70% of the film thickness) was observed under intense UV irradiation ( $950 \text{ mW}\cdot\text{cm}^{-2}$ , 320–390 nm). The mechanism is based on the intense light absorption by the complexes. Their unfavorable deexcitation by fluorescence leads to the conversion of the absorbed energy into heat, causing the dissociation of the metal–ligand bonds. This temporary cleavage of the supramolecular links under irradiation results in lower molecular weight species, with an increased mobility and a lower viscosity, these effects being enhanced by the simultaneously photoinduced heating of the sample (increase in temperature up to  $200^\circ\text{C}$ ). The properties are recovered when the UV irradiation is stopped due to the rapid reformation of the supramolecular links between the chains terminated with Mebip ligands. Stress–strain tests performed on thin samples revealed the possibility of a complete healing in terms of recovery of the mechanical properties,

depending on the composition of the sample. In a second contribution, Weder *et al.* adapted this combination of a photothermal effect with a supramolecular structure to nanocomposites [BIY 13]. These systems were based on PEB and cellulose nanocrystals (CNCs). PEB was functionalized with two terminal ureidopyrimidinone (UPy) groups. Hydroxyl groups on CNCs were substituted with the same group. The possible formation of hydrogen bonds between two UPy groups results in the formation of a network structure (Figure 12.10). Similarly to the previous example, UV irradiation ( $350 \text{ mW}\cdot\text{cm}^{-2}$ , 320–390 nm) enabled the temporary cleavage of the supramolecular cross-links. In a typical example, the healing of a scratch (depth:  $\sim 7 \mu\text{m}$ ) was observed by AFM in 20 s only. Besides self-healing polymers, the same group exploited the same PEBs terminated with Mebip or UPy terminal groups as supramolecular adhesives with reversible light-induced properties [HEI 14].

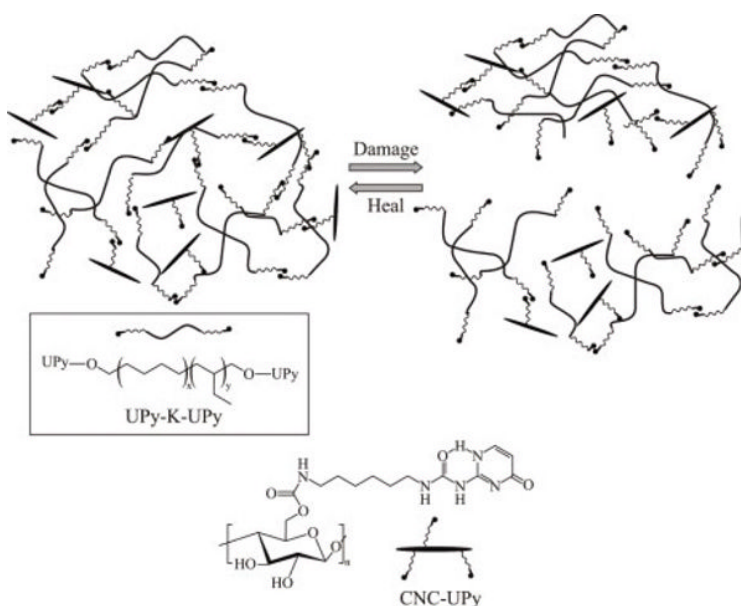


**Figure 12.10.** Schematic representation of the formation of a supramolecular nanocomposite based on UPy-K-UPy and UPy-decorated CNCs. Reproduced with permission from [BIY 13]

More recently, Ji *et al.* proposed another composite with healing properties, implying also a photothermal effect [YAN 14]. The fillers were

carbon nanotubes (CNTs). The polymer was a cross-linked epoxy, resulting from the reaction of bisphenol-A diglycidyl ether with adipic acid. Its structure thus comprised both ester junctions and pendant hydroxyl groups, which can react through transesterification reactions. Such networks come within the so-called concept of vitrimers, which combine a covalent network structure with features typical of supramolecular polymers, such as reprocessability, due to the dynamic exchange between covalent bonds [MON 11]. The  $T_g$  of the polymer was about  $40^\circ\text{C}$ . However, the important temperature to be considered in vitrimers is their topology-freezing transition temperature ( $T_v$ ): above  $T_v$ , the transesterification reactions are fast enough to ensure dynamic exchanges between covalent bonds and thus to enable a healing phenomenon. The  $T_v$  which was determined for the composite (CNTs at a concentration of 1 wt%) was about  $160^\circ\text{C}$ . This transition can be therefore exploited under irradiation if the resulting photothermal effect can lead to temperatures over  $T_v$ . In this study, the use of an intense light source (laser at 808 nm,  $15.2\text{ W}\cdot\text{cm}^{-2}$ ), combined with the strong absorption by the CNTs, resulted in an important photothermal effect which enabled to reach temperatures around  $180^\circ\text{C}$ , that is over  $T_v$ . A fast healing behavior ensued due to the dynamic transesterification reactions (Figure 12.11). A  $50\ \mu\text{m}$  width scratch in a film was totally healed after 10 s of irradiation only in these conditions. It was possible to heal larger scratches using longer irradiation times. The fast and important recovery of mechanical properties under irradiation was quantitatively confirmed by strain–stress measurements. In addition, it was found that the healing phenomenon was greatly enhanced and accelerated through the photothermal effect, compared to the one observed with a simple heating at the same temperature.

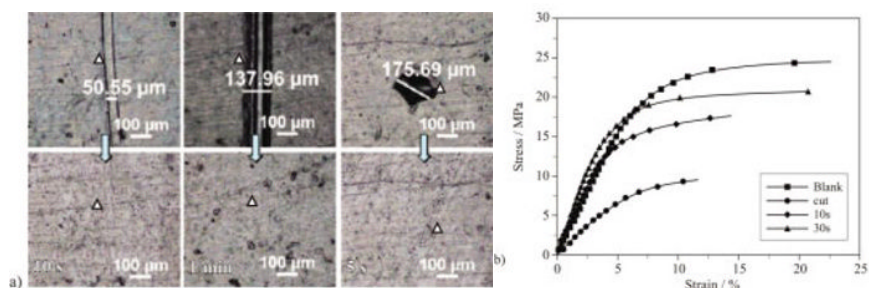


**Figure 12.11.** a) Light (intensity:  $15.2\text{ W}\cdot\text{cm}^{-2}$ ) triggered healing of CNT-vitrimer with narrow cut healed by irradiation for 10 s (left), wide cut healed by irradiation for 1 min (middle) and needle-pierced hole healed in 5 s (right). b) Stress–strain curves of CNT-vitrimer without cut, with cut and after healing via IR laser ( $15.2\text{ W}\cdot\text{cm}^{-2}$ ) irradiation for 10 s and 30 s. Reproduced with permission from [YAN 14]

In the aforementioned examples, a photothermal effect was used to trigger supramolecular remodeling or analogous dynamic exchanges between covalent bonds. Beyond these specific systems, it could be more simply applied in the same way to any un-cross-linked polymer so as to overcome the weak physical bonds existing between the chains.

### **12.5. Healing based on photothermally induced phase transitions or photo-isomerizations**

While the healing of thermosets and assimilated polymers necessarily implies the temporary dissociation of the chemical bonds or supramolecular links ensuring their network topology, a simple heating over their melting or glass transition temperature can be enough in the case of thermoplastic polymers. Heat brings the energy which is necessary for the mobility of the chains, enabling their disentanglement and the cleavage of weak bonds that can exist between them (hydrogen bonds,  $\pi$ -stacking, hydrophobic interactions, etc.). A photothermal effect could be therefore turned to good account in these polymers to initiate healing processes triggered by light.

This concept was recently applied by Zhao *et al.* who introduced gold nanoparticles (AuNPs) into poly(ethylene oxide) (PEO,  $M \approx 200\,000\text{ g.mol}^{-1}$ ,  $T_m \approx 63^\circ\text{C}$ ) as a crystalline polymer [ZHA 13a]. Compared to the work dealing with CNTs described in the previous section, the concentration of AuNPs was extremely low (0.05 wt% for the maximum value). The photothermal effect that was exploited here was the surface plasmon resonance of AuNPs. The complete healing of a scratch (width:  $\sim 100\ \mu\text{m}$ ) in a PEO film (thickness:  $50\ \mu\text{m}$ , 0.04 wt% in AuNPs) was reached after only 10 s of irradiation (laser diode at 532 nm,  $2.2\ \text{W.cm}^{-2}$ ), as observed by polarizing optical microscopy, which evidenced clearly the recrystallization in the scratched area (Figure 12.12). At this intensity, it was possible to reach temperatures as high as  $110^\circ\text{C}$ , thus far over the  $T_m$  of the PEO. Furthermore, comparative tensile tests were performed on thicker films ( $450\ \mu\text{m}$ ), some of them being cut into two pieces which were subsequently put into contact while the interfacial area was irradiated using the conditions mentioned above. It was found that the samples which were healed during 10 s exhibited mechanical properties very close to that of undamaged

samples. Low-density polyethylene (PE, density = 0.915;  $T_m \approx 103^\circ\text{C}$ ) was also investigated similarly in the same paper.

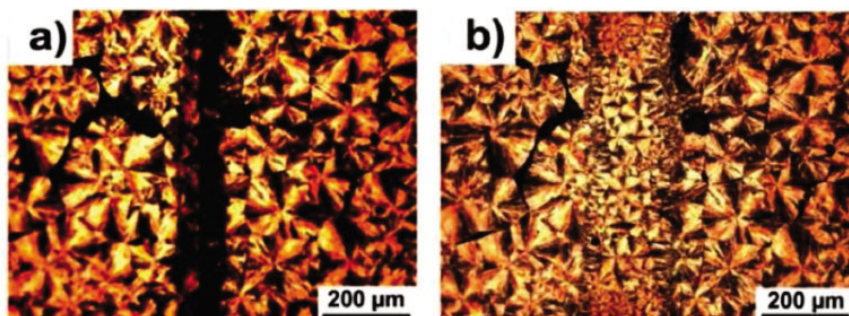


**Figure 12.12.** *a) Polarizing optical micrographs of a PEO/AuNP (0.04 wt%) film with a see-through damage made by razor blade cut and b) after localized optical healing by exposing the damaged area to laser ( $\lambda = 532 \text{ nm}$ ,  $2.2 \text{ W.cm}^{-2}$ ) at room temperature in air. Reproduced with permission from [ZHA 13a]*

The same group then published a second paper which described the synthesis of cross-linked PEOs in which AuNPs were embedded [ZHA 13b]. The network was synthesized by the radical cross-linking polymerization of a poly(ethylene glycol) diacrylate ( $M \approx 20\,000 \text{ g.mol}^{-1}$ ). AuNPs were coated with PEG chains ( $M \approx 2,000 \text{ g.mol}^{-1}$ ) for a better compatibility. Although a cut would irreversibly locally damage the covalent network structure, the melting of the crystalline domains ( $T_m \approx 60\text{--}62^\circ\text{C}$ ), due to the photothermal effect induced by AuNPs, followed by the recrystallization of the PEO chains is expected to permit healing. This was confirmed experimentally using samples that were cut and subsequently irradiated at the cut interface during 3 s (laser diode at 532 nm,  $13 \text{ W.cm}^{-2}$ ). A significant recovery of the original mechanical properties was observed, whereas the sample broke easily when it was heated for 3 min at  $140^\circ\text{C}$  instead of being irradiated. This difference was ascribed to the extent of the expansion phenomenon that occurs during melting: melting occurs locally in the case of the photothermal heating, favoring an expansion confined at the cut interface, whereas the free expansion that occurs in the case of a homogeneous heating does not enable the intimate contact between both sides of the cut. The polymers presented in [ZHA 13b] also exhibited light-triggered shape-memory behavior. More recently, this concept of self-healing polymers implying the photothermal melting of crystalline domains was also derived in the case of hydrogels

containing AuNPs [ZHA 14]. The polymer structure was based on cross-linked poly(*N,N*-dimethylacrylamide) using stearyl acrylate (SA) as a monomer. Pendant aliphatic chains were thus present along the primary chains of the network, enabling the formation of crystalline domains. These domains can be considered as physical cross-links. It is noteworthy that this system, which combines permanent covalent cross-links and reversible physical ones, is finally very similar to some systems presented in the previous section and implies additional cross-links considered as supramolecular interactions. A cut sample based on 24% of SA was photothermally healed upon irradiation (laser diode at 532 nm, 0.72 W, beam diameter:  $\sim 3$  mm) during 10 s.

The original mechanical properties were almost totally recovered. The introduction of fillers that can generate a photothermal effect, enabling the conversion of healable properties upon heating into a photo-healable behavior, appears to be a very general strategy, which can be adapted to many polymers.

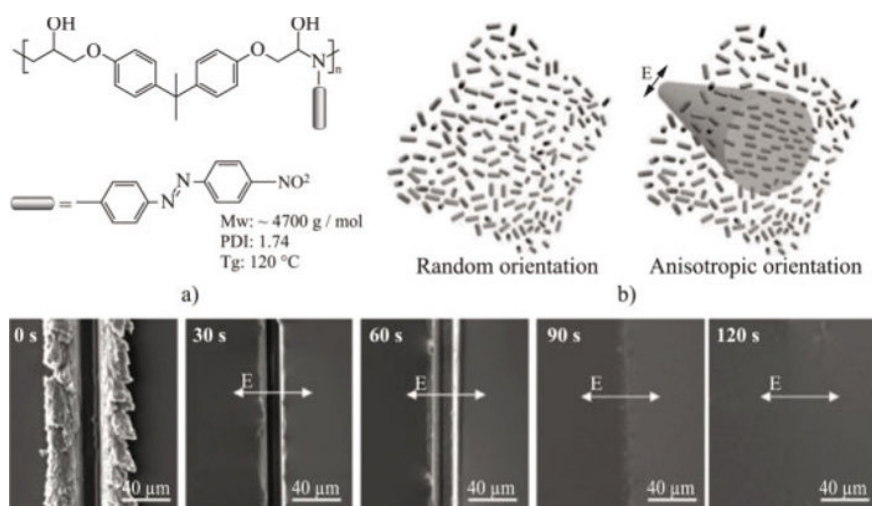


**Figure 12.13.** Light-powered structural healing of damaged azobenzene material: a) chemical structure of polydisperse orange 3 (PDO 3) azobenzene material. b) Schematic diagram showing the anisotropic molecular alignment of azobenzene molecules by light irradiation: the long-axis of azobenzene can be aligned in the direction perpendicular to the light polarization. c) SEM images taken at various stages of light-powered (*s*-polarization) healing of linearly cracked PDO 3 film (15  $\mu\text{m}$  width and 5  $\mu\text{m}$  depth). Reproduced with permission from [KAN 14]

Regarding un-cross-linked polymers, a recent article by Lee *et al.* reported another elegant strategy, which does not imply a photothermal effect [KAN 14]. In this contribution, they exploited the so-called photofluidization of polymers functionalized with pendant azobenzene groups that is an exploitation of the well-known photodimerization of these chromophores: under irradiation, the repeated photo-isomerization of the side groups between their *trans*- and *cis*-isomeric forms can give rise to the bulk diffusion of the polymer. This phenomenon, which is observed even under the  $T_g$  or the  $T_m$  of the polymer, was ascribed earlier to the molecular motions due to the free volume variation that occurs during the isomerization. Moreover, the diffusion process can be anisotropic using polarized light due to the orientation of the azobenzene chromophores along the direction perpendicular to the polarization. In this contribution, the polymer was an epoxy-based structure, synthesized using bisphenol-A diglycidyl ether and functionalized with disperse orange 3 pendant groups (Figure 12.13). Under polarized irradiation (laser at 532 nm,  $600 \text{ mW}\cdot\text{cm}^{-2}$ ), a  $20 \mu\text{m} \times 20 \mu\text{m}$  square post of the polymer was remodeled according to the direction of the light polarization. This anisotropic remodeling confirms that the observed photofluidization does not consist of a photothermal effect but is due to molecular motions resulting from the photo-isomerization of the azobenzene groups. This phenomenon was then exploited to heal a scratch (depth:  $5 \mu\text{m}$ , width:  $15 \mu\text{m}$ ) into a film of this polymer (thickness:  $5 \mu\text{m}$ , supported onto a  $70 \mu\text{m}$  thick polyethylene terephthalate film). A complete healing of the scratch was observed in only 120 s, still using the same irradiation conditions and with a polarization direction perpendicular to the scratch axis. A complete healing was also observed when a circular-polarized light was used, but with a longer irradiation time (150 s). Interestingly, a light-healable electrical conductor was derived from this polymer when it was filled with silver nanowires. The photofluidization effect enabled by the introduction of azobenzene chromophores appears as a very smart strategy toward a new class of light-triggered self-healing polymers.

## 12.6. Conclusion and perspectives

We have seen in this chapter that several novel approaches have been already successfully explored for the preparation of polymers being able to heal themselves under light irradiation when they are mechanically

damaged. While covalent macroscopic networks necessarily imply a temporary cleavage of the cross-links to generate enough mobility for the relaxation of the stress induced by the damage, thermoplastics can be more simply healed through a photothermal effect. This conversion of light into heat is, indeed, a very general strategy which could be adapted to many polymers considering their thermal properties ( $T_g$ ,  $T_m$ ...) through the use of various possible chemical groups or fillers (dyes, ligands, nanoparticles, etc.).

Some recent papers have also demonstrated that these strategies can no longer be strictly divided into two simple categories, which consist either in the methods applicable to thermoplastics or in the ones adapted to cross-linked polymers. To this respect, studies related to polymer networks based on supramolecular interactions or dynamic exchanges between covalent bonds constitute excellent examples of possible hybridization between these concepts. For instance, we have seen that the photothermal effect due to CNTs was efficiently applied to trigger the healing process of dynamic covalent networks. Similarly, the introduction of a photothermal effect into covalent networks implying thermally reversible cross-links, such as the one implying the Diels–Alder reaction, can easily be contemplated. A temporary de-cross-linking could also result from the conversion of light into another stimulus, such as pH or redox potential variation.

Several concepts could, however, be combined into the same system so as to overcome some specific limitations. For instance, the fast healing of a film under ambient light could imply an unwanted fragile or sticky behavior due to a permanently enhanced mobility of the chains. In this scenario, interpenetrated networks that would combine two distinct healing processes could be an interesting strategy to explore: a background mechanism that would occur as a slow healing process, combined with a possibly very fast one, which could be triggered only under very specific irradiation conditions and dedicated to the timely healing of some possible larger damages.

In any case, the absorption of light by the material implies a limited penetration depth. Thus, photo-triggered self-healing polymers will have to be applied necessarily as thin materials. These materials are already wanted for many potential applications, from obvious ones such as protective

coatings to smart films with a healing behavior including the recovery of other properties, such as conductivity.

## 12.7. Bibliography

- [AMA 11] AMAMOTO Y., KAMADA J., OTSUKA H. *et al.*, “Repeatable photoinduced self-healing of covalently cross-linked polymers through reshuffling of trithiocarbonate units”, *Angewandte Chemie International Edition*, vol. 50, no. 7, pp. 1660–1663, 2011.
- [AMA 12a] AMAMOTO Y., OTSUKA H., TAKAHARA A. *et al.*, “Changes in network structure of chemical gels controlled by solvent quality through photoinduced radical reshuffling reactions of trithiocarbonate units”, *ACS Macro Letters*, vol. 1, no. 4, pp. 478–481, 2012.
- [AMA 12b] AMAMOTO Y., OTSUKA H., TAKAHARA A. *et al.*, “Self-healing of covalently cross-linked polymers by reshuffling thiuram disulfide moieties in air under visible light”, *Advanced Materials*, vol. 24, no. 29, pp. 3975–3980, 2012.
- [BIL 13] BILLIET S., HILLEWAERE X.K.D., TEIXEIRA R.F.A. *et al.*, “Chemistry of crosslinking processes for self-healing polymers”, *Macromolecular Rapid Communications*, vol. 34, no. 4, pp. 290–309, 2013.
- [BIN 13] BINDER W.H., *Self-Healing Polymers: From Principles to Applications*, Wiley-VCH, Weinheim, 2013.
- [BIY 13] BIYANI M.V., FOSTER E.J., WEDER C., “Light-healable supramolecular nanocomposites based on modified cellulose nanocrystals”, *ACS Macro Letters*, vol. 2, no. 3, pp. 236–240, 2013.
- [BUR 11] BURNWORTH M., TANG L., KUMPFER J.R. *et al.*, “Optically healable supramolecular polymers”, *Nature*, vol. 472, no. 7343, pp. 334–337, 2011.
- [CAN 11] CANADELL J., GOOSSENS H., KLUMPERMAN B., “Self-healing materials based on disulfide links”, *Macromolecules*, vol. 44, no. 8, pp. 2536–2541, 2011.
- [CHE 02] CHEN X., DAM M.A., ONO K. *et al.*, “A thermally re-mendable cross-linked polymeric material”, *Science*, vol. 295, no. 5560, pp. 1698–1702, 2002.
- [CHU 04] CHUNG C.-M., ROH Y.-S., CHO S.-Y. *et al.*, “Crack healing in polymeric materials via photochemical [2 + 2] cycloaddition”, *Chemistry of Materials*, vol. 16, no. 21, pp. 3982–3984, 2004.
- [COR 08] CORDIER P., TOURNILHAC F., SOULIE-ZIAKOVIC C. *et al.*, “Self-healing and thermoreversible rubber from supramolecular assembly”, *Nature*, vol. 451, no. 7181, pp. 977–980, 2008.

- [COU 96] COURSAN M., DESVERGNE J.P., DEFFIEUX A., “Reversible photodimerisation of  $\omega$ -anthrylpolystyrenes”, *Macromolecular Chemistry and Physics*, vol. 197, no. 5, pp. 1599–1608, 1996.
- [FAI 11] FAIRBANKS B.D., SINGH S.P., BOWMAN C.N. *et al.*, “Photodegradable, photoadaptable hydrogels via radical-mediated disulfide fragmentation reaction”, *Macromolecules*, vol. 44, no. 8, pp. 2444–2450, 2011.
- [FRO 11] FROIMOWICZ P., FREY H., LANDFESTER K., “Towards the generation of self-healing materials by means of a reversible photo-induced approach”, *Macromolecular Rapid Communications*, vol. 32, no. 5, pp. 468–473, 2011.
- [GHO 09] GHOSH B., URBAN M.W., “Self-repairing oxetane-substituted chitosan polyurethane networks”, *Science*, vol. 323, no. 5920, pp. 1458–1460, 2009.
- [GHO 11] GHOSH B., CHELLAPPAN K.V., URBAN M.W., “Self-healing inside a scratch of oxetane-substituted chitosan-polyurethane (OXE-CHI-PUR) networks”, *Journal of Materials Chemistry*, vol. 21, no. 38, pp. 14473–14486, 2011.
- [GHO 12] GHOSH B., CHELLAPPAN K.V., URBAN M.W., “UV-initiated self-healing of oxolane-chitosan-polyurethane (OXO-CHI-PUR) networks”, *Journal of Materials Chemistry*, vol. 22, no. 31, pp. 16104–16113, 2012.
- [GUI 12] GUIMARD N.K., OEHLenschlaeger K.K., ZHOU J. *et al.*, “Current trends in the field of self-healing materials”, *Macromolecular Chemistry and Physics*, vol. 213, no. 2, pp. 131–143, 2012.
- [HAY 13] HAYES W., GREENLAND B.W., *Healable Polymer Systems*, RSC Polymer Chemistry Series No. 5, RSC Publishing, 2013.
- [HEI 14] HEINZMANN C., COULIBALY S., ROULIN A. *et al.*, “Light-induced bonding and debonding with supramolecular adhesives”, *ACS Applied Materials & Interfaces*, vol. 6, no. 7, pp. 4713–4719, 2014.
- [JI 14] JI S., CAO W., YU Y. *et al.*, “Dynamic diselenide bonds: exchange reaction induced by visible light without catalysis”, *Angewandte Chemie International Edition*, vol. 53, no. 26, pp. 6781–6785, 2014.
- [KAN 14] KANG H.S., KIM H.-T., PARK J.-K. *et al.*, “Light-powered healing of a wearable electrical conductor”, *Advanced Functional Materials*, vol. 24, no. 46, pp. 7273–7283, 2014.
- [KAU 14] KAUR G., JOHNSTON P., SAITO K. “Photo-reversible dimerisation reactions and their applications in polymeric systems”, *Polymer Chemistry*, vol. 5, no. 7, pp. 2171–2186, 2014.

- [KIS 14] KISKAN B., YAGCI Y., “Self-healing of poly(propylene oxide)-polybenzoxazine thermosets by photoinduced coumarin dimerization”, *Journal of Polymer Science Part A: Polymer Chemistry*, vol. 52, no. 20, pp. 2911–2918, 2014.
- [LIN 11] LING J., RONG M.Z., ZHANG M.Q., “Coumarin imparts repeated photochemical remendability to polyurethane”, *Journal of Materials Chemistry*, vol. 21, no. 45, pp. 18373–18380, 2011.
- [LIN 12] LING J., RONG M.Z., ZHANG M.Q., “Photo-stimulated self-healing polyurethane containing dihydroxyl coumarin derivatives”, *Polymer*, vol. 53, no. 13, pp. 2691–2698, 2012.
- [LIN 14] LING J., RONG M.Z., ZHANG M.Q., “Effect of molecular weight of PEG soft segments on photo-stimulated self-healing performance of coumarin functionalized polyurethanes”, *Chinese Journal of Polymer Science*, vol. 32, no. 10, pp. 1286–1297, 2014.
- [LIU 13] LIU Y.-L., CHUO T.-W., “Self-healing polymers based on thermally reversible Diels-Alder chemistry”, *Polymer Chemistry*, vol. 4, no. 7, pp. 2194–2205, 2013.
- [MON 11] MONTARNAL D., CAPELOT M., TOURNILHAC F. *et al.*, “Silica-like malleable materials from permanent organic networks”, *Science*, vol. 334, no. 6058, pp. 965–968, 2011.
- [OHI 13] OHISHI T., IKI Y., IMATO K. *et al.*, “Insertion metathesis depolymerization of aromatic disulfide-containing dynamic covalent polymers under weak intensity photoirradiation”, *Chemistry Letters*, vol. 42, no. 11, pp. 1346–1348, 2013.
- [OTS 10] OTSUKA H., NAGANO S., KOBASHI Y. *et al.*, “A dynamic covalent polymer driven by disulfide metathesis under photoirradiation”, *Chemical Communications*, vol. 46, no. 7, pp. 1150–1152, 2010.
- [SCO 05] SCOTT T.F., SCHNEIDER A.D., COOK W.D. *et al.*, “Photoinduced plasticity in cross-linked polymers”, *Science*, vol. 308, no. 5728, pp. 1615–1617, 2005.
- [SCO 06] SCOTT T.F., DRAUGHON R.B., BOWMAN C.N., “Actuation in crosslinked polymers via photoinduced stress relaxation”, *Advanced Materials*, vol. 18, no. 16, pp. 2128–2132, 2006.
- [SU 11] SU J., AMAMOTO Y., NISHIHARA M., TAKAHARA A. *et al.*, “Reversible cross-linking of hydrophilic dynamic covalent polymers with radically exchangeable alkoxyamines in aqueous media”, *Polymer Chemistry*, vol. 2, no. 9, pp. 2021–2026, 2011.

- [TEL 14] TELITEL S., AMAMOTO Y., POLY J. *et al.*, “Introduction of self-healing properties into covalent polymer networks via the photodissociation of alkoxyamine junctions”, *Polymer Chemistry*, vol. 5, no. 3, pp. 921–930, 2014.
- [WAN 14] WANG Z., YANG Y., BURTOVYY R. *et al.*, “UV-induced self-repairing polydimethylsiloxane-polyurethane (PDMS-PUR) and polyethylene glycol-polyurethane (PEG-PUR) Cu-catalyzed networks”, *Journal of Materials Chemistry A*, vol. 2, no. 37, pp. 15527–15534, 2014.
- [WHI 01] WHITE S.R., SOTTOS N.R., GEUBELLE P.H. *et al.*, “Autonomic healing of polymer composites”, *Nature*, vol. 409, no. 6822, pp. 794–797, 2001.
- [XU 13] XU J.-F., CHEN Y.-Z., WU L.-Z. *et al.*, “Dynamic covalent bond based on reversible photo [4 + 4] cycloaddition of anthracene for construction of double-dynamic polymers”, *Organic Letters*, vol. 15, no. 24, pp. 6148–6151, 2013.
- [YAN 14] YANG Y., PEI Z., ZHANG X. *et al.*, “Carbon nanotube-vitrimer composite for facile and efficient photo-welding of epoxy”, *Chemical Science*, vol. 5, no. 9, pp. 3486–3492, 2014.
- [YUA 11] YUAN C.E., RONG M.Z., ZHANG M.Q. *et al.*, “Self-healing of polymers via synchronous covalent bond fission/radical recombination”, *Chemistry of Materials*, vol. 23, no. 22, pp. 5076–5081, 2011.
- [ZHA 13a] ZHANG H., FORTIN D., XIA H. *et al.*, “Fast optical healing of crystalline polymers enabled by gold nanoparticles”, *Macromolecular Rapid Communications*, vol. 34, no. 22, pp. 1742–1746, 2013.
- [ZHA 13b] ZHANG H., ZHAO Y., “Polymers with dual light-triggered functions of shape memory and healing using gold nanoparticles”, *ACS Applied Materials & Interfaces*, vol. 5, no. 24, pp. 13069–13075, 2013.
- [ZHA 14] ZHANG H., HAN D., YAN Q. *et al.*, “Light-healable hard hydrogels through photothermally induced melting-crystallization phase transition”, *Journal of Materials Chemistry A*, vol. 2, no. 33, pp. 13373–13379, 2014.
- [ZHE 02] ZHENG Y., MICIC M., MELLO S.V. *et al.*, “PEG-based hydrogel synthesis via the photodimerization of anthracene groups”, *Macromolecules*, vol. 35, no. 13, pp. 5228–5234, 2002.
- [ZHE 12] ZHENG P., MCCARTHY T.J. “A surprise from 1954: siloxane equilibration is a simple, robust, and obvious polymer self-healing mechanism”, *Journal of the American Chemical Society*, vol. 134, no. 4, pp. 2024–2027, 2012.



---

## List of Authors

---

Julien BABINOT  
Institut de Chimie et des Matériaux  
Paris-Est (ICMPE)  
CNRS – UPEC  
Thiais  
France

Christopher BARNER-KOWOLLIK  
Preparative Macromolecular  
Chemistry  
Institut für Technische  
Chemie und Polymerchemie  
Karlsruhe Institute of  
Technology (KIT)  
Germany

Federico BELLA  
Politecnico di Torino  
Italy

Roberta BONGIOVANNI  
Politecnico di Torino  
Italy

Thomas BRÖMME  
Department of Chemistry and  
Institute of Coatings and Surface  
Chemistry  
Niederrhein University of Applied  
Sciences  
Krefeld  
Germany

Thanh-Tuân BUI  
Laboratoire de Physicochimie des  
Polymères et des Interfaces (LPPI)  
University of Cergy Pontoise  
France

James CRIVELLO  
Department of Chemistry and  
Chemical Biology  
Rensselaer Polytechnic Institute  
Troy  
USA

Guillaume DELAITTRE  
Preparative Macromolecular  
Chemistry  
Institut für Technische Chemie und  
Polymerchemie  
Karlsruhe Institute of Technology  
(KIT)  
Germany

Sean DORAN  
Faculty of Science and Letters  
Department of Chemistry  
Istanbul Technical University  
Turkey

Frédéric DUMUR  
Aix-Marseille University  
France

Steffen ERNST

FEW Chemicals GmbH  
Bitterfeld-Wolfen  
Germany

Christoph P. FIK

Dentsply DeTrey GmbH  
Konstanz  
Germany

Jean-Pierre FOUASSIER

Institut de Science des Matériaux de  
Mulhouse  
France

Didier GIGMES

Aix-Marseille University  
France

Anja S. GOLDMANN

Preparative Macromolecular  
Chemistry  
Institut für Technische Chemie und  
Polymerchemie  
Karlsruhe Institute of Technology  
(KIT)  
Germany

Fabrice GOUBARD

Laboratoire de Physicochimie des  
Polymères et des Interfaces (LPPI)  
University of Cergy Pontoise  
France

Gianmarco GRIFFINI

Politecnico di Milano  
Italy

Dietmar KEIL

FEW Chemicals GmbH  
Bitterfeld-Wolfen  
Germany

Joachim E. KLEE

Dentsply DeTrey GmbH  
Konstanz  
Germany

Jacques LALEVÉE

Institut de Science des Matériaux de  
Mulhouse  
France

Valérie LANGLOIS

Institut de Chimie et des Matériaux  
Paris-Est (ICMPE)  
CNRS – UPEC  
Thiais  
France

Maximilian MAIER

Dentsply DeTrey GmbH  
Konstanz  
Germany

Jan O. MUELLER

Preparative Macromolecular  
Chemistry  
Institut für Technische Chemie und  
Polymerchemie  
Karlsruhe Institute of Technology  
(KIT)  
Germany

Julien POLY

Institut de Science des Matériaux de  
Mulhouse  
France

Yue QI

School of Electrical, Electronic and  
Communications Engineering  
UCD Communications and  
Optoelectronic Research Centre  
SFI-Strategic Research Cluster in  
Solar Energy Conversion  
College of Engineering and  
Architecture  
University College Dublin  
Ireland

Knut REINER  
FEW Chemicals GmbH  
Bitterfeld-Wolfen  
Germany

Estelle RENARD  
Institut de Chimie et des Matériaux  
Paris-Est (ICMPE)  
CNRS – UPEC  
Thiais  
France

Xavier SALLENAVE  
Laboratoire de Physicochimie des  
Polymères et des Interfaces (LPPI)  
University of Cergy Pontoise  
France

Christian SCHMITZ  
Department of Chemistry and  
Institute of Coatings and Surface  
Chemistry  
Niederrhein University of Applied  
Sciences  
Krefeld  
Germany

John SHERIDAN  
School of Electrical, Electronic and  
Communications Engineering  
UCD Communications and  
Optoelectronic Research Centre  
SFI-Strategic Research Cluster in  
Solar Energy Conversion  
College of Engineering and  
Architecture  
University College Dublin  
Ireland

Bernd STREHMEL  
Department of Chemistry and  
Institute of Coatings and Surface  
Chemistry  
Niederrhein University of Applied  
Sciences  
Krefeld  
Germany

Mehmet Atilla TASDELEN  
Faculty of Engineering  
Department of Polymer Engineering  
Yalova University  
Turkey

Omer Suat TASKIN  
Faculty of Science and Letters  
Department of Chemistry  
Istanbul Technical University  
Turkey

Stefano TURRI  
Politecnico di Milano  
Italy

Davy-Louis VERSACE  
Institut de Chimie et des Matériaux  
Paris-Est (ICMPE)  
CNRS – UPEC  
Thiais  
France

Yusuf YAĞCI  
Istanbul Technical University  
Faculty of Science and Letters  
Department of Chemistry  
Istanbul  
Turkey



---

# Index

---

## A, B

acridinediones, 21, 66  
acridinium dyes, 55  
acyl  
  germanium compounds, 129, 130  
  phosphine oxides, 68, 127–129,  
  130  
addition-fragmentation  
  sensitization, 97  
alkoxyamine, 8, 87, 88, 405, 406  
allyl sulfide, 400–402  
amine, 8, 10, 11, 15, 17, 18, 21, 24–  
  26, 31, 32, 91, 94, 124–126, 128–  
  130, 133, 265, 281, 287, 292, 296,  
  307, 337  
anchoring groups, 188, 195, 205  
anionic polymerization, 45, 46, 83,  
  102, 106–108  
anthraquinone-derived  
  monomers, 337–339  
antibacterial properties, 344–347  
aryl azide photochemistry, 337  
bathochromic shifts, 134, 222, 239  
benzophenone, 7, 10, 63, 64, 69, 70,  
  88, 92, 297, 310, 329–331, 345  
borate, 8, 10, 11, 17, 20, 131, 225  
  photoinitiators, 131

## C

camphorquinone, 7, 11, 12, 68, 69,  
  93, 94, 124  
camphorquinone/amine system, 124–  
  127  
carbazoles, 62, 160  
cationic  
  photopolymerization, 2, 3, 5, 28,  
  29, 45, 57, 66, 69, 70, 102–105,  
  133–135  
  polymerization, 2, 45–47, 52, 53,  
  62–64, 68, 70, 102–105, 164  
cell  
  adhesion and compatibility, 348–  
  349  
  guiding, 280, 301  
cellulose, 280, 285, 296–303, 306,  
  307, 342, 347  
charge injection, 142, 145, 190, 197,  
  205  
color formation, 234, 235  
Computer to Plate (CtP), 16, 214,  
  216–239  
concentrator, 251, 371, 378, 379  
conjugated polymers, 141–149, 152,  
  162, 188, 197, 310, 312  
controlled/living polymerization, 87,  
  99, 100

crosslinking, 140, 150, 152, 155, 169, 309, 310, 382  
curcumin, 64  
cyanine, 10, 25, 224  
cycloaddition, 162, 280, 287, 288, 290, 291, 395, 397–400, 406, 407

## D

data storage, 251, 256, 260  
dental materials, 123  
depth of cure, 124, 130, 134  
dialkylphenacylsulfonium salts, 46, 47, 58, 60, 62  
diaryliodonium salts, 48, 52, 54–57, 59, 60, 63, 64, 66–69, 222  
diazonium salts, 46, 54, 297  
dichromated gelatin, 251  
diffusion, 10, 32, 153, 154, 217, 252–254, 257, 258, 267, 269, 270, 364, 416  
dimerization, 148, 283, 309, 311, 395, 399  
diode laser, 240, 242, 264, 265  
diphenyl iodonium salt, 10–12  
direct laser writing, 289  
diselenide, 404  
disulfide, 8, 292, 402–404  
dithienothiophene, 66  
donor-acceptor structure, 200  
downshifting, 365, 371–378  
durability, 188, 373, 378, 382, 384, 385  
dyes, 1  
dye-sensitized solar cell, 183, 184, 363, 371–378

## E, F

electrolyte, 184–187, 189, 194, 196, 204, 227–229, 372, 377  
electron-transfer  
  photosensitization, 51–55, 59  
  layer, 142

electropolymerisation, 196  
emissive layer, 142  
enzymes and proteins  
  immobilization, 347–348  
Eosin Y, 260  
eosine, 66, 69  
erythrosine b, 257  
europium, 200, 375  
ferrocenium salts, 4, 46  
fluoropolymer, 371, 374–378, 381–385  
free  
  radical promoted cationic  
    photopolymerization, 2  
  radical promoted  
    photosensitization, 66–70

## G, H

grafting  
  to, 300, 328, 337, 339, 350  
  from, 328, 329, 332, 335, 336, 340, 346, 347, 350  
halogen lamps, 23, 28  
hexaaryl bisimidazole, 130  
hole  
  transporter materials, 192  
  injection layer, 142  
holographic recording material, 253, 255, 271

## I, K

intramolecular photosensitization, 50  
iodide/triiodide couple, 185  
iodonium, 3, 8, 10, 11, 12, 14–17, 19–21, 25–28, 30, 31, 32, 89, 102–104, 133, 224, 225, 228, 229, 235, 236  
ketocoumarins, 66  
ketone, 6, 7, 9, 29, 69, 332

**L, M**

laser drying, 213  
LED, 5, 15, 16, 24, 27, 30, 33, 49, 65,  
66, 126, 127, 128, 152  
leuco form, 11  
light  
emitting electrochemical cells, 145  
emitting materials, 141–157  
harvesting large photoinitiators, 23  
low  
band gap, 199, 200  
viscosity monomers, 27, 34  
luminescent, 311, 361  
solar concentrator, 371, 378–385  
metallic oxide, 185  
methylene blue, 7, 10, 17, 26, 260  
metrology, 260

**N, O**

N-alkoxypyridinium salts, 47, 54, 59  
nanoparticles, 96, 153, 154, 189, 218,  
282, 290, 291, 332, 345, 346, 372,  
413, 417  
near infrared (NIR), 187, 215, 366  
network formation, 309  
NIR absorber, 215, 221, 239, 241,  
242  
nitroxide, 87–89, 298, 314, 405  
non-conjugated polymers, 149–154  
non-local photopolymerization driven  
diffusion, 251  
N-vinylcarbazole, 20, 62, 70  
one component system, 6–7, 9  
organic  
dye, 25, 187, 188, 196, 206, 369,  
370, 371, 373, 374, 375, 379,  
381, 382, 383  
dyes, 25, 187, 188, 196, 206, 369,  
370, 371, 373, 374, 379, 382  
light-emitting devices, 139

oxetane, 48, 143, 145, 160, 161, 164,  
167, 170, 309, 311, 407  
oxidation potential, 54, 195, 226  
oxime, 281, 283–287, 314  
oxolane, 407  
oxygen inhibition, 13, 14, 20, 21, 27,  
30, 102, 126, 134

**P**

panchromatic, 5, 29–30, 188  
phenacyl sulfide, 281, 291–293, 296,  
299, 314  
phencyclone, 281, 296, 314  
phenothiazines, 60, 61  
phloxine B, 260  
photo  
ATRP, 85, 89, 91–94, 97  
NMRP, 87–89  
RAFT, 97–102  
photocatalyst, 97, 297, 345  
photochemical cross-linking, 310  
photochemistry, 2, 46, 123, 219, 288,  
297, 337  
photoenol, 281, 288–291, 296, 299,  
305–307, 309, 312, 314  
photofluidization, 416  
photoinduced diels-alder  
reaction, 281  
photoiniferters, 19, 84–88, 101, 329,  
334–335, 350, 401, 404  
photoinitiated free radical  
polymerization, 45, 63, 123–133  
photoinitiating systems, 1, 12–32, 83,  
93, 106  
photoinitiators, 23, 46–57, 60  
photo-isomerization, 416  
photoligation, 291, 299, 305, 309,  
313  
photo-oxidation process, 333–334

photopatterning, 279, 284, 285, 301, 307, 314  
photopolymer, 64, 214–216, 218, 230, 236–238, 243, 251–262, 264–265, 267–269, 271  
photosensitivity, 7, 23, 33, 71, 131, 145, 160, 214  
photosensitizer, 2, 8, 46, 58, 60–66, 93, 126, 185, 187, 188, 197, 205, 257, 260–262, 264–267, 329, 331, 338, 342, 349  
photothermal effect, 411–417  
photovoltaics, 183, 361–371  
physical drying, 215, 239, 240  
polychromatic, 5, 14–16, 22, 25, 33, 236  
polyfluorene, 145–147, 206, 312  
polymer  
  network, 140, 150, 154, 161, 162, 381, 400, 405, 417  
  sensitizers, 197, 199  
polymeric metal complexes, 199  
polymer-sensitized solar cells, 188  
polymethine, 18, 219, 221, 225, 226, 230, 232, 233, 241  
polynuclear aromatic  
  hydrocarbons, 46, 56–59  
polyphenylenevinylene, 148, 206  
power efficiency, 155, 204  
printing, 5, 14, 17, 18, 32, 45, 213–217, 221, 232, 237, 239–243  
push-pull dyes, 22, 24

## Q, R

quantum yields, 46, 48, 128, 134, 287, 370  
quinoxalines, 65  
radiationless deactivation, 239  
radical  
  photopolymerization, 3, 5, 19, 63, 133, 257, 342  
  polymerization

recording media, 251, 260  
reduction potential, 7, 54, 97, 226  
rose bengal, 7, 10, 11, 260

## S

self-healing, 393  
sensitivity, 48–52, 60, 63, 66, 69, 94, 131, 215, 216, 218, 225, 228–230, 232, 236–239, 243, 259, 314, 342, 403  
silane, 8, 10, 12, 14, 16, 17, 19–21, 25–28, 30–32, 69, 108, 283, 284, 286, 288, 289, 292  
soft irradiation, 1, 5, 19–22, 23, 25, 33, 165  
solar energy, 183, 190, 362, 363, 378  
stimuli-responsive materials, 341–343  
sunlight, 5, 15, 19, 24, 25, 27, 33, 34, 91, 95, 183, 185, 313, 314, 364, 365, 372, 375, 378, 379, 384  
supramolecular cross-link, 411

## T

tetrazole, 281, 284–286, 296, 300–304, 313, 314  
thermally cross-linkable, 196  
thiol-ene photopolymerization, 2, 29  
thioxanthenes, 6, 15, 54, 63  
thiyl, 11, 29, 225, 336, 402–404  
three component systems, 10–12, 19, 21, 26  
time-of-flight secondary ion mass spectrometry, 282  
titanate initiators, 132  
triarylsulfonium salts, 46, 47, 50, 54, 56, 60, 63, 222, 329, 335–336  
triazine, 8–10, 15, 17, 21, 22, 25, 224, 228

triphenylamine, 22, 144, 167, 168,  
195–196  
trithiocarbonate, 100, 401  
two-component system, 7–10

## **U, V, X**

### **UV**

curing, 124, 151  
grafting, 337, 347, 348, 350

UV-VIS-NIR absorption, 219  
visible lights, 5, 7, 14–17, 19, 23, 28,  
34  
X-ray photoelectron spectroscopy  
(XPS), 282, 302



---

Other titles from

**ISTE**

in

Materials Science

---

## **2013**

BATHIAS Claude

*Fatigue Limit in Metals*

LEXCELLENT Christian

*Shape-memory Alloys Handbook*

## **2012**

DAVIM J. Paulo

*Wear of Advanced Materials*

DELHAES Pierre

*Carbon Science and Technology: From Energy to Materials*

GOUDEAU Philippe, GUINEBRETIERE René

*X-Rays and Materials*

SAANOUNI Khemais

*Damage Mechanics in Metal Forming: Advanced Modeling and Numerical Simulation*

VANBÉSIEN Olivier  
*Artificial Materials*

VERDU Jacques  
*Oxidative Ageing of Polymers*

## **2011**

BATHIAS Claude, PINEAU André  
*Fatigue of Materials and Structures: Application to Damage*

BATHIAS Claude, PINEAU André  
*Fatigue of Materials and Structures: Application to Design*

PRIESTER Luisette  
*Grain Boundaries and Crystalline Plasticity*

VIGNES Alain  
*Extractive Metallurgy 1: Basic Thermodynamics and Kinetics*

VIGNES Alain  
*Extractive Metallurgy 2: Metallurgical Reaction Processes*

VIGNES Alain  
*Extractive Metallurgy 3: Processing Operations and Routes*

## **2010**

BATHIAS Claude, PINEAU André  
*Fatigue of Materials and Structures VI / fundamental concepts*

CHATEIGNER Daniel  
*Combined Analysis*

CHEVALIER Yvon, VINH TUONG Jean  
*Mechanical Characterization of Materials and Wave Dispersion V2*

CHEVALIER Yvon, VINH TUONG Jean  
*Mechanical Characterization of Materials and Wave Dispersion*

DELHAES Pierre  
*Carbon-based Solids and Materials*

## **2009**

ALVAREZ-ARMAS Iris, DEGALLAIX-MOREUIL Suzanne  
*Duplex Stainless Steels*

DAVIM J. Paulo  
*Machining Composite Materials*

GALERIE Alain  
*Vapor Surface Treatments*

## **2008**

BATTAGLIA Jean-Luc  
*Heat Transfer in Materials Forming Processes*

BLONDEAU Régis  
*Metallurgy and Mechanics of Welding*

FRANÇOIS Dominique  
*Structural Components*

REYNE Maurice  
*Plastic Forming Processes*

TAKADOUM Jamal  
*Materials and Surface Engineering in Tribology*

## **2007**

BOCH Philippe, NIEPCE Jean-Claude  
*Ceramic Materials*

CRISTESCU Constantin  
*Materials with Rheological Properties*

## **2006**

LASSEN Tom, RÉCHO Naman  
*Fatigue Life Analyses of Welded Structures*



The design and development of dyes and chromophores has recently attracted much attention in various research fields such as materials, radiation curing, (laser) imaging, optics, medicine, microelectronics, nanotechnology, etc., and their use is widespread in polymer and materials science.

The authors of this book describe the basic principles and applications of dyes and chromophores within the polymer science and technology area and focus on the role played by these structures for the final properties of the polymer.

They provide a complete overview of the systems encountered and a thorough description of the mechanisms involved, thus providing the reader with all the necessary information in a single book.

The associated fields (optics, electronics, photovoltaics, materials, etc.) are largely emphasized and discussed and recently proposed systems are presented in detail. Up-to-date, promising and exciting developments are also illustrated.

**Jacques Lalevée** is Professor at Institut de Science des Matériaux de Mulhouse in France.

**Jean-Pierre Fouassier** was previously Professor at ENSCMu-UHA, Mulhouse, France.